MESON DISTRIBUTION AMPLITUDES

DISSERTATION
ZUR ERLANGUNG DES DOKTORGRADES
DER NATURWISSENSCHAFTEN (DR. RER. NAT.)
DER FAKULTÄT FÜR PHYSIK

DER UNIVERSITÄT REGENSBURG

vorgelegt von

Florian Anton Christoph Porkert

aus

Regensburg

im Jahr 2018

Promotionsgesuch eingereicht am: 20.06.2016
Die Arbeit wurde angeleitet von: Prof. Dr. Andreas Schäfer

Prüfungsausschuss:	Vorsitzender:	Prof. Dr. Jascha Repp
	1. Gutachter:	Prof. Dr. Andreas Schäfer
	2. Gutachter:	Prof. Dr. Vladimir M. Braun
	weiterer Prüfer:	PD Dr. Andrea Donarini

"Without a family, man, alone in the world, trembles with the cold."

—André Maurois (1885 – 1967)

Dedicated to my parents
Herta and Anton Porkert
with great gratitude

ABSTRACT

In this thesis we update the theoretical framework for the QCD calculations of $\gamma^*\gamma \to \eta$ and $\gamma^*\gamma \to \eta'$ transition form factors at large photon virtualities. This includes a full next-to-leading order analysis of perturbative corrections as well as charm quark contributions, while also taking into account $SU(3)$-flavor breaking effects and axial anomaly contributions to the power-suppressed twist-four distribution amplitudes. The related numerical analysis of the existing experimental data is performed with these improvements.

Moreover, we present an improved light-cone sum rule analysis of the $D, D_s \to \eta/\eta' l \nu_l$ transition form factors. In this context we argue, that these decays offer a very promising possibility to determine the leading Fock-state gluonic contribution of the η' meson in future experimental facilities, such as FAIR or Super-KEKB. We also provide a calculation for the corresponding branching ratios for B decays.

PUBLICATIONS

The research described in this thesis has been carried out in collaboration with Prof. Dr. Andreas Schäfer, Prof. Dr. Vladimir Braun, Dr. Nils Offen and Dr. Shahin Agaev.
Corresponding results have been published in the following articles [1–3].

Complete list of publications:

- S. S. Agaev, V. M. Braun, N. Offen and F. A. Porkert, "Light Cone Sum Rules for the $\pi^0\gamma^*\gamma$ Form Factor Revisited,"
  Phys. Rev. D **83** (2011) 054020
  [arXiv:1012.4671 [hep-ph]].
- S. S. Agaev, V. M. Braun, N. Offen and F. A. Porkert,
  "BELLE Data on the $\pi^0\gamma^*\gamma$ Form Factor: A Game Changer?,"
  Phys. Rev. D **86** (2012) 077504
  [arXiv:1206.3968 [hep-ph]].
- N. Offen, F. A. Porkert and A. Schäfer,
  "Light-cone sum rules for the $D_{(s)} \to \eta^{(\prime)} l \nu_l$ form factor,"
  Phys. Rev. D **88** (2013) 034023
  [arXiv:1307.2797 [hep-ph]].
- S. S. Agaev, V. M. Braun, N. Offen, F. A. Porkert and A. Schäfer,
  "Transition form factors $\gamma^*\gamma \to \eta$ and $\gamma^*\gamma \to \eta'$ in QCD,"
  Phys. Rev. D **90** (2014) 074019
  [arXiv:1409.4311 [hep-ph]].

CONTENTS

1 INTRODUCTION 1

2 QUANTUM CHROMODYNAMICS 5
- 2.1 Towards QCD 5
- 2.2 Symmetries and dynamics 8
- 2.3 Asymptotic freedom and perturbative QCD 15
- 2.4 QCD vacuum and operator product expansion 25
- 2.5 From symmetry currents to mesons 38
- 2.6 QCD and the Standard Model 48
  - 2.6.1 Aspects of weak interactions 48
  - 2.6.2 Hadronic matrix elements, form factors and branching fractions 55

3 MESON DISTRIBUTION AMPLITUDES 61
- 3.1 Mixing schemes and the $\eta - \eta'$ system 61
  - 3.1.1 Mixing effects and the $\eta - \eta'$ system 61
  - 3.1.2 Singlet-octet basis 63
  - 3.1.3 Quark-flavor basis 65
  - 3.1.4 Adaption to the language of distribution amplitudes 68
- 3.2 Conformal symmetry and twist-expansion 77
  - 3.2.1 General aspects of conformal symmetry 78
  - 3.2.2 Conformal towers 82
  - 3.2.3 Conformal operators in quantum chromodynamics (QCD) 86
- 3.3 Renormalization of the $\eta^{(\prime)}$ distribution amplitudes 90
  - 3.3.1 General remarks 90
  - 3.3.2 Leading-order evolution 92
  - 3.3.3 Next-to-leading order evolution 94
- 3.4 Higher twist $\eta^{(\prime)}$ distribution amplitudes 97
  - 3.4.1 General remarks 97
  - 3.4.2 Twist-three distribution amplitudes 98
  - 3.4.3 Twist-four distribution amplitudes 111

4 MESON PHOTON TRANSITION FORM FACTORS 131
- 4.1 pQCD approach 132
  - 4.1.1 Collinear factorization in QCD 132
  - 4.1.2 Leading order calculations 137
  - 4.1.3 Next-to-leading order calculations – light quark corrections 143
  - 4.1.4 Next-to-leading order – charm quark corrections 147
- 4.2 Light-cone sum rule approach 159
  - 4.2.1 Theoretical foundations 159
  - 4.2.2 Soft corrections vs. the large Q^2 limit 165
  - 4.2.3 Predictive power of QCD sum rules 166
  - 4.2.4 Twist-two spectral densities 166
  - 4.2.5 Twist-three, twist-four and meson mass corrections 169
  - 4.2.6 Rough estimate of twist-six corrections 170
- 4.3 Phenomenological analysis of $\eta^{(\prime)}$-meson-photon transitions 173
  - 4.3.1 The *BABAR* puzzle – part I 174
  - 4.3.2 The *BABAR* puzzle – part II 178
  - 4.3.3 The asymptotic limit for η and η' transition form factors 180

4.3.4 The time-like form factors 181
4.3.5 Numerical analysis of the space-like $\gamma^*\gamma \to (\eta, \eta')$ transition form factors 184

5 HEAVY TO LIGHT MESON TRANSITION FORM FACTORS 191
5.1 pQCD approach 191
5.1.1 Heavy-Meson Decay Constants 192
5.1.2 Perturbative calculations 195
5.2 Light-cone sum rules for heavy-to-light decays 208
5.2.1 General structure and special features 209
5.2.2 Leading-order and next-to-leading order spectral densities 210
5.3 Numerical evaluation 214
5.3.1 Choice of input parameters 214
5.3.2 Phenomenological results for $q^2 = 0$ 216
5.3.3 Parametrizations of heavy-to-light form factors 219
5.3.4 Heavy-to-light form factors and their shape $(q^2 \neq 0)$ 224

6 CONCLUSION 229

A APPENDIX – MISCELLANEOUS TOPICS 233
A.1 Pauli and Gell-Mann matrices 233
A.2 Dirac algebra and chiral projection operators 236
A.3 Operator identities 238
A.4 Restrictions on the Lagrangian 239
A.5 Elements of quantization 240
A.6 Feynman rules of QCD 241
A.7 Renormalization group – basics 243
A.8 Calculation of the chiral anomaly 243
A.9 Light-cone coordinates and projection operators 245
A.10 Construction of light-like vectors 247
A.11 Lie algebra of the conformal group 247
A.12 Polynomials and orthogonality relations 248
A.13 Asymptotic expansion 251
A.14 Fock states and light-cone wave functions 252
A.15 Short-distance correlation functions 254
A.16 Light-cone dominated correlation functions 255
A.17 SVZ-sum rule for the decay constant 258

B APPENDIX – CALCULATION SUPPLEMENTS 261
B.1 Scalar one-loop integrals 261
B.2 Passarino-Veltman decomposition – calculation example 265
B.3 The Borel transformation 267
B.4 Calculation of imaginary parts 271
B.5 Next-to-leading order quark-antiquark spectral densities 274
B.6 Fourier integrals 274
B.7 Two-gluon correlation function 275

C APPENDIX – RENORMALIZATION AND EVOLUTION 277
C.1 Evolution of the singlet decay constant 277
C.2 List of anomalous dimensions 278
C.3 Leading-order evolution kernels 283
C.4 Projection operators for the evolution procedure 285
C.5 Details of Kroll's formalism 285
C.6 Next-to-leading order singlet evolution 286

C.7 Equations of motion 288
C.8 Twist-three distribution amplitudes 291
C.9 Retrofitted higher twist Kaon distribution amplitudes 295

LIST OF FIGURES

Figure 1 Meson supermultiplet 6
Figure 2 Measurements of the Drell-ratio as a function of the e^+e^- center-of-mass energy 7
Figure 3 Measurements of the QCD color factors 8
Figure 4 Feynman diagram relevant for the axial anomaly 9
Figure 5 Feynman diagram: one-loop vacuum polarization 16
Figure 6 One-loop diagrams for the renormalization of α_S 18
Figure 7 Measurements of $\alpha_S(Q^2)$ 24
Figure 8 Generic example for bubble diagrams 26
Figure 9 Selected diagrams, including quark and gluon condensates 30
Figure 10 Example for a handbag diagram 36
Figure 11 Schematic overview of the Standard Model (SM) particles, based on [4] 49
Figure 12 Vertices of the electroweak interaction 50
Figure 13 Beta decay of a free quark 55
Figure 14 Leptonic decays of the charged pseudoscalar mesons π^- and D^- 57
Figure 15 Semileptonic weak decay $D^+ \to \pi^0 e^+ \nu_e$ 58
Figure 16 Determination of the mixing angle 68
Figure 17 Anomalous contribution to the twist-four distribution amplitude (DA) $\psi_{4M}^{(s)}(u)$ 126
Figure 18 Two-photon meson production and $e^+e^- \to M\gamma$ annihilation process 133
Figure 19 Factorization of the $F_{\gamma^*\gamma\to M}(Q^2)$ form factor at large Q^2 134
Figure 20 Example of higher twist diagrams 135
Figure 21 Soft photon corrections to the meson-photon transition form factor (TFF) 135
Figure 22 Twist-six correction to the $\eta^{(\prime)}$ TFF 143
Figure 23 next-to-leading order (NLO) Feynman diagrams of the $\gamma^*\gamma^{(*)} \to \bar{\psi}\psi$ amplitude 144
Figure 24 One-loop box diagrams contributing to the $\gamma^*\gamma^{(*)} \to gg$ amplitude 145
Figure 25 Central exclusive production of η and η' meson pairs in the perturbative regime 146
Figure 26 Schematic diagrams corresponding to $\mathcal{G}^2$ corrections in external fields 148
Figure 27 Conventions for N-point one-loop integrals 149
Figure 28 Hard subgraphs of Figure 24 a) and b) 153
Figure 29 Hard subgraph of Figure 24 c) 155
Figure 30 Analytic structure of $F^{\text{QCD}}_{\gamma^*\gamma^*\to M}(Q^2, -q_2^2)$ in the complex q_2^2-plane 163
Figure 31 Selected examples for twist-six corrections to Equation 731 in the factorization approximation 172
Figure 32 Comparison of the *BABAR* and Belle measurement [5, 6] for different models of the pion DA 174
Figure 33 Plot of various DA models 178
Figure 34 Comparison of the data on $\gamma^*\gamma \to \pi^0$ transitions with the non-strange component of $\eta^{(\prime)}$ TFFs $\gamma^*\gamma \to |\eta_q\rangle$ 179
Figure 35 Comparison of the experimental data on TFFs $\gamma^*\gamma \to (\eta, \eta')$ [7, 8] with a light-cone sum rule (LCSR) calculation 186
Figure 36 Impact of the gluon twist-two DA on the $\eta - \eta'$ system 188
Figure 37 Plot of a specific model (cf. Table 14) using a logarithmic scale in Q^2 189

Figure 38 Basic steps towards the QCD sum rules for a generic decay constant 196
Figure 39 Leading-order two- and three-particle contributions to the $D_s^+ \to \eta^{(\prime)} l^+ \nu_l$ transitions form factors 199
Figure 40 SU(3)-flavor singlet and octet contributions to the $D_s^+ \to \eta^{(\prime)} l^+ \nu_l$ transitions form factors 204
Figure 41 Next-to-leading order contributions to the $D_s^+ \to \eta^{(\prime)} l^+ \nu_l$ transitions form factors 207
Figure 42 Form factors $|f_+^{D_s \to \eta}(M^2)|$, $|f_+^{D_s \to \eta'}(M^2)|$ plotted as functions of M^2 216
Figure 43 $\left| f^+_{D_s^+ \eta'}(q^2) / f^+_{D_s^+ \eta}(q^2) \right|$ plotted as a function of q^2 218
Figure 44 Common extrapolation methods for the vector and scalar form factor 221
Figure 45 $f^+_{D_s^+ \eta}(q^2)$ plotted as a function of q^2 225
Figure 46 $f^+_{D_s^+ \eta'}(q^2)$ plotted as a function of q^2 226

LIST OF TABLES

Table 1 Symmetries of the classical (QCD) Lagrangian 40
Table 2 Ordering pattern of light pseudoscalar mesons 46
Table 3 Representation of the SM particles 51
Table 4 Elementary particles' weak hypercharge, electromagnetic charge and third component of their weak isospin 53
Table 5 Fundamental fields: collinear twist, conformal spin and spin projections 80
Table 6 Analogy: quantum mechanics and QCD 92
Table 7 Hadronic twist-three parameters 105
Table 8 Comparison of twist-three $\eta^{(\prime)}$ quark-flavor (QF) parameters for the input [9] and [10] 107
Table 9 Comparison of twist-three $\eta^{(\prime)}$ singlet-octet (SO) parameters for the input Table 8 111
Table 10 Hadronic twist-four parameters 121
Table 11 Numerical values of the coefficients $\widetilde{G}_n^k$ and $\widetilde{H}_n^k$, for $n, k \leqslant 10$ 169
Table 12 Models for the pion DA describing [5] and [6] 177
Table 13 First view coefficients "$f_{M;n}^{(p)}$" ($n=2,4$; $p=q,s,g$) 183
Table 14 Three sample models for the η and η' twist-two DAs 187
Table 15 Axial-vector currents j_μ^H for purely leptonic decays similar 192
Table 16 Currents entering Equation 946 195
Table 17 Numerical value of Equation 968 for $\mu_0 = 1.0$ GeV (fixed), and $\mu = 1.4$ GeV, $\mu = 1.5$ GeV or $\mu = 2.5$ GeV 205
Table 18 Input for the Ball-Zwicky model, parametrizing $f^+_{D_{(s)}\eta^{(\prime)}}(q^2)$ 224
Table 19 Branching fractions – comparison of LCSR results and experimental data 227
Table 20 Ratios of branching fractions – LCSR results and experimental data 227
Table 21 Mass coefficients in the SO and QF basis 235
Table 22 Pseudoscalar particles and their flavor structure 288
Table 23 Replacement rules, used for the derivation of twist-three kaon DAs 295

ACRONYMS

BMS	Bakulev-Mikhailov-Stefanis
BPST	Belavin-Polyakov-Schwartz-Tyupkin
BRST	Becchi-Rouet-Stora-Tyutin
ChPT	chiral perturbation theory
CKM	Cabibbo-Kobayashi-Maskawa
DA	distribution amplitude
DE	differential equation
DIS	deep inelastic scattering
EOM	equations of motion
ER-BL	Efremov-Radyushkin-Brodsky-Lepage
FF	form factor
FFNS	fixed flavor number scheme
FKS	Feldmann-Kroll-Stech
GMO	Gell-Mann-Okubo
GMOR	Gell-Mann-Oakes-Renner
HQET	heavy quark effective theory
IR	infrared
KS	Kogut-Soper
LB	Brodsky-Lepage
LCSR	light-cone sum rule
LEET	large energy effective theory
LFWF	light-front wave function
LO	leading-order
LSZ	Lehmann-Symanzik-Zimmermann
NLO	next-to-leading order
NNLO	next-to-next-to-leading order
OPE	operator product expansion
OZI	Okubo-Zweig-Iizuka

PCAC partially conserved axial current

pQCD perturbative quantum chromodynamics

PT perturbation theory

PV Passarino-Veltman

QCD quantum chromodynamics

QED quantum electrodynamics

QF quark-flavor

QFT quantum field theory

RG renormalization group

RGE renormalization group equation

SCET soft-collinear effective theory

SM Standard Model

SO singlet-octet

SSB spontaneous symmetry breaking

SVZ Shifman-Vainshtein-Zakharov

TFF transition form factor

UV ultraviolet

VEV vacuum expectation value

VFNS variable flavor number scheme

1 INTRODUCTION

"Thinking must never submit itself,
neither to a dogma,
nor to a party,
nor to a passion,
nor to an interest,
nor to a preconceived idea,
nor to anything whatsoever,
except to the facts themselves,
because for it to submit to anything else would be the end of its existence."

— Henri Poincaré (1854 – 1912)

For many years light pseudoscalar η and η' mesons were subject of numerous theoretical and experimental studies. Since they exhibit $\eta - \eta'$ mixing, driven by the famous $U(1)_A$ anomaly, these mesons play a key-role in the understanding of non-perturbative QCD. In particular, the confirmation of a large gluonic component in the η and η' wave functions would confirm our present understanding concerning the topological properties of QCD . Furthermore, a sound knowledge of the $\eta^{(\prime)}$ meson is important for several semileptonic weak decays that include charmed and beauty hadrons, e. g., $D_{(s)} \to \eta^{(\prime)} l \nu_l$. The latter are relevant for the determination of SM parameters.[1] It is, therefore, crucial for the search for physics beyond the SM in processes with η mesons in the final state.

As a very important source of information about the $\eta - \eta'$ system serves the "gold-plated" $\eta^{(\prime)} \to \gamma^* \gamma^{(*)}$ form factor (FF). The analogue process for the pion has been in the focus of theorists and experimentalists alike for over two decades and belongs to the most thoroughly investigated applications of QCD. Nevertheless, the (2009) *BABAR* [5] measurement of the pion photon TFF exhibited an unexpected scaling violation at large momentum transfer, known as the "*BABAR*-puzzle", posing the question whether hard exclusive hadron reactions are under theoretical control. This challenge led to a flurry of discussions about the applicability of collinear factorization in QCD and the non-perturbative structure of the meson itself. The (2012) Belle [6] measurement, where the scaling violation is less severe, took the pressure of theorists struggling to invent new non-perturbative mechanisms to resolve the puzzle. Also, recent *ab initio* calculations of the pion DA (cf. [11]) have become a viable method to help explaining the phenomenological findings. However, lattice QCD's attempt to establish theoretical control over the $\eta - \eta'$ mixing and $D^+_{(s)} \to \eta^{(\prime)} l^+ \nu_l$ weak decays are still in their infancy, since they are technically very challenging [12] and expensive to calculate. Especially the photon-meson TFFs can hardly be implemented in nowadays lattice studies. On the other hand, the same problems concerning the non-perturbative meson-mixing and the impact of the axial anomaly are also present in the analytical sector. To sort out all the relevant problems is very non-trivial and takes a lot of effort. In principle, the same program as carried out in the past for the pion case has to be adapted and extended for the $\eta^{(\prime)}$ mesons.

In contrast to the pion and kaons, the progress in the $\eta^{(\prime)}$-sector has been rather modest. No-

1 With SM we always refer to the Standard Model of particle physics.

table contributions concerning the $\eta - \eta'$ mixing for the corresponding decay constants have been made on the theoretical side using chiral perturbation theory (ChPT) calculations (cf. [13, 14]). The latter have been adapted and refined for phenomenological applications leading to the widely recognized Feldmann-Kroll-Stech (FKS) scheme [9, 15].
Apart from the mixing schemes, the work on the meson-photon TFF based on the collinear factorization assumption[2] culminated in the paper [20] of Kroll *et al.* which provides a NLO perturbative quantum chromodynamics (pQCD) calculation of the leading-twist contributions for vanishing quark-masses. Moreover, it includes a leading-order (LO) evolution of the involved DAs based on [21–27]. The related fit [28] to the *BABAR* [7] and CLEO [8] data belongs to the first attempts in finding a reliable model for the η and η' DAs which are represented by values for the first non-trivial moments of their Gegenbauer expansion. However, the corresponding findings for the pion DA in the same approach contradict several LCSR calculations and the latest available lattice results. As stated by the authors, the quoted Gegenbauer coefficients have to be seen as effective parameters which are perturbed by neglected possible mass and higher twist corrections. Therefore, a LCSRs approach would be helpful to test and extend these studies further. Such an approach includes the extension to higher twist effects as well as meson and quark-mass corrections. The former is more complicated compared to the pion because of the anomaly contributions and needs to be developed from scratch. Furthermore, NLO LCSRs for the gluonic DAs have to be calculated and the impact of heavy flavors in NLO pQCD corrections have to be analyzed. Apart from that, a NLO QCD renormalization adapted to the existing formalism has to be developed. Last but not least the $SU(3)_F$ breaking and the $\eta - \eta'$ mixing effects have to be included with, e. g., the help of a phenomenological approach. Similar to the pion case, the weak heavy-to-light decays are important for this complex of problems and have to be included into the considerations. In particular, the D_s system is an important item of the experimental program of current and planned hadron facilities, such as FAIR [29]. High precision experiments for semileptonic decay modes, including $B^+, D^+, D_s^+ \to \eta^{(\prime)} l^+ \nu_l$ are expected to become available in the near future. These will provide complementary and reliable information on $\eta - \eta'$ mixing as well as on the involved DAs.

As discussed in [30], the same mechanism responsible for the enhanced η' production exhibited by the weak decay[3] $D_s \to \rho^+ \eta'$ should also be present in Okubo-Zweig-Iizuka (OZI) suppressed diagrams where the η' is produced via gluons. Even though, a full treatment of the gluonic DA is beyond the scope of this Shifman-Vainshtein-Zakharov (SVZ) sum rules treatment, the effects have been estimated via phenomenological fits. A non-vanishing gluonic contribution seems very likely, and on these grounds the importance of the gluon fusion mechanisms for η' production has been emphasized. Another work devoted to the $D_s \to \eta^{(\prime)}$ transition was carried out in the LCSR formalism at LO accuracy for chiral currents (see [31]). Unfortunately, the interesting gluonic DA will only enter at NLO accuracy. Therefore, an analogous analysis as for the B decays (see [32]) is needed.

This is where our work begins, which is organized as follows: For the convenience of the reader, we start with a general introduction concerning quantum chromodynamics and weak interaction (cf. Chapter 2). In doing so, we lay the general foundations for the following chapters which focus on specific aspects of conformal symmetry (see Section 3.2) and QCD sum rules (e. g., Section 4.2, along with Section 5.1.1). Let us now mention some of the highlights of this work. As

2 There are two completely different approaches from D. Melikhov *et al.* (see [16–18]), a dispersion approach based on the constituent quark picture, and the work of O. Teryaev *et al.* (see [19]), who use an anomaly sum rule (developed for the octet channel). However, these methods lack the ability to extract information of the non-perturbative behavior of the $\eta^{(\prime)}$ DAs.

3 This decay is interesting for its unusual deviation between experiment and theory.

one bigger project, we will extend the studies of Kroll *et al.* [20, 28] which are based on the collinear factorization approach [33] (see Chapter 3 and Chapter 5). In view of the discussion given above, it is reasonable to go for a full and consistent NLO treatment of the η and η' DAs. To this end, we implement a complete NLO treatment of the scale dependence for $\eta^{(\prime)}$ DAs, including quark-gluon mixing (see Section 3.1, Section 3.3). Correspondingly, we calculate all relevant gluonic NLO QCD corrections contributing to the LCSRs for meson transition form factors. Here, we also take into account perturbative charm-quark contributions to the coefficient functions of the underlying two-gluon DAs (see Chapter 4 for details). Additionally, we provide a consistent treatment of strange quark mass and higher twist corrections[4] up to $\mathcal{O}(m_s)$ accuracy including an update of the $SU(3)_F$-breaking effects within twist-four DAs (cf. Section 3.4). In addition, we partially take into account contributions from the $U(1)_A$ anomaly and implement $\eta - \eta'$ mixing schemes in the twist-three, along with twist-four DAs (see Chapter 3). This is complemented by a verification of the applied QCD factorization approach at LO in the strong coupling constant (see Section 4.1.1). We further use these improvements for a numerical analysis of the current space-like and time-like TFF data, including a careful statistical analysis of the uncertainties, and the prospects to constrain the two-gluon $\eta^{(\prime)}$ DAs if more precise data on the FFs become available. In this sense, we were able to formulate a model for the η and η' mesons which is consistent with the available data. Moreover, we generalize the existing $D_s^+ \to \eta^{(\prime)} l^+ \nu_l$ analysis to NLO, including mass-corrections and two-gluon DA contributions. Furthermore, we extend the phenomenological evaluation to the D and B channel, providing results for the branching fractions obtained from the new DA models (see Chapter 5). Last but not least we identify a set of observables that is extremely sensitive to gluonic DAs (cf. Chapter 5).

Finally, in Chapter 6 we summarize the results of this work and give a brief outlook.

4 Here, we were able to restore collinear factorization.

2 QUANTUM CHROMODYNAMICS

"It is the last lesson of modern science,
that the highest simplicity of structure is produced,
not by few elements,
but by the highest complexity."

— Ralph Waldo Emerson (1803 – 1882)

The following chapter introduces the basics needed for this thesis. Apart from introducing QCD as the underlying theory of strong interaction, important technical and theoretical features, such as the operator product expansion (OPE) and axial anomaly are discussed in detail. Besides these topics, some background information concerning global symmetries of the QCD Lagrangian and implications on possible particle formation are mentioned. Furthermore, the most important features of the standard model are considered, including a short review concerning form factors and interpolating currents. In the subsequent chapters the mentioned aspects of strong and weak interaction are essential for approaching the η, along with η' mesons on a phenomenological and theoretical basis. Thus, they are particularly useful for an understanding of corresponding DA which are in the focus of this work.

2.1 TOWARDS QCD

Since the 1950s experimental high energy physics discovered a large and ever-growing number of strongly interacting particles, so-called "hadrons". Such a large number of particles seemed unlikely to be fundamental. The first attempts to understand the fundamental dynamics of the involved physical systems and (internal) symmetries have been deduced via group-theoretical considerations. In general, such symmetries are related to conserved quantum numbers and corresponding conservation laws which manifest themselves by the absence of certain processes, e. g., hydrogen does not decay into two photons due to the conservation of the baryon number "B". When realizing that the strong force is approximately independent of the electric charge carried by the hadron, the isospin has been introduced [34]. This is an internal $SU(2)$ symmetry in analogy to the (atomic) spin, where, e. g., the proton and the neutron form a (isospin) doublet like the spin "up" and "down" projections of a spin-$\frac{1}{2}$ particle. By extending the concept to other hadrons not only isospin doublets, but also triplets and isosinglets can be identified. In this way hadrons can be arranged according to their quantum numbers, such as the 3^{rd} of the isospin I_z or hypercharge[1] Y, implying characteristic multiplets (see Figure 1). After the discovery of the Λ baryons and the K mesons (their decays proceed with an unexpected lifetime [35]), the additive quantum number "strangeness" has been introduced which is conserved in strong interaction. Another important step has been done, when realizing, that the pseudoscalar meson octet (involving the lightest eight (π, K, η) mesons) can be related to weight diagrams implied by specific representations of the $SU(3)$ group. This led to the proposal of the "Eightfold Way" [38] which successfully predicted the Ω^- [39], but the fundamental representation of $SU(3)$ (which also would give triplet and sextet representations) cannot be identified with any known hadrons. Hence, the proposal of the quark model has been made in which all hadrons are built

1 Which at this point is the sum of the baryon number (for baryons 1 and for mesons 0) and the strangeness of the particle.

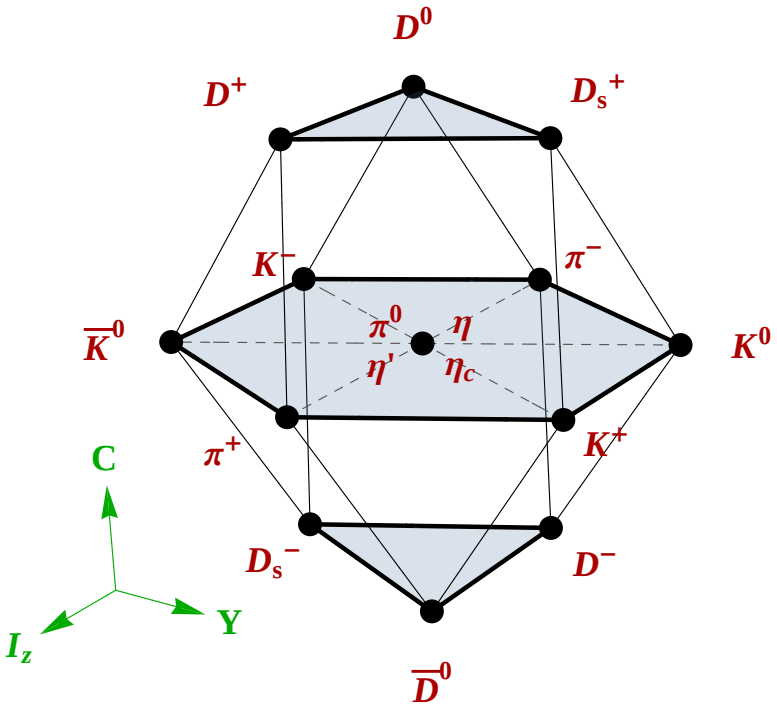

Figure 1: Meson supermultiplet (created with Wolfram *Mathematica*® 8 [36]), where each particle is arranged based on its quantum numbers, such as charm (C), hypercharge (Y) and the 3rd component of the isospin (I_z). According to the quark-model (i. e., on the valence quark level) corresponding positions in the (I_z, Y, C) space are given by $\pi^+ \sim (u\bar{d})$, $\pi^0 \sim \frac{1}{\sqrt{2}}(u\bar{u} - d\bar{d})$, $K^+ \sim (u\bar{s})$, $K^0 \sim (d\bar{s})$, $\eta \sim \frac{1}{\sqrt{6}}(u\bar{u} + d\bar{d} - 2s\bar{s})$, $\eta' \sim \frac{1}{\sqrt{3}}(u\bar{u} + d\bar{d} + s\bar{s})$, $\eta_c \sim (c\bar{c})$, $D^+ \sim (c\bar{d})$, $D^0 \sim (c\bar{u})$, $D_s^+ \sim (c\bar{s})$, etc. [37].

out of massive spin-$\frac{1}{2}$ quarks[2] which transform (restricted to three different quark species) as members of the fundamental representation of $SU(3)_F$. The quark model has several problems, restricting its status to a mere model rather than a full theory. First of all, the quarks "q" in the quark model are free fermions in contradiction to experiment where they have never been measured directly [42, 43]. Moreover, the hadrons are built out of $\bar{q}q$ (mesons) and qqq (baryons) states (and conjugates), while no evidence for possible qq, $qqqq$, etc., (not excluded by the quark model) bound states have been found. The third and most serious problem regards the decouplet baryon[3] with spin $\frac{3}{2}$. Here, particles like the Ω^- or Δ^{++} consist of three (valence) quarks of the same flavor with their spins aligned. Being a ground state the total angular momentum has to be zero and the spatial wave function will, therefore, be symmetric. Also the flavor and spin wave functions are totally symmetric leading to a violation of the Fermi-Dirac statistics and Pauli exclusion principle. Nevertheless, these theoretical shortcomings and paradoxes can be overcome by using another internal symmetry. A posteriori, quarks exhibit an intrinsic degree of freedom, usually referred to as color. Here, every quark flavor q_a comes in a color triplet ($a = 1, 2, 3$, i. e., "red, blue, green") producing, e. g., an antisymmetric part in the total wave function of the $|\Omega^-\rangle \sim |u_a u_b u_c\rangle \varepsilon^{abc}$ and the other baryons in question. In fact, studies of electron-positron

2 Quarks have been (indirectly) measured for the first time at the Stanford Linear Accelerator Center at 1967 (see [40] and references therein).

3 Those have total angular momentum $\frac{3}{2}$ (later on called $J^P = [\frac{3}{2}]^+$ state).

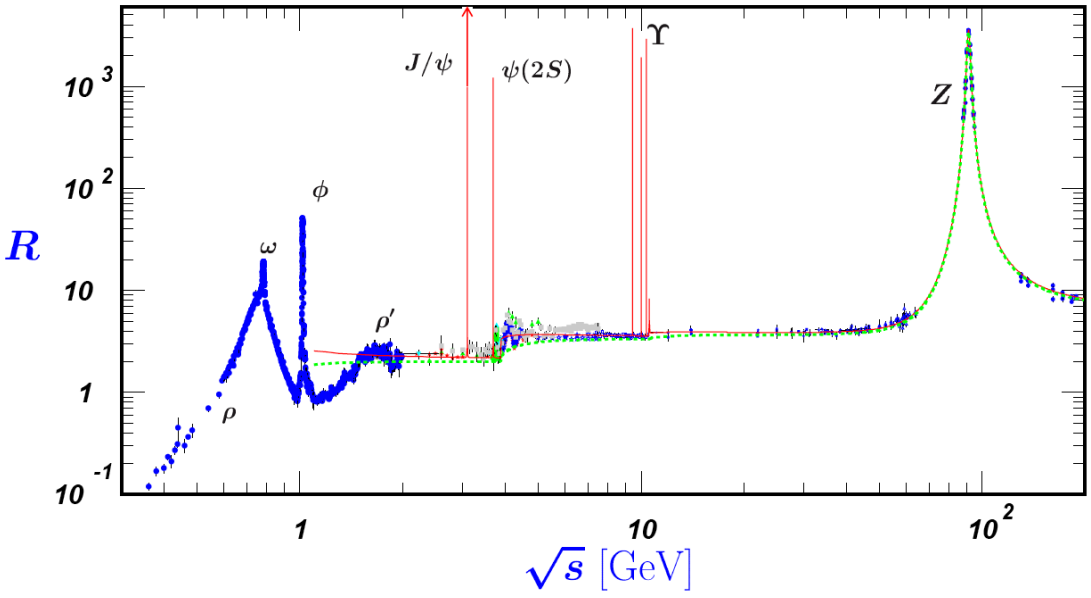

Figure 2: Measurements of the hadron-muon branching ratio (cf. Equation 1) as a function of the e^+e^- center-of-mass energy $\sqrt{s}$ (from [41, 42]).

annihilation to hadrons reveal, that the Drell-ratio [41, 42, 44, 45] (the ellipses denote neglected quantum and mass corrections, cf. Section 2.4)

$$R(s) = \frac{\sigma(e^+e^- \to \text{hadrons})}{\sigma(e^+e^- \to \mu^+\mu^-)} = N_c \sum_q e_q^2 + \dots , \tag{1}$$

depends on the quark specific fractions e_q of the proton electric charge e as well as the number of colors[4] N_c. Besides, the sum runs over all active flavors which can be produced at a given center-of-mass energy $\sqrt{s}$ (cf. Figure 2). The postulated value $N_c = 3$ is perfectly consistent with experiment (see[5] Figure 2 and Figure 3). However, the ratio of Equation 1 has to be seen as an approximation which does not yet include further quantum corrections in addition to the asymptotic ones. Nevertheless, besides e^+e^- annihilations there is another well-known process, relevant for this work, which bears indirect evidence for the color degree of freedom: the $\pi^0 \to 2\gamma$ decay. In particular, the neutral pion decay into two photons is driven by anomalous contributions to the divergence of corresponding axial-vector currents (see Figure 4). Hence, the lowest order calculation[6] results in the decay rate (cf. [45, 51, 52])

$$\Gamma\left(\pi^0 \to 2\gamma\right) = N_c^2 \left(e_u^2 - e_d^2\right)^2 \frac{\alpha_{QED}^2 m_\pi^3}{32\pi^3 f_\pi^2} , \tag{2}$$

where m_π refers to the neutral pion mass, $\alpha_{QED} = \frac{e^2}{4\pi}$ is the fine-structure constant and "f_π" corresponds to the pion decay constant, as extracted from the process $\pi \to \mu\nu$ ($f_\pi \approx 130.4$ MeV).

4 For the representation of color charges, we conveniently use red, green and blue, which implies the anti-colors cyan (anti-red), magenta (anti-green), as well as yellow (anti-blue) (see, e. g., Figure 11).

5 Apart from the resonances, the measured ratio R is almost flat, in agreement with Equation 1 for a given set of active flavors.

6 In the limit of vanishing quark masses and external momenta prediction from this Adler-Bell-Jackiw anomaly are rather precise, because higher-loop diagrams do not contribute (cf. [49, 50]).

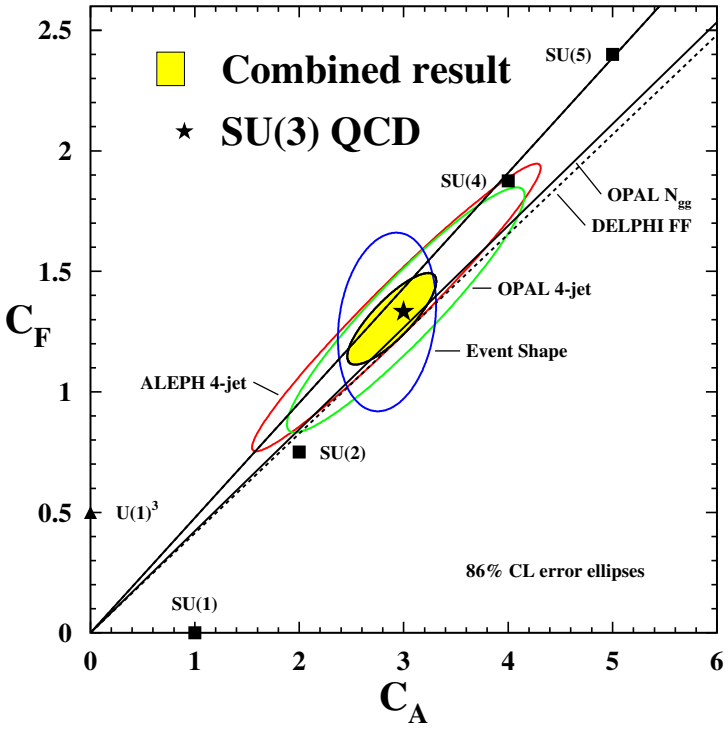

Figure 3: Measurements of the QCD color factors $C_A = N_c$ and C_f (cf. Section A.1), see also [46, 47].

According to this input, combined with $e_u = \frac{2}{3}$, $e_d = -\frac{1}{3}$ and $N_c = 3$, the implied theoretical prediction (see also [45]))

$$\Gamma\left(\pi^0 \to 2\gamma\right) \approx 7.6 \text{ eV} \tag{3}$$

is in very good agreement with experimental data [42, 45]

$$\Gamma\left(\pi^0 \to 2\gamma\right)\Big|_{\text{exp}} = (7.48 \pm 0.33) \text{ eV}\,. \tag{4}$$

Consequently, we may assume, that each quark flavor exists in three different colors. However, it must be emphasized that this new degree of freedom comes with the following phenomenological characteristics:

- only color singlet states are physically observable,
- quarks can only exist inside hadrons and can never be free.

These features of the strong interaction are known as color confinement. Hence, the color-symmetry is supposed to be exact. Furthermore, not only the Eightfold Way can be reproduced, but also the confinement restricts the physically observable states to products $3 \otimes \bar{3}$ and $3 \otimes 3 \otimes 3$ (mesons and baryons are singlet states of the group). Therefore, bound states, such as "$q\bar{q}$" or "qqq" and their combinations may exist, while others are ruled out.

2.2 SYMMETRIES AND DYNAMICS

Quantum chromodynamics represents a remarkable synthesis of the various ideas developed about hadron physics. That means it does not only reproduce elder developments, e. g., the

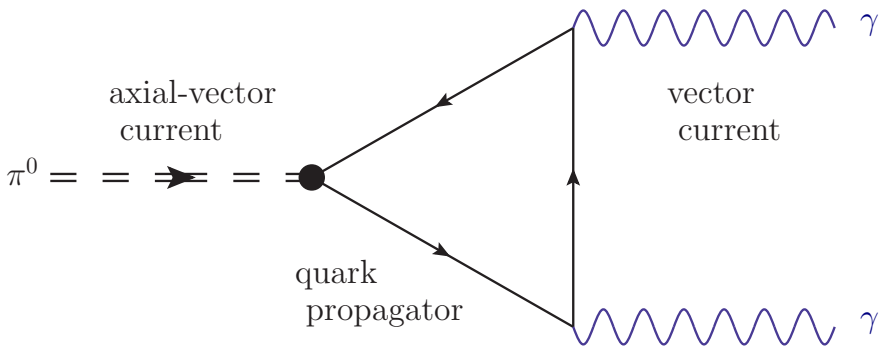

Figure 4: Feynman diagram relevant for the axial-anomaly, associated with the decay process $\pi^0 \to 2\gamma$. Solid, wave and double-dashed lines represent quarks, photons and external currents, respectively. Besides, the black dot corresponds to a vertex of the pion interpolating field. (Note that the Feynman diagrams shown in this work were created with *JaxoDraw* [48].)

Eightfold Way or current algebras, but reveals the origin of strong interaction in the corresponding energy realm[7].

One crucial step towards the theory of strong interaction has been done with the deep inelastic scattering (DIS) experiments of lepton-proton scattering. Here, a lepton[8] exchanges a highly virtual photon with a proton to probe its internal structure. These experiments also led to the discovery of Bjorken scaling [57, 58], the validation of the quark model and the confirmation of asymptotic freedom in QCD (see discussion below). The latter is connected with the strength of the strong interaction at different energy scales. Probed at asymptotically high energies, the observed strongly interacting particles behave as a collection of point-like, quasi-free constituents (cf. [59]). Therefore, such a property is called "asymptotic freedom", i. e., the coupling strength of the theory has to decrease at short distances. Theories with this property are called asymptotically free. This is a significant difference to the familiar quantum electrodynamics (QED) where the coupling strength decreases with distance due to dielectric screening by the cloud of virtual electron-positron pairs. That restricts the candidates for a possible quantum field theory (QFT) to theories with an anti-screening effect. In fact, no renormalizable field theory can be asymptotically free without non-abelian gauge fields [44, 60, 61], which are called "Yang-Mills theories". Therefore, the most distinctive feature of the strong interaction leads to a special class of QFT, because Yang-Mills theories are the only asymptotically free theory in four dimensions.

It has already been pointed out, that the source of the strong interaction is the color-charge. In analogy to (spinor) QED, QCD is formulated as a QFT with massive spin-$\frac{1}{2}$ fermions (quarks) interacting via vector bosons (spin-1), called the "gluons". Like the quarks also the gluons have been observed indirectly (see, e. g., [62] and references therein) with the properties discussed in the following section.

Let us start in the asymptotically free realm of the theory to construct the full QCD step by

7 According to the renormalization group (RG) ansatz (see, e. g., [53, 54] and references therein) one may regard (nearly) every quantum field theory with a cut-off scale as an effective field theory. That means it is futile to demand or expect that the theory will continue working at arbitrary short distances (high energies). At some point it will break down and has to be replaced by a more fundamental description (cf., e. g., [55, 56]).

8 A well established method of getting information on the structure of a particle is to use a structureless particle as a projectile which scatters off the particle in question.

step. In this way, the discussed features can be introduced systematically. As a starting point, there are six different quark species [63] (called "flavors") denoted by $\psi = u, d, s, c, b, t$ (see Section 2.6.1) and carrying the three-fold intrinsic degree of freedom color (color index $a = 1, 2, 3$) as well as spin-$\frac{1}{2}$ (Dirac-index $\alpha, \beta = 1, \ldots, 4$ – see Section A.2). Therefore, each flavor is expressed by a Dirac-spinor ψ^a_β with (bare) mass m_ψ satisfying the free Dirac equation (see, e. g., [45, 64])

$$\left[i \left(\gamma_\mu\right)_{\alpha\beta} \partial^\mu - m_\psi \delta_{\alpha\beta} \right] \psi^a_\beta(x) = 0 \tag{5}$$

in the asymptotically free regime. In order to make symmetries of the theory more obvious, we work with Lagrangian densities for the following considerations. So we start with the free Lagrangian[9]

$$\mathcal{L}_F^{(0)} = \sum_\psi \bar{\psi}^a_\alpha \delta^{ab} \left[i \left(\gamma_\mu\right)_{\alpha\beta} \partial^\mu - m_\psi \delta_{\alpha\beta} \right] \psi^b_\beta \tag{6}$$

and iteratively derive the full Lagrangian. In short, the form of this QCD Lagrangian density will be dictated by (gauge) symmetries and renormalizability (see Section A.4). Both requirements impose strong constraints on the form of a possible QCD Lagrangian.
Gauging the color symmetry formally is done by the hypothesis that the local transformation[10]

$$\psi^a_\alpha(x) \longmapsto \left[\exp\left\{ -i\theta^A(x) T^A \right\} \right]^{ab} \psi^b_\alpha(x) \,, \tag{7}$$

with rotation angles $\theta^A(x)$ and generators $\left\{T^A\right\}_{A=1,\ldots,8}$ of $SU(N_c = 3) \equiv SU(3)_c$, which leaves the physics invariant, i. e., this symmetry generates the underlying gauge interaction. The prototype for a gauge theory is QED with an inherent $U(1)$ symmetry, while Yang-Mills theories are based on non-abelian groups like $SU(N_c)$. This non-abelian nature of the gauge fields is responsible for the asymptotic freedom of the strong interaction. However, invariance under gauge transformation for dynamical quark fields is only possible after replacing ∂_μ in Equation 6 with the gauge covariant derivative in the fundamental representation (cf., e. g., [45, 64])

$$\left[D_\mu(x)\right]^{ab} = \delta^{ab} \left.\partial_\mu\right|_x - ig \mathcal{A}^A_\mu(x) \left[T^A\right]^{ab} \,. \tag{8}$$

Analogously, the covariant derivative in the adjoint representation can be defined:

$$\left[D_\mu(x)\right]^{AB} = \delta^{AB} \left.\partial_\mu\right|_x - ig \mathcal{A}^C_\mu(x) \left[\mathcal{T}^C\right]_{AB} \,, \tag{9}$$

where $\mathcal{T}^A$ are the generators in the adjoint representation (see Section A.1). It should be emphasized that the gauge fields $\left\{\mathcal{A}^A_\mu\right\}_{A=1,\ldots,8}$ are representing the eight different gluon species, while the parameter "g" denotes the coupling strength. The latter is the analogon to the electrical charge "e" of QED. Apart from renormalizability (see [45], Section A.4) gauge invariance can be ensured by the minimal coupling ansatz

$$\left[D_\mu(x)\right]^{ab} \psi^b_\alpha(x) \overset{\text{gauge}}{\longmapsto} \left[e^{-i\theta^A(x) T^A} \right]^{ab} \left[D_\mu(x)\right]^{bc} \psi^c_\alpha(x) \,, \tag{10}$$

implying, that the gluons $\left(\mathcal{A}_\mu(x) \equiv \mathcal{A}^A_\mu(x) T^A\right)$

$$\mathcal{A}_\mu(x) \overset{\text{gauge}}{\longmapsto} U(x) \left[\mathcal{A}^A_\mu(x) T^A - \frac{i}{g} U^\dagger(x) \left(\partial_\mu U(x)\right) \right] U^\dagger(x) \,, \quad U(x) \coloneqq \exp\left\{ -i\theta^A(x) T^A \right\} \tag{11}$$

9 Which implies the (classical) Euler-Lagrange Equation 5.
10 In other words, quarks transform as the fundamental representation of the color group $SU(3)_c$ (see Equation 7).

transform according to the adjoint representation of this gauge group. For infinitesimal angles[11], Equation 11 involves the structure constants f^{ABC} of the underlying gauge group $SU(3)_c$ (Section A.1):

$$\mathcal{A}_\mu^A \overset{\text{gauge}}{\longmapsto} \mathcal{A}_\mu^{A,\theta} \equiv \mathcal{A}_\mu^A - \frac{1}{g}\partial_\mu\theta^A + f^{ABC}\theta^B\mathcal{A}_\mu^C = \mathcal{A}_\mu^A - \frac{1}{g}\left[D_\mu\right]^{AB}\theta^B\,. \tag{12}$$

Thus, the quark-gluon interaction can be described by

$$\mathcal{L}_F = \sum_\psi \bar{\psi}_\alpha^a \left[i\left(\not{D}\right)_{\alpha\beta}^{ab} - m_\psi \delta_{\alpha\beta}\delta^{ab}\right]\psi_\beta^b\,, \tag{13}$$

which leads us to the gauge-fields. Similar to QED, the gluodynamics can be described via a corresponding gluon field strength tensor[12] [45, 64]

$$\mathcal{G}_{\mu\nu}(x) \coloneqq \mathcal{G}_{\mu\nu}^A(x)T^A = \frac{i}{g}\left[D_\mu, D_\nu\right] \Rightarrow \mathcal{G}_{\mu\nu}^A(x) = \partial_\mu\mathcal{A}_\nu^A(x) - \partial_\nu\mathcal{A}_\mu^A(x) + gf^{ABC}\mathcal{A}_\mu^B(x)\mathcal{A}_\nu^C(x), \tag{14}$$

which, in contrast to its electromagnetic counterpart, is itself not gauge invariant $\left(|\theta^B| \ll 1\right)$:

$$\mathcal{G}_{\mu\nu}(x) \overset{\text{gauge}}{\longmapsto} U(x)\mathcal{G}_{\mu\nu}(x)\,U^\dagger(x) \approx \mathcal{G}_{\mu\nu}^A + i\theta^B\left[T^B\right]^{AC}\mathcal{G}_{\mu\nu}^C\,. \tag{15}$$

This is a consequence of the non-abelian self-interaction (see Equation 14). Consequently, the related classical Lagrangian may incorporate terms proportional to $\mathrm{Tr}\{\mathcal{G}_{\mu\nu}\tilde{\mathcal{G}}^{\mu\nu}\}$ which apart from their covariance, represent $SU(3)_c$ invariant combinations of gauge fields. Incidentally, the dual field strength tensor is introduced for this purpose:

$$\tilde{\mathcal{G}}^{\mu\nu} = \frac{1}{2}\varepsilon^{\mu\nu\lambda\rho}\mathcal{G}_{\lambda\rho}\,. \tag{16}$$

Regardless of this difference to QED the gluonic interaction can be taken into account in a similar way with the same conventional prefactor to get[13]

$$\mathcal{L}_{\text{QCD}}^{(\text{cl.})} = \sum_\psi \bar{\psi}_\alpha^a\left[i\left(\not{D}\right)_{\alpha\beta}^{ab} - m_\psi\delta_{\alpha\beta}\delta^{ab}\right]\psi_\beta^b - \frac{1}{2}\,\mathrm{Tr}\{\mathcal{G}_{\mu\nu}\mathcal{G}^{\mu\nu}\}\,. \tag{17}$$

It is important to note that the gluons are massless[14], because a term proportional to $\mathcal{A}_\mu^A\mathcal{A}^{A,\mu}$ is not invariant under color symmetry, which is supposed to be exact. Furthermore, the minimal coupling of the gluons to the matter field has been constructed from the transformation properties of the gauge field. This is usually referred to as "universality". Other gauge invariant couplings such as, e. g., $\bar{\psi}\sigma_{\mu\nu}\mathcal{G}^{\mu\nu}\psi$ are ruled out by the requirement of renormalizability (see discussion in Section A.4). In order to point out the key features of QCD it is expedient to write the Lagrangian density Equation 17 in terms of the gauge fields. The interaction of gauge bosons with the elementary fermions of the theory is realized via (extracted from Equation 13)

$$\mathcal{L}_{\text{Int}} = g\mathcal{A}_\mu^A\mathcal{J}^{A,\mu} \quad \Leftrightarrow \quad \mathcal{L}_F = \mathcal{L}_F^{(0)} + \mathcal{L}_{\text{Int}}\,, \tag{18}$$

11 Equation 12 can be used in the subsequent quantization procedure.

12 Analogous to the electromagnetic interaction, we could define chromo-electric $E_i^A \coloneqq \mathcal{G}_{0i}^A$ as well as chromo-magnetic $B_i^A \coloneqq \frac{1}{2}\varepsilon_{ijk}\mathcal{G}_{jk}^A$ fields (see, e. g., [65]), which include the Levi-Civita symbol ε_{ijk} $(i,j,k = 1,2,3)$.

13 In this context, the superscript (cl.) in Equation 17 refers to its classical nature, i. e., the Lagrangian does not yet describe quantum interactions.

14 As discussed in [44], the symmetry in an asymptotically free theory is not broken spontaneously.

where $\mathcal{J}^{A,\mu}$ represents the color current of quarks. The latter is conserved due to the underlying exact color symmetry

$$\mathcal{J}^{A}_{\mu}(x) = \sum_{\psi} \bar{\psi}^{a}_{\alpha}(x)\,(\gamma_{\mu})_{\alpha\beta}\left[T^{A}\right]^{ab}\psi^{b}_{\beta}(x) \;\Rightarrow\quad \partial^{\mu}\mathcal{J}^{A}_{\mu}(x) = 0\,. \tag{19}$$

Similarly, the (conserved) electromagnetic current[15]

$$\mathcal{J}^{em}_{\mu} = \sum_{\psi} e_{\psi}\,\bar{\psi}^{a}_{\alpha}\,(\gamma_{\mu})_{\alpha\beta}\,\psi^{a}_{\beta} \qquad\qquad \Rightarrow\quad \partial^{\mu}\mathcal{J}^{em}_{\mu} = 0 \tag{20}$$

can be defined, dictating the admitted form of quark-photon interactions. Most importantly, the non-linear three- and four-gluon couplings within $\mathcal{L}_{QCD}$ generate the essential elements of asymptotic freedom:

$$\begin{aligned}\mathcal{L}_{G} = -\frac{1}{4}\mathcal{G}^{A}_{\mu\nu}\mathcal{G}^{A,\mu\nu} = &-\frac{1}{4}\left(\partial_{\mu}\mathcal{A}^{A}_{\nu} - \partial_{\nu}\mathcal{A}^{A}_{\mu}\right)\left(\partial^{\mu}\mathcal{A}^{A,\nu} - \partial^{\nu}\mathcal{A}^{A,\mu}\right)\\ &-\frac{g}{2}f^{ABC}\left(\partial_{\mu}\mathcal{A}^{A}_{\nu} - \partial_{\nu}\mathcal{A}^{A}_{\mu}\right)\mathcal{A}^{B,\mu}\mathcal{A}^{C,\nu}\\ &-\frac{g^{2}}{4}f^{ABE}f^{CDE}\mathcal{A}^{A}_{\mu}\mathcal{A}^{B}_{\nu}\mathcal{A}^{C,\mu}\mathcal{A}^{D,\nu}\,.\end{aligned} \tag{21}$$

Again, those selfinteractions arise due to the color-charge carried by gluons. So far, this is a classical Lagrangian. Thus, in order to quantize the theory, we have to somehow replace the classical fields with their quantum versions[16]. For a given Lagrangian gauge theory, this is done by choosing a gauge (usually referred to as gauge fixing). The latter is essential to remove ambiguities in defining the gauge fields. Let us exemplify this topic with the classical equation of motion for the (free) gluon field[17]

$$\begin{aligned}\mathcal{L}^{(0)}_{G} &= -\frac{1}{4}\left(\partial_{\mu}\mathcal{A}^{A}_{\nu} - \partial_{\nu}\mathcal{A}^{A}_{\mu}\right)\left(\partial^{\mu}\mathcal{A}^{A,\nu} - \partial^{\nu}\mathcal{A}^{A,\mu}\right)\\ &= -\frac{1}{2}\mathcal{A}^{A,\nu}\delta^{AB}\left[-\partial^{2}g_{\mu\nu} + \partial_{\mu}\partial_{\nu}\right]\mathcal{A}^{B,\mu}\\ &\equiv -\frac{1}{2}\mathcal{A}^{A,\nu}\widetilde{\mathcal{K}}^{AB}_{\mu\nu}\mathcal{A}^{B,\mu}\,.\end{aligned} \tag{22}$$

Here, the projection operator $\widetilde{\mathcal{K}}^{AB}_{\mu\nu}$ is not invertible (cf., e. g., [44]). The physical reason is that at this point all fields related by a gauge-transformation also propagate. Therefore, we have to make sure that only physical degrees of freedom propagate. In the classical electromagnetic case this can, e. g., be done by imposing the condition

$$\partial^{\mu}\mathcal{A}^{photon}_{\mu} = 0\,, \tag{23}$$

which is sufficient to ensure that (unphysical) longitudinal degrees of freedom do not interact with the (physical) transversal ones. For (classical) QCD, this ansatz would give rise to more complicated equations, similar to [66]:

$$\partial^{2}\left[\partial^{\rho}\mathcal{A}^{A}_{\rho}\right] + gf^{ABC}\mathcal{A}^{B}_{\mu}\partial^{\mu}\left[\partial^{\rho}\mathcal{A}^{C}_{\rho}\right] = 0\,, \tag{24}$$

15 When quantum fields are involved, the classical electromagnetic current of Equation 20 has to be replaced by its quantum version, i. e., $\mathcal{J}^{em}_{\mu} \to \sum_{\psi} e_{\psi}{:}\bar{\psi}^{a}_{\alpha}\,(\gamma_{\mu})_{\alpha\beta}\,\psi^{a}_{\beta}{:}$. Nevertheless, as long as their quantum nature is evident, we will not explicitly show the normal ordered form of involved fields and operators, i. e., corresponding symbols will be omitted.

16 We will not change the formal representation of the fields or Lagrangian density in this context (e. g., with operators).

17 Surface terms in the Lagrangian, which may arise after an integration by parts, are consequently omitted.

which include non-abelian terms, connecting longitudinal with transversal modes. While on the classical level these procedures may be sufficient to uniquely determine the involved gauge-fields, the situation is more complicated for quantum fields (see, e. g., [64, 67]). For instance, the full QCD Lagrangian can be derived from Equation 17 with the functional-integral formalism (see discussion in Section A.5). This approach canonically entails the gauge fixing conditions since the latter are necessary to avoid inherent divergences within the Feynman path integrals (cf. Section A.5). However, quantization is not at all a unique procedure, i. e., a multitude of equivalent methods[18] are known, e. g., stochastic formalism [45, 68], functional-integral formalism [45, 69] or the canonical operator formalism[19] [45, 70, 71]. This being said, let us start with the quantum Lagrangian of QCD as implied by the Faddeev-Popov method [45, 72]. This full quantum Lagrangian now includes unphysical auxiliary fields[20] and is invariant under a new extended local gauge transformation, the so-called Becchi-Rouet-Stora-Tyutin (BRST) symmetry (see, e. g., [44, 45]). Owing to the presence of these Faddeev-Popov ghosts, not only in the Lagrangian, but also in the BRST transformation, this symmetry may be regraded as a quantum version of the classical gauge transformation. In fact, the classical QCD Lagrangian is not invariant under BRST transformations, while the quantum Lagrangian is not invariant under local gauge transformations. Consequently, the BRST symmetry is the actual basis for developing the canonical operator formalism[21] (see, e. g., [45, Chapter 2.3]).

Let us list the components of the full QCD Lagrangian for a linear gauge fixing condition (with an auxiliary field $\mathcal{B}^A$)

$$G^\mu \mathcal{A}^A_\mu(x) = \mathcal{B}^A(x) \quad \Rightarrow \quad G^\mu \mathcal{A}^{A,\theta}_\mu(x) = \mathcal{B}^A(x)\,, \tag{25}$$

which yields a unique solution for every θ^A, for a given $\mathcal{A}^A_\mu$. On the Lagrangian level the gauge fixing condition can, e. g., be introduced by using the method of Lagrangian multipliers (defined as $\lambda = -\frac{1}{2\xi}$)

$$\mathcal{L}_{GF} = -\frac{1}{2\xi}\left[G^\mu \mathcal{A}^A_\mu\right]^2 . \tag{26}$$

This modification of the action implies (for a derivation see Section A.5) the Faddeev-Popov ghost term

$$\begin{aligned}\mathcal{L}_{FP} &= -\chi^{A*}\left[\delta^{AB}\, G^\mu \partial_\mu - g f^{ABC}\, G^\mu \mathcal{A}^C_\mu\right]\chi^B \\ &= -\chi^{A*}\, G^\mu\, [D_\mu]^{AB}\, \chi^B\end{aligned} \tag{27}$$

including the Faddeev-Popov ghost fields χ^A, χ^{A*} (see discussion in Section A.5) transform according to the adjoint representation of the color group. These unphysical fields have scalar propagators and obey the Fermi-Dirac statistics. As a matter of fact, they do not correspond to real particles, but are preserving unitarity. Ultimately they are responsible for the cancellation of unphysical polarizations of the gauge-bosons. Before coming back to this point, let us first collect the results of this discussion. At this point we are able to write down the full quantum Lagrangian density:

$$\mathcal{L}_{QCD} = \mathcal{L}_F + \mathcal{L}_G + \mathcal{L}_{GF} + \mathcal{L}_{FP}\,, \tag{28}$$

18 Here, we mean, that all these methods entail an equivalent description of nature.

19 This ansatz is somewhat tricky because a simple-minded replacement of the fields in Equation 17, while following the standard procedure (i. e., establish canonical commutation relations between the field operators and the conjugate canonical momenta) may produce contradictions (see discussion in [45, Chapter 2.2.1]).

20 Those are (complex) scalar fields obeying Fermi-Dirac statistics.

21 When starting with BRST symmetry, the full quantum Lagrangian can be derived from the corresponding transformations (see [45]).

which forms the basis of QCD.

The desired perturbative formulation of the theory will be achieved when the Feynman rules are at hand (see Section A.6). For this purpose it is useful to split up the full Lagrangian in Equation 28 into a part with non-interactive fields $\mathcal{L}^{(0)}_{\text{QCD}}$ and the separated interactive part $\mathcal{L}^{(1)}_{\text{QCD}}$:

$$\mathcal{L}_{\text{QCD}} = \mathcal{L}^{(0)}_{\text{QCD}} + \mathcal{L}^{(1)}_{\text{QCD}} \,. \tag{29}$$

While the former will provide the needed propagators of the different fields, the latter gives the vertices of the theory which specifies its structure. Moreover, it should be emphasized that $\mathcal{L}^{(1)}_{\text{QCD}}$ only includes terms at least of oder $\mathcal{O}(g)$. Let us only highlight a few features of this procedure needed in this work and refer to Section A.6 for the complete formulas. Two fundamentally different situations arise from Equation 29 depending on the choice of Equation 25:

- For covariant gauges, such as the Lorentz gauge $\left(G^\mu \to \partial^\mu\right)$ Equation 29 produces gluon propagators (see Equation 1144) with unphysical gluon polarizations $\varepsilon_\mu(k, \lambda = 0)$:

  $$d_{\mu\nu}(k,\xi) = \sum_{\lambda=0,\pm1} \varepsilon^*_\mu(k,\lambda)\, \varepsilon_\nu(k,\lambda) \,, \tag{30}$$

  where $d_{\mu\nu}(k,\xi)$ represents the involved tensor structure, while k^μ is the gluon four-momentum. Those contributions will be canceled by ghost-gluon interactions related to

  $$\mathcal{L}_{\text{FP}} = \partial^\mu \chi^{A*} \left[D_\mu\right]^{AB} \chi^B \,. \tag{31}$$

  In passing, we recognize that according to Equation 31 the Faddeev-Popov ghosts also obey the same Equation 24, as the scalar fields $\left[\partial^\rho \mathcal{A}^A_\rho\right]$. Unfortunately, in a perturbative approach each gluonic diagram may require an adequate ghost-correction which cancels the longitudinal part of the corresponding gluon contributions. When restricted to the diagrams of this work, no ghost-corrections are needed. For this specific situation the simple structure of the gluon propagator (using preferably the Feynman gauge $\xi = 1$) makes this gauge fixing the ideal choice.

- A completely different situation arises for non-covariant conditions $G^\mu \to n^\mu$, e. g.,

  $$n^\mu \mathcal{A}^A_\mu = 0 \quad \left(n^2 = 0\right) \,, \tag{32}$$

  where the ghost Lagrangian becomes independent of ghost-gluon interactions:

  $$\mathcal{L}_{\text{FP}} = -\chi^{A*} n^\mu \partial_\mu \chi^A \,. \tag{33}$$

  That means for this gauge fixing condition only physical gluon polarizations $\varepsilon_\mu k^\mu = 0$ and $\varepsilon_\mu n^\mu = 0$ exist. In this work we will also make use of Equation 32 via the Fock-Schwinger gauge[22]:

  $$(x - x_0)^\mu \, \mathcal{A}^A_\mu(x) = 0 \,. \tag{34}$$

  This specific choice is especially useful for the applied background field method, since this approach exploits the fact that the potential is directly expressible in terms of the gluon field strength tensor (cf. [64, 73–76]):

  $$\mathcal{A}^A_\mu(x) = \int_0^1 d\alpha \, \alpha x^\nu \mathcal{G}^A_{\nu\mu}(\alpha x) \,. \tag{35}$$

22 We will use $x^2 = 0$ for $\xi = 0$. Note, that x_0 is an arbitrary point playing the role of a gauge parameter.

We can now conclude this introductory discussion of the strong interaction. Combined with the named appendices the structure of QCD in terms of a perturbative formulation is at hand. In a next step the applicability of this formulation is discussed.

2.3 ASYMPTOTIC FREEDOM AND PERTURBATIVE QCD

In the previous part, we have pointed out one crucial property of QCD which is asymptotic freedom. This section is dedicated to derive this characteristic from the QCD Lagrangian and motivate its applicability in form of pQCD.

In order to calculate observables within QCD, a consistent technique has to be found which allows a systematic treatment of quantum corrections. Inspired by QED a canonical choice seems to be perturbation theory. The latter is in general applicable to theories, where the corresponding Lagrangian can be split up into an exactly solvable part and a perturbative part. In general, the theory might not possess an analytic solution, but the perturbative part exhibits a "small" parameter "α" which allows to approximate predictions of the theory in terms of a formal series. This perturbation series is an expansion in powers of the parameter α and constitutes usually only an asymptotic series (see Section A.13). In contrast to QED, where the fine structure constant is normally used as a fairly good expansion parameter $\alpha_{\text{QED}} = \frac{e^2}{4\pi} \approx \frac{1}{137}$, one has to justify if and when its analogon, the strong coupling constant $\alpha_S = \frac{g^2}{4\pi}$ fulfills the same requirements. The latter seems to be the physically most reasonable choice when looking at the structure of the Lagrangian in Equation 29 and anticipating that α_S is sufficiently small for adequate conditions. Therefore, when assuming α_S to be small, we make for a physical observable P the ansatz[23] (following [73]):

$$P \approx \sum_n C_n(\mathfrak{R}) \, [\alpha_S(\mathfrak{R})]^n \, , \tag{36}$$

which will be truncated in practice at some order[24] of $N \in \mathbb{R}_0$. In Equation 36 we introduced foresightfully a scheme-dependence $\mathfrak{R}$, because for finite N, both, α_S and C_n, depend on the "renormalization" scheme[25] in which they are calculated in. The latter, renormalization, is the actual key tool which is not only needed throughout this work, but in the context of QFTs in general. Most of the perturbatively calculable corrections, based on the Lagrangian in Equation 28, imply ultraviolet (UV) divergent loop integrals (see [45]). In order to get finite loop integrals, one has to regularize them, e. g., by introducing a UV cut-off $|k| \leqslant \Lambda$ for the involved loop momenta k^μ. When performing the resulting momentum integration there will be a divergent function of Λ (for the limit $\Lambda \to \infty$) and an additional finite part, which is cut-off independent in the limit $\Lambda \to \infty$. It is advantageous, if the regularization procedure is chosen in such a way that it respects Lorentz invariance and the symmetry of the problem[26]. Let us list at least two widely used schemes. The first is the covariant Pauli-Villars regularization which introduces a modified propagator with a sufficient number of internal momenta in the denominator to get a convergent loop integral [44]. Another method, applicable to the class of problems, we will face in this work is dimensional regularization. The basic idea of this scheme is to cure the UV diver-

23 In general, there is no rigorous non-perturbative definition of P in QCD available (cf. [77, 78]), i. e., it is unknown, whether the given divergent series expansion $\sim \sum_n C_n \alpha_S^n$ and the exact function $P(\alpha_S)$ are identical or not. Thus, it seems reasonable to interpret Equation 36 as an asymptotic series [77, 79], which approximates $P(\alpha_S)$ accordingly. See Section 2.4 for an extended discussion of this working assumption.

24 The dependence on $\mathfrak{R}$ will vanish for the observable as well as for infinite N.

25 In fact, two different schemes will give two different solutions for finite N. That means the C_n are not well-defined and the expansion Equation 36 is not unique, unless it is already the exact solution.

26 In fact, the cut-off procedure mentioned above would in certain circumstances break translation invariance [80, 81].

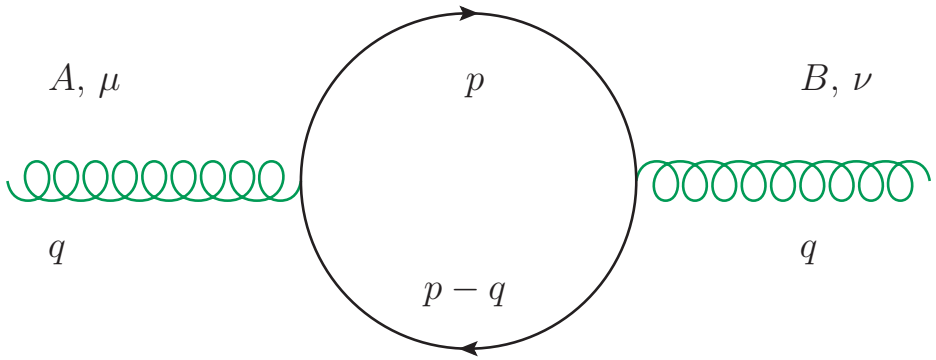

Figure 5: One-loop vacuum polarization Feynman diagram, with four-momenta "q", "p", as well as corresponding Lorentz indices "μ", "ν". Throughout this work, green curly lines represent gluons.

gences by changing the dimensionality of the space-time using analytical continuation (see [81]). In this way, the Feynman integrals become analytic functions of the new space-time dimension D, while divergences will be present as logarithms or inverse powers of $(4-D)$. This specific regularization preserves algebraic relations among Green's functions that do not depend on the space-time dimension. In particular, relations implied by the symmetries of the underlying theory, e. g., Ward identities [44] are preserved. To roughly sketch this method, let us have a look at the one-loop diagram shown in Figure 5 which is a correction to the gluon self energy. The ansatz for this diagram and a specific flavor ψ is[27] (see Section A.6):

$$i\Pi^{AB}_{\mu\nu}(q) = g^2 \int \frac{d^4p}{(2\pi)^4} \operatorname{Tr}\left\{ \gamma_\mu T^A \frac{i}{\not{p} - m_\psi} \gamma_\nu T^B \frac{i}{(\not{p} - \not{q}) - m_\psi} \right\}, \tag{37}$$

which gives a divergent loop integral. With dimensional regularization the so-called "renormalization scale" μ has to be introduced

$$\int \frac{d^4p}{(2\pi)^4} \to \int \frac{d^Dp}{(2\pi)^D} \quad \text{and} \quad g \to g\mu^{2-\frac{D}{2}} \tag{38}$$

to get the right dimension for the coupling. The introduction of an arbitrary mass scale is inevitable when subtracting divergences and can, therefore, be seen as a general feature of all regularization procedures. Its arbitrariness is caused by the corresponding regularization procedure, which can be haphazardly chosen. After evaluating the traces and solving the loop integral, only the Feynman parameter integral survives. With Lorentz invariance and the symmetry preserved the generalized Ward-Takahashi identities imply

$$i\Pi^{AB}_{\mu\nu}(q) = \delta^{AB}\left(q_\mu q_\nu - q^2 g_{\mu\nu}\right)\Pi\left(q^2\right), \tag{39}$$

with $\left(\text{define } \bar{x} := 1-x \text{ for } x \in [0,1]\right)$

$$\Pi\left(q^2\right) = \frac{g^2}{4\pi^2} \frac{\Gamma\left(\frac{4-D}{2}\right)}{[4\pi]^{\frac{D-4}{2}}} [\mu]^{4-D} \int_0^1 dx \, \frac{x\bar{x}}{\left[m_\psi^2 - x\bar{x}q^2\right]^{\frac{4-D}{2}}}. \tag{40}$$

27 The complete result includes a summation over all involved flavors.

For $D = 4 - 2\varepsilon$ and in the limit $\varepsilon \to 0$ the divergent part comes from the gamma function (with the Euler-Mascheroni constant γ_E)

$$\frac{\Gamma(\varepsilon)}{(4\pi)^{-\varepsilon}} = \left(\frac{1}{\varepsilon} - \gamma_E + \ln 4\pi\right) + \mathcal{O}(\varepsilon) \tag{41}$$

to get the desired form

$$\Pi\left(q^2\right) = \frac{[g\mu^\varepsilon]^2}{24\pi^2}\left[\left(\frac{1}{\varepsilon} - \gamma_E + \ln 4\pi\right) - 6\int_0^1 dx\, x\bar{x} \ln\left(\frac{m_\psi^2 - x\bar{x}q^2}{\mu^2}\right) + \mathcal{O}(\varepsilon)\right] . \tag{42}$$

When using the canonical choice of the renormalization scale given in Equation 38, the pole will always be accompanied by finite, transcendental terms "$-\gamma_E$", "$\ln 4\pi$" like in Equation 41. In the case of pQCD the standard choice is the so-called "modified minimal subtraction" ($\overline{MS}$) scheme. In contrast to the "minimal subtraction scheme", realized in Equation 42 when simply removing the ε-pole, one also has to choose a different renormalization scale [82]:

$$\mu = \mu^{\overline{MS}} \left(\frac{e^{\gamma_E}}{4\pi}\right)^{\frac{1}{2}} \tag{43}$$

in order to avoid the mentioned finite terms. Keeping them would produce (artificially) large coefficients in the perturbative expansion (see [82]). This example shows that there are not only different regularization schemes, but that a change in the auxiliary defined renormalization scale can be interpreted as a change of the underlying scheme[28].

At this point we have to dig deeper, because the following is vital for the theory of meson DAs and an understanding of QCD in general. First of all, it is possible to eliminate the divergent parts of the loop integrals from the very beginning by a redefinition of the fields and parameters of the Lagrangian. This so-called renormalization procedure can be constructed after choosing an adequate regularization scheme. For QCD this is realized when choosing dimensional regularization and by replacing the bare quantities with their renormalized counterparts [45] (use the abbreviation $\mathcal{Z}(\mathfrak{R}) = \mathcal{Z}$ when in the scheme $\mathfrak{R}$):

$$\left.\begin{aligned} A^{a,\mu} = \mathcal{Z}_3^{1/2} A_{\mathfrak{R}}^{a,\mu}\,, \quad \psi = \mathcal{Z}_2^{1/2}\psi_{\mathfrak{R}}\,, \quad \chi^a = \tilde{\mathcal{Z}}_3^{1/2}\chi_{\mathfrak{R}}^a\,, \\ g = \mathcal{Z}_g\, g_{\mathfrak{R}}\,, \qquad \xi = \mathcal{Z}_3\,\xi_{\mathfrak{R}}\,, \qquad m = \mathcal{Z}_m\, m_{\mathfrak{R}}\,. \end{aligned}\right\} \tag{44}$$

Here, we assume a covariant gauge (e. g., Lorentz gauge, with the gauge parameter ξ) to also include possible ghost fields into our considerations. Applying Equation 44 to the original Lagrangian $\mathcal{L}$ results in a renormalized Lagrangian

$$\mathcal{L} = \mathcal{L}_{\mathfrak{R}} + \mathcal{L}_{\mathfrak{C}}\,, \tag{45}$$

where $\mathcal{L}_{\mathfrak{R}}$ has the same structure like $\mathcal{L}$, but with the fields replaced by their renormalized equivalents. Moreover, the counter-term Lagrangian $\mathcal{L}_{\mathfrak{C}}$ will be cast in such a way that it includes all the renormalization constants. The Feynman rules for $\mathcal{L}_{\mathfrak{R}}$ alone would have the same structure like those of $\mathcal{L}$ except for the replacements of the bare with the corresponding renormalized quantities. However, the Lagrangian density $\mathcal{L}_{\mathfrak{C}}$ gives an overall modification of the complete Feynman rules of the renormalized Lagrangian. According to the loop order, the renormalization constants will be adequately chosen to absorb the divergences. This means, in accordance with the renormalization program, all the divergences of the Green's functions are subtracted systematically order by order in perturbation theory. Let us illustrate the full one-loop self energy

28 Obviously, one has to work consistently in a chosen scheme order by order. At the end of the day different schemes give the same results up to a fixed order in Equation 36.

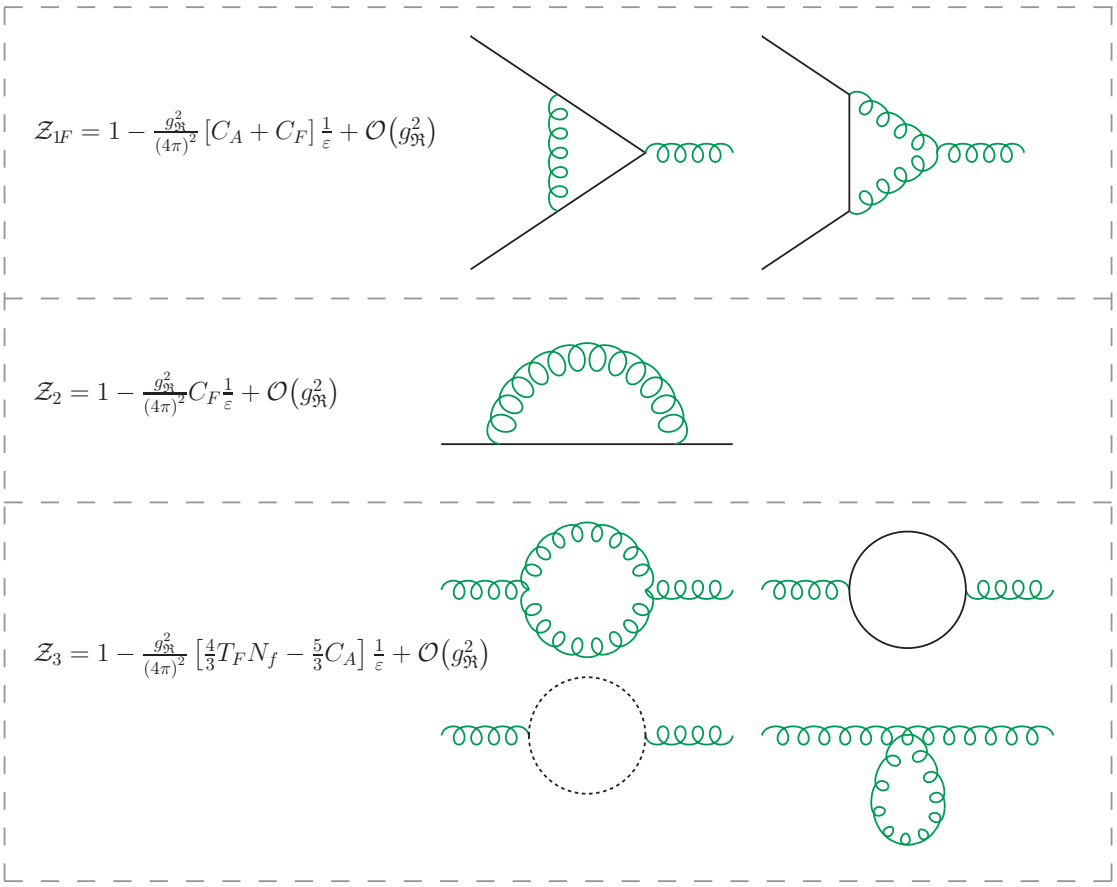

Figure 6: One-loop diagrams and renormalization constants (using Feynman gauge) for the QCD β-function [45, 82]. The dashed line represents a ghost.

of the gluon (see Figure 6 for $\mathcal{Z}_3$). The result for Feynman gauge (in the $\overline{\text{MS}}$ scheme) reads

$$\Pi^{(\text{full})}\left(q^2\right) = \frac{g_{\mathfrak{R}}^2}{(4\pi)^2}\left[\frac{4}{3} T_F N_f - C_A \frac{5}{3}\right]\frac{1}{\varepsilon} + \mathcal{Z}_3 - 1 + \dots , \tag{46}$$

where the ellipses stand for finite terms and neglected higher order corrections in the coupling constant. Note, that Equation 46 has still the same tensorial structure as found in Equation 39 which does not allow for a mass term. Hence, gluons remain massless under radiative corrections as required. The extracted (one-loop) renormalization constants are listed in Figure 6. They have been chosen such that the corresponding poles of the summed diagrams cancel. Obviously, a different choice of the renormalization procedure would produce a distinct set of renormalization constants (distinguished from the former by attaching a prime). The set of all possible renormalization constants could be used to generate the so-called RG which describes the (abelian) group of transformations responsible for the change between renormalization schemes (see Section A.7). For example, we may write for a finite renormalization of the coupling constant:

$$g_{\mathfrak{R}} = z_g\left(\mathfrak{R}, \mathfrak{R}'\right) g_{\mathfrak{R}'} , \quad \text{with} \quad z_g\left(\mathfrak{R}, \mathfrak{R}'\right) = \frac{\mathcal{Z}_g(\mathfrak{R})}{\mathcal{Z}_g(\mathfrak{R}')} , \tag{47}$$

which can be written as a formal series [45, 73]

$$z_g(\mathfrak{R},\mathfrak{R}') = \sum_{n=0}^{\infty} z_g^{(n)}(\mathfrak{R},\mathfrak{R}') \left[\alpha_{S,\mathfrak{R}}\right]^n . \tag{48}$$

This leaves the question how much the physical predictions of the theory depend on the mentioned arbitrariness in subtracting the divergences. In other words, the renormalized theory has to be warranted by some underlying mechanism to give unique physical predictions independent of the renormalization scale μ. Let us assume, that the physical quantity $P \equiv P(p, g_{\mathfrak{R}}, m_{\mathfrak{R}}, \mu)$ (p represents an aggregate of external momenta) of Equation 36 is given for a fixed scheme $\mathfrak{R}$. Since obtained from a unique Lagrangian, it should be invariant under finite renormalizations:

$$P(p, g_{\mathfrak{R}}, m_{\mathfrak{R}}, \mu) = P'(p, g_{\mathfrak{R}'}, m_{\mathfrak{R}'}, \mu') , \tag{49}$$

where $g_{\mathfrak{R}'}$ and $m_{\mathfrak{R}'}$ are the renormalized coupling constant and mass in the scheme $\mathfrak{R}'$ different from $g_{\mathfrak{R}}$ and $m_{\mathfrak{R}}$. Because of this connection, the coupling constant and mass in one scheme can be expressed as an implicit function of the corresponding quantities in another scheme [45]:

$$\left.\begin{aligned} g_{\mathfrak{R}'} &= g_{\mathfrak{R}'}(g_{\mathfrak{R}}, m_{\mathfrak{R}}) , \\ m_{\mathfrak{R}'} &= m_{\mathfrak{R}'}(g_{\mathfrak{R}}, m_{\mathfrak{R}}) . \end{aligned}\right\} \tag{50}$$

When comparing the measured observable with the corresponding quantity $P^{(\prime)}$, the values of $g_{\mathfrak{R}}^{(\prime)}$ and $m_{\mathfrak{R}}^{(\prime)}$ can be determined by an adequate fitting procedure. The resulting values of $g_{\mathfrak{R}}^{(\prime)}$ and $m_{\mathfrak{R}}^{(\prime)}$ must satisfy Equation 50. In this way P and P' describe the same physics. Unfortunately, knowing only the first "N" orders of the perturbation expansion Equation 36 prohibits a direct confirmation of this strategy. In fact, when choosing the scheme with the smaller value of $g_{\mathfrak{R}}$ as expansion parameter the two predictions differ

$$P(p, g_{\mathfrak{R}}, m_{\mathfrak{R}}, \mu) - P'(p, g_{\mathfrak{R}'}, m_{\mathfrak{R}'}, \mu') = \mathcal{O}\left(g_{\mathfrak{R}}^{N+2}\right) \tag{51}$$

in a finite higher-order correction. This motivates the renormalization scheme-dependence of perturbative predictions of physical quantities. Particularly, for QCD this causes a non-negligible difference and one has practically no means for estimating the size of the neglected orders a priori. However, there are several ways to reduce the scheme-dependence of the result by choosing an adequate scheme for each problem[29]. For instance, the $\overline{MS}$ scheme shows a very good convergence for e^+e^--annihilations and $\gamma\gamma$-scattering [45]. Fortunately, not only the asymptotic freedom of QCD, but also the assumed one-loop accuracy will tame the scheme-dependence for the processes investigated in this work. In fact, Equation 48 (after equating coefficients) implies a scheme independence of the LO and NLO results of perturbative calculations, i. e., in terms of Equation 36 and Equation 48 [45, 73]:

$$\left.\begin{aligned} C_0(\mathfrak{R}) &= C_0(\mathfrak{R}') , \\ C_1(\mathfrak{R}) &= C_1(\mathfrak{R}') , \\ C_2(\mathfrak{R}) &= C_2(\mathfrak{R}') + 2z_g^{(0)}(\mathfrak{R},\mathfrak{R}')\, C_1(\mathfrak{R}') . \end{aligned}\right\} \tag{52}$$

This is a general statement for perturbative results, however, not all higher order coefficients $C_{n\geqslant 2}(\mathfrak{R})$ are necessarily scheme-dependent, as shown for the QCD "beta function" (see below).

29 For an advanced discussion of, e. g., the Stevenson criterion see [45].

In the following step we recall the scale dependence of the renormalized coupling constant and renormalized operators in general. The latter is essential for the theory of DAs which we want to study later on. Restricted to infinitesimal changes of the mass scale Equation 47 reduces to a differential equation (DE)[30], expressing the response of the Green's functions and parameters to the change of the renormalization scale μ. Such DEs are called renormalization group equation (RGE)s. One should note, that those RGEs are in principle independent of perturbation theory, therefore, they can be used to supplement perturbative results. Moreover, the RGEs are mere representations of the fact that the bare parameters are scale-independent unique constants (see [45] for further details). Thus, the RGEs guarantee that the theory is based on a unique Lagrangian although the renormalized theory appears to possess an arbitrariness due to the possible change of the renormalization scale [45]. In other words, the renormalized theory is warranted by these RGEs to give unique physical predictions independent of the renormalization scale μ. Beginning with the coupling constant $g_{\mathfrak{R}}$ the corresponding RGE is (cf. [44, 45])

$$\frac{\partial g}{\partial \mu} = 0 \quad \Rightarrow \quad \mu \frac{\partial g_{\mathfrak{R}}}{\partial \mu} = \beta(\varepsilon, g_{\mathfrak{R}}) \,, \tag{53}$$

with the QCD beta or Gell-Mann-Low function [45] $(\varepsilon \to 0)$

$$\beta(\varepsilon, g_{\mathfrak{R}}) = -\varepsilon g_{\mathfrak{R}} - \frac{1}{\mathcal{Z}_g}\left(\mu \frac{\partial \mathcal{Z}_g}{\partial \mu}\right) g_{\mathfrak{R}} \tag{54}$$

controlling the RG flow of $g_{\mathfrak{R}}(\mu)$. Analogously, the ansatz of scale independence for the bare mass in dimensional regularization

$$\frac{\partial m}{\partial \mu} = 0 \quad \Rightarrow \quad \mu \frac{\partial m_{\mathfrak{R}}}{\partial \mu} = -m_{\mathfrak{R}} \gamma_m(\varepsilon, g_{\mathfrak{R}}) \tag{55}$$

implies the RGE of the quark-masses. In this context the renormalization group function γ_m (for a definition see, e. g., [45, 82]):

$$\gamma_m(g_{\mathfrak{R}}, \xi_{\mathfrak{R}}) = \frac{\mu}{\mathcal{Z}_m^{1/2}} \frac{\partial \mathcal{Z}_m^{1/2}}{\partial \mu} = -\frac{\mu}{m_{\mathfrak{R}}} \frac{\partial m_{\mathfrak{R}}}{\partial \mu} \tag{56}$$

is called the anomalous dimension of the mass m (flavor not specified at this point). The renormalization functions are finite because the divergences cancel in the limit $\varepsilon \to 0$. This also holds for the involved anomalous dimensions (for fixed m, g, ξ)

$$\delta(g_{\mathfrak{R}}, \xi_{\mathfrak{R}}) = \mu \frac{\partial \xi_{\mathfrak{R}}}{\partial \mu} = -2\xi_{\mathfrak{R}} \gamma_G(g_{\mathfrak{R}}, \xi_{\mathfrak{R}}) \tag{57}$$

$$\gamma_G(g_{\mathfrak{R}}, \xi_{\mathfrak{R}}) = \frac{\mu}{2\mathcal{Z}_3} \frac{\partial \mathcal{Z}_3}{\partial \mu} \tag{58}$$

$$\gamma_F(g_{\mathfrak{R}}, \xi_{\mathfrak{R}}) = \frac{\mu}{2\mathcal{Z}_2} \frac{\partial \mathcal{Z}_2}{\partial \mu} \tag{59}$$

in the RGE [45, 82]

$$\left[\mu \frac{\partial}{\partial \mu} + \beta(g_{\mathfrak{R}}, \xi_{\mathfrak{R}}) \frac{\partial}{\partial g_{\mathfrak{R}}} - \gamma_m(g_{\mathfrak{R}}, \xi_{\mathfrak{R}})\, m_{\mathfrak{R}} \frac{\partial}{\partial m_{\mathfrak{R}}} \right.$$
$$\left. + \delta(g_{\mathfrak{R}}, \xi_{\mathfrak{R}}) \frac{\partial}{\partial \xi_{\mathfrak{R}}} - n_G \gamma_G(g_{\mathfrak{R}}, \xi_{\mathfrak{R}}) - n_F \gamma_F(g_{\mathfrak{R}}, \xi_{\mathfrak{R}}) \right] \Gamma_{n_G n_F} = 0 \tag{60}$$

30 This corresponds to the Lie DEs of Lie groups [83].

of the truncated connected Green's function[31] $\Gamma_{n_G n_F}(p, g_{\mathfrak{R}}, m_{\mathfrak{R}}, \xi_{\mathfrak{R}}, \mu)$ with n_G external gluon and n_F quark legs in momentum space[32]. Equation 60 is the so-called 't Hooft-Weinberg equation which is an important tool to derive fundamental properties of QCD. In general, the RGE has a specific form, corresponding to the chosen renormalization scheme. Therefore, instead of the 't Hooft-Weinberg equation also the Callan-Symanzik, Greorgi-Politzer and Gell-Mann-Low equations are mentioned in the literature (see [45] for a detailed discussion). Actually, it is possible to show that in the asymptotic regime or in the massless limit all of them will provide the same solution [45]. However, this leads to another advantage of our choice. While in the named limits the solutions can be straightforwardly obtained, the general situation is somewhat dire. The Gell-Mann-Low equation is based on a scheme that uses physical on-shell quark masses[33] and an off-shell subtraction scheme for the fields and coupling which leads to a simpler appearance of the RGE, because of the implied absence of γ_m. On the other hand, it is impossible to give a general expression for the solution [45]. This is not the case for the 't Hooft-Weinberg equation, where a general solution can be easily obtained. In this context, a special feature of the chosen MS (and $\overline{\text{MS}}$) scheme is the decoupling of $m_{\mathfrak{R}}$ and $g_{\mathfrak{R}}$, i. e., the RGE can be solved independently [45]. This results from the structure of the corresponding renormalization constants which in the MS (and $\overline{\text{MS}}$) scheme only depend on the renormalized gauge coupling. Moreover, this scheme has the remarkable property that the β function and γ_m are gauge-independent (see also [45]). In general, the renormalization group functions depend on the gauge ξ and, hence, they are no physical quantities. It is, however, possible to extract useful physical consequences by observing the (analytic) behavior of these functions. Here, the β-function is of primary importance for the asymptotic freedom of QCD due to its control of the scale dependence of the strong coupling. It should be noticed, that besides the quark-gluon interaction, the strong coupling can also be defined via the three three-gluon vertex. However, when imposing Slavnov-Taylor identities [45, 84, 85] it is possible to show that both quantities coincide. Based on Figure 6, we may, therefore, introduce

$$g\bar{\psi}\mathcal{A}^A T^A \psi = \mathcal{Z}_{1F} g_{\mathfrak{R}} \bar{\psi}_{\mathfrak{R}} \mathcal{A}^A_{\mathfrak{R}} T^A \psi_{\mathfrak{R}}\,, \tag{61}$$

with the renormalization factors

$$\mathcal{Z}_{1F} = \mathcal{Z}_g \mathcal{Z}_2 \mathcal{Z}_3^{1/2} \quad \Leftrightarrow \quad \mathcal{Z}_g = \mathcal{Z}_{1F} \mathcal{Z}_2^{-1} \mathcal{Z}_3^{-1/2}\,. \tag{62}$$

A formal expansion in the renormalized[34] $\alpha_{S,\mathfrak{R}}$ gives for $\mathcal{Z}_g$ (N_f: number of active flavors):

$$\mathcal{Z}_g = 1 - \frac{\alpha_{S,\mathfrak{R}}}{4\pi}\frac{1}{\varepsilon}\frac{11C_A - T_R N_f}{6} + \mathcal{O}\left(\alpha^2_{S,\mathfrak{R}}\right) \tag{63}$$

at one loop accuracy[35]. Inserting Equation 63 into Equation 54 [45]

$$\begin{aligned}\beta(\varepsilon, g_{\mathfrak{R}}) &= -\varepsilon g_{\mathfrak{R}} + \frac{11C_A - 4T_R N_f}{3}\frac{g^2_{\mathfrak{R}}}{(4\pi)^2}\frac{1}{\varepsilon}\beta(\varepsilon, g_{\mathfrak{R}}) + \mathcal{O}\left(g^5_{\mathfrak{R}}\right)\\ &= -\frac{1}{(4\pi)^2}\frac{11C_A - 4T_R N_f}{3} g^3_{\mathfrak{R}} + \mathcal{O}\left(g^5_{\mathfrak{R}}, \varepsilon\right)\end{aligned} \tag{64}$$

31 That is constructed from a connected Green's function by amputating the propagators from all external lines. Here, a connected Green's function is one without disjoint pieces, i. e., any part of it is joint to the remaining part by at least one propagator.

32 It is futile to consider external ghost-lines.

33 Quarks in QCD are most unlikely to be observed in isolation due to the confinement mechanism. Therefore, it is ambiguous to talk about quark masses on their mass shell.

34 Here, we use the MS-scheme to shorten the expressions.

35 Note that the dependence on the gauge-parameter in $\mathcal{Z}_g$ would cancel anyway. Therefore, the expressions in Figure 6 have been abbreviated using Feynman gauge.

gives the first coefficient of the perturbative expansion of the QCD beta function. The expressions in Equation 64 include three different color factors [43, 45] (see Section A.1 for details):

$$C_f = \frac{N_c^2 - 1}{2N_c}, \quad C_A = N_c, \quad T_R = \frac{1}{2}, \tag{65}$$

which can be associated with a gluon emission from quarks, a gluon emission from gluons, or a gluon that splits into a quark-antiquark pair, respectively. For this work we rewrite Equation 64 according to (omitting the subscript "$\mathfrak{R}$")

$$\mu^2 \frac{\partial \alpha_S}{\partial \mu^2} = -\alpha_S \left[\beta_0 \frac{\alpha_S}{4\pi} + \beta_1 \left(\frac{\alpha_S}{4\pi} \right)^2 + \mathcal{O}\left(\alpha_S^3 \right) \right] \equiv \beta(\alpha_S) , \tag{66}$$

$$\alpha_S\left(\mu^2\right) = \frac{g(\mu)^2}{4\pi} \tag{67}$$

and expand it up to NLO. In this context, α_S is an equivalent of the fine structure constant. Most importantly, the first two coefficients of the QCD beta function (restricted to $SU(3)_c$)

$$\beta_0 = 11 - \frac{2}{3} N_f, \quad \beta_1 = 102 - \frac{38}{3} N_f \tag{68}$$

are scheme independent [45] and indicate the asymptotic freedom. The latter occurs for $\beta(g) < 0$ which requires, e. g., for the leading order terms of Equation 66 $11 C_A - 4 T_R N_f > 0$, or equivalently $2\, N_f < 33$. Since QCD involves at most six (active) quark flavors, this requirement is certainly fulfilled. Furthermore, the origin of the asymptotic freedom at this level can be traced back to the three-gluon coupling. This is in contrast to QED where the coupling would grow $(\beta(e) > 0)$ with the renormalization scale. In fact, the natural choice for the renormalization procedure in QED is an on-shell scheme, where the parameters of the theory can be replaced by, e. g., the electrical charge or the fine structure constant. Unfortunately, there is no comparable method for QCD. On the other hand, the validity of QCD perturbation theory is an a posteriori result of the RGE applied to the case of a large momentum scales. This brings us to the concept of the running coupling[36]. Here, the typical momentum scale of the process under consideration q^μ is introduced, by choosing a new parameter (taken for space-like momenta $-q^2 > 0$)

$$\frac{1}{\lambda} = e^t \equiv \sqrt{-\frac{q^2}{\mu^2}} . \tag{69}$$

The running coupling $\bar{g}(t)$ (analogously the running mass, etc.) can be introduced via a new renormalization scale μ/λ instead of μ which will then be held constant. This implies the modified Equation 53:

$$\frac{\mu}{\lambda} \frac{d\,\bar{g}}{d\left(\frac{\mu}{\lambda}\right)} = \beta(\bar{g}) \quad \Leftrightarrow \quad \frac{d\,\bar{g}}{d\,t} = \beta(\bar{g}) , \tag{70}$$

with the formal solution $\left(\bar{\beta}_0 \equiv \frac{\beta_0}{(4\pi)^2}, \bar{\beta}_1 \equiv \frac{\beta_1}{(4\pi)^4}, \text{etc.} \right)$

$$(t - t_0) = \int_{\bar{g}(t_0)}^{\bar{g}(t)} dg' \, \frac{1}{\beta(g')} = \frac{1}{2} \int_{\bar{g}^2(t_0)}^{\bar{g}^2(t)} \frac{d\lambda}{\lambda^2} \, \frac{-1}{\bar{\beta}_0 + \bar{\beta}_1 \lambda + \mathcal{O}(\lambda^2)} . \tag{71}$$

36 For consistency reasons, this concept is not elaborated with α_S, but an equivalent auxiliary function $\bar{g}$ instead.

Here, the standard choice is $t_0 = 0$ with $\bar{g}(0) = g$ at the fixed reference scale μ. The latter can be chosen arbitrarily, e. g., $\mu \to \mu_0 = 1$ GeV. For this work we will truncate the expansion of the beta function[37] at NLO accuracy to get (cf. Equation 71)

$$\frac{1}{\bar{g}^2} + \frac{\bar{\beta}_1}{\bar{\beta}_0} \log\left(\frac{\bar{\beta}_0 \bar{g}^2}{1 + \bar{\beta}_1 \bar{g}^2/\bar{\beta}_0}\right) = \bar{\beta}_0 \log\left(\frac{-q^2}{\Lambda^2_{\text{QCD}}}\right), \tag{72}$$

with the QCD scale parameter [45]

$$\Lambda_{\text{QCD}} = \mu e^{-\frac{1}{2\bar{\beta}_0 g^2}} \left(\frac{1 + \bar{\beta}_1 g^2/\bar{\beta}_0}{\bar{\beta}_0 g^2}\right)^{\frac{\bar{\beta}_1}{2\bar{\beta}_0^2}}. \tag{73}$$

The parameter g has been effectively replaced by Λ_{QCD}. This is an example of the so-called dimensional transmutation, where a dimensionless parameter, on which physical quantities can depend in a non-trivial way, is traded for a dimensional one (see [44, 86] and references therein). The physical mechanism providing this connection is given by quantum corrections of the underlying QFT. Consequently, the two-loop result for $\alpha_S(Q^2)$ $(Q^2 = -q^2)$ can be extracted from Equation 72 when assuming $-q^2 \gg \Lambda^2_{\text{QCD}}$, i. e.,

$$\bar{g}^2 = \frac{1}{\bar{\beta}_0 \log\left(-\frac{q^2}{\Lambda^2_{\text{QCD}}}\right)} \left[1 - \frac{\bar{\beta}_1}{\bar{\beta}_0^2} \frac{\log\left(\log\left(-\frac{q^2}{\Lambda^2_{\text{QCD}}}\right)\right)}{\log\left(-\frac{q^2}{\Lambda^2_{\text{QCD}}}\right)}\right]. \tag{74}$$

We see that the celebrated property of asymptotic freedom can be deduced from Equation 74 accordingly:

$$\lim_{Q^2 \to +\infty} \alpha_S\left(Q^2\right) = 0. \tag{75}$$

Thus, for sufficiently large space-like Q^2, a perturbative expansion in α_S can be justified. Furthermore, let us consider the observable P to be a dimensionless quantity depending on a single large scale $Q^2 \gg \Lambda_{\text{QCD}}$ (assume the massless limit)

$$\mu^2 \frac{d}{d\mu^2} P\left(\frac{Q^2}{\mu^2}, \alpha_S\right) = \left[\mu^2 \frac{\partial}{\partial \mu^2} + \beta(\alpha_S) \frac{\partial}{\partial \alpha_S}\right] P\left(\frac{Q^2}{\mu^2}, \alpha_S\right) = 0, \tag{76}$$

with $\alpha_S = \alpha_S(\mu^2)$. The choice $\mu^2 = Q^2$ minimizes the dependence on an arbitrary scale at a fixed order in perturbation theory [87]. Moreover, it reveals that all the scale dependence comes from the running coupling:

$$P\left(\frac{Q^2}{\mu^2}, \alpha_S\right) = P\left(1, \alpha_S\left(Q^2\right)\right). \tag{77}$$

For quantitative calculations a value for Λ_{QCD} has to be found, e. g., extracted from experimental data [46, 73, 87] (cf. Figure 7). One has to note, that Λ_{QCD} is an effective parameter which has to be chosen according to the used loop order and active flavors. This is due to the decoupling theorem which states that flavors with $m_\psi^2 \gg Q^2$ are not relevant in this energy realm. This can be seen for the mentioned example Equation 42 $(Q^2 = -q^2)$

$$\int_0^1 dx\, x\bar{x} \ln\left(\frac{m_\psi^2 - x\bar{x}q^2}{\mu^2}\right) = \begin{cases} \frac{1}{6}\log\left(\frac{Q^2}{\mu^2}\right) + \mathcal{O}\left(\frac{m_\psi^2}{\mu^2}, \frac{m_\psi^2}{Q^2}\right) & , Q^2, \mu^2 \gg m_\psi^2 \\ \frac{1}{6}\log\left(\frac{m_\psi^2}{\mu^2}\right) + \frac{1}{30}\frac{Q^2}{m_\psi^2} + \mathcal{O}\left(\frac{\mu^2}{m_\psi^2}, \frac{Q^2}{m_\psi^2}\right) & , m_\psi^2 \gg Q^2, \mu^2 \end{cases}. \tag{78}$$

37 The QCD β-function is known up to four loop accuracy [45].

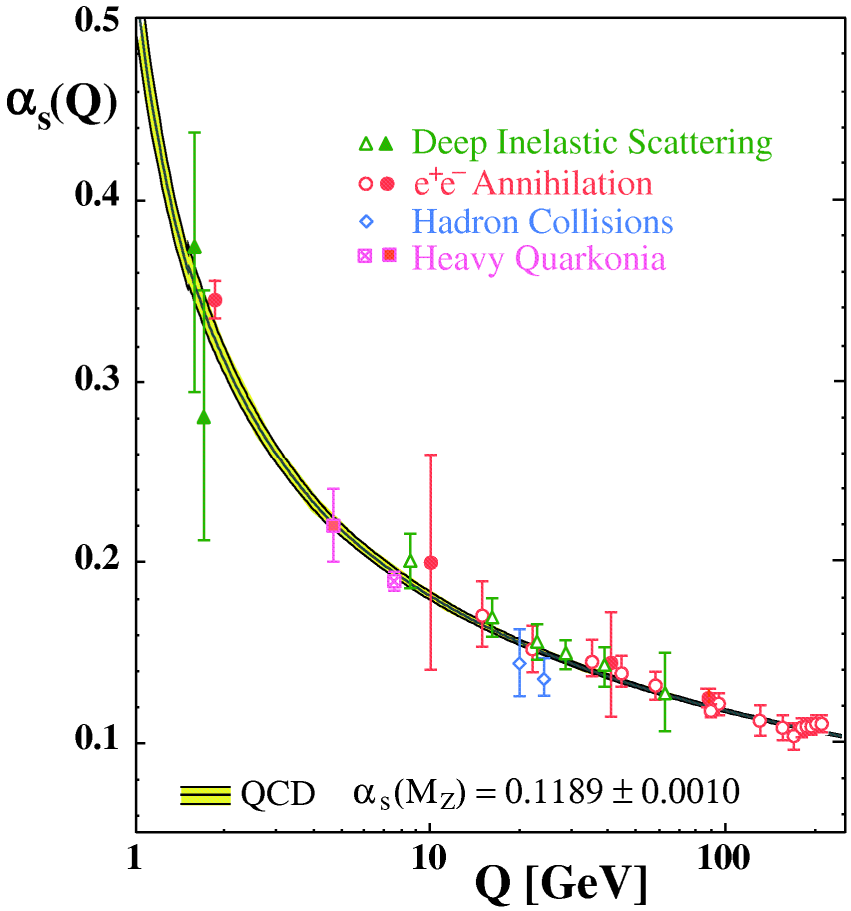

Figure 7: Measurements of $\alpha_S(Q)$ as a function of the respective energy scale Q (picture taken from [46, 87]). Open symbols indicate (resummed) NLO, and filled symbols NNLO QCD calculations used in the respective analysis. The curves are the QCD predictions for the combined world average value of $\alpha_S(m_{Z^0})$, in 4-loop approximation and using 3-loop threshold matching at the heavy quark pole masses $m_c = 1.5$ GeV and $m_b = 4.7$ GeV (for details, see [46, 87]).

In general, the neglected terms can also include $\mathcal{O}\left(\left(Q^2/m_\psi^2\right)^m \log^n\left(Q^2/m_\psi^2\right)\right)$ corrections (cf. [73]; $n, m \in \mathbb{N}_0$). A simple solution for the problem of taking this into account is the introduction of an effective number of (active) flavors:

$$N_f\left(Q^2\right) = \sum_{\psi=u,d,\ldots} \theta\left(Q^2 - m_\psi^2\right) \tag{79}$$

and adapt the QCD scale parameter to this approach

$$\Lambda_{QCD} \to \Lambda_{QCD}(N_f) \; . \tag{80}$$

For this work we will use

$$\Lambda_{QCD}(N_f = 4) = 326 \text{ MeV} \, , \tag{81}$$

while values of Λ_{QCD} for different numbers of active flavors can be found via a matching of the different expressions of the running coupling (cf. [73]). Last but not least a closer look at

Equation 72 reveals a divergence for the limit $Q^2 \to \Lambda^2_{\text{QCD}}$ which is present already at leading-order ($\beta_1 \to 0$). In fact, this Landau pole[38] reveals a breakdown of perturbation theory at a momentum scale close to the QCD scaling parameter. Due to the confinement mechanism and the immanent hadronization this energy realm has to be studied with a different approach, which can access the non-perturbative regime.

2.4 QCD VACUUM AND OPERATOR PRODUCT EXPANSION

This section is dedicated to a heuristic description of the OPE and selected QCD vacuum effects, as required for Chapter 4 and Chapter 5. Furthermore, all NLO anomalous dimensions, which are necessary for the development, i. e., normalization of $\eta^{(\prime)}$ DAs (see Chapter 3) will be introduced below.

The previous subsection has been concluded with a dedicated discussion concerning anti-screening effects and their impact on the (perturbative) QCD coupling constant. In this context, the QCD scale parameter has been obtained which can be used to roughly separate the perturbatively accessible sector from non-perturbative field configurations[39]. Accordingly, apart from possible special cases, the framework given by a perturbative ansatz that only covers asymptotically free parton interactions (see Section 2.3), is not applicable beyond energy scales of relative order $\sim \Lambda_{\text{QCD}}$, i. e., at distances, where quarks and gluons are either confined inside hadrons or QCD vacuum fluctuations become relevant. Fortunately, a consistent method to separate and systematically take into account those large as well as short distance contributions is given by the Wilson-Zimmermann OPE (cf. [89–94]), along with its generalizations.

In fact, there exist a multitude of conceivable situations where this technique can be implemented, e. g., short distance or hard exclusive processes (see [95–97]). For instance, the total annihilation cross section[40] (as encountered in Equation 1) at leading order in the electromagnetic interaction[41] [98, 99]

$$\begin{aligned}\frac{8\pi^2\alpha^2_{\text{QED}}}{q^6} L^{\mu\nu} W_{\mu\nu}(q) &= \frac{16\pi^2\alpha^2_{\text{QED}}}{q^6} L^{\mu\nu}\,\text{Im}\{\Pi_{\mu\nu}(q)\} \\ &= \frac{16\pi^2\alpha^2_{\text{QED}}}{q^2}\,\text{Im}\Big\{\Pi\Big(q^2\Big)\Big\} \equiv \sigma\big(e^+e^- \to \text{hadrons}\big) \end{aligned} \tag{82}$$

has been widely studied and belongs to this important class of problems. Therefore, this is an ideal example to illustrate the involved methods and explain, why the OPE can be seen as an extension of a pure perturbative ansatz (cf. Equation 36). However, at this level of accuracy Equation 82 can be factorized into an unpolarized leptonic (u and v are related lepton spinors, see Section A.2)

$$\begin{aligned} L_{\mu\nu} &= -\frac{1}{4}\sum_{s,s'}\big[\bar{u}\big(k',s'\big)\,\gamma_\mu v(k,s)\big]\big[\bar{v}(k,s)\,\gamma_\nu u\big(k',s'\big)\big] \\ &= \big(k\cdot k'\big)\,g_{\mu\nu} - k_\mu k'_\nu - k'_\mu k_\nu + \mathcal{O}(m_l)\,, \end{aligned} \tag{83}$$

38 The Landau pole beyond perturbation theory has been studied for QED in the context of a lattice approach [88].

39 In other words, at distances $\sim 1/\Lambda^2_{\text{QCD}}$ the confinement mechanism becomes dominant which cannot be described by Feynman diagrams of any order.

40 In Equation 82 the unpolarized case has been assumed, corresponding to a forward scattering amplitude, where initial and final spins as well as momenta are equal. Besides, all possible lepton mass corrections have been neglected.

41 Here, the optical theorem has been applied (cf. [64, 98]).

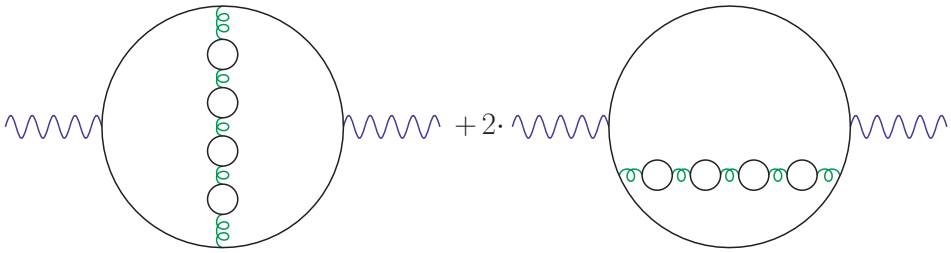

Figure 8: Two simple "bubble" diagrams contributing to the Adler function. By inserting any number of fermion loops into a single gluon line, the corresponding set of bubble-chain diagrams can be generated (see [77, 95, 105] for details).

as well as a hadronic tensor

$$W_{\mu\nu}(q) = \int d^4x\, e^{iq\cdot x} \langle 0| \left[J^{\text{em}}_\mu(x), J^{\text{em}}_\nu(0) \right] |0\rangle \,, \tag{84}$$

with the virtual photon four-momentum $q^\mu = k^\mu - k'^\mu$. Thus, it is more common to consider the associated vacuum-polarization tensor, i. e., two-point correlation function (see, e. g., [95, 97])

$$\Pi_{\mu\nu}(q) = i \int d^4x\, e^{iq\cdot x} \langle 0| \, T\{ J^{\text{em}}_\mu(x)\, J^{\text{em}}_\nu(0) \} \, |0\rangle = \left(q_\mu q_\nu - q^2 g_{\mu\nu} \right) \Pi\left(q^2\right) \,, \tag{85}$$

which entails the $\left(Q^2 \coloneqq -q^2\right)$ Adler function[42] [101]

$$D\left(Q^2\right) \coloneqq -4\pi^2 q^2 \frac{d}{dq^2} \Pi\left(q^2\right) \,. \tag{86}$$

Consequently, all dynamical effects are encoded in a single amplitude. Besides, for kinematical configurations that imply a large Euclidean photon virtuality $Q^2 \gg \Lambda^2_{\text{QCD}}$ (see Section A.15) the vacuum polarization $\Pi\left(q^2\right)$, along with $D\left(Q^2\right)$ turn out to be genuine short distance objects[43] (e. g., [97]).

Therefore, one could expect a sufficient suppression of long distance effects which would at first glance justify an approach similar to Equation 36. Unfortunately, even if the interaction between elementary degrees of freedom is weak, soft corrections cannot be completely avoided. For instance, among the possible multiloop corrections to $D\left(Q^2\right)$, the so-called bubble-chain diagrams (see Figure 8) play a special role (cf. [102–104]). In this context a corresponding exact solution for fixed loop momenta was found by Neubert [105]. For illustrative purposes (following [78]), however, it is more expedient to analyze a simple interpolating expression [78, 106], collecting all bubble insertions into the gluon lines[44] $\left(C_1 \in \mathbb{C}\right)$

$$D\left(Q^2\right)\Big|_{\text{bubble}} = C_1 Q^2 \int_0^\infty dk^2 \frac{k^2 \alpha_S\left(k^2\right)}{\left(k^2 + Q^2\right)^3} \,. \tag{87}$$

42 The given tensor structure of Equation 85 results from Ward identities similar to $q^\mu \Pi_{\mu\nu} = 0$, i. e., as dictated by the conservation of the electromagnetic current (see [100]).

43 In general, this may refer to a set of graphs where all internal lines have momenta $|k| \sim |Q|$, i. e., that are off-shell by order $\sim Q^2$ (see [100]).

44 Based on a perturbative (LO) description of $\alpha_S\left(Q^2\right) = \alpha_S\left(k^2\right)\left(1 - \frac{\beta_0 \alpha_S\left(Q^2\right)}{4\pi} \log\left(\frac{Q^2}{k^2}\right)\right)$, the integration over k^2 in Equation 87 is problematic, since its integrand exhibits a Landau pole at $k^2 = \Lambda^2_{\text{QCD}}$. As discussed below, the related integral $\sim \int_0^{\Lambda^2_{\text{QCD}}} dk^2 \frac{k^2 \alpha_S\left(k^2\right)}{\left(Q^2 + k^2\right)^3}$ implies a factorial divergence (cf. Equation 88).

Similar to the actual solution (cf. [105]), this toy model possesses a factorially divergent perturbative series[45], e. g., as presented within the limits $k^2 \ll Q^2$ and $k^2 \gg Q^2$ $\left(y := 2\log(Q^2/k^2) =: -\tilde{y}\right.$, while Q^2 is fixed and $\alpha_S \equiv \alpha_S(Q^2)\big)$

$$\begin{aligned}\left[D\left(Q^2\right)\Big|_{\text{bubble}}\right]_{\text{IR}} &= C_1 \frac{\alpha_S}{4} \sum_{n=0}^{\infty} \sum_{m=1}^{\infty} (-1)^{m+1} m\,(m+1) \left(\frac{\beta_0 \alpha_S}{8\pi}\right)^n \int_0^{\infty} dy\, y^n e^{-\frac{y}{2}(m+1)} \\ &= C_1 \frac{\alpha_S}{2} \sum_{n=0}^{\infty} \left(\frac{\beta_0 \alpha_S}{8\pi}\right)^n n! + \dots , \end{aligned} \tag{88}$$

$$\begin{aligned}\left[D\left(Q^2\right)\Big|_{\text{bubble}}\right]_{\text{UV}} &= C_1 \frac{\alpha_S}{4} \sum_{n=0}^{\infty} \sum_{m=1}^{\infty} (-1)^{m+n+1} m\,(m+1) \left(\frac{\beta_0 \alpha_S}{8\pi}\right)^n \int_0^{\infty} d\tilde{y}\, \tilde{y}^n e^{-\frac{\tilde{y}}{2} m} \\ &= C_1 \alpha_S \sum_{n=0}^{\infty} (-1)^n \left(\frac{\beta_0 \alpha_S}{4\pi}\right)^n n! + \dots . \end{aligned} \tag{89}$$

According to their position in momentum space [77, 78], the related divergences are called IR or UV renormalons, respectively. Focusing on the infrared domain, Equation 88 leads to the emergence of what we later on may identify as a gluon condensate (see [78, 107]). More precisely, for the discussed Adler function, the leading IR renormalon corresponds to a "soft" operator $\mathcal{O}_G = \alpha_S \mathcal{G}^A_{\mu\nu} \mathcal{G}^{A,\mu\nu}$ (see [77, 108]) which will be absorbed[46] by the associated[47] vacuum expectation value (VEV) $\langle \alpha_S \mathcal{G}^2 \rangle$. In a nutshell, this may be explained as follows (cf. [77, 78, 95, 96]):

- The coefficients of Equation 88 contain integrals[48] which are saturated by values close to [78]

$$y \sim n \Leftrightarrow k^2 \sim Q^2 e^{-\frac{n}{2}} . \tag{90}$$

  Consequently, at sufficiently large $n \geqslant N_* = 2\log\left(Q^2/\Lambda^2_{\overline{\text{QCD}}}\right)$ [78] the factorial divergence is of purely formal nature, since all related Feynman diagrams cease to properly represent the underlying non-abelian dynamics within this strongly coupled infrared domain [77, 78].

45 In fact, Equation 87 can be written as

$$D\left(Q^2\right)\Big|_{\text{bubble}} = \left[D\left(Q^2\right)\Big|_{\text{bubble}}\right]_{\text{IR}} + \left[D\left(Q^2\right)\Big|_{\text{bubble}}\right]_{\text{UV}} ,$$

with the formal expansions

$$\left[D\left(Q^2\right)\Big|_{\text{bubble}}\right]_{\text{IR}} = C_1 \frac{\alpha_S}{2Q^2} \sum_{n=0}^{\infty} \sum_{m=1}^{\infty} (-1)^{m+1}\, m\,(m+1) \left(\frac{\beta_0 \alpha_S}{4\pi}\right)^n \int_0^{Q^2} dk^2 \left(\frac{k^2}{Q^2}\right)^m \left(\log\left(\frac{Q^2}{k^2}\right)\right)^n ,$$

$$\left[D\left(Q^2\right)\Big|_{\text{bubble}}\right]_{\text{UV}} = C_1 \frac{\alpha_S}{2Q^2} \sum_{n=0}^{\infty} \sum_{m=1}^{\infty} (-1)^{m+1}\, m\,(m+1) \left(\frac{\beta_0 \alpha_S}{4\pi}\right)^n \int_{Q^2}^{\infty} dk^2 \left(\frac{Q^2}{k^2}\right)^{m+1} \left(\log\left(\frac{Q^2}{k^2}\right)\right)^n .$$

46 In general, the actual uncertainty due to infrared renormalons is numerically smaller than the corresponding gluon condensate contribution (cf. [107, 109]). This could be caused by distortion effects of the Green's function within the IR domain (see discussion in [107]).

47 In order to justify this statement, let us illustrate some arguments, as given by [77, 108]:

- A posteriori (see discussion below), the only hard momentum scale $\sim |Q|$ can be factored out which leaves only soft field configurations. Therefore, the given IR parameter should be related to a (soft) local operator.
- Since there are no external hadrons involved, this boils down to a vacuum matrix element of that operator.
- The leading IR renormalon singularities in question are caused by a single gluon line. Thus, the required operator has to be bilinear in the gluon fields. However, the lowest dimensional operator allowed by Lorentz and gauge invariance is proportional to $\mathcal{G}^A_{\mu\nu} \mathcal{G}^{A,\mu\nu}$.

Consequently, the leading infrared contribution to the Adler function is given by $\langle 0 | \alpha_S \mathcal{G}^A_{\mu\nu} \mathcal{G}^{A,\mu\nu} | 0 \rangle$. In general, IR renormalons are related to properties of higher-dimensional operators which in the present case are embedded within condensates (see, e. g., [77] for an extended discussion).

48 For $m \in \mathbb{N}$ and $\text{Re}\,(n) > -1$ one has $\int_0^{\infty} dy\, y^n \exp\left(-\frac{y}{2} m\right) = \left(\frac{2}{m}\right)^{n+1} \Gamma(n+1)$.

- As discussed in [77, 78, 110], N_* should, therefore, be interpreted as the optimal truncation point (cf. Section A.13) (ellipses represent the truncated tail of this series, cf. [110, 111])

$$\left[D\left(Q^2\right)\Big|_{\text{bubble}} \right]_{\text{IR}} \mapsto C_1 \frac{\alpha_S}{2} \sum_{n=0}^{\lceil N_* \rceil} \left(\frac{\beta_0 \alpha_S}{8\pi} \right)^n n! + \dots , \tag{91}$$

  yielding an exponentially small ambiguity for the definition of this asymptotic expansion which scales as[49] (see Section A.13)

$$\left[\Delta D\left(Q^2\right)\Big|_{\text{bubble}} \right]_{\text{IR}} \sim \exp\left(-\frac{8\pi}{\beta_0 \alpha_S\left(Q^2\right)} \right) \sim \frac{\Lambda_{\text{QCD}}^4}{Q^4} . \tag{92}$$

- Most importantly, the tail of this asymptotic expansion does not have to be ignored. Instead, it gives rise to non-perturbative contributions of $\mathcal{O}(\Lambda_{\text{QCD}}^4/Q^4)$ after introducing the following ansatz. Similar to renormalization itself, which requires an UV cut-off to define an associated renormalizable field theory, the concept of infrared factorization is crucial in QCD (cf. [77, 112]). This (as roughly mentioned before) can, therefore, also be found in the OPE [90] and comparable approaches, such as perturbative factorization [113], which are both based on a systematic separation of IR and UV contributions. In practical terms, this is done by introducing an auxiliary momentum scale μ (normalization point) that formally separates all fluctuations with frequencies higher (hard) or lower (soft) than μ (see [78, 95, 111]).

With regard to the Adler function and related loop integrals, we realize, that by excluding any integration over the IR domain, a modified NLO pQCD result is implied[50] [107]:

$$D\left(Q^2\right)\Big|_{\{k^2>\mu^2\}} = 1 + \frac{\alpha_S\left(Q^2\right)}{\pi} + \frac{\pi}{3} g_2 \alpha_S\left(\mu^2\right) \frac{\mu^4}{Q^4} + \dots . \tag{93}$$

Thus, this rigid-cut-off scheme entails an additional term proportional to μ^4, as we may anticipate from Equation 92. We note, that analogous to the discussed renormalization scheme-dependence (cf. Section 2.3), all physical quantities are independent of the normalization point, i. e., corresponding counter terms should emerge from neglected soft corrections. Since the latter are affected by QCD vacuum effects, the standard Feynman rules (cf. Section A.6) have to be extended accordingly (see discussion below and [95, 107, 114]), e. g., by including contributions resulting from VEVs of local operators (see Equation 99):

$$D\left(Q^2\right)\Big|_{\{k^2<\mu^2\}} = -\frac{\pi}{3Q^4} \langle \alpha_S G^2 \rangle . \tag{94}$$

A posteriori, those modifications are sufficient to characterize the involved soft modes which in the present case are represented by [107] ($g_1, g_2 \in \mathbb{R}$)

$$\langle \alpha_S G^2 \rangle \approx g_1 \Lambda_{\text{QCD}}^4 + g_2 \mu^4 \alpha_S\left(\mu^2\right) . \tag{95}$$

Thus, together with Equation 95 the dependence on μ cancels. In this context two basic requirements for μ arise [95, 107]:

49 As mentioned in [77] (see also [78, 95, 96]), the physics of power corrections is unrelated to α_S and lies within the small-momentum behavior of associated skeleton diagrams (i. e., primitive one-particle irreducible graphs). Therefore, for qualitative purposes Equation 92 remains valid (cf. [77, 78]), even though the infrared dynamics are not accessible.

50 Here, we apply the physically more intuitive rigid-cut-off factorization, while later on the dimensional regularization will be used.

a) Since we intent to calculate hard contributions (as far as possible) perturbatively, μ must be sufficiently large to ensure $\alpha_S(\mu^2) \ll 1$.

b) On the other hand, only if μ is small enough possible soft/hard admixtures within hard/-soft corrections are numerically insignificant (cf. Equation 95, Equation 93).

Provided, that point a) and b) are fulfilled simultaneously (e. g., $\Lambda^2_{\text{QCD}} \ll \mu^2 \ll Q^2$), there is actually no need to explicitly introduce μ, i. e., as done above, via a cut-off (cf. [77, 93, 107]). Instead, it is more convenient to implement factorization by using dimensional regularization (see [77, 115, 116]). In particular, within the latter case Feynman integrals contributing to hard corrections are integrated over all possible loop momenta, while the normalization point dependence of involved VEVs can be determined by RG equations.

This prompts us to generally expect contributions of the form $\sim C_i(Q^2/\mu^2)\,\langle 0|\mathcal{O}_i(\mu)|0\rangle$, with hard coefficient functions C_i and soft operators $\mathcal{O}_i$ ($i \in \mathbb{N}$). Most remarkably, the perturbative analysis necessitates[51] the presence of certain non-perturbative "condensates" in QCD (see [77, 78, 96] for an extended discussion). Nevertheless, not all condensates can be found in this way. For instance, operators, which do not occur at any finite order in pQCD, such as the chiral condensate are invisible to this method (see also [77, 78]). Consequently, one is led to introduce a more formal approach, such as the OPE. Originally, this method has been developed for the analysis of products of composite operators (cf. [89–94, 109]). According to [89–92, 98], each operator product and corresponding singularities are expressed as a sum of well-defined non-singular operators, along with singular complex functions. The latter are usually called Wilson coefficients [44, 90].

In the context of this work, two distinct versions of the OPE have to be discussed. However, instead of a cumbersome general proof, we only explain the underlying coarse structure using suitable examples.

- SHORT DISTANCE OPERATOR PRODUCT EXPANSION: Let us start with the short distance case, formulated for the product of two local operators $\mathcal{A}(x)$ and $\mathcal{B}(x)$, e. g., representing some problem specific interpolating currents. At small distances[52] a product of two local operators should itself resemble a local operator. This is the original motivation behind this bookkeeping device [44]. Formally we may write (see, e. g., [44, 73, 98])

$$\lim_{|x-y|\to 0} \left\{ \mathcal{A}(x)\,\mathcal{B}(y) \right\} \approx \sum_n C_n(x-y,\mu_F)\,\mathcal{Q}_n\left(\tfrac{1}{2}(x+y),\mu_F\right), \tag{96}$$

  with the perturbatively calculable Wilson coefficients C_n and a complete set of local regular operators $\{\mathcal{Q}_n\}_{n\in\mathbb{N}_0}$. In fact, for renormalizable theories it has been proven, that the expansion in Equation 96 is valid within the limit $x \to y$ to any finite order of perturbation theory (see, e. g., [44, 45] and references therein). Besides, the given local operators have the same quantum numbers as $\left\{\mathcal{A}(x)\,\mathcal{B}(y)\right\}$. Furthermore, we have the normalization point μ_F separating hard from soft fluctuations. Thus, the short distance behavior of the Wilson coefficients can be deduced from corresponding RGEs (see [98] for details), implying[53]

$$\lim_{|x|\to 0} C_n(x,\mu_F) \sim |x|^{d_{\mathcal{Q}_n}-d_{\mathcal{A}}-d_{\mathcal{B}}} \log\left(\frac{1}{|x|}\right)^{\frac{c_{\mathcal{A}}+c_{\mathcal{B}}-c_{\mathcal{Q}_n}}{2}}. \tag{97}$$

51 As discussed above, without introducing specific condensates, the perturbative series cannot be defined unambiguously.

52 That means compared to the characteristic length of the system.

53 For simplicity, we assume the massless case. A generalization, including operator mixing can be found in [98]. Roughly speaking, for $|x| \ll m^{-1}$ (m is a generic mass parameter) we would encounter terms similar to [44] $\log(|x|) \to \log(|x|m)\,(1+\mathcal{O}(|x|m))$.

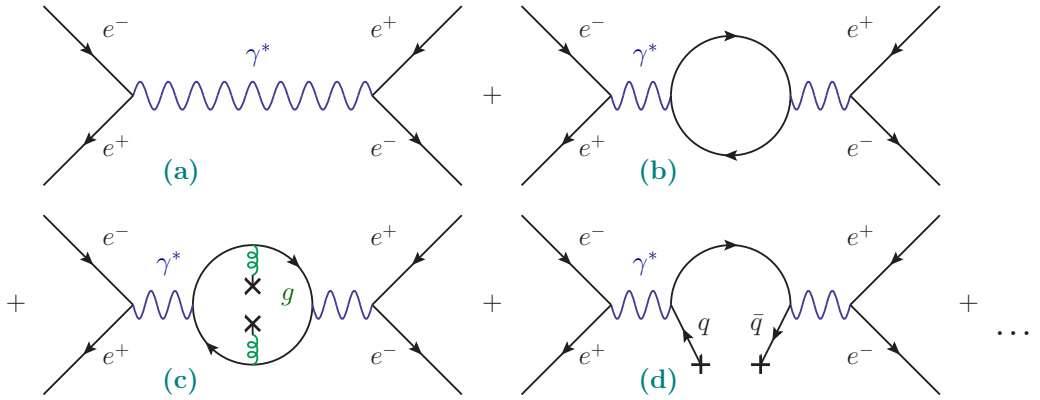

Figure 9: Selected diagrams contributing to Equation 85, including gluon and quark condensate corrections, as illustrated by figure (c) and (d), respectively. Crosses represent vacuum condensates.

Here, $d_{\mathcal{Q}_n}$, $d_{\mathcal{A}}$ and $d_{\mathcal{B}}$ are the canonical mass dimensions of the operator $\mathcal{Q}_n$, $\mathcal{A}$ as well as $\mathcal{B}$, respectively. Similarly, the coefficients c_X $\left(X = \mathcal{Q}_n, \mathcal{A}, \mathcal{B}\right)$ are associated to the anomalous dimensions $\gamma_X(g) = c_X g^2 + \mathcal{O}\left(g^3\right)$ (see [45, 98]). This reveals the ordering of the singularities: the higher the dimension of $\mathcal{Q}_n$ the less singular are the coefficients C_n. Hence, operators with the smallest dimension dominate the short distance expansion.

In a broader context, the OPE, therefore, serves as a tool to handle composite operators which are in general not always well-defined mathematical objects (see, e. g., discussion in [45, Chapter 4]. On a phenomenological level, the mentioned perturbative framework is only applicable if at least some of the involved partons have sufficiently high virtualities to guarantee a small strong coupling constant (see also Section A.15). However, even for such specifically chosen processes a pure perturbative calculation would be insufficient, since the mentioned quarks and gluons are still affected by the QCD vacuum, along with the confinement mechanism. Accordingly, the initial and final state in Equation 85 represents the real (not perturbative) QCD vacuum state (cf. [64, 73–76, 95, 97, 109, 114, 117]. Correspondingly, the calculation of Equation 85 has to include effects due to soft quarks and gluons populating the QCD vacuum (cf. Figure 9). For instance, Equation 85 gives rise to[54] (cf. [64, 73–76]; the ellipses represent neglected higher order corrections)

$$
\begin{aligned}
\Pi_{\mu\nu}(q) &= i\int d^4x\, e^{iq\cdot x} \sum_{\psi} e_\psi^2 \Big[\langle 0|\bar{\psi}(x)\gamma_\mu \overbrace{\psi(x)\bar{\psi}}(0)\gamma_\nu \psi(0)|0\rangle \\
&\quad + \langle 0|\bar{\psi}(x)\gamma_\mu \underbrace{\psi(x)\bar{\psi}}(0)\gamma_\nu \psi(0)|0\rangle + \langle 0|\bar{\psi}(x)\gamma_\mu \underbrace{\psi(x)\bar{\psi}(0)\gamma_\nu \psi}(0)|0\rangle \Big] + \dots \\
&= i\int d^4x\, e^{iq\cdot x} \sum_{\psi} e_\psi^2 \left[-\frac{2x_\mu x_\nu - g_{\mu\nu}x^2}{x^8}\frac{N_c}{\pi} \right. \\
&\quad \left. - \frac{2x_\mu x_\nu + g_{\mu\nu}x^2}{x^4}\left(\frac{\langle \frac{\alpha_S}{\pi} G^A_{\mu\nu} G^{A,\mu\nu}\rangle}{96\pi^2} + \frac{N_c m_\psi \langle\bar{\psi}\psi\rangle}{12\pi^2} \right) \right] + \dots \\
&= \left(q_\mu q_\nu - g_{\mu\nu} q^2\right) \Pi\left(q^2\right) , \qquad (98)
\end{aligned}
$$

54 In Equation 99, a pure perturbative ansatz would only be exact up to $\mathcal{O}(1/q^4)$ accuracy.

together with the amplitude

$$\Pi\left(q^2\right) = \sum_{\psi} e_{\psi}^2 \left[\frac{N_c}{12\pi^2} \log\left(\frac{\mu^2}{-q^2}\right) + \frac{1}{12q^4} \langle \tfrac{\alpha_s}{\pi} \mathcal{G}^A_{\mu\nu} \mathcal{G}^{A,\mu\nu} \rangle + \frac{2N_c}{3q^4} m_{\psi} \langle \bar{\psi}\psi \rangle \right] + \dots . \tag{99}$$

The latter includes[55] the associated vacuum expectation values [74, 97, 118]

$$\langle 0|\bar{\psi}^a_{\alpha}(x)\psi^b_{\beta}(0)|0\rangle = \langle \bar{\psi}\psi \rangle \left[\frac{\delta^{ab}\delta_{\beta\alpha}}{12} - \frac{m_{\psi}}{48i}\delta^{ab}\left[\not{x}\right]_{\beta\alpha} \right] + \mathcal{O}\left(x^2\right) , \tag{100}$$

$$\langle 0|\mathcal{G}^A_{\alpha\beta}(0)\,\mathcal{G}^B_{\rho\sigma}(0)|0\rangle = \frac{\langle \mathcal{G}^A_{\mu\nu}\mathcal{G}^{A,\mu\nu}\rangle}{96}\delta^{AB}\left(g_{\alpha\rho}g_{\beta\sigma} - g_{\alpha\sigma}g_{\beta\rho}\right) , \tag{101}$$

of occurring local operators (see discussion below). Here, we can only mention selected aspects of the QCD vacuum related to the used approach, as the ultimate solution of QCD and the resulting complete picture concerning vacuum fields are unknown (see, e. g., [119]). From a phenomenological point of view, these soft fields fluctuate with a typical long-distance scale $\Lambda_{\text{vac}} \sim \Lambda_{\text{QCD}}$ [97]. A quark-antiquark pair, created by an external current at some point and absorbed at another point has to interact with these soft fields, according to the specific problem studied.

For Equation 85 (vacuum-to-vacuum) and the set-up $Q^2 \gg \Lambda^2_{\text{QCD}}$ the average distance between the quark-antiquark emission and absorption is essentially smaller than the characteristic scale of the vacuum fluctuations. Therefore, the fast oscillating quark-antiquark fields perceive the slow vacuum fluctuations as an almost static average of a soft background field [97]. At the same time this short distance probe of the long-distance fields does not significantly disturb the vacuum state. Therefore, an explicit ansatz for the interaction of, e. g., quarks with momenta $\sim \sqrt{Q^2}$ and the vacuum can be expressed as a scattering process. This means, the highly energetic quarks and gluons are scattered by external static fields composed of soft quarks and gluons. Again (cf. [74, 97]), one has to keep in mind the specific flavor structure of this interaction:

- LIGHT QUARKS:
  - vacuum gluons are emitted and absorbed by virtual gluons;
  - quarks/antiquarks are interchanged with their vacuum counterparts;
  - combined (soft) quark-gluon interaction;
- HEAVY QUARKS:
  - here only the interaction with the vacuum gluons is important.

This means, that heavy and light corrections effectively have a quite different structure (cf. [97]). While in loop corrections of light flavors masses can be safely neglected, heavy quark masses have to be included without exception. Also, due to their large mass $m_{c,b,t} \gg \Lambda_{\text{QCD}}$ the heavy flavors are far off-shell even at the momentum scale Λ_{vac}. Therefore, their interaction with the soft fields of the vacuum proceeds mainly via gluon interaction. In terms of the OPE Equation 85 takes the form[56] (modulo the tensor structure)

$$\Pi\left(q^2\right) = C_0\left(Q^2\right) + \sum_{n>0} C_n\left(Q^2,\mu\right) \langle 0|\mathcal{O}_n(\mu)|0\rangle , \tag{102}$$

55 While the mentioned first contraction in Equation 99 leads to LO perturbation theory (PT) and gluon condensate contributions, the second and third term correspond (at this accuracy) to quark condensate corrections. Besides, the ellipses stand for higher order admixtures, including additional condensates and mass corrections.

56 Sometimes, the short hand notation $\langle 0|\mathcal{O}_n(\mu)|0\rangle = \langle \mathcal{O}_n(\mu)\rangle$ is used.

with the local gauge invariant operators[57] $\mathcal{O}_n$, composed of soft fields (for instance $\mathcal{O}_3 = \bar{\psi}\psi$, $\mathcal{O}_4 = \frac{\alpha_S}{\pi} G^A_{\mu\nu} G^{A,\mu\nu}$, $\mathcal{O}_5 = g\bar{\psi}\sigma^{\mu\nu} G_{\mu\nu}\psi$, etc.) that form non-vanishing vacuum condensates. The latter parametrize the averaged vacuum characteristics, i. e., the concrete structure of the vacuum fields is irrelevant at this point. Thus, the vacuum fields are treated as external fields [74]. The vacuum condensates are an example of (almost purely) non-perturbative parameters. Therefore, numerical values for the condensate densities can only be calculated from first principle[58], i. e., one has to use methods like lattice[59] QCD (see, e. g., [122]). At present the most common method (see [109]) is to fit the corresponding QCD sum rule to experimental data and extract the values for the condensates. We need several of these condensates throughout this work. Starting with the quark condensate [123, 124] ($\psi = u$, d and for $SU(3)_F$ symmetry also including $\psi = s$ [97])

$$\langle\bar{\psi}\psi\rangle(\mu = 2\text{ GeV}) = \left[-0.246\,{}^{-0.019}_{+0.028}\right]^3\ \text{GeV}^3\,, \tag{103}$$

which is the order-parameter of (spontaneous) chiral-symmetry breaking in QCD and was already known before the development of QCD sum rules. Also, we will need the gluon condensate (related to the QCD vacuum energy-density [95])

$$\langle\tfrac{\alpha_S}{\pi} G^A_{\mu\nu} G^{A,\mu\nu}\rangle(\mu{=}2\text{ GeV}) = \left[0.012\,{}^{-0.012}_{+0.006}\right]\ \text{GeV}^4 \tag{104}$$

and the parametrization for mixed (quark-gluon) condensates [125]

$$m_0^2(\mu{=}1\text{ GeV}) = \frac{\langle g\bar{\psi}\sigma^{\mu\nu} G_{\mu\nu}\psi\rangle}{\langle\bar{\psi}\psi\rangle} = (0.8 \pm 0.2)\ \text{GeV}^2\,. \tag{105}$$

Admittedly, the accuracy of the numerical values for the condensate densities is not very high[60] and ranges between five to thirty percent. In particular, when using less conservative estimates as we did in this work (see [97] and references therein). Fortunately, uncertainties caused by condensate contributions for the quantities calculated in this work is less than four percent (see Chapter 5). As mentioned above, the heavy flavors do not form condensates, but interact with the soft fluctuations of the vacuum via gluons. Therefore, the interaction of heavy quarks with condensates of gluons or light quarks will appear only in higher orders[61] of α_S. Moreover, dimensional counting reveals, that $\langle 0|\mathcal{O}_n|0\rangle \sim \Lambda_{\text{vac}}^{d_n}$ (cf. [74]), which means that the n^{th} term of the series in Equation 102 $\sim \sqrt{\Lambda^2_{\text{vac}}/Q^2}^{\,d_n}$ is suppressed for $Q^2 \gg \Lambda^2_{\text{QCD}}$, as assumed. Therefore, already at intermediate $Q^2 \sim 1\text{ GeV}^2$ the expansion given in Equation 102 can be safely truncated after a few terms. In fact, condensates with canonical dimensions larger than six usually play a minor role in the existing calculations (see [97]). In addition to the condensates there exist other vacuum fluctuations at short distances $\sim 1/\sqrt{Q^2}$ which are able to absorb the whole momentum of the external quark current (cf. [97]). These effects are known as direct instantons (cf. [127]) and for the vector currents under consideration they may become important only for operators with dimension larger than ten (see discussion in [97]). Therefore, they will not play any role in the truncated OPE we were discussing. Another possible issue concerns the key point of the OPE which is the separation of hard and soft scales. In this context it is possible to get a certain amount of double counting, e. g., due to the soft tails of the perturbative contributions overlapping with the long-distance parametrizations. For some cases a rearrangement of the OPE into

57 According to Equation 102 $C_0(Q^2)$ corresponds to the coefficient of the unit operator $\mathcal{O}_0 = \mathbb{1}$.
58 Also, attempts exist to calculate the condensates with models of the instanton vacuum [120, 121].
59 Still, very little is known about higher dimensional condensates and lattice studies mainly focus on the chiral condensate.
60 Despite the technical and experimental challenges considerable improvements are possible (cf. [94]).
61 This is a reason, why correlation functions of heavy quark currents can be used to study, e. g., the gluon condensate [97, 126]. The latter then is the dominant condensate term in the OPE.

a practical version [95] can reduce this overlap, but for the discussed cases the double counting will be numerically insignificant [97].

Since our work mainly deals with light-cone dominated processes, we have to extend the discussion to this specific setting. Thus, it is mandatory to introduce the light-cone[62] OPE:

- LIGHT-CONE OPERATOR PRODUCT EXPANSION: It has the generic form [44]

$$\lim_{x^2\to 0} \mathcal{A}\left(\tfrac{x}{2}\right) \mathcal{B}\left(-\tfrac{x}{2}\right) \approx \sum_i C_i(x)\, \mathcal{O}_i\left(\tfrac{x}{2}, -\tfrac{x}{2}\right) , \tag{106}$$

with singular complex functions $C_i(x)$ and the regular bilocal operators $\mathcal{O}_i(x,y)$, which in our case will turn out to be the so-called QCD string operators (see Chapter 3 and [75]). The Taylor expansion of such a non-local operator can be expressed as [44]

$$\mathcal{O}_i\left(\tfrac{x}{2}, -\tfrac{x}{2}\right) = \sum_j x^{\mu_1} \cdots x^{\mu_j}\, \mathcal{O}^{(j,i)}_{\mu_1 \dots \mu_j}(0) , \tag{107}$$

so that Equation 106 can also be written in terms of local operators

$$\lim_{x^2\to 0} \mathcal{A}\left(\tfrac{x}{2}\right) \mathcal{B}\left(-\tfrac{x}{2}\right) \approx \sum_{i,j} C_i^{(j)}\left(x^2\right) x^{\mu_1} \cdots x^{\mu_j}\, \mathcal{O}^{(j,i)}_{\mu_1 \dots \mu_j}(0) . \tag{108}$$

When choosing a basis[63] $\left\{\mathcal{O}^{(j,i)}_{\mu_1 \dots \mu_j}\right\}_i$ consisting of symmetric traceless tensors with j Lorentz indices, the (Lorentz-) spin[64] j can be assigned to each operator [44, 98]. In fact, a naive dimensional analysis reveals for the light-cone behavior of the Wilson coefficients

$$\lim_{x^2\to 0} C_i^{(j)}\left(x^2\right) \sim \left[\sqrt{x^2}\right]^{d_{i,j}-j-d_{\mathcal{A}}-d_{\mathcal{B}}} \left[\ln\left(x^2 m^2\right)\right]^p , \tag{109}$$

where $d_{j,i}$ is the mass-dimension of $\mathcal{O}^{(j,i)}_{\mu_1 \dots \mu_j}$. Besides, m is a generic mass parameter and p a corresponding real number, see [44]. Hence, the leading term of Equation 108 corresponds to the lowest value of $(d_{i,j} - j)$. This combination is in general called the twist (cf. Section 3.2) of a given light-cone operator, i. e.,

> "(geometrical) twist = (canonical) dimension − (Lorentz) spin" .

Accordingly, the operators with the lowest twist dominate the involved light-cone expansion. Here, we did not yet include possible RG effects (see [64, 98]), which are discussed below.

62 More precisely, we use a specific version of the light-cone OPE which is usually referred to as conformal OPE [128].
63 This operator basis may include an infinite number of terms, contributing to the given operator product.
64 Strictly speaking, the related spin characterizes the corresponding representation of the homogenous Lorentz group (see, e. g., [44, 98]).

Furthermore, for the investigation of pseudoscalar singlet mesons we need the anomalous dimensions of related twist-two operators. For this purpose, one may study the product of two electromagnetic currents[65] [129–131] (ellipses represent neglected higher order corrections):

$$\begin{aligned}\lim_{x^2\to 0} J^{em}_\mu(x)\, J^{em}_\nu(0) \approx \left(-g_{\mu\nu}\partial^2+\partial_\mu\partial_\nu\right)\frac{1}{x^2}\sum_{m=0}^{\infty}\sum_i C^m_{i,1}\left(x^2,\mu^2,g\right) x_{\mu_1}\cdots x_{\mu_m}\mathcal{O}^{\mu_1\cdots\mu_m}_i(0)\\ -\left(g_{\mu\mu_1}g_{\nu\mu_2}\partial^2-g_{\mu\mu_1}\partial_\nu\partial_{\mu_2}-g_{\nu\mu_2}\partial_\mu\partial_{\mu_1}+g_{\mu\nu}\partial_{\mu_1}\partial_{\mu_2}\right)\times\\ \times\sum_{m=2}^{\infty}\sum_i C^m_{i,2}\left(x^2,\mu^2,g\right) x_{\mu_3}\cdots x_{\mu_m}\mathcal{O}^{\mu_1\cdots\mu_m}_i(0)\\ -i\varepsilon_{\mu\nu\lambda\mu_1}\partial^\lambda\frac{1}{x^2}\sum_{m=1}^{\infty}\sum_i E^m_{i,1}\left(x^2,\mu^2,g\right) x_{\mu_2}\cdots x_{\mu_m}\mathcal{R}^{\mu_1\cdots\mu_m}_i(0)+\ldots,\end{aligned}\tag{110}$$

where we deal with renormalized quantities, denoted by the renormalization scale μ^2. In Equation 110 we only consider contributions of twist-two operators. The index i of $\mathcal{O}^{\mu_1\cdots\mu_m}_i$ and $\mathcal{R}^{\mu_1\cdots\mu_m}_i$ stands for the representation of the flavor $SU(N_f)_F$ group which is used to model the flavor structure of the non-singlet (NS) contributions "$\mathcal{R}^{\mu_1\cdots\mu_m}_{(NS,A);q}$" in the OPE. Therefore, T^A stand for the generators of the $SU(N_f)$ group in an adequate matrix representation, i. e., when restricted to $N_f=3$ the standard Gell-Mann matrices will be used to define $T^A=\frac{1}{2}\lambda^A$. Also there will be flavor singlet (S) contributions "$\mathcal{R}^{\mu_1\cdots\mu_m}_{S;q}$" which are important in the context of this work that is devoted to study eta mesons. The latter have to be described theoretically by contributions of flavor singlet admixtures and parity-odd operators. As can be seen in the following, the singlet sector receives contributions from quark $\mathcal{R}^{\mu_1\cdots\mu_m}_{S;q}$ and gluon operators $\mathcal{R}^{\mu_1\cdots\mu_m}_{S;g}$ because both have the same quantum numbers. This implies, that they mix under renormalization. For the parity-odd sector, in QCD there are three classes of gauge-invariant twist-two operators (near $x^2\approx 0$):

$$\left.\begin{aligned}\mathcal{R}^{\mu_1\cdots\mu_m}_{(NS,A);q} &= i^m\hat{S}\left\{\overline{\Psi}\gamma_5\gamma^{\mu_1}D^{\mu_2}\cdots D^{\mu_m}T^A\Psi-(\text{traces})\right\},\\ \mathcal{R}^{\mu_1\cdots\mu_m}_{S;q} &= i^m\hat{S}\left\{\overline{\Psi}\gamma_5\gamma^{\mu_1}D^{\mu_2}\cdots D^{\mu_m}\Psi-(\text{traces})\right\},\\ \mathcal{R}^{\mu_1\cdots\mu_m}_{S;g} &= i^m\hat{S}\left\{\mathrm{Tr}\left\{\tilde{G}^{\mu_1\alpha}D^{\mu_2}\cdots D^{\mu_{m-1}}G_\alpha{}^{\mu_m}\right\}-(\text{traces})\right\},\end{aligned}\right\}\tag{111}$$

with $\Psi(x)=(u(x),d(x),s(x),\ldots)^T$, the vector of the first $1\leqslant N\leqslant N_f$ quark-spinors. Those operators are irreducible representations of the Lorentz group, i. e., they are traceless and symmetric in the Lorentz indices $\mu_1,\ldots,\mu_m$. Therefore, the operator $\hat{S}$ in front of the curly brackets of Equation 111 implies the symmetrization of all involved indices, while the term "(traces)" represents the adequate subtractions in order to produce a traceless operator. Furthermore, the operators $\mathcal{O}^{\mu_1\cdots\mu_m}_i$ correspond to the parity-even case (e. g., for the description of vector mesons) and the corresponding anomalous dimensions have been calculated in [129, 132–139]. For the renormalization the flavor structure has to be specified. Actually, the singlet and the non-singlet cases decouple. To sketch the ansatz (for a full treatment see [129]) for deriving the anomalous dimensions, one starts with a formal definition of the partonic operator matrix element [129]

$$\langle j,p,s|\mathcal{R}^{\mu_1\cdots\mu_n}_{k;i}|j,p,s\rangle = A^{(n)}_{k;ij}\left(p^2,\mu^2,g,\xi\right)\hat{S}\{(s^{\mu_1}p^{\mu_2}\cdots p^{\mu_n})-(\text{traces})\},\tag{112}$$

65 For the correct pole structure in Equation 110 one has to replace $x^2\to x^2-i\varepsilon x_0$ [129].

with spin s and indices $k = NS, S$ and $i, j = q, g$. The coefficients $A^{(n)}_{k;ij}$ are derived from the Fourier transform into momentum space of the connected Green's functions [129] (i. e., one where external lines are amputated)

$$\langle 0|T\Big\{\bar{\varphi}_j(x)\,\mathcal{R}^{\mu_1\cdots\mu_n}_{k;i}(0)\,\varphi_j(y)\Big\}|0\rangle\Big|_{\text{connected}}\,. \tag{113}$$

Here, $\varphi_i(x)$ stands either for the quark $\psi(x)$, or gluon fields $\mathcal{A}^A_\mu(x)$. Therefore, the corresponding Callan-Symanzik equation can be written as (for details see [129])

$$\left[\mu\frac{\partial}{\partial\mu}+\beta(g)\,\frac{\partial}{\partial g}+\delta(\xi,g)\,\frac{\partial}{\partial\xi}+\gamma^{(m)}_{NS;qq}\right]A^{(m)}_{NS;qq}\left(p^2,\mu^2,g,\xi\right)=0 \tag{114}$$

$$\left[\left(\mu\frac{\partial}{\partial\mu}+\beta(g)\,\frac{\partial}{\partial g}+\delta(\xi,g)\,\frac{\partial}{\partial\xi}\right)\delta_{ij}+\gamma^{(m)}_{S;ij}\right]A^{(m)}_{S;jk}\left(p^2,\mu^2,g,\xi\right)=0\,. \tag{115}$$

In [129] the renormalization constants $Z_{NS;qq}$ and $Z_{S;ij}\equiv(\mathfrak{Z}_S)_{ij}$ have been calculated up to α_S^2 accuracy, leading to the desired result

$$\gamma^{(m)}_{NS;qq}=\beta(g,\varepsilon)\,Z^{-1}_{NS;qq}\frac{d}{dg}Z_{NS;qq} \tag{116}$$

$$\gamma^{(m)}_{S;ij}=\beta(g,\varepsilon)\left(\mathfrak{Z}_S^{-1}\right)_{ik}\frac{d}{dg}Z_{S;kj}\,. \tag{117}$$

The anomalous dimensions arise from the perturbative series

$$\gamma^{(m)}_{k;ij}=\gamma^{(0),(m)}_{k;ij}\frac{\alpha_S}{4\pi}+\gamma^{(1),(m)}_{k;ij}\left(\frac{\alpha_S}{4\pi}\right)^2+\mathcal{O}\left(\alpha_S^3\right)\,. \tag{118}$$

Accordingly, they have been adapted to the rest of the formalism and can be found in Section C.2. In fact, the discussed anomalous dimensions are essential for the intended renormalization of $\eta^{(\prime)}$ DAs (see Chapter 3).

Let us come back to the question, whether it makes sense to describe a light-cone dominated process with a tower of condensates or not. For an illustration we consider the pion electromagnetic form factor at leading-twist accuracy and LO in α_S, as discussed in [140]. This process (see Figure 10) can be described with the correlation function

$$\mathcal{T}_{\mu\nu}(p,q)=i\int d^4x\,e^{iq\cdot x}\langle 0|T\Big\{\mathcal{J}^5_\mu(0)\,\mathcal{J}^{em}_\nu(x)\Big\}|\pi^+(p)\rangle\,, \tag{119}$$

with the pion interpolation current $\mathcal{J}^5_\mu=\bar{d}\gamma_\mu\gamma_5 u$, the electromagnetic current $\mathcal{J}^{em}_\mu$ as well as the pion momentum p ($p^2=m_\pi^2$) and the photon virtuality $Q^2=-q^2$ (which is fixed). The contribution of the pion intermediate state also depends on the invariant variable $s=(p-q)^2$ which implies the parametrization

$$\mathcal{T}_{\mu\nu}(p,q)=\frac{2if_\pi\,(p-q)_\mu\,p_\nu}{m_\pi^2-(p-q)^2}F_\pi\left(Q^2\right)\,, \tag{120}$$

where F_π is the pion electromagnetic form factor, containing all the process specific information, e. g., on the electromagnetic pion structure. Besides, this form factor can be calculated in full

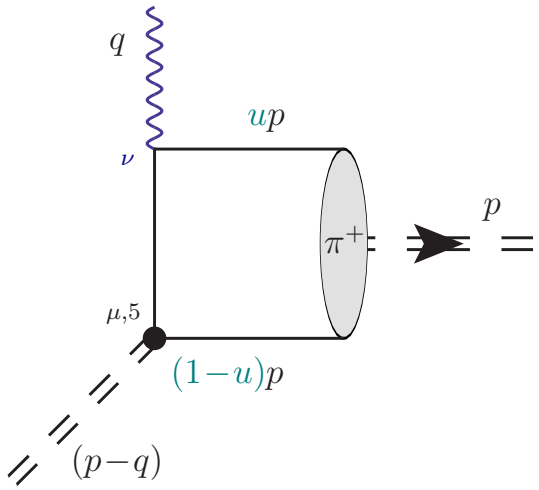

Figure 10: A generic tree-level contribution to the correlation function in Equation 119. Within this "hand-bag" diagram the blob represents non-perturbative effects related to the pion DA, while the interpolating axial-vector current $\mathcal{J}^5_\nu$ is depicted by a dashed double line.

analogy to the $\pi^0\gamma^{(\star)}\gamma^*$ transition form factor which makes it an interesting testing ground for us. The tree-level leading-twist correction for massless (u, d) quarks reads:

$$\begin{aligned}\mathcal{T}_{\mu\nu}(p,q) &= i\int d^4x\, e^{iq\cdot x}\Big\{e_u\langle 0|\bar{d}(0)\gamma_\mu\gamma_5\overbrace{u(0)\bar{u}}(x)\gamma_\nu u(x)|\pi^+(p)\rangle \\ &\quad - e_d\langle 0|\bar{d}(x)\gamma_\nu\overbrace{d(x)\bar{d}}(0)\gamma_\mu\gamma_5 u(0)|\pi^+(p)\rangle\Big\} \\ &= \int d^4x\,\frac{e^{iq\cdot x}}{2\pi^2x^4}x^\alpha S_{\mu\nu\alpha\beta}\Big\{e_u\langle 0|\bar{d}(0)\gamma^\beta\gamma_5 u(x)|\pi^+(p)\rangle \\ &\quad - e_d\langle 0|\bar{d}(x)\gamma^\beta\gamma_5 u(0)|\pi^+(p)\rangle\Big\}\,, \end{aligned} \tag{121}$$

with the tensor structure

$$S_{\mu\nu\alpha\beta} = g_{\mu\alpha}g_{\nu\beta} + g_{\nu\alpha}g_{\mu\beta} - g_{\mu\nu}g_{\alpha\beta}\,. \tag{122}$$

At this point it should be emphasized, that Equation 121 is written with an abbreviation for the matrix elements (cf.[64, 73–76])

$$\langle 0|\bar{\psi}(x)\gamma_\mu\gamma_5\varphi(y)|M(p)\rangle \equiv \langle 0|\bar{\psi}_{cl}(x)\gamma_\mu\gamma_5\,[x,y]_{cl}\,\varphi_{cl}(y)|M(p)\rangle\,, \tag{123}$$

where ψ, φ are specific (light) quark flavors, M is the meson under consideration and $[x,y]$ represents the path-ordered exponent (cf. Equation 1153) to ensure gauge-invariance of this non-local object. In Equation 123 soft field configurations[66] are assumed, denoted by the subscript "cl". This factorized form of the correlation function can be seen as a consequence of the light-cone OPE (cf. Equation 106), where Equation 123 denote corresponding soft contributions. Let us try to describe the soft corrections with a formal expansion into a Taylor series of the matrix-

66 In other words, the fields are assumed to be slowly varying.

elements in Equation 121. For a symmetric interval[67] the operators of this expansion are given by [140]

$$\bar{\mathcal{O}}^{(n)}_{\mu\mu_1\cdots\mu_n} = \bar{d}(0)\gamma_\mu\gamma_5 i\overset{\leftrightarrow}{D}_{\mu_1}\cdots i\overset{\leftrightarrow}{D}_{\mu_n} u(0)\,, \tag{124}$$

$$\langle 0|\bar{d}(x)\gamma_\mu\gamma_5 u(-x)|\pi^+(p)\rangle = \sum_n \frac{(-i)^n}{n!} x^{\mu_1}\cdots x^{\mu_n}\langle 0|\bar{\mathcal{O}}^{(n)}_{\mu\mu_1\cdots\mu_n}|\pi^+(p)\rangle\,, \tag{125}$$

with the covariant derivative[68] $\overset{\leftrightarrow}{D}_\mu = \overset{\leftarrow}{D}_\mu - \vec{D}_\mu$ (see Section 3.4.3). When choosing the expansion point accordingly, the operators Equation 124 can be expressed as a linear combination of $\mathcal{R}^{\mu\mu_1\ldots\mu_n}_{(NS,1);q}$ and $\mathcal{R}^{\mu\mu_1\ldots\mu_n}_{(NS,2);q}$, plus higher twist corrections. Therefore, similar to Equation 112, the matrix elements of the local operators can be parametrized according to $(x^2 \approx 0)$

$$x^{\mu_1}\cdots x^{\mu_n}\langle 0|\bar{\mathcal{O}}^{(n)}_{\mu\mu_1\cdots\mu_n}|\pi^+(p)\rangle = i f_\pi p_\mu\,(p\cdot x)^n\,\langle\!\langle \mathcal{O}^{(n)}_\pi\rangle\!\rangle + \ldots\,, \tag{126}$$

where the ellipses stand for other Lorentz-structures (i. e., contributions of higher twist). When inserting Equation 126 in Equation 121, one gets[69] $\left(\text{using } x = \frac{Q^2}{s+Q^2},\ s = (p-q)^2\right)$ [140]

$$\mathcal{T}_{\mu\nu}(p,q) = i f_\pi \frac{p_\mu p_\nu}{Q^2}\frac{2x}{\xi_x}\left\{1 + \frac{2x}{\xi_x}\sum_{n=1}^{\infty}\langle\!\langle \mathcal{O}^{(2n)}_\pi\rangle\!\rangle\left(\frac{x+\bar{x}}{x-\bar{x}}\right)^{2n-1}\right\} + \ldots\,, \tag{127}$$

with the useful definitions[70] $(x \in [0,1])$

$$\xi_x = x - \bar{x}\,,\quad \bar{x} = 1 - x\,. \tag{128}$$

A sensible evaluation of F_π requires the application of a Borel transformation (see Section B.3) which entails an additional variable M^2, i. e., the so-called Borel parameter [140] (omitting higher twist and continuum subtractions, see Section 4.2):

$$F_\pi\left(Q^2\right) = e^{-\frac{Q^2}{M^2}}\left\{1 + \sum_{n=1}^{\infty}\langle\!\langle \mathcal{O}^{(2n)}_\pi\rangle\!\rangle\sum_{k=1}^{2n}\binom{2n-1}{k-1}\frac{1}{\Gamma(k+1)}\left(\frac{-2Q^2}{M^2}\right)^k\right\}. \tag{129}$$

A major motivational reason for this step is given by an implicit suppression of all except low-lying resonances and higher order OPE contributions (for an elaborate discussion see Section 4.2). This has been further studied in the context of QCD sum rules (cf. Chapter 4, Chapter 5), which represent a well-known analytic technique (inter alia) devised for the calculation of QCD observables, as named above. Indeed, the SVZ sum rules (see Section 5.1.1) have been widely used for this purpose. The representation Equation 129, however, turns out to be inadequate for light-cone dominated problems, because the two required conditions are contradictory unless Q^2 is sufficiently small [140]. Indeed, for a sufficient suppression of higher resonances (e. g., a_1 meson intermediate state, etc.) the Borel parameter has to be held within the predetermined window (see also Section B.3) $1\ \text{GeV}^2 \leqslant M^2 \leqslant 2\ \text{GeV}^2$. On the other hand, Equation 129 enhances the OPE's higher order terms by factors of $\left[Q^2\right]^k$ and for $Q^2 > M^2$ the entire expansion breaks down. A solution to this problem has been worked out in [140–143]. In a nutshell, one may escape those

67 Due to translation invariance, this may be chosen without loss of generality.

68 Here, $\overset{\leftarrow}{D}_\mu$ and $\vec{D}_\mu$ only acts on fields on the left, or the right-hand side of the derivative, respectively.

69 Only operators with even numbers of derivatives, i. e., n contribute due to G-parity.

70 In the next chapters, we will restrict the use of Equation 128 to the case $x \in [0,1]$. Then, "x" may be interpreted as a longitudinal (anti-) quark momentum fraction, while "$p\,\xi_x$" is playing the role of a quark-antiquark relative longitudinal momentum (cf. Section 3.1.4).

calamities, by abandoning the (formal) short distance OPE and instead write all results directly in a factorized form, with coefficient functions and so-called DAs:

$$\langle\!\langle \mathcal{O}_\pi^{(n)}(\mu) \rangle\!\rangle = \int_0^1 \mathrm{d}u\, \xi_u^n \phi_\pi(u,\mu)\ , \tag{130}$$

which themselves parametrize non-local matrix elements[71], such as (up to twist-two)

$$\langle 0|\bar{d}(x)\gamma_\nu\gamma_5 u(-x)|\pi^+(p)\rangle\big|_{x^2\approx 0} = \mathrm{i} f_\pi p_\mu \int_0^1 \mathrm{d}u\, e^{\mathrm{i}\xi_u p\cdot x}\phi_\pi(u,\mu\sim 1/\sqrt{x^2})\ . \tag{131}$$

Correspondingly, the related leading-twist LO QCD corrections can then be conflated to

$$\mathcal{T}_{\mu\nu}(p,q) = 2\mathrm{i} f_\pi p_\mu p_\nu \int_0^1 \mathrm{d}\,u\, \frac{u\phi_\pi(u)}{\bar{u}Q^2 - us} + \ldots \tag{132}$$

implying a rather compact LCSR [144] (omitting continuum subtractions)

$$F_\pi\Big(Q^2\Big) = \int_0^1 \mathrm{d}\,u\,\phi_\pi(u)\exp\Big(-\tfrac{\bar{u}Q^2}{uM^2}\Big)\ . \tag{133}$$

This ansatz works perfectly well, especially within the limit $Q^2 \to \infty$. In fact, one can consistently perform every stage of the underlying calculation within this non-local approach [75]. Hence, light-cone dominated processes, such as the hard exclusive processes considered within this work, favor a description in terms of light-cone DAs. In particular, the latter also allow a deeper insight into the examined meson's non-perturbative structure and will be subject of a detailed discussion in Chapter 3.

2.5 FROM SYMMETRY CURRENTS TO MESONS

Before being able to investigate hadron properties, the apparent gap between a formal description in terms of quarks and gluons and the observables of the hadronic world has to be bridged. Due to the absence of a rigorous analytic solution of QCD, relating the fundamental degrees of freedom to the measurable particle spectrum, an effective description has to be employed. This inevitably will be problem dependent, i. e., when assigning a specific flavor structure to a hadron[72] for its classification, the characteristic parameters (e. g., involved quantum numbers of the particle under consideration) have to be kept obvious throughout the analysis. Nevertheless, in this subsection, the basics needed for a process independent approach will be introduced, allowing nontrivial statements about the hadrons parton structure.

Let us start with the global symmetries of the QCD Lagrangian. In general conservation laws lead to conserved currents and charges. Those and the implied commutation relations are useful to classify the possible particle spectrum. To clarify this issue, one has to study the invariance of the underlying Lagrangian[73]

$$\mathcal{L}(\phi_i(x), \partial_\mu\phi_i(x))\ , \tag{134}$$

such as $\mathcal{L} \equiv \mathcal{L}_{\mathrm{QCD}}$, under the global transformations

$$\phi_i \mapsto \exp\Big\{\mathrm{i}\Gamma^A\theta_A\Big\}_{ij}\,\phi_j\ , \tag{135}$$

71 A dedicated discussion may be found in Chapter 3.
72 For instance, when probing its flavor structure with a specific quark current.
73 With the generic fields ϕ_i standing for the fundamental fields of the theory.

with the generators Γ^A (e. g., of $SU(N)$ or $U(N)$) and the global (space-time independent) angles θ_A. For QCD both indices i, j may refer to a given flavor. Because of Noether's theorem [145, 146], any continuous symmetry transformation similar to Equation 135, which leaves the action invariant, implies the existence of a conserved current [44]

$$\mathcal{J}^A_\mu = -i\frac{\delta\mathcal{L}}{\delta(\partial^\mu\phi_i)}\left[\Gamma^A\right]_{ij}\phi_j \quad \Rightarrow \quad \partial^\mu\mathcal{J}^A_\mu = 0\,, \tag{136}$$

with the associated conserved charge[74]

$$Q^A(x_0) = \int d^3x\, \mathcal{J}^A_0(x) \quad \Rightarrow \quad \frac{d}{dx_0}Q^A = 0\,. \tag{137}$$

The underlying symmetry together with the canonical commutation relation (at equal time) implicate the charge algebra [44]

$$\left[Q^A(x_0), Q^B(x_0)\right] = if^{ABC}Q^C(x_0)\,, \tag{138}$$

with the structure constants f^{ABC} of the corresponding symmetry group. Similar extensions to symmetry currents are called current algebra which have been a powerful tool in the development of QCD [147, 148] and beyond. As a matter of fact, QCD can be described with two or three dynamical light quark flavors at low energies. To a good approximation, one may consider them as massless $m_\psi \approx 0$ ($\psi = u, d, s$), even though we will see that mass corrections become important for further theoretical considerations. Therefore, this digression into a hypothetical world of N_f massless flavors[75] has to be seen as a useful gedankenexperiment, giving us better insight into the (non-perturbative) QCD dynamics. Later on the results can be retrofitted with the corresponding mass corrections. For instance, the quark mass corrections can be treated perturbatively when the scales under consideration are much larger than the light masses m_ψ. To exemplify this case, we may consider the quark propagator Equation 1142, while assuming $\frac{m_\psi}{\Lambda_{QCD}} \ll 1$:

$$iS_\psi(x,0) = i\frac{\Gamma\left(\frac{D}{2}\right)\not{x}}{2\pi^{\frac{D}{2}}\left[-x^2\right]^{\frac{D}{2}}} + m_\psi\frac{\Gamma\left(\frac{D-2}{2}\right)\mathbb{1}_4}{4\pi^{\frac{D}{2}}\left[-x^2\right]^{\frac{D-2}{2}}} - m_\psi^2 i\frac{\Gamma\left(\frac{D-2}{2}\right)\not{x}}{8\pi^{\frac{D}{2}}\left[-x^2\right]^{\frac{D-2}{2}}} + \mathcal{O}\left(m_\psi^3\right)\,. \tag{139}$$

Moreover, the massless (classical) QCD Lagrangian with N_f active (light) flavors

$$\mathcal{L}^{(cl.)}_{QCD} = -\frac{1}{4}\mathcal{G}^A_{\mu\nu}\mathcal{G}^{A,\mu\nu} + \sum_{f=1}^{N_f}\overline{\Psi}_f i\not{D}\Psi_f\,, \tag{140}$$

with "f" being its flavor index that numbers the elements of the N_f-tuples[76]

$$\Psi = (u, d, \ldots)^T\,, \quad \overline{\Psi} = (\bar{u}, \bar{d}, \ldots)\,, \tag{141}$$

has the following symmetries [44, 55, 76, 146]

$$U(1)_V \times U(1)_A \times SU(N_f)_L \times SU(N_f)_R \tag{142}$$

as listed in Table 1. In the context of massless particles it is convenient to define the frame

74 Provided that surface terms at infinity are negligibly small.

75 The remaining "heavy flavors" are assumed to be non-dynamical which is accomplished by setting their masses to infinitely large values.

76 We choose a configuration of the components in $\Psi = (\ldots, \Psi_i, \ldots, \Psi_j, \ldots)^T$ such that $m_i < m_j\ \forall i, j$ is fulfilled.

symmetry	transformation	current	quantum level
$U(1)_V$	$\Psi_f \mapsto e^{i\alpha}\Psi_f \ (\alpha \in \mathbb{R})$	$\mathcal{J}^{(B)}_\mu = \frac{1}{3}\sum_f \overline{\Psi}_f \gamma_\mu \Psi_f$	baryon number conservation
$U(1)_A$	$\Psi_f \mapsto e^{i\alpha\gamma_5}\Psi_f \ (\alpha \in \mathbb{R})$	$\mathcal{J}^{(A)}_{\mu 5} = \sum_f \overline{\Psi}_f \gamma_\mu \gamma_5 \Psi_f$	anomalous
$SU(N_f)_L \times SU(N_f)_R$	$\Psi_{f,L} \mapsto [U_L]_{fg}\Psi_{g,L}$ $\Psi_{f,R} \mapsto [U_R]_{fg}\Psi_{g,R}$	$\mathcal{J}^A_{\mu L} = \overline{\Psi}_{f,L}\gamma_\mu [T^A]_{fg}\Psi_{g,L}$ $\mathcal{J}^A_{\mu R} = \overline{\Psi}_{f,R}\gamma_\mu [T^A]_{fg}\Psi_{g,R}$	spontaneously broken

Table 1: Symmetries of the classical QCD Lagrangian (see Equation 140). Here, T^A denote the generators of $SU(N_f)$, $U_R = \exp\left[i\gamma_5 \theta^A_R T^A\right]$ and $U_L = \exp\left[i\theta^A_L T^A\right]$ for θ^A_R, $\theta^A_L \in \mathbb{R}$ (cf. [55, 146]).

independent decomposition of the Dirac spinor (see Section A.2)

$$\Psi_{f,X} = P_X \Psi_f \quad (X = L, R) \,, \tag{143}$$

with the chiral projection operators (specified in $D = 4$)

$$P_R = \frac{1}{2}\left(\mathbb{1}_4 + \gamma_5\right) \,, \quad P_L = \frac{1}{2}\left(\mathbb{1}_4 - \gamma_5\right) \tag{144}$$

into left- and right-handed spinors

$$\Psi_f = \Psi_{f,R} + \Psi_{f,L} \,. \tag{145}$$

Then the dynamics of the left- and right-handed quarks decouples (for the limit $m_{u,d,s} \to 0$ and $m_{c,b,t} \to \infty$)

$$\mathcal{L}^{(cl.)}_{QCD} = \sum_{f=1}^{N_f} \left[\overline{\Psi}_{f,R} i\not{D}\Psi_{f,R} + \overline{\Psi}_{f,L} i\not{D}\Psi_{f,L}\right] - \frac{1}{4}\mathcal{G}^A_{\mu\nu}\mathcal{G}^{A,\mu\nu} \tag{146}$$

on the Lagrangian level[77]. Additionally, the corresponding action of Equation 140 exhibits an invariance under a global scale transformation (see discussion in Chapter 3), but we first will focus on the axial $U(1)_A$ and the chiral $SU(3)$ flavor symmetries.
In fact, exact symmetries give rise to exact conservation laws, i. e., in this case both the Lagrangian and the related vacuum are invariant under the specific symmetry [149]. Nevertheless, not all symmetries of the classical Lagrangian are preserved at quantum level[78], i. e., QCD possesses quantum anomalies. An anomaly free symmetry is the $U(1)_V$ vector symmetry which is responsible for the baryon number conservation within QCD processes [55]. However, the $U(1)_A$ axial symmetry which can be also written as the following rotations of the left- and right-handed fields in opposite directions (cf. Equation 1090)

$$e^{i\alpha}\Psi_{f,R} + e^{-i\alpha}\Psi_{f,L} = e^{i\alpha\gamma_5}\Psi_f \tag{147}$$

is anomalous at the quantum level. The related axial[79] (or Adler-Bell-Jackiw, or triangle) anomaly can be seen in the divergence of the (external) axial vector current $\mathcal{J}^{(A)}_{5\mu}$ and is of major importance when studying $\eta^{(\prime)}$ mesons. There are several ways to calculate the axial anomaly, e. g.,

77 Here, one uses $\bar{\psi}_{R,L} i\not{D}\psi_{R,L} = \frac{1}{2}\left[\bar{\psi} i\not{D}\psi \pm \bar{\psi} i\gamma_\mu\gamma_5 D^\mu \psi\right]$ for every active flavor ψ.
78 That means, when quantum corrections are included.
79 Due to Equation 147, it is self-evident to call the corresponding axial anomaly also chiral anomaly.

by evaluating the corresponding triangle diagram similar to Figure 4 (cf. [52]). In particular, it is wise to use the so-called Schwinger or point splitting renormalization (ε-splitting) [150, 151]. This scheme [55, 66, 150] introduces a gauge-invariant UV regularization prescription for the axial vector currents, by replacing the original current $\mathcal{J}^{(A)}_{5\mu}(x)$ with their regularized counterparts

$$\mathcal{J}^{(A),\text{reg.}}_{\mu 5}(x) = \lim_{|\varepsilon_\mu|\to 0} \sum_f \overline{\Psi}_f(x+\varepsilon)\,\gamma_\mu\gamma_5\,[x+\varepsilon, x-\varepsilon]\,\Psi_f(x-\varepsilon)\ . \tag{148}$$

Consequently, the generic form of the chiral anomaly (for a calculation see Section A.8) in terms of the axial current (see Equation 148) with N_f light flavors is

$$\partial^\mu \mathcal{J}^{(A),\text{reg.}}_{\mu 5}(x) = N_f \frac{\alpha_S}{4\pi} \mathcal{G}^A_{\mu\nu}(0)\,\widetilde{\mathcal{G}}^{A,\mu\nu}(0) + 2\,\overline{\Psi}_f i\gamma_5\,[\hat{m}]^{fg}\Psi_g\,, \tag{149}$$

with the $N_f \times N_f$ mass matrix [152]

$$\hat{m} = \text{diag}(m_u, m_d, \ldots)\ . \tag{150}$$

It is important to outline the connection of the axial anomaly with the complex non-perturbative structure of QCD. We can only do this in passing and, therefore, have to focus on the major highlights relevant for this work. First, let us consider a world without quarks. In contrast to other QFTs, the field theoretical degrees of freedom in QCD are not only oscillator like[80], but exhibit a direction in the (infinite dimensional) space of (gauge) fields along which the Yang-Mills system can tunnel [44]. For instance, the zero-energy states may be connected with each other by (quantum mechanical) tunneling transitions. Consider the so-called Chern-Simons current which plays an important role in the description of the QCD vacuum via instanton[81] calculus:

$$K^\mu = \frac{\alpha_S}{4\pi}\varepsilon^{\mu\nu\rho\sigma}\mathcal{A}^A_\nu\left[\left(\partial_\rho\mathcal{A}^A_\sigma\right) - \frac{g}{3}f^{ABC}\mathcal{A}^B_\rho\mathcal{A}^C_\sigma\right]\ . \tag{151}$$

The corresponding Chern-Simons charge

$$\mathcal{K}(x_0) = \int d^3x\, K_0(x) \tag{152}$$

can be related to the Pontryagin-index (or winding number) which classifies the different topological sectors of QCD [55, 152]. An analysis[82] of $\mathcal{K}$ reveals a (quasi) periodic Bloch boundary condition of the vacuum "fields" ϕ_{vac} (cf. [55])

$$\phi_{vac}(\mathcal{K}+1) = e^{i\theta}\phi_{vac}(\mathcal{K})\ , \tag{153}$$

with $\theta \in [0, 2\pi]$, a hidden parameter, called the vacuum angle. The latter would be a global fundamental constant, characterizing the boundary conditions of the θ-vacuum

$$|\theta\rangle = \sum_{n\in\mathbb{Z}} e^{in\theta}|n\rangle\,, \tag{154}$$

with $|n\rangle$ the n^{th} zero energy state corresponding to $\mathcal{K} = n$ (cf. [55]). According to the genuine form of the θ-vacuum and the given topological structure of Yang-Mills theories, the vacuum transition $|\theta\rangle \to |\theta'\rangle$ (with $\theta \neq \theta'$) can be taken into account with the additional term

$$\mathcal{L}_\theta = \frac{\theta}{2}\left(\frac{\alpha_S}{4\pi}\mathcal{G}^A_{\mu\nu}\widetilde{\mathcal{G}}^{A,\mu\nu}\right) \tag{155}$$

80 That means, having a single ground state.

81 In a manner of speaking, a field configuration $\mathcal{A}^A_\mu$ continuously interpolating between the states (cf. Equation 152) $\mathcal{K}(x_0 \to -\infty) = n \in \mathbb{Z}$ and $\mathcal{K}(x_0 \to +\infty) = n+1$ (with minimal action) in Euclidean time, i. e., the least action tunneling trajectory, is called the Belavin-Polyakov-Schwartz-Tyupkin (BPST) instanton [55].

82 According to [55] a Hamiltonian formulation of the Yang-Mills theory can be developed, allowing a separation of an associated potential energy term $\mathcal{V}(\mathcal{K})$. The latter exhibits a periodicity in the variable $\mathcal{K}$, i. e., along the $\mathcal{K}$-direction.

in the effective QCD Lagrangian density (for a construction cf. [44]). Equation 155 includes the only gauge-invariant Lorentz scalar operator (in $D=4$) that can be constructed from $\mathcal{A}^A_\mu$, violating parity and time-reversal symmetry[83]. On the other hand, the operator $\mathcal{G}\widetilde{\mathcal{G}}$ can be expressed as a total derivative of the gauge-dependent Chern-Simons current

$$\partial_\mu K^\mu = \frac{\alpha_S}{8\pi}\mathcal{G}^A_{\mu\nu}\widetilde{\mathcal{G}}^{A,\mu\nu}\,, \tag{156}$$

and, therefore, one could believe that Equation 155 can have no impact on the action after all.[84] However, due to the instanton field this is not the case [44]. Being aware of that, the seemingly unavoidable inclusion of $\mathcal{L}_\theta$ into the QCD Lagrangian would introduce (for $\theta \neq 0, \pi$ cf. [55]) a measurable P (parity), and (therefore) CP (combination of both charge conjugation and parity) breaking of strong interaction. Nevertheless, it is known experimentally that both, P and CP, are conserved symmetries for strong interaction to a very high degree of accuracy. In fact, estimates (see [55] and references therein) for the vacuum angle give values very close to zero $\theta \leqslant 10^{-9}$ [153]. This gives rise to the strong CP problem (cf. [55, 154, 155]). On phenomenological grounds, one could simply assume $\theta \equiv 0$, but in the presence of (nearly) massless quarks the mentioned axial anomaly will purge those theoretical tensions. In order to get to this deeper insight, a different gauge-independent operator, based on the Chern-Simons charge can be defined

$$Q = \mathcal{K}(x_0 \to +\infty) - \mathcal{K}(x_0 \to -\infty) \equiv \Delta\mathcal{K}\,. \tag{157}$$

This so-called topological charge Q has the local representation

$$Q = \frac{\alpha_S}{8\pi}\int d^4x\, \mathcal{G}^A_{\mu\nu}\widetilde{\mathcal{G}}^{A,\mu\nu}\,, \tag{158}$$

which can be related to Chern-Simons current

$$Q = \int d^4x\, \partial^\mu K_\mu = \int_{-\infty}^{+\infty} dx_0 \int d^3x\, \partial_0 K_0 = \lim_{\alpha\to\infty}\int d^3x\, K_0(x_0,\vec{x})\Big|_{x_0=-\alpha}^{x_0=+\alpha} = \Delta\mathcal{K} \tag{159}$$

via the Gauss formula [55] $(i = 1,2,3)$

$$\int_\Omega d^4x\, \partial_i K_i = \int_{\partial\Omega} d\mathcal{S}_i\, K_i \to 0\,. \tag{160}$$

Again, for the theory of instantons and QCD vacuum structure Equation 158 is an important quantity, labeling distinct topologies of the vacuum (cf. [44, 55]). Furthermore, when coming back to a formulation of QCD with N_f light quark flavors, the following relations are implied by the immanent axial anomaly (cf. Equation 137):

$$\begin{aligned}\int d^4x\, \partial^\mu \mathcal{J}^{(A)}_{\mu 5}(x) &= \int_{-\infty}^{+\infty} dx_0 \int d^3x\, \partial_0 \mathcal{J}^{(A)}_{05}(x) = \lim_{x_0\to\infty}\{Q_5(x_0) - Q_5(-x_0)\} \\ &= 2N_f Q = 2N_f \Delta\mathcal{K}\end{aligned} \tag{161}$$

83 Before the discovery of instantons it was believed that QCD naturally conserves P and CP [55].

84 Equation 156 can be easily verified, e. g., via a short calculation

$$\begin{aligned}\partial_\mu K^\mu &\sim \frac{\alpha_S}{8\pi}\varepsilon^{\mu\nu\rho\sigma}\,\mathrm{Tr}\{4\,[\partial_\mu \mathcal{A}_\nu][\partial_\rho \mathcal{A}_\sigma] + 4ig\,[\partial_\mu \mathcal{A}_\nu]\,[\mathcal{A}_\rho, \mathcal{A}_\sigma]\} \\ &= \frac{\alpha_S}{8\pi}\varepsilon^{\mu\nu\rho\sigma}\,\mathrm{Tr}\{(2\,[\partial_\mu \mathcal{A}_\nu] + ig\,[\mathcal{A}_\mu, \mathcal{A}_\nu])(2\,[\partial_\rho \mathcal{A}_\sigma] + ig\,[\mathcal{A}_\rho, \mathcal{A}_\sigma])\} \\ &= \frac{\alpha_S}{8\pi}\varepsilon^{\mu\nu\rho\sigma}\,\mathrm{Tr}\{\mathcal{G}_{\mu\nu}\mathcal{G}_{\rho\sigma}\}\,.\end{aligned}$$

relating the change of the chiral charge with the topological charge of the gauge field. The latter is better known in the context of the Atiyah-Singer index theorem (see [156] and references therein). This famous theorem may be interpreted as follows [55]: the number of fermion zero modes (i.e., $\not{D}\psi = 0$, with ψ normalizable) is related to the topological charge of the gauge fields via

$$Q = n_R - n_L \,, \tag{162}$$

where "$n_{R,L}$" is the number of (normalizable) zero modes of positive/negative (or right-/left-handed) chirality. Therefore, on quantum level left- and right-handed zero modes are not conserved separately. Moreover, in the presence of massless fermions the possible θ-term in the Lagrangian becomes unobservable, even for finite θ. This is a consequence of the axial anomaly which allows us to rewrite $\mathcal{L}_\theta$ as a total derivative of the gauge-invariant quantity $\mathcal{J}^{(A)}_{\mu 5}$

$$\mathcal{L}_\theta \sim \partial^\mu \mathcal{J}^{(A)}_{\mu 5} \tag{163}$$

and, therefore, $\mathcal{L}_\theta$ will drop out of the effective action[85]. In conclusion we will treat P and CP as conserved within QCD modulo small perturbations.
The other class of chiral transformations affects the flavor structure of the possible particles. According to the $SU(N_f)_R \times SU(N_f)_L$ symmetry of the (classical) Lagrangian Equation 146

$$\Psi_{f,X} \mapsto \exp\left[iT^A \theta^A_X\right]_{fg} \Psi_{g,X} \,, \quad X = R,\, L \tag{164}$$

with the symmetry currents (now omitting the flavor index of Ψ_X)

$$\mathcal{J}^A_{\mu X} = \overline{\Psi}_X \gamma_\mu T^A \Psi_X \tag{165}$$

implying the charge algebra [44]

$$\left[Q^A_X(x_0)\,, Q^B_X(x_0)\right] = i f^{ABC} Q^C_X(x_0) \tag{166}$$

$$\left[Q^A_R(x_0)\,, Q^A_L(x_0)\right] = 0 \,. \tag{167}$$

Equivalently, the invariance under the $SU(N_f)$ transformations

$$\Psi_f \mapsto \exp\left[iT^A \theta^A\right]_{fg} \Psi_g \tag{168}$$

$$\Psi_f \mapsto \exp\left[iT^A \gamma_5 \theta^A\right]_{fg} \Psi_g \tag{169}$$

can be considered, which lead to the more convenient (rescaled[86]) Noether currents (later on generalized to $A = 0, 1, \ldots, N_f^2 - 1$)

$$\mathcal{J}^A_\mu = \overline{\psi}\gamma_\mu \sqrt{2} T^A \psi \quad = \sqrt{2}\left(\mathcal{J}^A_{\mu R} + \mathcal{J}^A_{\mu L}\right) \tag{170}$$

$$\mathcal{J}^A_{\mu 5} = \overline{\psi}\gamma_5\gamma_\mu \sqrt{2} T^A \psi = \sqrt{2}\left(\mathcal{J}^A_{\mu R} - \mathcal{J}^A_{\mu L}\right) \tag{171}$$

and corresponding conserved axial "Q^A_5" as well as vector "Q^A_V" charges

$$Q^A_V = Q^A_R + Q^A_L \,, \tag{172}$$

$$Q^A_5 = Q^A_R - Q^A_L \,. \tag{173}$$

85 More generally, in a theory with light quarks ($m_{quark} \approx 0$) all θ dependent effects must be proportional to the corresponding quark masses (cf. [157]).

86 For convenience, we have rescaled the standard currents by a factor of "$\sqrt{2}$".

The latter are important for the low energy realm of QCD. For instance, the related charge algebra[87] of Equation 173 will be of use in the following:

$$\left[Q_5^A(x_0), Q_5^B(x_0)\right] = if^{ABC} Q_V^C(x_0) \,. \tag{174}$$

On classical level, the divergences of the involved Noether currents $(A = 1, \ldots, N_f^2 - 1)$

$$\partial^\mu \left(j_{\mu R}^A \mp j_{\mu L}^A\right) = \overline{\psi}\left[T^A, \hat{m}\right]_\pm i\gamma_5 \psi = \pm \sum_{f,f'} (m_f \pm m_{f'})\, \overline{\psi}_f i\gamma_5 \left[T^A\right]_{ff'} \psi_{f'} \tag{175}$$

are quasi conserved[88] (see [152] and Section A.1 for an extended discussion). In contrast to the classical Lagrangian density (see Equation 146), the physical vacuum $|0\rangle$ will not respect the continuous global symmetry as induced by Equation 164, i. e., the chiral symmetry appears to be spontaneously broken. The anatomy of the latter

$$SU(N_f)_R \times SU(N_f)_L \to SU(N_f)_V \tag{176}$$

can only be depicted together with the chiral (or quark) condensate

$$\langle \overline{\psi}\psi \rangle = \langle \overline{\psi}_R \psi_L + \overline{\psi}_L \psi_R \rangle \neq 0 \,, \tag{177}$$

which turns out to be the relevant order parameter[89] of the spontaneously broken chiral symmetry. Furthermore, the remaining vector symmetry is only realized approximately in nature, due to finite quark-masses. Even though the chiral symmetry is spontaneously broken, Equation 175 also holds on the quantum level, implying the general identity for local axial-vector currents

$$\begin{aligned} \partial^\mu j_{\mu 5}^A &= \overline{\psi}\left[\sqrt{2}T^A, \hat{m}\right]_+ i\gamma_5 \psi + \delta^{0A} 2\sqrt{3}\omega \\ &= \sum_{f,f'} (m_f + m_{f'})\, \overline{\psi}_f i\gamma_5 \left[\sqrt{2}T^A\right]_{ff'} \psi_{f'} + \delta^{0A} 2\sqrt{3}\omega \,, \end{aligned} \tag{178}$$

where "ω" is the topological charge density (see also [152])

$$\omega = \frac{\alpha_S}{8\pi} G_{\mu\nu}^A \widetilde{G}^{A,\mu\nu} \,. \tag{179}$$

This being said, let us also approach the symmetry breaking from a phenomenological perspective[90]. Therefore, the realization of the chiral symmetry has to be questioned again. From a spectroscopical point of view a Wigner-Weyl realization [158]

$$Q_V^A|0\rangle = 0 = Q_5^A|0\rangle \,, \tag{180}$$

i. e., a total symmetry between positive and negative parity states is excluded due to the observed particle spectrum. In fact, no parity doublets[91] can be seen in nature, e. g., for pseudoscalar mesons, or the nucleon no chirality partner can be seen. Instead the Nambu-Goldstone realization of the chiral symmetry can be found in nature:

$$Q_V^A|0\rangle = 0 \neq Q_5^A|0\rangle \tag{181}$$

87 This is just a reformulation of Equation 166 and Equation 167. Therefore, it would be redundant to provide the corresponding charge algebra of Q_V^A and Q_5^A.

88 For non-vanishing quark masses the chiral symmetry is also explicitly broken, which is caused by mass terms similar to $\mathcal{L}_{\text{mass}} = \sum_{f=1}^{N_f} m_f \left[\overline{\Psi}_{f,R}\Psi_{f,L} + \overline{\Psi}_{f,L}\Psi_{f,R}\right]$.

89 It is the analogon of, e. g., the magnetization, which is the order parameter of the spontaneous $O(3)$ symmetry breaking of a ferromagnet.

90 The outcome will be equivalent to the abstract statement of Equation 177, but in this way the interesting components of the particle spectrum can be related to the involved operators heuristically.

91 Such a doublet would consist out of states of positive and negative parity, with equal masses.

implying that the axial symmetry is spontaneously broken (cf. [44, 55, 76]). The latter leads to the famous Goldstone theorem [159–161], which states (cf. [149]):

- GOLDSTONE THEOREM: When an exact continuous global symmetry (of a manifestly Lorentz invariant theory) is spontaneously broken, the theory contains one massless (or light, if the symmetry is not exact) scalar particle in the spectrum of possible excitations for each broken generator of the original symmetry group.

This means, for each generator failing to annihilate the vacuum $Q_5^A|0\rangle \neq 0$, there must exist a massless boson with the quantum numbers of the generator Q_5^A (cf. [73]). Hence, this theorem may serve us as a guiding light towards the desired formalism which is connecting the abstract QCD operators and particles of the Hilbert space. Let us first investigate the properties of the Goldstone bosons with the aid of the (classical) energy-momentum tensor (where the summation runs over all fields of the QCD Lagrangian)

$$\Theta^{\mu\nu} = \sum_i \frac{\partial \mathcal{L}}{\partial (\partial_\mu \phi_i)} \partial^\nu \phi_i - g^{\mu\nu}\mathcal{L}\,, \tag{182}$$

which is generated by (infinitesimal) space-time translations (cf. [73, 128]). Even though its form on classical level is fixed by Noether's theorem, the quantum version is not unique due to possible ambiguities in the definition of $\mathcal{L}$. Moreover, the intended gauge-independence[92] has to be introduced by modifying $\Theta^{\mu\nu}$ appropriately (for a thorough discussion see [73, 98] and references therein). According to the supposed properties of Equation 181, combined with the QCD Hamiltonian density [73]

$$\mathcal{H}(x_0, \vec{x}) = \Theta^{00}(x_0, \vec{x})\,, \tag{183}$$

a conserved charge $Q_\mathcal{J}$ of a (quasi) conserved symmetry current $\mathcal{J}_\mu$ entails the commutation relation[93]

$$[Q_\mathcal{J}(x_0)\,, \mathcal{H}(x_0, \vec{x})] = 0\,. \tag{184}$$

Therefore, with the definition of the $N_f^2 - 1$ states via the axial charges (the ellipses stand for heavier excitations with the same quantum numbers)

$$Q_5^A|0\rangle = |\phi^A\rangle + \dots \tag{185}$$

and the assumed form of the Schrödinger equation [76]

$$\mathcal{H}|0\rangle = \mathcal{E}_0|0\rangle \tag{186}$$

Equation 184 immediately implies

$$\mathcal{H}|\phi^A\rangle = \mathcal{E}_0|\phi^A\rangle\,, \quad \forall A = 1, \dots, N_f^2 - 1\,, \tag{187}$$

i. e., the $|\phi^A\rangle$ are energetically degenerate (with the vacuum state) and thus represent massless particles. Moreover, applying Equation 174 to the vacuum state reveals the bosonic nature of $|\phi^A\rangle$, while the transformation properties of the $\{Q_5^A\}_{A=1,\dots,N_f^2-1}$ identifies them as pseudoscalar particles. In fact, for $N_f \leqslant 3$ the lightest pseudoscalar mesons can be identified as (quasi) Goldstone bosons[94] (cf. Table 2) which can be better understood when approaching the

92 A direct application of Equation 182 does not necessarily yield a gauge-invariant energy-momentum tensor [73].

93 When including finite mass terms $\mathcal{H}_m = \sum_{f=1}^{N_f} m_f \overline{\psi}_f \psi_f$ in the $\mathcal{H}$, the l.h.s. of Equation 184 will be proportional to the total derivative of $\mathcal{J}_\mu$ [73].

94 Note, that according to the representation of the generators, the fields in Equation 185 do not have to embody the actual meson states, but can, e. g., be a superposition of them.

symmetry group	representation	particle multiplet	singlet particle
$SU(2)_F$	$2 \otimes \bar{2} = 3 \oplus 1$	(π^+, π^0, π^-)	$\sigma \sim \frac{1}{\sqrt{2}}(u\bar{u} + d\bar{d})$
$SU(3)_F$	$3 \otimes \bar{3} = 8 \oplus 1$	$\left(\pi^+, \pi^0, \pi^-, K^+, K^0, \overline{K}^0, K^-, \eta\right)$	η'

Table 2: Ordering pattern of light pseudoscalar meson states, including the hypothetical state σ.

problem again from a spectroscopical point of view. Light-quark meson spectroscopy eponymously studies [162–169] mesons with a valence content made out of up, down and strange quarks. Therefore, the simplest and preferred classification scheme in this context is the quark model[95] [41], i. e., the meson is modeled as a positronium-like [170] quark-antiquark system of quasi free constituents[96]. When focusing on QCD processes, the meson can be expressed in terms of conserved quantum numbers, like parity (P), charge conjugation (C), G-parity (G), total angular momentum (J), or isospin (I), which in their entirety can be written as $\left(I^G\right) J^{PC}$, e. g., pseudoscalar mesons have 0^{-+} (cf. [169]). Accordingly, along with their masses, (decay) width as well as decay modes, etc., it is the explicit flavor structure which allows us to uniquely identify a particular meson. In QFT one can connect hadron properties with the internal quark-gluon structure by applying an operator "$\mathcal{O}_X$" with the right quantum numbers and transformation properties to the vacuum state (see Goldstone theorem) and project the desired meson state "M" (with momentum P_μ and mass $m_M^2 = P^2$) out of the generated tower of states. This procedure leads to matrix elements with the generic form "$\langle 0|\mathcal{O}_X|M(P)\rangle$" which obviously fulfill the desired purpose to connect the parton content with the meson under consideration. Consequently, the simplest operator $\mathcal{O}_X$ to build a meson state (flavor, color and Dirac-indices not contracted) can be constructed from (cf. Equation 1095, Equation 1096)

$$\begin{aligned}\overline{\psi}^a_{f',\alpha'}\psi^b_{f,\alpha} = \frac{1}{4}\Big\{ &(\mathbb{1})_{\alpha\alpha'}\left[\overline{\psi}^a_{f'}\psi^b_f\right] - (i\gamma_5)_{\alpha\alpha'}\left[\overline{\psi}^a_{f'} i\gamma_5 \psi^b_f\right] + (\gamma_\mu)_{\alpha\alpha'}\left[\overline{\psi}^a_{f'}\gamma^\mu\psi^b_f\right] \\ &- (\gamma_\mu\gamma_5)_{\alpha\alpha'}\left[\overline{\psi}^a_{f'}\gamma^\mu\gamma_5\psi^b_f\right] + \frac{1}{2}(\sigma_{\mu\nu}\gamma_5)_{\alpha\alpha'}\left[\overline{\psi}^a_{f'}\sigma^{\mu\nu}\gamma_5\psi^b_f\right]\Big\} . \end{aligned} \tag{188}$$

According to the given quantum numbers of the meson "M", Equation 188 additionally has to be retrofitted with the adequate color and flavor structures, e. g., by a gauge link $[x,0]^{ab}$ (for gauge-invariance) and a combination[97] such as $\sum_{A=0}^{N_f^2-1} c_A \left[T^A\right]_{f'f}$ (cf. Section A.1). In this way all possible flavor structures can be generated. For example, the neutral pion π^0 can be modeled, by using the operator

$$\overline{\psi}^a_{f',\alpha'}(x)\,[x,0]^{ab}\left[\sqrt{2}T^3\right]_{f'f}\psi^b_{f,\alpha}(0) . \tag{189}$$

After taking the matrix element

$$\langle 0|\overline{\psi}^a_{f',\alpha'}(x)\,[x,0]^{ab}\left[\sqrt{2}T^3\right]_{f'f}\psi^b_{f,\alpha}(0)|\pi^0(P)\rangle \tag{190}$$

the only allowed Lorentz structures are proportional to $i\gamma_5$, $\gamma_\mu\gamma_5$, $\sigma_{\mu\nu}\gamma_5$ due to the supposed parity conservation in QCD. All other structures have to vanish when taking into account the pseudoscalar nature (transformation properties) of the pion. For the η and η' the situation is more

95 This choice makes it easier to connect the quantum numbers of the meson with the observed particle properties.
96 In fact, this is just a toy model to represent specific spectroscopic parameters of non-exotic mesons (cf. [41]). It cannot be used to fully describe the underlying meson structure.
97 Consequently, the matrix elements can be expressed in terms of (non-local) Noether currents.

complicated, because they actually are a superposition of the flavor octet and singlet currents. The latter implies additional pure gluonic admixtures and, therefore, a priori, the existence of non-vanishing matrix elements of the type[98]

$$\langle 0|\mathcal{G}^{A}_{\mu\nu}(x)\,[x,0]\,\widetilde{\mathcal{G}}^{A}_{\rho\omega}(0)|\eta^{(\prime)}(P)\rangle\,. \tag{191}$$

Analogously, matrix elements of multi-particle states can be derived, by further combining additional quark and gluon fields. Fortunately, for the problems addressed in this work, only composite operators consisting out of the fewest possible number of fields will contribute.

One should again emphasize that the non-vanishing matrix elements are caused by the non-perturbative effects related to the physical vacuum[99]. That this is the case for the quark-antiquark type, expressed with Equation 190, is a consequence of the immanent chiral symmetry breaking. However, can we expect non-vanishing gluonic matrix elements like Equation 191? For a general argumentation we have to briefly raise the topic of the $\eta - \eta'$ mass splitting. As discussed the Goldstone theorem for "$N_f = 3$" predicts eight bosons which appear to be massless in the limit of vanishing quark masses. The latter results from Gell-Mann-Oakes-Renner (GMOR) relations (see, e. g., [73]), such as[100] (cf. [171] and references therein)

$$m_q\,\langle\bar{\psi}\psi\rangle = -\frac{f_\pi^2}{2}\,m_\pi^2\left(1+\mathcal{O}\left(m_\pi^2\right)\right)\,, \tag{192}$$

$$(m_q+m_s)\left(\langle\bar{s}s\rangle+\langle\bar{\psi}\psi\rangle\right) = -2f_K^2\,m_K^2\left(1+\mathcal{O}\left(m_K^2\right)\right)\,, \tag{193}$$

$$m_q = \frac{1}{2}\,(m_u+m_d)\,, \tag{194}$$

which are a result of the spontaneous chiral symmetry breaking. Here, m_P is the meson mass $(P=\pi,K)$, while f_P is its corresponding decay constant. In contrast, the $U(1)_A$ symmetry give rise neither to another Goldstone boson, nor a conserved quantum number [152]. Instead, the η' emerges, which is much heavier than all other mesons of the pseudoscalar octet, actually too massive to be identified as a Goldstone boson at all. A possible explanation might be the presence of the chiral anomaly, i. e., the η' mass does not have to vanish in the massless limit $\hat{m}\to 0$. However, for this to be true on theoretical level and in order to reproduce the observed $\eta-\eta'$ mass splitting the (anomalous) Ward identity (cf. Equation 178) alone is not sufficient. That means (for the chosen approach), one additionally needs to ask for non-vanishing matrix elements of the topological charge density which represent a coupling of the nontrivial vacuum effects to the η' meson (see [152, 172] and references therein). Since "ω" (cf. Equation 179) is a total divergence (of a gauge independent current), it will vanish to any finite order of perturbation theory [64]. The latter implies that the $U(1)_A$ problem cannot be solved by perturbative gluons alone. That the needed solution really lies in the non-perturbative sector of QCD, which inevitably is connected to the nontrivial topological features of the theory, has been suggested by several authors. For instance, [173, 174] pointed out, that infrared enhanced gluons may be the source of the large η' mass. Moreover, they have argued that the non-perturbative phenomena responsible for the confinement mechanism are also preventing the η' from being realized as another Goldstone boson. This approach has been refined by [175], suggesting the described

98 The operator Equation 191 obviously also generates the local gluonic operators of Equation 111. The latter will mix with the corresponding flavor singlet operators via renormalization.

99 Due to the fact that Q_5^A as well as the currents $J^A_{\mu 5}$ are Wick-ordered products of field operators, they give no finite contribution when applied to the perturbative vacuum ($|\emptyset\rangle$) $Q_5^A|\emptyset\rangle = 0 = J^A_{\mu 5}|\emptyset\rangle$. This is true to all orders of perturbation theory [64].

100 The quark masses and the condensate acquire opposite renormalization, therefore, we do not have to distinguish between bare and renormalized quantities when focusing on their products $m_q\langle\bar{q}\,q\rangle = m_{q,\mathcal{R}}\langle\bar{q}\,q\rangle_{\mathcal{R}}$.

instanton calculus as a solution, including the non-conservation of the axial vector current as a source for non-zero η' mass in the chiral limit [173, 175–177]. However, there also exists an alternative approach initiated by [178, 179] and [180], who proposed an expansion of QCD in (powers of) $N_f N_c^{-1}$. It turns out that in the formal limit[101] $N_c \to \infty$, the η' mass should be of order $\mathcal{O}(N_c^{-1})$. Additionally, a realization of the general N_c^{-1} counting rules, as imposed by [178, 179] can be introduced into the theory via a ghost state (cf. [180]). The latter corresponds to a massless unphysical pole of the correlation function [152]

$$q_\mu q_\nu \langle K^\mu K^\nu \rangle \neq 0\,, \quad \tau_0 = \int d^4x \, \langle 0|T\{\omega(x)\,\omega(0)\}|0\rangle \neq 0\,, \tag{195}$$

which generates a finite topological susceptibility[102] (τ_0). The term "unphysical" in this context means, that the ghost pole does not correspond to an (experimentally) observable glueball state [152], since K^μ is gauge-dependent.
Finally, Equation 195 is essential for a finite [152] matrix element

$$\langle 0|\omega|\eta'\rangle \neq 0\,. \tag{196}$$

Recent lattice studies (see [183, 184]) also support Equation 196, including a significant correlation with the topological susceptibility.

Consequently, this justifies the intended thorough phenomenological investigation of involved (non-local) matrix-elements, in particular those involving gluonic operators similar to $\mathcal{G}^A_{\mu\nu}\widetilde{\mathcal{G}}^A_{\rho\omega}$. Most importantly, based on the latest high precision measurements, a subsequent numerical evaluation can extract quantitative information on the mentioned non-perturbative quantities from the related data.

2.6 QCD AND THE STANDARD MODEL

Although we mainly deal with effects related to QCD phenomena in this work, specific aspects of the electroweak theory cannot be completely avoided. Therefore, in the following section, we will roughly record some basic facts about the weak interaction. An appropriate presentation of this topic may, e. g., be found in the standard literature [64, 98, 146, 149, 185–188].

2.6.1 *Aspects of weak interactions*

The SM[103] successfully describes three of the four known fundamental forces in the universe, i. e., the electromagnetic, weak and strong interaction, while excluding gravity.[104] That includes a classification of all known elementary particles which can be arranged into three generations of fermionic matter (cf. Table 3), a set of corresponding gauge bosons and the scalar Higgs boson (see Figure 11). According to their inherent charges, the different fermions participate in all possible interactions which are mediated by the corresponding gauge bosons. Some of the latter, are charged themselves and may, therefore, exchange related force carriers with other particles. An overview is provided by Figure 12. On a theoretical level, the following milestones during

101 A similar ansatz for describing the $\eta - \eta'$ mixing has been used by Leutwyler [13, 14, 181, 182] (cf. Section 3.1).
102 Another possible interpretation of τ_0 is the mean square winding number per unit volume [152].
103 Here, we always refer to the SM of particle physics.
104 Concerning its predictive power, which is expected to fail at Planck scales [189, 190], the SM has to be seen as an effective field theory. This statement is further supported by the apparent deficiencies of the SM, such as the hierarchy problem or the exclusion of gravitation (for a more complete list see, e. g., [189, 191, 192] and references therein). Accordingly, there are a variety of theories beyond the SM trying to solve these shortcomings, e. g., models with warped extra dimensions or by applying a completely different framework, such as supersymmetry or string theory (cf. [193–196]).

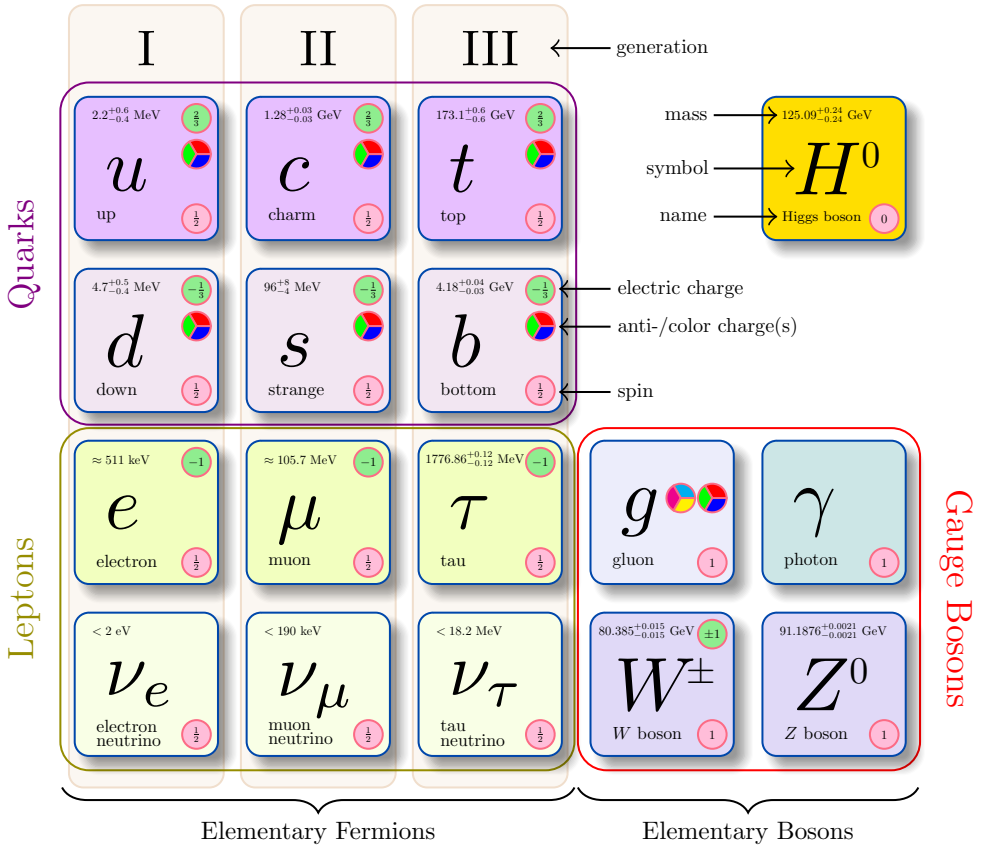

Figure 11: Schematic illustration [4] of all SM particles, including three generations of fermions, force carrying gauge bosons and the massive scalar Higgs boson. In this context, the light quark masses m_u, m_d and m_s are estimates of so-called "current quark masses" within the mass-independent $\overline{MS}$ scheme at a scale $\mu \approx 2$ GeV (cf. [37]). Similarly, m_c as well as m_b are the "running" masses in the same scheme. The top quark mass, on the other hand, results from "direct measurements" (see [42, 197]).

the development of a self-consistent SM have been achieved:

- Proof of asymptotic freedom (see previous discussion) [181, 199, 200],
- Unification of weak and electromagnetic interaction [201, 202],
- Proof of renormalizability [203–205] via the Higgs mechanism [206–209].

These achievements have to be seen in the context of a similarly rapid development in experimental physics (see, e. g., [149]). For instance, the Gorter-Rose method (in low-temperature physics) [210, 211] made it possible to perform the famous Wu experiment [212], which confirmed the hypothesis, that parity is broken in the electroweak interactions [213]. Moreover, weak kaon decays [214] showed clear evidence for a violation of CP-symmetry.[105]

105 Hence, in contrast to QED, along with QCD, which are vectorial (see, e. g., [119, 215]) and preserve P and C separately, the electroweak theory is chiral, i. e., violating both P as well as C. In other words, by construction left- and right-handed fields have to be treated differently (see Section A.2).

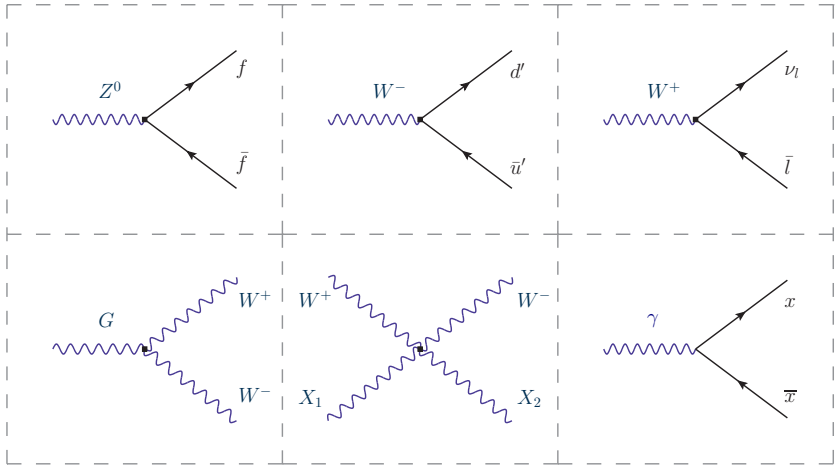

Figure 12: Compilation of possible electroweak interactions within the SM which are mediated by gauge bosons (see, e. g., [198]). Here, "f" stands for any (SM) fermion, while "x" is restricted to electrically charged particles. Furthermore, u′ (d′) only includes up (down)-type quarks and "l" represents a (charged) SM lepton with a corresponding neutrino ν_l. In this context, wave lines represent electroweak gauge bosons, while black squares depict related vertices. Accordingly, "G" is either a photon γ, or a Z^0 boson. The quartic gauge interactions are such that charge conservation for the involved $X_{1,2}$ (i. e., $X_{1,2} = Z^0, W^\pm, \gamma$) holds.

In order to find an effective Lagrangian of nature's electroweak interactions, the following ingredients must be specified:

1) GAUGE GROUP: The required gauge group which is a direct product "$SU(2)_L \times U(1)_Y$" of an abelian $U(1)_Y$ and a non-abelian $SU(2)_L$ group. Both imply (local) transformations in the flavor space (see, e. g., [186]), similar to (Y being the field's hypercharge – see Table 4)

$$D_L^i(x) \longmapsto e^{i\frac{Y}{2}\theta_Y(x)} \exp\left(i\tfrac{\sigma_a}{2}\theta_L^a(x)\right) D_L^i(x) \equiv e^{i\frac{Y}{2}\theta_Y(x)} U_L(x)\, D_L^i(x)\,, \tag{197}$$

$$s_R^i(x) \longmapsto e^{i\frac{Y}{2}\theta_Y(x)} s_R^i(x)\,, \tag{198}$$

with $D_L^i \in \{Q_L^i, L_L^i\}$ and $s_R^i \in \{u_R^i, d_R^i, e_R^i, \nu_R^i\}$ ($i = 1,2,3$). Here, the fundamental representation of $SU(2)_L$ involves the standard Pauli matrices $\{\sigma_1, \sigma_2, \sigma_3\}$ (cf. Section A.1). Moreover, when requiring the free Lagrangian density (omitting the sterile right-handed neutrinos)

$$\mathcal{L}_{\text{free}}^{(\text{weak})} = \overline{L}_L^i i\not{\partial} L_L^i + \overline{Q}_L^i i\not{\partial} Q_L^i + \bar{u}_R^i i\not{\partial} u_R^i + \bar{d}_R^i i\not{\partial} d_R^i + \bar{e}_R^i i\not{\partial} e_R^i\,, \tag{199}$$

to be invariant under the named local gauge transformations, the standard derivatives "∂_μ" have to be replaced by covariant ones[106] (see, e. g., [186])

$$D_\mu D_L^i(x) = \left[\partial_\mu \mathbb{1}_2 + ig'\frac{Y}{2}B_\mu(x)\,\mathbb{1}_2 + ig\frac{\sigma_a}{2}W_\mu^a(x)\right] D_L^i(x)\,, \tag{200}$$

$$D_\mu s_R^i(x) = \left[\partial_\mu + ig'\frac{Y}{2}B_\mu(x)\right] s_R^i(x)\,. \tag{201}$$

106 When demanding $D_\mu D_L^i(x)$ (or $D_\mu s_R^i(x)$) to transform in exactly the same way as $D_L^i(x)$ (or $s_R^i(x)$), one gets for the transformation properties of the gauge-fields (cf. [186]):

$$B_\mu(x) \mapsto B_\mu(x) - \tfrac{1}{g'}\partial_\mu\theta_Y(x)\,, \quad W_\mu^a(x)\,\tfrac{\sigma_a}{2} \mapsto U_L(x)\,W_\mu^a(x)\,\tfrac{\sigma_a}{2}\,U_L^\dagger(x) + \tfrac{i}{g}\left(\partial_\mu U_L(x)\right) U_L^\dagger(x)\,.$$

	Leptons		Quarks	
	left-handed	right-handed	left-handed	right-handed
1st generation	$\begin{pmatrix}\nu_e\\ e^-\end{pmatrix}_L =: L_L^1$	$e_R^- =: e_R^1$ $\nu_{eR} =: \nu_R^1$	$\begin{pmatrix}u\\ d\end{pmatrix}_L =: Q_L^1$	$u_R =: u_R^1$ $d_R =: d_R^1$
2nd generation	$\begin{pmatrix}\nu_\mu\\ \mu^-\end{pmatrix}_L =: L_L^2$	$\mu_R^- =: e_R^2$ $\nu_{\mu R} =: \nu_R^2$	$\begin{pmatrix}c\\ s\end{pmatrix}_L =: Q_L^2$	$c_R =: u_R^2$ $s_R =: d_R^2$
3rd generation	$\begin{pmatrix}\nu_\tau\\ \tau^-\end{pmatrix}_L =: L_L^3$	$\tau_R^- =: e_R^3$ $\nu_{\tau R} =: \nu_R^3$	$\begin{pmatrix}t\\ b\end{pmatrix}_L =: Q_L^3$	$t_R =: u_R^3$ $b_R =: d_R^3$

Table 3: According to the canonical matter representation, each generation of left-handed fermions is collected in doublets, while right-handed particles form singlets (see, e. g., [188]).

The emerging new Lagrangian is invariant under Equation 197 and Equation 198, but exhibits four new gauge fields, i. e., one for each generator[107] of the underlying symmetry groups. In particular, it now contains interactions of the fermion fields with the gauge bosons:

$$\mathcal{L}_{CC}^{weak} = -g\overline{Q}_L^i \gamma^\mu W_\mu^a \frac{\sigma_a}{2} Q_L^i - g\bar{L}_L^i \gamma^\mu W_\mu^a \frac{\sigma_a}{2} L_L^i \,, \tag{202}$$

which is almost, what we need. Most importantly, the gauge symmetry forbids mass terms that explicitly break gauge invariance[108]. Massive gauge fields, on the other hand, would by design imply the phenomenologically required short range of weak interactions. Unfortunately, as discussed above, the symmetry group $SU(2)_L \times U(1)_Y$ is only capable to describe an interacting system of massless fermions and gauge bosons. Consequently, more is needed to describe electroweak phenomena.

II) MATTER REPRESENTATIONS: As already anticipated, the representation of all required fields under this gauge group has to be chosen (cf. Table 3 or [149, 215] for a detailed discussion). That "choice", however, is necessary for the consistency of this theory. In fact, the cancellation of gauge anomalies within this Glashow-Weinberg-Salam theory [203, 216, 217] is only possible if quarks and leptons appear in equal numbers and by organizing themselves into successive generations, as listed in[109] Table 3 (cf. [64]).

III) SPONTANEOUS SYMMETRY BREAKING: The pattern of SSB, i. e., "$SU(2)_L \times U(1)_Y \to U(1)_{EM}$" has to be determined. As mentioned before, this boils down to an adaption of the Higgs mechanism, which on the one hand preserves renormalizability, while on the other hand allows an inclusion of mass terms [203–209]. In fact, due to their short range, the physical $W^\pm$ and Z^0 bosons should be quite heavy particles. In order to generate masses [185, 186, 203],

107 Their transformation properties and field strength tensors exhibit similarities to photon and gluon-fields:

$$B_{\mu\nu} = \partial_\mu B_\nu - \partial_\nu B_\mu \,, \quad W_{\mu\nu}^a = \partial_\mu W_\nu^a - \partial_\nu W_\mu^a - g\varepsilon_{abc} W_\mu^b W_\nu^c \,,$$

which imply the kinetic Lagrangian (cf. also [186])

$$\mathcal{L}_{kin}^{(weak)} = -\frac{1}{4} B_{\mu\nu} B^{\mu\nu} - \frac{1}{4} W_{\mu\nu}^a W^{a,\mu\nu} \,.$$

108 For a chiral theory fermion mass terms are problematic, since they would additionally mix right- and left-handed fermion components: $\bar{\psi}\psi = \bar{\psi}_R \psi_L + \bar{\psi}_L \psi_R$.

109 The mentioned quantum numbers within Table 3 refer to states before the spontaneous symmetry breaking (SSB).

one may consider a $SU(2)_L$ doublet of complex scalar fields "ϕ" $\left(Y_\phi = 1,\, T_3 = -1/2\right)$ and its C-conjugate $\phi^C = i\sigma_2\phi^*$:

$$\phi(x) \coloneqq \begin{pmatrix} \phi^{(+)}(x) \\ \phi^{(0)}(x) \end{pmatrix} \quad \Rightarrow \quad \phi^C(x) = \begin{pmatrix} \phi^{(0)}(x)^* \\ -\phi^{(-)}(x) \end{pmatrix}, \tag{203}$$

combined with a gauged Lagrangian, that includes Goldstone's sombrero potential [159]:

$$\mathcal{L}_H = (D_\mu\phi)^\dagger D^\mu\phi - \mu^2\phi^\dagger\phi - h\left[\phi^\dagger\phi\right]^2, \quad \left(\mu^2 < 0 < h\right), \tag{204}$$

$$D_\mu\phi(x) = \left[\partial_\mu \mathbb{1}_2 + ig'\frac{Y_\phi}{2}B_\mu(x)\,\mathbb{1}_2 + ig\frac{\sigma_a}{2}W^a_\mu(x)\right]\phi(x)\,. \tag{205}$$

Being invariant under local $SU(2)_L \times U(1)_Y$ transformations, $\mathcal{L}_H$ together with the corresponding Yukawa-type[110] [64, 98, 218] density ($c^{(k)}_{ij}$ are Yukawa couplings)

$$\mathcal{L}_Y = -c^{(d)}_{ij}\left(\overline{Q}^i_L\phi\right)d^j_R - c^{(u)}_{ij}\left(\overline{Q}^i_L\phi^C\right)u^j_R - c^{(e)}_{ij}\left(\overline{L}^i_L\phi\right)e^j_R + \text{h.c.} \tag{206}$$

can be incorporated into the total effective Lagrangian. Furthermore, the classical ground state of Equation 204 may be associated with the vacuum

$$\left|\langle 0|\phi^{(0)}|0\rangle\right| = \sqrt{\frac{-\mu^2}{2h}} =: \frac{v}{\sqrt{2}}, \tag{207}$$

allowing us to canonically reformulate Equation 203, i. e.,

$$\phi(x) = \exp\left(i\theta^a(x)\,\frac{\sigma_a}{2}\right)\frac{1}{\sqrt{2}}\begin{pmatrix} 0 \\ v + H(x) \end{pmatrix} \tag{208}$$

via the four real fields $H(x)$ and $\theta^a(x)$ $(a = 1, 2, 3)$. In other words, according to Equation 204 there is an infinite set of degenerate states with minimal energy (cf. Equation 207) which transform under $SU(2)_L$ rotations as the members of a doublet. If one of those states is selected arbitrarily as this system's ground state, the given symmetry is spontaneously broken. Using the (local) $SU(2)_L$ invariance, any dependence on the $\theta^a(x)$ can be removed. Hence, due to this local gauge symmetry the otherwise generated three massless Goldstone bosons can be removed (see [219] for a more elaborate discussion of this topic). Therefore, when taking the physical (unitary) gauge $\theta^a(x) \equiv 0$, with[111] [185, 186]

$$W_\mu \coloneqq \frac{1}{\sqrt{2}}\left(W^1_\mu + iW^2_\mu\right) \quad \Leftrightarrow \quad W^\dagger_\mu = \frac{1}{\sqrt{2}}\left(W^1_\mu - iW^2_\mu\right), \tag{209}$$

$$Z_\mu \coloneqq \cos(\theta_W)\,W^3_\mu - \sin(\theta_W)\,B_\mu\,, \tag{210}$$

$$A_\mu \coloneqq \sin(\theta_W)\,W^3_\mu + \cos(\theta_W)\,B_\mu\,, \tag{211}$$

$$\cos(\theta_W) \coloneqq \frac{g}{\sqrt{g^2 + g'^2}} \quad \Leftrightarrow \quad \sin(\theta_W) = \frac{g'}{\sqrt{g^2 + g'^2}}\,, \tag{212}$$

the kinetic part of Equation 204 gives rise to (see, e. g., [185, 186])

$$(D_\mu\phi)^\dagger D^\mu\phi \longrightarrow \frac{1}{2}\left(\partial_\mu H\right)\partial^\mu H + (v + H)^2\left\{\frac{g^2}{4}W^\dagger_\mu W^\mu + \frac{g^2}{8\cos^2(\theta_W)}Z_\mu Z^\mu\right\}. \tag{213}$$

110 This is a gauge-invariant fermion-scalar coupling (see, e. g., [64]).

111 The parameter θ_W is usually referred to as Weinberg angle.

doublet/singlet	el. charge Q	weak hypercharge Y	T_3 of weak isospin
$Q_L^i =: \begin{pmatrix} u_L^i \\ d_L^i \end{pmatrix}$	$\begin{pmatrix} \frac{2}{3} \\ -\frac{1}{3} \end{pmatrix}$	$\begin{pmatrix} \frac{1}{3} \\ \frac{1}{3} \end{pmatrix}$	$\begin{pmatrix} \frac{1}{2} \\ -\frac{1}{2} \end{pmatrix}$
$L_L^i =: \begin{pmatrix} \nu_L^i \\ e_L^i \end{pmatrix}$	$\begin{pmatrix} 0 \\ -1 \end{pmatrix}$	$\begin{pmatrix} -1 \\ -1 \end{pmatrix}$	$\begin{pmatrix} \frac{1}{2} \\ -\frac{1}{2} \end{pmatrix}$
(e_R^i, u_R^i, d_R^i)	$(-1, \frac{2}{3}, -\frac{1}{3})$	$(-2, \frac{4}{3}, -\frac{2}{3})$	$(0, 0, 0)$

Table 4: Listed are (cf. [188]) the weak hypercharge (Y), electromagnetic charge (Q) and third component (T_3) of the weak isospin (T) for each ($i = 1, 2, 3$) left-chiral fermion doublet ($T = \frac{1}{2}$) as well as right-chiral fermion singlets ($T = 0$). The definitions satisfy $Y = 2(Q - T_3)$.

This means, that the gauge fields representing $W^\pm$ and Z^0 have acquired masses:

$$M_Z \cos(\theta_W) = M_W := \frac{1}{2} v g \,. \tag{214}$$

When demanding $Y = 2(Q - T_3)$ (cf. Table 4) and $g \sin(\theta_W) = g' \cos(\theta_W) \equiv e$, QED can be recovered from the effective Lagrangian after introducing SSB (see, e. g., [185, 186, 220]). As expected, $U(1)_{EM}$ is an unbroken symmetry and A_μ describes a massless photon field.

With these puzzle pieces the most general renormalizable Lagrangian describing electroweak interactions can be formulated. Since the Glashow-Iliopoulos-Maiani mechanism (cf. [221, 222]) leads to a strong suppression of flavor-changing neutral currents within the SM, we may focus on the Yukawa sector and Equation 202. In the unitary gauge Equation 206 can be written as [186, 215] ($i, j = 1, 2, 3$)

$$\mathcal{L}_Y = -\left(1 + \frac{H}{v}\right) \left\{ \bar{d}_L'^i M_{ij}^{(d)} d_R'^j + \bar{u}_L'^i M_{ij}^{(u)} u_R'^j + \bar{e}_L'^i M_{ij}^{(e)} e_R'^j + \text{h.c.} \right\} , \tag{215}$$

with corresponding complex mass matrices ($a \in \{u, d, e\}$):

$$M_{ij}^{(a)} = \frac{v}{\sqrt{2}} c_{ij}^{(a)} \,. \tag{216}$$

Those are in general not diagonal and may contain unphysical parameters. Fortunately, by moving to the mass basis, i. e., when applying a bi-unitary transformation, such as

$$\widehat{M}_{ij}^{(a)} = \left[V_L^{(a)}\right]_{ik} M_{kl}^{(a)} \left[V_R^{\dagger(a)}\right]_{lj} = \begin{cases} \text{diag}(m_d, m_s, m_b) \,, & a = d, \\ \text{diag}(m_u, m_c, m_t) \,, & a = u, \\ \text{diag}(m_e, m_\mu, m_\tau) \,, & a = e, \end{cases} \tag{217}$$

those parameters can be absorbed into the unitary matrices $V_{L,R}^{(a)}$ $\left(V_{L,R}^{(a)} V_{L,R}^{\dagger(a)} = \mathbb{1}_3\right)$, which rotate left-chiral and right-chiral fields accordingly (cf. [186, 215]; $a = d, u, e$), i. e.,

$$a_{L,R}^i = \left[V_{L,R}^{(a)}\right]_{ij} a_{L,R}'^j \,. \tag{218}$$

Let us now assume the mass basis. Besides a simpler representation of the Yukawa Lagrangian and an unchanged neutral-current part, we see an important modification in the charged current component (cf. Equation 202). Here, off-diagonal terms arise[112]:

$$\mathcal{L}_{CC} \supset -\frac{g}{\sqrt{2}} W_\mu^\dagger \bar{u}_L'^i \gamma^\mu d_L'^i + \text{h.c.} \longrightarrow -\frac{g}{\sqrt{2}} W_\mu^\dagger \bar{u}_L^i \gamma^\mu \underbrace{\left[V_L^{(u)} V_L^{(d)\dagger}\right]_{ij}}_{=:[V_{CKM}]_{ij}} d_L^j + \text{h.c.}\,, \tag{219}$$

which exhibit the famous Cabibbo-Kobayashi-Maskawa (CKM) matrix[113] [223, 224]:

$$\mathcal{L}_{CCW} = -\frac{g}{2\sqrt{2}} \left\{ W_\mu^\dagger \left[\bar{u}_i \gamma^\mu \left(\mathbb{1} - \gamma_5\right) [V_{CKM}]_{ij}\, d_j + \bar{\nu}_i \gamma^\mu \left(\mathbb{1} - \gamma_5\right) e_i \right] + \text{h.c.} \right\} . \tag{220}$$

This unitary matrix has four physical parameters (i. e., always three mixing "angles" and a complex phase) [215, 225, 226], which are encoded in

$$V_{CKM} = \begin{pmatrix} V_{ud} & V_{us} & V_{ub} \\ V_{cd} & V_{cs} & V_{cb} \\ V_{td} & V_{ts} & V_{tb} \end{pmatrix} . \tag{221}$$

Accordingly, one canonically parametrizes (cf. [225]) Equation 221 via three (real) Euler angles θ_{ij} $(i < j;\ i,j = 1,2,3)$, which can be chosen to lie in the first quadrant (i. e., $s_{ij} := \sin(\theta_{ij}) \leqslant 1$, $c_{ij} := \cos(\theta_{ij}) \leqslant 1$). Along with a phase parameter "δ", that is responsible for all CP violations[114] within the SM, one gets [225, 229]:

$$\Rightarrow V_{CKM}^{(\text{std.})} = \begin{pmatrix} c_{12}c_{13} & s_{12}c_{13} & s_{13}e^{i\delta} \\ -s_{12}c_{23} - c_{12}s_{23}s_{13}e^{i\delta} & c_{12}c_{23} - s_{12}s_{23}s_{13}e^{i\delta} & s_{23}c_{13} \\ s_{12}s_{23} - c_{12}c_{23}s_{13}e^{i\delta} & -c_{12}s_{23} - s_{12}c_{23}s_{13}e^{i\delta} & c_{23}c_{13} \end{pmatrix} . \tag{222}$$

For numerical values and other parametrizations (such as the Wolfenstein parametrization) see, e. g., [225]. Moreover, the underlying hierarchy[115] [42, 225] $s_{13} \ll s_{23} \ll s_{12} \ll 1$ exhibits a dominance of the diagonal components which translates into a higher transition probability for the related flavors. Consequently, CP violation mainly occurs in interactions between the first and third generation[116]. In fact, a phase-convention-independent quantity, which measures the amount of CP violation in the SM, is given by (adapted to Equation 222; see, e. g., [215, 225, 226])

$$J = c_{12}c_{23}c_{13}^2 s_{12}s_{23}s_{12}\sin(\delta) . \tag{223}$$

112 A complete discussion of the effective Lagrangian which cover gauge fixing contributions can, e. g., be found in [188, 198].

113 In this context we may use $\begin{pmatrix} u_1 & u_2 & u_3 \\ d_1 & d_2 & d_3 \end{pmatrix} = \begin{pmatrix} u & c & t \\ d & s & b \end{pmatrix}$ as well as $\begin{pmatrix} \nu_1 & \nu_2 & \nu_3 \\ e_1 & e_2 & e_3 \end{pmatrix} = \begin{pmatrix} \nu_e & \nu_\mu & \nu_\tau \\ e & \mu & \tau \end{pmatrix}$.

114 As mentioned before, the electroweak theory is by construction parity violating. Furthermore, applying the charge conjugation operator to a left-handed field transforms it into a right-handed one, i. e., this theory also violates C parity. A detailed analysis concerning CP violation may be found in [215, 227, 228]. The implication of this discussion can be summarized as follows (from [215]): *"a physical complex parameter that is measured to be nontrivial implies CP violation."*

115 Besides, for phenomenological applications (see [226]), one may also set $c_{13} = c_{23}$ and use $s_{12} = |V_{us}|$, $s_{13} = |V_{ub}|$, $s_{23} = |V_{cb}|$, along with δ as the four independent parameters.

116 I. e., the matrix element $[V_{CKM}]_{ij}$ indicates the probability of a transition from one quark flavor "i" into another one "j" (or analogously "$j \to i$"). According to the experimentally confirmed pattern, one may interpret these transition probabilities as follows (see, e. g., [230]):

- The heavier two neighboring families are, the less likely transitions between their quarks will occur.
- Transitions between families, that are not adjacent, are the least likely.

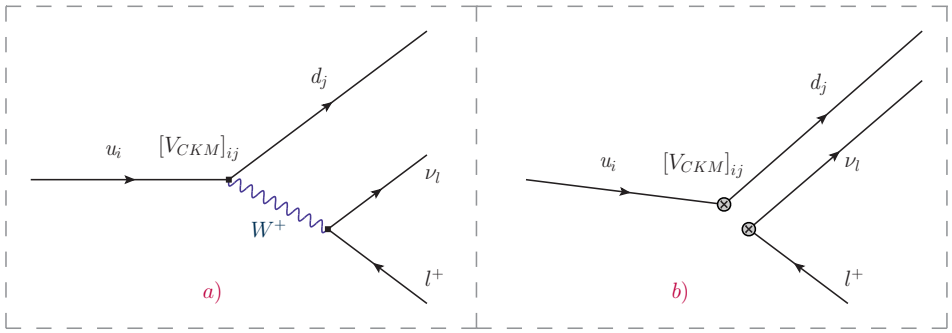

Figure 13: Semileptonic tree-level decay of a free u_i quark within the full a) and an effective b) theory (e. g., [226]). The latter includes an effective vertex (cross in a circle) that couples quarks to leptons, with a sufficiently small momentum transfer $|k^2| \ll M_W^2$.

This so-called Jarlskog invariant "J" [231] depends on each physical mixing angle, i. e., for its existence at least three fermion generations are necessary. In other words, not less than three generations are needed to have CP violation within the SM.

For an extended and more comprehensive review, which is beyond this brief introduction of the required basic concepts, we again refer to[117] [64, 98, 146, 149, 185–188]. Besides, the semileptonic decays, which are particularly important for this work, will be further elaborated in the next subsection.

2.6.2 *Hadronic matrix elements, form factors and branching fractions*

In this subsection, we introduce the spectator model and some of the basics concerning hadronic matrix elements, form factors as well as branching fractions needed for Chapter 5.

Among other things, flavor changing weak decays, such as "$H \to H' l^- \bar{\nu}_l$" or "$H' \to H l^+ \nu_l$" (H, H' being two adequate hadrons[118], cf. [186]), are in general studied to improve our knowledge on CKM parameters, because those processes can be associated with the corresponding quark transitions "$d_j \to u_i l^- \bar{\nu}_l$" and "$u_i \to d_j l^+ \nu_l$" (see Figure 13). In this context heavy to light transitions, such as $B \to \pi$ or $D \to K$ and the related form factors become relevant. Accordingly, a proper theoretical description of these processes and observables has to be found.

The typical momentum transfer k^2 in hadronic weak decays, which involve a heavy-to-light quark transition, should be on the same order as the associated large parton mass (e. g., [230]). Therefore, it is not unreasonable to expect that the semileptonic features of these heavy flavor

117 Here, also the omitted discussion concerning the unitary triangle can be found.

118 Flavor changing weak decays may, e. g., involve charged pions, kaons or charmed (D) and B mesons. Possible exceptions are given by flavored neutral mesons, i. e., with a vanishing total flavor quantum number. They usually exhibit an additional electromagnetic decay mode, such as the $\gamma^* \gamma^{(*)} \to P$ $(P = \pi^0, \eta, \eta', \ldots)$ transitions.

transitions are mainly reflected by short distance dynamics. For instance, the "free" quark case, as depicted in Figure 13, boils down to $\left(G_F = \sqrt{2}g^2/8M_W^2 \text{ is the Fermi coupling constant}\right)$

$$\begin{aligned} &i\frac{g}{2\sqrt{2}}\left(\bar{u}_i\gamma_\alpha\left(\mathbb{1}-\gamma_5\right)d_j\right)\frac{-ig^{\alpha\beta}}{k^2-M_W^2+i0^+}i\frac{g}{2\sqrt{2}}\left(\bar{l}\gamma_\beta\left(\mathbb{1}-\gamma_5\right)\nu_l\right)V_{u_id_j} \\ &\approx -i\frac{G_F}{\sqrt{2}}\left[\bar{u}_i\gamma^\mu\left(\mathbb{1}-\gamma_5\right)d_j\right]\left[\bar{l}\gamma_\mu\left(\mathbb{1}-\gamma_5\right)\nu_l\right]V_{u_id_j} \quad \left(|k^2| \ll M_W^2\right) . \end{aligned} \tag{224}$$

However, in contrast to the involved leptons, quarks are affected by the confinement mechanism and only their hadronized "reaction products" can be observed as free particles. In other words, the fundamental fields of flavor physics (and its effective Lagrangian) are not necessarily the experimentally measured particles. Thus, similar to the strong interaction, one may separate long and short distance interactions via a factorization ansatz. This means, all long distance effects are absorbed in hadron matrix elements, while short distance interactions are associated with the corresponding effective weak Hamiltonian[119] (e. g., [226, 230, 232]). A possible manifestation of such an approximation is given by the spectator model[120] [235, 236], relying on the following assumptions and restrictions (see also [230]):

- The initial hadron is replaced by its valence quark configuration, i. e., higher Fock states are neglected.
- Possible soft gluon interactions[121] that accompany the weak process are omitted.
- The sum of all possible hadron states is replaced with final states of free quarks which have been emitted by the decay.

In the context of a heavy quark expansion[122] (cf. [233, 240–243]), this model would be represented by the corresponding leading term, while all $\mathcal{O}\left(m_Q^{-2}\right)$ corrections were neglected. For our purpose, we may employ this approach in a modified way. As a conceptual model let us consider the process[123] $\pi^- \to \mu^-\bar{\nu}_\mu$ at tree-level (see Figure 14), which is described by

$$\begin{aligned} &\langle\pi^-|[\bar{u}\gamma_\alpha\left(\mathbb{1}-\gamma_5\right)d]\left[\bar{\nu}_\mu\gamma^\alpha\left(\mathbb{1}-\gamma_5\right)\mu\right]|\mu^-\bar{\nu}_\mu\rangle \\ &= \langle\pi^-|\bar{u}\gamma_\alpha\left(\mathbb{1}-\gamma_5\right)d|0\rangle\left[\bar{v}_\nu\gamma^\alpha\left(\mathbb{1}-\gamma_5\right)u_\mu\right] , \end{aligned} \tag{225}$$

where "u" and "v" are the usual Dirac spinors (e. g., [64, 146]). That leaves the matrix element

$$\langle\pi^-|\bar{u}\gamma_\mu\left(\mathbb{1}-\gamma_5\right)d|0\rangle = \langle\pi^-|(\bar{u}d)_{V-A}|0\rangle = 2\langle\pi^-|\bar{u}_L\gamma_\mu d_L|0\rangle . \tag{226}$$

While the $(V-A)$ structure of weak interaction (cf. [226]) is still present in Equation 226, only its parity-odd component[124]

$$\langle\pi^-(P)\,|\bar{u}(x)\,\gamma_\mu\gamma_5 d(x)|0\rangle = -iP_\mu f_\pi e^{iP\cdot x} \tag{227}$$

119 In Equation 224, we have already encountered an example, i. e., $\mathcal{H}_{\text{eff}}^{(\beta)} \sim \frac{G_F}{\sqrt{2}}\left[\bar{u}_i\gamma^\mu\left(\mathbb{1}-\gamma_5\right)d_j\right]\left[\bar{l}\gamma_\mu\left(\mathbb{1}-\gamma_5\right)\nu_l\right]$ of an effective Hamiltonian (see, e. g., [226]).

120 The spectator model predicts equal total decay rates and lifetimes for pseudoscalar D or B mesons, such as $\left(D^+, D^0, D_s^+\right)$ or $\left(B^+, B^0, B_s^+\right)$, respectively. In reality, however, especially D meson lifetimes can considerably deviate from these predictions, possibly due to neglected $\mathcal{O}\left(m_c^{-2}\right)$ corrections (cf. [37, 233, 234]).

121 When including soft gluon corrections, one may face a multitude of related non-perturbative phenomena (see, e. g., [234, 237] and references therein). In principle, a finite heavy quark mass m_Q may cause additional non-spectator effects (cf [234]), which are (fortunately) suppressed by extra powers of m_Q^{-1}. Therefore, the spectator model works well for B decays, but seems in general less adequate for applications to charmed mesons. Such contributions, however, are beyond the present analysis. For a review, which describes spectator as well as non-spectator effects in the framework of an heavy-quark effective theory (cf. [238]) see, e. g., [239].

122 This is roughly speaking an expansion in inverse powers of the given generic heavy flavor m_Q.

123 This is the primary decay mode of a pion which has a branching ratio of about 99.99% (cf. [37]). Hence, it is a standard example and has been considered many times before (see, e. g., [64, 244, 245]).

124 More precisely, the pseudoscalar pion is created via a left-handed current out of the parity-even vacuum. Due to parity conservation in QCD, only the parity-odd component of $\bar{u}_L\gamma_\mu d_L$ can contribute.

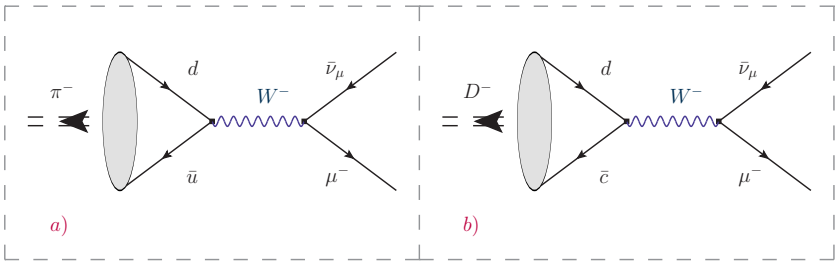

Figure 14: Based on the spectator model, figure a) shows the weak annihilation process $\pi^- \to \mu^- \bar{\nu}_\mu$, while the analogous leptonic decay $D^- \to \mu^- \bar{\nu}_\mu$ of a charmed meson is depicted in figure b).

can contribute $\left(P^2 = m_\pi^2\right)$. The latter encodes all relevant non-perturbative information which are contained in the pion decay constant f_π. For Chapter 5, we have to consider the more complicated $D_{(s)}^- \to \eta^{(\prime)} l^- \bar{\nu}_l$ as well as analogous $B^+ \to \eta^{(\prime)} l^+ \bar{\nu}_l$ decays. When focusing on the pseudoscalar charmed D^- meson[125], similar matrix elements as for the pion case can be introduced (see Figure 14). For instance, we may define (see also Section 5.1.1)

$$\langle D^-(P)\,|\bar{c}(x)\,\gamma_\mu\gamma_5\,d(x)|0\rangle = -iP_\mu f_D\, e^{iP\cdot x}\,, \tag{228}$$

which includes the (charmed) axial vector current

$$j_\mu^{D^-} \coloneqq \bar{c}\gamma_\mu\gamma_5 d\,, \quad \Rightarrow \quad \partial^\mu j_\mu^{D^-} = (m_c + m_d)\,\bar{c}i\gamma_5 d =: j_5^{D^-}\,. \tag{229}$$

In the current QCD sum rule literature, however, neither Equation 228 nor Equation 229 are common. Instead, it is customary to consider the divergence of $j_\mu^{D^-}$, implying

$$(m_c + m_d)\,\langle D^-(P)\,|\bar{c}(x)\,i\gamma_5 d(x)|0\rangle = m_D^2 f_D\, e^{iP\cdot x} \tag{230}$$

as well as (when neglecting $m_d \ll m_c$) the renormalization group invariant operator

$$j_{D^-} \coloneqq m_c \bar{c} i\gamma_5 d\,. \tag{231}$$

As a result, this canonical interpolation current for the D^- meson assures RG invariance, when it is used within certain products, such as[126] (cf. [246])

$$\mathcal{O}_{D^-}(x,0) \coloneqq T\left\{\bar{d}(x)\,\gamma_\mu c(x)\,, j_{D^-}(0)\right\}\,. \tag{232}$$

For correlation functions based on Equation 232 (cf. Chapter 5) this has the important consequence, that UV-renormalized hard amplitudes "$T_{hard}^{(r)}$" can be obtained from their unrenormalized counterparts "T_{hard}", simply by replacing the unrenormalized heavy quark mass in T_{hard} with the corresponding renormalized one (see [246]). This allows an uncomplicated handling of (charm quark) mass terms within the corresponding pQCD calculations (cf. Chapter 5).

125 After replacing $\bar{c} \leftrightarrow \bar{b}$, $d \leftrightarrow u$ and $D^- \leftrightarrow B^+$, the named definitions do also apply for B mesons. This is also true for $D^- \leftrightarrow D_s^-$, which additionally requires $d \leftrightarrow s$.

126 In [246] unrenormalized quark currents analogous to j_{D^-}, $V_\mu^{D^-} = \bar{d}\gamma_\mu c$ and the bare quark mass m_c have been considered. The corresponding renormalized quantities emerge after defining $j_{D^-} \to Z_5\,[j_{D^-}]^{(r)}$, $V_\mu^{D^-} \to Z_V\left[V_\mu^{D^-}\right]^{(r)}$ as well as $m_c \to Z_m\,[m_c]^{(r)}$, together with the renormalization constants [246] (in the $\overline{MS}$-scheme):
$Z_V = 1$, $Z_5 = \left(1 + \frac{3}{\varepsilon}\frac{\alpha_S C_F}{4\pi}\right)$ and $Z_m = \left(1 - \frac{3}{\varepsilon}\frac{\alpha_S C_F}{4\pi}\right)$. This means, that the overall renormalization factor $Z_\mathcal{O}$ of $\mathcal{O}_{D^-}(x,0)$ is $Z_\mathcal{O} \equiv Z_5 Z_V Z_m = 1 + \mathcal{O}(\alpha_S^2)$.

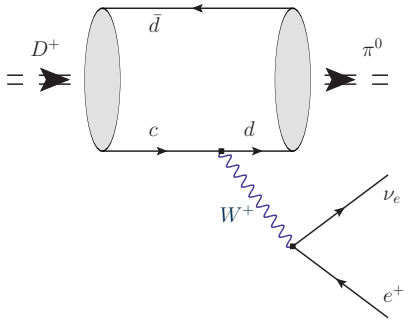

Figure 15: A typical application of the spectator model: the semileptonic weak decay $D^+ \to \pi^0 e^+ \nu_e$.

Moreover, in the context of $H \to H' l \bar{\nu}_l$ transitions several new hadronic form factors arise. Based on the spectator model, weak decays of charmed mesons are driven by the underlying heavy quark dynamics, whereas the involved light flavor is a mere spectator (see Figure 15). Therefore, the associated decay amplitude (cf. Equation 225) can be written as (see also [186])

$$\mathcal{A}\left(H \to H' l \bar{\nu}_l\right) \approx \frac{G_F}{\sqrt{2}} V_{u_i d_j} \left[\bar{u}(p_l)\, \gamma_\mu \left(\mathbb{1} - \gamma_5\right) v(p_{\nu_l})\right] \langle H' | \bar{u}_i \gamma^\mu \left(\mathbb{1} - \gamma_5\right) d_j | H \rangle \,. \tag{233}$$

For H and H' being two (on-shell) pseudoscalar mesons, parity conservation excludes the axial vector contribution given by $\bar{u}_i \gamma^\mu \gamma_5 d_j$. Combined with Lorentz invariance the a priori unknown strong dynamics of Equation 233 can be parametrized via [186, 247] $\left(q^\mu := (p - p')^\mu;\, t = q^2\right)$

$$\langle H'(p') \left| \bar{u}_i \gamma^\mu d_j \right| H(p) \rangle = \mathcal{C}_{HH'} \left\{ (p + p')^\mu \, f_{HH'}^+(t) + q^\mu \, f_{HH'}^-(t) \right\} , \tag{234}$$

which introduces[127] the Clebsch-Gordan coefficient $\mathcal{C}_{HH'}$ and two form factors $f_{HH'}^{\pm}$. Alternatively, we may perform a Lorentz decomposition according to $\left(\Sigma^\mu := (p + p')^\mu\right)$

$$\mathcal{C}_{HH'}^{-1} \langle H'(p') \left| \bar{u}_i \gamma^\mu d_j \right| H(p) \rangle = \left[\Sigma^\mu - \frac{m_H^2 - m_{H'}^2}{q^2} q^\mu \right] f_{HH'}^+(t) + \frac{m_H^2 - m_{H'}^2}{q^2} q^\mu \, f_{HH'}^0(t) \,, \tag{235}$$

with the scalar form factor[128]

$$f_{HH'}^0(t) = f_{HH'}^+(t) + \frac{q^2}{m_H^2 - m_{H'}^2} f_{HH'}^-(t) \,. \tag{236}$$

The mentioned coefficients $\mathcal{C}_{HH'}$ arise due to certain symmetries (cf. [248]) which are present in the named meson transitions and ultimately reduce the number of independent form factors (see, e. g., [248–257] for a dedicated discussion). As a heuristic example, one may consider the two weak decays $K^+ \to \pi^+ \bar{\nu}\nu$ and $K^+ \to \pi^0 e^+ \nu_e$ which can be related with each other by using an approximate isospin symmetry[129] (e. g., [226]):

$$\langle \pi^+ | \bar{s} \gamma_\mu \left(\mathbb{1} - \gamma_5\right) d | K^+ \rangle = \sqrt{2} \langle \pi^0 | \bar{s} \gamma_\mu \left(\mathbb{1} - \gamma_5\right) u | K^+ \rangle \,. \tag{237}$$

127 As discussed in [215], the operator $\bar{u}_i \gamma^\mu d_j$ is in general acting on the isospin space, similar to the usual $SU(2)_I$ ladder operators. This, however, may relate different processes and particles via Clebsch-Gordan factors.

128 When contracting Equation 234 with $\frac{q_\mu}{(m_H - m_{H'})(m_H + m_{H'})}$, Equation 236 can be derived.

129 Based on Section 2.6.1, the rare kaon decay $K^+ \to \pi^+ \bar{\nu}\nu$ requires at least one loop to occur, because there are no flavor-changing neutral currents at tree level within the SM. For instance, it can be realized via a corresponding penguin diagram.

Consequently, both processes could be described via one set of form factors and the named Clebsch-Gordan coefficient "$\sqrt{2}$". We can circumvent a general discussion based on heavy quark symmetries and heavy-to-light form factors (cf. [248, 249, 256, 257]) when focusing on $f^{+}_{HH'}$, which turns out to be the main hadronic input for the intended phenomenological study of decay rates and branching fractions in Chapter 5.

In fact, the contribution of $f^{-}_{HH'}$ is kinematically suppressed within the electron and muon decay modes (see, e. g., [146, 186] or [215]). Qualitatively, may be seen, when reconsidering Equation 233, which implies $\left(q = p_l + p_{\nu_l};\, \not{p}_l u(p_l) = m_l u(p_l),\, \not{p}_{\nu_l} v(p_{\nu_l}) = 0\right)$

$$f^{-}_{HH'}(t)\left[\bar{u}(p_l)\,\not{q}\,(\mathbb{1}-\gamma_5)\,v(p_{\nu_l})\right] \sim m_l\,. \tag{238}$$

Thus, $f^{-}_{HH'}$ is subdominant compared to $f^{+}_{HH'}$. This becomes even more evident, when studying partial decay rates, such as [37] $\left(k_1 := p_l,\, m_1 := m_l,\, k_2 := p_{\nu_l},\, m_2 := 0,\, k_3 := p',\, m_3 := m_{H'};\right)$:[130]

$$d\,\Gamma\left(H \to H' l \bar{\nu}_l\right) = \frac{1}{2m_H}\left|\mathcal{A}\left(H \to H' l \bar{\nu}_l\right)\right|^2 (2\pi)^4\,\delta^{(4)}(q-k_1-k_2)\prod_{i=1}^{3}\frac{d^3\,k_i}{(2\pi)^3\,2E_{k_i}}\,, \tag{239}$$

which are given in terms of the Lorentz-invariant matrix element $\mathcal{A}$ (cf. Equation 233):

$$\left|\mathcal{A}\left(H \to H' l \bar{\nu}_l\right)\right|^2 = \frac{G_F^2}{2}|V_{u_i d_j}|^2 \mathcal{C}^2_{HH'} H^{\mu\nu}(p,p')\,L_{\mu\nu}(k_1,k_2)\,. \tag{240}$$

The latter implies a hadronic

$$H^{\mu\nu}(p,p') = \left(f^{+}_{HH'}(t)\,\Sigma^{\mu} + f^{-}_{HH'}(t)\,q^{\mu}\right)\left(f^{+}_{HH'}(t)^{*}\Sigma^{\nu} + f^{-}_{HH'}(t)^{*}q^{\nu}\right) \tag{241}$$

as well as a leptonic tensor[131] (s, s' are indicating the otherwise suppressed spin state)

$$\begin{aligned} L_{\mu\nu}(k_1,k_2) &= \sum_{s,s'}\left[\bar{u}^{s}(k_1)\,\gamma_\mu\,(\mathbb{1}-\gamma_5)\,v^{s'}(k_2)\right]\left[\bar{v}^{s'}(k_2)\,\gamma_\nu\,(\mathbb{1}-\gamma_5)\,u^{s}(k_1)\right] \\ &= 2\left[\mathrm{Tr}\{\not{k}_1\gamma_\mu\not{k}_2\gamma_\nu\} - \mathrm{Tr}\{\not{k}_1\gamma_\mu\not{k}_2\gamma_\nu\gamma_5\}\right] \\ &= 8\left(g_{\alpha\mu}g_{\beta\nu} + g_{\alpha\nu}g_{\beta\mu} - g_{\alpha\beta}g_{\mu\nu} - \cancel{i\varepsilon_{\mu\nu\alpha\beta}}\right)k_1^{\alpha}k_2^{\beta} =: T^{(\mathrm{aux})}_{\mu\nu;\alpha\beta}\,k_1^{\alpha}k_2^{\beta}\,. \end{aligned} \tag{242}$$

According to Equation 240 all terms containing $f^{-}_{HH'}$ (similarly for $\mu \leftrightarrow \nu$), i. e.,

$$L^{\mu\nu}(k_1,k_2)\,q_\mu = 8m_l^2 k_2^{\nu}\,, \quad L^{\mu\nu}(k_1,k_2)\,q_\mu q_\nu = 4m_l^2\left(q^2 - m_l^2\right)\,, \tag{243}$$

are accompanied by extra powers of the quadratic lepton mass. Hence, after solving the phase space integrals, the mentioned kinematical suppression of these terms becomes obvious. This can be done in two stages (see, e. g., [64, 146, 257–260]):

i) By employing the auxiliary integral for massless leptons

$$I^{\mu\nu}(q) = \int d^3k_1 \int d^3k_2\,\delta^{(4)}(q-k_1-k_2)\,\frac{k_1^{\mu}k_2^{\nu}}{E_{k_1}E_{k_2}} = \frac{\pi}{6}\left(q^2 g^{\mu\nu} + 2q^{\mu}q^{\nu}\right)\,, \tag{244}$$

130 In Equation 239, one uses the rest frame of particle H $\left(E_p = \sqrt{m_H^2 + \vec{p}^{\,2}}\right)$.

131 Since $L_{\mu\nu}$ is contracted with $H^{\mu\nu}$, the totally antisymmetric tensor within Equation 242 will not contribute to the given amplitude. Moreover, in Equation 242 we sum over the (final) lepton polarizations (see, e. g., [146]). Hence, completeness relations, such as Equation 1088 and Equation 1089 can be used.

one may obtain the following partial result (omitting $\mathcal{O}(m_l^2)$ contributions):

$$(2\pi)^4 \prod_{i=1}^{2} \int \frac{d^3 k_i}{(2\pi)^3\, 2E_{k_i}} L_{\mu\nu}(k_1, k_2)\, H^{\mu\nu}(p, p')\, \delta^{(4)}(q - k_1 - k_2)$$
$$= \frac{1}{16\pi^2} I^{\alpha\beta}(q)\, T^{(aux)}_{\mu\nu;\alpha\beta}\, H^{\mu\nu}(p, p') = \frac{\lambda(t, m_H^2, m_{H'}^2)}{3\pi} \left| f^+_{HH'}(t) \right|^2 . \tag{245}$$

Here, we make use of the triangle function, as defined in Equation 1310.

ii) When modifying the phase space integration by inserting the condition $q^\mu \equiv (p - p')^\mu$ via an associated delta distribution, one gets

$$\int \frac{d^3 k_3}{(2\pi)^3\, 2E_{k_3}} \delta\Big(q^2 - (p - k_3)^2\Big) = \frac{\sqrt{\lambda(t, m_H^2, m_{H'}^2)}}{16\pi^2 m_H^2} , \tag{246}$$

which is the missing puzzle piece.

After these steps, it is straightforward to derive the following (master) formula:

$$\frac{d\,\Gamma(H \to H' l \bar{\nu}_l)}{d\,q^2} = \frac{G_F^2 |V_{u_i d_j}|^2}{192\pi^3 m_H^3} \lambda^{3/2}\Big(t, m_H^2, m_{H'}^2\Big) \left| f^+_{HH'}(t) \right|^2 + \mathcal{O}\Big(m_l^2\Big) . \tag{247}$$

As can be seen from Equation 247, all terms proportional m_l^2 are additionally suppressed by meson mass corrections. Consequently, for $l = e, \mu$ admixtures of $f^-_{HH'}$ can be safely neglected.

Together with Equation 247, this subsection, therefore, provides the basis for a phenomenological investigation of corresponding form factors and branching fractions, as set out in Chapter 5.

3 MESON DISTRIBUTION AMPLITUDES

"Mixing one's wines may be a mistake,
but old and new wisdom mix admirably."

— Bertolt Brecht (1898 – 1956)

In this chapter, we study η and η' light-cone DAs via the approximate conformal symmetry in QCD. The theoretical updates provided with this part are as follows:

i) For the mentioned $\eta^{(\prime)}$ DAs, we present a complete NLO treatment of the corresponding scale dependence (see Section 3.3.3).

ii) Moreover, we consider a consistent treatment of quark mass corrections up to $\mathcal{O}(m_s)$ accuracy. This includes an update of the $SU(3)_F$-breaking effects in the twist-four DAs (see Section 3.4.3, along with Section C.9).

iii) Most importantly, we partially take into account the anomalous contributions and implement $\eta-\eta'$ mixing schemes into the twist-four DAs (see Section 3.1 as well as Section 3.4.3).

With these improvements, it is possible to study hard exclusive processes, that include $\eta^{(\prime)}$ mesons, with a previously unknown level of accuracy (cf. [3] for more details).

3.1 MIXING SCHEMES AND THE $\eta-\eta'$ SYSTEM

In this subsection, we will discuss selected mixing schemes which are needed for a sound description of the $\eta-\eta'$ system.
Hence, we start with a short review of the FKS scheme and an illustration of its previous implementation into hard exclusive processes. Most importantly, we then present our own ansatz, developed for an application to higher twist effects at a wide range of momentum transfer (see Chapter 4, along with Chapter 5).

3.1.1 *Mixing effects and the $\eta-\eta'$ system*

To begin with, the flavor structure of the neutral η and η' mesons have to be determined. In an ideal world with three massless light and three infinitely heavy quark species the η' meson would be a pure flavor singlet [152, 225, 261], while the η would have a flavor octet structure. In the real world, however, the effects of finite quark masses as well as the impact of the axial anomaly have to be taken into account. Both phenomenons lead to a mixing of the neutral mesons among each other (see [152] and references therein). Therefore, the $\eta-\eta'$ system[1] has to be fenced off from possible admixtures of, e. g., the π^0 and the heavy η_c or η_b mesons.
Starting with the light part of the spectrum, isospin violating mixing effects of π^0 with $\eta^{(\prime)}$ may be relevant, when $\mathcal{O}(m_u-m_d)$ corrections are not negligible anymore. For the processes in question the mass difference of up and down quarks is sufficiently smaller than the generic energy scale $(\mu_0 \approx 1\,\text{GeV})$ and can therefore be safely discarded. In general, the isospin limit $m_u = m_d$

1 A priori, one may assume a non-negligible mixing of the η and η' mesons due to the perceptible breaking of $SU(3)_F$ symmetry in nature.

is a very good approximation to the real world, therefore, π^0 is an almost pure isotriplet. On the other hand, the mixing effects of the η or η' with heavier neutral pseudoscalar mesons (like η_c or η_b) induced by the $U(1)_A$ anomaly are, however, less important, when compared to the effects within the $\eta-\eta'$ system. The reason for the latter lies in the general anomalous Ward-identity (similar to Equation 178) since the non-anomalous terms dominate in this case [152].
For the sake of clarity, we therefore assume exact isospin symmetry, including the distinction $m_u = m_d \ll m_s$, while disregarding heavy quark mass contributions ($m_Q \to \infty$, for $Q = c, b, t$) to the low-energy mixing phenomenology (cf. [9, 15, 152, 225, 261]). Furthermore, in this limit the π^0 actually resembles a pure isotriplet and is, therefore, also an ideal testing ground for theoretical considerations, which later on can be extended to more complex pseudoscalar mesons.

In order to quantify the mixing in the $\eta-\eta'$ system, one has to define appropriate mixing[2] parameters which can be related to the physical observables. Inspired by the quark-model[3] approach for the $\eta-\eta'$-mixing [44, 225], one could try to extend the concept of state mixing to the QFT level. Therefore, let us first consider a toy model ansatz based on the (local) operators

$$j_5^A = \overline{\psi}\sqrt{2}T^A i\gamma_5\psi \quad (A = 0, 1, \dots, 8) \,, \tag{248}$$

where we may assume that j_5^0 as well as j_5^8 will both couple to the physical states $|\eta\rangle$ and $|\eta'\rangle$. The latter would imply $\left(\text{for } A = 0, 8\right)$

$$j_5^A|0\rangle = \alpha_\eta^A|\eta\rangle + \alpha_{\eta'}^A|\eta'\rangle + \dots \,, \tag{249}$$

with the complex numbers α_η^A and $\alpha_{\eta'}^A$. Note, that for the sake of a better consistency, we also include T^0, which is proportional to the unity matrix (see Section A.1). Based on the physical spectrum of Equation 249 we could further define the hypothetical states:

$$|\overline{\eta}_8\rangle = \left[\cos\vartheta_0|\eta\rangle + \sin\vartheta_0|\eta'\rangle\right]\cos\gamma + \sin\gamma\,|r\rangle \,, \tag{250}$$
$$|\overline{\eta}_0\rangle = \left[\cos\vartheta_8|\eta'\rangle - \sin\vartheta_8|\eta\rangle\right]\cos\gamma' + \sin\gamma'|r\rangle \,, \tag{251}$$

which ideally either couple to j_5^8 or j_5^0. In fact, both states[4] decouple with respect to the current densities (cf. Section 3.1.2)

$$\langle 0|J_{\mu5}^A|\overline{\eta}_B(P)\rangle \sim i\delta^{AB}P_\mu \quad (A, B = 0, 8) \,. \tag{252}$$

Moreover, $|r\rangle$ is a residual state, i. e., collecting contributions of higher excitations, and so forth. When assuming orthonormal states, such as $\langle\eta|\eta\rangle = 1 = \langle\eta'|\eta'\rangle$, $\langle\eta|\eta'\rangle = 0$, etc. we would get[5]

$$\langle\overline{\eta}_8|\overline{\eta}_8\rangle = \cos^2\gamma\left[\cos^2\vartheta_0 + \sin^2\vartheta_0\right] + \sin^2\gamma = 1 = \langle\overline{\eta}_0|\overline{\eta}_0\rangle \,, \tag{253}$$

along with the projection

$$\langle\overline{\eta}_8|\overline{\eta}_0\rangle = \sin\gamma\sin\gamma' + \cos\gamma\cos\gamma'\sin(\vartheta_0 - \vartheta_8) \,. \tag{254}$$

Here, a finite overlap may, e. g., be caused by non-trivial admixtures of gluonic contributions into the hypothetical states $\{|\overline{\eta}_A\rangle\}_{A=8,0}$. Nevertheless, the standard approach (cf. [152, 225] for

2 In this context, mixing does not mean some sort of meson oscillation (e. g., $B-\overline{B}$ oscillations [262]), but rather a formal superposition of states.
3 Within the quark-model, it is possible to construct pure, i. e., orthogonal singlet and octet states, while mixing-effects correspond to mere rotations.
4 The definitions of Equation 250 and Equation 251 are compatible with Equation 257, when rescaled $|\overline{\eta}_A\rangle = \cos(\vartheta_0 - \vartheta_8)\,|\eta_A\rangle$, together with $\vartheta_A \to \theta_A$ $(A = 0, 8)$.
5 Usually, one uses $\gamma = 0 = \gamma'$ along with the state mixing ansatz $\vartheta_0 = \theta = \vartheta_8$ (cf. [15]).

a review) favors a single mixing angle "θ", relating the mesonic states via an orthogonal transformation (cf. Section 3.1.2, Section 3.1.3) to a predefined basis. Therefore, densities, such as "$\langle 0|\mathcal{J}^A_{\mu 5}|\eta_B(P)\rangle$" ($A, B = 0, 8$), a priori do no longer follow the corresponding (single angle) state mixing, but exhibit a more complicated mixing scheme (cf. Section 3.1.2, Section 3.1.3). Consequently, in general Equation 252 will not be valid anymore, depending on the chosen basis.

Accordingly, there exist several approaches in the literature (see, e. g., [152, Chapter 3] and references therein) claiming to provide a proper description of the $\eta - \eta'$ mixing parameters. Let us pick the two most popular and sophisticated concepts available which form the basis for further developments on the DA level later on.
The first approach is based on ChPT [13, 14, 182] which favors a description in terms of the SO parameters[6] [182]. However, the second approach elaborates the mixing parameters in terms of the QF basis by using well-defined operator identities (e. g., the anomalous Ward-identity) and sandwiches them between a physical meson and the vacuum state[7]. Yet, both approaches can be formulated in a similar way (as done by [152, 261]) when combining the language of ChPT with that of local matrix elements.
In a nutshell, the low-energy physics of light pseudoscalar mesons can (successfully) be described by an effective Lagrangian [14] for QCD. The latter reflects a systematic expansion in powers of small momenta and masses of the (almost) Goldstone bosons "π, K, η". Since the η' meson cannot be classified as an additional Goldstone boson (due to its large mass) it is not straight forward to include it as an additional degree of freedom in the effective Lagrangian. Nevertheless, Leutwyler and Kaiser have worked out a strategy to include the η', based on the formal limit $N_c \to \infty$. Here, the anomaly term Equation 178 vanishes and the η' (formally) becomes a 9^{th} Goldstone boson. As discussed in [152, 263], a consistent effective Lagrangian for the dynamics of the (light) pseudoscalar nonet can be constructed, including $SU(3)_F$-breaking effects $\big($introduced with the matrix $\hat{\chi} \sim \hat{m}$ – see [152] and references therein$\big)$ as well as chiral condensate and anomaly contributions, combined with finite quark- and meson mass-corrections[8]. Moreover, the Lagrangian has been retrofitted with OZI-violating corrections, which come into play via the parameters Λ_1 and Λ_2, while the anomalous coupling to the photon field is realized with the Wess-Zumino-Witten term (cf. [152] and [13]). In other words the complete low-energy behavior of QCD has been modeled with this effective Lagrangian which allows a thorough analytical treatment of the mixing parameters. We will list the needed results of this approach in the following.

3.1.2 *Singlet-octet basis*

It is more convenient to describe the mixing phenomenology via decay constants rather than formal states of the Hilbert space. Those decay constants are defined by the matrix elements of axial vector currents[9] (cf. Equation 171)

$$\langle 0|\mathcal{J}^A_{\mu 5}|M(P)\rangle = i f^A_M P_\mu \,, \tag{255}$$

6 By knowing the low-energy physics of QCD in the pseudoscalar sector, one would be able to predict the mixing parameters of a chosen scheme. The latter ultimately encode information on how the particles of the system are interwoven.
7 This approach has been refined by [9, 15, 152, 261], who also rewrote it in the language of ChPT.
8 Finite quark-masses combined with corrections of the chiral condensate give rise to GMOR-relations. The latter may be used for the introduction of meson-mass corrections.
9 This parametrization (cf. Equation 255) is justified by the assumed Lorentz invariance.

implying four independent decay constants f_M^A ($M = \eta, \eta'$; $A = 0, 8$) for the $\eta - \eta'$ system. Moreover, for each pair of decay constants to a given current, a mixing angle can be defined [13, 152, 182, 263]:

$$\frac{f_\eta^8}{f_{\eta'}^8} = \cot\theta_8 \,, \quad \frac{f_\eta^0}{f_{\eta'}^0} = -\tan\theta_0 \,. \tag{256}$$

The latter can be used to define two basic decay constants f_8, f_0 by [13, 182]

$$\mathcal{F}_{SO} = \begin{pmatrix} f_\eta^8 & f_\eta^0 \\ f_{\eta'}^8 & f_{\eta'}^0 \end{pmatrix} = U(\theta_8, \theta_0)\,\mathrm{diag}(f_8, f_0) \,, \tag{257}$$

with the mixing matrix

$$U(\theta_8, \theta_0) = \begin{pmatrix} \cos\theta_8 & -\sin\theta_0 \\ \sin\theta_8 & \cos\theta_0 \end{pmatrix} , \tag{258}$$

which again leaves four independent parameters θ_8, θ_0 and f_8, f_0. Especially, the definitions leading to Equation 258 are chosen in such a way that the case of vanishing mixing angles resembles a $SU(3)_F$ symmetric world. This may be illustrated with the state mixing ansatz[10]

$$\begin{pmatrix} |\eta\rangle \\ |\eta'\rangle \end{pmatrix} = U(\theta, \theta) \begin{pmatrix} |\eta_8\rangle \\ |\eta_0\rangle \end{pmatrix} \xrightarrow{\theta \to 0} \begin{pmatrix} |\eta_8\rangle \\ |\eta_0\rangle \end{pmatrix} . \tag{259}$$

Most important, let us list the non-trivial features and relations among the SO mixing parameters brought up by the ChPT approach (see, e. g., [152, 263]), describing the low-energy QCD dynamics [13, 152, 182].

- SINGLET DECAY CONSTANT: The ChPT ansatz (up to NLO) reveals that OZI-violating effects are related to the singlet decay constants [152]

$$\sum_{M=\eta,\eta'} f_M^0 f_M^0 = f_0^2 = \frac{2}{3}\left(f_K^2 + f_\pi^2\right) + \Lambda_1 f_\pi^2 \,, \tag{260}$$

  where Λ_1 can, e. g., be determined phenomenologically. Moreover, as pointed out by [13, 152, 184] the singlet decay constants are scale dependent[11]:

$$\left[\mu \frac{d}{d\mu} - \gamma_A\right] f_M^0 = 0 \,, \tag{261}$$

  with the anomalous dimension[12]

$$\gamma_A(\alpha_S) = \sum_{m=1}^{\infty} \left(\frac{\alpha_S}{2\pi}\right)^m \gamma_A^{(m-1)} = -4N_f \left(\frac{\alpha_S}{2\pi}\right)^2 + \mathcal{O}\left(\alpha_S^3\right) . \tag{262}$$

  Numerically the scale dependence of f_M^0 (for moderate scales) should be relatively small because it is a sub-leading effect. However, we will work out a full NLO (in α_S) approach of the photon-transition form factor where the scale dependence of the singlet decay constant may proof its phenomenological relevance for high energies (see Section 4.3).

10 Additionally, the ansatz given by Equation 259 does not reproduce the canonical definition [44] (including $|\eta_A\rangle = |\phi^A\rangle$ for $A = 8, 0$) $\langle 0|J_{\mu 5}^A(0)|\phi^B(P)\rangle = i\delta^{AB} f_B P_\mu$, but implies [261] $\langle 0|J_{\mu 5}^0(0)|\eta_8(P)\rangle = i f_0 \sin(\theta - \theta_0)\, P_\mu$ along with $\langle 0|J_{\mu 5}^8(0)|\eta_0(P)\rangle = i f_8 \sin(\theta_8 - \theta)\, P_\mu$.

11 The RGE of Equation 261 will be solved in Section 3.3.

12 According to Equation 261, Λ_1 has to be replaced by a scale dependent parameter $\Lambda_1(\mu^2)$ (cf. [152]).

- SCALE INDEPENDENT QUANTITIES: Up to the assumed order of accuracy the combinations

$$\sum_{M=\eta,\eta'} f_M^8 f_M^8 = f_8^2 = \frac{4}{3}\left(f_K^2 - f_\pi^2\right) , \tag{263}$$

$$\sum_{M=\eta,\eta'} f_M^8 f_M^0 = f_8 f_0 \sin(\theta_8 - \theta_0) = -\frac{2\sqrt{2}}{3}\left(f_K^2 - f_\pi^2\right) , \tag{264}$$

are not affected by OZI rule violating effects (i. e., they are independent of Λ_i) [13, 152, 182, 263]. This means, when taking into account flavor symmetry breaking effects, a universal mixing angle $\left(\text{e. g., } \theta_P \equiv \theta_{8,0}\right)$ is no longer justified. Due to the impact of the axial anomaly (cf. discussion in [152, Chapter 3.1]), the mixing angles θ_8 and θ_0 are "small" quantities, however, their difference cannot be neglected:

$$0 \ll \left|\frac{\theta_8 - \theta_0}{\theta_8 + \theta_0}\right| \lesssim 1 . \tag{265}$$

Therefore, when working in the SO basis $\theta_8 \neq \theta_0$ has to be used. Moreover, it is important to note that θ_0 is not scale dependent (similar to θ_8), because the renormalization factors in Equation 256 actually cancel [152].

Let us come back to the basis of physical states $M_{1,2} = \eta, \eta'$. When constructing the matrix [152]

$$\left(\sum_{A=8,0} f_{M_1}^A f_{M_2}^A\right)_{M_1,M_2=\eta,\eta'} \stackrel{?}{=} \operatorname{diag}\left(f_\eta^2, f_{\eta'}^2\right) \tag{266}$$

in the physical basis, it will only be diagonal for special cases, like the $SU(3)_F$ symmetric limit. Otherwise, i. e., as long as mixing effects are incorporated, the $\eta - \eta'$ system cannot be adequately described by individual decay constants f_η, $f_{\eta'}$ (cf. [152] for a detailed discussion).

3.1.3 *Quark-flavor basis*

A different parametrization of the $\eta - \eta'$ system is using a change of basis in the subspace[13] spanned by

$$\begin{pmatrix} \lambda^q \\ \lambda^s \end{pmatrix} = \underbrace{\begin{pmatrix} \sqrt{\frac{2}{3}} & \sqrt{\frac{1}{3}} \\ \sqrt{\frac{1}{3}} & -\sqrt{\frac{2}{3}} \end{pmatrix}}_{\equiv \mathcal{U}} \begin{pmatrix} \lambda^0 \\ \lambda^8 \end{pmatrix} , \tag{267}$$

with the involutory matrix $\mathcal{U}$ $\left(\text{i. e., } \mathcal{U}^2 = \mathbb{1}_2\right)$ and the definitions

$$\lambda^q = \operatorname{diag}(1,1,0) , \quad \lambda^s = \operatorname{diag}\left(0,0,\sqrt{2}\right) . \tag{268}$$

In terms of independent axial vector currents Equation 267 implies the change

$$\left\{ \begin{array}{l} J_{\mu 5}^8 = \frac{1}{\sqrt{6}}\left[\bar{u}\gamma_\mu\gamma_5 u + \bar{d}\gamma_\mu\gamma_5 d - 2\bar{s}\gamma_\mu\gamma_5 s\right] \\ J_{\mu 5}^0 = \frac{1}{\sqrt{3}}\left[\bar{u}\gamma_\mu\gamma_5 u + \bar{d}\gamma_\mu\gamma_5 d + \bar{s}\gamma_\mu\gamma_5 s\right] \end{array} \right\} \Leftrightarrow \left\{ \begin{array}{l} J_{\mu 5}^q = \frac{1}{\sqrt{2}}\left[\bar{u}\gamma_\mu\gamma_5 u + \bar{d}\gamma_\mu\gamma_5 d\right] \\ J_{\mu 5}^s = \bar{s}\gamma_\mu\gamma_5 s \end{array} \right\} , \tag{269}$$

13 Strictly speaking, this refers to the linear hull "$\operatorname{span}(\{\lambda^8, \lambda^0\})_C$" and "$\operatorname{span}(\{\lambda^q, \lambda^s\})_C$".

i. e., instead of $SU(3)_F$ singlet and octet currents, the set of quark-flavor currents is used, eponymously for the corresponding QF-basis. The related decay constants are defined (analogously to Equation 255) via the matrix elements $(R = q, s)$

$$\langle 0|J^R_{\mu 5}|M(P)\rangle = i f^R_M P_\mu \,. \tag{270}$$

As discussed in [152], the choice of Equation 267 will also entail new bare fields φ^q and φ^s (instead of φ^8 and φ^0 – cf. [152, 263]) in the effective Lagrangian of low energy QCD. Within the QF-basis the matrix $\hat{\chi}$ [152, 263], which induces (as discussed above) $SU(3)_F$ symmetry breaking into the effective Lagrangian, is diagonal[14] [152]. Therefore, the physical states would be close to φ^q and φ^s if it was not about the $U(1)_A$ anomaly.
The impact of the axial anomaly on the particle spectrum in this context may be seen, when considering the ϕ and ω mesons, which are the analogue of the $\eta - \eta'$ system in the vector meson sector. While the $U(1)_A$ anomaly induces a significant mixing in the pseudoscalar sector, there is only a small deviation from the ideal mixing-angle for the $\phi - \omega$ system[15]. Therefore, from a phenomenological point of view, the QF-basis seems to be a more natural choice than the SO-basis.

However, the construction of the QF-mixing scheme is similar to the SO-basis [152, 261] (again making use of Equation 258):

$$\mathcal{F}_{QF} = \begin{pmatrix} f^q_\eta & f^s_\eta \\ f^q_{\eta'} & f^s_{\eta'} \end{pmatrix} = U(\phi_q, \phi_s)\, \mathrm{diag}(f_q, f_s) \,, \tag{271}$$

with the mixing angles

$$\frac{f^q_\eta}{f^q_{\eta'}} = \cot\phi_q \,, \quad \frac{f^s_\eta}{f^s_{\eta'}} = -\tan\phi_s \,. \tag{272}$$

Yet, there are several decisive differences between these two schemes.

- SCALE DEPENDENT QUANTITIES: ChPT calculations implicate the following relations [14, 152]:

$$\sum_{M=\eta,\eta'} f^q_M f^q_M = f_q^2 = f_\pi^2 + \frac{2}{3} f_\pi^2 \Lambda_1 \tag{273}$$

$$\sum_{M=\eta,\eta'} f^q_M f^s_M = f_q f_s \sin(\phi_q - \phi_s) = \frac{\sqrt{2}}{3} f_\pi^2 \Lambda_1 \tag{274}$$

$$\sum_{M=\eta,\eta'} f^s_M f^s_M = f_s^2 = 2 f_K^2 - f_\pi^2 + \frac{1}{3} f_\pi^2 \Lambda_1 \,. \tag{275}$$

  At first glance, according to the obvious scale dependence[16] of, e. g., f_q and f_s, a consistent description within the QF-basis seems to be more complicated than in the SO-scheme (there only f_0 has to be renormalized).

- DIFFERENCES BETWEEN THE SCHEMES: Before jumping to a conclusion, the following characteristics have to be taken into account:

14 For $\hat{\chi} = \mathrm{diag}(\chi_1, \chi_2, \chi_3)$, the expression in the QF-basis looks like: $\hat{\chi} = \frac{\chi_1+\chi_2}{2}\lambda^q + \frac{\chi_1-\chi_2}{2}\lambda^3 + \frac{\chi_3}{\sqrt{2}}\lambda^s$.
15 The latter is also consistent with the OZI-rule (cf. [152]).
16 As discussed, the parameter $\Lambda_1(\mu^2) = \frac{1}{f_\pi^2}\left(f_0^2(\mu^2) - \frac{2}{3}\left[f_K^2 + f_\pi^2\right]\right)$ indirectly comes with a scale dependence (cf. Equation 260).

i) The difference $\phi_q \neq \phi_s$ is caused by an OZI-rule violating ($\Lambda_1 \neq 0$) effect and not by $SU(3)_F$ flavor breaking ($f_K \neq f_\pi$) contributions.

ii) Unlike the SO case (cf. Equation 265), both mixing angles within the QF scheme themselves are not small quantities [152], but with the addition that their difference is relatively small:

$$\left| \frac{\phi_q - \phi_s}{\phi_q + \phi_s} \right| \ll 1 \,. \tag{276}$$

According to Equation 276, the difference between these parameters is considered as a subleading correction ($|\phi_q - \phi_s| < 5°$, cf. [9, 152]), i. e., up to $\mathcal{O}(\Lambda_1)$ the assumption $\phi_q \approx \phi \approx \phi_s$ is justified. Therefore, Equation 271 can be rewritten in terms of one mixing angle ϕ [152]

$$\begin{pmatrix} f_\eta^q & f_\eta^s \\ f_{\eta'}^q & f_{\eta'}^s \end{pmatrix} = U(\phi)\,\mathrm{diag}(f_q, f_s) + \mathcal{O}(\Lambda_1) \,, \tag{277}$$

with the (modified) rotation matrix[17]

$$U(\phi) = \begin{pmatrix} \cos\phi & -\sin\phi \\ \sin\phi & \cos\phi \end{pmatrix} . \tag{278}$$

Obviously, in this approach the $SU(3)_F$ amounts to the ideal angle $\varphi_0 = \arctan\left(\sqrt{2}\right) \approx 54.7°$. As discussed in the following (also cf. [152]), this simplified parametrization in the QF-basis will (necessarily) lead to a more complicated set of constants in another basis.

Undoubtedly, the assumption of an exact common mixing angle can only be uphold when assuming the strict OZI-rule to be true. The latter becomes rigorous in the formal limit $N_c \to \infty$ or (also) for a vanishing strong coupling (i. e., at asymptotically large energies). Therefore, process independent mixing parameters can only be determined and at the same time valid up to $\mathcal{O}(N_c^{-1})$ corrections[18].

A consequent use of the OZI-rule leads to the so-called FKS-scheme. That means, all OZI violating parameters will be neglected, while topological effects, e. g., due to τ_0, will be kept. Moreover, possible scale dependencies (of the mixing parameters) and all other amplitudes involving quark-antiquark annihilations will also be discarded. We will use the term "strict FKS-scheme" for this rigorous ansatz.

Furthermore, the following parameters are the outcome of a thorough phenomenological analysis (see Figure 16) based on the strict FKS-scheme of a better part of the existing data [9, 152]:

$$\begin{aligned} f_8 &= (1.26 \pm 0.04) f_\pi \,, \quad \theta_8 = -21.2° \pm 1.6° \,, \\ f_0 &= (1.17 \pm 0.03) f_\pi \,, \quad \theta_0 = -9.2° \quad \pm 1.7° \,, \end{aligned} \tag{279}$$

$$\Leftrightarrow \quad \begin{aligned} f_q &= (1.07 \pm 0.02) f_\pi \,, \quad \phi = 39.3° \pm 1.0° \,, \\ f_s &= (1.34 \pm 0.06) f_\pi \,, \, (\Lambda_1 = 0) \,. \end{aligned} \tag{280}$$

17 Equation 278 is related to Equation 258 via $U(\phi) \equiv U(\phi, \phi)$.
18 In this context the parameters $\Lambda_{1,2}$ are of order N_c^{-1} (cf. [152]).

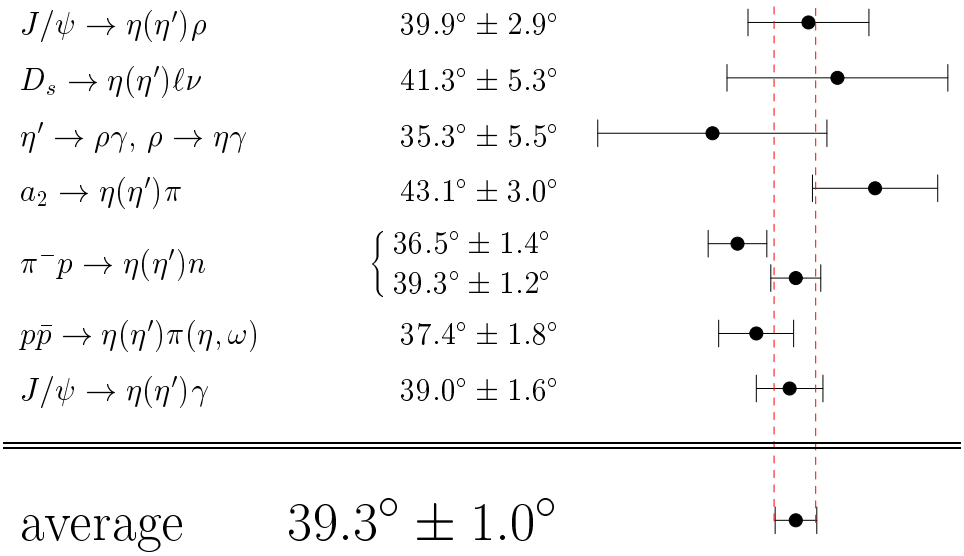

Figure 16: Based on [9, 152] and references therein, the mixing angle ϕ has been determined from several experimental processes. The picture is borrowed from [264].

Here, the error bars correspond to the experimental uncertainties, while the systematic errors (e. g., from neglecting OZI-rule violating effects) have not been included. Other analysis, such as [10], are exploiting more recent data, but use only a subset of the processes investigated in [15]. This yields the following results [3, 10]:

$$\begin{aligned} f_q &= (1.09 \pm 0.03) f_\pi\,, \quad \phi = 40.7° \pm 1.4° \\ f_s &= (1.66 \pm 0.06) f_\pi\,. \end{aligned} \tag{281}$$

Accordingly, the difference between Equation 280 and Equation 281 may be viewed as an intrinsic uncertainty of the FKS approximation (cf. discussion in [3]). For the sake of consistency with previous studies, e. g., [20, 265], we adopt the numbers shown in Equation 280 as default values when implementing our numerical evaluations (cf. Section 4.3).

3.1.4 *Adaption to the language of distribution amplitudes*

The primary goal of this subsection is to formulate an adequate description of the $\eta - \eta'$ system on the level of DAs. Therefore, the discussed mixing schemes have to be implemented into the standard framework for DA.

A legitimate way to introduce the language of DAs is to start with the concept of light-front wave function (LFWF). The latter arises from the solutions of a corresponding Hamiltonian eigenvalue problem, similar to [266]

$$\mathcal{H}_{\rm LC}\,|\Psi\rangle = M^2 |\Psi\rangle\,, \tag{282}$$

that includes a given particle state $|\Psi\rangle$ with invariant mass M^2. Besides, the involved light-cone Hamiltonian[19]

$$\mathcal{H}_{LC} = P_\mu P^\mu = P^- P^+ - \vec{P}_\perp^2 \tag{283}$$

is usually defined within an "intrinsic frame", i. e., $\vec{P}_\perp = \vec{0}$ (see [266] for details). Here, the conventions of [128] are used, i. e., corresponding "+" and "−" components can be defined $P_+ \equiv P_\mu n^\mu$, $P_- \equiv P_\mu \bar{n}^\mu$ via two independent light-like four vectors $n^2 = 0 = \bar{n}^2$ $\left(n \cdot \bar{n} = 1\right)$, while possible orthogonal projections $\vec{P}_\perp$ related to $P_\perp^\mu \equiv g^{\mu\alpha} P^\beta g^\perp_{\alpha\beta}$ (see Section A.9 or Section 3.2 for details) additionally require

$$g^\perp_{\mu\nu} = g_{\mu\nu} - n_\mu \bar{n}_\nu - n_\nu \bar{n}_\mu \,. \tag{284}$$

The underlying light-cone quantization[20] can then be formulated independently of the Lorentz frame [266], implicating a very simple vacuum structure. In fact, there is no spontaneous creation of massive fermions in the light-cone quantized vacuum (cf. [266] and references therein). Consequently, for the eigenvectors of Equation 282, the Fock expansion turns out to be extremely useful, because all constituents in a physical eigenstate are directly related to the state and not to disconnected vacuum fluctuations [266]. Thus, it is reasonable for a given eigenstate of Equation 282

$$|\Psi\rangle \equiv |\Psi; M, P^+, \vec{P}_\perp, S^2, S_3, h\rangle \tag{285}$$

to be calculated in terms of a complete set of (eigen-) functions $\{|\mu_n\rangle\}_n$ [266]

$$\sum_n \int d[\mu_n] \; |\mu_n\rangle\langle\mu_n| = \mathbb{1} \,, \tag{286}$$

with the projections [266] on the basis[21] states

$$\Psi_{n/h(M,P^+,\vec{P}_\perp,S^2,S_3)}(\mu) = \langle \mu_n | \Psi \rangle \,, \tag{287}$$

which are usually referred to as wave functions.
Here, the associated quantum numbers of the particular hadron "h" (cf. Equation 285, Equation 287), such as the generalized spin-squared S^2, or the longitudinal projection S_3, along with its charge, parity, etc., including the kinematical set-up are supposed to be obvious in the context of a given case. Therefore, it is convenient to omit any further reference after their introduction.
As discussed in Section 2.5, a reasonable choice of basis should connect the quark content with the hadron state under consideration. Therefore, one can construct the complete basis of Fock states, by applying products of (free) field creation operators to the vacuum state (numbered with $n = 0$) [266]:

$$\begin{array}{lll} n = 1 & : & |q\bar{q}; k_i^+, \vec{k}_{\perp i}, \lambda_i\rangle \,, \\ n = 2 & : & |q\bar{q}g; k_i^+, \vec{k}_{\perp i}, \lambda_i\rangle \,, \\ n = 3 & : & |gg; k_i^+, \vec{k}_{\perp i}, \lambda_i\rangle \,, \\ \vdots & \vdots & \vdots \end{array} \tag{288}$$

19 The Hamilton (cf. Equation 283) has been written in generic light-cone coordinates.
20 Unlike the equal-time Hamiltonian formalism, this technique uses a quantization on a null plane, i. e., a plane tangential to the light-cone (cf. [266] and references therein).
21 The choice is also denoted by "μ" which is additionally referring to specific sets of arguments characteristic for the basis.

with the momenta k_i^+, $\vec{k}_{\perp i}$ and helicities λ_i of the i^{th} constituent[22] (of one of the N_n partons corresponding to the n^{th} Fock state). It is noteworthy that each Fock state $|\mu_n\rangle \equiv |n; k_i^+, \vec{k}_{\perp i}, \lambda_i\rangle$ is an eigenstate of the operators P^+, $\vec{P}_\perp$, with the eigenvalues[23] [266]

$$\vec{P}_\perp = \sum_{i=1}^{N_n} \vec{k}_{\perp i}\,, \quad P^+ = \sum_{i=1}^{N_n} k_i^+ \quad \left(k_i^+ > 0\right) . \tag{289}$$

Moreover, along with the transverse parton momenta $\vec{k}_{\perp i}$ (relative to the direction of the meson) it is convenient to define the (boost invariant) longitudinal momentum fraction [266]

$$x_i = \frac{k_i^+}{P^+} \quad \text{with} \quad x_i \in (0,1) . \tag{290}$$

The latter is a consequence of Equation 289 which also gives

$$\sum_{i=1}^{N_n} x_i = 1 \quad \text{as well as} \quad \sum_{i=1}^{N_n} \vec{k}_{\perp i} = \vec{0} \tag{291}$$

when working within the intrinsic frame $\vec{P}_\perp = \vec{0}$. Unfortunately, the involved quantities may become ill-defined in the case $\vec{k}_{\perp i}^2 \to \infty$ ("UV singularities") or for longitudinal momenta close to the end points[24], i. e., $x_i \to 0$ or $x_i \to 1$ ("end-point singularities"). As a solution, one may introduce a cut-off or similar regularization procedures [266]. Being aware of this subtlety, a meson state "$|M\rangle$" can be written as a sum over all Fock space sectors (cf. [266])

$$|M(P)\rangle = \sum_{n=1}^{\infty} \int [d\,\mu_n]\, |n; x_i P^+, \vec{k}_{\perp i} + x_i \vec{P}_\perp, \lambda_i\rangle \Psi_{n/M}\left(x_i, \vec{k}_{\perp i}, \lambda_i\right) , \tag{292}$$

with the phase-space integration

$$\int [d\,\mu_n] = \sum_{\lambda_i} \int \prod_{i=1}^{N_n} dx_i \prod_{j=1}^{N_n} d^2 k_{\perp j}\, \delta\left(1 - \sum_{k=1}^{N_n} x_k\right) \delta^{(2)}\left(\sum_{l=1}^{N_n} \vec{k}_{\perp l}\right) . \tag{293}$$

The coefficient functions $\Psi_{n/M}$ of Equation 292 are then called LFWF (cf. [267]). This representation allows a phenomenological study of the hadrons anatomy, due to the obvious relation of the Fock states $|\mu_n\rangle$ to the probability (cf. [268])

$$\mathcal{P}_n = \int [d\,\mu_n] \left|\Psi_{n/M}\left(x_i, \vec{k}_{\perp i}, \lambda_i\right)\right|^2 \tag{294}$$

of being measured. In this context the process and gauge-independent distribution amplitude (cf. [268]) can be defined as an integral over transverse momenta of the meson's Bethe-Salpeter wave function. Exemplified for the pion (via the $n = 1$ Fock state coefficient) the DA may be written as (cf. [268])

$$\Phi_\pi\left(x, Q^2\right) = \int_0^{Q^2} \frac{d^2 \vec{k}_\perp}{16\pi^3} \Psi_{\bar{q}q/\pi}\left(x, \vec{k}_\perp\right) , \tag{295}$$

22 The running index "i" obviously depends on the involved other constituents of the specific Fock state. Equation 288 lists the genuine examples without specifying a nongeneric flavor structure. All other Fock states can be constructed from them by adding additional gluons and quark-antiquark pairs.

23 Note, that for the vacuum we would get $\vec{P}_\perp|0\rangle = \vec{0}_\perp$ and $P^+|0\rangle = 0$ [266].

24 In this case one of the partons carries almost the full meson momentum, while the others become soft.

which then evidently is the probability amplitude for finding the pion as a quark-antiquark pair with momentum fractions $x_q = x$ and $x_{\bar{q}} = \bar{x}$ (cf. Equation 291). Similar arguments hold for meson DAs of higher Fock states or different flavor structure.

One main advantage of the presented light-cone formalism and DAs (cf. [142, 269–275]) in particular results from their versatile applicability to hard exclusive reactions. In this context it is possible to formally calculate and extract many related hadronic properties without an explicit knowledge of the underlying non-perturbative mechanisms, such as meson mixing effects or confinement itself. Explicitly, this can be done by means of a formalism developed especially for that purpose which is based (inter alia) on the collinear factorization approach (see Chapter 4). Accordingly, for a better compatibility with the latter, it is advantageous to define DAs via corresponding matrix elements.

Following the previous approach [20, 152, 268], all DAs involved in this work can be defined as the Fourier transform of adequate matrix elements similar to[25] (by default we may for example set $M = \eta, \eta'$ and $A = 0, 8$)

$$i\Phi_M^A\left(x,\mu^2\right) = \int \frac{dz^-}{2\pi} e^{i\xi_x P\cdot z} \langle 0|\overline{\Psi}(-z)\left[T^A\right]\frac{\gamma^+\gamma_5}{\sqrt{N_c}}\Psi(z)|M(P)\rangle\Big|_{z^2=0;\,\mu^2}, \tag{296}$$

$$\Phi_M^g\left(x,\mu^2\right) = \int \frac{dz^-}{2\pi} e^{i\xi_x P\cdot z} \frac{2}{P^+\sqrt{N_c^2-1}} \langle 0|\mathcal{G}^{+\zeta}(-z)\,\widetilde{\mathcal{G}}_{\zeta+}(z)|M(P)\rangle\Big|_{z^2=0;\,\mu^2}. \tag{297}$$

The mentioned constraints refer to:

i) The implied assumption of the constituents' (e. g., the quark-antiquark pair) light-like separation is expressed by $z^\mu = z^- n^\mu$, using the vector n^μ, which defines the plus components (cf. Equation 1172 in Section A.9) of arbitrary four-vectors.

ii) Moreover, an UV cut-off (similar to Equation 295) for the implicitly assumed $\vec{k}_\perp$-integration has been introduced which is also present in the definitions Equation 296 as well as Equation 297. Thus, only Fock states with (kinetic) invariant mass squared $M^2 \leqslant \mu^2$ contribute (see, e. g., [20, 266, 271]).

For later use we will rescale the definitions Equation 296 and Equation 297 to get $(N_f \equiv 3)$

$$\phi_M^A\left(x,\mu^2\right) = \frac{2\sqrt{2N_c}}{f_M^A}\Phi_M^A\left(x,\mu^2\right) \tag{298}$$

$$\phi_M^g\left(x,\mu^2\right) = \sigma\frac{2\sqrt{2N_c}}{f_M^0}\Phi_M^g\left(x,\mu^2\right), \tag{299}$$

with $\sigma = \sqrt{\frac{N_f}{C_f}}$ (cf. [20, 32]). The definitions given in Equation 296, Equation 297 can then be inverted [20] and generalized to get (cf. [3])

$$\langle 0|\overline{\Psi}(z_2 n)\,\not{n}\gamma_5 T^A \Psi(z_1 n)|M(P)\rangle\Big|_{n^2=0;\mu^2} = i\,(P\cdot n)\,\frac{f_M^A}{\sqrt{2}}\int_0^1 dx\, e^{-iz_{21}^x\,(P\cdot n)}\,\phi_M^A\left(x,\mu^2\right), \tag{300}$$

$$\langle 0|\mathcal{G}_{n\xi}(z_2 n)\,\widetilde{\mathcal{G}}^{n\xi}(z_1 n)|M(P)\rangle\Big|_{n^2=0;\mu^2}, = (P\cdot n)^2\,\frac{C_f f_M^0}{2\sqrt{3}}\int_0^1 dx\, e^{-iz_{21}^x\,(P\cdot n)}\,\phi_M^g\left(x,\mu^2\right), \tag{301}$$

25 In order to abbreviate the expressions, we omit the obvious Wilson lines.

where we employ the abbreviation $\mathcal{G}_{n\xi} = n^\mu \mathcal{G}_{\mu\xi}$ as well as

$$z_{21}^x = \bar{x} z_2 + x z_1 \,, \quad z_{21} = z_2 - z_1 \,. \tag{302}$$

While Equation 301 is very effective when working with the so called background field method (cf. Section 4.1.3), an alternative parametrization, such as[26]

$$\langle 0|\mathcal{A}_\alpha^A(z_2 n)\,\mathcal{A}_\beta^B(z_1 n)|M(P)\rangle\Big|_{n^2=0;\mu^2} = \varepsilon_{\alpha\beta\rho\sigma}\frac{n^\rho P^\sigma}{(P\cdot n)}\frac{C_f f_M^0}{32\sqrt{3}}\delta^{AB}\int_0^1 dx\, e^{-iz_{21}^x (P\cdot n)}\frac{\phi_M^g(x,\mu^2)}{x\bar{x}} \tag{303}$$

seems more efficient if choosing a perturbative approach (see, e. g., Chapter 4). Yet, both approaches are equivalent, because Equation 303 results from the conversion of Equation 301 (cf. [20, 276, 277]), after applying[27] [276]

$$\mathcal{A}_\mu^A(z;x) = x^\nu \int_0^\infty d\sigma\, \mathcal{G}_{\mu\nu}^A(z+\sigma x) \,, \quad x^\mu \mathcal{A}_\mu^A(z;x) = 0 \,. \tag{304}$$

Furthermore, the internal symmetries of the η and η' dictate[28] that the DAs of Equation 298, Equation 299 satisfy the symmetry relations

$$\phi_M^A\left(x,\mu^2\right) = \phi_M^A\left(\bar{x},\mu^2\right) \tag{305}$$

$$\phi_M^g\left(x,\mu^2\right) = -\phi_M^g\left(\bar{x},\mu^2\right) \,. \tag{306}$$

Exemplified for Equation 305, the explanation is very intuitive. Here, the momentum fraction of the quark $\left(x_q = x\right)$ will be exchanged with the one of the antiquark $\left(x_{\bar{q}} = \bar{x}\right)$ which has no impact on the system due to the meson's positive C-parity[29]. Consequently, Equation 305 will hold. Similar arguments may be found for Equation 306, but we have to postpone a dedicated analysis to Section 3.2 and Section 3.3 where the internal structure of DAs is unfolded.

According to the discussion in Section 2.5, the named matrix elements may be used to interpolate flavorless neutral mesons like[30] the π^0 $(A=3)$ or η and η' (e. g., choose $A=8,0$), particularly when including the particle mixing. Therefore, we have to come back to the pivotal issue of this chapter which is the adaption of the FKS scheme to the language of DAs. Ideally, the latter should also reduce the total number of required parameters.

To realize the need for such a program, it is useful to outline the overall concept and the available information. In principle, it would be a formidable task to investigate the six different quark-$\phi_M^A\left(x,\mu^2\right)$ and related two independent gluon-amplitudes $\phi_M^g\left(x,\mu^2\right)$, since such a study offers the opportunity to extract (non-perturbative) information about the $\eta-\eta'$ system (including the mixing mechanism) at the level of DAs (see also [20]). Due to the simple transition between different bases, e. g.,[31] (when combining Equation 267 with Equation 300, assuming $\varphi_0 = \arctan(\sqrt{2})$ and $M=\eta,\eta'$)

$$\begin{aligned} f_M^8\phi_M^8 &= \sqrt{\tfrac{1}{3}} f_M^q \phi_M^q - \sqrt{\tfrac{2}{3}} f_M^s \phi_M^s \,, \\ f_M^0\phi_M^0 &= \sqrt{\tfrac{2}{3}} f_M^q \phi_M^q + \sqrt{\tfrac{1}{3}} f_M^s \phi_M^s \,, \end{aligned} \tag{307}$$

26 One prominent reason for this are the standard Feynman rules themselves which rather involve vector potentials $\mathcal{A}_\mu$ than field-strength tensors $\mathcal{G}_{\mu\nu}$.

27 Equation 304 corresponds to the light-cone gauge.

28 The relation Equation 305 would also hold for the π^0 when choosing $A=3$ (assuming no mixing with the η).

29 For a charged pseudoscalar meson like the $\pi^\pm$ an additional $SU(2)_I$ rotation in flavor space would be needed to recreate the original set-up. Therefore, the full G-parity has to be assumed in this case.

30 This means, that for charged particles like the $\pi^\pm$ replacements in Equation 296 according to $\sqrt{2}T^A \to \left[T^1 \mp iT^2\right]$ have to be made.

31 Equation 307 is exact for strictly light-like separation of the partons.

or equivalently (while omitting any scale dependence in the notation)

$$\begin{pmatrix} f_M^8 \phi_M^8 \\ f_M^0 \phi_M^0 \end{pmatrix} = U(\varphi_0) \begin{pmatrix} f_M^q \phi_M^q \\ f_M^s \phi_M^s \end{pmatrix} \tag{308}$$

a simultaneous study of different phenomena, such as the rather nontrivial $SU(3)_F$-breaking effects in the $\eta - \eta'$ system as well as the interplay of OZI-rule violation and the $U(1)_A$ anomaly in the pseudoscalar channel would then be a possible scenario. Unfortunately, the quality of the present data is insufficient to fix that many parameters at an acceptable level of accuracy. Thus, the limited fidelity of the experimental data on the one hand has to be accompanied by a sensible strategy to reduce the number of theoretical parameters on the other hand. In order to overcome this calamity the following strategy [20, 32] has become quite popular:

i) It has been suggested [20] to assume that there are only small deviations of the quark DAs from their asymptotic form ϕ_{as}:

$$\phi_M^A\left(x, \mu^2\right) \approx \phi_{as}(x) \,. \tag{309}$$

The latter has the universal structure (cf. Section 3.2)

$$\phi_{as}(x) = 6x\bar{x} \,. \tag{310}$$

Instead of assuming an exact relation for Equation 309, where particle independence would hold trivially, the following ansatz has been made ($M = \eta, \eta'$):

$$\phi_M^A\left(x, \mu^2\right) = \phi_A\left(x, \mu^2\right) \,, \quad A = 0, 8, g \,. \tag{311}$$

ii) A posteriori (see discussion below), the choices made in Equation 311 lead to OZI-rule violating admixtures in the supposedly pure states $\{|\eta_R\rangle\}_{R=q,s}$ if no additional assumptions are employed. Fortunately, the OZI-rule may be restored when choosing, e. g.,

$$\phi_8\left(x, \mu^2\right) = \phi_0\left(x, \mu^2\right) = \phi_q\left(x, \mu^2\right) = \phi_s\left(x, \mu^2\right) \tag{312}$$

at some fixed scale μ^2. Admittedly [20, 32], Equation 312 can only hold approximately, e. g., when $\phi_A \approx \phi_{as}$ is valid, and for a limited range of the factorization scale[32] where $\phi_8 \approx \phi_0$ is justified. Therefore, and in order to guarantee the approximate validity of the OZI-rule, Equation 312 has been replaced with the assumption

$$\left| \frac{\phi_{opp}\left(x, \mu^2\right)}{\phi_{as}(x)} \right| \ll 1 \,, \quad \forall x \in [0, 1] \,. \tag{313}$$

Here, the "wrong-flavor" DA [32] is defined via[33]

$$\phi_{opp}\left(x, \mu^2\right) = \frac{\sqrt{2}}{3} \left(\phi_0\left(x, \mu^2\right) - \phi_8\left(x, \mu^2\right) \right) \,. \tag{314}$$

Acknowledging this ansatz, but being aware of its limitations, a refined approach should be consistent within a chosen basis and additionally allow for an applicability to a wide range of renormalization scales. Thus, the key strategy lies in the combination of the FKS-scheme with

32 Due to evolution effects, Equation 312 cannot hold for all scales (cf. Section 3.3).
33 The DA of Equation 314 is obviously generated by OZI-rule violating interactions.

the reinstated particle independence of certain DAs. Given that the small spatial separation of the parton pairs dominates the behavior of hard processes, it has been further suggested by [9, 15, 20, 278] to embed the particle dependence and the mixing behavior of the valence Fock components solely into the decay constants[34]. Therefore, and in order to reduce the number of unconstrained parameters it seems natural to assume that the physical states are related to the flavor states by an orthogonal rotation[35]:

$$\begin{pmatrix} |\eta\rangle \\ |\eta'\rangle \end{pmatrix} = U(\phi) \begin{pmatrix} |\eta_q\rangle \\ |\eta_s\rangle \end{pmatrix} . \tag{315}$$

This state mixing[36] assumption implies that the same mixing pattern valid for the decay constants (cf. Equation 271) also applies to the flavor DAs

$$\begin{pmatrix} f_\eta^q \, \phi_\eta^q & f_\eta^s \, \phi_\eta^s \\ f_{\eta'}^q \phi_{\eta'}^q & f_{\eta'}^s \phi_{\eta'}^s \end{pmatrix} = U(\phi) \, \mathrm{diag}(f_q \phi_q, f_s \phi_s) \tag{316}$$

including the same mixing angle "ϕ" of the FKS scheme. In fact, this is a far reaching conjecture that allows one to reduce the total number of needed (twist-two) DAs by assigning the particle dependence to the corresponding mixing scheme. Therefore, instead of four quark DAs implied by the physical states there remain two DAs ϕ_q and ϕ_s suggested by the flavor states, i. e., we effectively have the relations

$$\phi_M^R\left(x, \mu^2\right) \equiv \phi_R\left(x, \mu^2\right) , \quad \forall M = \eta, \eta' : R = q, s . \tag{317}$$

Furthermore, for the sake of consistency with the state mixing, we assume for the gluonic matrix elements that (see also Section A.14)

$$\langle 0 | \mathcal{G}_{n\xi}(z_2 n) \, \widetilde{\mathcal{G}}^{n\xi}(z_1 n) | \eta_q \rangle = \langle 0 | \mathcal{G}_{n\xi}(z_2 n) \, \widetilde{\mathcal{G}}^{n\xi}(z_1 n) | \eta_s \rangle , \tag{318}$$

which is compatible with the ansatz (see calculation in Section A.14)

$$\phi_M^g\left(x, \mu^2\right) = \phi_g\left(x, \mu^2\right) , \quad \forall M = \eta, \eta' \tag{319}$$

of one remaining gluonic DA for the whole $\eta - \eta'$ system.

At this point the number of unconstrained parameters has been successfully reduced by 50% together with a self-consistent choice of the basis (cf. Section A.14).

We can now develop a strategy for handling the scale dependence of involved DAs. In a nutshell it is possible to extend the approximations given by Equation 317, along with Equation 319 via a combination of Equation 308 and Equation 316, resulting in the corresponding scheme specific expression for the (twist-two) SO DAs (at a fixed[37] scale $\mu_0 = 1$ GeV):

$$\begin{pmatrix} f_\eta^8 \, \phi_\eta^8 & f_\eta^0 \, \phi_\eta^0 \\ f_{\eta'}^8 \phi_{\eta'}^8 & f_{\eta'}^0 \phi_{\eta'}^0 \end{pmatrix} = U(\phi) \, \mathrm{diag}(f_q \phi_q, f_s \phi_s) \, U^T(\varphi_0) . \tag{320}$$

34 According to Equation 300, the decay constants play the role of wave functions at the origin (also cf. [20]).
35 For a phenomenological discussion of the state mixing approach see Section 4.3.
36 Commonly, this term is only used, when there is only one mixing angle.
37 In fact, it is natural to assume that the FKS scheme refers to a low renormalization scale, due to its low energy nature (cf. Chapter 5).

Since the flavor octet and singlet DAs have a different scale dependence [3], Equation 320 cannot hold to all scales. Consequently, one has to consider Equation 320 as an instruction how to translate the (now) reduced number of parameters in the QF basis, which is assumed to be valid for a low renormalization scale $\mu_0^2 = 1\ \mathrm{GeV}^2$, where the (strict) FKS scheme is supposed to hold into the SO scheme, where results for higher scales are obtainable by QCD evolution. In this way we solve two problems at the same time:

i) We preserve the particle dependence within the SO scheme and accordingly it is possible to (consistently) take into account $SU(3)_F$ corrections[38].

ii) Moreover, within the SO basis a proper renormalization scheme can be developed (cf. Section 3.3) in order to extend Equation 320 to arbitrary scales $\mu \in \mathbb{R}_0^+$ (sufficiently high). Thus, OZI-rule violating effects can be taken into account without restricting the choices of the DA parameters (cf. Equation 313), enabling an advanced phenomenological study (cf. Section 4.3).

However, there are more non-vanishing matrix elements that can be considered (see Section 2.5). In fact, for an overall consistent treatment of the associated DAs also deviations from the light-cone have to be taken into account [39]. Therefore, Equation 300 has to be rewritten in terms of a series expansion around the light-cone $(n^2 \approx 0)$. Fortunately, only the first few powers of the almost light-like distances between the constituents are relevant for the kinematical set-up as provided by hard exclusive processes. Hence, Equation 300 may be extended to[40] $(A = 0, \ldots, N_f^2 - 1)$:

$$\begin{aligned}
&\langle 0|\overline{\Psi}(z_2 n)\,\gamma_\mu\gamma_5 T^A \Psi(z_1 n)|M(P)\rangle\Big|_{n^2\approx 0;\mu^2} \\
&= i\frac{f_M^A}{\sqrt{2}}\int_0^1 dx\, e^{-iz_{21}^x (P\cdot n)}\left\{P_\mu\left[\phi_M^A\left(x,\mu^2\right) + z_{21}^2 n^2 \widetilde{\phi}_{4M}^A\left(x,\mu^2\right) + \mathcal{O}\left(n^4\right)\right]\right. \\
&\quad \left. + z_{21}^2\left(n_\mu (n\cdot P) - P_\mu n^2\right)\left[\int_0^x du\, \widetilde{\psi}_{4M}^A\left(u,\mu^2\right) + \mathcal{O}\left(n^2\right)\right]\right\}, \qquad (321)
\end{aligned}$$

where $\widetilde{\phi}_{4M}^A$ and $\widetilde{\psi}_{4M}^A$ are higher twist DAs which may be redefined (cf. [3, 257]) via[41]

$$\phi_{4M}^A\left(x,\mu^2\right) = 16\left[\widetilde{\phi}_{4M}^A\left(x,\mu^2\right) - \int_0^x du\, \widetilde{\psi}_{4M}^A\left(u,\mu^2\right)\right], \qquad (322)$$

$$\psi_{4M}^A\left(x,\mu^2\right) = -2\frac{d}{dx}\widetilde{\psi}_{4M}^A\left(x,\mu^2\right). \qquad (323)$$

The latter are generated via integration by parts of the original DAs, i. e., by using identities similar to

$$-i\int_0^1 dx\, e^{-iz_{21}^x (P\cdot n)}\left[\int_0^x du\, \phi(u)\right] = \int_0^1 dx\, \frac{e^{-iz_{21}^x (P\cdot n)}}{z_{21}(P\cdot n)}\phi(x) - \frac{e^{-iz_1 (P\cdot n)}}{z_{21}(P\cdot n)}\int_0^1 dx\, \phi(x), \qquad (324)$$

38 An assumption like Equation 311 would clearly complicate this agenda (cf. Section 4.3).

39 Here, both, the DAs belonging to matrix elements with the Lorentz structures $\sim \sigma_{\mu\nu}\gamma_5$, $i\gamma_5$ and the terms of $\mathcal{O}(z_{21}^2 n^2)$ are of higher twist (cf. Section 3.4).

40 In contrast to other attempts (cf. [279]) Equation 321 is the standard expansion, which reveals up to this order two distinct Lorentz structures, implying an equal number of different higher twist DAs. Moreover, we use the abbreviation $n^2 \approx 0$ instead of $z_{21}^2 n^2 \approx 0$ to emphasize the underlying light-cone expansion.

41 For the pion case (cf. [280]) also the notation $g_1(x,\mu^2) = \widetilde{\phi}_{4\pi}^3(x,\mu^2)$ and $g_2(x,\mu^2) = \widetilde{\psi}_{4\pi}^3(x,\mu^2)$ is in use.

which are in general valid for an adequate (e. g., continuously differentiable) function $\phi(x)$. This leads to the standard representation (cf. [1, 3, 281]) of Equation 321:

$$\begin{aligned}
&\langle 0|\overline{\Psi}(z_2 n)\,\gamma_\mu\gamma_5 T^A \Psi(z_1 n)|M(P)\rangle\Big|_{n^2\approx 0;\mu^2}\\
&= i\frac{f_M^A}{\sqrt{2}}\int_0^1 dx\, e^{-iz_{21}^x (P\cdot n)}\left\{P_\mu\left[\phi_M^A\left(x,\mu^2\right)+z_{21}^2 n^2\widetilde{\phi}_{4M}^A\left(x,\mu^2\right)\right]\right.\\
&\quad\left.+\,i z_{21}\left(n_\mu - P_\mu\frac{n^2}{P\cdot n}\right)\widetilde{\psi}_{4M}^A\left(x,\mu^2\right)+\mathcal{O}\left(z_{21}^4 n^4\right)\right\}\\
&= iP_\mu\frac{f_M^A}{\sqrt{2}}\int_0^1 dx\, e^{-iz_{21}^x (P\cdot n)}\left[\phi_M^A\left(x,\mu^2\right)+\frac{z_{21}^2 n^2}{16}\phi_{4M}^A\left(x,\mu^2\right)\right]\\
&\quad+\frac{i}{2}\frac{n_\mu}{P\cdot n}\frac{f_M^A}{\sqrt{2}}\int_0^1 dx\, e^{-iz_{21}^x (P\cdot n)}\psi_{4M}^A\left(x,\mu^2\right)+\mathcal{O}\left(z_{21}^4 n^4\right)\,.
\end{aligned}\tag{325}$$

For the involved higher twist DAs all possible surface terms vanish (see also Section 3.4). Furthermore, up to the intended order of accuracy, Equation 325 allows a consistent parametrization of all the two-particle matrix elements[42] for pseudoscalar mesons (omitting Wilson lines)

$$\begin{aligned}
&\langle 0|\overline{\psi}^a_{f',\alpha'}(z_2 n)\,\psi^b_{f,\alpha}(z_1 n)\,|M(P)\rangle\\
&= \frac{\delta^{ab}}{12}\sum_{A=0}^{N_f^2-1}\left(\sqrt{2}T^A\right)_{ff'}\left\{-(i\gamma_5)_{\alpha\alpha'}\langle 0|\overline{\psi}(z_2 n)\sqrt{2}T^A i\gamma_5\psi(z_1 n)\,|M(P)\rangle\right.\\
&\quad-(\gamma_\mu\gamma_5)_{\alpha\alpha'}\langle 0|\overline{\psi}(z_2 n)\sqrt{2}T^A\gamma^\mu\gamma_5\psi(z_1 n)\,|M(P)\rangle\\
&\quad\left.+\frac{1}{2}(\sigma_{\mu\nu}\gamma_5)_{\alpha\alpha'}\langle 0|\overline{\psi}(z_2 n)\sqrt{2}T^A\sigma^{\mu\nu}\gamma_5\psi(z_1 n)\,|M(P)\rangle\right\}
\end{aligned}\tag{326}$$

via higher twist DAs. In general, the corresponding amplitudes can be defined by[43]

$$\begin{aligned}
&\langle 0|\overline{\psi}(z_2 n)\,i\gamma_5 T^A\psi(z_1 n)\,|M(P)\rangle\Big|_{n^2=0;\mu^2}\\
&= \frac{f_M^A}{\sqrt{2}}h_{3M}^A\int_0^1 dx\, e^{-iz_{21}^x (P\cdot n)}\phi_{3M}^{A;p}\left(x,\mu^2\right)\,,
\end{aligned}\tag{327}$$

$$\begin{aligned}
&\langle 0|\overline{\psi}(z_2 n)\,\sigma_{\mu\nu}\gamma_5 T^A\psi(z_1 n)\,|M(P)\rangle\Big|_{n^2=0;\mu^2}\\
&= -\frac{iz_{21}}{6}\frac{f_M^A}{\sqrt{2}}h_{3M}^A\left(P_\mu n_\nu - P_\nu n_\mu\right)\int_0^1 dx\, e^{-iz_{21}^x (P\cdot n)}\phi_{3M}^{A;\sigma}\left(x,\mu^2\right)\,,
\end{aligned}\tag{328}$$

with the auxiliary parameter "h_{3M}^A" as specified in Section 3.4. Analogously, the three particle DAs can be found and defined when parametrizing the non-vanishing matrix elements implied by $\overline{\psi}^a_{f',\alpha'}(x)\,g\mathcal{G}^A_{\mu\nu}(y)\,\psi^b_{f,\alpha}(z)$. In contrast to the pure quark-antiquark structure, the field-strength tensor can also be replaced by its dual form which allows other non-vanishing Lorentz structures.

42 This is similar to Equation 188, but has been retrofitted with possible flavor and the predetermined color structures.
43 Possible normalization conditions will be specified in the following subsections.

For instance, the latter entails a contribution $\sim \varepsilon_{\alpha\beta\mu\nu}\,(\gamma_\lambda)_{\alpha\alpha'}$, effectively generating the dual field-strength tensor "attached" to a vector-current. Therefore, the associated DAs are given by[44]

$$\begin{aligned}
&\langle 0|\overline{\psi}(z_2 n)T^A \sigma_{\mu\nu}\gamma_5 g\mathcal{G}_{\alpha\beta}(z_3 n)\,\psi(z_1 n)\,|M(P)\rangle\Big|_{n^2\approx 0;\mu^2}\\
&= i\frac{f_{3M}^A}{\sqrt{2}}\Big(p_\alpha p_\mu g^\perp_{\nu\beta} - p_\alpha p_\nu g^\perp_{\mu\beta} - (\alpha\leftrightarrow\beta)\Big)\Phi_{3M}^A(\underline{z}, p\cdot n) + \dots\,, \qquad (329)\\
&\langle 0|\overline{\psi}(z_2 n)T^A \gamma_\mu\gamma_5 g\mathcal{G}_{\alpha\beta}(z_3 n)\,\psi(z_1 n)\,|M(P)\rangle\Big|_{n^2\approx 0;\mu^2}\\
&= \frac{f_M^A}{\sqrt{2}}\,p_\mu\big(p_\alpha n_\beta - p_\beta n_\alpha\big)\frac{1}{p\cdot n}\Phi_{4M}^A(\underline{z}, p\cdot n) + \frac{f_M^A}{\sqrt{2}}\Big(p_\beta g^\perp_{\alpha\mu} - p_\alpha g^\perp_{\beta\mu}\Big)\Psi_{4M}^A(\underline{z}, p\cdot n) + \dots\,, \qquad (330)\\
&\langle 0|\overline{\psi}(z_2 n)T^A \gamma_\mu i g\widetilde{\mathcal{G}}_{\alpha\beta}(z_3 n)\,\psi(z_1 n)\,|M(P)\rangle\Big|_{n^2\approx 0;\mu^2}\\
&= \frac{f_M^A}{\sqrt{2}}\,p_\mu\big(p_\alpha n_\beta - p_\beta n_\alpha\big)\frac{1}{p\cdot n}\widetilde{\Phi}_{4M}^A(\underline{z}, p\cdot n) + \frac{f_M^A}{\sqrt{2}}\Big(p_\beta g^\perp_{\alpha\mu} - p_\alpha g^\perp_{\beta\mu}\Big)\widetilde{\Psi}_{4M}^A(\underline{z}, p\cdot n) + \dots\,, \qquad (331)
\end{aligned}$$

where "p_μ" represents another light-cone vector[45] (see Section A.10 for details):

$$p_\mu = P_\mu - \frac{n_\mu m_M^2}{2\,(n\cdot P)} + \mathcal{O}\big(n^2\big)\,. \qquad (332)$$

Besides, the ellipses stand for higher twist contributions, beyond the accuracy of this work. Moreover, the shorthand notation ($m\in\mathbb{N}$ according to the number of involved partons)

$$\mathcal{F}(\underline{z}, p\cdot n) = \int \mathcal{D}\underline{\alpha}\, e^{-i[\alpha_1 z_1 + \alpha_2 z_2 + \dots + \alpha_m z_m](p\cdot n)}\mathcal{F}(\underline{\alpha}) \qquad (333)$$

implied by Equation 292 and Equation 293 using the corresponding integration measure

$$\int \mathcal{D}\underline{\alpha}\,\phi(\underline{\alpha}) = \left[\prod_{i=1}^{m}\int_0^1 d\alpha_i\right]\delta\Big(1 - \sum_{j=1}^{m}\alpha_j\Big)\phi(\underline{\alpha})\,, \qquad (334)$$

with the auxiliary test function "$\phi(\underline{\alpha})\equiv\phi(\alpha_1,\dots,\alpha_m)$".

Apparently, such a large number of additional DAs would undermine our intended strategy to reduce the redundancies if it would entail an equal number of new, unconstrained parameters. However, in the following subsections the internal structure of the given non-perturbative amplitudes is studied, revealing the interconnectedness of the named DAs with each other. Therefore, this interrelation, given by the very nature of QCD itself prevents the emergence of such spurious "new" parameters. As a result, the discussed approach will not be compromised when including higher twist corrections.

3.2 CONFORMAL SYMMETRY AND TWIST-EXPANSION

In Chapter 2 the self-consistency of QCD has been discussed with the result that this theory indeed has no internal, but only external anomalies (cf. [55]). Apart from the already reviewed axial anomaly, QCD in the chiral limit also possesses the so-called conformal or scale anomaly.

44 It is still very common to use the abbreviation $\underline{z} = (z_1,\dots,z_n)$ for a n-tuple of numbers.

45 With the given kinematics, p_μ defines the minus-direction $\bar{n}_\mu = p_\mu/p\cdot n$, complementary to the corresponding plus-direction n_μ (cf. Section A.9, Section A.10).

Although the conformal symmetry of QCD is broken by the scale anomaly and finite quark masses, its study provides powerful tools for practical applications and puts strong constraints on the structure of DAs. Therefore, the following review[46] is essential for the subsequent investigation of meson DAs (see Section 3.4.2, along with Section 3.4.3).

3.2.1 *General aspects of conformal symmetry*

By definition, the conformal group is formed via those coordinate transformations in four-dimensional Minkowski space which preserve angles and leave the light-cone invariant. This means, the intended transformations only change the scale of the metric

$$g'_{\mu\nu}(x) = \omega(x)\, g_{\mu\nu}(x) \tag{335}$$

and conserve the space-time interval

$$ds^2 = g_{\mu\nu}(x)\, dx^\mu\, dx^\nu\,. \tag{336}$$

More precisely, the conformal group proves to be an extension of the Pointcaré group [128, 282–286] which may be understood on the level of Lie algebras (cf. Section A.11). Here, the ten familiar generators of the Pointcaré group

$$\begin{aligned} \mathbf{P}_\mu &\rightarrow (4 \text{ translations}) \\ \mathbf{M}_{\mu\nu} &\rightarrow (6 \text{ Lorentz rotations}) \end{aligned} \tag{337}$$

are generalized with five more operators

$$\begin{aligned} \mathbf{D} &\rightarrow (1 \text{ dilatation}) \\ \mathbf{K}_\mu &\rightarrow (4 \text{ special conformal transformations})\,. \end{aligned} \tag{338}$$

The latter manifest themselves not only in the obvious (global) scale transformation (called dilatation), or inversions

$$x^\mu \xrightarrow[(\text{dil.})]{} \lambda x^\mu \quad (\lambda \in \mathbb{R}\backslash\{0\})\,, \quad x^\mu \xrightarrow[(\text{inv.})]{} \frac{x^\mu}{x^2}\,, \tag{339}$$

but also in the class of so-called special conformal transformations[47]

$$x^\mu \xrightarrow[(\text{inv.})]{} \frac{x^\mu}{x^2} \xrightarrow[(\text{tran.})]{} \frac{x^\mu + a^\mu x^2}{x^2} \xrightarrow[(\text{inv.})]{} \frac{x^\mu + a^\mu x^2}{1 + 2a\cdot x + a^2 x^2}\,. \tag{340}$$

Besides, the group theoretical properties of conformal symmetry one also has to address its field-theoretical aspects.

When starting at classical level, the question of the necessary and sufficient conditions under which the theory is conformally invariant has to be answered. Accordingly, the follow-up question would then concern the interplay of these requirements with possible quantum anomalies. Therefore, commencing with the conformal symmetry at classical level, the Noether's theorem applied to the QCD Lagrangian Equation 17 in the chiral limit implies the existence of fifteen

46 The study of conformal symmetry constitutes an important contribution to physics in general. However, we have to restrict ourselves to the needed aspects, thereby, closely following [128].

47 The transformation Equation 340 is obviously a combination of inversions and translations: $x^\mu \rightarrow a^\mu + x^\mu$ (with "a^μ" a constant four-vector).

conserved currents with the corresponding conserved charges $\mathbf{P}_\mu$, $\mathbf{M}_{\mu\nu}$, $\mathbf{D}$ and $\mathbf{K}_\mu$ that are nothing else, but the named generators (cf. Equation 337, Equation 338) of the conformal group. Remarkably, the symmetry currents can be expressed in terms of the so-called improved energy-momentum tensor $\theta_{\mu\nu}$ (cf. [128] and references therein) which is traceless, symmetric, and divergenceless,

$$g^{\mu\nu}\theta_{\mu\nu}(x)|_{\text{class.}} = 0\,,\quad \theta_{\mu\nu}(x) = \theta_{\nu\mu}(x)\,,\quad \partial^\mu\theta_{\mu\nu}(x) = 0\,, \tag{341}$$

when assuming a classical set-up. Furthermore, the tensor $\theta_{\mu\nu}$ allows a very compact representation of the symmetry currents associated with the dilatation and special conformal transformations [128]:

$$\mathcal{J}^\mu_{\mathbf{D}} = x_\nu\theta^{\mu\nu}\,,\quad \mathcal{J}^\mu_{\mathbf{K},\alpha} = \left(2x_\nu x_\alpha - x^2 g_{\nu\alpha}\right)\theta^{\mu\nu}\,. \tag{342}$$

Correspondingly, Equation 342 entails the necessary and sufficient condition for a theory to be conformally invariant[48] which is fulfilled if and only if $\theta_{\mu\nu}$ is divergenceless and traceless. On quantum level[49], however, the improved energy-momentum tensor remains divergenceless and symmetric, while its trace will exhibit the famous conformal anomaly (cf. [128, 287–289])

$$\partial_\mu\mathcal{J}^\mu_{\mathbf{D}}(x) = \frac{\beta(g)}{2g}\mathcal{G}^{\mathcal{A}}_{\mu\nu}(x)\,\mathcal{G}^{\mathcal{A},\mu\nu}(x)\,. \tag{343}$$

As discussed in Chapter 2, the related effects may be taken care of within a suitable renormalization procedure.[50] In the following, the inclusion of conformal symmetry breaking and quantum effects will be formulated separately. Therefore, the development of a customized renormalization procedure will later on (cf. Section 3.3) supplement the results of this chapter.

Infinitesimal symmetry transformations, such as

$$x^\mu \to x^\mu + \varepsilon^\mu,\quad \phi(x) \to \left[1 + \varepsilon_\mu\delta^\mu_{\mathbf{P}}\right]\phi(x) \tag{344}$$

are related to the generators, that in general act on generic fundamental fields ϕ. According to [128, 284, 290] those are given by

$$\delta^\mu_{\mathbf{P}}\phi(x) = i[\mathbf{P}^\mu,\phi(x)] = \partial^\mu\phi(x)\,, \tag{345}$$
$$\delta^{\mu\nu}_{\mathbf{M}}\phi(x) = i[\mathbf{M}^{\mu\nu},\phi(x)] = (x^\mu\partial^\nu - x^\nu\partial^\mu - \mathbf{\Sigma}^{\mu\nu})\phi(x)\,, \tag{346}$$
$$\delta_{\mathbf{D}}\phi(x) = i[\mathbf{D},\phi(x)] = (x\cdot\partial + l)\phi(x)\,, \tag{347}$$
$$\delta^\mu_{\mathbf{K}}\phi(x) = i[\mathbf{K}^\mu,\phi(x)] = \left(2x^\mu x\cdot\partial - x^2\partial^\mu + 2lx^\mu - 2x_\nu\mathbf{\Sigma}^{\mu\nu}\right)\phi(x)\,, \tag{348}$$

where "l" denotes the related scaling dimension of ϕ. At the classical level l coincides with the field's canonical dimension l^{can}, while quantum corrections entail a difference $l - l^{\text{can}}$, which is usually referred to as anomalous dimension (see, e. g., [128] for a detailed discussion). Moreover, $\mathbf{\Sigma}^{\mu\nu}$ represents the spin generator. For quark ψ or gluon fields $\mathcal{A}_\mu$, this operator may be written as [128, 290]

$$\mathbf{\Sigma}_{\mu\nu}\psi = \frac{i}{2}\sigma_{\mu\nu}\psi\,,\quad \mathbf{\Sigma}_{\mu\nu}\mathcal{A}_\alpha = g_{\nu\alpha}\mathcal{A}_\mu - g_{\mu\alpha}\mathcal{A}_\nu\,, \tag{349}$$

48 In other words, this is the case, when the currents Equation 342 are conserved.

49 The underlying regularization procedure introduces an intrinsic mass-scale with the related dimensionful UV cut-off which inevitably breaks the scale invariance.

50 Obviously, there are subtleties, e. g., those related to the gauge-fixing, which may break the conformal invariance. See [128] for details.

COMPONENT	$\mathcal{G}_{+\perp}$	$(\mathcal{G}_{+-}, \mathcal{G}_{\perp\perp})$	$\mathcal{G}_{-\perp}$	ψ_+	ψ_-
spin-projection "s"	$+1$	0	-1	$+\frac{1}{2}$	$-\frac{1}{2}$
conformal spin "j"	$\frac{3}{2}$	1	$\frac{1}{2}$	1	$\frac{1}{2}$
collinear twist "t"	1	2	3	1	2

Table 5: Relevant components of the fundamental fields (cf. also [128, 290]).

while gluonic field-strength tensors $\mathcal{G}_{\alpha\beta}$ require [290]

$$\mathbf{\Sigma}_{\mu\nu}\mathcal{G}_{\alpha\beta} = g_{\mu\alpha}\mathcal{G}_{\beta\nu} + g_{\beta\nu}\mathcal{G}_{\alpha\mu} - (\alpha \leftrightarrow \beta) \,. \tag{350}$$

Similar to the (quantization) axis of the atomic spin, the Lorentz spin of a fundamental field can be projected along a distinguished direction. Referring to the assumed phenomenological set-up of partons, that are collinearly propagating along the same direction $\bar{n}^\mu$ ($\bar{n}^2 = 0$), one may consider the corresponding quantum fields ϕ as living on the light-cone ($n^2 = 0$)

$$\phi(x) \to \phi(\alpha n) \quad (\alpha \in \mathbb{R}) \,. \tag{351}$$

Here, the shorthand notation $\phi(\alpha n) \equiv \phi(\alpha)$ is commonly used [128, 290]. In this context, one may assume a fixed spin projection "s" of those fields on, e. g., the "+"-direction (cf. Section A.9):

$$\mathbf{\Sigma}_{+-}\phi(\alpha) = s\,\phi(\alpha) \,. \tag{352}$$

In fact, for the gluon field one may, therefore, formulate

$$\mathbf{\Sigma}_{+-}\mathcal{A}_+ = s_+\mathcal{A}_+ \,, \quad \mathbf{\Sigma}_{+-}\mathcal{A}_- = s_-\mathcal{A}_+ \,, \quad \mathbf{\Sigma}_{+-}\mathcal{A}_\perp = s_\perp\mathcal{A}_\perp \,, \tag{353}$$

an eigenvalue problem similar to Equation 352, i. e., with the spin projections $s_\pm = \pm 1$ and $s_\perp = 0$. Analogously, for $\mathcal{G}_{\alpha\beta}$ the indices may be combined to components with definite spin projections (cf. Table 5). Thus, in the context of conformal symmetry, the standard quark spinors are not the fundamental fields. Correspondingly, the different spin projections have to be separated, e. g., with the standard projection operators (cf. Section A.9)

$$\Pi_\pm = \frac{1}{2}\gamma_\mp\gamma_\pm \tag{354}$$

leading to the plus or minus components of the underlying quark fields

$$\psi_\pm = \Pi_\pm\psi \,. \tag{355}$$

The latter have definite spin projections (cf. Equation 349, Equation 352)

$$\mathbf{\Sigma}_{+-}\psi_\pm = \pm\frac{1}{2}\psi_\pm \tag{356}$$

and are, therefore, the actual fundamental fields of conformal symmetry (cf. Table 5). Besides, when restricted to this collinear setting (along $\bar{n}^\mu$), all relevant conformal transformations can be mapped onto the light-cone. In other words, the special conformal transformation of Equation 340 (set $a^\mu = a\bar{n}^\mu$, $a \in \mathbb{R}$) boils down to

$$x_- \to \frac{x_-}{1 + 2ax_-} \,. \tag{357}$$

This also applies to the translation and dilatation $(c \in \mathbb{R})$

$$x_- \to x_- + c\,, \quad x_- \to \lambda x_-\,. \tag{358}$$

Consequently, the four-dimensional conformal group can be reduced to its collinear subgroup $SL(2,\mathbb{R})$, generating Möbius transformations[51] $(ad - bc = 1)$:

$$\alpha \to \frac{a\alpha + b}{c\alpha + d}\,, \tag{359}$$

that ultimately imply the correspondence [128]

$$\phi(\alpha) \to (c\alpha + d)^{-2j}\, \phi\left(\frac{a\alpha + b}{c\alpha + d}\right)\,. \tag{360}$$

Here, "j" is the so-called conformal spin (see discussion below), which is composed of the spin projection s and the scaling dimension l of the field ϕ (such as $l_\psi = 3/2$, $l_{\mathcal{A}} = 1$, etc. for $D = 4$)

$$j = \frac{1}{2}\,(l + s)\,. \tag{361}$$

Similar to the quantum mechanical angular momentum, the needed analogon of the spherical harmonics[52] may be found when studying the collinear subalgebra of the (full) conformal algebra (cf. Section A.11). The latter is formed by the projections $\mathbf{P}_+$, $\mathbf{M}_{-+}$, $\mathbf{D}$ and $\mathbf{K}_-$, which can be either combined to [292, 293]

$$\mathbf{L}_0 = \frac{i}{2}\,(\mathbf{D} + \mathbf{M}_{-+})\,, \quad \mathbf{L}_1 = \frac{i}{4}\,(\mathbf{K}_- - 2\mathbf{P}_+)\,, \quad \mathbf{L}_2 = -\frac{1}{4}\,(\mathbf{K}_- + 2\mathbf{P}_+)\,, \tag{362}$$

or more commonly to the ladder operators

$$\mathbf{L}_\pm = \mathbf{L}_1 \pm i\mathbf{L}_2\,. \tag{363}$$

It is easy to check (by applying Equation 1191-Equation 1197), that these operators fulfill the commutation relations

$$[\mathbf{L}_0, \mathbf{L}_\pm] = \pm\mathbf{L}_\pm\,, \quad [\mathbf{L}_+, \mathbf{L}_-] = 2\,\mathbf{L}_0\,. \tag{364}$$

The latter also give rise to a set of corresponding differential operators[53]

$$[\mathbf{L}_a, \phi(\alpha)] \equiv L_a \phi(\alpha) \quad (a = +, -, 0)\,, \tag{365}$$

that are fully compatible with the described formalism (cf. Equation 361)

$$\begin{aligned} [\mathbf{L}_-, \phi(\alpha)] &= \left(\alpha^2 \partial_+ + \alpha\,(l + s)\right) \phi(\alpha) \equiv L_- \phi(\alpha) \\ &\Rightarrow j \equiv \tfrac{1}{2}\,(l + s)\,. \end{aligned} \tag{366}$$

Moreover, the local field operator ϕ with fixed spin projection turns out to be an eigenstate

$$\sum_{a=0,1,2} [\mathbf{L}_a, [\mathbf{L}_a, \phi(\alpha)]] = j\,(j-1)\,\phi(\alpha) \equiv L^2 \phi(\alpha) \tag{367}$$

51 Under the right conditions (cf. Equation 359), the Möbius transformation reproduces the transformation of Equation 357 and Equation 358.

52 These ultraspherical polynomials [291] form the basis for a quantitative description of DAs.

53 As discussed in [128], these operators satisfy $SL(2)$ commutation relations analogous to those of Equation 364, however, with an extra minus sign.

of the quadratic Casimir operator ($i = 0, 1, 2$)

$$L^2 = L_0^2 + L_1^2 + L_2^2 = L_0^2 - L_0 + L_- L_+ \,, \quad \left[L^2, L_i\right] = 0 \,. \tag{368}$$

One remaining operator is given by [128]

$$\mathbf{E} = \frac{i}{2}\left(\mathbf{D} - \mathbf{M}_{-+}\right) \,. \tag{369}$$

It commutes with all operators $\{\mathbf{L}_i\}_{i=0,1,2}$. In fact, $\mathbf{E}$ is counting the collinear twist "t" of the field "ϕ":

$$[\mathbf{E}, \phi(\alpha)] = t\,\phi(\alpha) \,, \quad t = l - s \,. \tag{370}$$

This means instead of the "geometric" twist[54], which refers to the full conformal group (cf. [128, 294]), "t" is restricted to the collinear subgroup.

3.2.2 *Conformal towers*

In order to build the basic machinery needed to describe the genuine non-perturbative structures of DAs, the concept of conformal towers[55] is essential.

The simplest case of a conformal tower can be constructed with the eigenvalue equations [128]

$$[\mathbf{L}_-, \phi(\alpha)]|_{\alpha=0} = 0 \,, \quad [\mathbf{L}_0, \phi(\alpha)]|_{\alpha=0} = j\phi(0) \,, \tag{371}$$

where $\mathbf{L}_-$ acts as an annihilation operator, and $\phi(0)$ is an eigenstate of $\mathbf{L}_0$ with eigenvalue j. Furthermore, by iteratively applying the raising operator $\mathbf{L}_+$ we get:

$$\mathcal{O}_k = [\mathbf{L}_+, \ldots, [\mathbf{L}_+, [\mathbf{L}_+, \phi(\alpha)]] \ldots]\,\big|_{\alpha=0} = \left[\left(-\frac{d}{d\,\alpha}\right)^k \phi(\alpha)\right]\Bigg|_{\alpha=0} \,. \tag{372}$$

Consequently, the commutation relations given in Equation 364 lead to the corresponding characteristic properties of $\mathcal{O}_k$ [128]:

$$\left[\mathbf{L}_+, \mathcal{O}_k\right] = \mathcal{O}_{k+1} \,, \tag{373}$$

$$\left[\mathbf{L}_0\,, \mathcal{O}_k\right] = (k + j)\,\mathcal{O}_k \,, \tag{374}$$

$$\left[\mathbf{L}_-, \mathcal{O}_k\right] = \sum_{l=1}^{k} -2\,(k - l + j)\,\mathcal{O}_k = -k\,(k + 2j - 1)\,\mathcal{O}_k \,. \tag{375}$$

As a result, Equation 372 can be used in the context of a Taylor expansion

$$\phi(\alpha) = \sum_{k=0}^{\infty} \frac{\alpha^k}{k!} \left(\frac{d^k}{d^k \alpha}\phi(\alpha)\right)\Bigg|_{\alpha=0} = \sum_{k=0}^{\infty} \frac{(-\alpha)^k}{k!}\mathcal{O}_k \,, \tag{376}$$

allowing us to express light-cone fields in terms of local operators and their derivatives. In other words, the key ingredients of this construction are:

54 Beyond that, the term "dynamical twist" (τ) can be found in the literature [294, 295] which counts powers $Q^{2-\tau}$ of the process specific energy-momentum transfer "Q". Due to its lack of universality and Lorentz covariance, we are not using this concept within this work.

55 They are a result of the attempt to construct a complete set of states (i. e., a basis), built of fundamental fields and their derivatives.

i) Finding the highest weight vector on the $SL(2,\mathbb{R})$ representation space (cf. [128], i. e., those operators that fulfill Equation 374.

ii) The latter then procreates higher operators[56] $\mathcal{O}_k$ via the raising operator $\mathbf{L}_+$ (cf. Equation 372).

Most importantly, the rather cumbersome structure of composite operators can be expressed via specific polynomials. For instance, the tower of local operators can be rewritten as

$$\mathcal{O}_k = \left[\mathcal{P}_k\left(\tfrac{d}{d\alpha}\right)\phi(\alpha)\right]\Big|_{\alpha=0} , \quad \mathcal{P}_k(u) = [-u]^k . \tag{377}$$

Therefore, the algebra of generators acting on each operator $\mathcal{O}_k$ can be replaced by an equivalent algebra of differential operators acting on the space of characteristic polynomials.[57] Accordingly, this approach either requires adequate operators $\widetilde{L}_0$, $\widetilde{L}_\pm$

$$\left[\widetilde{L}_0\mathcal{P}_k\left(\frac{d}{d\alpha}\right)\phi(\alpha)\right]\Big|_{\alpha=0} \equiv \mathcal{P}_k\left(\frac{d}{d\alpha}\right)[L_0\phi(\alpha)]|_{\alpha=0} \tag{378}$$

$$\left[\widetilde{L}_\pm\mathcal{P}_k\left(\frac{d}{d\alpha}\right)\phi(\alpha)\right]\Big|_{\alpha=0} \equiv \mathcal{P}_k\left(\frac{d}{d\alpha}\right)[L_\mp\phi(\alpha)]|_{\alpha=0} \tag{379}$$

acting on the (vector) space of polynomials[58] via [128]

$$\widetilde{L}_-\mathcal{P}(u) = [-u]\,\mathcal{P}(u) , \tag{380}$$

$$\widetilde{L}_0\mathcal{P}(u) = \left[u\frac{d}{du} + j\right]\mathcal{P}(u) , \tag{381}$$

$$\widetilde{L}_+\mathcal{P}(u) = \left[u\frac{d^2}{du^2} + 2j\frac{d}{du}\right]\mathcal{P}(u) , \tag{382}$$

or a substitution similar to [128, 292, 293] $\left(\text{i. e., } \partial_\kappa \equiv \frac{d}{d\kappa}\right)$

$$\kappa^n \to \frac{[-u]^n}{\Gamma(n+2j)} \Rightarrow \widetilde{\mathcal{P}}_n(\kappa) \to \mathcal{P}_n(u) . \tag{383}$$

The latter allows us to use the original operator structures, implying[59]:

$$\begin{aligned} L_-\widetilde{\mathcal{P}}_n(\kappa) &= -\partial_\kappa\widetilde{\mathcal{P}}_n(\kappa) , \\ L_0\widetilde{\mathcal{P}}_n(\kappa) &= (\kappa\partial_\kappa + j)\,\widetilde{\mathcal{P}}_n(\kappa) , \\ L_+\widetilde{\mathcal{P}}_n(\kappa) &= \left(\kappa^2\partial_\kappa + 2j\kappa\right)\widetilde{\mathcal{P}}_n(\kappa) . \end{aligned} \tag{384}$$

In a nutshell, the techniques that apply to the one particle case can be generalized to products of several fundamental fields $\phi_{j_1},\dots,\phi_{j_n}$

$$\mathcal{O}(\alpha_1,\dots,\alpha_n) = \phi_{j_1}(\alpha_1)\cdots\phi_{j_n}(\alpha_n) \quad (n\in\mathbb{N}) , \tag{385}$$

with given collinear spins $j_1,\dots,j_n$. Here, the involved fields live on the light-cone $\left(n^2=0,\ \phi_{j_k}(\alpha_k)\equiv\phi_{j_k}(\alpha_k n)\right)$ and we assume $\alpha_i\neq\alpha_j$ (for $i\neq j$). Besides, the cases $n=2$ and $n=3$ of

56 These operators have a larger eigenvalue (see Equation 374) of the conformal spin projection on the zero axis, than the corresponding highest weight vector $\mathcal{O}_k = \phi(0)$.

57 In this context, the relevant structure of $\mathcal{O}_k$ is encoded in associated characteristic polynomials.

58 Here, $\mathcal{P}(u)$ may be formed with the monomials from Equation 377: $\mathcal{P}(u)=\sum_{k=0}^{m}\alpha_k\mathcal{P}_k(u)$ $(\alpha_k\in\mathbb{R})$.

59 At this point it should be emphasized that even though the operator structure of Equation 384 may coincide with that in Equation 365, the operators $L_\pm$ acting on the characteristic polynomials is the adjoint to $L_\mp$ (related to the operators).

particular interest for us, and we will discuss the former example in detail. When analyzing the generic short distance expansion [128]

$$\lim_{|\alpha_1-\alpha_2|\to 0} \mathcal{O}(\alpha_1,\alpha_2) = \phi_{j_1}(\alpha_1)\,\phi_{j_2}(\alpha_2)\,, \tag{386}$$

one encounters a set of local operators similar to [128, 296]

$$\mathcal{O}_n(0) = \mathcal{P}_n\big(\partial_{\alpha_1},\partial_{\alpha_2}\big)\,\phi_{j_1}(\alpha_1)\,\phi_{j_2}(\alpha_2)\,. \tag{387}$$

In this context, the homogenous polynomials $\mathcal{P}_n(u_1,u_2)$ of degree n arise (cf. Section A.12). Apparently, the $\mathcal{O}_n$ in Equation 387 do not have simple properties under conformal transformations. Hence, a complete basis of local operators has to be constructed, forming a conformal tower. As it turns out (cf. [128]), the collinear transformation of two-particle operators (such as Equation 386) corresponds to independent transformations of the underlying fields[60]. Therefore, the group generators can be constructed from the one-particle case[61] (cf. Equation 362)

$$\mathbb{L}_a = \mathbf{L}_{1,a} + \mathbf{L}_{2,a} \quad (a = 0,1,2)\,, \tag{388}$$

with the corresponding quadratic Casimir operator

$$\mathbb{L}^2 = \sum_{a=0}^{2} \big(\mathbf{L}_{1,a} + \mathbf{L}_{2,a}\big)^2\,. \tag{389}$$

Consequently, for the definition of an adequate local (conformal) operator[62] $\mathbb{O}_n$ the same transformation properties that apply to a fundamental field under the collinear conformal group have to be imposed:

$$\begin{aligned} \big[\mathbb{L}^2,\mathbb{O}_n\big] &= j\,(j-1)\,\mathbb{O}_n\,,\\ \big[\mathbb{L}_0,\mathbb{O}_n\big] &= (j_1+j_2+n)\,\mathbb{O}_n\,,\\ \big[\mathbb{L}_-,\mathbb{O}_n\big] &= 0\,. \end{aligned} \tag{390}$$

Owing to the representation

$$\mathbb{L}^2 = \mathbb{L}_0^2 - \mathbb{L}_0 + \mathbb{L}_+\mathbb{L}_- \tag{391}$$

of the Casimir operator Equation 390 entails

$$j = j_1 + j_2 + n\,. \tag{392}$$

Thus, as long as j_1, j_2 and n are given, the label j is redundant. Furthermore, when knowing the conformal operator $\mathbb{O}_n$, it is convenient to construct[63] the related complete basis in terms of a conformal tower of operators ($k, n \in \mathbb{N}_0$)

$$\mathbb{O}_{n,n+k} = \underbrace{[\mathbb{L}_+,\ldots,[\mathbb{L}_+,[\mathbb{L}_+}_{k-\text{times}},\mathbb{O}_n]]\ldots] = (-\partial_+)^k\,\mathbb{O}_n\,. \tag{393}$$

In fact, for the given set-up, the explicit structure of the conformal operator may be most easily found, when using the adjoint representation of the ladder operators (cf. Section A.11), which

60 This is analogous to the quantum mechanical problem of spin summation, yet with another symmetry group.
61 For a definition of the remaining ladder operators Equation 363 may be applied to Equation 388.
62 Again, those shall consist of the two fundamental fields and their derivatives.
63 In full analogy to the one-particle case.

is similar to Equation 384. According to Equation 390, the desired characteristic polynomial[64] $\widetilde{\mathbb{P}}_n^{j_1 j_2}(\kappa_1, \kappa_2)$, fulfills the partial DE (cf. Equation 1199)

$$L_- \widetilde{\mathbb{P}}_n^{j_1 j_2}(\kappa_1, \kappa_2) \equiv \left(-\partial_{\kappa_1} - \partial_{\kappa_2}\right) \widetilde{\mathbb{P}}_n^{j_1 j_2}(\kappa_1, \kappa_2) = 0\,, \tag{394}$$

which has the solution[65] (modulo an arbitrary constant)

$$\widetilde{\mathbb{P}}_n^{j_1 j_2}(\kappa_1, \kappa_2) \sim (\kappa_2 - \kappa_1)^n = \sum_{n_1+n_2=n} \binom{n}{n_1} (-\kappa_1)^{n_1}\, \kappa_2^{n_2}\,. \tag{395}$$

In order to define the differential operator $\mathbb{O}_n^{j_1,j_2}$ one may perform a change of variables

$$(-\kappa_1)^{n_1}\, \kappa_2^{n_2} \to \frac{(-u_1)^{n_1}\, u_2^{n_2}}{\Gamma(n_1 + 2j_1)\, \Gamma(n_2 + 2j_2)}\,, \tag{396}$$

which implies the final form of the desired characteristic polynomials [128]

$$\begin{aligned} \mathbb{P}_n^{j_1 j_2}(u_1, u_2) &= \sum_{n_1+n_2=n} \binom{n}{n_1} \frac{[-u_1]^{n_1}\, u_2^{n_2}}{\Gamma(n_1 + 2j_1)\, \Gamma(n_2 + 2j_2)} \\ &= (u_1 + u_2)^n\, P_n^{(2j_1-1, 2j_2-1)}\left(\tfrac{u_2-u_1}{u_1+u_2}\right)\,. \end{aligned} \tag{397}$$

Those are given in terms of the Jacobi polynomials $P_n^{(a,b)}(x)$ [291]. According to the replacements[66] $u_1 \to \overleftarrow{\partial}_+$, $u_2 \to \overrightarrow{\partial}_+$ we, therefore, get the corresponding set of local conformal operators:

$$\mathbb{O}_n^{j_1,j_2}(x) = \partial_+^n \left[\phi_{j_1}(x)\, P_n^{(2j_1-1,2j_2-1)}\left(\frac{\overrightarrow{\partial}_+ - \overleftarrow{\partial}_+}{\overrightarrow{\partial}_+ + \overleftarrow{\partial}_+}\right) \phi_{j_2}(x)\right]\,. \tag{398}$$

The latter may be used as a blueprint for the conformal expansion of leading twist two-particle meson DAs (see below). Besides, this procedure can be generalized to products of more than two fundamental fields (see [128] for details). However, there exist several solutions for the actual construction of the characteristic polynomials which is a consequence of possible ambiguities in summing up the different conformal spins (of fundamental fields) to an overall spin [128]. In particular, for the product of three fields the required characteristic polynomials have to fulfill [128]

$$L_- \widetilde{\mathbb{P}}_n(\kappa_1, \kappa_2, \kappa_3) \equiv -\sum_{i=1}^{3} \partial_{\kappa_i} \widetilde{\mathbb{P}}_n(\kappa_1, \kappa_2, \kappa_3) = 0\,, \tag{399}$$

which can be solved via polynomials similar to (modulo a constant) [128]

$$\widetilde{\mathbb{P}}_n(\kappa_1, \kappa_2, \kappa_3) \sim (\kappa_3 - \kappa_2)^{n_1} (\kappa_2 - \kappa_1)^{n_2} \quad (n = n_1 + n_2)\,. \tag{400}$$

In particular, a possible solution is given by the so-called Appell polynomials [142], but also other bases may be used[67]. Another point, which is crucial for the handling of DAs, concerns possible

64 The notation has to be retrofitted with superscripts j_1, j_2, which explicitly show the collinear spin of the involved fundamental fields.

65 Here, we apply the multinomial theorem (cf. Section A.12).

66 The total derivative may be written as $\partial_+ = \overleftarrow{\partial}_+ + \overrightarrow{\partial}_+$.

67 To avoid ambiguities, we do not attribute to a specific basis, but show the truncated expansions explicitly. We will resume this discussion in Section 3.4.2.

orthogonality relations among the characteristic polynomials and the associated interplay of the corresponding conformal operators with the "conformal scalar product", e. g., for the two-particle conformal operators [128]:

$$\langle 0|\mathrm{T}\left\{\mathbb{O}_n^{j_1 j_2}(x)\,\mathbb{O}_m^{j_1 j_2}(0)\right\}|0\rangle \sim \delta_{nm}\,. \tag{401}$$

The latter is an important consequence of conformal symmetry in general, i. e., for a conformally invariant theory the correlation function of two conformal operators vanishes, unless they have the same conformal spin [128]. In terms of characteristic polynomials, Equation 401 is equivalent to the orthogonality relation

$$\int_0^1 du_1 \int_0^1 du_2\, \delta\left(1-\sum_{i=1}^{2} u_i\right) u_1^{2j_1-1} u_2^{2j_2-1}\, \mathbb{P}_n^{j_1 j_2}(u_1,u_2)\, \mathbb{P}_m^{j_1 j_2}(u_1,u_2) = \mathcal{N}\,\delta_{nm}\,, \tag{402}$$

with[68] an appropriate weight function and an adequate normalization constant "$\mathcal{N}$". The named Appell polynomials, however, are not mutually orthogonal, suggesting the use of orthogonal polynomials instead[69] (cf. [128, 142, 297]).

3.2.3 *Conformal operators in QCD*

According to the previous discussion, it is now evident how to decompose the relevant two- and three-particle states into towers of conformal operators. For instance, the standard quark-antiquark operators such as ($\Gamma = i\gamma_5$, $\gamma_\mu\gamma_5$, etc.)

$$\mathcal{O}_\Gamma^A(z_2 n, z_1 n) = \overline{\Psi}(z_2 n)\,[z_2 n, z_1 n]\,\mathrm{T}^A \Gamma\, \Psi(z_1 n) \tag{403}$$

formally give rise to states with definite spin projections (omitting the given flavor and color structures)

$$\overline{\Psi}\,\Gamma\,\Psi = \underbrace{\overline{\Psi}_+\,\Gamma\,\Psi_+}_{\text{twist-2}} + \underbrace{\overline{\Psi}_+\,\Gamma\,\Psi_- + \overline{\Psi}_-\,\Gamma\,\Psi_+}_{\text{twist-3}} + \underbrace{\overline{\Psi}_-\,\Gamma\,\Psi_-}_{\text{twist-4}} \tag{404}$$

and consequently also well-defined (collinear) twist. Therefore, the different Lorentz structures "Γ" are implying DAs of a specific twist, while the resulting knowledge of the collinear spin structure determines the underlying conformal operators and the correlated infinite dimensional representation of the conformal group.

Focusing on the two-particle components[70] one finds:

1) For the operator given in Equation 403 (with $\Gamma = \gamma_\mu\gamma_5$), one may extract the leading twist-two contribution

$$\overline{\Psi}\,\gamma_+\gamma_5\,\Psi = \overline{\Psi}_+\,\gamma_+\gamma_5\,\Psi_+ \tag{405}$$

68 As discussed in [128] the underlying conformal Ward identities not only put strong constrain on possible Green's functions, but also imply Equation 401. Therefore, an ansatz purely based on conformal Ward identities can be worked out (cf. [128]) which also reveals the structure of the characteristic polynomials as well as Equation 402.

69 Contributions of three-particle DAs in this work are embedded in other higher twist (two-particle) DAs which, in principle, allows the use of Equation 402 and makes specific choices of a base in the three-particle case at first glance unnecessary. The clean separation of contributions with different conformal spin, however, is facilitated with a suitable choice of basis.

70 The related higher twist DAs will be derived in Section 3.4.

via an associated projection, with the conformal spin $j_{\Psi} = 1 = j_{\overline{\Psi}}$. The latter implies[71] a set of (rescaled) conformal operators [128]

$$\begin{aligned}\widetilde{\mathbb{O}}_n^{1,1}(x) &= (i\partial_+)^n \left[\overline{\Psi}(x)\,\gamma_+\gamma_5\, P_n^{(1,1)}\left(\frac{\overrightarrow{D}_+ - \overleftarrow{D}_+}{\overrightarrow{D}_+ + \overleftarrow{D}_+}\right)\Psi(x)\right] \\ &\sim (i\partial_+)^n \left[\overline{\Psi}(x)\,\gamma_+\gamma_5\, C_n^{(3/2)}\left(\frac{\overleftrightarrow{D}_+}{\overleftrightarrow{\partial}_+}\right)\Psi(x)\right], \end{aligned} \tag{406}$$

where $C_n^{(\alpha)}(x)$ are the so-called Gegenbauer polynomials (cf. Section A.12), which are a special case of the Jacobi polynomials[72] [291]

$$C_n^{(\alpha)}(x) = \frac{(2\alpha)_n}{\left(\alpha+\frac{1}{2}\right)_n} P_n^{(\alpha-1/2,\alpha-1/2)}(x)\,. \tag{407}$$

Moreover, the standard short hand notation

$$\partial_\mu = \overrightarrow{\partial}_\mu + \overleftarrow{\partial}_\mu = \overrightarrow{D}_\mu + \overleftarrow{D}_\mu\,, \tag{408}$$

$$\overleftrightarrow{D}_\mu = \overrightarrow{D}_\mu - \overleftarrow{D}_\mu\,, \tag{409}$$

is commonly used in the context of an interacting theory (cf. Equation 406).

11) For, the two gluon case[73] (cf. Equation 301 or equivalently Equation 303) one obtains the local twist-two operators [128]

$$\mathbb{G}_n^{3/2,3/2}(x) = (i\partial_+)^n \left[\mathcal{G}^A_{+\perp}(x)\, C_n^{(5/2)}\left(\frac{\overleftrightarrow{D}_+}{\overleftrightarrow{\partial}_+}\right)\mathcal{G}^A_{+\perp}(x)\right]. \tag{410}$$

After the decomposition into generic fields with fixed Lorentz spin projections on the light-cone, an explicit expansion of the DAs in terms of an (irreducible) representation of $SL(2,\mathbb{R})$ can be constructed. For example, the general contribution to an m-particle[74] DA ($m \in \mathbb{N}$)

$$\langle 0|\phi_{j_1}(\alpha_1)\cdots\phi_{j_m}(\alpha_m)|M(P)\rangle \sim \int [d\,\underline{u}]\; e^{iP\cdot n\left(\sum_{i=1}^m \alpha_i u_i\right)}\phi(\underline{u})\,, \tag{411}$$

with the lowest possible conformal spin (projection) $j = \sum_{i=1}^m j_i$ is given by the "asymptotic distribution amplitude" [128, 269]

$$\phi_{AS}(u_1,\ldots,u_m) = \frac{\Gamma\left(2\sum_{l=1}^m j_l\right)}{\prod_{i=1}^m \Gamma(2j_i)} \prod_{k=1}^m u_k^{2j_k-1}\,, \tag{412}$$

which is chosen such that

$$\int [d\,\underline{u}]\; \phi_{AS}(\underline{u}) = 1\,. \tag{413}$$

When applied to Equation 406 and Equation 410, whilst using the phase space condition in Equation 291, Equation 412 not only allows us to recover Equation 310, but we also obtain (what we want to call) the canonical form of the asymptotic twist-two gluon DA:

$$\phi_{as}^g(u) = 30u^2\bar{u}^2\,. \tag{414}$$

71 For the interacting theory the common derivatives in Equation 398 are replaced by their covariant counterparts.

72 Here, $(x)_n = x\,(x+1)\cdots(x+n-1)$ is the rising factorial.

73 Analogous to the quark-antiquark case Equation 301 is also accompanied by higher twist DAs (cf. Section 3.4), which corresponds to two gluon states with different helicities than shown in Equation 410 (cf. [128]).

74 Here, the definition of Equation 334 is extended to (cf. [128]) the measure $\int [d\,\underline{u}] = \int_0^1 du_1 \ldots \int_0^1 d\,u_m\, \delta\left(1 - \sum_{i=1}^m u_i\right)$.

Higher states in conformal spin will enter the DAs as a product of the asymptotic form with adequate polynomials [128, 291, 298], e. g., those that are mutually orthogonal with the weight function (proportional to) ϕ_{as} (cf. Equation 402).

For instance, (similar to the standard approach in [128]), the plus-projection of Equation 300 stretched over the symmetric light-like ($n^2 = 0$) interval $z_2 = 1 = -z_1$ implies the well-known local expansion (cf. Section 2.4)

$$\langle 0|\overline{\Psi}(0)\, T^A \gamma_+\gamma_5 \left(i \overset{\leftrightarrow}{D}_+\right)^n \Psi(0)|M(P)\rangle\Big|_{\mu^2} = i P_+^{n+1} \frac{f_M^A}{\sqrt{2}} \int_0^1 dx\, \xi_x^n \phi_M^A\left(x,\mu^2\right) , \tag{415}$$

with the relevant operators [128]

$$\mathcal{O}^A_{n-k,k} = (i\partial_+)^k \left[\overline{\Psi}(0)\, T^A \gamma_+\gamma_5 \left(i \overset{\leftrightarrow}{D}_+\right)^n \Psi(0)\right] . \tag{416}$$

The related conformal operators are substantially given by Equation 406, retrofitted with the explicit flavor structure (labeled with "A")

$$\mathbb{O}^{1,1}_{n,A}(x) = (i\partial_+)^n \left[\overline{\Psi}(x)\, T^A\, \gamma_+\gamma_5\, C_n^{(3/2)}\left(\frac{\overset{\leftrightarrow}{D}_+}{\overset{\leftrightarrow}{\partial}_+}\right) \Psi(x)\right] . \tag{417}$$

According to Equation 415, one finds the corresponding generalization[75] with regard to the reduced matrix elements of Equation 417:

$$\int_0^1 dx\, C_n^{(3/2)}(x)\, \phi_M^A\left(x,\mu^2\right) = \langle\langle \mathbb{O}^{1,1}_{n,A}\left(\mu^2\right)\rangle\rangle , \tag{418}$$

$$i f_M^A P_+^{n+1} \langle\langle \mathbb{O}^{1,1}_{n,A}\left(\mu^2\right)\rangle\rangle = \langle 0|\mathbb{O}^{1,1}_{n,A}(0)|M(P)\rangle\Big|_{\mu^2} . \tag{419}$$

As a result of conformal symmetry, Equation 418 suggests an expansion of the two-particle DAs in terms of Gegenbauer polynomials (cf. orthogonality relations and normalization constants $N_n^{(3/2)}$ Section A.12):

$$\phi_M^A\left(x,\mu^2\right) = 6x\bar{x} \sum_{n=0}^{\infty} c_{n,M}^{(A)}\left(\mu^2\right) C_n^{(3/2)}\left(\xi_x\right) , \tag{420}$$

$$c_{n,M}^{(A)}\left(\mu^2\right) = \frac{\langle\langle \mathbb{O}^{1,1}_{n,A}\left(\mu^2\right)\rangle\rangle}{6 N_n^{(3/2)}} , \tag{421}$$

with the non-perturbative Gegenbauer coefficients $c_{n,M}^{(A)}(\mu^2)$. Only the zeroth coefficient of $\phi_M^A(x,\mu^2)$ is fixed by the standard choice for the otherwise arbitrary normalization condition

$$\int_0^1 dx\, \phi_M^A\left(x,\mu^2\right) = 1 \quad \Leftrightarrow \quad c_{0,M}^{(A)}\left(\mu^2\right) = 1 . \tag{422}$$

As discussed in Section 3.3, the anomalous dimensions[76] of the conformal operators rise logarithmically with the conformal spin (cf. also [128]). Therefore, the operators with higher spin are strongly suppressed[77] at large scales μ^2, leading to the exact limit

$$\lim_{\mu^2\to\infty} \phi_M^A\left(x,\mu^2\right) = \phi_{as}(x) , \tag{423}$$

75 To make it more obvious, Equation 415 exhibits a projection $\int_0^1 dx\, \xi_x^n \phi_M^A(x,\mu^2) = 2\int_{-1}^1 d\xi\, \xi^n \phi_M^A\left(\frac{1}{2}(1+\xi),\mu^2\right)$ on monomials.

76 Those also determine the scale dependence of the Gegenbauer coefficients.

77 According to [1, 281, 299] this is not the case for hadronic scales.

which has to be fulfilled[78]. Thus, the definition in Equation 422 ensures compatibility with the rest of all findings. Analogously, the assumed transformation properties[79] and structure of the underlying conformal operators provided in Equation 410 lead to the (canonical) ansatz[80]

$$\phi_M^{(g)}\left(x,\mu^2\right) = 30x^2\bar{x}^2 \sum_{n=1}^{\infty} c_{2n,M}^{(g)}\left(\mu^2\right) C_{2n-1}^{(5/2)}\left(\xi_x\right) \tag{424}$$

for the twist-two gluon DA defined in Equation 301. However, in contrast to Equation 420, $\phi_M^{(g)}$ has no finite scale-independent asymptotic form, i. e., for asymptotically large scales one gets (cf. also [22, 23, 300])

$$\lim_{\mu^2\to\infty} \phi_M^g\left(x,\mu^2\right) = 0\,. \tag{425}$$

Furthermore, the lack of normalizability

$$\int_0^1 dx\, \phi_M^g\left(x,\mu^2\right) = 0 \tag{426}$$

allows also non-canonical choices $\phi_M^g \to \alpha\,\phi_M^g$ ($\alpha \in \mathbb{R}\backslash\{0\}$), which leads to alternative definitions[81] $\left(c_{n,M}^{(g)} \to \frac{1}{\alpha} c_{n,M}^{(g)}\right)$ of the Gegenbauer coefficients (cf. [20, 28]). In other words, the definition in Equation 424 ensures that the gluonic $\left(c_{n,M}^{(g)}\right)$ and quark $\left(c_{n,M}^{A}\right)$ Gegenbauer coefficients are of the same magnitude (cf. Section 4.3).

Before we proceed, let us emphasize the following points:

I) The conformal expansion is formal, in the sense, that its convergence (a priori) cannot be concluded from symmetry considerations alone [128]. However, in the context of QCD factorization (cf. Chapter 4) or phenomenological applications (cf. Section 4.3) one implicitly assumes and uses convergent expansions (for further discussion cf. [128]).

II) The validity of the (renormalized) Gegenbauer expansion is not compromised when including finite quark masses [128, 271]; although the latter will break the conformal symmetry (already at classical level). This is a consequence of the RG approach (cf. Chapter 2), where the UV divergent contributions to the corresponding matrix elements (cf., e. g., [20]) are canceled by mass-independent counter-terms [128].

III) Moreover, the mentioned expansion (cf. Equation 420)

$$\phi_M\left(x,\mu^2\right) = 6x\bar{x}\left[1 + \sum_{n>0} c_{n,M}\left(\mu^2\right) C_n^{(3/2)}(\xi_x)\right] \tag{427}$$

is generic for all leading twist quark-antiquark meson DAs. According to the flavor structure and transformation properties, they only differ in the expansion coefficients and involved anomalous dimensions. For instance, in the case of π^0 and $\eta^{(\prime)}$ the odd coefficients have to vanish (cf. Equation 305), while for the kaon they also encode non-vanishing $SU_F(3)$ breaking effects (cf. [271]).

78 Equation 423 is among the most important and most rigorously proven results of QCD (cf. [144]).
79 These are a consequence of, e. g.Equation 303 when interchanging the partons.
80 The validity of Equation 424 becomes clear in the context of the RG approach (cf. Section 3.3).
81 Earlier approaches [20, 28, 32] have been using the factor $\alpha = 1/30$.

In general, the conformal partial wave expansion (cf. Section 3.3) provides a sensible approach for the consistent inclusion of higher twist DAs. In fact, the latter are related with each other in a non-trivial way which puts further constraints on the underlying parameters. Such a discussion has to be postponed to Section 3.4. In the next step, the two-loop evolution of the quark singlet and gluon DAs has to be constructed.

3.3 RENORMALIZATION OF THE $\eta^{(\prime)}$ DISTRIBUTION AMPLITUDES

In the previous Section 3.2 the structure of leading twist two-particle DAs, based on conformal symmetry, has been analyzed. As a result, the Gegenbauer expansion has been imposed, which dictates the DA's general anatomy, while the non-perturbative information and scale dependence is encoded in the Gegenbauer coefficients.

Correspondingly, this section is dedicated to formulate the required NLO evolution of the η and η' twist-two meson DAs. For this purpose, we will reformulate the existing work of [20, 26, 129] and adapt it to our needs. The latter results in a new self-consistent representation of the $\eta^{(\prime)}$ DAs scale dependence.

3.3.1 *General remarks*

According to the discussion of Chapter 2 a reasonable inclusion of quantum corrections into our considerations requires a proper renormalization procedure.

Correspondingly, the UV divergent contributions, characterizing the asymptotic behavior of the non-local operator products (such as in Equation 300 or Equation 301), may be collected within an adequate normalization factor $\mathcal{Z}$, which then connects the unrenormalized DA Φ_M^{ur} with its renormalized counterpart Φ_M [20]:

$$\Phi_M^{\text{ur}}(x) = \int_0^1 dx' \, \mathcal{Z}\left(x, x'; \alpha_S\left(\mu_F^2\right)\right) \Phi_M\left(x', \mu_F^2\right) . \tag{428}$$

Furthermore, the acquired renormalization scale dependence[82] is thus governed by the so-called Efremov-Radyushkin-Brodsky-Lepage (ER-BL) evolution equation[83] [301–303]

$$\mu^2 \frac{\partial}{\partial \mu^2} \Phi_M\left(x, \mu^2\right) = \int_0^1 dy \, V\left(x, y; \alpha_S\left(\mu^2\right)\right) \Phi_M\left(y, \mu^2\right) , \tag{429}$$

which itself is defined by the purely perturbative kernels $V^{(k)}(x, y)$ [20, 27, 304], that are belonging to the expansion (in α_S) [20]

$$\begin{aligned} &- \int_0^1 dx' \, \mathcal{Z}^{-1}\left(x, x'; \alpha_S\left(\mu^2\right)\right) \left[\mu^2 \frac{\partial}{\partial \mu^2} \mathcal{Z}^{-1}\left(x', y; \alpha_S\left(\mu^2\right)\right)\right] \\ &= V\left(x, y; \alpha_S\left(\mu^2\right)\right) = \sum_{k=1}^{\infty} \left[\frac{\alpha_S\left(\mu^2\right)}{4\pi}\right]^k V^{(k)}(x, y) . \end{aligned} \tag{430}$$

Obviously, an overall consistent solution to a physical problem requires a set of kernels and, consequently, a renormalization procedure of an adequate loop order (cf. Section 2.3). In particular,

82 In this context, the factorization point "μ_F^2" also represents the scale, at which the separation between soft and hard contributions takes place (cf. Chapter 2). Accordingly, the DAs not only get scale, but also (subtraction) scheme-dependent.

83 Equation 429 results from Equation 428 when applying the operator "$\mu^2 \frac{\partial}{\partial \mu^2}$".

a full NLO (cf. [3, 281]) treatment of, e. g., a transition form factor depends on a renormalization approach, with a two-loop order accuracy. For a solution of Equation 429, however, one should start at LO in the strong coupling, while interpreting the ER-BL equation as an eigenvalue problem[84]. The advantage of this approach is immanent because at LO, the operator renormalization is driven by tree-level counter terms [128], i. e., up to this level of accuracy all symmetry properties of the classical theory are retained. This implies, that (at LO) operators with different conformal spin cannot mix (cf. Equation 433) and the Callan-Symanzik equation, that governs the renormalization scale dependence, is the Ward identity of the dilatation operator (cf. [128]). In other words, the eigenfunctions of Equation 429 are nothing else, but the Gegenbauer polynomials multiplied with their associated weight-functions (cf. Section C.3). Alternatively, these arguments may be confirmed by a brute force calculation based on the analytical composition of the evolution kernels (cf. Section C.3), which encode the very structure of QCD interaction at asymptotic energies.

Accordingly, one may surmise a deeper truth behind these findings, underlining the relevance of our favored ansatz, i. e., to reconstruct the DAs order by order from their conformal moments. The latter, on the other hand, are related (e. g., after rearranging Equation 417) to the leading twist forward matrix elements of Equation 111 via operators like $\mathcal{O}^{A}_{n,0}$ (cf. Equation 416), which arise from a local expansion of the corresponding matrix elements, such as Equation 300 or Equation 301. In the case of DAs, however, there is no restriction to the forward case alone, but one also has to include the mixing (cf. [128]) with operators containing total derivatives (cf. Equation 416, Equation 417). Therefore, it is not possible to simply take the OPE's (cf. Equation 112 with Equation 118) anomalous dimensions, but in general has to modify them first[85] (cf. Section C.2). Knowing both: the forward anomalous dimensions (cf. Equation 118) as well as the corresponding modification procedure (cf. Section C.2) completes the search for the needed eigenvalues of Equation 429 and allows a reformulation of the eigenvalue problem. In a nutshell, conformal symmetry leads to a separation of longitudinal and transversal degrees of freedom, which may be exemplified for the LO octet renormalization[86] (cf. Section C.2, Section C.3):

$$\mu^2 \frac{\partial}{\partial \mu^2} \phi_M^{(8)}\left(x, \mu^2\right) = -\frac{\alpha_s\left(\mu^2\right)}{4\pi} \int_0^1 dy \left[V_{NS}^{(1)}(x,y)\, \phi_M^{(8)}\left(y, \mu^2\right)\right] \tag{431}$$

$$\Rightarrow \mu^2 \frac{\partial}{\partial \mu^2} c_{n,M}^{(8)}\left(\mu^2\right) = -\frac{\alpha_s\left(\mu^2\right)}{4\pi} \gamma_n^{(0)} c_{n,M}^{(8)}\left(\mu^2\right) , \tag{432}$$

with the solution and LO RG factor "$\mathcal{E}_n^{LO}$" ($n \geqslant 0$):

$$c_{n,M}^{(8)}\left(\mu^2\right) = c_{n,M}^{(8)}\left(\mu_0^2\right) \left[\frac{\alpha_s(\mu^2)}{\alpha_s(\mu_0^2)}\right]^{\frac{\gamma_n^{(0)}}{\beta_0}} \equiv c_{n,M}^{(8)}\left(\mu_0^2\right) \mathcal{E}_n^{LO}\left(\mu^2, \mu_0^2\right) . \tag{433}$$

This forms a close analogy to non-relativistic quantum mechanics [128] in a spherically symmetric potential (cf. Table 6), justifying the name: partial conformal wave expansion (cf. Section 4.3).

84 Other solutions, such as contour or numerical integration [26] would also be possible, but are leading astray from our preferred Gegenbauer ansatz.

85 This means, the formalism, that is taking care of the mixing effects, uses specific conventions to which the forward anomalous dimensions have to be adapted.

86 This corresponds to Equation 429, when replacing $\mathbf{\Phi}_M \to \phi_M^8$ and $\mathbf{V} \to -\frac{\alpha_s}{4\pi} q q V_D^{(1)}$.

ASPECTS	QUANTUM MECHANICS	QUANTUM CHROMODYN.
symmetry	$O(3)$	$SL(2,\mathbb{R})$
separation	radial & angular (d.o.f)	transversal & longitudinal
differential equation	1-dim. Schrödinger eqn.	1-dim. RG eqn.
irreducible representation	spherical harmonics	ultraspherical harmonics

Table 6: The corresponding symmetry leads to a separation of variables: one (angular/longitudinal component) denoted by an irreducible representation of the symmetry group; the other one (radial/-transversal coordinate) governed by a DE.

3.3.2 *Leading-order evolution*

According to Section 3.1.1, the η and η' meson DAs exhibit flavor octet as well as singlet components, which in principle evolve independently from each other. In practice, however, the (LO) non-singlet evolution may be interpreted as a special case of the (one-loop) singlet renormalization, when focusing on its pure structure[87].

Therefore, it is possible to harmonize both cases, permitting us to use the existing octet evolution[88] as a role model and adjust the singlet case to it. This strategy ensures that both classes of quark-antiquark DAs may be treated on an equal footing (cf. Section 4.3), i. e., their Gegenbauer coefficients do not exhibit extra scaling factors due to non-canonical choices within the renormalization procedure.
For instance, the LO octet evolution kernel coincides with ${}^{qq}V_D^{(1)}$ (cf. Section C.3) of the singlet ER-BL equation[89] [20, 26]

$$\mu^2 \frac{d}{d\mu^2} \begin{pmatrix} \phi_M^{(0)}(x,\mu^2) \\ \phi_M^{(g)}(x,\mu^2) \end{pmatrix} = \frac{\alpha_S(\mu^2)}{4\pi} \int_0^1 dy\, \boldsymbol{V}^{(1)}(x,y) \begin{pmatrix} \phi_M^{(0)}(x,\mu^2) \\ \phi_M^{(g)}(x,\mu^2) \end{pmatrix}, \tag{434}$$

which is defined by $\left(\sigma = \sqrt{C_f/N_f}\right)$

$$\boldsymbol{V}^{(1)}(x,y) = -\begin{pmatrix} {}^{qq}V_D^{(1)}(x,y) & {}^{qg}V_D^{(1)}(x,y)\,\sigma^{-1} \\ {}^{gq}V_D^{(1)}(x,y)\,\sigma & {}^{gg}V_D^{(1)}(x,y) \end{pmatrix}. \tag{435}$$

Furthermore, Equation 434 implies a RG equation for the corresponding Gegenbauer coefficients

$$\mu^2 \frac{d}{d\mu^2} \begin{pmatrix} c_{n,M}^{(0)}(\mu^2) \\ c_{n,M}^{(g)}(\mu^2) \end{pmatrix} = -\frac{\alpha_S(\mu^2)}{4\pi} \left[\mathbf{T}_n^{-1} \boldsymbol{\gamma}_n^{D(0)} \mathbf{T}_n\right] \begin{pmatrix} c_{n,M}^{(0)}(\mu^2) \\ c_{n,M}^{(g)}(\mu^2) \end{pmatrix} \quad (n \geqslant 0), \tag{436}$$

that includes the transformation matrix (cf. discussion in Section A.12 and Section C.5)

$$\mathbf{T}_n = \operatorname{diag}\left(6\, N_n^{(3/2)},\, 30\, N_{n-1}^{(5/2)}\right). \tag{437}$$

87 In the NLO case, a similar connection may be found on the level of anomalous dimensions (cf. Section C.2).
88 The octet case matches the π^0 evolution which is known up to NLO accuracy [1].
89 The evolution of the singlet decay constant is a NLO effect (cf. Equation 261). Therefore, up to LO accuracy, it may be treated as a constant.

The latter compensates differences in the definitions of quark and gluon Gegenbauer coefficients which lead to distinct off-diagonal elements in the (diagonal) anomalous dimension matrix (cf. Section C.2)

$$\boldsymbol{\gamma}_n^{D(m)} = \begin{pmatrix} {}^{qq}\gamma_n^{D(m)} & {}^{qg}\gamma_n^{D(m)} \\ {}^{gq}\gamma_n^{D(m)} & {}^{gg}\gamma_n^{D(m)} \end{pmatrix} \quad (m \geqslant 0) \,. \tag{438}$$

In order to solve Equation 436, however, it is convenient to diagonalize the related anomalous dimension matrix, by defining the $\pm$-modes

$$\vec{c}_{n,M}\left(\mu^2\right) = \begin{pmatrix} c_{n,M}^{(0)}\left(\mu^2\right) \\ c_{n,M}^{(g)}\left(\mu^2\right) \end{pmatrix} = \mathbf{D}_n \begin{pmatrix} c_{n,M}^{(+)}\left(\mu^2\right) \\ c_{n,M}^{(-)}\left(\mu^2\right) \end{pmatrix} , \tag{439}$$

with the change of basis matrix[90]

$$\mathbf{D}_n = \begin{pmatrix} \frac{{}^{gq}\gamma_n^{(0)}}{\gamma_n^{(+)} - {}^{qq}\gamma_n^{(0)}} \frac{5N_f}{C_f} & 1 \\ 1 & \frac{{}^{qg}\gamma_n^{(0)}}{\gamma_n^{(-)} - {}^{gg}\gamma_n^{(0)}} \frac{C_f}{5N_f} \end{pmatrix} \tag{440}$$

and the special case "$n=0$":

$$\vec{c}_{0,M}(\mu_0) = (1,0)^T \,. \tag{441}$$

Consequently, Equation 440 entails a decoupling

$$\begin{aligned} \mu^2 \frac{d}{d\,\mu^2} \mathbf{D}_n^{-1} \vec{c}_{n,M}\left(\mu^2\right) &= -\frac{\alpha_S\left(\mu^2\right)}{4\pi} \left(\mathbf{D}_n^{-1} \left[\mathbf{T}_n^{-1} \boldsymbol{\gamma}_n^{D(0)} \mathbf{T}_n\right] \mathbf{D}_n\right) \mathbf{D}_n^{-1} \vec{c}_{n,M}\left(\mu^2\right) \\ &= -\frac{\alpha_S\left(\mu^2\right)}{4\pi} \operatorname{diag}\left(\gamma_n^{(+)}, \gamma_n^{(-)}\right) \mathbf{D}_n^{-1} \vec{c}_{n,M}\left(\mu^2\right) \end{aligned} \tag{442}$$

of the RG equations corresponding to $c_{n,M}^{(\pm)}$, such that each has a structure analogous to Equation 432. Therefore, the evolution of the $\pm$-Gegenbauer coefficients is given by Equation 433 when simultaneously interchanging $c_{n,M}^{(8)} \leftrightarrow c_{n,M}^{(\pm)}$ and $\gamma_n^{(0)} \leftrightarrow \gamma_n^{(\pm)}$ with the eigenvalues of $\boldsymbol{\gamma}_n^{D(0)}$:

$$\gamma_n^{(\pm)} = \frac{{}^{qq}\gamma_n^{(0)} + {}^{gg}\gamma_n^{(0)} \pm \sqrt{\left({}^{qq}\gamma_n^{(0)} - {}^{gg}\gamma_n^{(0)}\right)^2 + 4\,{}^{gq}\gamma_n^{(0)}\,{}^{qg}\gamma_n^{(0)}}}{2} \,. \tag{443}$$

Fortunately, this rather cumbersome procedure may be automatized by introducing the projection operators (cf. Section C.4)

$$\mathbf{P}_n^{\pm} = \frac{\pm 1}{\gamma_n^{(+)} - \gamma_n^{(-)}} \left(\boldsymbol{\gamma}_n^{D(0)} - \gamma_n^{(\mp)} \mathbb{1}_2\right) , \tag{444}$$

which allow a closed form of the singlet evolution. This means, the LO scale dependence of $c_{n,M}^{(a)}$ ($a = 0, g$) may be described order by order in conformal spin via

$$\vec{c}_{n,M}\left(\mu^2\right) = \mathbf{T}_n^{-1} \mathcal{E}_n^{LO}\left(\mu^2, \mu_0^2\right) \mathbf{T}_n \vec{c}_{n,M}\left(\mu_0^2\right) , \tag{445}$$

where the LO evolution operator is given by

$$\mathcal{E}_n^{LO}\left(\mu^2, \mu_0^2\right) = \sum_{a=\pm} \left[\frac{\alpha_S\left(\mu^2\right)}{\alpha_S\left(\mu_0^2\right)}\right]^{\frac{\gamma_n^{(a)}}{\beta_0}} \mathbf{P}_n^a \,. \tag{446}$$

90 A similar concept has been used in [20].

3.3.3 *Next-to-leading order evolution*

When turning to the NLO evolution of the $\eta^{(\prime)}$ DAs, the very general formalism of [26, 27, 304] as well as the parity-odd anomalous dimensions have to be combined and adapted to our needs. We will only highlight the crucial steps of this rather technical procedure in order to introduce the necessary abbreviations (cf. Section C.2, Section C.6). It should be emphasized, however, that this revisited evolution procedure allows a broad phenomenological application and at the same time a simple numerical implementation. Both points are vital for this work.

As a guideline, we start with the NLO scale dependence of the Gegenbauer coefficients belonging to the flavor-octet contributions. The latter is given by [3, 305–311]

$$c_{n,M}^{(8)}(\mu) = c_{n,M}^{(8)}(\mu_0)\,\mathcal{E}_n^{\mathrm{NLO}}(\mu,\mu_0) + \frac{\alpha_S(\mu)}{2\pi}\sum_{k=0}^{n-2} c_{k,M}^{(8)}(\mu_0)\,\mathcal{E}_k^{\mathrm{LO}}(\mu,\mu_0)\,d_n^k(\mu,\mu_0)\,, \tag{447}$$

with the NLO RG factor $\mathcal{E}_n^{\mathrm{NLO}}$ and the off-diagonal mixing coefficients d_n^k (cf. Section C.2). In a nutshell, the d_n^k describe the mixing of Gegenbauer coefficients with those of smaller conformal spin, i. e., (conformal) operators with less total derivatives only mix with counterparts, that contain more total derivatives (cf. [128]). A similar set-up applies to the singlet case[91], when the NLO evolution kernels acquire an additional off-diagonal contribution [27]

$$\mathbf{V}^{(m)}(x,y) = \mathbf{V}^{\mathrm{D}(m)}(x,y) + \mathbf{V}^{\mathrm{ND}(m)}(x,y) \quad (m \geqslant 2) \tag{448}$$

implying an isomorphic structure for the corresponding anomalous dimensions[92] [26] (cf. Section C.3)

$$\int_0^1 dx\, C_j^{\nu(a)}(\xi_x)\;{}^{ab}\Big[\mathbf{V}\Big(x,y;\alpha_S\Big(\mu^2\Big)\Big)\Big] = -\frac{1}{2}\sum_{k=0}^{j}{}^{ab}\Big[\gamma_{jk}\Big(\alpha_S\Big(\mu^2\Big)\Big)\Big]\,C_k^{\nu(b)}(\xi_y)\,. \tag{449}$$

This means, the (general) coefficients

$$\gamma_{jk}^{(m)} = \delta_{jk}\gamma_j^{\mathrm{D}(m)} + \gamma_{jk}^{\mathrm{ND}(m)} \tag{450}$$

of the asymptotic expansion [3, 26]

$$\gamma_{jk}\Big(\alpha_S\Big(\mu^2\Big)\Big) = \sum_{m=1}^{\infty}\left(\frac{\alpha_S(\mu^2)}{2\pi}\right)^m \gamma_{jk}^{(m)} \tag{451}$$

is not only possessing the already mentioned diagonal anomalous dimensions (cf. Equation 438), but (for $m \geqslant 2$) also exhibits finite non-diagonal contributions[93] (cf. Section C.2):

$$\gamma_{jk}^{\mathrm{ND}(m)} = \begin{pmatrix} {}^{qq}\gamma_{jk}^{\mathrm{ND}(m)} & {}^{qg}\gamma_{jk}^{\mathrm{ND}(m)} \\ {}^{gq}\gamma_{jk}^{\mathrm{ND}(m)} & {}^{gg}\gamma_{jk}^{\mathrm{ND}(m)} \end{pmatrix} \Rightarrow \gamma_{jk}^{\mathrm{ND}(1)} \equiv \mathfrak{M}_j^k\,. \tag{452}$$

This rather complicated structure of the NLO kernel has to be taken into account when trying to derive the analogon for Equation 447 within the singlet sector. Fortunately, the general solution

91 For the singlet case, the analogon of d_n^k will be a matrix-operator $\mathfrak{D}_n^k$.

92 The different channels are labeled by $\nu(a) = \begin{cases} 3/2\,, & \text{for } a = q \\ 5/2\,, & \text{for } a = g \end{cases}$ (cf. Section C.3).

93 Note, that $\mathfrak{M}_j^k$ is the analog of Equation 1399.

of the ER-BL Equation 429 is known [26, 27] to be given in terms of a partial conformal wave expansion[94] (cf. Section C.6 for a detailed discussion) such as[95]

$$\boldsymbol{\Phi}_M\left(x,\mu^2\right) = \begin{pmatrix} f_M^{(0)}(\mu^2)\phi_M^{(0)}(x,\mu^2) \\ f_M^{(0)}(\mu^2)\phi_M^{(g)}(x,\mu^2) \end{pmatrix} = \sum_{n=0}^{\infty} f_M^{(0)}\left(\mu^2\right) \boldsymbol{\Psi}_n(x)\, \vec{c}_{n,M}\left(\mu^2\right) , \tag{453}$$

with the (modified) LO partial conformal wave matrix

$$\boldsymbol{\Psi}_n(x) = \operatorname{diag}\left(6x\bar{x}C_n^{(3/2)}(\xi_x)\,, 30\,[x\bar{x}]^2\, C_{n-1}^{(5/2)}(\xi_x)\right) . \tag{454}$$

At an arbitrary scale μ with respect to a reference scale μ_0, where the Gegenbauer coefficients are defined, Equation 453 may be written as

$$\begin{aligned} \boldsymbol{\Phi}_M\left(x,\mu^2\right) = &\sum_{n=0}^{\infty} \boldsymbol{\Psi}_n(x)\, \mathbf{L}_n^{(1)}\left(\mu^2,\mu_0^2\right) \boldsymbol{\Phi}_{n,M}\left(\mu_0^2\right) \\ &+ \sum_{n=0}^{\infty}\sum_{k=n}^{\infty} \boldsymbol{\Psi}_k(x)\, \mathbf{L}_{kn}^{(2)}\left(\mu^2,\mu_0^2\right) \boldsymbol{\Phi}_{n,M}\left(\mu_0^2\right) . \end{aligned} \tag{455}$$

In Equation 455 the auxiliary matrix operators (cf. Section C.6)

$$\mathbf{L}_n^{(1)}\left(\mu^2,\mu_0^2\right) = \mathbf{T}_n^{-1}\, \mathcal{E}_n^{\mathrm{NLO}}\left(\mu^2,\mu_0^2\right) \mathbf{T}_n \tag{456}$$

$$\mathbf{L}_{kn}^{(2)}\left(\mu^2,\mu_0^2\right) = \frac{\alpha_S\left(\mu^2\right)}{2\pi} \left[\mathbf{T}_k^{-1}\mathcal{D}_k^n\left(\mu^2,\mu_0^2\right) \mathcal{E}_n^{\mathrm{LO}}\left(\mu^2,\mu_0^2\right) \mathbf{T}_n\right] \tag{457}$$

and the moments

$$\boldsymbol{\Phi}_{n,M}\left(\mu_0^2\right) = f_M^{(0)}\left(\mu_0^2\right) \vec{c}_{n,M}\left(\mu_0^2\right) \tag{458}$$

have been introduced. The applicability of Equation 455 in its present form, however, seems to be limited. Due to its double series, the intended numerical implementation of model DAs (cf. Section 4.3) could get aggravated Fortunately, the formal structure of $\mathcal{M}_j^k$ allows for a decisive simplification of Equation 455, when employing Equation 457. The latter implicates ($n, k \in \mathbb{N}_0$)

$$\begin{aligned} \sum_{n=0}^{\infty}\sum_{k=n}^{\infty} \boldsymbol{\Psi}_k \mathbf{L}_{kn}^{(2)} \boldsymbol{\Phi}_{n,M} &= \sum_{n=0}^{\infty}\sum_{k=0}^{\infty} \boldsymbol{\Psi}_k \mathbf{L}_{kn}^{(2)} \boldsymbol{\Phi}_{n,M} - \sum_{n=0}^{\infty}\sum_{k=0}^{n-1} \boldsymbol{\Psi}_k \mathbf{L}_{kn}^{(2)} \boldsymbol{\Phi}_{n,M} \\ &= \sum_{n=0}^{\infty} \boldsymbol{\Psi}_n \sum_{k=0}^{\infty} \mathbf{L}_{nk}^{(2)} \boldsymbol{\Phi}_{k,M} - \sum_{n=0}^{\infty}\sum_{k=0}^{n-1} \boldsymbol{\Psi}_k \mathbf{L}_{kn}^{(2)} \boldsymbol{\Phi}_{n,M} \\ &= \sum_{n=0}^{\infty} \boldsymbol{\Psi}_n \sum_{k=0}^{n-2} \mathbf{L}_{nk}^{(2)} \boldsymbol{\Phi}_{k,M} , \end{aligned} \tag{459}$$

because Equation 457 a priori fulfills (given that $\mu \neq \mu_0$)

$$\mathbf{L}_{kn}^{(2)} \neq 0 \quad \Leftrightarrow \quad k \geqslant 2+n . \tag{460}$$

94 In this context, we do not refer to the convergence of any involved DA, i. e., every series will be treated as a (formal) power series.

95 The formalism has been constructed in such a way that at the reference scale "μ_0^2" there are no radiative corrections (cf. Section C.6).

Therefore, the evolution of moments may be expressed via ($n \geqslant 0$)

$$\boldsymbol{\Phi}_{n,M}(\mu) = \mathbf{L}_n^{(1)}(\mu,\mu_0)\,\boldsymbol{\Phi}_{n,M}(\mu_0) + \sum_{k=0}^{n-2} \mathbf{L}_{nk}^{(2)}(\mu,\mu_0)\,\boldsymbol{\Phi}_{k,M}(\mu_0)\,, \tag{461}$$

which is almost the intended result. Nevertheless, when aiming for a phenomenological evaluation (with a close analogy between the singlet and octet case) Equation 461 has to be modified. Accordingly, the present simultaneous evolution of Gegenbauer moments and the singlet decay constant should be separated. In order to recognize this connection, we may compare the solution of Equation 261 with Equation 461 at $n=0$:

i) When assuming $\alpha_S(Q) \ll 1$ ($Q = \mu, \mu_0$), we find for the related singlet decay constant (cf. Section C.1):

$$f_M^0(\mu) = f_M^0(\mu_0)\left[1 + \frac{2N_f}{\pi\beta_0}\left(\alpha_S(\mu) - \alpha_S(\mu_0)\right)\right]. \tag{462}$$

ii) Owing to the structure of Equation 458 and Equation 1463 within the limit

$$\begin{aligned}\lim_{n\to 0} \boldsymbol{\Phi}_{n,M}(\mu) &= \lim_{n\to 0}\left\{\mathbf{L}_n^{(1)}(\mu,\mu_0)\,\boldsymbol{\Phi}_{n,M}(\mu_0)\right\} \\ &= f_M^0(\mu_0)\left[1 + \frac{\alpha_S(\mu)-\alpha_S(\mu_0)}{2\pi\beta_0}\,(4N_f)\right]\vec{c}_{0,M}(\mu_0)\end{aligned} \tag{463}$$

Equation 462 can be reproduced.

In general, however, it is quite tricky assigning each contribution to its related source. For the study of $\eta^{(\prime)}$ mesons it is, therefore, useful to separate both cases from each other from the start. Consequently, the NLO kernels (cf. Equation 448), or at least the corresponding anomalous dimensions have to be adapted. According to the chain rule, a modified evolution kernel, only evolves the singlet DAs

$$\mu^2\frac{d}{d\,\mu^2}\begin{pmatrix}\phi_M^{(0)}(x,\mu^2)\\ \phi_M^{(g)}(x,\mu^2)\end{pmatrix} = \int_0^1 dy\,\widetilde{\mathbf{V}}\Big(x,y;\alpha_S\left(\mu^2\right)\Big)\begin{pmatrix}\phi_M^{(0)}(x,\mu^2)\\ \phi_M^{(g)}(x,\mu^2)\end{pmatrix}, \tag{464}$$

has the structure (cf. Equation 262, Equation 430)

$$\widetilde{\mathbf{V}}\Big(x,y;\alpha_S\left(\mu^2\right)\Big) = \mathbf{V}\Big(x,y;\alpha_S\left(\mu^2\right)\Big) - \frac{1}{2}\delta^{(4)}(x-y)\,\gamma_A\left(\alpha_S\left(\mu^2\right)\right). \tag{465}$$

Strictly speaking, only the diagonal contributions of Equation 430 are affected, leading to the shift $\left(m \geqslant 1;\, \boldsymbol{\gamma}_n^{D(0)} \equiv \boldsymbol{\gamma}_n^{(0)}\right)$

$$\boldsymbol{\gamma}_n^{D(m)} \to \boldsymbol{\gamma}_n^{D(m)} + \gamma_A^{(m)}\mathbb{1}_2 \equiv \boldsymbol{\gamma}_n^{(m)}, \tag{466}$$

which also entail adjusted eigenvalues (cf. Equation 449). Therefore, after replacing $\boldsymbol{\gamma}_n^{D(1)}$ with $\boldsymbol{\gamma}_n^{(1)}$ and modifying the NLO evolution operator $\mathcal{E}_j^{NLO}$ (cf. Section C.6), we get the desired analogon of Equation 447 for the flavor singlet sector[96] ($n \geqslant 2$):

$$\begin{aligned}\vec{c}_{n,M}\left(\mu^2\right) &= \mathbf{T}_n^{-1}\,\mathcal{E}_n^{NLO}\left(\mu^2,\mu_0^2\right)\mathbf{T}_n\,\vec{c}_{n,M}\left(\mu_0^2\right) \\ &\quad + \frac{\alpha_S\left(\mu^2\right)}{2\pi}\sum_{k=0}^{n-2}\mathbf{T}_n^{-1}\mathcal{D}_n^k\left(\mu^2,\mu_0^2\right)\mathcal{E}_k^{LO}\left(\mu^2,\mu_0^2\right)\mathbf{T}_k\,\vec{c}_{k,M}\left(\mu_0^2\right).\end{aligned} \tag{467}$$

In conclusion, Equation 462 combined with Equation 467 determine the NLO evolution of the $\eta^{(\prime)}$ meson twist-two DAs. Fortunately, the latter can also be incorporated in the study of higher twist effects, as discussed in the following subsection.

96 Due to G-parity, only those $\vec{c}_{n,M}$ with an even index "n" are non-vanishing.

3.4 HIGHER TWIST $\eta^{(\prime)}$ DISTRIBUTION AMPLITUDES

According to Section 2.4 higher twist corrections can be related to OPE contributions that are in general suppressed by extra powers of the assumed large momentum transfer and may, therefore, be considered negligible for many processes. For the intended investigation of hard exclusive processes, however, QCD predictions sometimes rely rather heavily on soft and higher twist corrections, in particular, when studying regions of moderate momentum transfer[97] [1, 281].

Consequently, we are obliged to carry out a systematic study of higher twist η and η' DAs, which takes into account the relevant meson mass and $\mathcal{O}(m_s)$ corrections as well as $SU(3)_F$-breaking effects related to the anomalous Ward identities, such as Equation 178.

3.4.1 *General remarks*

Towards a consistent description of higher twist effects two important questions emerge (cf. [128] for an extended discussion):

i) Can the QCD factorization ansatz be extended to the corresponding power suppressed corrections?

ii) Is it possible to incorporate all the relevant hadronic quantities, without causing an uncontrollable number of independent non-perturbative parameters?

While point i) has to be answered anew for each process individually (cf. Chapter 4), the second issue ii) can be solved on general grounds by an approximation of the higher twist DAs via a sensible extension of the partial conformal wave expansion approach.

In a nutshell, a central component of this technique (cf. [128, 143, 269, 274, 313–316]) is provided by exact non-local operator identities, known as equations of motion (EOM) (e. g., [313]). The latter allow to constrain superfluous degrees of freedom within the higher twist operators[98], such as the minus projections of Equation 404, and, correspondingly, entail recurrence relations between the involved DAs. Since these relations of moments have to be fulfilled identically, they also give rise to the desired solutions of higher twist DAs.

More specifically, the following steps are essential in setting up and solving the named recurrence relations:

1) In order to constrain all involved DAs, one has to derive a sufficient number of EOM (cf. Section C.7) first.

2) Corresponding definitions of the former are applicable when taking the EOM at (quasi) light-like separations and sandwiching them between adequate particle states.

3) After a possibly needed shift of coordinates, all resulting equations can be rewritten in terms of recurrence relations of moments. The latter are related to the reduced matrix

97 When focusing on the $\eta^{(\prime)}$ TFF, rather numerous measurements of this region exist (e. g., [312]), making it a valuable source of information on the corresponding DAs.

98 It has been shown that in the context of light-cone quantization [277] not all field components represent independent degrees of freedom. Instead, only the "+"-projections of the spinor fields and selected components of the four-potentials may be considered as free variables.

elements of Equation 418, because the n^{th} moment ($n \in \mathbb{N}_0$) of an arbitrary test function ϕ (on $[0,1]$) is given by:

$$M_n^\phi = \int_0^1 dx\, \xi_x^n \phi(x) \,. \tag{468}$$

4) As a final step, one may transform the relations of moments into (ordinary) DEs, and make use of the leading twist DA's conformal expansions.

In particular, the conformal expansion ansatz in point 4) is crucial for the systematic calculation of higher twist distributions. This results from the fact that standard EOM (cf. Section C.7) do not contain any quantum corrections, i. e., they exhibit all symmetries of the classical theory. Therefore, only operators with the same transformation properties are related, implying, that this technique exclusively connects contributions with the same conformal spin. Consequently, the higher twist DAs may be solved order by order in conformal spin, suggesting a formal expansion in terms of orthogonal polynomials. This new series, however, will (in general) not qualify as a conformal expansion anymore because its coefficients may contain contributions with different conformal spin, depending on the leading twist input[99].

Thus, for this approach to be consistent the specific order of accuracy has to be stated explicitly. According to the present state of the art [128, 142, 143, 274, 313–315], we restrict ourselves to a calculation of higher twist DAs up to NLO in conformal spin. There are two main reasons for this (apparent) limitation: one is phenomenological (cf. Section 4.3), the other theoretical. When focusing on the second aspect, it has to be emphasized, that higher twist DAs are in general numerous and not only interconnected by EOM alone. For instance, a proper calculation of twist four distributions has to include operators containing total derivatives in a systematic way (cf. [128]). A key issue in this context [314, 315] is to take into account contributions such as

$$\partial^2 \mathcal{O}_n^{\alpha_1 \cdots \alpha_n} \tag{469}$$

as well as (with the Lorentz indices $\alpha_1, \ldots, \alpha_n$ explicitly shown)

$$\partial_{\alpha_1} \mathcal{O}_n^{\alpha_1 \cdots \alpha_n} \tag{470}$$

of specific (leading twist) conformal operators $\mathcal{O}_n^{\alpha_1 \cdots \alpha_n}$. Notably, the class of contributions belonging to Equation 470 has to be treated order by order in conformal spin [315], providing nontrivial relations between the corresponding parameters [143]. Along these lines, a proliferation of new parameters[100] may be averted to some extend. However, the basic problem, which weakens the descriptive power of this approach, would remain. That is the inevitable appearance of additional non-perturbative parameters[101] which come along with an increasing order of conformal spin. Therefore, it is pivotal for this work to start with as few parameters as possible and extend the ansatz to the phenomenologically possible limits.

3.4.2 *Twist-three distribution amplitudes*

As a matter of fact, twist-three pseudoscalar meson DAs have been the object of several theoretical [271, 275, 317, 318] and phenomenological investigations, such as $B, D_{(s)} \to \pi, K$ (see [2, 319–322]

99 As discussed in the next subsection, one reason for that may, e. g., be found in the conventional definition of some higher twist DAs.

100 For instance, in the form of redundancies.

101 Which are at this point unconstrained.

and references therein), where they are belonging to the dominant contributions.
Nevertheless, the bulk part of this previous work is focusing on pions and kaons, while a reliable and consistent treatment of higher twist DAs for the $\eta - \eta'$ system is still missing.
Hence, with this subsection we attempt to further improve the aforementioned general survey by adding $\eta^{(\prime)}$ twist-three DAs, which (formally) include mass terms, anomaly contributions, as well as mixing effects. Moreover, we will partially discuss the choice of basis and the resulting impact on the (theoretical) applicability.

When considering the general remarks of Section 3.4.1 it seems reasonable to first identify the relevant higher twist DAs, before proceeding with the steps 1) to 4). Let us start with the two particle case. According to[102] Section 3.2.3, the only possible twist-three quark antiquark operators are featuring states with definite spin projections $s_{\overline{\Psi}} = \pm\frac{1}{2}$ and $s_{\Psi} = \mp\frac{1}{2}$. Therefore, it is convenient to define the pseudoscalar densities:

$$\overline{\Psi}(z_2 n)\, i\gamma_\pm\gamma_\mp\gamma_5\sqrt{2}T^A\Psi(z_1 n) = 2\overline{\Psi}_\pm(z_2 n)\, i\gamma_5\sqrt{2}T^A\Psi_\mp(z_1 n)\,, \tag{471}$$

with $j_{\overline{\Psi}} = 1$ $\left(j_{\overline{\Psi}} = \frac{1}{2}\right)$ and $j_{\Psi} = \frac{1}{2}$ $(j_{\Psi} = 1)$, respectively. Subsequently, the associated (auxiliary) twist-three DAs (cf. [128])

$$\langle 0|\overline{\Psi}(z_2 n)\, i\gamma_+\gamma_-\gamma_5 T^A\Psi(z_1 n)\,|M(P)\rangle\Big|_{n^2=0;\mu} = \frac{f_M^A}{\sqrt{2}}h_{3M}^A\int_0^1 dx\, e^{-iz_{21}^x(P\cdot n)}\phi_{\uparrow\downarrow}^{A;M}(x,\mu)\,, \tag{472}$$

$$\langle 0|\overline{\Psi}(z_2 n)\, i\gamma_-\gamma_+\gamma_5 T^A\Psi(z_1 n)\,|M(P)\rangle\Big|_{n^2=0;\mu} = \frac{f_M^A}{\sqrt{2}}h_{3M}^A\int_0^1 dx\, e^{-iz_{21}^x(P\cdot n)}\phi_{\downarrow\uparrow}^{A;M}(x,\mu)\,, \tag{473}$$

may be defined. According to Equation 398 for the interacting theory, and Equation 412, the underlying conformal operator structure implies the expansions (cf. [128] and Section A.12):

$$\phi_{\uparrow\downarrow}^{A;M}\left(x,\mu^2\right) = 2\bar{x}\sum_{n=0}^{\infty}\kappa_n^{A;M}\left(\mu^2\right)P_n^{(1,0)}(\xi_x)\,, \tag{474}$$

$$\phi_{\downarrow\uparrow}^{A;M}\left(x,\mu^2\right) = 2x\sum_{n=0}^{\infty}\overline{\kappa}_n^{A;M}\left(\mu^2\right)P_n^{(0,1)}(\xi_x)\,. \tag{475}$$

Fortunately, (as mentioned in Section 3.4.1) all expansion coefficients can be related to other involved non-perturbative parameters[103] when using adequate EOM (cf. Section C.7). The latter, however, are usually formulated in terms of the pseudoscalar (cf. Equation 327) and tensor (see Equation 328) twist-three distributions, whose Lorentz structures resemble the generally accepted standard choices [45, 64, 323–326]. In fact, the set of DAs $\left\{\phi_{\uparrow\downarrow}^{A;M}, \phi_{\downarrow\uparrow}^{A;M}\right\}$ can be converted into (cf. [128]) $\left\{\phi_{3M}^{A;p}, \phi_{3M}^{A;\sigma}\right\}$ and vice versa, by using the transformations[104]:

$$\phi_{3M}^{A;p}\left(x,\mu^2\right) = \frac{1}{2}\left(\phi_{\uparrow\downarrow}^{A;M}\left(x,\mu^2\right) + \phi_{\downarrow\uparrow}^{A;M}\left(x,\mu^2\right)\right)\,, \tag{476}$$

$$\frac{d}{dx}\phi_{3M}^{A;\sigma}\left(x,\mu^2\right) = 3\left(\phi_{\uparrow\downarrow}^{A;M}\left(x,\mu^2\right) - \phi_{\downarrow\uparrow}^{A;M}\left(x,\mu^2\right)\right)\,, \tag{477}$$

which results from Equation 1075 and integration by parts[105]. Therefore, without loss of generality, we may use Equation 327 and Equation 328 instead of Equation 472 as well as Equation 473. For this purpose, the formal structure of $\phi_{3M}^{A;\sigma}$ along with $\phi_{3M}^{A;p}$ has to be deduced from the given

102 At this point we want to resume the discussion of Section 3.2.3, with emphasize on the blueprint of Equation 404.
103 As shown below, this will reduce the total number of relevant input parameters.
104 The obvious counterparts to Equation 477 and Equation 476 are Equation 1518 along with Equation 1519.
105 A posteriori, all surface terms of the tensor twist-three quark-antiquark DAs vanish.

conformal expansions Equation 472, Equation 473, and their coefficients. Apparently, an explicit calculation (cf. Equation 1520) as carried out below will reveal for the first view expansion coefficients ($0 \leqslant n \leqslant 3$)

$$\kappa_n^{A;M} = (-1)^n \, \overline{\kappa}_n^{A;M} \, . \tag{478}$$

This is completely analogous to the pion case [142] which inspires us to (formally) extend Equation 478 to an additional $n=4$, while still truncating all coefficients with $n \geqslant 5$. When including Equation 478 into our considerations, we get[106] (cf. Section A.12)

$$\begin{aligned} \phi_{3M}^{A;p}(x) &= \kappa_0^{A;M} + \left(\kappa_2^{A;M} - \kappa_1^{A;M}\right) C_2^{(1/2)}(\xi_x) \\ &\quad + \left(\kappa_4^{A;M} - \kappa_3^{A;M}\right) C_4^{(1/2)}(\xi_x) + \frac{\kappa_{\log}^{A;M}}{2} \log x\bar{x} + \dots \, , \end{aligned} \tag{479}$$

$$\begin{aligned} \phi_{3M}^{A;\sigma}(x) &= 6x\bar{x} \left(\kappa_0^{A;M} - \kappa_1^{A;M} - \frac{\kappa_{\log}^{A;M}}{2} + \frac{\kappa_2^{A;M} - \kappa_3^{A;M}}{6} C_2^{(3/2)}(\xi_x) + \frac{\kappa_4^{A;M}}{15} C_4^{(3/2)}(\xi_x) \right) \\ &\quad + 3x\bar{x} \, \kappa_{\log}^{A;M} \log x\bar{x} + \dots \, . \end{aligned} \tag{480}$$

In Equation 479 and Equation 480 the occurrence of logarithmic contributions has been anticipated which also give finite admixtures to the constant polynomial's prefactor[107]. The remaining polynomial contributions, however, are a natural consequence of Equation 478 and Equation 1221 – Equation 1223. In other words, the conformal expansions Equation 474 and Equation 475 imply a power series representation of $\phi_{3M}^{A;p}$ and $\phi_{3M}^{A;\sigma}$ in terms of Gegenbauer polynomials $C_n^{(1/2)}$ and $C_n^{(3/2)}$, respectively (cf. [128, 142]). As addressed in Section 3.4.1, the resulting expressions (i. e., Equation 479 along with Equation 480) cannot be classified as conformal expansions anymore, because the involved polynomial's prefactors are differences of coefficients with neighboring conformal spins (cf. [128]).

Other possible twist-three DAs may arise from the quark-antiquark-gluon (light-cone) operators

$$\overline{\psi}_+ \sigma_{\mu\nu} \gamma_5 \mathcal{G}_{+\perp} \sqrt{2} T^A \psi_+ \, , \tag{481}$$

with $j_{\overline{\Psi}} = 1 = j_\Psi$ and $j_\mathcal{G} = 3/2$. Evidently Equation 481 has the non-vanishing component $\overline{\psi} \sigma_{+\perp} \gamma_5 \mathcal{G}_{+\perp} \sqrt{2} T^A \psi$ which corresponds to the leading twist projection of Equation 329 (cf. also [128, 142]). Therefore, the asymptotic form of $\Phi_{3M}^A(\underline{\alpha})$ (cf. Equation 412) is proportional to $\sim 360 \alpha_1 \alpha_2 \alpha_3^2$, while contributions with conformal spin $j \geqslant 7/2$ can be absorbed into the full conformal expansion[108] [271]:

$$\Phi_{3M}^A(\underline{\alpha}) = 360 \alpha_1 \alpha_2 \alpha_3^2 \left[1 + \lambda_{3M}^A (\alpha_1 - \alpha_2) + \omega_{3M}^A \tfrac{1}{2} (7\alpha_3 - 3) + \dots \right] , \tag{482}$$

which implies the corresponding non-perturbative coefficients [271]

$$\langle 0 | \overline{\psi} T^A \sigma_+{}^\zeta \gamma_5 \, [iD_+, g\mathcal{G}_{+\zeta}] \, \psi - i \tfrac{3}{7} \partial_+ \overline{\psi} T^A \sigma_+{}^\zeta \gamma_5 g \mathcal{G}_{+\zeta} \psi | M(P) \rangle = \sqrt{2} i \left[f_{3M}^A \omega_{3M}^A \right] \tfrac{3}{28} P_+^3 \, , \tag{483}$$

106 When inserting $\kappa_{\log}^{A;M} = 0$, $\kappa_0^{A;M} = R$, $\kappa_1^{A;M} = 0$, $\kappa_2^{A;M} = 30\omega^{7/2}$, $\kappa_3^{A;M} = 3\omega^{9/2}$ and $\kappa_4^{A;M} = \frac{3}{2}\left[4\omega_1^{11/2} - \omega_2^{11/2}\right]$ the results of [142] are reproduced (see also [128]).

107 The latter arise when integrating the logarithmic contributions of Equation 477.

108 For the derivation of Equation 482, we adapt all relevant standard definitions of [271] to our needs, by retrofitting the involved matrix elements with adequate flavor structures.

as well as

$$\langle 0|\overline{\psi}\,T^A i\overleftarrow{D}_+\sigma_+{}^\zeta\gamma_5 g\mathcal{G}_{+\zeta}\psi - \overline{\psi}\,T^A\sigma_+{}^\zeta\gamma_5 g\mathcal{G}_{+\zeta} i\overrightarrow{D}_+\psi|M(P)\rangle = \sqrt{2}i\left[f_{3M}^A\lambda_{3M}^A\right]\tfrac{1}{14}P_+^3\,, \quad (484)$$

and (cf. Equation 329, [271])

$$\langle 0|\overline{\psi}\,T^A\sigma_+{}^\zeta\gamma_5 g\mathcal{G}_{+\zeta}\psi|M(P)\rangle = \sqrt{2}if_{3M}^A P_+^2\,. \quad (485)$$

While for π^0 and $\eta^{(\prime)}$ mesons the structure proportional to[109] $Y^{(12)3}_{9/2,3}(\underline{\alpha})$ (cf. Equation 1227) is prohibited, due to G-parity, it will be present in the context of kaons (cf. Section C.9). Furthermore, the associated LO evolution is given by[110] (cf. [75, 327–329]):

$$f_{3M}^A\left(\mu^2\right) = \left[\frac{\alpha_S\left(\mu^2\right)}{\alpha_S\left(\mu_0^2\right)}\right]^{\frac{55}{9\beta_0}} f_{3M}^A\left(\mu_0^2\right) + \dots\,, \quad (486)$$

$$\left[f_{3M}^A\omega_{3M}^A\right]\left(\mu^2\right) = \left[\frac{\alpha_S\left(\mu^2\right)}{\alpha_S\left(\mu_0^2\right)}\right]^{\frac{104}{9\beta_0}} \left[f_{3M}^A\omega_{3M}^A\right]\left(\mu_0^2\right) + \dots\,, \quad (487)$$

$$\left[f_{3M}^A\lambda_{3M}^A\right]\left(\mu^2\right) = \left[\frac{\alpha_S\left(\mu^2\right)}{\alpha_S\left(\mu_0^2\right)}\right]^{\frac{139}{18\beta_0}} \left[f_{3M}^A\lambda_{3M}^A\right]\left(\mu_0^2\right) + \dots\,. \quad (488)$$

Besides discarded higher order corrections, the ellipses also represent possible admixtures of "$f_M^A c_{n,M}^{(A)}$" ($n \leqslant 2$) multiplied by a quark mass of appropriate flavor. When included into the mentioned higher twist DAs, those mixing effects are of $\mathcal{O}\left(m_\psi^2\right)$. Hence, they are beyond the phenomenological scope of this work and will be neglected in our numerical evaluations.

Additional mixing effects may occur when incorporating contributions of higher conformal spin into Equation 482. In fact, the three-particle representations of the collinear conformal group are degenerate (see [128] and references therein), i. e., there may exist several different operators with the same conformal spin[111]. Consequently, one would face RG effects of similar complexity as described in Section 3.3 (cf. [142]). For the discussed reasons, however, we begin with contributions up to NLO in conformal spin.

Let us now derive the general relations among the named $\eta^{(\prime)}$ DAs, followed by a discussion of the resulting constraints on the former.
For this purpose we implement the aforementioned EOM (cf. Section C.7), which have been adapted to our specific needs, such as the essential incorporation of the $\eta-\eta'$ mixing, or the straightforward applicability of different bases. When combining the former with Equation 327–

109 Using the given input $j_1, j_2 = 1$ and $j_3 = 3/2$.
110 In fact, these mixing effects arise from the light-ray-operator technique (cf. [75]). Owing to this formalism, valid combinations of f_{3M}^A, λ_{3M}^A, and ω_{3M}^A are restricted to the cases Equation 483 as well as Equation 484.
111 As explicitly shown by [142], for $j = 11/2$ (cf. Equation 482) there exist two distinct structures with unequal non-perturbative coefficients. The latter already mix at LO.

Equation 329, a system of integral equations between the two- and three particle DAs can be devised[112] ($n^2=0$):

$$P_+\int_0^1 dx\, e^{i\xi_x P_+}\phi_{3M}^{A;\sigma}(x) = -3i\int_0^1 dx\, e^{i\xi_x P_+}\xi_x\phi_{3M}^{A;p}(x) - 6R_{3M}^A P_+\int_{-1}^1 dv\,\Phi_{3M}^A(\underline{z},P_+) + 3i\sum_{B\in I}\left[\rho_-^M\right]^{AB}\int_0^1 dx\, e^{i\xi_x P_+}\phi_M^B(x)\,, \tag{489}$$

$$\int_0^1 dx\, e^{i\xi_x P_+}\phi_{3M}^{A;p}(x) = \int_0^1 dx\, e^{i\xi_x P_+}\left[1+\frac{i}{3}\xi_x P_+\right]\phi_{3M}^{A;\sigma}(x) - 2iR_{3M}^A P_+\int_{-1}^1 dv\, v\,\Phi_{3M}^A(\underline{z},P_+) + \sum_{B\in I}\left[\rho_+^M\right]^{AB}\int_0^1 dx\, e^{i\xi_x P_+}\phi_M^B(x)\,, \tag{490}$$

which include the definitions[113] (cf. Equation 1070, Equation 1071)

$$R_{3M}^A = \frac{f_{3M}^A}{f_M^A h_{3M}^A}\,,\quad \left[\rho_+^M\right]^{AB} = \frac{\alpha_{AB}\, f_M^B}{f_M^A h_{3M}^A}\,,\quad \left[\rho_-^M\right]^{AB} = \frac{\beta_{AB}\, f_M^B}{f_M^A h_{3M}^A}\,. \tag{491}$$

As an intermediate step ($n\neq 0$, $\underline{z}=(-1,1,v)$), it is convenient [313] to introduce recurrence relations[114]:

$$n\, M_{n-1}^{\phi_{3M}^{A;\sigma}} = 3\, M_{n+1}^{\phi_{3M}^{A;p}} - 3\sum_{B\in I}\left[\rho_-^M\right]^{AB} M_n^{\phi_M^B} - 6nR_{3M}^A\int_{-1}^1 dv\,\ll(\alpha_1-\alpha_2-v\,\alpha_3)^{n-1}\gg, \tag{492}$$

$$(3+n)\, M_n^{\phi_{3M}^{A;\sigma}} = 3\, M_n^{\phi_{3M}^{A;p}} - 3\sum_{B\in I}\left[\rho_+^M\right]^{AB} M_n^{\phi_M^B} + 6nR_{3M}^A\int_{-1}^1 dv\, v\,\ll(\alpha_1-\alpha_2-v\,\alpha_3)^{n-1}\gg, \tag{493}$$

for the involved moments (cf. Equation 468) as well as [142, 313]

$$(-i)^n\,\frac{\partial^n}{\partial\tau^n}\Phi_{3M}^A(\underline{z},\tau)\Big|_{\tau=0} = \int\mathcal{D}\underline{\alpha}\,[-\underline{z}\cdot\underline{\alpha}]^n\,\Phi_{3M}^A(\underline{\alpha}) \equiv \ll(-\underline{z}\cdot\underline{\alpha})^n\gg, \tag{494}$$

112 When focusing on the SO and QF basis, the index "I" is restricted to $I=\{0,1,\ldots,8\}$ and $I=\{q,s,1,\ldots,7\}$, respectively (cf. Section C.7).

113 In Section A.1 the abbreviations α_{AB} and β_{AB} have been introduced which arise canonically in the context of EOM (cf. Table 21, Equation 1072).

114 Here, we are using the standard choice $\underline{z}=(-1,1,v)$, which includes a dependence on v.

by expanding Equation 489 and Equation 490 in powers of "P_+". In this context, the self-evident transformation of the measure[115]

$$\int_0^1 dx\, \xi_x^n\, \varphi_{3M}^{A;(1)}(x) \equiv \int_0^1 dx\, \xi_x^n \left[\int_0^x d\alpha_1 \int_0^{\bar{x}} d\alpha_2\, \frac{2\Phi_{3M}^A(\underline{\alpha})}{\alpha_3} \Big|_{\alpha_3=1-\alpha_1-\alpha_2} \right]$$
$$= \int_{-1}^1 dv \ll (\alpha_1 - \alpha_2 - v\,\alpha_3)^n \gg , \tag{495}$$

$$\int_0^1 dx\, \xi_x^n\, \varphi_{3M}^{A;(2)}(x) \equiv \int_0^1 dx\, \xi_x^n \left[\int_0^x d\alpha_1 \int_0^{\bar{x}} d\alpha_2\, \frac{2\,(\alpha_1 - \alpha_2 - \xi_x)\,\Phi_{3M}^A(\underline{\alpha})}{\alpha_3^2} \Big|_{\alpha_3=1-\alpha_1-\alpha_2} \right]$$
$$= \int_{-1}^1 dv\, v \ll (\alpha_1 - \alpha_2 - v\,\alpha_3)^n \gg , \tag{496}$$

not only enables an overall harmonized notation, but simultaneously induces the useful auxiliary functions[116] $\varphi_{3M}^{A;(1)}$ and $\varphi_{3M}^{A;(2)}$. When further following the canonical approach (cf. [142, 330]), the two-particle twist-three DAs $\phi_{3M}^{A;p}$ and $\phi_{3M}^{A;\sigma}$ have to be expressed via the related leading twist DAs. Accordingly, Equation 492 and Equation 493 may be combined to

$$M_n^{\phi_{3M}^{A;p}} = \frac{n-1}{n+1} M_{n-2}^{\phi_{3M}^{A;p}} + 2\,(n-1)\, R_{3M}^A \left[M_{n-2}^{\varphi_{3M}^{A;(1)}} + \frac{n-2}{n+1} M_{n-3}^{\varphi_{3M}^{A;(2)}} \right]$$
$$+ \sum_{B\in I} \left[\rho_-^M\right]^{AB} M_{n-1}^{\phi_M^B} - \frac{n-1}{n+1} \sum_{B\in I} \left[\rho_+^M\right]^{AB} M_{n-2}^{\phi_M^B} + \mathcal{N}\delta_{n0}\,, \tag{497}$$

$$M_n^{\phi_{3M}^{A;\sigma}} = \frac{n-1}{n+3} M_{n-2}^{\phi_{3M}^{A;\sigma}} + \frac{6}{n+3} R_{3M}^A \left[n\, M_{n-1}^{\varphi_{3M}^{A;(2)}} + (n-1)\, M_{n-2}^{\varphi_{3M}^{A;(1)}} \right]$$
$$- \frac{3}{n+3} \left[\sum_{B\in I} \left[\rho_+^M\right]^{AB} M_n^{\phi_M^B} - \sum_{B\in I} \left[\rho_-^M\right]^{AB} M_{n-1}^{\phi_M^B} \right] + \mathcal{N}\delta_{n0}\,, \tag{498}$$

which includes an arbitrary normalization condition, expressed by the associated constant "$\mathcal{N}$". The latter will give rise to initial conditions when transforming Equation 497 and Equation 498 into (ordinary) DE. For instance, Equation 497 implies the first order equation (cf. Section C.8)

$$4x\bar{x}\, \frac{d}{dx} \phi_{3M}^{A;p}(x) = \mathcal{L}_{3M}^{A;p}(x)\,, \tag{499}$$

together with (cf. Section C.8)

$$\mathcal{L}_{3M}^{A;p}(x) = R_{3M}^A \left[\xi_x \frac{d^2 \varphi_{3M}^{A;(1)}(x)}{dx^2} - 2\, \frac{d\varphi_{3M}^{A;(1)}(x)}{dx} + \frac{d^2 \varphi_{3M}^{A;(2)}(x)}{dx^2} \right]$$
$$+ \sum_{B\in I} \left[\rho_+^M\right]^{AB} \frac{d\phi_M^B(x)}{dx} + \sum_{B\in I} \left[\rho_-^M\right]^{AB} \left[2\phi_M^B(x) - \xi_x \frac{d\phi_M^B(x)}{dx} \right], \tag{500}$$

which allows a separation according to the specific input and prefactors. Therefore, a general solution of Equation 499 ("$C_0^{\mathcal{L}}$" is the corresponding constant of integration)

$$\phi_{3M}^{A;p}(x) = \frac{1}{4} \int_0^x dv\, \frac{1}{\bar{v}} \mathcal{L}_{3M}^{A;p}(v) - \frac{1}{4} \int_x^1 dv\, \frac{1}{v} \mathcal{L}_{3M}^{A;p}(v) + C_0^{\mathcal{L}} \tag{501}$$

115 Equation 495 and Equation 496 provide the transition between the formalism of [142] and [271].

116 Up to the assumed accuracy, $\varphi_{3M}^{A;(1)}$ and $\varphi_{3M}^{A;(2)}$ are proportional to $x^2\bar{x}^2$, while their first derivatives are $\sim x\bar{x}$. Therefore, the appearing surface terms vanish.

may be written as $(\mathcal{N} \overset{!}{=} 1)$

$$\phi_{3M}^{A;p}(x) = 1 + R_{3M}^{A}\phi_{3M}^{A;(g)}(x) + \sum_{B\in I}\left[\rho_{+}^{M}\right]^{AB}\phi_{3M}^{B;(+)}(x) + \sum_{B\in I}\left[\rho_{-}^{M}\right]^{AB}\phi_{3M}^{B;(-)}(x)\,, \tag{502}$$

with the partial solutions (cf. Section C.8)

$$\begin{aligned}\phi_{3M}^{A;(g)}(x) = {}& \frac{1}{4}\int_0^x dv\,\frac{1}{\bar v}\left[\xi_v\frac{d^2\varphi_{3M}^{A;(1)}(v)}{dv^2} - 2\frac{d\varphi_{3M}^{A;(1)}(v)}{dv} + \frac{d^2\varphi_{3M}^{A;(2)}(v)}{dv^2}\right]\\ & - \frac{1}{4}\int_x^1 dv\,\frac{1}{v}\left[\xi_v\frac{d^2\varphi_{3M}^{A;(1)}(v)}{dv^2} - 2\frac{d\varphi_{3M}^{A;(1)}(v)}{dv} + \frac{d^2\varphi_{3M}^{A;(2)}(v)}{dv^2}\right]\,,\end{aligned} \tag{503}$$

$$\phi_{3M}^{A;(+)}(x) = \frac{1}{4}\int_0^x dv\,\frac{1}{\bar v}\left[\frac{d}{dv}\phi_M^A(v)\right] - \frac{1}{4}\int_x^1 dv\,\frac{1}{v}\left[\frac{d}{dv}\phi_M^A(v)\right]\,, \tag{504}$$

$$\phi_{3M}^{A;(-)}(x) = \frac{1}{4}\int_0^x dv\,\frac{1}{\bar v}\left[2\phi_M^A(v) - \frac{d}{dv}\phi_M^A(v)\right] - \frac{1}{4}\int_x^1 dv\,\frac{1}{v}\left[2\phi_M^A(v) + \frac{d}{dv}\phi_M^A(v)\right]\,, \tag{505}$$

as implied by the related normalization condition

$$\int_0^1 dx\,\phi_{3M}^{A;p}(x) \overset{!}{=} 1\,. \tag{506}$$

Hence, the expressions up to NLO in conformal spin are given by

$$\phi_{3M}^{A;(g)}(x) = 30C_2^{(1/2)}(\xi_x) + 10\lambda_{3M}^{A}C_3^{(1/2)}(\xi_x) - 3\omega_{3M}^{A}C_4^{(1/2)}(\xi_x)\,, \tag{507}$$

$$\begin{aligned}\phi_{3M}^{A;(+)}(x) = {}& 3 + 18c_{2,M}^{(A)} + \frac{27}{2}c_{1,M}^{(A)}C_1^{(1/2)}(\xi_x) + 15c_{2,M}^{(A)}C_2^{(1/2)}(\xi_x)\\ & + \frac{3}{2}\left(1 + 3c_{1,M}^{(A)} + 6c_{2,M}^{(A)}\right)\log\bar x + \frac{3}{2}\left(1 - 3c_{1,M}^{(A)} + 6c_{2,M}^{(A)}\right)\log x,\end{aligned} \tag{508}$$

$$\begin{aligned}\phi_{3M}^{A;(-)}(x) = {}& -9c_{1,M}^{(A)} - \left(\frac{3}{2} + 27c_{2,M}^{(A)}\right)C_1^{(1/2)}(\xi_x) - 3c_{1,M}^{(A)}C_2^{(1/2)}(\xi_x)\\ & - \frac{9}{2}c_{2,M}^{(A)}C_3^{(1/2)}(\xi_x) - \frac{3}{2}\left(1 + 3c_{1,M}^{(A)} + 6c_{2,M}^{(A)}\right)\log\bar x\\ & - \frac{3}{2}\left(1 - 3c_{1,M}^{(A)} + 6c_{2,M}^{(A)}\right)\log x\,.\end{aligned} \tag{509}$$

Analogously, for Equation 498 we get the first order DE (cf. Section C.8)

$$4\xi_x\phi_{3M}^{A;\sigma}(x) + 4x\bar x\frac{d}{dx}\phi_{3M}^{A;\sigma}(x) = \mathcal{L}_{3M}^{A;\sigma}(x)\,, \tag{510}$$

with the general solution[117] ("$\overline{C}_0^{\mathcal{L}}$" is a constant)

$$\phi_{3M}^{A;\sigma}(x) = \frac{x\bar x}{4}\left[\int_0^x dv\left(\frac{1}{\bar v^2} + \frac{2}{\bar v}\right)\mathcal{L}_{3M}^{A;\sigma}(v) - \int_x^1 dv\left(\frac{1}{v^2} + \frac{2}{v}\right)\mathcal{L}_{3M}^{A;\sigma}(v)\right] + x\bar x\,\overline{C}_0^{\mathcal{L}}\,, \tag{511}$$

including (cf. Section C.8):

$$\begin{aligned}\mathcal{L}_{3M}^{A;\sigma}(x) = {}& -6R_{3M}^{A}\left(\xi_x\frac{d\varphi_{3M}^{A;(2)}(x)}{dx} + \frac{d\varphi_{3M}^{A;(1)}(x)}{dx}\right)\\ & - 6\sum_{B\in I}\left[\rho_{+}^{M}\right]^{AB}\xi_x\phi_M^B(x) + 6\sum_{B\in I}\left[\rho_{-}^{M}\right]^{AB}\phi_M^B(x)\,.\end{aligned} \tag{512}$$

117 Here, we use $\frac{1}{v^2\bar v^2} = \left(\frac{1}{v^2} + \frac{2}{v}\right) + \left(\frac{1}{\bar v^2} + \frac{2}{\bar v}\right)$.

PION	μ_0	KAON	μ_0
$f_{3\pi}$	$0.0045(15)\,\mathrm{GeV}^2$	f_{3K}	$0.0045(15)\,\mathrm{GeV}^2$
$\omega_{3\pi}$	$-1.5(7)$	ω_{3K}	$-1.2(7)$
$\lambda_{3\pi}$	0	λ_{3K}	$1.6(4)$

Table 7: Hadronic twist-three parameters for the pion and kaon case, taken from [271, 331] (at the reference scale $\mu_0 = 1$ GeV).

In particular, Equation 511 can be written as:

$$\phi_{3M}^{A;\sigma}(x) = 6\,x\bar{x} + R_{3M}^{A}\widetilde{\phi}_{3M}^{A;(g)}(x) + \sum_{B\in I}\left[\rho_{+}^{M}\right]^{AB}\widetilde{\phi}_{3M}^{B;(+)}(x) + \sum_{B\in I}\left[\rho_{-}^{M}\right]^{AB}\widetilde{\phi}_{3M}^{B;(-)}(x)\,, \tag{513}$$

together with[118]

$$\begin{aligned}\widetilde{\phi}_{3M}^{A;(g)}(x) = -\frac{3}{2}x\bar{x}\Bigg[&\int_0^x dv\left(\frac{1}{\bar{v}^2}+\frac{2}{\bar{v}}\right)\left[\xi_v\frac{d\varphi_{3M}^{A;(2)}(v)}{dv}+\frac{d\varphi_{3M}^{A;(1)}(v)}{dv}\right]\\ &-\int_x^1 dv\left(\frac{1}{v^2}+\frac{2}{v}\right)\left[\xi_v\frac{d\varphi_{3M}^{A;(2)}(v)}{dv}+\frac{d\varphi_{3M}^{A;(1)}(v)}{dv}\right]\Bigg]\,,\end{aligned} \tag{514}$$

$$\widetilde{\phi}_{3M}^{A;(+)}(x) = -\frac{3}{2}x\bar{x}\left[\int_0^x dv\,\frac{1}{\bar{v}^2}\phi_M^A(v)+\int_x^1 dv\,\frac{1}{v^2}\phi_M^A(v)\right]\,, \tag{515}$$

$$\widetilde{\phi}_{3M}^{A;(-)}(x) = \frac{3}{2}x\bar{x}\left[\int_0^x dv\,\frac{2\bar{v}+1}{\bar{v}^2}\phi_M^A(v)-\int_x^1 dv\,\frac{2v+1}{v^2}\phi_M^A(v)\right]\,. \tag{516}$$

Thus, the resulting NLO expressions are:

$$\widetilde{\phi}_{3M}^{A;(g)}(x) = 6x\bar{x}\left[5\left(1-\frac{\omega_{3M}^{A}}{10}\right)C_2^{(3/2)}(\xi_x)+\lambda_{3M}^{A}C_3^{(3/2)}(\xi_x)\right]\,, \tag{517}$$

$$\begin{aligned}\widetilde{\phi}_{3M}^{A;(+)}(x) = 6x\bar{x}\Bigg[&\frac{3}{2}+15c_{2,M}^{(A)}+3c_{1,M}^{(A)}C_1^{(3/2)}(\xi_x)+\frac{3}{2}c_{2,M}^{(A)}C_2^{(3/2)}(\xi_x)\Bigg]\\ &+9x\bar{x}\left(1-3c_{1,M}^{(A)}+6c_{2,M}^{(A)}\right)\log x+9x\bar{x}\left(1+3c_{1,M}^{(A)}+6c_{2,M}^{(A)}\right)\log\bar{x}\,,\end{aligned} \tag{518}$$

$$\begin{aligned}\widetilde{\phi}_{3M}^{A;(-)}(x) = -6x\bar{x}\Bigg[&\frac{15}{2}c_{1,M}^{(A)}+\frac{15}{2}c_{2,M}^{(A)}C_1^{(3/2)}(\xi_x)\Bigg]\\ &+9x\bar{x}\left(1-3c_{1,M}^{(A)}+6c_{2,M}^{(A)}\right)\log x-9x\bar{x}\left(1+3c_{1,M}^{(A)}+6c_{2,M}^{(A)}\right)\log\bar{x}\,.\end{aligned} \tag{519}$$

Together with adequate rules of replacement (cf. Section C.9) our results also reproduce the findings of [271, 332]. This means, we not only confirm the general structures Equation 502 and Equation 513, but also replicate Equation 503-Equation 505 as well as Equation 514-Equation 516. Another important point is that $\mathcal{L}_{3M}^{A;p}$ and $\mathcal{L}_{3M}^{A;\sigma}$ receive contributions of different source terms which in general split up into three categories (cf. also [313]):

- Contributions of genuine twist-three, i. e., those related to the corresponding three particle DAs.

118 In essence, the identities $\left(\frac{1}{v^2}+\frac{2}{v}\right)\xi_v = 4-\frac{1}{v^2}$ and $\left(\frac{1}{\bar{v}^2}+\frac{2}{\bar{v}}\right)\xi_v = \frac{1}{\bar{v}^2}-4$ imply additional corrections $\sim 6x\bar{x}$ to Equation 515. The latter, however, may be canceled via adequate constants of integration (cf. Equation 511).

- Terms affiliated to quark mass corrections.
- Wandzura-Wilczek type contributions [295, 313, 333] of twist-two operators.

While the latter are present in the pion and kaon case, their $\eta^{(\prime)}$ meson's counterpart is altered by effects related to the axial anomaly. This presents a substantial problem when trying to estimate the named twist-three (NLO) parameters due to a lack of information about the corresponding flavor singlet contribution. In fact, no SVZ sum rule or lattice calculation for, e. g., f_{3M}^R or ω_{3M}^R ($R = q, s$) were available until recently (see discussion in [334]). The latter, however, are vital for a meaningful definition of $\phi_{3M}^{A;p}$ and $\phi_{3M}^{A;\sigma}$, forcing us to adopt, e. g., pion or kaon parameters (cf. Table 7) as possible crude estimates. This may be done via the state mixing assumption (cf. Section 3.1.1), i. e., Equation 485 gives rise to a particle independent constant f_{3R} ($R = q, s$):

$$\langle 0|\overline{\psi}\, T^R \sigma_+^{\ \zeta} \gamma_5 g \mathcal{G}_{+\zeta} \psi|\eta_R(P)\rangle = \sqrt{2} i f_{3R} P_+^2\,, \tag{520}$$

which then may be identified with (at the scale $\mu_0 = 1$ GeV)

$$f_{3s} \approx f_{3K}\,, \quad f_{3q} \approx f_{3\pi}\,. \tag{521}$$

Analogously, the parameters (cf. also [335])

$$\omega_{3s} \approx \omega_{3K}\,, \quad \omega_{3q} \approx \omega_{3\pi} \tag{522}$$

can be estimated (cf. Table 7). As shown below, the NLO (and beyond) conformal contributions are suppressed by extra factors of quark masses, while the leading corrections are proportional to (cf. Section C.8 for the SO analogon)

$$f_M^R h_{3M}^R =: \frac{h_M^R}{2m_R} \quad (R = q, s) \tag{523}$$

and do, therefore, not suffer from such effects. Fortunately, all parameters $\{h_M^R\}_{R,M}$ are accessible via the Ward identities of Equation 178, which imply[119]

$$\begin{aligned} m_M^2 f_M^A &= \sum_{B \in I_{SO}} \alpha_{AB} f_M^B h_{3M}^B + \sqrt{3} a_M \delta^{A0} \\ &= \sum_{B \in I_{QF}} \alpha_{AB} f_M^B h_{3M}^B + \sqrt{2} a_M \delta^{Aq} + a_M \delta^{As}\,, \end{aligned} \tag{524}$$

when using the densities (cf. partially conserved axial current (PCAC) relations for Equation 171, Equation 179 and Equation 248)

$$\langle 0|\partial^\mu j_{\mu 5}^A|M(P)\rangle = m_M^2 f_M^A\,, \tag{525}$$

$$\langle 0|j_5^A|M(P)\rangle = f_M^A h_{3M}^A\,, \tag{526}$$

$$\langle 0|2\omega|M(P)\rangle = a_M\,. \tag{527}$$

Besides, we will also use $(R = q, s)$

$$a_R = \langle 0|2\omega|\eta_R(P)\rangle\,. \tag{528}$$

In the assumed $SU(2)_I$ limit Equation 524 boils down to (cf. Table 21)

$$H_M^A = m_M^2 F_M^A - a_M\,, \tag{529}$$

119 Again, we make use of the abbreviations $I_{SO} = \{0, 1, \ldots, 8\}$ and $I_{QF} = \{q, s, 1, \ldots, 7\}$.

PARAMETER	FOR [9]	FOR [10]
h_q	0.0017 ± 0.0038	-0.0135 ± 0.0043
h_s	0.0876 ± 0.0057	0.1116 ± 0.0063
a_η	0.0221 ± 0.0021	0.0302 ± 0.0024
$a_{\eta'}$	0.0568 ± 0.0018	0.0666 ± 0.0021
f_η^q	108.47 ± 2.55	108.25 ± 3.75
f_η^s	-111.18 ± 5.51	-141.80 ± 6.52
$f_{\eta'}^q$	88.78 ± 2.52	93.11 ± 3.68
$f_{\eta'}^s$	135.84 ± 6.38	164.86 ± 6.89
h_η^q	0.0013 ± 0.0029	-0.0102 ± 0.0033
h_η^s	-0.0547 ± 0.0034	-0.0728 ± 0.0034
$h_{\eta'}^q$	0.0011 ± 0.0024	-0.0088 ± 0.0027
$h_{\eta'}^s$	0.0678 ± 0.0048	0.0846 ± 0.0059

Table 8: Comparison of decay constants (in [MeV]) as well as pseudoscalar densities along with anomaly matrix elements (both in $[\text{GeV}]^3$) for different input values Equation 280 and Equation 281, i. e., [9, 10].

with the abbreviations ($M = \eta, \eta'$)

$$H_M^A = \begin{cases} h_M^s, & A = s \\ \frac{h_M^q}{\sqrt{2}}, & A = q \end{cases}, \quad F_M^A = \begin{cases} f_M^s, & A = s \\ \frac{f_M^q}{\sqrt{2}}, & A = q \end{cases}, \tag{530}$$

which additionally allow a simplified definition[120] of the involved DAs (cf. discussion in [3, 281]). Furthermore, when imposing the state mixing ansatz (cf. Equation 278, Equation 315)

$$\begin{pmatrix} h_\eta^q & h_\eta^s \\ h_{\eta'}^q & h_{\eta'}^s \end{pmatrix} = U(\phi)\,\mathrm{diag}(h_q, h_s) \tag{531}$$

the particle independent densities[121]

$$h_q \coloneqq 2m_q \langle 0|j_5^q|\eta_q(P)\rangle\,, \quad h_s \coloneqq 2m_s \langle 0|j_5^s|\eta_s(P)\rangle\,, \tag{532}$$

arise. In practice, however, h_q and h_s have to be used with caution because Equation 532 implies[122]

$$\frac{h_q}{m_q} \sim \frac{h_s}{m_s}\,. \tag{533}$$

Therefore, a consistent treatment of twist-three effects requires an appropriate implementation

120 Due to an effective decoupling of light and strange flavors within the QF basis, the $\eta^{(\prime)}$ DAs may be defined analogously to the π^0 case (cf. [3, 281]).

121 In this context, all OZI rule violating contributions, such as "$\langle 0|j_5^s|\eta_q\rangle$", are neglected.

122 For instance, when assuming $m_q \to 0$ along with $h_q \to 0$, inconsistencies with h_q/m_q may arise. This is particularly relevant for twist-six corrections.

of quark-mass corrections. The latter has also been pointed out by [265] who suggested the following parametrization of Equation 532:

$$H_q = F_s \sin\phi\cos\phi\left(m_\eta^2 - m_{\eta'}^2\right) + F_q\left(m_\eta^2\cos^2\phi + m_{\eta'}^2\sin^2\phi\right), \tag{534}$$

$$H_s = F_q \sin\phi\cos\phi\left(m_\eta^2 - m_{\eta'}^2\right) + F_s\left(m_\eta^2\sin^2\phi + m_{\eta'}^2\cos^2\phi\right), \tag{535}$$

written in our notation. Evidently, Equation 534 and Equation 535 emerge from Equation 529 after eliminating a_η along with $a_{\eta'}$. Conversely, when eliminating Equation 532 within the four resulting equations of Equation 529, one gets (cf. also [265]):

$$a_\eta = \left(m_\eta^2 - m_{\eta'}^2\right)\sin\phi\cos\phi\left(F_q\sin\phi - F_s\cos\phi\right), \tag{536}$$

$$a_{\eta'} = \left(m_{\eta'}^2 - m_\eta^2\right)\sin\phi\cos\phi\left(F_q\cos\phi + F_s\sin\phi\right). \tag{537}$$

Nevertheless, these parametrization have to be taken with a grain of salt because Equation 534-Equation 537 are including m_η as well as $m_{\eta'}$, which themselves can be expressed via the mixing angle "ϕ" (cf. [152, 265]). Thus, replacing $m_{\eta^{(\prime)}}$ with their physical values [42]

$$m_\eta = 547.862(18)\ \text{MeV}, \quad m_{\eta'} = 957.78(6)\ \text{MeV} \tag{538}$$

may lead to inconsistencies that imply large cancellations and errors for h_q. In particular, this can be seen when comparing Equation 534-Equation 537 for different input values of (f_q, f_s, ϕ) (cf. Table 8). Notably, with Table 8 we not only reproduce the results of [265], but additionally provide a similar error analysis for [10]. Most strikingly, the different set-up of [10] implies a significant decrease in all error estimates related to h_q. An alternative approach is given by (LO) ChPT [14, 182, 265], suggesting a positive, albeit small numerical value for the pseudoscalar densities[123] (cf. Chapter 5 for applications):

$$h_q = f_q m_\pi^2 \approx 0.0025\ \text{GeV}^3, \tag{539}$$

$$h_s = f_s\left(2m_K^2 - m_\pi^2\right) \approx 0.086\ \text{GeV}^3. \tag{540}$$

The latter are actually linked to the Gell-Mann-Okubo (GMO) mass formulas (cf. [9, 44])

$$m_{qq}^2 \approx m_\pi^2, \quad m_{ss}^2 \approx 2m_K^2 - m_\pi^2, \tag{541}$$

for the corresponding (hypothetical) states $|\eta_q\rangle$ and $|\eta_s\rangle$ (cf. Equation 315). In general, a possible mass shift due to admixtures of the axial anomaly has to be included. Hence, we get the generic $(SU(2)_I$ limit) expressions:

$$h_q = f_q m_{qq}^2, \quad h_s = f_s m_{ss}^2. \tag{542}$$

In fact, Equation 542 enables an additional cross-check with previous studies. For instance, Equation 270 and Equation 271 imply

$$\mathcal{M}^2\mathcal{F}_{QF}\,\mathrm{diag}\left(\tfrac{1}{f_q}, \tfrac{1}{f_s}\right) = \begin{pmatrix} \frac{1}{f_q}\langle 0|\partial^\mu J^q_{\mu 5}|\eta\rangle & \frac{1}{f_s}\langle 0|\partial^\mu J^s_{\mu 5}|\eta\rangle \\ \frac{1}{f_q}\langle 0|\partial^\mu J^q_{\mu 5}|\eta'\rangle & \frac{1}{f_s}\langle 0|\partial^\mu J^s_{\mu 5}|\eta'\rangle \end{pmatrix}, \tag{543}$$

with the mass matrix

$$\mathcal{M}^2 = \mathrm{diag}\left(m_\eta^2, m_{\eta'}^2\right). \tag{544}$$

123 In this strict limit, one would also have to assume $f_q = f_\pi$, $f_s = \sqrt{2f_K^2 - f_\pi^2}$.

Furthermore, a multiplication with the inverse rotation matrix Equation 278 leads to a decomposition of all physical into ideal states [9]:

$$U^{\dagger}(\phi)\,\mathcal{M}^2 U(\phi) = \mathcal{M}^2_{qs}\,, \tag{545}$$

with the unitary matrix (cf. [9, 152])

$$\mathcal{M}^2_{qs} = \begin{pmatrix} \frac{H_q + a_q}{F_q} & \frac{a_q}{F_s} \\ \frac{a_s}{F_q} & \frac{H_s + a_s}{F_s} \end{pmatrix}. \tag{546}$$

As a result, one obtains (using $\mathcal{M}^2_{qs} = \left[\mathcal{M}^2_{qs}\right]^{\dagger}$) the symmetry breaking parameter [9, 152, 261]

$$y = \frac{f_q}{f_s} = \sqrt{2}\frac{a_s}{a_q}\,. \tag{547}$$

Moreover, due to the single mixing angle, $\mathcal{M}^2$ and $\mathcal{M}^2_{qs}$ are related by a similarity transformation, justifying an interpretation of Equation 546 as a mass matrix. After evaluating the trace and determinant of Equation 545 we get

$$m^2_{\eta'} = \frac{2m^2_{ss}\left(m^2_{\eta} - m^2_{ss}\right) + y^2 m^2_{qq}\left(m^2_{\eta} - m^2_{qq}\right)}{\left(2+y^2\right)m^2_{\eta} - y^2 m^2_{qq} - 2m^2_{ss}}\,, \tag{548}$$

which reproduces the improved Schwinger mass formula[124] [152]

$$m^2_{\eta'} = m^2_{\pi} + \frac{4\left(m^2_K - m^2_{\pi}\right)\left(2m^2_K - m^2_{\eta} - m^2_{\pi}\right)}{4m^2_K - \left(2+y^2\right)m^2_{\eta} - \left(2-y^2\right)m^2_{\pi}}\,, \tag{549}$$

when inserting Equation 541 into Equation 548. The gain of these equations is twofold:

i) while Equation 548 may be used for a consistency check of the parameters in Table 8,

ii) Equation 549 gives an opportunity to roughly cross-check experimental values of $m_{\eta'}$ (cf. Equation 538) with the symmetry breaking parameters Equation 547.

As an illustration, let us compare the three relevant data sets of Equation 280, Equation 281 as well as LO ChPT with Equation 538. Evidently, Equation 548 acquires a rather large error, but the corresponding mean values almost perfectly coincide with Equation 538:

$$m_{\eta'}\big|_{\text{Equation 280}} \approx 957.78\,, \quad m_{\eta'}\big|_{\text{Equation 281}} \approx 957.69\,, \tag{550}$$

indicating a good consistency of the associated parameters in Table 8. At the same time, Equation 549 favors the FKS parameters ($y = 0.80$) as well as LO ChPT predictions ($y = 0.71$), while [10] in this context seems less applicable ($y = 0.66$). That is a reasonable result because the named LO ChPT predictions are nothing else, but an implementation of the strict FKS scheme for twist-three parameters (cf. Equation 531, Equation 539, Equation 540 and [152])

$$\begin{pmatrix} h^q_{\eta} & h^s_{\eta} \\ h^q_{\eta'} & h^s_{\eta'} \end{pmatrix} = U(\phi)\,\mathrm{diag}\Big(f_q\, m^2_{\pi}, f_s\left(2m^2_K - m^2_{\pi}\right)\Big)\,. \tag{551}$$

However, the validity of this approach has to be tested against phenomenology (cf. [152]), depending on the physical context (see, e. g., Section 4.3 or Chapter 5). Before proceeding, let us

124 The original version of Schwinger's mass formula [152, 336] will be recovered for $y \to 1$. Besides, [42] and Equation 549 would imply the phenomenological value $y \approx 0.77$.

note, that the numerically small values of h_M^R ($R = q, s$; $M = \eta, \eta'$) in their present arrangement within Equation 502 and Equation 513, e. g.,

$$\left[\rho_+^\eta\right]^{qq} = \frac{4m_q^2 f_\eta^q}{h_\eta^q}\,, \quad R_{3\eta}^q = \frac{2m_q f_{3\eta}^q}{h_\eta^q}\,, \tag{552}$$

may lead to (numerical) instabilities. Therefore, it seems self-evident to absorb all h_M^R-factors into the DAs:

$$h_M^R \phi_{3M}^{R;\sigma}(x) =: \overline{\phi}_{3M}^{R;\sigma}(x)\,, \quad h_M^R \phi_{3M}^{R;p}(x) =: \overline{\phi}_{3M}^{R;p}(x)\,, \tag{553}$$

implicating the NLO result[125]:

$$\begin{aligned}\overline{\phi}_{3M}^{R;p}(x) &= h_M^R + 12m_R^2 f_M^R\left(1 + 6c_{2,M}^{(R)}\right) + 60\left(m_R f_{3M}^R + m_R^2 f_M^R c_{2,M}^{(R)}\right) C_2^{(1/2)}(\xi_x) \\ &\quad - 6m_R f_{3M}^R \omega_{3M}^R C_4^{(1/2)}(\xi_x) + 6m_R^2 f_M^R\left(1 + 6c_{2,M}^{(R)}\right)\log x\bar{x}\,, \end{aligned} \tag{554}$$

$$\begin{aligned}\overline{\phi}_{3M}^{R;\sigma}(x) &= 6x\bar{x}\Big[h_M^R + 6m_R^2 f_M^R\left(1 + 10c_{2,M}^{(R)}\right) \\ &\quad + \left(10m_R f_{3M}^R - m_R f_{3M}^R \omega_{3M}^R + 6m_R^2 f_M^R c_{2,M}^{(R)}\right) C_2^{(3/2)}(\xi_x)\Big] \\ &\quad + 36x\bar{x}m_R^2 f_M^R\left(1 + 6c_{2,M}^{(R)}\right)\log x\bar{x}\,. \end{aligned} \tag{555}$$

Correspondingly, the normalization conditions are given by[126]

$$\int_0^1 dx\, \overline{\phi}_{3M}^{R;p}(x) = h_M^R\,, \tag{556}$$

$$\int_0^1 dx\, \overline{\phi}_{3M}^{R;\sigma}(x) = h_M^R - 4m_R^2 f_M^R\,. \tag{557}$$

Due to different $SU(3)_F$ corrections[127] within the corresponding Ward identities and EOM, one cannot simply convert these findings for the SO basis. Accordingly, the associated SO twist-three DAs (cf. Equation 1514 and Equation 1515) exhibit a more elaborate formal structure, compared to the QF case. As a matter of fact, both cases only, coincide exactly in the strict $SU(3)_F$ limit (cf. for instance Equation 1516, Equation 1517 and Equation 554, Equation 555). Disregarding their mere formal structure, all involved higher order parameters are crucial for the actual definition of $\phi_{3M}^{A;p}$ and $\phi_{3M}^{A;\sigma}$. As discussed before, at the moment non-perturbative quantities, such as f_{3M}^A, etc. can only be roughly estimated. Within the QF basis, one may hope that all corresponding ambiguities are sufficiently suppressed [3] (when compared to the leading contribution)

$$\frac{2m_s f_{3s}}{h_s} \sim 0.01\,. \tag{558}$$

125 Owing to their equivalent structure in the $SU(2)_I$ limit, the corresponding EOM (cf. Section C.7) for $R = q, s$ imply analogous DAs. Hypothetical G-parity breaking contributions have been excluded.

126 Notably, $\overline{\phi}_{3M}^{R;p}$ and $\overline{\phi}_{3M}^{R;\sigma}$ are interconnected via Equation 476 as well as Equation 477. Therefore, the normalization of Equation 556 cannot be altered without affecting Equation 557 and vice versa.

127 For instance, in the assumed $SU(2)_I$ limit, the singlet and octet currents not only couple with each other via the axial anomaly, but also by (quark) mass terms.

PARAMETER	FOR [9]	FOR [10]
h_η^8	0.0443 ± 0.0313	-0.0696 ± 0.0358
h_η^0	-0.0009 ± 0.0233	-0.0969 ± 0.0266
$h_{\eta'}^8$	-0.0257 ± 0.0260	-0.1417 ± 0.0295
$h_{\eta'}^0$	0.0228 ± 0.0193	-0.0532 ± 0.0218

Table 9: Estimates for the SO twist-three pseudoscalar densities (in $[\text{GeV}]^3$) of Equation 559 and Equation 560, as implied by Table 8, i. e., [9, 10].

It is yet unclear, how to translate this strategy for the SO basis. As a matter of fact, according to Table 8 already our best numerical estimates for the leading factors

$$h_M^8 = h_M^q\left(\frac{1}{3\sqrt{3}} + \frac{2}{3\sqrt{3}}\frac{m_s}{m_q}\right) - h_M^s\left(\frac{2\sqrt{2}}{3\sqrt{3}} + \frac{\sqrt{2}}{3\sqrt{3}}\frac{m_q}{m_s}\right), \tag{559}$$

$$h_M^0 = h_M^q\left(\frac{2\sqrt{2}}{3\sqrt{3}} + \frac{\sqrt{2}}{3\sqrt{3}}\frac{m_s}{m_q}\right) + h_M^s\left(\frac{1}{3\sqrt{3}} + \frac{2}{3\sqrt{3}}\frac{m_q}{m_s}\right), \tag{560}$$

are prone to large uncertainties, cf. Table 9. Here, the experimental value [42, 225]

$$\frac{m_s}{m_q} = 27.5 \pm 1.0 \tag{561}$$

has been used (for masses at $\mu_0 \approx 2$ GeV). Moreover, Equation 559 along with Equation 560 effectively exclude our preferred ansatz with $m_q \to 0$ and $m_s \neq 0$. Another important phenomenological reason to abandon the SO basis in the context of higher twist DAs concerns the applicability of the state mixing ansatz[128]. When used for twist-three DAs (similar for "$\sigma \leftrightarrow p$"):

$$\begin{pmatrix} \overline{\phi}_{3\eta}^{q;\sigma}(x,\mu) & \overline{\phi}_{3\eta}^{s;\sigma}(x,\mu) \\ \overline{\phi}_{3\eta'}^{q;\sigma}(x,\mu) & \overline{\phi}_{3\eta'}^{s;\sigma}(x,\mu) \end{pmatrix} = U(\phi)\,\mathrm{diag}\Big(\overline{\phi}_{3q}^{\sigma}(x,\mu), \overline{\phi}_{3s}^{\sigma}(x,\mu)\Big), \tag{562}$$

all particle dependencies are consequently shifted into the underlying mixing scheme, while (four) universal DAs absorb the remaining non-perturbative information ($R = q, s$):

$$\overline{\phi}_{3R}^{p}(x) = h_R + 60 m_R f_{3R} C_2^{(1/2)}(\xi_x) + \dots, \tag{563}$$

$$\overline{\phi}_{3R}^{\sigma}(x) = 6x\bar{x}\left[h_R + 10 m_R f_{3R} C_2^{(3/2)}(\xi_x) + \dots\right]. \tag{564}$$

Here, we introduce truncated DAs, neglecting the numerically small $\mathcal{O}(m_R^2)$ and $\mathcal{O}(m_R f_{3R})$ corrections ($R = q, s$). Those will also be omitted for consistency with the calculation of twist-four corrections (cf. Section 3.4.3).

3.4.3 *Twist-four distribution amplitudes*

This subsection completes our theoretical investigations concerning higher twist distributions by a detailed discussion and an update of twist-four light pseudoscalar meson DAs. Those also play an important role in the intended investigation of the $\eta^{(\prime)}$ photon TFF (cf. Chapter 4, Section 4.3),

128 Given that this is true (cf. Section 4.3), the total number of twist-three two-particle DAs can be halved.

urging us to develop a phenomenologically applicable formalism. Hence, we focus on a description within the QF basis.
In order to derive models for the two- and three-particle DAs up to NLO in conformal spin, we follow the classifications and notations in [271, 314] adapted to our case. Contrary to previous studies (e. g., [269, 271, 314]), we will take into account quark mass corrections as well as anomalous contributions to the twist-four DAs. While the former may also be used for the flavor octet sector, the latter represent an entirely new subject. In fact, we are not aware of any related study beyond twist-two accuracy.
The presentation is, therefore, divided into two distinct segments. In the first part, we ignore any anomalous contributions, while within the second all corresponding results are retrofitted via a simple substitution rule.

Let us begin with a general classification of the four possible (cf. Equation 330, Equation 331) three-particle twist-four DAs and their NLO parameters. Note, that all these DAs for light flavors are defined by the same expressions with the generic substitution of corresponding quark fields and superscripts "$s \to q$". Therefore, without loss of generality we may in our notation focus on the strange case. According to G-parity[129], the DAs Φ^R_{4M} and Ψ^R_{4M} ($R = q, s$) are symmetric under the interchange of the quark momenta, i. e., $\alpha_1 \leftrightarrow \alpha_2$, whereas $\widetilde{\Phi}^R_{4M}$ and $\widetilde{\Psi}^R_{4M}$ are symmetric. This puts further constraints on the allowed conformal expansion, resulting from the spin structure of the underlying light-cone operators, such as

$$\bar{s}(z_2 n)\, \gamma_\mu \gamma_5 g \mathcal{G}_{\alpha\beta}(z_3 n)\, s(z_1 n)\ , \tag{565}$$

$$\bar{s}(z_2 n)\, \gamma_\mu i g \widetilde{\mathcal{G}}_{\alpha\beta}(z_3 n)\, s(z_1 n)\ . \tag{566}$$

For instance, the projection "$(\mu, \alpha, \beta) = (+, +, -)$" is uniquely related to $j_{\overline{\Psi}} = 1 = j_{\Psi}$, along with $j_{\mathcal{G}} = 1$. Consequently, both DAs

$$\langle 0|\bar{s}(z_2 n)\, \gamma_+ \gamma_5 g \mathcal{G}_{+-}(z_3 n)\, s(z_1 n)|M(P)\rangle = P_+ F_M^{(s)} \Phi^{(s)}_{4M}(\underline{z}, P_+)\ , \tag{567}$$

$$\langle 0|\bar{s}(z_2 n)\, \gamma_+ i g \widetilde{\mathcal{G}}_{+-}(z_3 n)\, s(z_1 n)|M(P)\rangle = P_+ F_M^{(s)} \widetilde{\Phi}^{(s)}_{4M}(\underline{z}, P_+)\ , \tag{568}$$

exhibit the conformal NLO expansion (similar for $\widetilde{\Phi}^R_{4M}(\underline{z}, P_+)$)

$$\Phi^{(s)}_{4M}(\underline{z}, P_+) = 120 \alpha_1 \alpha_2 \alpha_3 \left[\phi^{(s)}_{0,M} Y^{(12)3}_{3,2}(\underline{\alpha}) - \frac{1}{2} \phi^{(s)}_{2,M} Y^{(12)3}_{4,2}(\underline{\alpha}) - \frac{1}{2} \phi^{(s)}_{1,M} Y^{(12)3}_{4,3}(\underline{\alpha}) \right]\ , \tag{569}$$

which due to the named symmetry properties reduces to (cf. Equation 1227)

$$\Phi^{(s)}_{4M}(\underline{z}, P_+) = 120 \alpha_1 \alpha_2 \alpha_3 \left[\phi^{(s)}_{1,M}\, (\alpha_1 - \alpha_2) \right]\ , \tag{570}$$

$$\widetilde{\Phi}^{(s)}_{4M}(\underline{z}, P_+) = 120 \alpha_1 \alpha_2 \alpha_3 \left[\tilde{\phi}^{(s)}_{0,M} + \tilde{\phi}^{(s)}_{2,M}\, (3\alpha_3 - 1) \right]\ . \tag{571}$$

A more complicated situation arises for "$(\mu, \alpha, \beta) = (\perp, \perp, +)$", where the projection (cf. Section A.9)

$$\gamma^\perp_\mu = \gamma_\mu - n_\mu \gamma_- - \bar{n}_\mu \gamma_+ \tag{572}$$

129 As stated before, for the assumed flavorless meson, G-parity boils down to C-parity. Nevertheless, in the context of light pseudoscalar mesons, we instead keep the most general term.

produces a mixture of different quark-spin states $s_\Psi = \pm\frac{1}{2}$ together with $s_{\overline{\Psi}} = \mp\frac{1}{2}$, while $\mathcal{G}_{+\perp}$ corresponds to $s_\mathcal{G} = 1$. Therefore, for a clean separation of the different spin projections, one has to introduce adequate auxiliary DAs, being (e. g., [271], Section A.11)

$$\langle 0|\bar{s}(z_2 n)\, ig\widetilde{\mathcal{G}}_{\alpha\beta}(z_3 n)\, \gamma_+\gamma_\mu\gamma_- s(z_1 n)|M(P)\rangle = F_M^{(s)} \left(p_\beta g^\perp_{\alpha\mu} - p_\alpha g^\perp_{\beta\mu}\right) \Psi^{\uparrow\downarrow}_{M,s}(\underline{z}, P_+)\,, \quad (573)$$

$$\langle 0|\bar{s}(z_2 n)\, ig\widetilde{\mathcal{G}}_{\alpha\beta}(z_3 n)\, \gamma_-\gamma_\mu\gamma_+ s(z_1 n)|M(P)\rangle = F_M^{(s)} \left(p_\beta g^\perp_{\alpha\mu} - p_\alpha g^\perp_{\beta\mu}\right) \Psi^{\downarrow\uparrow}_{M,s}(\underline{z}, P_+)\,, \quad (574)$$

which are related to $\Psi^{(s)}_{4M}$ and $\widetilde{\Psi}^{(s)}_{4M}$ via (cf. [271])

$$\widetilde{\Psi}^{(s)}_{4M}(\underline{\alpha}) = -\frac{1}{2}\left[\Psi^{\uparrow\downarrow}_{M,s}(\underline{\alpha}) + \Psi^{\downarrow\uparrow}_{M,s}(\underline{\alpha})\right], \quad (575)$$

$$\Psi^{(s)}_{4M}(\underline{\alpha}) = +\frac{1}{2}\left[\Psi^{\uparrow\downarrow}_{M,s}(\underline{\alpha}) - \Psi^{\downarrow\uparrow}_{M,s}(\underline{\alpha})\right], \quad (576)$$

due to the matrix identities Equation 1181 and Equation 1182. The definitions Equation 573 and Equation 574 are immediately implying $\left(j_{\overline{\Psi}} = 1 = j_1,\, j_\Psi = \frac{1}{2} = j_2,\, j_\mathcal{G} = \frac{3}{2} = j_3\right)$

$$\begin{aligned}\Psi^{\uparrow\downarrow}_{M,s}(\underline{\alpha}) &= 60\alpha_2\alpha_3^2\left[\psi^{(s)}_{0,M} Y^{(1,2)3}_{3,3/2}(\underline{\alpha}) - \frac{\psi^{(s)}_{1,M} + \psi^{(s)}_{2,M}}{3} Y^{(1,2)3}_{4,3/2}(\underline{\alpha})\right.\\ &\quad \left. + \frac{\psi^{(s)}_{2,M} - 2\psi^{(s)}_{1,M}}{2} Y^{(1,2)3}_{4,5/2}(\underline{\alpha})\right]\\ &= 60\alpha_2\alpha_3^2\left[\psi^{(s)}_{0,M} + \psi^{(s)}_{1,M}(\alpha_3 - 3\alpha_1) + \psi^{(s)}_{2,M}\left(\alpha_3 - \tfrac{3}{2}\alpha_2\right)\right], \end{aligned} \quad (577)$$

along with $\left(j_{\overline{\Psi}} = \frac{1}{2},\, j_\Psi = 1,\, j_\mathcal{G} = \frac{3}{2}\right)$

$$\begin{aligned}\Psi^{\downarrow\uparrow}_{M,s}(\underline{\alpha}) &= 60\alpha_1\alpha_3^2\left[\overline{\psi}^{(s)}_{0,M} Y^{(1,2)3}_{3,3/2}(\underline{\alpha}) - \frac{\overline{\psi}^{(s)}_{1,M} + \overline{\psi}^{(s)}_{2,M}}{3} Y^{(1,2)3}_{4,3/2}(\underline{\alpha})\right.\\ &\quad \left. - \frac{\overline{\psi}^{(s)}_{2,M} - 2\overline{\psi}^{(s)}_{1,M}}{2} Y^{(1,2)3}_{4,5/2}(\underline{\alpha})\right]\\ &= 60\alpha_1\alpha_3^2\left[\overline{\psi}^{(s)}_{0,M} + \overline{\psi}^{(s)}_{1,M}(\alpha_3 - 3\alpha_2) + \overline{\psi}^{(s)}_{2,M}\left(\alpha_3 - \tfrac{3}{2}\alpha_1\right)\right], \end{aligned} \quad (578)$$

when neglecting contributions of conformal spin $J \geqslant 5$ (see Equation 1227). In Equation 577 and Equation 578 we have chosen all coefficients accordingly to reproduce the notation of [271]. Evidently, we get the G-parity relation (cf. [271, 314])

$$\Psi^{\uparrow\downarrow}_{M,s}(\alpha_1, \alpha_2, \alpha_3) = \Psi^{\downarrow\uparrow}_{M,s}(\alpha_2, \alpha_1, \alpha_3) \;\Rightarrow\; \psi^{(s)}_{k,M} = \overline{\psi}^{(s)}_{k,M} \;(k \leqslant 2)\,, \quad (579)$$

which allows us to formulate the NLO expansions

$$\Psi^{(s)}_{4M}(\underline{\alpha}) = -30(\alpha_1 - \alpha_2)\alpha_3^2\left[\psi^{(s)}_{0,M} + \psi^{(s)}_{1,M}\alpha_3 + \frac{1}{2}\psi^{(s)}_{2,M}(5\alpha_3 - 3)\right], \quad (580)$$

$$\begin{aligned}\widetilde{\Psi}^{(s)}_{4M}(\underline{\alpha}) &= -30\alpha_3^2\left[\psi^{(s)}_{0,M}(1-\alpha_3) + \psi^{(s)}_{1,M}(\alpha_3(1-\alpha_3) - 6\alpha_1\alpha_2)\right.\\ &\quad \left. + \psi^{(s)}_{2,M}\left(\alpha_3(1-\alpha_3) - \frac{3}{2}\left(\alpha_1^2 + \alpha_2^2\right)\right)\right], \end{aligned} \quad (581)$$

with a reduced set of non-perturbative parameters (cf. also [2, 271]). Still, this general parametrization of three-particle twist-four DAs up to NLO in conformal spin, a priori, involves $6\times2\times2=24$ new non-perturbative quantities for the $\eta-\eta'$ system in the QF basis. Fortunately, these coefficients are related by QCD equations of motion [269].

The actual determination of such operator relations is, therefore, an important part of this project. Hence, we show the essential steps towards the needed results.
One of these relations is rather non-trivial and involves the divergence (in the mathematical sense) of the spin-three conformal operator

$$O^{(\bar{s}s)}_{\mu\alpha\beta} = \left[\bar{s}\overleftrightarrow{D}_\alpha\overleftrightarrow{D}_\beta\gamma_\mu\gamma_5 s - \frac{1}{5}\partial_\alpha\partial_\beta\bar{s}\gamma_\mu\gamma_5 s\right]_{\text{sym}} - \text{traces}\,. \tag{582}$$

Here, the symmetrization in all Lorentz indices and subtraction of traces is necessary to get an irreducible representation of the Lorentz group. When ignoring possible anomalous contributions, the needed calculation is similar to that for a pion-like system. For instance, the expansion of "$\bar{u}(-x)\,\gamma_\mu\gamma_5 d(x)$" includes local operators, such as

$$\mathcal{O}^{(\bar{u}d)}_{\mu\alpha\beta} = \left[\bar{u}\overleftrightarrow{D}_\alpha\overleftrightarrow{D}_\beta\gamma_\mu\gamma_5 d\right]_{\text{sym}} - \text{traces}\,, \tag{583}$$

which resembles one component of Equation 582, after replacing "u, d" with "s". Explicitly, Equation 583 takes the form

$$\frac{1}{6}\left[S^{\alpha_1\alpha_2\alpha_3}_{\mu\alpha\beta} - \frac{1}{3}\mathbb{T}_{\alpha\beta\mu\alpha_4}\mathbb{T}^{\alpha_1\alpha_2\alpha_3\alpha_4}\right]\widetilde{\mathcal{O}}^{(\bar{u}d)}_{\alpha_1\alpha_2\alpha_3} = \mathcal{O}^{(\bar{u}d)}_{\mu\alpha\beta}\,, \tag{584}$$

when using the abbreviations

$$\widetilde{\mathcal{O}}^{(\bar{u}d)}_{\alpha_1\alpha_2\alpha_3} = \bar{u}\,\widetilde{\mathcal{R}}_{\alpha_1\alpha_2\alpha_3}\gamma_5 d\,,\quad \widetilde{\mathcal{R}}_{\alpha_1\alpha_2\alpha_3} = \overleftrightarrow{D}_{\alpha_1}\overleftrightarrow{D}_{\alpha_2}\gamma_{\alpha_3}\,, \tag{585}$$

along with ($S^{\alpha_1\alpha_2\alpha_3}_{\mu\alpha\beta} \equiv S_{\mu\alpha\beta;\mu_1\mu_2\mu_3}\,g^{\mu_1\alpha_1}\,g^{\mu_2\alpha_2}\,g^{\mu_2\alpha_2}$)

$$\begin{aligned} S_{\mu_1\mu_2\mu_3;\alpha_1\alpha_2\alpha_3} &= g_{\mu_1\alpha_1}\left(g_{\mu_2\alpha_2}g_{\mu_3\alpha_3} + g_{\mu_3\alpha_2}g_{\mu_2\alpha_3}\right) \\ &\quad + g_{\mu_2\alpha_1}\left(g_{\mu_1\alpha_2}g_{\mu_3\alpha_3} + g_{\mu_3\alpha_2}g_{\mu_1\alpha_3}\right) \\ &\quad + g_{\mu_3\alpha_1}\left(g_{\mu_2\alpha_2}g_{\mu_1\alpha_3} + g_{\mu_1\alpha_2}g_{\mu_2\alpha_3}\right)\,, \end{aligned} \tag{586}$$

$$\begin{aligned} \mathbb{T}^{\alpha_1\alpha_2\alpha_3\alpha_4} &= \frac{1}{2}g^{\mu_1\mu_2}g^{\mu_3\alpha_4}S^{\alpha_1\alpha_2\alpha_3}_{\mu_1\mu_2\mu_3} \\ &= g^{\alpha_1\alpha_2}g^{\alpha_3\alpha_4} + g^{\alpha_1\alpha_3}g^{\alpha_2\alpha_4} + g^{\alpha_1\alpha_4}g^{\alpha_2\alpha_3}\,. \end{aligned} \tag{587}$$

Those may find general application, such as (when acting on pion momenta)

$$\begin{aligned} \mathcal{X}_{\mu\alpha\beta} &= \frac{1}{6}\left[S^{\alpha_1\alpha_2\alpha_3}_{\mu\alpha\beta} - \frac{1}{3}\mathbb{T}_{\alpha\beta\mu\alpha_4}\mathbb{T}^{\alpha_1\alpha_2\alpha_3\alpha_4}\right]P_{\alpha_1}P_{\alpha_2}P_{\alpha_3} \\ &= P_\mu P_\alpha P_\beta - \frac{1}{6}m_\pi^2\left(P_\mu g_{\alpha\beta} + P_\alpha g_{\mu\beta} + P_\beta g_{\mu\alpha}\right)\,, \end{aligned} \tag{588}$$

$$\mathcal{X}_{\alpha\beta} = \frac{3}{32}\left[S^{\alpha_1\alpha_2\alpha_3}_{\mu\alpha\beta} - \frac{1}{3}\mathbb{T}_{\alpha\beta\mu\alpha_4}\mathbb{T}^{\alpha_1\alpha_2\alpha_3\alpha_4}\right]P_{\alpha_1}P_{\alpha_2}g^{\mu}_{\alpha_3} = P_\alpha P_\beta - \frac{1}{4}m_\pi^2 g_{\alpha\beta}\,. \tag{589}$$

Due to their length, we have to omit the complete expressions for all occurring traces and will instead discuss only the vital components, e. g.,

$$\mathbb{T}_{\alpha_1\alpha_2\alpha_3\mu}\,\widetilde{\mathcal{R}}^{\alpha_1\alpha_2\alpha_3} = \gamma_\mu\overleftrightarrow{D}^2 + \overleftrightarrow{\not{D}}\overleftrightarrow{D}_\mu + \overleftrightarrow{D}_\mu\overleftrightarrow{\not{D}} =: \mathcal{R}_\mu\,. \tag{590}$$

The actual calculation makes intensified use of operator and matrix identities as listed in Section A.2 and Section A.3. For example, the latter allow us to rewrite an operator

$$\bar{u}\Big[\gamma_\mu \overleftrightarrow{\not{D}}\overleftarrow{\not{D}} - \overrightarrow{\not{D}}\overleftrightarrow{\not{D}}\gamma_\mu\Big]\gamma_5 d = \partial^\rho \bar{u}\Big[\gamma_\mu \overleftrightarrow{\not{D}}\gamma_\rho - \gamma_\rho \overleftrightarrow{\not{D}}\gamma_\mu\Big]\gamma_5 d - \bar{u}\Big[i m_d \gamma_\mu \overleftrightarrow{\not{D}} - i m_u \overleftrightarrow{\not{D}}\gamma_\mu\Big]\gamma_5 d\,, \quad (591)$$

in terms of a divergence and mass terms. Accordingly, after some algebra, we get

$$\bar{u}\,\mathcal{R}_\mu\gamma_5 d = \bar{u}\Big[4g\widetilde{\mathcal{G}}_{\mu\rho}\gamma^\rho\gamma_5 + 2i(m_d - m_u)\overleftrightarrow{D}_\mu - \gamma_\mu \partial^\rho \partial_\rho\Big]\gamma_5 d\,, \quad (592)$$

modulo omitted corrections of $\mathcal{O}(m_q^2)$ and $\mathcal{O}(m_u - m_d)$. The (mathematical) four divergence of Equation 583 then requires[130]

$$\partial_\alpha\,\mathcal{R}_\beta = \partial_\alpha\Big[4\bar{u}g\widetilde{\mathcal{G}}_{\beta\rho}\gamma^\rho d - \partial^2\bar{u}\gamma_\beta\gamma_5 d + 2(m_d - m_u)\,\bar{u}\overleftrightarrow{D}_\beta i\gamma_5 d\Big]\,, \quad (593)$$

$$\partial^\mu\,\mathcal{R}_\mu = 4\partial^\mu\bar{u}g\widetilde{\mathcal{G}}_{\mu\rho}\gamma^\rho d - (m_u + m_d)\,\partial^2\bar{u}i\gamma_5 d + \dots\,, \quad (594)$$

as well as

$$\partial^\mu\bar{u}\Big\{\overleftrightarrow{D}_\alpha, \overleftrightarrow{D}_\beta\Big\}\gamma_\mu\gamma_5 d = -4ig\bar{u}\gamma^\rho\gamma_5\Big[\mathcal{G}_{\rho\beta}\overrightarrow{D}_\alpha - \overleftarrow{D}_\alpha\mathcal{G}_{\rho\beta} + (\alpha\leftrightarrow\beta)\Big]d + 2m_q\bar{u}i\gamma_5\Big\{\overleftrightarrow{D}_\alpha, \overleftrightarrow{D}_\beta\Big\}d\,, \quad (595)$$

along with (again discarding not required corrections)

$$\begin{aligned}\partial^\mu\bar{u}\Big\{\overleftrightarrow{D}_\mu, \overleftrightarrow{D}_\beta\Big\}\gamma_\alpha\gamma_5 d = {}& 4ig\bar{u}\gamma^\rho\gamma_5\Big[\mathcal{G}_{\alpha\rho}\overrightarrow{D}_\beta - \overleftarrow{D}_\beta\mathcal{G}_{\alpha\rho} + (\alpha\leftrightarrow\beta)\Big]d \\ & - 4g\partial^\rho\bar{u}\gamma^\sigma\Big[g_{\alpha\beta}\widetilde{\mathcal{G}}_{\rho\sigma} + g_{\rho\beta}\widetilde{\mathcal{G}}_{\sigma\alpha} + g_{\sigma\beta}\widetilde{\mathcal{G}}_{\alpha\rho}\Big]d - 8im_q\bar{u}\sigma_{\alpha\xi}\gamma_5 g\mathcal{G}^\xi{}_\beta\, d.\end{aligned} \quad (596)$$

Here, only symmetric contributions in "(α,β)" have been kept, while also considering the relation

$$\begin{aligned}2im_q\bar{u}g\mathcal{G}^\xi{}_\alpha\sigma_{\xi\beta}\gamma_5 d = {}& ig\bar{u}\gamma^\rho\gamma_5\Big[\mathcal{G}_{\rho\alpha}\overrightarrow{D}_\beta - \overleftarrow{D}_\beta\mathcal{G}_{\rho\alpha}\Big]d - ig\bar{u}\gamma_\beta\gamma_5\Big[\mathcal{G}_{\rho\alpha}\overrightarrow{D}^\rho - \overleftarrow{D}^\rho\mathcal{G}_{\rho\alpha}\Big]d \\ & + \partial^\rho\bar{u}\gamma^\sigma g\Big[g_{\alpha\beta}\widetilde{\mathcal{G}}_{\rho\sigma} + g_{\alpha\rho}\widetilde{\mathcal{G}}_{\sigma\beta} + g_{\alpha\sigma}\widetilde{\mathcal{G}}_{\beta\rho}\Big]d - \bar{u}\gamma^\sigma\mathcal{D}_\alpha g\widetilde{\mathcal{G}}_{\sigma\beta}\,d\,.\end{aligned} \quad (597)$$

In Equation 597 a special covariant derivative "$\mathcal{D}_\rho$" has been introduced which solely acts on the involved field strength tensor, i. e.,

$$\big[\mathcal{D}_\rho, \mathcal{G}_{\alpha\beta}\big] \equiv \mathcal{D}_\rho\mathcal{G}_{\alpha\beta}\,. \quad (598)$$

Besides, Equation 597 gives rise to the operator relation

$$2im_q\mathcal{Q}_3^{\alpha\beta} = \mathcal{V}_1^{\alpha\beta} - \mathcal{V}_2^{\alpha\beta} + \mathcal{V}_3^{\alpha\beta} - i\partial^\alpha\mathcal{U}^\beta + \partial^\rho\bar{u}\gamma^\alpha g\widetilde{\mathcal{G}}^\beta{}_\rho\, d - \cancel{ig^{\alpha\beta}\partial^\rho\mathcal{U}_\rho}^{\text{(surface term)}} - \text{traces}\,, \quad (599)$$

which relies on the definitions[131] $\big(n^2 = 0,\, n^\mu\mathcal{G}_{\mu\nu} \equiv \mathcal{G}_{+\nu}\big)$

$$\mathcal{U}_+ = i\bar{u}\gamma^\rho g\widetilde{\mathcal{G}}_{\rho+}\,d\,, \quad (600)$$

$$\mathcal{Q}_3^{++} = \bar{u}\sigma_{\rho+}\gamma_5\mathcal{G}^\rho{}_+\,d\,, \quad (601)$$

$$\mathcal{V}_1^{++} = i\bar{u}\gamma_\rho\gamma_5\Big[g\mathcal{G}^\rho{}_+\overrightarrow{D}_+ - \overleftarrow{D}_+ g\mathcal{G}^\rho{}_+\Big]d\,, \quad (602)$$

$$\mathcal{V}_2^{++} = i\bar{u}\gamma_+\gamma_5\Big[g\mathcal{G}_{\rho+}\overrightarrow{D}^\rho - \overleftarrow{D}^\rho g\mathcal{G}_{\rho+}\Big]d\,, \quad (603)$$

$$\mathcal{V}_3^{++} = \bar{u}\gamma^\rho\Big[iD_+, ig\widetilde{\mathcal{G}}_{\rho+}\Big]d\,. \quad (604)$$

130 Here, we only mention the relevant contributions, while neglecting other $\mathcal{O}(m_q^2)$ corrections (e. g., denoted by ellipses).
131 Those are given in a contracted form, in order to erase all traces.

Together with the pion matrix elements $(k=1,2,3)$

$$\langle 0|U_\mu|\pi^-(P)\rangle = P_\mu f_\pi \delta_\pi^2 , \tag{605}$$

$$\Leftrightarrow \langle 0|i\bar{u}\gamma_\alpha g\widetilde{\mathcal{G}}_{\beta\rho} d|\pi^-(P)\rangle = -\frac{1}{3} f_\pi \delta_\pi^2 \left[P_\beta g_{\alpha\rho} - P_\rho g_{\alpha\beta}\right] ,$$

$$\langle 0|\mathcal{Q}_3^{\alpha\beta}|\pi^-(P)\rangle = 2 i f_{3\pi}\left[P^\alpha P^\beta - \frac{1}{4} m_\pi^2 g^{\alpha\beta}\right] , \tag{606}$$

$$\langle 0|\mathcal{V}_k^{\alpha\beta}|\pi^-(P)\rangle = f_\pi \delta_\pi^2 \lambda_k^\pi \left[P^\alpha P^\beta - \frac{1}{4} m_\pi^2 g^{\alpha\beta}\right] , \tag{607}$$

Equation 599 further implies $(\delta_\pi^2 = (0.18 \pm 0.06)\ \text{GeV}\ [271])$

$$\lambda_2^\pi = \lambda_1^\pi + \lambda_3^\pi - \frac{2}{3} + 4 m_q \frac{f_{3\pi}}{f_\pi \delta_\pi^2} , \tag{608}$$

which may be seen as a showcase for our search of possible associations between local operators, such as Equation 600–Equation 604. Correspondingly, the resulting divergence

$$\begin{aligned} 6\,\partial^\mu \mathcal{O}^{(\bar{u}d)}_{\mu\alpha\beta} = &-12 i \bar{u}\gamma^\rho\gamma_5 \left[g\mathcal{G}_{\rho\beta}\overrightarrow{D}_\alpha - \overleftarrow{D}_\alpha g\mathcal{G}_{\rho\beta}\right] d - 4\partial^\rho \bar{u}\gamma_\beta g\widetilde{\mathcal{G}}_{\alpha\rho} d \\ &- 8 i m_q \bar{u}\sigma_{\alpha\rho}\gamma_5 g\mathcal{G}^\rho{}_\beta d - \frac{8}{3}\partial_\beta \bar{u}\gamma^\sigma g\widetilde{\mathcal{G}}_{\sigma\alpha} d \\ &+ \frac{1}{3}\partial_\beta\partial^2 \bar{u}\gamma_\alpha\gamma_5 d + 2 m_q \bar{u} i\gamma_5 \overleftrightarrow{D}_\alpha \overleftrightarrow{D}_\beta d \\ &- \frac{2}{3}(m_d - m_u)\,\partial_\beta \bar{u} i\gamma_5 \overleftrightarrow{D}_\alpha d + (\alpha \leftrightarrow \beta) - \text{traces} \end{aligned} \tag{609}$$

of Equation 583 represents an indispensable source of further operator relations, while in this context the actual structure of occurring traces, e. g., terms proportional to $g_{\alpha\beta}\partial^\rho \bar{u}\gamma^\sigma g\widetilde{\mathcal{G}}_{\rho\sigma} d$, $g_{\alpha\beta}\partial^\mu \bar{u}\gamma^\rho g\widetilde{\mathcal{G}}_{\mu\rho} d$, $g_{\alpha\beta} m_q \partial^2 \bar{u} i\gamma_5 d$, etc., becomes unimportant. Owing to Equation 609, the divergence of Equation 582 may now be deduced (modulo anomaly terms) by simply adding

$$\Delta_{\alpha\beta} = -\frac{1}{5}\partial^\mu \left\{\left[\mathcal{S}^{\alpha_1\alpha_2\alpha_3}_{\mu\alpha\beta} - \frac{1}{3}\mathbb{T}_{\alpha\beta\mu\alpha_4}\mathbb{T}^{\alpha_1\alpha_2\alpha_3\alpha_4}\right]\mathcal{M}_{\alpha_1\alpha_2\alpha_3}\right\} , \tag{610}$$

$$\mathcal{M}_{\mu\nu\rho} = \partial_\mu\partial_\nu \bar{u}\gamma_\rho\gamma_5 d . \tag{611}$$

Again, it is sufficient to analyze[132]

$$\mathcal{S}_\mu = \gamma_\mu \partial^2 + 2\not{\partial}\partial_\mu , \tag{612}$$

$$\mathcal{S}^{\alpha_1\alpha_2\alpha_3}_{\mu\alpha\beta}\mathcal{M}_{\alpha_1\alpha_2\alpha_3} = \bar{u}\left[2\gamma_\beta\partial_\alpha\partial_\mu + 2\gamma_\alpha\partial_\mu\partial_\beta + 2\gamma_\mu\partial_\alpha\partial_\beta\right]\gamma_5 d , \tag{613}$$

which gives us

$$\Delta_{\alpha\beta} = \left[-\frac{2}{15} m_q \partial_\alpha\partial_\beta \bar{u} i\gamma_5 d - \frac{1}{3}\partial_\beta\partial^2 \bar{u}\gamma_\alpha\gamma_5 d + (\alpha \leftrightarrow \beta)\right] - \text{traces}, \tag{614}$$

132 For this setting, $\bar{u}\,\mathcal{S}_\mu\gamma_5 d = g^{\xi\zeta}\left(\mathcal{M}_{\xi\zeta\mu} + \mathcal{M}_{\zeta\mu\xi} + \mathcal{M}_{\mu\xi\zeta}\right)$ represents a basic building block of the traces.

while ignoring all traces $\sim g_{\alpha\beta} m_q \partial^2 \bar{u} i\gamma_5 d$. Ultimately, we obtain the result (Equation 582 written for two different flavors)

$$\begin{aligned} 6\,\partial^\mu \mathcal{O}^{(\bar{u}d)}_{\mu\alpha\beta} &= -12 i\bar{u}\gamma^\rho\gamma_5 \Big[g\mathcal{G}_{\rho\beta}\overrightarrow{D}_\alpha - \overleftarrow{D}_\alpha g\mathcal{G}_{\rho\beta}\Big] d - 4\partial^\rho \bar{u}\gamma_\beta g\widetilde{\mathcal{G}}_{\alpha\rho} d \\ &\quad - 8 i m_q \bar{u}\sigma_{\alpha\rho}\gamma_5 g\mathcal{G}^\rho{}_\beta\, d - \frac{8}{3}\partial_\beta \bar{u}\gamma^\sigma g\widetilde{\mathcal{G}}_{\sigma\alpha} d \\ &\quad - \frac{2}{15} m_q \partial_\alpha\partial_\beta \bar{u} i\gamma_5 d + 2 m_q \bar{u} i\gamma_5 \overleftrightarrow{D}_\alpha \overleftrightarrow{D}_\beta d \\ &\quad - \frac{2}{3}(m_d - m_u)\,\partial_\beta \bar{u} i\gamma_5 \overleftrightarrow{D}_\alpha d + (\alpha \leftrightarrow \beta) - \text{traces}\,. \end{aligned} \tag{615}$$

As addressed before, the quark mass corrections $\sim \mathcal{O}(m_\psi)$ are a new result, extending our knowledge of the light pseudoscalar meson sector (e. g., [271]), see Section C.9. This is the case, since Equation 615 may be used to relate the NLO three-particle parameters of Equation 570, Equation 571, Equation 580 and Equation 581 with each other. For this purpose we start with the two-particle (pion) DAs

$$\langle 0|\bar{u}(-x)\,\gamma_\mu\gamma_5\, d(x)|\pi^-(P)\rangle = i f_\pi P_\mu \int_0^1 du\, e^{-i\xi_u (P\cdot x)} \phi_\pi(u)\,, \tag{616}$$

$$2 m_q \langle 0|\bar{u}(-x)\, i\gamma_5\, d(x)|\pi^-(P)\rangle = f_\pi m_\pi^2 \int_0^1 du\, e^{-i\xi_u (P\cdot x)} \phi_{3\pi}^p(u)\,, \tag{617}$$

$$\int_0^1 du\, \phi_\pi(u) = 1 = \int_0^1 du\, \phi_{3\pi}^p(u)\,, \tag{618}$$

and expand it around "$|x_\rho| \to 0$". The expansion up to "$\mathcal{O}(\xi_u^2)$" ensures, to receive nontrivial relations between the NLO parameters of

$$\phi_\pi(u) = 6u\bar{u}\left[1 + a_2^\pi\, C_2^{(3/2)}(\xi_u)\right]\,, \tag{619}$$

$$\phi_{3\pi}^p(u) = 1 + 30\,\eta_{3\pi}\, C_2^{(1/2)}(\xi_u)\,, \tag{620}$$

$$\eta_{3\pi} = \frac{2 m_q f_{3\pi}}{f_\pi m_\pi^2}\,, \tag{621}$$

and Equation 605–Equation 607. Accordingly, on the one hand we have (cf. Equation 588)

$$\begin{aligned} &x^\mu x^\alpha x^\beta \langle 0|\left[\bar{u}\overleftrightarrow{D}_\alpha \overleftrightarrow{D}_\beta \gamma_\mu\gamma_5 d - \frac{1}{5}\partial_\alpha\partial_\beta \bar{u}\gamma_\mu\gamma_5 d\right]_{\text{sym}} |\pi^-(P)\rangle \\ &= i f_\pi x^\mu x^\alpha x^\beta \mathcal{X}_{\mu\alpha\beta} \int_0^1 du\, \phi_\pi(u)\left[\xi_u^2 - \frac{1}{5}\right]\,, \end{aligned} \tag{622}$$

which entails (cf. Equation 589)

$$\langle 0|\partial^\mu \mathcal{O}^{(\bar{u}d)}_{\mu\alpha\beta}|\pi^-(P)\rangle = -\frac{2}{3} f_\pi m_\pi^2\, \mathcal{X}_{\alpha\beta} \int_0^1 du\, \phi_\pi(u)\left[\xi_u^2 - 1\right]\,. \tag{623}$$

Again, the local expansions

$$\langle 0|\bar{u} i\gamma_5 d|\pi^-(P)\rangle = \frac{f_\pi m_\pi^2}{2 m_q}\,, \tag{624}$$

$$x^\alpha x^\beta \langle 0|\bar{u}\overleftrightarrow{D}_\alpha \overleftrightarrow{D}_\beta i\gamma_5 d|\pi^-(P)\rangle = \frac{f_\pi m_\pi^2}{2 m_q} x^\alpha x^\beta \mathcal{X}_{\alpha\beta} \int_0^1 du\, \xi_u^2 \phi_{3\pi}^p(u)\,, \tag{625}$$

produce another conditional equation for $\langle 0|\partial^\mu O^{(\bar u d)}_{\mu\alpha\beta}|\pi^-(P)\rangle$ when inserted in Equation 615. After combining both approaches, we get the solutions:

$$\lambda_1^\pi = \frac{1}{9} - \frac{1}{45}\frac{m_\pi^2}{\delta_\pi^2}\left(1 - \frac{18}{7}a_2^\pi\right) - 2m_q\frac{f_{3\pi}}{f_\pi\delta_\pi^2}\,, \tag{626}$$

$$\lambda_2^\pi = -\frac{5}{9} + \lambda_3^\pi - \frac{1}{45}\frac{m_\pi^2}{\delta_\pi^2}\left(1 - \frac{18}{7}a_2^\pi\right) + 2m_q\frac{f_{3\pi}}{f_\pi\delta_\pi^2}\,. \tag{627}$$

A similar technique may be applied to the three-particle DAs, i. e., exploiting their local expansions (up to $\mathcal{O}(z^2)$), such as

$$\begin{aligned}&\langle 0|\bar u(z)\,\gamma_\mu\gamma_5 g\mathcal{G}_{\alpha\beta}(vz)\,d(-z)|\pi^-(P)\rangle\\ &= \langle 0|\bar u\gamma_\mu\gamma_5 g\mathcal{G}_{\alpha\beta}\,d|\pi^-(P)\rangle + z^\rho\langle 0|\bar u\gamma_\mu\gamma_5\Big[\overleftarrow{D}_\rho g\mathcal{G}_{\alpha\beta} + v\mathcal{D}_\rho g\mathcal{G}_{\alpha\beta} - g\mathcal{G}_{\alpha\beta}\overrightarrow{D}_\rho\Big]d|\pi^-(P)\rangle,\end{aligned} \tag{628}$$

$$\begin{aligned}&\langle 0|\bar u(z)\,\gamma_\mu ig\widetilde{\mathcal{G}}_{\alpha\beta}(vz)\,d(-z)|\pi^-(P)\rangle\\ &= \langle 0|\bar u\gamma_\mu ig\widetilde{\mathcal{G}}_{\alpha\beta}\,d|\pi^-(P)\rangle + z^\rho\langle 0|\bar u\gamma_\mu i\Big[\overleftarrow{D}_\rho g\widetilde{\mathcal{G}}_{\alpha\beta} + v\mathcal{D}_\rho g\widetilde{\mathcal{G}}_{\alpha\beta} - g\widetilde{\mathcal{G}}_{\alpha\beta}\overrightarrow{D}_\rho\Big]d|\pi^-(P)\rangle,\end{aligned} \tag{629}$$

in combination with (cf. Equation 330, Equation 331 and[133] Equation 333 up to[134] $\mathcal{O}((p\cdot z)^2)$)

$$\begin{aligned}&\langle 0|\bar u(z)\,\gamma_\mu\gamma_5 g\mathcal{G}_{\alpha\beta}(vz)\,d(-z)|\pi^-(P)\rangle\\ &= p_\mu(p_\alpha z_\beta - p_\beta z_\alpha)\frac{1}{p\cdot z}f_\pi\Big[i(p\cdot z)\tfrac{2}{21}\phi_1^\pi\Big]\\ &\quad + \Big(p_\beta g^\perp_{\alpha\mu} - p_\alpha g^\perp_{\beta\mu}\Big)f_\pi\Big[i(p\cdot z)\tfrac{1}{14}\big(\psi_2^\pi - \psi_1^\pi - \tfrac{7}{3}\psi_0^\pi\big)\Big]\,,\end{aligned} \tag{630}$$

$$\begin{aligned}&\langle 0|\bar u(z)\,\gamma_\mu ig\widetilde{\mathcal{G}}_{\alpha\beta}(vz)\,d(-z)|\pi^-(P)\rangle\\ &= p_\mu(p_\alpha z_\beta - p_\beta z_\alpha)\frac{1}{p\cdot z}f_\pi\Big[\tilde\phi_0^\pi - i(p\cdot z)\tfrac{v}{3}\big(\tilde\phi_0^\pi + \tfrac{2}{7}\tilde\phi_2^\pi\big)\Big]\\ &\quad - \Big(p_\beta g^\perp_{\alpha\mu} - p_\alpha g^\perp_{\beta\mu}\Big)f_\pi\Big[\psi_0^\pi - i(p\cdot z)\tfrac{v}{14}\big(7\psi_0^\pi + \psi_1^\pi + \psi_2^\pi\big)\Big]\,.\end{aligned} \tag{631}$$

Already the local limit of Equation 631, i. e.,

$$\begin{aligned}\lim_{|z|\to 0}\langle 0|\bar u(z)\,\gamma_\mu ig\widetilde{\mathcal{G}}_{\alpha\beta}(vz)\,d(-z)|\pi^-(P)\rangle &= -\big(p_\beta g_{\alpha\mu} - p_\alpha g_{\beta\mu}\big)f_\pi\psi_0^\pi\\ &\quad + \frac{p_\mu}{p\cdot z}(p_\alpha z_\beta - p_\beta z_\alpha)f_\pi\big[\tilde\phi_0^\pi - \psi_0^\pi\big] + \ldots\end{aligned} \tag{632}$$

reveals the necessary condition

$$\tilde\phi_0^\pi = \psi_0^\pi\,, \tag{633}$$

needed for the cancellation of a (formal) singularity at "$p\cdot z\to 0$". The remaining components of Equation 632 can be related to "$\mathcal{U}_\mu$" (cf. Equation 605) via a contraction with "$g^{\alpha\mu}$", implicating

$$\psi_0^\pi = -\frac{1}{3}\delta_\pi^2\,. \tag{634}$$

Furthermore, Equation 628 effectively reduces to[135]

$$\begin{aligned}&z^\rho\langle 0|\bar u\gamma_\mu\gamma_5\Big[\overleftarrow{D}_\rho g\mathcal{G}_{\alpha\beta} + \cancel{v\mathcal{D}_\rho g\mathcal{G}_{\alpha\beta}} - g\mathcal{G}_{\alpha\beta}\overrightarrow{D}_\rho\Big]d|\pi^-(P)\rangle\\ &= ip_\mu(p_\alpha z_\beta - p_\beta z_\alpha)f_\pi\tfrac{2}{21}\phi_1^\pi + ip\cdot z\Big(p_\beta g^\perp_{\alpha\mu} - p_\alpha g^\perp_{\beta\mu}\Big)f_\pi\big[\tfrac{1}{14}\psi_2^\pi - \tfrac{1}{14}\psi_1^\pi - \tfrac{1}{6}\psi_0^\pi\big]\end{aligned} \tag{635}$$

133 The pion case may be deduced from Equation 570, Equation 571 and Equation 580, Equation 581 via the replacement ($k\in\mathbb{N}_0$) $\phi^{(s)}_{k,M}\to\phi^\pi_k$, $\tilde\phi^{(s)}_{k,M}\to\tilde\phi^\pi_k$ and $\psi^{(s)}_{k,M}\to\psi^\pi_k$.

134 In this expansion, we neglect all contributions of $\mathcal{O}((p\cdot z)^2)$ to match the accuracy of Equation 628 and Equation 629.

135 There are no terms proportional to "v" on the r. h. s., hence corresponding terms on the l. h. s. may be dropped.

at NLO in conformal spin, which is related to $\mathcal{V}_1^{\alpha\beta}$ (cf. Equation 607) after a contraction with "$z^\beta g^{\mu\alpha}$":

$$\lambda_1^\pi \delta_\pi^2 = -\tfrac{2}{21}\phi_1^\pi - \tfrac{1}{3}\psi_0^\pi - \tfrac{1}{7}\psi_1^\pi + \tfrac{1}{7}\psi_2^\pi\,. \tag{636}$$

Similarly, when considering the general parametrization

$$\begin{aligned}&\langle 0|\bar{u}\gamma_\mu\gamma_5\Big[\overleftarrow{D}_\rho g\mathcal{G}_{\alpha\beta} - g\mathcal{G}_{\alpha\beta}\overrightarrow{D}_\rho\Big]d|\pi^-(P)\rangle\\ &= P_\rho\big(P_\beta g_{\alpha\mu} - P_\alpha g_{\beta\mu}\big)A + P_\mu\big(P_\beta g_{\alpha\rho} - P_\alpha g_{\beta\rho}\big)B\\ &\quad + \big(g_{\alpha\mu}g_{\beta\rho} - g_{\alpha\rho}g_{\beta\mu}\big)C + i\varepsilon_{\rho\mu\alpha\beta}D\,,\end{aligned} \tag{637}$$

a contraction with "$z^\beta z^\rho g^{\mu\alpha}$" and "$z^\beta z^\mu g^{\rho\alpha}$" not only entails

$$if_\pi\delta_\pi^2\lambda_1^\pi = 3A + B\,, \tag{638}$$

$$if_\pi\delta_\pi^2\lambda_2^\pi = 3B + A\,, \tag{639}$$

but also implies

$$A = if_\pi\big[\tfrac{1}{14}\psi_2^\pi - \tfrac{1}{14}\psi_1^\pi - \tfrac{1}{6}\psi_0^\pi\big]\,, \tag{640}$$

$$B = if_\pi\big[\tfrac{1}{6}\psi_0^\pi + \tfrac{1}{14}\psi_1^\pi - \tfrac{1}{14}\psi_2^\pi - \tfrac{2}{21}\phi_1^\pi\big]\,, \tag{641}$$

after equating coefficients with Equation 635. As a result, we get another useful relation:

$$\big(\lambda_1^\pi + \lambda_2^\pi\big)\,\delta_\pi^2 = -\tfrac{8}{21}\phi_1^\pi\,. \tag{642}$$

Equivalently, the contributions proportional to "v", i. e.,

$$\begin{aligned}&\langle 0|\bar{u}\gamma_\mu i\Big[\mathcal{D}_\rho g\widetilde{\mathcal{G}}_{\alpha\beta}\Big]d|\pi^-(P)\rangle\\ &= -ip_\mu\big(p_\alpha z_\beta - p_\beta z_\alpha\big)f_\pi\big[\tfrac{1}{3}\tilde{\phi}_0^\pi + \tfrac{2}{21}\tilde{\phi}_2^\pi\big]\\ &\quad + ip\cdot z\Big(p_\beta g^\perp_{\alpha\mu} - p_\alpha g^\perp_{\beta\mu}\Big)f_\pi\big[\tfrac{1}{2}\psi_0^\pi + \tfrac{1}{14}\psi_1^\pi + \tfrac{1}{14}\psi_2^\pi\big] + \ldots\,,\end{aligned} \tag{643}$$

are connected to "$\mathcal{V}_3^{\alpha\beta}$" (cf. Equation 607) via

$$\begin{aligned}&\langle 0|\bar{u}\gamma_\mu i\Big[\mathcal{D}_\rho g\widetilde{\mathcal{G}}_{\alpha\beta}\Big]d|\pi^-(P)\rangle\\ &= P_\rho\big(P_\beta g_{\alpha\mu} - P_\alpha g_{\beta\mu}\big)\widetilde{A} + P_\mu\big(P_\beta g_{\alpha\rho} - P_\alpha g_{\beta\rho}\big)\widetilde{B}\\ &\quad + \big(g_{\alpha\mu}g_{\beta\rho} - g_{\alpha\rho}g_{\beta\mu}\big)\widetilde{C} + i\varepsilon_{\rho\mu\alpha\beta}\widetilde{D}\,,\end{aligned} \tag{644}$$

when contracting Equation 644 with "$z^\rho z^\beta g^{\mu\alpha}$" and "$z^\beta z^\mu g^{\rho\beta}$", resulting in

$$\widetilde{A} = -\frac{3}{8}if_\pi\delta_\pi^2\lambda_3^\pi\,, \tag{645}$$

$$\widetilde{B} = +\frac{1}{8}if_\pi\delta_\pi^2\lambda_3^\pi\,. \tag{646}$$

After equating coefficients with Equation 631, Equation 644 implies

$$\delta_\pi^2\lambda_3^\pi = -\tfrac{4}{3}\tilde{\phi}_0^\pi - \tfrac{8}{21}\tilde{\phi}_2^\pi\,, \tag{647}$$

$$0 = \tilde{\phi}_0^\pi + \tfrac{2}{7}\tilde{\phi}_2^\pi - \psi_0^\pi - \tfrac{1}{7}\psi_1^\pi - \tfrac{1}{7}\psi_2^\pi\,. \tag{648}$$

Hence, we get

$$\delta_\pi^2\left(\lambda_1^\pi-\tfrac{1}{9}\right)=-\tfrac{2}{21}\phi_1^\pi-\tfrac{1}{7}\psi_1^\pi+\tfrac{1}{7}\psi_2^\pi\,, \tag{649}$$

$$\delta_\pi^2\left(\lambda_1^\pi+\lambda_2^\pi\right)=-\tfrac{8}{21}\phi_1^\pi\,, \tag{650}$$

$$\delta_\pi^2\left(\lambda_3^\pi-\tfrac{4}{9}\right)=-\tfrac{8}{21}\tilde{\phi}_2^\pi\,, \tag{651}$$

$$0=2\tilde{\phi}_2^\pi-\psi_1^\pi-\psi_2^\pi\,, \tag{652}$$

implying the equivalence between the parameter sets $\{\lambda_1^\pi,\lambda_2^\pi,\lambda_3^\pi\}\Leftrightarrow\{\phi_1^\pi,\psi_1^\pi,\psi_2^\pi\}$. Due to the structure of Equation 600 and Equation 604, λ_3^π is linked to:

$$\begin{aligned}&\langle 0|\bar{u}\Big[iD_\mu,ig\widetilde{\mathcal{G}}_{\nu\xi}\Big]\gamma^\xi d-\tfrac{4}{9}i\partial_\mu\bar{u}ig\widetilde{\mathcal{G}}_{\nu\xi}\gamma^\xi d|\pi^-(P)\rangle\\&=f_\pi\delta_\pi^2\omega_{4\pi}\left[P_\mu P_\nu-\frac{1}{4}m_\pi^2 g_{\mu\nu}\right]+\text{“twist 5”}\,,\end{aligned} \tag{653}$$

via (e.g., [271, 281])

$$\omega_{4\pi}=\frac{4}{9}-\lambda_3^\pi\,. \tag{654}$$

Analogously, the QF (NLO) parameters can be related to [3]

$$\begin{aligned}&\langle 0|\bar{s}\Big[iD_\mu,ig\widetilde{\mathcal{G}}_{\nu\xi}\Big]\gamma^\xi s-\tfrac{4}{9}i\partial_\mu\bar{s}ig\widetilde{\mathcal{G}}_{\nu\xi}\gamma^\xi s|M(P)\rangle\\&=f_M^{(s)}\delta_M^{2(s)}\omega_{4M}^{(s)}\left[P_\mu P_\nu-\frac{1}{4}m_M^2 g_{\mu\nu}\right]+\text{“twist 5”}\end{aligned} \tag{655}$$

as well as [3]

$$\langle 0|\bar{s}\gamma^\rho ig\widetilde{\mathcal{G}}_{\rho\mu}s|M(P)\rangle=P_\mu f_M^{(s)}\delta_M^{2(s)}\,. \tag{656}$$

This allows us to rephrase Equation 634 and Equation 649–Equation 652 into the result [3]

$$\tilde{\phi}_{0,M}^{(s)}=\psi_{0,M}^{(s)}=-\frac{1}{3}\delta_M^{2(s)}, \tag{657}$$

$$\tilde{\phi}_{2,M}^{(s)}=\frac{21}{8}\delta_M^{2(s)}\omega_{4M}^{(s)}\,, \tag{658}$$

$$\phi_{1,M}^{(s)}=\frac{21}{8}\left[\delta_M^{2(s)}\omega_{4M}^{(s)}+\frac{2}{45}m_M^2\left(1-\frac{18}{7}c_{2,M}^{(s)}\right)\right], \tag{659}$$

$$\psi_{1,M}^{(s)}=\frac{7}{4}\left[\delta_M^{2(s)}\omega_{4M}^{(s)}+\frac{1}{45}m_M^2\left(1-\frac{18}{7}c_{2,M}^{(s)}\right)+4m_s\frac{f_{3M}^{(s)}}{f_M^{(s)}}\right], \tag{660}$$

$$\psi_{2,M}^{(s)}=\frac{7}{4}\left[2\delta_M^{2(s)}\omega_{4M}^{(s)}-\frac{1}{45}m_M^2\left(1-\frac{18}{7}c_{2,M}^{(s)}\right)-4m_s\frac{f_{3M}^{(s)}}{f_M^{(s)}}\right], \tag{661}$$

modulo anomaly terms. In consequence, the number of anticipated new twist-four parameters has been reduced to $2\times2\times2=8$ in general and dwindles even more when assuming the state mixing ansatz (cf. Equation 315). After employing the latter, we would be left with only four extra parameters[136] (cf. Equation 315, Table 10)

$$\delta_{4q}^2\approx\delta_{4\pi}^2\,,\quad \delta_{4s}^2\approx\delta_{4K}^2\,,\quad \omega_{4q}\approx\omega_{4\pi}\,,\quad \omega_{4s}\approx\omega_{4K}\,, \tag{662}$$

136 This is analogous to Equation 277, when replacing the decay constants either with $f_M^{(s)}\leftrightarrow f_M^{(s)}\delta_M^{2(s)}$ (similar for “$q\leftrightarrow s$”) or $f_M^{(s)}\leftrightarrow f_M^{(s)}\delta_M^{2(s)}\omega_{4M}^{(s)}$.

PION	μ_0	KAON	μ_0
δ_π^2	$0.18(6)\,\mathrm{GeV}^2$	δ_K^2	$0.20(6)\,\mathrm{GeV}^2$
$\kappa_{4\pi}$	0	κ_{4K}	$-0.09(2)$
$\omega_{4\pi}$	0.2(1)	ω_{4K}	0.2(1)

Table 10: Hadronic twist-four parameters for the pion and kaon case, taken from [269, 271, 337] (at the reference scale $\mu_0 = 1$ GeV).

which are renormalized at LO via [271] (analogously for "$q \leftrightarrow s$")

$$\left[\delta_M^{2(s)}\right]\left(\mu^2\right) \approx L(\mu,\mu_0)\left[\delta_M^{2(s)}\right]\left(\mu_0^2\right) + \frac{1}{8}m_M^2\left(1 - L(\mu,\mu_0)\right), \tag{663}$$

$$\left[\omega_{4M}^{(s)}\delta_M^{2(s)}\right]\left(\mu^2\right) \approx L(\mu,\mu_0)^{\frac{45}{16}}\left[\omega_{4M}^{(s)}\delta_M^{2(s)}\right]\left(\mu_0^2\right), \tag{664}$$

with the factor $L(\mu,\mu_0) \equiv \left[\alpha_s(\mu^2)/\alpha_s(\mu_0^2)\right]^{\frac{32}{9\beta_0}}$. While this takes care of all needed three particle DAs, there are still the corresponding two-particle twist-four distributions $\psi_{4M}^{(s)}$ and $\widetilde{\phi}_{4M}^{(s)}$ (cf. Equation 325). Due to strategic reasons, such as the explicit calculation of updated twist-four octet meson DAs (cf. Section C.9), we will start with the pion case, as a generic example, followed by the anticipated extension to the singlet case. Similar to the mentioned twist-three case, all two-particle twist-four DAs may be calculated on the basis of non-local operator identities, e. g., Equation 1487 and Equation 1488. For $\psi_{4\pi}$, we, therefore, get $\left(n^2 = 0,\, n^\mu P_\mu = P_+\right)$

$$\begin{aligned}\int_0^1 dx\, e^{i\xi_x P_+}\psi_{4\pi}(x) = &\int_0^1 dx\, e^{i\xi_x P_+} 2m_\pi^2\left[\phi_{3\pi}^p(x) - \phi_\pi(x)\right] \\ &+ \int_{-1}^1 dv\, 2\,(iP_+)\left[2\Psi_{4\pi}(v,P_+) - \Phi_{4\pi}(v,P_+)\right],\end{aligned} \tag{665}$$

which implies the relation[137]

$$M_n^{\psi_{4\pi}} = 2m_\pi^2\left[M_n^{\phi_{3\pi}^p} - M_n^{\phi_\pi}\right] + n\, M_{n-1}^{\varphi_{4\pi}^{(3)}}, \tag{666}$$

formulated with the auxiliary DA (cf. Equation 1522, Equation 1523)

$$\varphi_{4\pi}^{(3)}(x) = \int_0^x d\alpha_1 \int_0^{\bar{x}} d\alpha_2\, \frac{4[2\Psi_{4\pi}(\underline{\alpha}) - \Phi_{4\pi}(\underline{\alpha})]}{\alpha_3}\bigg|_{\alpha_3 = 1-\alpha_1-\alpha_2}. \tag{667}$$

The corresponding solution is then given by (cf. Equation 1494)

$$\psi_{4\pi}(x) = 2m_\pi^2\left[\phi_{3\pi}^p(x) - \phi_\pi(x)\right] - \frac{1}{2}\frac{d}{dx}\varphi_{4\pi}^{(3)}(x)\,. \tag{668}$$

Analogously, Equation 1482 entails the equation

$$\begin{aligned}iP_+\int_0^1 dx\, e^{i\xi_x P_+}\phi_{4\pi}(x) = &\int_0^1 dx\, e^{i\xi_x P_+}\left[\left(\xi_x + \frac{3}{iP_+}\right)\psi_{4\pi}(x)\right. \\ &\left. + 2m_\pi^2\left(\xi_x\phi_\pi(x) + \frac{m_u - m_d}{m_u + m_d}\phi_{3\pi}^p(x)\right)\right] \\ &+ 2iP_+\int_{-1}^1 dv\, v[2\Psi_{4\pi}(v,P_+) - \Phi_{4\pi}(v,P_+)],\end{aligned} \tag{669}$$

137 Similar to the twist-three two particle DAs, $\psi_{4M}^{(s)}$ and $\widetilde{\phi}_{4M}^{(s)}$, can be calculated in terms of three-particle (twist-four) distributions as well as the named DAs of lower twist.

which evokes a (formal) recursion relation

$$n\,M_{n-1}^{\phi_{4\pi}} = \frac{n+4}{n+1} M_{n+1}^{\psi_{4\pi}} + 2n\,M_{n-1}^{\varphi_{4\pi}^{(4)}} + 2m_\pi^2 \left(M_{n+1}^{\phi_\pi} + \frac{m_u - m_d}{m_u + m_d} M_n^{\phi_{3\pi}^p} \right) , \tag{670}$$

for $\phi_{4\pi}$. In other words, when using $(\alpha_3 = 1 - \alpha_1 - \alpha_2)$

$$\varphi_{4\pi}^{(4)}(x) = \int_0^x d\alpha_1 \int_0^{\bar{x}} d\alpha_2 \, \frac{2\,[\alpha_1 - \alpha_2 - \xi_x]}{\alpha_3^2} \, [2\Psi_{4\pi}(\underline{\alpha}) - \Phi_{4\pi}(\underline{\alpha})] , \tag{671}$$

Equation 670 gives rise to the ordinary DE

$$\begin{aligned} \frac{d^2}{dx}\phi_{4\pi}(x) = {} & 12\,\psi_{4\pi}(x) - 2\frac{d}{dx}\xi_x \Big(\psi_{4\pi}(x) + 2m_\pi^2 \phi_\pi(x) \Big) \\ & - 4m_\pi^2 \frac{m_u - m_d}{m_u + m_d} \frac{d}{dx} \phi_{3\pi}^p(x) + 2\frac{d^2}{dx^2} \varphi_{4\pi}^{(4)}(x) , \end{aligned} \tag{672}$$

that exhibits a substantial difference to [271, Equation 4.28]. A literature search supports this finding: in [319] the needed correction has been formulated as follows (based on [271])

$$^{[271]}\psi_{4\pi}(x) \to {}^{[271]}\psi_{4\pi}(x) + m_\pi^2 \phi_\pi(x) . \tag{673}$$

The latter is in agreement with Equation 672. Thus, the full solution is given by

$$\phi_{4\pi}(x) = -x \int_0^1 dv \int_0^v dw\, \phi_{4\pi}''(w) + \int_0^x dv \int_0^v dw\, \phi_{4\pi}''(w) . \tag{674}$$

On these grounds, we may obtain the required two-particle DAs $\psi_{4M}^{(s)}$ and $\psi_{4M}^{(s)}$ (likewise "$q \leftrightarrow s$") without anomalous contributions. The corresponding expressions can conveniently be separated in genuine twist-four contributions and meson mass corrections (for a numerical evaluation see Section 4.3):

$$\psi_{4M}^{(s)}(x) = \psi_{4M}^{(s)\,\text{twist}}(x) + m_M^2 \psi_{4M}^{(s)\,\text{mass}}(x) , \tag{675}$$

together with

$$\psi_{4M}^{(s)\,\text{twist}}(x) = \frac{20}{3}\delta_M^{2(s)} C_2^{(1/2)}(\xi_x) + 30 m_s \frac{f_{3M}^{(s)}}{f_M^{(s)}} \left(\frac{1}{2} - 10x\bar{x} + 35x^2\bar{x}^2 \right) , \tag{676}$$

$$\psi_{4M}^{(s)\,\text{mass}}(x) = \frac{17}{12} - 19x\bar{x} + \frac{105}{2}x^2\bar{x}^2 + c_{2,M}^{(s)} \left(\frac{3}{2} - 54x\bar{x} + 225x^2\bar{x}^2 \right) . \tag{677}$$

Similarly for

$$\phi_{4M}^{(s)}(x) = \phi_{4M}^{(s)\,\text{twist}}(x) + m_M^2 \phi_{4M}^{(s)\,\text{mass}}(x) , \tag{678}$$

we get

$$\begin{aligned} \phi_{4M}^{(s)\,\text{twist}}(x) = {} & \frac{200}{3}\delta_M^{2(s)} x^2\bar{x}^2 + 21\delta_M^{2(s)}\omega_{4M}^{(s)} \Big\{ x\bar{x}\,(2 + 13x\bar{x}) \\ & + 2\left[x^3 \left(10 - 15x + 6x^2 \right) \log x + (x \leftrightarrow \bar{x}) \right] \Big\} \\ & + 20 m_s \frac{f_{3M}^{(s)}}{f_M^{(s)}} x\bar{x} \left[12 - 63x\bar{x} + 14x^2\bar{x}^2 \right] , \end{aligned} \tag{679}$$

along with

$$\phi_{4M}^{(s)\,\mathrm{mass}}(x) = x\bar{x}\left[\frac{88}{15}+\frac{39}{5}x\bar{x}+14x^2\bar{x}^2\right] - c_{2,M}^{(s)}\,x\bar{x}\left[\frac{24}{5}-\frac{54}{5}x\bar{x}+180x^2\bar{x}^2\right] + \left(\frac{28}{15}-\frac{24}{5}c_{2,M}^{(s)}\right)\left[x^3\left(10-15x+6x^2\right)\log x+(x\leftrightarrow\bar{x})\right] . \tag{680}$$

Notably, Equation 675–Equation 680 are a new result and supersede the corresponding expressions in [271] and [319] (cf. Section C.9 for the updated kaon case).

Let us now include the anomalous contributions into our considerations. In general, the operator identities Equation 615, Equation 1482 and Equation 1483, are only valid in their present form when considering unrenormalized operators. Hence, an extended full NLO analysis would have to include $\mathcal{O}(\alpha_S)$ renormalization factors[138] (cf. [82, 338]) for the involved light-cone operators (cf. discussion in [3]). Those RG corrections, however, have to match the problem specific OPE's accuracy. For instance, twist-four corrections of the latter have to be of a similar order in "α_S", as the renormalization factors. Given that, only LO twist-four effects are included, all $\mathcal{O}(\alpha_S)$ corrections created by the corresponding operator renormalization should be neglected. Hence, we have to separate all relevant "LO" contributions of the axial anomaly from actual (multi-particle) NLO RG corrections.
On the other hand, we have to avoid possible ill-defined contributions, that are conceivable in the context of axial-vector currents (cf. [3]). E. g., by their nature, both involved EOM (analogously for "$q\leftrightarrow s$"; see Section C.7)

$$\frac{\partial}{\partial x_\mu}\bar{s}(x)\,\gamma_\mu\gamma_5 s(-x) = -i\int_{-1}^{1}\mathrm{d}v\,\bar{s}(x)\,vx_\rho g\mathcal{G}^{\rho\mu}(vx)\,\gamma_\mu\gamma_5 s(-x)\ , \tag{681}$$

$$\partial^\mu\{\bar{s}(x)\,\gamma_\mu\gamma_5 s(-x)\} = -i\int_{-1}^{1}\mathrm{d}v\,\bar{s}(x)\,x_\rho g\mathcal{G}^{\rho\mu}(vx)\,\gamma_\mu\gamma_5 s(-x) + 2m_s\bar{s}(x)\,i\gamma_5 s(-x)\ , \tag{682}$$

are exact for $|x_\rho|\neq 0$, while the limit $x_\rho\to 0$ has to be taken with great caution (cf. Section A.8). Particularly, light-ray operators that enter the definitions of DAs (e. g., Equation 682) are generating functions of renormalized local operators which themselves may give rise to identities such as Equation 149.

In analogy to Schwinger's split point regularization (cf. Section A.8) we may, therefore, apply a regularized version of the light-ray operators, refined by shifting all compatible operators slightly off the light-cone ($n^2=0$), i. e.,

$$\bar{s}\,(z_1 n)\,[z_1 n, z_2 n]\,\gamma_\mu\gamma_5 s(z_2 n) \mapsto \bar{s}\,(x_1)\,[x_1,x_2]\,\gamma_\mu\gamma_5 s(x_2)\ , \tag{683}$$

with the notation (setting $x^2\neq 0$)

$$x_2^\mu := z_2 n^\mu - x^\mu\,,\quad x_1^\mu := z_1 n^\mu + x^\mu\,,\quad \Delta^\mu := x_1^\mu - x_2^\mu\,, \tag{684}$$

$$\Delta^2 = (x_1-x_2)^2 = (z_{12}n+2x)^2 = x^2\,,\quad (x\cdot n)=0\,. \tag{685}$$

138 It should be mentioned, that such an endeavor would be considerable and has only been partially attempted (mostly leading twist effects) during the last decades of development within this sector of QCD (e. g., [311, 338]). Moreover, a similar complex of problems has been discussed in the context of three-particle pion DAs (cf. [332]), whose evolution is largely unknown (e. g., [339] and references therein). Indeed, the evolution of two- and three-particle twist-four operators is significantly more complicated, than the twist-two counterpart, due to mixing effects with all other multi-particle operators that have proper quantum numbers (cf. [3]).

Hence, Equation 682 (cf. Equation 1484) transforms into

$$\begin{aligned}\partial^{\mu}\{\bar{s}(z_1 n{+}x)\,\gamma_\mu\gamma_5 s(z_2 n{-}x)\} = -i\int_0^1 dv\,\bar{s}(z_1 n{+}x)\,\Delta_\rho g\mathcal{G}^{\rho\mu}(z_{21}^v n{+}\xi_v x)\,\gamma_\mu\gamma_5 s(z_2 n{-}x)\\ +2m_s\bar{s}(z_1 n{+}x)\,i\gamma_5 s(z_2 n{-}x)\,,\end{aligned}\tag{686}$$

whose three-particle components are a source of anomalous contributions. For instance, when using[139] [75]

$$\begin{aligned}\overbrace{\psi(x_2)\,\bar{\psi}}(x_1) = -i\frac{\not{\Delta}}{2\pi^{D/2}}\frac{\Gamma\left(\frac{D}{2}\right)}{\left[-\Delta^2\right]^{D/2}}[x_2,x_1]\\ -\frac{\Delta^\rho}{8\pi^{D/2}}\frac{\Gamma\left(\frac{D}{2}{-}1\right)}{\left[-\Delta^2\right]^{D/2-1}}\int_0^1 du\Big[ig\widetilde{\mathcal{G}}_{\rho\sigma}(ux_2{+}\bar{u}x_1)\,\gamma^\sigma\gamma_5\\ -u\bar{u}\,(\Delta{\cdot}D)\,\mathcal{G}_{\rho\sigma}(ux_2{+}\bar{u}x_1)\,\gamma^\sigma\Big]\,,\end{aligned}\tag{687}$$

Equation 686 engenders the new anomaly term[140]

$$\begin{aligned}&\mathcal{O}_\chi(z_1 n{+}x, z_2 n{-}x)\\ &:= i\int_0^1 dv\,\underbrace{\bar{\psi}(z_1 n{+}x)\,\Delta^\alpha g\mathcal{G}_{\alpha\mu}(z_{21}^v n{+}\xi_v x)\,\gamma_\mu\gamma_5\psi}(z_2 n{-}x)\\ &= i\int_0^1 dv\,\Delta^\alpha\,\mathrm{Tr}\big\{\gamma^\mu\gamma_5 iS_\psi(z_2 n{-}x, z_1 n{+}x)\,g\mathcal{G}_{\alpha\mu}(z_{21}^v n{+}\xi_v x)\big\}\\ &= \frac{\alpha_S}{4\pi}\int_0^1 dv\int_0^1 du\,\frac{\Delta^\alpha\Delta^\rho}{\Delta^2}\mathcal{G}^A_{\alpha\xi}(z_{21}^v n{+}\xi_v x)\,\widetilde{\mathcal{G}}^{A,\xi}_\rho(z_{12}^u n{-}\xi_u x)\,.\end{aligned}\tag{688}$$

Indeed, Equation 688 procreates a plethora of different contributions, e. g., by using the proper light-cone expansions (modulo $\mathcal{O}(x^2)$)

$$\mathcal{G}_{\alpha\beta}(z_{21}^v n{+}\xi_v x) = \mathcal{G}_{\alpha\beta}(z_{21}^v n) + \xi_v x^\xi\left[D_\xi\mathcal{G}_{\alpha\beta}\right](z_{21}^v n) + \dots\,,\tag{689}$$

$$\widetilde{\mathcal{G}}_{\alpha\beta}(z_{12}^u n{-}\xi_u x) = \widetilde{\mathcal{G}}_{\alpha\beta}(z_{12}^u n) - \xi_u x^\xi\left[D_\xi\widetilde{\mathcal{G}}_{\alpha\beta}\right](z_{12}^u n) + \dots\,,\tag{690}$$

along with

$$\mathcal{G}_{\rho\alpha}(x_1)\,\widetilde{\mathcal{G}}^\rho{}_\mu(x_2) + \widetilde{\mathcal{G}}^\rho{}_\mu(x_1)\,\mathcal{G}_{\rho\alpha}(x_2) = \frac{1}{2}g_{\alpha\mu}\widetilde{\mathcal{G}}_{\rho\xi}(x_1)\,\mathcal{G}^{\rho\xi}(x_2)\,,\tag{691}$$

$$\Rightarrow \mathcal{G}_{\rho\xi}(x_1)\,\widetilde{\mathcal{G}}^{\rho\xi}(x_2) = \widetilde{\mathcal{G}}_{\rho\xi}(x_1)\,\mathcal{G}^{\rho\xi}(x_2)\,.\tag{692}$$

Certainly, the Equation 691 enables a decisive simplification of several contributions, e. g.,

$$\left[D^\alpha\mathcal{G}^A_{n\mu}\right](z_{21}^v n)\,\widetilde{\mathcal{G}}^{A,\mu}_\alpha(z_{12}^u n) = \frac{1}{2}(n{\cdot}D)\widetilde{\mathcal{G}}^A_{\alpha\mu}(z_{21}^v n)\,\mathcal{G}^{A,\alpha\mu}(z_{12}^u n)\,,\tag{693}$$

$$\begin{aligned}\mathcal{G}^A_{\alpha\mu}(z_{21}^v n)\left[D^\alpha\widetilde{\mathcal{G}}^{A,\mu}_n\right](z_{12}^u n) = \frac{1}{2}\widetilde{\mathcal{G}}^A_{\alpha\mu}(z_{21}^v n)\,(n{\cdot}D)\mathcal{G}^{A,\alpha\mu}(z_{12}^u n)\\ -\widetilde{\mathcal{G}}^A_{n\mu}(z_{21}^v n)\left[D^\alpha\mathcal{G}^{A,\mu}_\alpha\right](z_{12}^u n)\,.\end{aligned}\tag{694}$$

139 The ellipses in Equation 687 correspond to $\mathcal{O}(\log x^2)$, not contributing in the relevant limit $x_\rho\to 0$.
140 The mass terms of $\mathcal{O}(m_\psi)$ cannot contribute to $\mathcal{O}_\chi$ (cf. Equation 139).

After a further simplifications, we get up to $\mathcal{O}(x^2)$

$$\begin{aligned}\mathcal{O}_\chi(x_1,x_2) = \frac{\alpha_s}{4\pi}\int_0^1 dv\int_0^1 du\, \mathcal{G}^A_{\mu\nu}(z^v_{21}n)\,\widetilde{\mathcal{G}}^{A,\mu\nu}(z^u_{12}n)\\ + \frac{\alpha_s}{8\pi}z_{12}\int_0^1 dv\int_0^1 du\left[\xi_u\widetilde{\mathcal{G}}^A_{n\mu}(z^v_{21}n)\left[D^\alpha\mathcal{G}^{A,\mu}_\alpha\right](z^u_{12}n)\right.\\ + \xi_v\left[D^\alpha\mathcal{G}^A_{\alpha\mu}\right](z^v_{21}n)\,\widetilde{\mathcal{G}}^{A,\mu}_n(z^u_{12}n) + \frac{1}{2}\xi_v\,(n{\cdot}D)\,\widetilde{\mathcal{G}}^A_{\alpha\mu}(z^v_{21}n)\,\mathcal{G}^{A,\alpha\mu}(z^u_{12}n)\\ - \frac{1}{2}\xi_u\widetilde{\mathcal{G}}^A_{\alpha\mu}(z^v_{21}n)\,(n{\cdot}D)\,\mathcal{G}^{A,\alpha\mu}(z^u_{12}n)\\ \left. - \frac{1}{2}z_{12}^2\xi_u\xi_v\left[D^\alpha\mathcal{G}^A_{n\mu}\right](z^v_{21}n)\left[D_\alpha\widetilde{\mathcal{G}}^{A,\mu}_n\right](z^u_{12}n)\right] + \dots\,,\end{aligned} \tag{695}$$

where we omit all terms, that do not survive the symmetric limit

$$\frac{x^\alpha x^\beta}{x^2} \longrightarrow \frac{1}{4}g^{\alpha\beta}\,. \tag{696}$$

As a result, terms similar to

$$z_{12}\,(n{\cdot}D)\,\mathcal{G}^A_{\alpha\mu}(z^u_{12}n) = -\partial_u\mathcal{G}^A_{\alpha\mu}(z^u_{12}n)\,, \tag{697}$$

$$z_{12}\,(n{\cdot}D)\,\widetilde{\mathcal{G}}^A_{\alpha\mu}(z^v_{21}n) = +\partial_v\widetilde{\mathcal{G}}^A_{\alpha\mu}(z^v_{21}n)\,, \tag{698}$$

within Equation 695 vanish. However, a multitude of finite $\mathcal{O}(\alpha_s)$ corrections to the three-particle DAs, such as

$$\left[D^\alpha\mathcal{G}^A_{\alpha\mu}\right](z^v_{21}n)\,\widetilde{\mathcal{G}}^{A,\mu}_n(z^u_{12}n) = i\sum_\psi\bar\psi(z^v_{21}n)\,\gamma^\mu ig\widetilde{\mathcal{G}}_{n\mu}(z^u_{12}n)\,\psi(z^v_{21}n)\,, \tag{699}$$

$$\widetilde{\mathcal{G}}^A_{n\mu}(z^v_{21}n)\left[D^\alpha\mathcal{G}^{A,\mu}_\alpha\right](z^u_{12}n) = i\sum_\psi\bar\psi(z^u_{12}n)\,\gamma^\mu ig\widetilde{\mathcal{G}}_{n\mu}(z^v_{21}n)\,\psi(z^u_{12}n)\,, \tag{700}$$

along with

$$D^2\mathcal{G}_{n\mu} = 2i\left[\mathcal{G}_{n\alpha},\mathcal{G}^\alpha{}_\mu\right] + (n{\cdot}D)\,D^\alpha\mathcal{G}_{\alpha\mu} - D_\mu D^\alpha\mathcal{G}_{\alpha n}\,. \tag{701}$$

remain. Those produce the anticipated NLO corrections to quark-antiquark-gluon and three-gluon terms. Consequently, an extended EOM result for higher twist corrections is given by

$$\begin{aligned}\partial^\mu\left\{\bar\psi(z_1n)\,\gamma_\mu\gamma_5\psi(z_2n)\right\} = -i\int_0^1 dv\,\bar\psi(z_1n)\,z_{12}n^\rho g\mathcal{G}_{\rho\mu}(z^v_{21}n)\,\gamma^\mu\gamma_5\psi(z_2n)\\ + \frac{\alpha_s}{4\pi}\int_0^1 dv\int_0^1 du\,\mathcal{G}^A_{\mu\nu}(z^v_{21}n)\,\widetilde{\mathcal{G}}^{A,\mu\nu}(z^u_{12}n)\\ + 2m_\psi\bar\psi(z_1n)\,i\gamma_5\psi(z_2n)\,,\end{aligned} \tag{702}$$

where we have taken the "$|x_\rho|\to 0$" limit, while using

$$\frac{\alpha_s}{4\pi}\int_0^1 dv\int_0^1 du\,\mathcal{G}^A_{\mu\nu}(z^v_{21}n)\,\widetilde{\mathcal{G}}^{A,\mu\nu}(z^u_{12}n) = \frac{\alpha_s}{16\pi}\int_{-1}^1 d\alpha\int_{-1}^1 d\beta\,\mathcal{G}^A_{\mu\nu}(\alpha n)\,\widetilde{\mathcal{G}}^{A,\mu\nu}(\beta n)\,. \tag{703}$$

Compared to the pion case, this modification only affects $\psi^{(s)}_{4M}$ (as well as "$q\leftrightarrow s$") directly, represented by admixtures of a new twist-four gluonic DA ($n^2=0$)

$$\langle 0|\tfrac{\alpha_s}{4\pi}\mathcal{G}^A_{\mu\nu}(z_2n)\,\widetilde{\mathcal{G}}^{A,\mu\nu}(z_1n)|M(P)\rangle = a_M\int_0^1 dx\,e^{-iz^x_{21}P{\cdot}n}\phi^{(g)}_{4M}(x)\,. \tag{704}$$

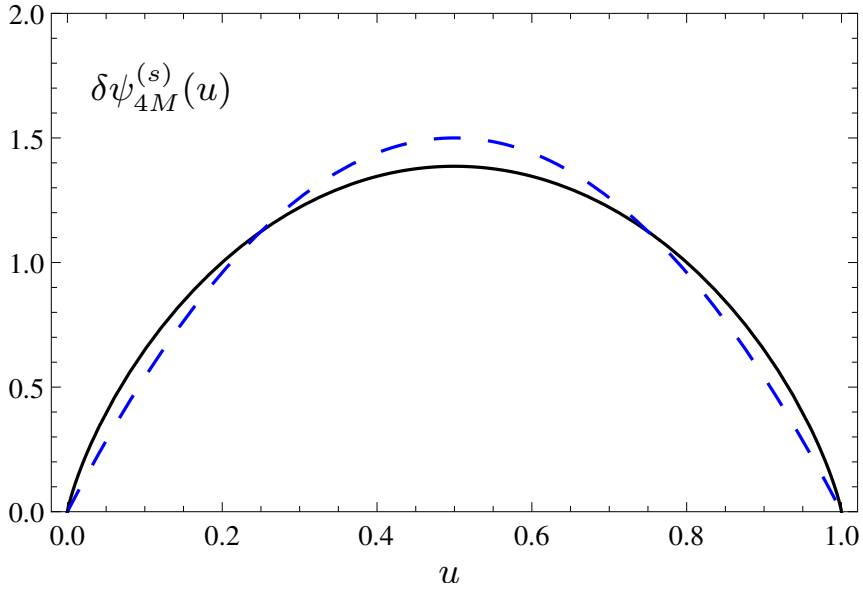

Figure 17: The anomalous contribution Equation 726 to the twist-four DA "$\psi^{(s)}_{4M}(u)$" (continuous line) compared to the asymptotic (leading-twist) DA "$6u\bar{u}$" (dashed line).

Naively, the associated leading twist components, e. g., ($j_1 = 1 = j_2$) those corresponding to $\mathcal{G}^A_{+-}\widetilde{\mathcal{G}}^A_{-\perp} \sim \mathcal{G}^A_{+-}\mathcal{G}^A_{\perp\perp}$ would imply a conformal expansion similar to[141]

$$\phi^{(g)}_{4M}\left(x,\mu^2\right) = 6x\bar{x}\sum_{n=0}^{\infty} a^{(g)}_{n,M}\left(\mu^2\right) C_n^{(3/2)}(\xi_x)\,, \tag{705}$$

with a necessarily non-vanishing asymptotic form[142] (cf. Equation 527)

$$\phi^{(g)}_{4M}(x) \longrightarrow 6x\bar{x} \quad \Leftrightarrow \quad a^{(g)}_{0,M} = 1\,. \tag{706}$$

Specifically, Equation 706 presupposes the normalization condition

$$\int_0^1 dx\, \phi^{(g)}_{4M}(x) = 1\,, \tag{707}$$

while Equation 692 implies

$$\phi^{(g)}_{4M}(x) = \phi^{(g)}_{4M}(\bar{x})\,, \tag{708}$$

i. e., an expansion with only even Gegenbauer moments "$a^{(g)}_{n,M}$" (cf. Equation 706). This newly found DA is intrinsically connected to effects of the axial anomaly and may, therefore, shed light on the topological structure of QCD in general (cf. Section 2.5). Thus, any information on its shape might be valuable for further studies. On the other hand, a calculation of the correlation function

$$\begin{aligned}\Pi(p) &= i\int d^4y\, e^{-ipy}\langle 0|\mathcal{G}_{\mu\nu}(z_1 n)\,\widetilde{\mathcal{G}}^{\mu\nu}(z_2 n)\,\mathcal{G}_{\alpha\beta}(y)\,\widetilde{\mathcal{G}}^{\alpha\beta}(y)|0\rangle \\ &= \int_0^1 dx\, e^{-z_{21}^x pn}\phi^{(g)}_{4M}(x)\,\mathcal{N}\left(p^2\right)\,,\end{aligned} \tag{709}$$

141 In this context Equation 705 has to be regarded as a (formal) toy model.
142 Due to the definition Equation 527, Equation 706 is the only possible choice.

in a free theory (cf. Section B.7 for details) suggests[143] a constant asymptotic DA

$$\mathcal{N}\left(p^2\right) = -D\frac{2^{4-D}}{\pi^{D/2}}\Gamma\left(-\tfrac{D}{2}\right)\left[-p^2\right]^{\frac{D}{2}}\,, \tag{710}$$

$$\phi_{4M}^{(g)}(x)\Big|_{as} = 1\,. \tag{711}$$

Being the only substantial evidence of its shape, we should express Equation 711 via the toy model Equation 705 (at, e. g., $\mu_0^2 = 1\ \text{GeV}^2$), by using the Gegenbauer coefficients [281]

$$a_{n,M}^{(g)}\left(\mu_0^2\right) = \frac{2\,(2n+3)}{3\,(n+1)\,(n+2)}\,. \tag{712}$$

Let us, therefore, study the impact of a flat (asymptotic) DA Equation 711 on the other higher twist two-particle distributions in more detail. In this context Equation 702 implies[144] (cf. Equation 665)

$$\begin{aligned}
&\int_0^1 dx\, e^{i\xi_x P_+}\left[\psi_{4M}^{(s)}(x) - 2\frac{H_M^{(s)}}{F_M^{(s)}}\phi_{3M}^{(s);p}(x) + 2m_M^2\phi_M^{(s)}(x)\right]\\
&= \frac{a_M}{2F_M^{(s)}}\int_0^1 dx\int_{-1}^1 d\alpha\int_{-1}^1 d\beta\, e^{-i(\bar{x}\alpha+x\beta)P_+}\phi_{4M}^{(g)}(x) + \dots\\
&= \frac{a_M}{2F_M^{(s)}}\frac{1}{(iP_+)^2}\int_0^1 dx\left[e^{iP_+} + e^{-iP_+} - 2e^{i\xi_x P_+}\right]\frac{\phi_{4M}^{(g)}(x)}{x\bar{x}} + \dots\,,
\end{aligned} \tag{713}$$

which may be transformed into

$$\int_0^1 dx\, e^{i\xi_x P_+}\delta\psi_{4M}^{(s)}(x) = \frac{a_M}{F_M^{(s)}}\int_0^1 dx\,\frac{e^{i\xi_x P_+}}{iP_+}\varphi_{4M}^{(g)}(x)\,, \tag{714}$$

when using the relation

$$\int_u^1 dv\, e^{i\xi_v P_+} - \int_0^u dv\, e^{i\xi_v P_+} = \frac{1}{2}\frac{1}{iP_+}\left[e^{iP_+} + e^{-iP_+} - 2e^{i\xi_u P_+}\right] \tag{715}$$

as well as[145] (for a test function $\phi(x)$ on $x \in [0,1]$)

$$\int_0^1 du\,\left[\int_u^1 dv\, e^{i\xi_v P_+}\right]\phi(u) = \int_0^1 du\, e^{i\xi_u P_+}\left[\int_0^u dv\,\phi(v)\right]\,, \tag{716}$$

$$\int_0^1 du\,\left[\int_0^u dv\, e^{i\xi_v P_+}\right]\phi(u) = \int_0^1 du\, e^{i\xi_u P_+}\left[\int_u^1 dv\,\phi(v)\right]\,, \tag{717}$$

143 This estimate is relevant for sufficiently large reference scales, and should be taken as a qualitative lead for an extended analysis.

144 Here, the ellipses represent omitted three-particle DAs.

145 Equation 716 and Equation 717 are written in such a way that all surface terms (for a general function ϕ) vanish.

along with the auxiliary[146] DAs ($\alpha_3 = 1 - \alpha_1 - \alpha_2$)

$$\delta\psi^{(s)}_{4M}(x) = \psi^{(s)}_{4M}(x) - 2\frac{H^{(s)}_M}{F^{(s)}_M}\phi^{(s);p}_{3M}(x) + 2m^2_M\phi^{(s)}_M(x) - \frac{d}{dx}\int_0^x d\alpha_1 \int_0^{\bar{x}} d\alpha_2 \, \frac{2\left[\Phi^{(s)}_{4M}(\underline{\alpha}) - 2\Psi^{(s)}_{4M}(\underline{\alpha})\right]}{\alpha_3}\,, \tag{718}$$

$$\delta\overline{\psi}^{(s)}_{4M}(x) = 2\frac{a_M}{F^{(s)}_M}\delta\psi^{(s)}_{4M}(x)\,, \tag{719}$$

$$\varphi^{(g)}_{4M}(x) = \int_0^x du\, \frac{\phi^{(g)}_{4M}(u)}{u\bar{u}} - \int_x^1 du\, \frac{\phi^{(g)}_{4M}(u)}{u\bar{u}}\,. \tag{720}$$

The latter cannot be normalized

$$\int_0^1 dx\, \varphi^{(g)}_{4M}(x) = 0\,, \tag{721}$$

but naturally gives rise to (cf. Equation 714)

$$(n+1)\, M_n^{\delta\overline{\psi}^{(s)}_{4M}} = \frac{a_M}{F^{(s)}_M} M_{n+1}^{\varphi^{(g)}_{4M}} \tag{722}$$

$$\Rightarrow \frac{d}{dx}\delta\overline{\psi}^{(s)}_{4M}(x) = [\delta(\bar{x}) - \delta(x)]\, \delta\overline{\psi}^{(s)}_{4M}(x) - \varphi^{(g)}_{4M}(x)\,, \tag{723}$$

with the formal solution (assuming[147] $x \in (0,1)$)

$$\delta\overline{\psi}^{(s)}_{4M}(x) = -\int_0^x du\, \varphi^{(g)}_{4M}(u)\,. \tag{724}$$

According to Equation 724, the gluonic DA $\phi^{(g)}_{4M}$ (cf. Equation 705) with arbitrary Gegenbauer coefficients implies a truncated expansion

$$\delta\overline{\psi}^{(s)}_{4M}(x) = 6x\bar{x}\left[1 + \frac{1}{6}a^{(g)}_{2,M}C_2^{(3/2)}(\xi_x) + \frac{1}{15}a^{(g)}_{4,M}C_4^{(3/2)}(\xi_x) + \frac{1}{28}a^{(g)}_{6,M}C_6^{(3/2)}(\xi_x) + \frac{1}{45}a^{(g)}_{8,M}C_8^{(3/2)}(\xi_x) + \frac{1}{66}a^{(g)}_{10,M}C_{10}^{(3/2)}(\xi_x) + \dots\right], \tag{725}$$

which exhibits a strong suppression of higher order terms. Thus, when assuming an approximately flat DA $\phi^{(g)}_{4M}$ (see Equation 705), we get for the corresponding exact solution[148] (cf. Equation 724)

$$\delta\overline{\psi}^{(s)}_{4M}(x) = -\lim_{\varepsilon\to 0^+}\int_0^x dv\left[\int_\varepsilon^v du\, \frac{1}{u\bar{u}} - \int_v^{\bar{\varepsilon}} du\, \frac{1}{u\bar{u}}\right] = -2\left[x\log x + \bar{x}\log\bar{x}\right], \tag{726}$$

which yields the asymptotic form

$$\delta\overline{\psi}^{(s)}_{4M}(x) \longrightarrow 6x\bar{x}\,. \tag{727}$$

146 In fact, Equation 718 is a mere reformulation of Equation 702.

147 The assumption $x \in [0,1)$ eradicates all extra factors related to the integrand in Equation 724, such as $\sim e^{\theta(-\bar{x})-\theta(x)}$, or $\sim e^{\theta(u)-\theta(-\bar{u})}$.

148 A different approach towards the exact solution has been discussed in [3].

The numerical difference between these two expressions is indeed very small, see Figure 17. Nevertheless, the modified relation (see Equation 718) in its present form would lead to inconsistencies, with regard to the normalization of $\psi_{4M}^{(s)}(x)$. Owing to the numerically small deviations (cf. Figure 17)

$$-2m_M^2 F_M^{(s)} \phi_M^{(s)}(x) + 2a_M \delta\overline{\psi}_{4M}^{(s)}(x) \approx -2\left(m_M^2 F_M^{(s)} - a_M\right) \phi_M^{(s)}(x) = -2H_M^{(s)} \phi_M^{(s)}(x)\,, \quad (728)$$

however, all effects of anomalous contributions may be collected within a proper redefinition of those meson mass corrections, which are related to twist-two DAs. In other words, when applying the substitution (analogously for "$q \leftrightarrow s$")

$$m_M^2 F_M^{(s)} \longmapsto H_M^{(s)} \quad (729)$$

to all occurring higher twist terms, we not only restore the condition

$$\int_0^1 dx\, \psi_{4M}^{(s)}(x) = 0\,, \quad (730)$$

but also guarantee the FKS mixing scheme to hold within higher twist effects, e. g., of the $\eta^{(\prime)}$ TFF at low momentum transfer (cf. Chapter 4). Furthermore, as demonstrated in Section 4.3, this assumption does not contradict the existing data.

4 MESON PHOTON TRANSITION FORM FACTORS

"The study of light has resulted in achievements of insight, imagination and ingenuity unsurpassed in any field of mental activity; it illustrates, too, better than any other branch of physics, the vicissitudes of theories."

— Sir J. J. Thomson (1856 – 1940)

Due to its well-known quantum electrodynamical properties[1], the photon may be considered as an ideal probe to study more complicated particles, such as hadrons (e. g., [340, 341]). Notably, among the plethora of possible processes to carry out such an analysis, the (high energy) photon-photon collisions play an important role. The latter are mainly studied at e^+e^- colliders (e. g., [342–347]) and provide a remarkable laboratory for testing the SM (e. g., [346]) and QCD phenomena in particular, such as resonances (see, e. g., [348, 349]), heavy quarkonia, exclusive two-photon reactions, (time-like) Compton scattering, hard QCD Jets, photon structure functions, etc., to name only a small selection of popular topics.
In this chapter, we focus on the photon-meson TFFs, which represent an ideal testing ground for models of involved DAs. For this purpose a rather wide range of photon virtualities have to be measured, ideally including large momentum transfers (cf. Section 4.3). Only recently, these requirements have been fulfilled in the context of η and η' TFFs (see discussion in Section 4.3), allowing a broad phenomenological insight into the η–η' system. Hence, unlike the well-studied pion case, only a rather limited number of theoretical publications are available for the $\eta^{(\prime)}$ FF. As mentioned before, one of the most recent and substantial contributions came from [20, 28], featuring (among other things):

a) A reexamination of the formalism for treating twist-two $\eta^{(\prime)}$ DAs, including a LO evolution.

b) An updated $\mathcal{O}(\alpha_S)$ calculation of the $\eta^{(\prime)}$-photon TFF in the real photon limit, at leading twist accuracy.

c) An estimate for the lowest Gegenbauer coefficient of ϕ_M^A $(A = 0, 8, g;\ M = \eta, \eta')$ based on [8, 350] as well as [7, 351].

While point a) has been discussed in Chapter 3, we now turn to subitem b) and examine c) within Section 4.3. In the following, we extend earlier approaches via several improvements, especially:

- We consistently take into account strange-quark mass contributions up to $\mathcal{O}(m_s)$ accuracy, including $SU(3)_F$-breaking corrections in twist-four DAs.
- In this context, we explicitly prove the cancellation of possible end-point divergences within the higher twist LO corrections, for generally shaped twist-three DAs.
- We also extend and test the result of [20, Equation B7, B8] by performing all corresponding calculations with two instead of one non-vanishing photon virtualities.

1 In contrast to QED, the photon within QCD can interact both as a point-like particle as well as a collection of partons (cf. Equation 20). Thus, more complicated theoretical methods are involved Section 4.2.

- Moreover, we include charm-quark (NLO) contributions to the twist-two two-gluon DA's coefficient function.

Combined with the methods developed in Section 3.3.3, these new results provide a consistent NLO treatment of the $\eta^{(\prime)}$ FF. Additionally, in this context, the photon's long distance behavior (real photon limit) needs to be taken into account. For this reason, we also implement the first NLO LCSR analysis of the $\eta^{(\prime)}$ meson-photon TFF.

Equipped with these tools, we can carry out a phenomenological analysis (see Section 4.3), which further reveals the non-perturbative effects within the $\eta{-}\eta'$ system, in particular their DAs.

4.1 PQCD APPROACH

Corresponding to Section 2.4, the OPE represents an initial point for our analytical investigations of hard exclusive processes (e. g., [352, 353]). Accordingly, after judiciously choosing a normalization point "μ^2" we may assume a consistent separation of long and short distances. Thus, the Wilson coefficients, or at least their analogue (see, e. g., Equation 737) are mostly determined by pQCD, while all soft functions become (approximate) genuine non-perturbative quantities. Nevertheless, it is evidently impossible to fully calculate the infinite α_S-series for all coefficient functions, let alone the infinitely many higher twist contributions, belonging to the underlying light-cone OPE. Therefore, in the next subsection, we will discuss the schematic realization of such a truncated (light-cone) OPE in the context of hard exclusive processes, while focusing on meson transition FFs.

4.1.1 *Collinear factorization in QCD*

In this subsection the theoretical basis for the subsequent calculation of hard exclusive processes are discussed in some detail. For consistency reasons[2], the main ideas will first be illustrated for the well studied π^0-case and later on adapted to our needs. Additionally, a better part of the required formalism and definitions will be summarized.

A key issue to use and understand pQCD is the idea of factorization (e. g., [33, 265, 301, 302, 354–358]). This is the property that some amplitudes or cross-sections may be expressed as a product[3] of two or more factors which themselves only depend on physics taking place on a single momentum scale[4]. Furthermore, the process under consideration is supposed to involve a large momentum transfer "Q", and corrections to the factorized form are then suppressed by inverse powers of Q.

In particular, the FF "$F_{\gamma^*\gamma^*\to M}(q_1^2, q_2^2)$", which relates two virtual photons "$\gamma^*(q_1)\,\gamma^*(q_2)$" with a (light) pseudoscalar meson "$M(P)$", plays a crucial role in the studies of hard exclusive processes. This arises from its simple structure which involves only one hadron and the intrinsic relation to the axial anomaly. Hence, especially the $\gamma^*\gamma^{(*)}\pi^0$ TFF has been an object of intensive research (e. g., [1, 281, 302] and references therein) and may serve us as a guide for the $\eta^{(\prime)}$ TFF. As an important result of [33, 301], a kinematical set-up that includes (two) large photon virtualities would allow a reasonable comparison of pQCD predictions with possible experimental data (e. g., [8, 359]) and, therefore, could provide important information on the shape of the involved meson DAs. Experimentally, however, a setting with only one highly virtual and another (almost)

2 No comparable studies exist for the $\eta^{(\prime)}$-case.
3 In general, this product is given by a matrix product or a convolution.
4 Synonymously, "distance scale" could be used in this context.

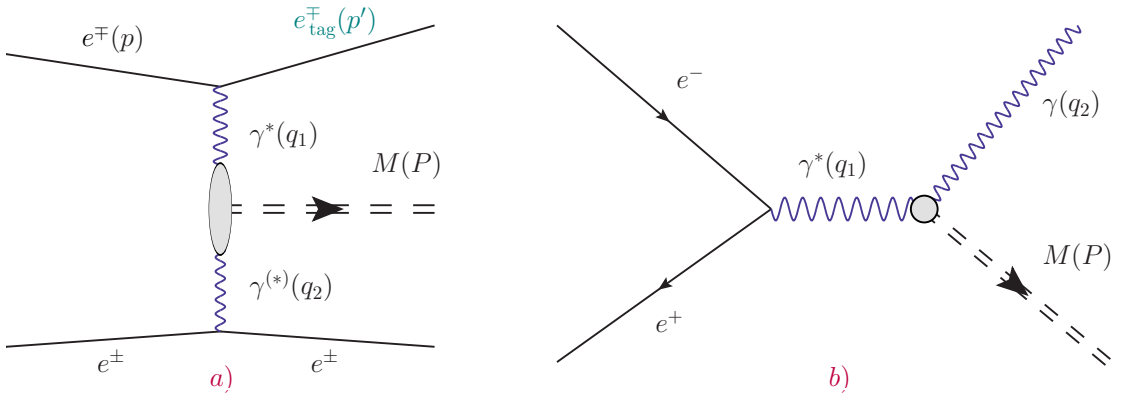

Figure 18: Diagram a) depicts the two-photon fusion reaction $e^+e^- \to e^+e^-M$ ($M = \pi^0, \eta, \eta'$). For this process the corresponding differential cross section can be measured in the single tag mode (cf. [5, 6, 8, 359]), i. e., one of the outgoing electrons/positrons (tagged) is detected $\left(Q^2 = -(p-p')^2 \gg 0\right)$, whereas its untagged counterpart is scattered at a small angle $\left(q^2 \approx 0\right)$. Besides, the meson is fully reconstructed. Diagram b) illustrates the corresponding $e^+e^- \to \gamma^* \to M\gamma$ transition. Most importantly, this annihilation process can be measured at very high center-of-mass energies of the e^+e^- system (cf. [351]).

real photon "$\gamma^{(*)}(q_2)$" is favorable, see Figure 18. In this situation[5], we also need reliable estimates of possible "soft" corrections to the (lowest order) handbag diagram a) in Figure 20, which are usually caused by gluon radiation or higher twist effects (cf. b), c), d) of Figure 20). Hence, a more elaborate picture for the factorization of $F_{\gamma^*\gamma^* \to M}$ emerges, see Figure 19. Let us first introduce the required notation. Since the latter describes a meson transition into two (in general virtual) photons, it is defined by a matrix element of two electromagnetic currents (cf. Equation 20), such as

$$\int d^4x\, e^{-iq_1\cdot x} \langle M(P)|\, T\{j^{em}_\mu(x)\, j^{em}_\nu(0)\}\,|0\rangle = ie^2 \varepsilon_{\mu\nu\alpha\beta}\, q_1^\alpha q_2^\beta F_{\gamma^*\gamma^* \to M}\left(q_1^2, q_2^2\right), \tag{731}$$

with $P^\mu = q_1^\mu + q_2^\mu$ and $P^2 = m_M^2$. When considering space-like FFs, both virtualities are negative, implying positive values for

$$Q^2 := -q_1^2, \quad q^2 := -q_2^2, \tag{732}$$

while the experimentally relevant situation corresponds to the assumption

$$0 \lesssim q^2 \ll Q^2. \tag{733}$$

Moreover, seeing that most of the equations are written for $q^2 = 0$, we introduce the abbreviation:

$$F_{\gamma^*\gamma \to M}\left(Q^2\right) = F_{\gamma^*\gamma^* \to M}\left(q_1^2 = -Q^2, q_2^2 = 0\right). \tag{734}$$

On these grounds, let us now briefly examine the general behavior of Equation 734 by means of the well studied π^0-case (e. g., [362] and references therein). Given, that the experimentally preferred set-up, with sufficiently large Q^2 to apply pQCD is realized, then Equation 731 resembles

5 Here, the missing mass in an event of this measured meson-electron system is close to zero (cf. [360, 361]). Moreover, being part of a specific decay chain, the meson is usually observed via its decay products. If the latter are fully detected, the corresponding meson (decay) is said to be "fully reconstructed" [361].

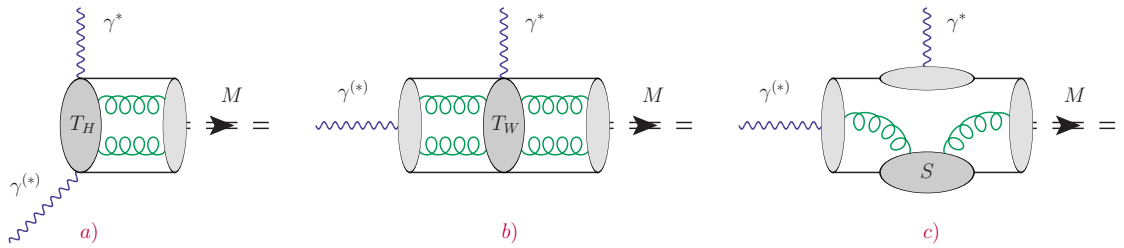

Figure 19: Schematic structure of the QCD factorization for the $F_{\gamma^*\gamma\to M}(Q^2)$ FF at large Q^2 (e. g., [281, 362]).

a light-cone dominated object (cf. Section A.16 for details). This well defined setting, allows a consistent decomposition into light-ray operators (e. g., [75]), i. e., the OPE can be constructed in a systematic way. Most importantly, in that case a power-like behavior of $F_{\gamma^*\gamma\to M}(Q^2)$ can be assumed. The latter may be generated by three basic regimes, as shown in Figure 19:

- REGION a): Notably, the dominant contributions are provided by this regime, which corresponds to a large virtuality flow through a (perturbatively calculable) hard subgraph "T_H", containing both photon vertices.[6] According to power counting estimates, the large-Q^2 behavior of such configurations is given by (e. g., [362–364])

$$F^{\text{region a)}}_{\gamma^*\gamma\to M}\left(Q^2\right) = \mathcal{O}\left(\frac{1}{Q^2}\right) . \tag{735}$$

In fact, the leading twist corrections for $M=\pi^0$ can be written (see Section 4.1.2 for $M=\eta^{(\prime)}$) in terms of a hard scattering formula[7] [3, 281, 365–367] (cf. Section 4.1.3)

$$F_{\gamma^*\gamma\to\pi^0}\left(Q^2\right) = \frac{\sqrt{2}f_\pi}{3}\int_0^1 dx\, T_H^{(3)}\left(x, Q^2; \mu, \alpha_S(\mu)\right)\phi_\pi(x,\mu) , \tag{736}$$

$$\begin{aligned} T_H^{(3)}\left(x, Q^2; \mu, \alpha_S(\mu)\right) = \frac{1}{xQ^2}\Bigg\{1 + C_f\frac{\alpha_S(\mu)}{2\pi}\left[\frac{1}{2}\log^2 x - \frac{1}{2}\frac{x}{\bar{x}}\log x - \frac{9}{2}\right. \\ \left. + \left(\frac{3}{2} + \log x\right)\log\frac{Q^2}{\mu^2}\right]\Bigg\} + \mathcal{O}\left(\alpha_S^2\right) , \end{aligned} \tag{737}$$

which may be seen as a prototype for the general factorized form. As an illustration, the generic structure of this region is given by an expression similar to (e. g., [332])

$$F_{\gamma^*\gamma\to M}\left(Q^2\right) = \sum_n \prod_i \int_0^1 du_i\, w_n(\underline{u})\, T_H^{(n)}\left(\underline{u}, Q^2; \mu, \alpha_S(\mu)\right)\phi_{n,M}(\underline{u},\mu) , \tag{738}$$

$$\begin{aligned} n &: \text{(collinear) twist,} \\ w_n &: \text{adequate weight function,} \\ T_H^{(n)} &: \text{process specific "hard" amplitude,} \\ \phi_{n,M} &: \text{universal "soft" DA,} \end{aligned}$$

6 By construction, the contributions of region a) involve a time ordered product of two electromagnetic currents at small light-like separations [3, 281]. Hence, they can be studied by Wilson's OPE.

7 Besides the $\overline{\text{MS}}$ scheme, where T_H is known up to NLO, for the pion-case it is available up to NNLO in a conformal scheme, see [311]. For Equation 737 we applied the symmetry properties of Equation 305 (e. g., with $A=3$).

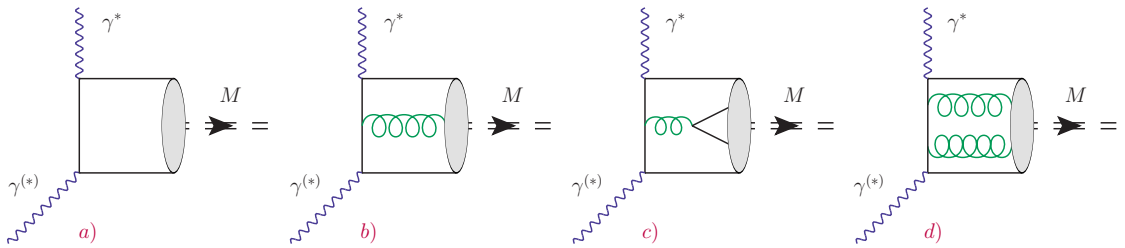

Figure 20: An example of leading (e. g., a)) and higher twist diagrams (such as b), c), along with d)), contributing to the meson TFF. This includes three-particle twist four corrections, as implied by diagram b).

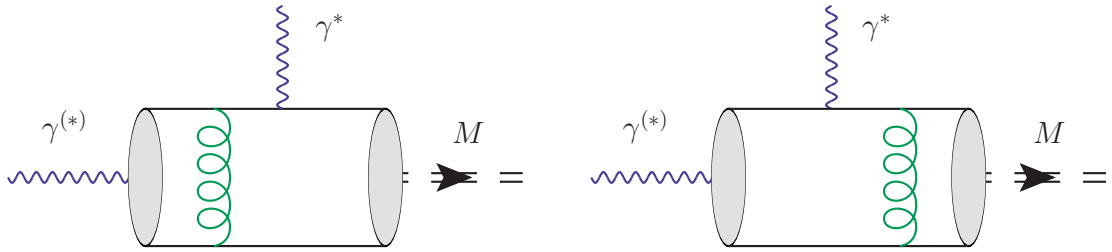

Figure 21: Typical contribution to region b). These diagrams represent a convolution of the involved hard scattering kernel with the (soft) twist-two photon and twist-three pion DAs (cf. Equation 740).

due to the underlying light-cone OPE. Nonetheless, in general the actual realization of collinear factorization may not be presumed, but must be proven for each contribution individually. E. g., an explicit calculation reveals for the[8] π^0 TFF [281] (at $\mathcal{O}(\alpha_s^0)$ and up to NLO in conformal spin)

$$F_{\gamma^*\gamma\to\pi^0}\left(Q^2\right) = \frac{\sqrt{2}f_\pi}{3Q^2}\int_0^1 dx\left[\frac{\phi_\pi(x)}{x} - \frac{1}{Q^2}\frac{\mathbb{F}_\pi(x)}{x^2}\right] = \frac{\sqrt{2}f_\pi}{Q^2}\left[1 + a_2^\pi - \frac{80}{27}\frac{\delta_\pi^2}{Q^2}\right] + \dots . \tag{739}$$

Here, $\mathbb{F}_\pi(x)$ serves as a collection of the higher twist corrections up to twist-four. Besides, Equation 739 provides an estimate for higher twist corrections. Those seem to be sizable for $Q^2 \sim 1\ \text{GeV}^2 - 5\ \text{GeV}^2$, while they may be safely neglected in the large-Q^2 limit.

- REGION b): Since at least one photon virtuality is small, we have to take into account a long distance photon propagation in the q_2-channel as well. This regime involves large momenta flowing through a central subgraph "T_W" (cf. Figure 19), which contains the virtual photon vertices, see Figure 21. At lowest order, this subgraph corresponds to a hard gluon exchange, similar to the leading pQCD contribution of the (pion) electromagnetic FF (e. g., [33, 301]). Hence, we may expect [281] corrections such as

$$F_{\gamma^*\gamma\to\pi^0}\left(Q^2\right) = \frac{\sqrt{2}f_\pi}{3Q^4}\frac{16\pi\alpha_s\chi\langle\bar{\psi}\psi\rangle^2}{9f_\pi^2}\int_0^1 dx\frac{\phi_{3\pi}^p(x)}{x}\int_0^1 dy\frac{\phi_\gamma(y)}{\bar{y}}. \tag{740}$$

Here, we use the quark condensate's magnetic susceptibility (e. g., [274, 281])

$$\chi \approx \frac{2}{m_\rho^2} \approx 3.3\ \text{GeV}^{-2}, \tag{741}$$

8 In this context, we use the abbreviation $c_{2,\pi} \equiv a_2^\pi$.

along with $\phi_\gamma(x) \approx 6x\bar{x}$, being the leading twist (asymptotic) photon DA [274]. In particular, both integrals over the quark momentum fractions are logarithmically divergent at the end-points, i. e., for $x \to 0$ and $y \to 1$. This signals an overlap with the soft region c) (e. g., [281]). Moreover, the contributions of this region [362, 364] (cf. Equation 740)

$$F^{\text{region b)}}_{\gamma^*\gamma\to M}\left(Q^2\right) = \mathcal{O}\left(\frac{1}{Q^4}\right), \tag{742}$$

may be significant for $Q^2 \approx 5\ \text{GeV}^2$, i. e., sufficiently soft momentum transfer. For instance, the regularized (asymptotic) version of Equation 740 (e. g., assuming $Q^2 \approx \mu_{\text{IR}}^2 = 1\ \text{GeV}^2$)

$$\begin{aligned}&\frac{16\pi\alpha_s\chi\langle\bar{\psi}\psi\rangle^2}{27 f_\pi^2 Q^4}\int_0^1 dx \frac{\phi^p_{3\pi}(x)}{x}\int_0^1 dy \frac{\phi_\gamma(y)}{\bar{y}}\\ &\approx \frac{0.2\ \text{GeV}^2}{Q^4}\left[\log^2\left(\frac{\mu_{\text{IR}}^2+Q^2}{\mu_{\text{IR}}^2}\right) - \frac{Q^2}{\mu_{\text{IR}}^2+Q^2}\log\left(\frac{\mu_{\text{IR}}^2+Q^2}{\mu_{\text{IR}}^2}\right)\right],\end{aligned} \tag{743}$$

with an *ad hoc* IR cut-off scale μ_{IR}, is only relevant in a region of relatively small momenta Q^2 (i. e., $Q^2 \gtrsim \mu_{\text{IR}}^2$).

- REGION c): This region belongs to the Feynman mechanism, which constitutes a highly asymmetric momentum distribution, where a passive (observer) quark becomes soft. Similar to region b), this sector is subleading [362]:

$$F^{\text{region c)}}_{\gamma^*\gamma\to M}\left(Q^2\right) = \mathcal{O}\left(\frac{1}{Q^4}\right). \tag{744}$$

In terms of the standard terminology, $F_{\gamma^*\gamma\to M}\left(Q^2\right)$ within this regime is given by an overlap of non-perturbative wave functions, describing the involved initial and final states. Based on the Brodsky-Lepage formula [301, 362], that may be illustrated for the related quark-antiquark contribution[9]

$$(\vec{\varepsilon}_\perp \times \vec{q}_\perp)\, F^{\bar{q}q}_{\gamma^*\gamma\to\pi^0}\left(Q^2\right) = \frac{f_\pi}{4\pi^3\sqrt{3}}\int_0^1 dx \int d^2k_\perp \frac{(\vec{\varepsilon}_\perp \times (x\vec{q}_\perp + \vec{k}_\perp))}{(x\vec{q}_\perp+\vec{k}_\perp)^2 - i0^+}\Psi_{\bar{q}q/\pi}\left(x, \vec{k}_\perp\right), \tag{745}$$

where $\vec{q}_\perp$ ($\vec{q}_\perp^{\,2} = Q^2$) and $\vec{\varepsilon}_\perp$ are two orthogonal vectors in the transverse plane. In the absence of any further knowledge, a convenient model for $\Psi_{\bar{q}q/\pi}$ [362, 368–370] is given by the Gaussian ansatz

$$\Psi_{\bar{q}q/\pi}\left(x, \vec{k}_\perp\right) = \frac{4\pi^2}{\sigma\sqrt{6}}\frac{\phi_\pi(x)}{x\bar{x}}\exp\left(-\frac{\vec{k}_\perp^{\,2}}{2\sigma x\bar{x}}\right), \tag{746}$$

which includes an additional width parameter "σ".[10] Given that $\sum_{n=0}^{\infty} a_{2n}^\pi$ is convergent we may use (e. g., [362])

$$\sigma = \frac{4\pi^2 f_\pi^2}{3}\int_0^1 dx \frac{\phi_\pi(x)}{x}. \tag{747}$$

9 In this context "$\times$" denotes the standard vector-product (e. g., Section A.9 and [128, 362]).

10 In general, specific normalization conditions for the wave function $\Psi_{\bar{q}q/\pi}$ may be chosen, e. g., such implied by an adequate integration via $\int_0^1 dx$ or $\int_0^1 dx \int d^2k_\perp$. Particularly, Equation 747 is a result of such constraints (cf. [362]). Other approaches exist, which also define reasonable conditional equations for σ, including cases, where $\sum_{n=0}^{\infty} a_{2n}^\pi$ is not convergent (see [362] and references therein).

Based on Equation 746, one may carry out the $k_\perp^2$-integration within Equation 745, which results [362] in the Musatov-Radyushkin model:

$$F^{\bar{q}q}_{\gamma^*\gamma\to\pi^0}\left(Q^2\right) = \frac{\sqrt{2}f_\pi}{3Q^2}\int_0^1 dx \frac{\phi_\pi(x)}{x}\left[1 - e^{-\frac{xQ^2}{2\bar{x}\sigma}}\right] . \tag{748}$$

While the first term in Equation 748 corresponds to a LO pQCD contribution, the second term is exponentially small in Q^2 and can, therefore, not be seen in any (finite) order of the OPE (e. g., [281, 362]). Hence, it may be associated to the (entirely) soft contribution of region c).

According to the previous discussion, two important issues in the subsequent calculations may arise:

i) Can higher order or mass corrections to the correlation function be factorized?

ii) Is it possible to consistently include soft contributions from region b) and c)?

Therefore, the following subsections are devoted to the explicit proof of collinear factorization at the intended accuracy. Throughout this proof we keep two non-vanishing photon virtualities. This strategy results from the anticipated application of the LCSR method. The latter allows a systematical inclusion of soft effects related to region b) and c) (see Section 4.2), in an (almost) model-independent way.

4.1.2 *Leading order calculations*

In this subsection we introduce all necessary leading order results for the $\eta^{(\prime)}$-TFF, including some details concerning their calculation. Being mostly the result of standard methods, we omit lengthy intermediate steps and only focus on corner posts such as the corresponding ansatz along with several necessary tools.

Reconsidering the introductory example of Equation 121, we most conveniently get the required tree-level contributions, by performing all possible contractions within Equation 731 up to $\mathcal{O}\left(\alpha_S^0\right)$ accuracy. On these grounds, the desired LO corrections result from

$$\begin{aligned}&\langle M(P)|\, T\left\{j_\mu^{em}(x)\, j_\nu^{em}(0)\right\}|0\rangle\big|_{LO}\\ &= \sum_\psi e_\psi^2 \left(\langle M(P)|\bar{\psi}(x)\,\gamma_\mu i S_\psi(x,0)\,\gamma_\nu\psi(0)\,|0\rangle + \langle M(P)|\bar{\psi}(0)\,\gamma_\nu i S_\psi(0,x)\,\gamma_\mu\psi(x)\,|0\rangle\right) ,\end{aligned} \tag{749}$$

which is at this point formally similar to the π^0 TFF [281]. Evidently, in contrast to the pion case, with one predetermined flavor structure, a more elaborate situation emerges for the $\eta{-}\eta'$ system. Based on our ansatz for the inclusion of mixing effects (see Section 3.1), we in general have to decompose all occurring light-ray operators into currents with definite flavor content, depending on the chosen basis. While we were able to establish an analogy between the pion and the QF case due to a decoupling of light and strange contributions (cf. [3]), we would face a different situation, when choosing the SO basis.[11] Here, both, light and strange corrections may belong to a singlet or an octet state at the same time. Therefore, we have to use at least once a completeness relation, such as Equation 1066 which implies the closed form solution for

11 Note, that all OZI rule violations are neglected within the QF basis.

this decomposition procedure. In order to exemplify that issue, let us consider a generic quark-antiquark contribution (cf. Equation 749) with the flavor structure $\mathcal{F}_{\text{em}} = \text{diag}(e_u^2, e_d^2, e_s^2)$. As a result, we get (cf. Equation 188)

$$\begin{aligned}
\overline{\psi}_\alpha^a \mathcal{F}_{\text{em}} \psi_\beta^b &= \sum_{A=0}^{8} \sqrt{2}\,\text{Tr}\left\{\mathcal{F}_{\text{em}} T^A\right\} \overline{\psi}_\alpha^a \sqrt{2} T^A \psi_\beta^b \\
&= \frac{2}{\sqrt{3}}\left[e_u^2 + e_d^2 + e_s^2\right] \overline{\psi}_\alpha^a \sqrt{2} T^0 \psi_\beta^b + \sqrt{\frac{2}{3}}\left[e_u^2 + e_d^2 - 2e_s^2\right] \overline{\psi}_\alpha^a \sqrt{2} T^8 \psi_\beta^b \\
&\quad + \sqrt{2}\left[e_u^2 - e_d^2\right] \overline{\psi}_\alpha^a \sqrt{2} T^3 \psi_\beta^b \\
&= 2e_s^2 \overline{\psi}_\alpha^a \sqrt{2} T^s \psi_\beta^b + \sqrt{2}\left[e_u^2 + e_d^2\right] \overline{\psi}_\alpha^a \sqrt{2} T^q \psi_\beta^b + \sqrt{2}\left[e_u^2 - e_d^2\right] \overline{\psi}_\alpha^a \sqrt{2} T^3 \psi_\beta^b \,, \qquad (750)
\end{aligned}$$

which resembles a recurring pattern within the following calculation. For instance, when applied to the real photon limit, we get

$$\begin{aligned}
F_{\gamma^*\gamma\to M}\left(Q^2\right) &= \frac{f_M^{(8)}}{3\sqrt{6}} \int_0^1 du\, T_H^{(8)}\left(u, Q^2; \mu, \alpha_S(\mu)\right) \phi_M^{(8)}(u,\mu) \\
&\quad + \frac{2f_M^{(0)}}{3\sqrt{3}} \int_0^1 du\, T_H^{(0)}\left(u, Q^2; \mu, \alpha_S(\mu)\right) \phi_M^{(0)}(u,\mu) \\
&\quad + \frac{2f_M^{(0)}}{3\sqrt{3}} \int_0^1 du\, T_H^{(g)}\left(u, Q^2; \mu, \alpha_S(\mu)\right) \phi_M^{(g)}(u,\mu) \,, \qquad (751)
\end{aligned}$$

together with (cf. [3, 20] and Equation 737)

$$T_H^{(0)}\left(u, Q^2; \mu, \alpha_S(\mu)\right) = T_H^{(8)}\left(u, Q^2; \mu, \alpha_S(\mu)\right) \equiv 2T_H^{(3)}\left(u, Q^2; \mu, \alpha_S(\mu)\right) \,, \qquad (752)$$

$$\begin{aligned}
T_H^{(g)}\left(u, Q^2; \mu, \alpha_S(\mu)\right)\Big|_{\text{light}} &= -C_f \frac{\alpha_S(\mu)}{2\pi} \left\{ \frac{2\log(u)}{\bar{u}^2 Q^2} \log\left(\frac{Q^2}{\mu^2}\right) \right. \\
&\quad \left. + \frac{2\log(u)}{u\bar{u}Q^2}\left[3 - \frac{2}{\bar{u}} + \frac{u}{2\bar{u}}\log(u)\right] \right\} + \mathcal{O}\left(\alpha_S^2\right) \,, \qquad (753)
\end{aligned}$$

in analogy to Equation 736 and Equation 737. Another substantial difference to the π^0-case concerns finite quark and meson mass corrections. Unlike earlier approaches (e. g., [20, 281]) we also have to consistently include those contributions which are generated by the hard scattering kernels. Hence, we can, a priori, not neglect any terms that potentially produce $\mathcal{O}(m_\psi)$ or $\mathcal{O}(m_M)$ admixtures within T_H. Accordingly, Equation 731 has to be calculated via the massive quark-propagator[12] (e. g., [75, 371, 372] and Equation 1142)

$$\begin{aligned}
&\langle 0|T\left\{\psi(x)\,\bar{\psi}(0)\right\}|0\rangle \\
&= iS_\psi(x) - ig\int \frac{d^4k}{(2\pi)^4}\, e^{-ikx} \int_0^1 du \left[\frac{1}{2}\frac{\not{k} + m_\psi}{(m_\psi^2 - k^2)^2} G^{\mu\nu}(ux)\,\sigma_{\mu\nu} + \frac{u\,x_\mu}{m_\psi^2 - k^2} G^{\mu\nu}(ux)\,\gamma_\nu\right] \,, \qquad (754)
\end{aligned}$$

effectively producing the anticipated light-cone OPE. Consequently, the latter exhibits contributions of less singular terms $\sim 1/x^2$, $\log x^2$, etc., as compared to the leading contribution $\sim 1/x^4$ (e. g., [3] and Equation 139), which in effect can be related to higher twist DAs. Hence, they may be referred to as higher twist corrections. Essentially, those subleading expressions are one source of

12 Equation 754 corresponds to the light-cone expansion of a massive quark propagator in the QCD background field [74, 75, 371].

power corrections proportional to $1/[Q^2]^k$ ($k \in \mathbb{N}$, $k \geqslant 2$) to the $\eta^{(\prime)}$ TFF (cf. Section 4.1.1). Indeed, the leading twist-two corrections arise from (modulo higher order terms)

$$T\{j^{em}_\mu(x)\, j^{em}_\nu(0)\} = \left[\sum_\psi e_\psi^2 \int \frac{d^4k}{(2\pi)^4 i} \frac{e^{-ik\cdot(x-0)}}{m_\psi^2 - k^2} \bar\psi(x)\, \gamma_\mu \not{k} \gamma_\nu \psi(0)\right] + \left[\begin{matrix} x \leftrightarrow 0 \\ \mu \leftrightarrow \nu \end{matrix}\right] + \dots , \quad (755)$$

as implied by the most singular part of Equation 1142. Together with adequate matrix relations (cf. Section A.1), e. g.,

$$\bar\psi(x)\, \gamma_\mu \not{k} \gamma_\nu \psi(0) = i\varepsilon_{\mu\nu\alpha\beta} k^\alpha \bar\psi(x)\, \gamma^\beta \gamma_5 \psi(0) + \dots , \quad (756)$$

the characteristic tensor structure may then be separated from the actual QCD amplitude[13]

$$\begin{aligned}
&i\varepsilon_{\mu\nu\alpha\beta}\, q_1^\alpha q_2^\beta F^{QCD;(tw2)}_{\gamma^*\gamma^*\to M}\left(Q^2, q^2\right) \\
&= 2\sum_\psi e_\psi^2 \int d^4x \int \frac{d^4k}{(2\pi)^4 i} \frac{e^{-ix\cdot(k+q_1)}}{m_\psi^2 - k^2} \langle M(P)\, |\bar\psi(x)\, \gamma_\mu \not{k} \gamma_\nu \psi(0)| 0\rangle \\
&= 2\varepsilon_{\mu\nu\alpha\beta} P^\beta \sum_\psi e_\psi^2 F_M^{(\psi)} \int_0^1 du\, \phi_M^{(\psi)}(u) \int d^4x \int \frac{d^4k}{(2\pi)^4 i} k^\alpha \frac{e^{ix\cdot[uP-k-q_1]}}{m_\psi^2 - k^2} \\
&= 2i\varepsilon_{\mu\nu\alpha\beta}\, q_1^\alpha q_2^\beta \sum_\psi e_\psi^2 F_M^{(\psi)} \int_0^1 du\, \frac{\phi_M^{(\psi)}(u)}{m_\psi^2 - [uP - q_1]^2} \,. \qquad (757)
\end{aligned}$$

Besides, the safely negligible $\mathcal{O}\left(m_\psi^2\right)$ terms, Equation 757 additionally gives rise to specific meson mass corrections, that are basically also present in higher twist contributions. Generally speaking, we face hard scattering kernels proportional to ($k \in \mathbb{N}$)

$$\begin{aligned}
\left[m_\psi^2 - [uP - q_1]^2\right]^{-k} &= \left[\bar u Q^2 + u q^2 + u\bar u m_M^2 + m_\psi^2\right]^{-k} \\
&= \left[\frac{1}{\left[\bar u Q^2 + u q^2\right]^k} - \frac{k u \bar u m_M^2}{\left[\bar u Q^2 + u q^2\right]^{k+1}} + \mathcal{O}\left(\frac{m_M^2}{[Q^2]^{2+k}}\right)\right] + \mathcal{O}\left(m_\psi^2\right), \quad (758)
\end{aligned}$$

which (after omitting quark-mass terms) can be expanded into a formal power series in the variable "m_M^2/Q^2". This approach ensures a better compatibility with the given definition of twist (cf. Chapter 3). Therefore, unlike the π^0-case, specific amplitudes may feature modified convolution integrals such as

$$F^{QCD;(tw2)}_{\gamma^*\gamma^*\to M}\left(Q^2, q^2\right) = 2\sum_\psi e_\psi^2 F_M^{(\psi)} \int_0^1 du \left[\frac{1}{\bar u Q^2 + u q^2} - \frac{u\bar u m_M^2}{\left[\bar u Q^2 + u q^2\right]^2}\right] \phi_M^{(\psi)}(u) \,, \quad (759)$$

13 For convenient reference the amplitude in Equation 757 carries a superscript "tw2", because it is related to a twist-two DA.

that should be included at the intended level of accuracy. Similarly, the corresponding twist-three two-particle corrections, i. e.,

$$\begin{aligned}
&i\varepsilon_{\mu\nu\alpha\beta}\,q_1^\alpha q_2^\beta F^{\mathrm{QCD};(\mathrm{tw3})}_{\gamma^*\gamma^*\to M}\left(Q^2,q^2\right)\\
&= 2\sum_\psi e_\psi^2\int d^4x\int\frac{d^4k}{(2\pi)^4 i}\,\frac{m_\psi e^{-ix\cdot(k+q_1)}}{m_\psi^2-k^2}\langle M(P)\,|\bar\psi(x)\,\gamma_\mu\gamma_\nu\psi(0)|0\rangle\\
&= i\varepsilon_{\mu\nu\alpha\beta}\sum_\psi e_\psi^2\int d^4x\int\frac{d^4k}{(2\pi)^4}\,\frac{m_\psi e^{-ix\cdot(k+q_1)}}{m_\psi^2-k^2}\langle M(P)\,|\bar\psi(x)\,\sigma^{\alpha\beta}\gamma_5\psi(0)|0\rangle\\
&= i\varepsilon_{\mu\nu\alpha\beta}\,q_1^\alpha q_2^\beta\left[\frac{2e_s^2}{6}\int_0^1 du\frac{\overline{\phi}^{(s);\sigma}_{3M}(u)}{\left[\bar uQ^2+uq^2\right]^2}+\frac{\sqrt{2}\,(e_u^2+e_d^2)}{6}\int_0^1 du\frac{\overline{\phi}^{(q);\sigma}_{3M}(u)}{\left[\bar uQ^2+uq^2\right]^2}\right],
\end{aligned}\tag{760}$$

have been beyond the scope of earlier approaches (e. g., [20, 281]). Correspondingly, we have to pay special attention to their behavior. Yet, another possible twist-three contribution could originate from mass corrections related to the three-particle DA $\Phi^A_{3M}(\underline{\alpha})$ (cf. Equation 329). As a matter of convenience, we may check this lead by expanding the gluonic part of Equation 754 up to $\mathcal{O}(m_\psi)$:

$$\begin{aligned}
&\langle 0|T\left\{\psi(x)\,\bar\psi(0)\right\}|0\rangle\big|_{\mathrm{gluons}}\\
&= g\int\frac{d^4k}{(2\pi)^4 i}\,e^{-ik\cdot x}\int_0^1 du\left[\left(\frac{1}{2}\frac{\not k}{k^4}\sigma_{\mu\nu}-\frac{ux_\mu}{k^2}\gamma_\nu\right)\mathcal{G}^{\mu\nu}(ux)+\frac{1}{2}\frac{m_\psi}{k^4}\sigma_{\mu\nu}\mathcal{G}^{\mu\nu}(ux)\right]+\mathcal{O}\left(m_\psi^2\right)\\
&= \frac{ig\mu^{2-D/2}}{16\pi^{D/2}}\frac{\Gamma\left(\frac{D}{2}-1\right)}{\left[-x^2\right]^{D/2-1}}\int_0^1 du\,(\not x\sigma_{\mu\nu}-4iux_\mu\gamma_\nu)\,\mathcal{G}^{\mu\nu}(ux)\\
&\quad+m_\psi\frac{g\mu^{2-D/2}}{32\pi^{D/2}}\frac{\Gamma\left(\frac{D}{2}-2\right)}{\left[-x^2\right]^{D/2-2}}\int_0^1 du\,\sigma_{\mu\nu}\mathcal{G}^{\mu\nu}(ux)+\mathcal{O}\left(m_\psi^2\right)
\end{aligned}\tag{761}$$

and analyze their possible contribution to $F^{\mathrm{QCD}}_{\gamma^*\gamma^*\to M}$ via

$$\gamma_\mu\sigma_{\alpha\beta}\gamma_\nu\mathcal{G}^{\alpha\beta}=2i\mathcal{G}_{\mu\nu}-2\gamma_5\widetilde{\mathcal{G}}_{\mu\nu}+2\sigma_{\mu\xi}\mathcal{G}^\xi{}_\nu+2\sigma_{\nu\xi}\mathcal{G}^\xi{}_\mu+g_{\mu\nu}\sigma_{\alpha\beta}\mathcal{G}^{\alpha\beta}\,.\tag{762}$$

By reformulating Equation 329

$$\begin{aligned}
&\langle M(P)\,|\overline{\psi}(z_2n)\sqrt{2}T^A\sigma_{\mu\nu}g\mathcal{G}_{\alpha\beta}(z_3n)\,\psi(z_1n)\,|0\rangle\\
&= f_{3M}^A\left(\varepsilon_{\mu\nu\xi\alpha}p_\beta-\varepsilon_{\mu\nu\xi\beta}p_\alpha\right)p^\xi\left[\Phi^A_{3M}(\underline{z},p\cdot n)\right]^*+\ldots,
\end{aligned}\tag{763}$$

it becomes evident that Equation 762 does not contribute to the intended higher twist accuracy. This also includes twist-four three-particle terms of $\mathcal{O}(m_\psi)$ which are absent within the LO FF due to their non matching tensor structure (cf. Equation 330, Equation 331). Likewise, at $\mathcal{O}(\alpha_S^0)$ Equation 754 does not imply any additional $\mathcal{O}(m_\psi)$ corrections related to $\phi^{(\psi)}_{4M}$. Hence, the relevant "twist-four" amplitude (cf. ansatz of Equation 757) boils down to

$$\begin{aligned}
F^{\mathrm{QCD};(\mathrm{tw4})}_{\gamma^*\gamma^*\to M}\left(Q^2,q^2\right)&=\sum_\psi\frac{e_\psi^2}{2}\int_0^1 du\frac{F_M^{(\psi)}\phi_{4M}^{(\psi)}(u)}{\left[\bar uQ^2+uq^2+u\bar um_M^2\right]^2}\\
&=\sum_\psi\frac{e_\psi^2}{2}\int_0^1 du\frac{F_M^{(\psi)}\phi_{4M}^{(\psi)}(u)}{\left[\bar uQ^2+uq^2\right]^2}+\mathcal{O}\left(\frac{m_M^2}{[Q^2]^3}\right).
\end{aligned}\tag{764}$$

After discarding all $\mathcal{O}(m_M^2/[Q^2]^3)$ admixtures, Equation 764 is formally analogous to the corresponding results of, e. g., [281]. That is also true for three-particle twist-four contributions which are obtained by evaluating diagram b) of Figure 20 (see also [373]), i. e.,

$$\int_0^1 du \int \mathcal{D}\underline{\alpha} \frac{\widetilde{\Phi}_{4M}^{A}(\underline{\alpha}) + \xi_v \Phi_{4M}^{A}(\underline{\alpha})}{[(\alpha_1 + v\alpha_3)\,P - q_1]^4} = \int_0^1 du \frac{\rho_{4M}^{A}(u)}{[uP - q_1]^4}\,, \tag{765}$$

together with ($\alpha_3 = 1 - \alpha_1 - \alpha_2$)

$$\rho_{4M}^{A}(u) = \int_0^u d\alpha_1 \int_0^{\bar{u}} \frac{d\alpha_2}{\alpha_3} \left[\widetilde{\Phi}_{4M}^{A}(\underline{\alpha}) + \frac{\xi_u - \alpha_1 + \alpha_2}{\alpha_3} \Phi_{4M}^{A}(\underline{\alpha})\right], \tag{766}$$

while discarding all additional meson mass corrections, as implied by the associated denominator. Again, the resulting amplitude is of similar appearance as her pion counterpart (e. g., [280, 281, 352])

$$F_{\gamma^*\gamma^*\to M}^{\text{QCD;(tw4)}}\left(Q^2, q^2\right)\Big|_{3PP} = -2 \sum_{\psi} e_\psi^2 F_M^{(\psi)} \int_0^1 du \frac{\rho_{4M}^{(\psi)}(u)}{\left[\bar{u}Q^2 + uq^2\right]^2}\,. \tag{767}$$

The distinctive differences between the mentioned mesons manifest themselves in their internal structure determined by the corresponding DAs.
The latter can be obtained from an analysis of the scaled LO $\eta^{(\prime)}$-TFF[14]:

$$\begin{aligned} Q^2 F_{\gamma^*\gamma\to M}^{\text{QCD}}\left(Q^2\right)\Big|_{\text{LO}} = 2 \sum_{\psi=u,d,s} e_\psi^2 F_M^{(\psi)} \int_0^1 \frac{du}{u} \Bigg\{ & \phi_M^{(\psi)}(u) \\ & - \frac{1}{Q^2}\left[\bar{u} m_M^2 \phi_M^{(\psi)}(u) - \frac{1}{6uF_M^{(\psi)}} \overline{\Phi}_{3M}^{(\psi);\sigma}(u) + \frac{1}{u} \mathbb{A}_{4M}^{(\psi)}(u)\right]\Bigg\}\,, \end{aligned} \tag{768}$$

where "$\mathbb{A}_{4M}^{(\psi)}$" collects all contributing twist-four[15] DAs:

$$\mathbb{A}_{4M}^{(\psi)}(u) = \frac{1}{4}\phi_{4M}^{(\psi)}(u) - \rho_{4M}^{(\psi)}(u)\,. \tag{769}$$

Therefore, by proofing the related collinear factorization assumption, we may get further insight into the particle's non-perturbative behavior[16]. Within the real photon limit "$q^2 \to 0$", however, several contributions of Equation 768 become ill-defined when taken separately. For instance, at NLO in conformal spin[17], both terms

$$\begin{aligned} \mathbb{A}_{4M}^{(\psi)}(u) = u\bar{u}\left(60\frac{m_\psi f_{3M}^{(\psi)}}{f_M^{(\psi)}} + \frac{h_M^{(\psi)}}{f_M^{(\psi)}}\right) + u^2\bar{u}^2\left(\frac{80}{3}\delta_M^{2(\psi)} - \frac{h_M^{(\psi)}}{f_M^{(\psi)}}\left[\frac{13}{12} - \frac{21}{2}c_{2,M}^{(\psi)}\right]\right. \\ \left. -315\frac{m_\psi f_{3M}^{(\psi)}}{f_M^{(\psi)}}\right) + u^3\bar{u}^3\left(\frac{h_M^{(\psi)}}{f_M^{(\psi)}}\left[\frac{7}{2} - 45c_{2,M}^{(\psi)}\right] + 70\frac{m_\psi f_{3M}^{(\psi)}}{f_M^{(\psi)}}\right)\,, \end{aligned} \tag{770}$$

as well as (expanded in powers of $[u\bar{u}]^k$, $k \in \mathbb{N}_0$)

$$-\frac{\overline{\Phi}_{3M}^{(\psi);\sigma}(u)}{6f_M^{(\psi)}} = -u\bar{u}\left(60\frac{m_\psi f_{3M}^{(\psi)}}{f_M^{(\psi)}} + \frac{h_M^{(\psi)}}{f_M^{(\psi)}}\right) + 300u^2\bar{u}^2\frac{m_\psi f_{3M}^{(\psi)}}{f_M^{(\psi)}}\,, \tag{771}$$

14 In Equation 768 all contributions have been combined with the correct prefactors.
15 Here, $\mathbb{A}_{4M}^{(\psi)}$ is the η–η' analogon of $\mathbb{F}_\pi$ (cf. Equation 739).
16 Especially, the interdependence of all involved higher twist DAs can be studied in this context.
17 Explicit expressions may be found in Chapter 3.

exhibit end-point divergences (highlighted in blue) caused by the corresponding convolution integrals $\sim\int_0^1 du\,\frac{\bar{u}}{u}$. Nevertheless, the explicit calculation of Equation 768 yields a finite result[18]

$$\begin{aligned} Q^2 F^{\text{QCD}}_{\gamma^*\gamma\to M}\left(Q^2\right)\Big|_{\text{LO}} &= 2\sum_\psi e_\psi^2 F_M^{(\psi)}\Bigg[3\left(1+c_{2,M}^{(\psi)}\right)-\frac{1}{Q^2}\Bigg[\frac{h_M^{(\psi)}}{f_M^{(\psi)}}\left(2+3c_{2,M}^{(\psi)}\right) \\ &\quad+\left\{\frac{80}{3}\delta_M^{2(\psi)}-\frac{h_M^{(\psi)}}{f_M^{(\psi)}}\left(\frac{67}{360}-\frac{5}{4}c_{2,M}^{(\psi)}\right)+\frac{200-203}{2}\frac{m_\psi f_{3M}^{(\psi)}}{f_M^{(\psi)}}\right\}\Bigg]\Bigg] \qquad (772) \\ &= 2\sum_\psi e_\psi^2 F_M^{(\psi)}\Bigg\{3\left(1+c_{2,M}^{(\psi)}\right)-\frac{1}{Q^2}\Bigg[\frac{h_M^{(\psi)}}{f_M^{(\psi)}}\left(2+3c_{2,M}^{(\psi)}\right) \\ &\quad+\frac{80}{3}\delta_M^{2(\psi)}-\frac{h_M^{(\psi)}}{f_M^{(\psi)}}\left(\frac{67}{360}-\frac{5}{4}c_{2,M}^{(\psi)}\right)-\frac{3}{2}\frac{m_\psi f_{3M}^{(\psi)}}{f_M^{(\psi)}}\Bigg]\Bigg\}\,. \qquad (773) \end{aligned}$$

Notably, Equation 773 entails the following conclusions:

- FACTORIZATION: The singularity at $u\to 0$ in Equation 771 exactly cancels with that of Equation 770 because both originate from similar twist-three operators[19]. Notably, this cancellation is general and does not depend on the twist-three DAs' shape.
- CONSISTENCY CHECK: Moreover, Equation 773 represents another successful consistency check for our ansatz as formulated in Equation 729.
- FKS SCHEME: When assuming the FKS mixing scheme all ratios ($R=q,s$)

$$\frac{h_M^R}{f_M^R}=\frac{h_R}{f_R}\,, \qquad (774)$$

become independent of the meson state $M=\eta,\eta'$. Consequently, the $1/Q^2$ corrections of Equation 773 (in square brackets) also get particle independent. Moreover, while (cf. [3], Table 8)

$$\frac{h_M^{(s)}}{f_M^{(s)}}=(0.50\pm 0.04)\ \text{GeV}^2 \qquad (775)$$

should be taken into account, the complementary ratio for light quarks is compatible with zero (cf. discussion in [3]).

- DOMINANT ADMIXTURES: Similar to Equation 739, the higher twist corrections of Equation 773 are dominated by the contributions proportional to $\delta_M^{2(\psi)}$, whereas the residual twist-three admixtures[20] $\sim m_\psi f_{3M}^{(\psi)}/f_M^{(\psi)}$ are numerically negligible.

Based on Equation 773 and Section 4.1.1 we obtain a rough estimate of the considered higher twist contributions (at $\mathcal{O}(\alpha_s^0)$) when inserting the given numbers (see [3] and Chapter 3)

$$F^{\text{QCD}}_{\gamma^*\gamma\to M}\left(Q^2\right)=\left[1-\frac{0.9\ \text{GeV}^2}{Q^2}\right]F^{\text{QCD;(tw2)}}_{\gamma^*\gamma\to M}\left(Q^2\right)\,. \qquad (776)$$

18 In Equation 772 the finite contributions of Equation 771 have been highlighted in orange, while the rest of Equation 772 (inside curly brackets) corresponds to all non-singular corrections resulting from Equation 770. Note that the scale dependence is not written out explicitly, but is always implied.

19 As discussed in Section 3.4.3, there are counterparts to $\overline{\Phi}_{3M}^{(\psi);\sigma}$ within $\mathbb{A}_{4M}^{(\psi)}$, that are generated by adequate EOM.

20 These originate from contributions of twist-three quark-antiquark-gluon matrix elements.

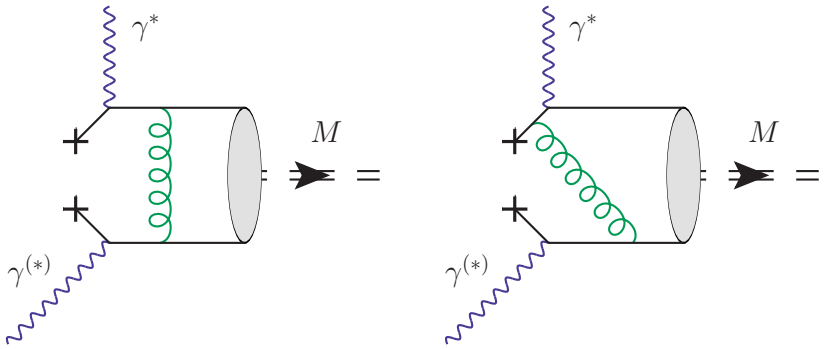

Figure 22: Assortment of conceivable twist-six contributions to the $\eta^{(\prime)}$ TFF (cf. [140, 281]). Here, a possible non-perturbative quark-vacuum interaction is taken into account, via the inclusion of quark condensate terms (cf. [64, 73–76]).

As expected, these corrections are only relevant in the small-Q^2 region. Conversely, one can show that contributions of arbitrary twist may produce $1/Q^2$ terms as well (see [281, 373] for a detailed discussion), indicating that the light-cone dominance of Equation 731 with one virtual and one real photon does not hold beyond leading power accuracy. An estimate of, e. g., the twist-six corrections [373] results in a small positive $1/Q^2$ contribution that is enhanced via an additional logarithmic factor (see [3, 373]).

For the $\eta^{(\prime)}$-TFF, this approach would have to be retrofitted with $\mathcal{O}(m_\psi)$ terms, originating from the (massive) quark propagator and quark condensates[21] (see Figure 22). Still, the general mismatch of twist- and power-counting remains. This is caused by the fact that to power accuracy one must consider contributions of large light-cone distances between the currents (e. g., similar to Equation 740) that are not "seen" in the twist expansion (see discussion in [3]). Up to $\mathcal{O}(\alpha_S^0)$, such terms conceivably imply only a numerically small alteration within Equation 776 and the resulting TFF as a whole. Consequently, it is reasonable to focus on the more pressing issue of how NLO gluonic corrections can be included into our considerations. Hence, this will be a key aspect of the following subsections.

4.1.3 *Next-to-leading order calculations – light quark corrections*

In this subsection, we focus on the calculation of α_S-corrections related to gluonic DAs at leading-twist accuracy and for light-quark flavors. Particularly, we assume two non-vanishing photon virtualities, while performing all relevant analytical computations within the framework of pQCD in external fields[22] (see [64, 73–76]).

The main challenge is rooted in a key feature of the $\eta{-}\eta'$ system: its possible two-gluon content. As depicted in Figure 23, each meson of the pseudoscalar octet (cf. Figure 1) can be exited via a quark-antiquark pair. According to Chapter 3, η and η' mesons may also be created by a photon-photon fusion into two gluons. This (short-distance) mechanism (see Figure 24), however, is suppressed by an extra factor of α_S, when compared to the subprocess $\gamma^*\gamma^{(*)} \to \bar{\psi}\psi$ ($\psi = u, d, s$),

21 Evidently, a distinction between light and strange flavor condensates requires non-vanishing quark-mass terms. However, in order to find all possible $\mathcal{O}(m_\psi)$ corrections, the quark propagator (expanded in an external field) has to be reconsidered as well. A priori, this requires a rather costly calculation with an expectedly small numerical impact.

22 The corresponding results have also been tested by means of "standard" pQCD methods (i. e., those mentioned in [112]).

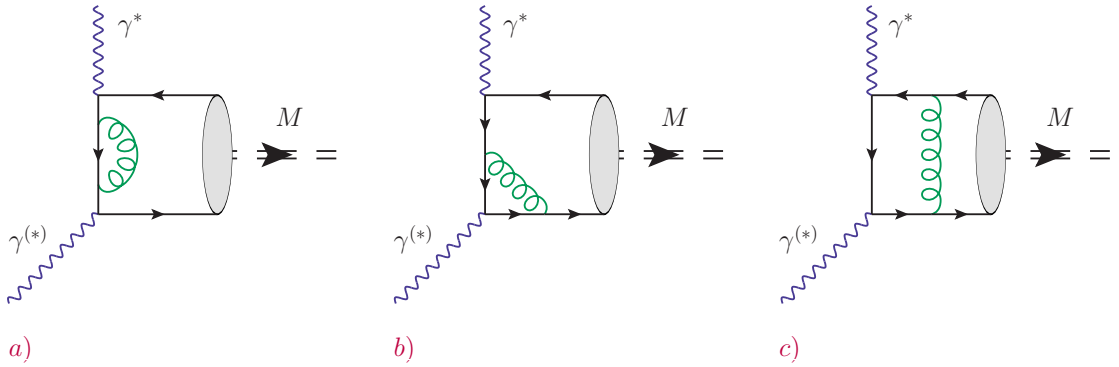

Figure 23: Sample of NLO Feynman diagrams contributing to the $\gamma^*\gamma^{(*)} \to M$ amplitude (e. g., $M = \pi^0, \eta, \eta'$). Complementary diagrams can be obtained by reversing the fermion flow's direction.

which may already be realized at LO in pQCD. Consequently, we naively might expect a strong suppression of the gluonic DAs ϕ_M^g within hard exclusive processes when compared to quark distributions such as ϕ_M^R ($R = q, s$). A consistent inclusion of all described NLO contributions in combination with the $\mathcal{O}(\alpha_s^2)$ RG corrections a posteriori leads to non-negligible effects, especially within $F_{\gamma^*\gamma\to\eta'}$ (see Section 4.3). Therefore, after those adjustments, this process exhibits a strong[23] sensitivity to both quark and gluon DAs. Besides, another conceivable process which in principle could be used as a promising testing ground for the twist-two $\eta^{(\prime)}$ meson DAs, is given by ($M_1, M_2 = \eta, \eta'$)

$$\gamma^*\gamma^* \to M_1 M_2 \,. \tag{777}$$

As discussed in [300], such a central exclusive pair production of pseudoscalar mesons would potentially display a high sensitivity to gluonic components of the η and η' mesons (for details see also [374–377]). In particular, it is an example, where the two-gluon components enter at the same order as quark-antiquark Fock states (see Figure 25). Hence, when corresponding data gets available, this process should be recalculated within a model-independent approach. For the time being, let us focus on the calculation of Figure 24.

In pQCD, the formation of η or η' mesons out of light (at $\mathcal{O}(\alpha_{QED})$) via an intermediate two-gluon state is given by corresponding NLO box-diagrams, such as those within Figure 24. When considering quark loop effects of light flavors, a calculation in external fields seems to be preferable. A major reason for this choice may be found in the resulting transformation of loop into Fourier integrals (cf. Section B.6) which are (at least for the current problem) easier to solve. For this purpose, the NLO diagrams of Figure 24 have to be reinterpreted and treated as follows:

i) According to[24] Figure 26, the diagrams a) and b) of Figure 24 correspond to a product of two propagators: one free, the other one emitting two soft gluons. Analogously, the remaining diagram c) may be regarded as a quark propagation from x^μ to $y^\mu = 0$ and back, each time accompanied by an emission of a slowly oscillating gluon field[25].

ii) Furthermore, all emerging contributions $\sim G_{\alpha\beta} G_{\mu\nu}$, $\widetilde{G}_{\alpha\beta} G_{\mu\nu}$, or $G_{\alpha\beta} \widetilde{G}_{\mu\nu}$, have to be taken into account. Similar to Figure 9, the latter are non-perturbative objects, but instead of forming condensates, they hadronize into $\eta^{(\prime)}$ mesons.

23 This may be seen on the level of Gegenbauer coefficients, as specified in Section 4.3.

24 In order to point out the difference between gluon condensates (see Figure 9 and [74]) and soft gluonic contributions to Equation 731, we retrofit the latter with a blob.

25 The corresponding expressions for quark propagators are collected in [64, 73–76].

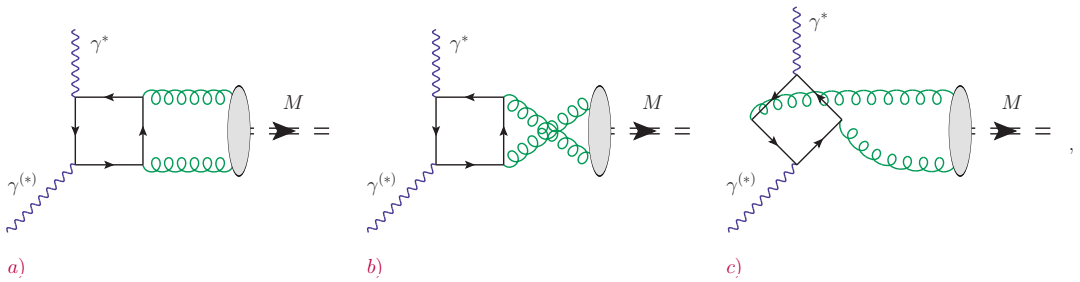

Figure 24: Short distance gluon fusion mechanism for the $\eta^{(\prime)}$ meson creation. Distinct one-loop box-diagrams of the corresponding $\gamma^*\gamma^{(*)} \to M$ ($M = \eta, \eta'$) amplitude.

Thus, for the actual calculation it becomes necessary to unfold the tensor structure of Equation 301, e. g., via $(n^2 = 0)$

$$\langle 0|\mathcal{G}_{\alpha\beta}(z_2 n)\, \mathcal{G}_{\mu\nu}(z_1 n)|M(P)\rangle = f_M^{(0)} T_{\alpha\beta;\mu\nu} \int_0^1 dx\, e^{-i z_{21}^x (P\cdot n)} \phi_M^{(g)}(x)\,, \tag{778}$$

$$\langle 0|\widetilde{\mathcal{G}}_{\alpha\beta}(z_2 n)\, \mathcal{G}_{\nu\mu}(z_1 n)|M(P)\rangle = f_M^{(0)} \widetilde{T}_{\alpha\beta;\mu\nu} \int_0^1 dx\, e^{-i z_{21}^x (P\cdot n)} \phi_M^{(g)}(x)\,, \tag{779}$$

as well as

$$\langle 0|\mathcal{G}_{\alpha\beta}(z_2 n)\, \widetilde{\mathcal{G}}_{\mu\nu}(z_1 n)|M(P)\rangle = f_M^{(0)} \widetilde{T}_{\alpha\beta;\mu\nu} \int_0^1 dx\, e^{-i z_{21}^x (P\cdot n)} \phi_M^{(g)}(x)\,. \tag{780}$$

Where, in analogy to Equation 101, the Lorentz structures are given by

$$\widetilde{T}_{\alpha\beta;\mu\nu} = \frac{C_f}{4\sqrt{3}} \left[p_\alpha \left(p_\mu g_{\beta\nu} - p_\nu g_{\beta\mu} \right) + p_\beta \left(p_\nu g_{\alpha\mu} - p_\mu g_{\alpha\nu} \right) \right], \tag{781}$$

$$T_{\alpha\beta;\mu\nu} = -\frac{1}{2} \varepsilon_{\mu\nu}{}^{\omega\tau} \widetilde{T}_{\alpha\beta;\omega\tau} = \frac{C_f}{4\sqrt{3}} p^\xi \left(p_\alpha \varepsilon_{\beta\xi\mu\nu} - p_\beta \varepsilon_{\alpha\xi\mu\nu} \right), \tag{782}$$

where p^μ is a light-like vector constructed from n^μ and P^μ (see Section A.10).[26] In order to

26 Since we only want to take into account leading twist corrections, other possible parametrizations, such as

$$T^{\text{alt}}_{\alpha\beta;\omega\tau} = \frac{C_f}{4\sqrt{3}} p^\xi \left(P_\beta \varepsilon_{\omega\tau\alpha\xi} - P_\alpha \varepsilon_{\omega\tau\beta\xi} + P_\omega \varepsilon_{\alpha\beta\tau\xi} - P_\tau \varepsilon_{\alpha\beta\omega\xi} \right),$$

along with $\left(\widetilde{T}^{\text{alt}}_{\alpha\beta;\mu\nu} = \frac{1}{2} \varepsilon_{\mu\nu}{}^{\omega\tau} T^{\text{alt}}_{\alpha\beta;\omega\tau}\right)$

$$\widetilde{T}^{\text{alt}}_{\alpha\beta;\mu\nu} = \frac{C_f}{4\sqrt{3}} \left\{ 2 \left[P_\beta \left(P_\mu g_{\nu\alpha} - P_\nu g_{\mu\alpha} \right) + P_\alpha \left(P_\nu g_{\mu\beta} - P_\mu g_{\nu\beta} \right) \right] + P^2 \left(g_{\mu\alpha} g_{\nu\beta} - g_{\nu\alpha} g_{\mu\beta} \right) \right\},$$

are excluded. The latter are contaminated with $\mathcal{O}(m_M^2)$ contributions which could be interpreted as higher twist effects (Equation 784).

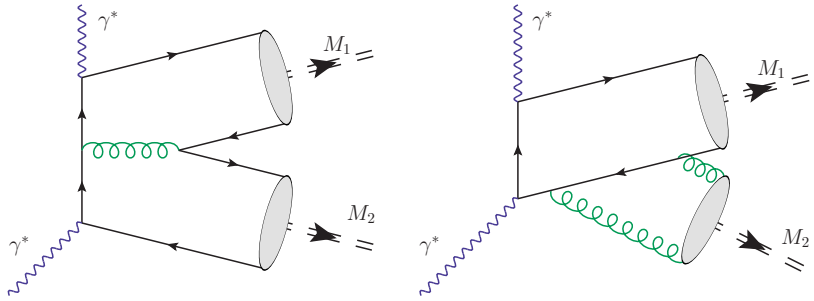

Figure 25: Representative Feynman diagrams for the $\gamma^*\gamma^* \to M_1 M_2$ ($M_1, M_2 = \eta, \eta'$) transition (e. g., [300, 348]), belonging to two distinct classes of characteristic perturbative subprocesses, i. e., $\gamma^*\gamma^* \to \bar{\psi}\psi\bar{\chi}\chi$ or $\gamma^*\gamma^* \to \bar{\psi}\psi gg$ ($\psi, \chi = u, d, s$).

demonstrate the need for Equation 778–Equation 780, let us, e. g., consider diagram b) of Figure 26, whose two-gluon leading twist contributions can be reduced to

$$\begin{aligned}
&\int d^D x\, e^{-iq_1\cdot x} \langle M(P)|\, \mathrm{Tr}\{ iS_\psi(0,x)\, \gamma_\mu iS_\psi(x,0)\, \gamma_\nu \}\, |0\rangle \\
&= g^2 \mu^{4-D} \int d^D x\, e^{-iq_1\cdot x} \int_0^1 du\, \langle M(P)|\, \mathrm{Tr}\Bigg\{ \frac{\Gamma\left(\frac{D}{2}\right) \not{x}}{2\pi^{D/2} i \left[-x^2\right]^{D/2}} \gamma_\mu \times \\
&\quad \times \Bigg[\frac{4i\Gamma\left(\frac{D}{2}-1\right) \not{x}}{16\pi^{D/2} \left[-x^2\right]^{D/2-1}} \int_0^u dv\, \bar{u} x^\alpha v x^\beta \mathcal{G}_{\alpha\xi}(ux)\, \mathcal{G}_\beta{}^\xi(vx) \\
&\quad + \frac{i\Gamma\left(\frac{D}{2}-2\right)}{16\pi^{D/2} \left[-x^2\right]^{D/2-2}} \Big(u\bar{u} x^\alpha \gamma^\beta \Big[\mathcal{G}_{\beta\xi}(ux)\, \mathcal{G}_\alpha{}^\xi(ux) - (\alpha \leftrightarrow \beta) \Big] \\
&\quad + \frac{1}{2} \int_0^u dv \Big[(2\bar{u}\xi_v + 1)\, x^\alpha \mathcal{G}_{\alpha\xi}(ux)\, \mathcal{G}^\xi{}_\lambda(vx)\, \gamma^\lambda + (1 - 2v\xi_u)\, \gamma^\alpha \mathcal{G}_{\alpha\xi}(ux)\, \mathcal{G}^\xi{}_\lambda(vx)\, x^\lambda \\
&\quad + i x^\alpha \widetilde{\mathcal{G}}_{\alpha\xi}(ux)\, \mathcal{G}^\xi{}_\lambda(vx)\, \gamma^\lambda \gamma_5 + i\, (\xi_v + 2\bar{u})\, x^\alpha \mathcal{G}_{\alpha\xi}(ux)\, \widetilde{\mathcal{G}}^\xi{}_\lambda(vx)\, \gamma^\lambda \gamma_5 \Big] \Big) \Bigg] \gamma_\nu \Bigg\} |0\rangle\,. \qquad (783)
\end{aligned}$$

When combined with all other corrections, we get[27] a result proportional to ($a := uv + \bar{u}w$)

$$\begin{aligned}
&\int_0^1 du \int_0^1 dv \int_0^1 dw\, \Theta(w-v)\, \frac{(v-w)\left(\xi_a \cancel{m_M^2} + Q^2 - q^2\right)}{\left[a\bar{a}\cancel{m_M^2} + \bar{a}Q^2 + aq^2\right]^{4-D/2}} \phi_M^{(g)}(u) \\
&= \int_0^1 du \left[\int_0^u dv \frac{v^2 \left(\xi_v \cancel{m_M^2} + Q^2 - q^2\right)}{\left[v\bar{v}\cancel{m_M^2} + \bar{v}Q^2 + vq^2\right]^{4-D/2}} - \int_{\bar{u}}^1 dv \frac{\bar{v}^2 \left(\xi_v \cancel{m_M^2} + Q^2 - q^2\right)}{\left[v\bar{v}\cancel{m_M^2} + \bar{v}Q^2 + vq^2\right]^{4-D/2}} \right] \frac{\phi_M^{(g)}(u)}{2u^2}\,, \qquad (784)
\end{aligned}$$

from which we may extract the hard scattering kernel[28] $\left(c_1(\mu,\varepsilon) := \frac{[4\pi\mu^2]^\varepsilon \Gamma(2-\varepsilon)\Gamma(2+\varepsilon)\Gamma(-\varepsilon)}{\Gamma(2-2\varepsilon)}\right)$

$$T_H^G\left(u, Q^2, q^2\right) = \frac{C_f \alpha_S}{2\pi} c_1(\mu,\varepsilon)\, \frac{1}{u^2} \left[\int_0^u dv \frac{v^2(Q^2-q^2)}{\left[\bar{v}Q^2 + vq^2\right]^{2+\varepsilon}} - \int_{\bar{u}}^1 dv \frac{\bar{v}^2(Q^2-q^2)}{\left[\bar{v}Q^2 + vq^2\right]^{2+\varepsilon}} \right]. \qquad (785)$$

27 For the calculation of Equation 784 we (partially) took into account $\mathcal{O}(m_M^2)$ corrections.
28 Now including all prefactors, while suppressing the underlying scale dependencies.

The corresponding ε-expansion[29]

$$T_H^G\left(u, Q^2, q^2\right) = \frac{1}{\varepsilon} T_{div}^g\left(u, Q^2, q^2\right) + T_H^g\left(u, Q^2, q^2\right)\Big|_{light} + \mathcal{O}(\varepsilon) \,, \tag{786}$$

implies two (new) coefficient functions[30], i. e.,

$$\begin{aligned} T_{div}^g\left(u, Q^2, q^2\right) = {} & \frac{2}{u^2\bar{u}^2\left[Q^2-q^2\right]^2} \frac{C_f \alpha_S}{2\pi} \Bigg[u^2 Q^2 \log\left(\frac{uQ^2+\bar{u}q^2}{Q^2}\right) \\ & - \bar{u}^2 q^2 \log\left(\frac{uQ^2+\bar{u}q^2}{q^2}\right) \Bigg] \,, \end{aligned} \tag{787}$$

$$\begin{aligned} T_H^g\left(u, Q^2, q^2\right)\Big|_{light} = {} & \frac{-1}{u^2\bar{u}^2\left[Q^2-q^2\right]^2} \frac{C_f \alpha_S}{2\pi} \Bigg\{ u^2 Q^2 \log\left(\frac{uQ^2+\bar{u}q^2}{Q^2}\right) \times \\ & \times \left[\log\left(\frac{uQ^2+\bar{u}q^2}{\mu^2}\right) + \log\left(\frac{Q^2}{\mu^2}\right)\right] \\ & - \bar{u}^2 q^2 \log\left(\frac{uQ^2+\bar{u}q^2}{q^2}\right) \left[\log\left(\frac{uQ^2+\bar{u}q^2}{\mu^2}\right)\right. \\ & \left. + \log\left(\frac{q^2}{\mu^2}\right)\right] + 2\left[Q^2 u(3\bar{u}-2)\log\left(\frac{uQ^2+\bar{u}q^2}{Q^2}\right)\right. \\ & \left. - q^2\bar{u}\,(3u-2)\log\left(\frac{uQ^2+\bar{u}q^2}{q^2}\right)\right] \Bigg\} \,, \end{aligned} \tag{788}$$

where especially the second one is relevant for our subsequent considerations. Besides, within the limit "$q^2 \to 0$" Equation 788 reproduces a major result of [20], namely:

$$\lim_{q^2\to 0} T_H^G\left(u, Q^2, q^2\right) = C_f \frac{\alpha_S}{2\pi} \frac{2\log(u)}{\bar{u}^2 Q^2} \left\{ \frac{1}{\varepsilon} - \left[\frac{1}{u} - 3 + \frac{1}{2}\log(u) + \log\left(\frac{Q^2}{\mu^2}\right)\right]\right\} \,. \tag{789}$$

Therefore, Equation 786 represents the generalization of Equation 789 to $q^2 \neq 0$, as needed for the anticipated LCSR approach (see Section 4.2).

4.1.4 *Next-to-leading order – charm quark corrections*

In this subsection, we focus on methods and results concerning the calculation of heavy quark effects related to the $\eta^{(\prime)}$ TFF. These effects are especially important for large momentum transfers where they enhance the most interesting two-gluon DAs decisively (see Section 4.3). Hence, for this work, their inclusion is mandatory.

An inclusion of heavy flavor contributions into the selected QCD factorization formalism in principle requires a reconsideration of the (physical) factorization scale "μ". The latter can either be (much) larger, $\mu \gg m_h$, or smaller, $\mu \ll m_h$ than a given quark mass "m_h" ($h = c, b, t$). Consequently, two distinct approaches arise (cf. [3, 378–382]):

i) The decoupling, or fixed flavor number scheme (FFNS) which presumes a large quark mass (i. e., $\Lambda_{QCD} \ll \mu \ll m_h, Q$) of similar order as the photon virtuality Q^2, predetermines all

29 Here, we by default use the $\overline{MS}$-scheme (e. g., Equation 43).

30 While neglecting irrelevant contributions, such as "$2u\bar{u}\left(q^2 - Q^2\right)$" in Equation 787, which disappear after a convolution with ϕ_M^g.

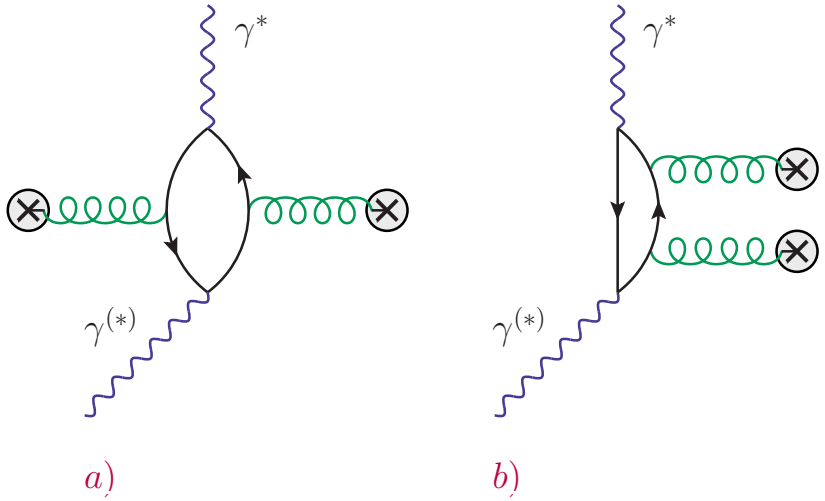

Figure 26: Schematic diagrams, depicting the radiation of soft gluons (cf. [74]), similar to Figure 9. In contrast to the latter, these soft gluonic fields hadronize into η or η' mesons.

"light" quark species via $m_{\text{light}} < m_h$. For this scenario it is natural to write the involved structure functions as a convolution of (hard) coefficient functions and (soft) parton densities that only involve light flavors (cf. [3]).

ii) Another possibility is given by assuming the hierarchy

$$\Lambda_{\text{QCD}}, m_h \ll \mu \ll Q\,, \tag{790}$$

and write the FF as a sum of active (heavy) flavors[31]. This ansatz is usually called the variable flavor number scheme (VFNS).

Within this subsection and beyond, we favor scheme i) which retains the entire heavy quark dependence in the coefficient functions. That ensures a standard one-scale calculation, incorporating $(m_h^2/Q^2)^n$ $(n \in \mathbb{N}_0)$ terms as well (e. g., [383]). Nonetheless, for $Q^2 \gg m_h^2$ the coefficient functions involve potentially large logarithms $\sim \log(Q^2/m_h^2)$ which a priori should be resummed systematically (e. g., [3, 380, 381]). Such improvements, however, are not likely to be large and their numerical impact on the TFF should be negligible (cf. discussion in [3, 281]). Thus, we may now focus on those techniques which allow a systematic calculation of heavy flavor corrections to the (NLO) hard scattering kernels of Equation 751. A major reason for using such an approach lies in its high degree of automation. The latter is indispensable when considering "real life" loop calculations which at some point may produce an unmanageable number of terms. Hence, our computations have been implemented in Wolfram *Mathematica*® 8 [36], employing the TRACER 1.1 [384] and FEYNCALC 8.1.0 [385, 386] packages[32] for the decomposition of traces and resulting tensor integrals. Due to the inherent limitations[33] as set by FEYNCALC 8.1.0, a bulk part of the actual

31 Their number changes according to the scale (cf. Section 2.3).

32 The FEYNCALC 8.1.0 package enables a symbolic computation of specific tensor integrals (cf. [385, 387]).

33 In this context, the used FEYNCALC 8.1.0 version provides a function called "`OneLoop`" which hitherto has been the only implemented tool for a tensor decomposition of one-loop integrals. Most importantly, the tensor integrals' maximal processable rank has been limited to three, while the output was written in terms of (formal) Passarino-Veltman (PV) coefficient functions. Therefore, its use has to be seen as a workaround, needed for our semiautomatic ansatz. This being said, an updated version of FEYNCALC 9 has been released recently (cf. [386]) which reportedly overcomes some of those limitations.

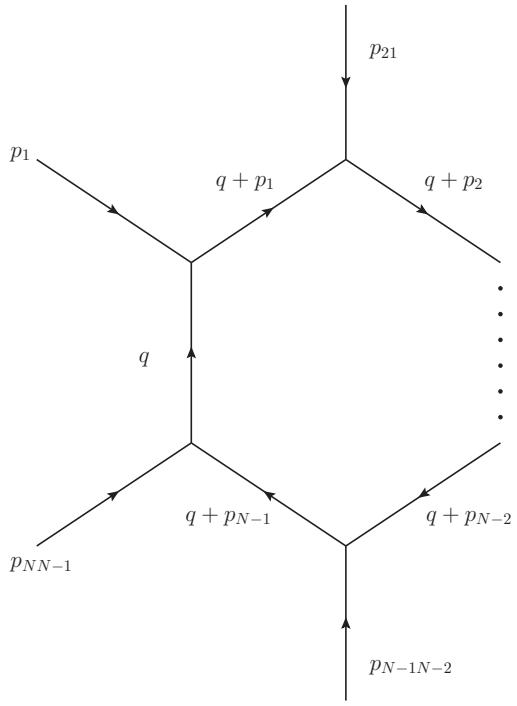

Figure 27: Conventions for N-point integrals, having the momenta $p_1, \ldots, p_{N-1}$ and q (e. g., [388]).

calculation has been kept independent of the underlying algorithm which allowed an additional cross-check with a different reduction method.

4.1.4.1 *Reduction algorithm*

In order to discuss the main features of these reduction methods in detail, let us first review some common facts about loop integrals.

Subsequently, the general classification of one-loop integrals in D dimensions (cf. Figure 27), assumes N $(N \in \mathbb{N})$ propagators in the denominator, together with P $(P \in \mathbb{N}_0)$ integration momenta within the corresponding numerator. Therefore, they happen to be UV divergent for $P+D-2N \geqslant 0$ (e. g., [388]). As discussed in Chapter 2, those divergences can be regulated for $D \neq 4$, while within a renormalizable theory we may assume $P \leqslant N$ (see also [44, 388]). Thus, considering a given problem and loop order, one faces a finite number of divergent integrals. Moreover, all encountered one-loop (tensor) integrals, such as [388]

$$T^N_{\mu_1 \ldots \mu_P}(p_1, \ldots, p_{N-1}; m_0, \ldots, m_{N-1}) \coloneqq \frac{(2\pi\mu)^{4-D}}{i\pi^2} \int d^D k \, \frac{k_{\mu_1} \cdots k_{\mu_P}}{D_0 D_1 \cdots D_{N-1}} \,, \tag{791}$$

with denominator factors[34] $(j = 1, \ldots, N-1)$

$$D_0 \coloneqq k^2 - m_0^2 + i0^+ \equiv D_0\left(m_0^2\right) \,, \quad D_j \coloneqq (k+p_j)^2 - m_j^2 + i0^+ \equiv D_j\left(m_j^2\right) \,, \tag{792}$$

34 Like before "$i0^+$" is an infinitesimal imaginary part (i. e., if $\phi : \mathbb{C} \to \mathbb{C}$ is a test function with $x \mapsto \phi(x)$, then $\phi(x+i0^+) \equiv \lim_{\varepsilon \to 0^+} \phi(x+i\varepsilon)$), which is needed to regulate singularities of the integral. Besides, it ensures causality (e. g., [64]) and (after integration) determines the correct imaginary parts of resulting Spence functions or logarithms.

only depend on the external momenta (p_0^μ vanishes)

$$p_{j0}^\mu \coloneqq p_j^\mu \,, \quad p_{ij}^\mu \coloneqq p_i^\mu - p_j^\mu \tag{793}$$

and the involved quark-masses m_k ($k = 0, \ldots, N-1$). Accordingly, their Lorentz covariance allows an efficient decomposition into scalar integrals "T_0^L" ($L \leqslant N$), multiplied by tensors constructed from corresponding four-momenta (cf. Equation 793) and, in some cases, the metric tensor. A well established method based on this circumstance is given by the PV algorithm[35] [388, 394–400]. In its essence, this procedure can be roughly summarized as follows:

i) The Lorentz covariance of Equation 791 formally implies [388, 394]

$$T^N_{\mu_1 \ldots \mu_P}(p_1, \ldots, p_{N-1}; m_0, \ldots, m_{N-1}) = \sum_{i_1, \ldots, i_P = 0}^{N-1} T^N_{i_1 \ldots i_P} p_{i_1 \mu_1} \cdots p_{i_P \mu_P} \,, \tag{794}$$

where we have introduced the auxiliary four-vectors p_0^μ. The latter give rise to totally symmetric tensors, constructed from $g_{\mu\nu}$ via[36]

$$\prod_{j=1}^{P} p_{0\mu_j} \longmapsto \begin{cases} g_{\{\mu_1\mu_2} g_{\mu_3\mu_4} \cdots g_{\mu_{P-1}\mu_P\}} & , P \text{ even} \\ 0 & , P \text{ odd} \end{cases} . \tag{795}$$

Notably, for $N \geqslant 5$ and a sufficient number of linear independent external momenta $\{\tilde{p}_1, \ldots, \tilde{p}_4\} \subseteq \{p_1, \ldots, p_{N-1}\}$ Equation 794 can be replaced by [388, 394]

$$T^N_{\mu_1 \ldots \mu_P}(p_1, \ldots, p_{N-1}; m_0, \ldots, m_{N-1}) = \sum_{i_1, \ldots, i_P = 1}^{4} T^N_{i_1 \ldots i_P} \tilde{p}_{i_1 \mu_1} \cdots \tilde{p}_{i_P \mu_P} \,, \tag{796}$$

which, similar to Equation 794, includes unique scalar coefficient functions $T^N_{i_1 \ldots i_P}$. Those are symmetric under any exchange of arguments and related indices, such as

$$(p_k, m_k, i_k) \leftrightarrow (p_j, m_j, i_j) \,, \tag{797}$$

because the underlying one-loop integrals are themselves invariant with regard to similar transformations concerning their propagators. Besides, when recording an explicit result, one conveniently denotes T^N by the Latin alphabet's N^{th} letter, i. e., $T^1 \equiv A$, $T^2 \equiv B$, and so forth.

ii) Most importantly, the emerging invariant coefficients within Equation 794 can then be iteratively reduced to scalar integrals T_0^L which in principle[37] boil down to a basic set of PV functions, as represented by A_0, B_0, C_0 and D_0 (cf. Section B.1).

The first step towards this favored reduction algorithm affects all scalar products within a given loop integrand's numerator which naturally can be expressed in terms of denominator factors (e. g., [388, 394])

$$k \cdot p_j = \frac{1}{2} \left[D_j - D_0 - f_j \right] \,, \quad f_j = p_j^2 - m_j^2 + m_0^2 \,, \tag{798}$$

$$k^2 = D_0 + m_0^2 \,. \tag{799}$$

35 This commonly used term only mentions two of the many trailblazers in perturbative QFT (e. g., [44, 388]). In particular, its application to NLO calculations of electroweak phenomena and the related renormalization of the SM (e. g., [44, 388–391]) lead to an ongoing development within this field. Only recently, the linked problem of (scalar) one-loop integrals has been reexamined [392, 393] and is only now assumed to be completely solved.

36 Within Equation 795 the bracket notation (cf. [401]) indicates a symmetrization over Lorentz indices included in those brackets, e. g., $g_{\{\mu_1\mu_2} g_{\mu_3\mu_4\}} = g_{\mu_1\mu_2} g_{\mu_3\mu_4} + g_{\mu_1\mu_3} g_{\mu_2\mu_4} + g_{\mu_1\mu_4} g_{\mu_2\mu_3}$ (see also [388]).

37 Except some special cases, every N-point scalar integral ($N \geqslant 5$) can be reduced to a set of four-point integrals, i. e., D_0s in four space-time dimensions (cf. [388, 394, 402–404]).

To that effect, Equation 798 and Equation 799 entail two essential relations (cf. Equation 791)

$$R^{N,k}_{\mu_1\dots\mu_{P-1}} \coloneqq T^N_{\mu_1\dots\mu_P} p_k^{\mu_P} = \frac{1}{2}\left[T^{N-1}_{\mu_1\dots\mu_{P-1}}[k] - T^{N-1}_{\mu_1\dots\mu_{P-1}}[0] - f_k T^N_{\mu_1\dots\mu_{P-1}}\right], \tag{800}$$

$$R^{N,00}_{\mu_1\dots\mu_{P-2}} \coloneqq T^N_{\mu_1\dots\mu_P} g^{\mu_{P-1}\mu_P} = T^{N-1}_{\mu_1\dots\mu_{P-2}}[0] + m_0^2 T^N_{\mu_1\dots\mu_{P-2}}, \tag{801}$$

when employing the common definition[38] (cf. [388, 394]; $n = 0, 1, \dots, N$)

$$T^N_{\mu_1\dots\mu_P}[n] \coloneqq \frac{(2\pi\mu)^{4-D}}{i\pi^2}\int d^D k \, \frac{k_{\mu_1}\cdots k_{\mu_P}}{D_0 D_1 \cdots D_N} D_n \,. \tag{802}$$

Additional contractions with external momenta, accompanied by another Lorentz decomposition of involved tensor integrals within Equation 800 and Equation 801, such as $(M \leqslant N-1)$

$$R^{N,k}_{\mu_1\dots\mu_{P-1}} = \sum_{i_1,\dots,i_{P-1}=0}^{M} R^{N,k}_{i_1\dots i_{P-1}} p_{i_1\mu_1}\cdots p_{i_{P-1}\mu_{P-1}}, \tag{803}$$

$$R^{N,00}_{\mu_1\dots\mu_{P-2}} = \sum_{i_1,\dots,i_{P-2}=0}^{M} R^{N,00}_{i_1\dots i_{P-2}} p_{i_1\mu_1}\cdots p_{i_{P-2}\mu_{P-2}}, \tag{804}$$

give rise (see also e. g., [388, 394]) to a multitude of linear equations for the relevant coefficient functions, formally resulting in [388] (see also Section B.2)

$$T^N_{00 i_1\dots i_{P-2}} = \frac{1}{D+P-2-M}\left[R^{N,00}_{i_1\dots i_{P-2}} - \sum_{k=1}^{M} R^{N,k}_{k i_1\dots i_{P-2}}\right], \tag{805}$$

$$T^N_{k i_1\dots i_{P-1}} = \left(X_M^{-1}\right)_{kk'}\left[R^{N,k'}_{i_1\dots i_{P-1}} - \sum_{r=1}^{P-1}\delta^{k'}_{i_r} T^N_{00 i_1\dots i_{r-1} i_{r+1}\dots i_{P-1}}\right]. \tag{806}$$

I. e., this set further decomposes into disjoint sub-sets of (up to) $N-1$ equations for each tensor integral which can be solved, if the inverse matrix (cf. [388, 405])

$$X_M^{-1} = \begin{pmatrix} p_1^2 & p_1\cdot p_2 & \cdots & p_1\cdot p_M \\ p_2\cdot p_1 & p_2^2 & \cdots & p_2\cdot p_M \\ \vdots & \vdots & \ddots & \vdots \\ p_M\cdot p_1 & p_M\cdot p_2 & \cdots & p_M^2 \end{pmatrix}^{-1} \tag{807}$$

exists. Hence, the related invariant functions then yield tensor integrals (cf. Equation 805, Equation 806) with viewer indices and propagator factors (see [388, 394, 405] for details). In this way, the bulk part of all required tensor integrals can be iteratively rewritten in terms of scalar integrals and predetermined Lorentz tensors (see[39] Section B.2). Nevertheless, there are a few problematic cases which have to be circumvented[40] (e. g., [388, 394]), for instance:

1) If $(X_{N-1})_{ij} = p_i\cdot p_j$ $(i,j = 1,\dots,N-1$; cf. Equation 807$)$ becomes singular, the described PV algorithm breaks down. At best, this is caused by linearly dependent (external) momenta which correspondingly can be left out in the Lorentz decomposition and Equation 807. That implies a smaller matrix $X_{M'}$ $(M' \leqslant N-1)$, which, if it is non-singular, restores the algorithm.

38 Having an external momentum in its first propagator, the case $n = 0$ has to be treated with caution. In order to restore Equation 791, the integration measure of $T^N_{\mu_1\dots\mu_P}[0]$ has to be shifted accordingly, e. g., via $k \to k - p_1$.

39 An explicit application of this method can be found in Section B.2, where we calculate the first view tensor integrals.

40 Consistent with this rough sketch of the PV reduction algorithm, we only list the most relevant scenarios.

2) If the Gram determinant $\det X_{N-1}$ is zero, but without linearly dependent four-momentum vectors, a different reduction method has to be used (e. g., [402, 403]).

3) Another "worst case" scenario occurs $\left(\text{relevant for } N \geqslant 5\right)$ when the Cayley determinant [388, 394] "$\det Y$", as defined by

$$(Y)_{ij} \equiv Y_{ij} \coloneqq m_i^2 + m_j^2 - p_{ij}^2 \,, \tag{808}$$

is vanishing. Consequently, the related N-point one-loop integral has either to be calculated directly, or a different reduction procedure has to be applied (see [388, 402–404]).

Specifically, point 1) and 2) are relevant for the consecutive calculation of (leading-twist) charm-quark effects due to occurring collinear momenta.

However, before proceeding, it should be mentioned, that the complementary Duplančić–Nižić algorithm (see [406] for details), which we have used as a nontrivial cross-check, is additionally based on integration-by-parts identities (e. g., [407–410]) in combination with the discussed Lorentz decomposition (cf. [406]). This leads to different recursion relations for scalar integrals, without restrictions regarding the external momenta[41] (cf. [406, 416]). The resulting reduction method [406, 407] is particularly useful for multi-leg calculations which include Feynman integrals with massless internal lines (cf. [406]).

4.1.4.2 *Calculation of charm quark corrections*

For an explicit derivation of relevant heavy flavor corrections we may now resort to the discussed reduction algorithm and introduced tensor integral formalism (cf. Section 4.1.4.1). Fortunately, this profoundly facilitates a detailed delineation of intermediate steps towards our result, even though the latter is actually independent of any decomposition method.

In order to get there, let us start with the following ansatz:

- The gluonic corrections to Equation 751 can be calculated with one single non-vanishing photon virtuality $Q^2 \gg 0$, i. e., q_2^μ can be treated as a given light-like vector.
- Furthermore, when focusing on leading twist NLO contributions, we may neglect all $\mathcal{O}\left(m_M^2\right)$ corrections from the very beginning.

Both points combined allow an efficient tensor decomposition due to the corresponding cancellation of involved integrals and coefficient functions, as indirectly implied by $P^2, q^2 = 0$. Yet, the very same set-up can also cause a breakdown of our preferred PV reduction algorithm, in particular, when applying the QCD factorization (cf. Section 4.1.1) approach which may generate additional collinear four-momenta[42] within related subgraphs. Consequently, a reasonable choice of the interrelated momentum configuration is imperative, as discussed below.

In any case, the eligible heavy quark NLO corrections require an adequate reevaluation of all

41 Additionally, the involved generalized recursion relations connect scalar integrals in a different number of dimensions with each other [407, 411–415]. Therefore, this algorithm also has a different set of master integrals.

42 Notably, a collinear setting permits the reformulation of scalar four-point integrals in terms of three-point PV functions and their derivatives (see Equation 835).

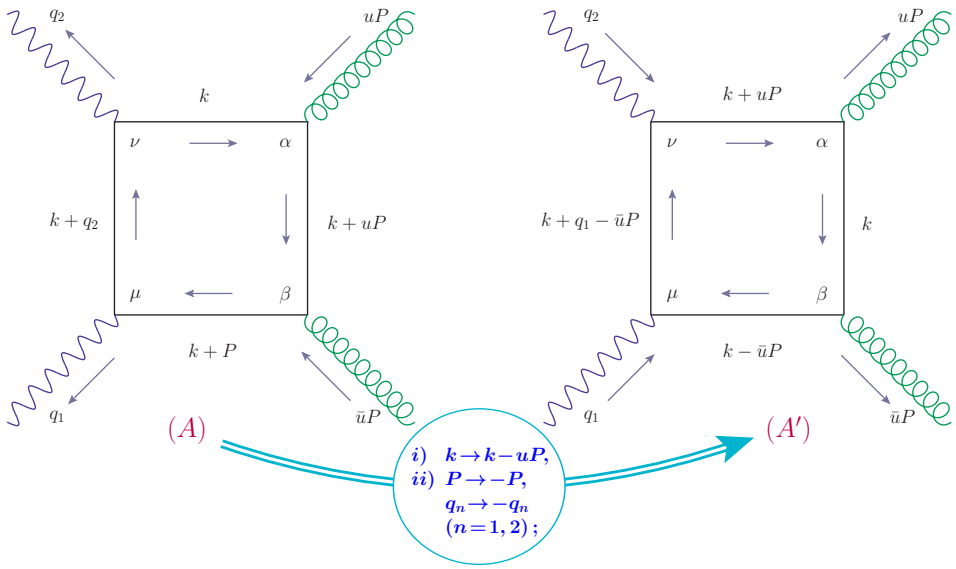

Figure 28: Two basic possibilities for the hard subgraph of Figure 24 a) (or b), respectively). The corresponding translation "$k^\mu \to k^\mu - uP^\mu$", followed by a reversal of all "external" gauge particles' momenta transforms diagram (A) into (A′).

related one-loop diagrams, i. e., those given by Figure 24. When starting with Figure 24 a), a standard pQCD analysis of the embedded hard subgraph leads to the intermediate result[43]

$$M_{\mu\nu}^{(A)} := \sum_\psi e_\psi^2 g^2 \mu^{4-D} \int d^D y \int d^D z \left[\prod_{j=1}^{4} \int \frac{d^D k_j}{(2\pi)^D}\right] e^{ix\cdot(k_1-k_2)+iy\cdot(k_3-k_4)+iz\cdot(k_2-k_3)} \times$$
$$\times \frac{\mathrm{Tr}\{(\not{k}_1+m_\psi)\gamma_\mu(\not{k}_2+m_\psi)\not{A}(z)(\not{k}_3+m_\psi)\not{A}(y)(\not{k}_4+m_\psi)\gamma_\nu\}}{\prod_{l=1}^4 \left[k_l^2-m_\psi^2+i0^+\right]}\,, \tag{809}$$

which can then be further examined via the collinear factorization ansatz (cf. Equation 738). Depending on the essential definition[44] (see Equation 731)

$$F_{\mu\nu}^{(A)}(q_1,q_2) := \int d^D x\, e^{-iq_1\cdot x} \langle M(P)|M_{\mu\nu}^{(A)}|0\rangle\,, \tag{810}$$

as well as (cf. Equation 303)

$$\langle M(P)\,|\mathcal{A}_\alpha(z)\,\mathcal{A}_\beta(y)|0\rangle\big|_{(z-y)^2=0} \sim \varepsilon_{\alpha\beta\sigma\rho}\frac{P^\sigma(z^\rho-y^\rho)}{P\cdot(z-y)} f_M^0 \int_0^1 du\, e^{iP\cdot(uy+\bar{u}z)}\frac{\phi_M^g(u)}{u\bar{u}}\,, \tag{811}$$

Equation 809 implies (modulo constant factors)

$$F_{\mu\nu}^{(A)} \sim \sum_\psi e_\psi^2 C_f \frac{\alpha_S}{2\pi}\frac{f_M^0}{Q^2}\varepsilon^{\alpha\beta}{}_{\rho\tau} q_1^\rho q_2^\tau \int_0^1 du\,\frac{\phi_M^g(u)}{u\bar{u}} I_{\mu\nu;\alpha\beta}^{(A,\psi)}(u;q_1,q_2)\,, \tag{812}$$

43 In contrast to the background field method (cf. Section 4.1.3), a pQCD ansatz, e. g., as given by Equation 809 involves combinations of soft gluon fields "$\mathcal{A}_\mu$", instead of field-strength tensors "$\mathcal{G}_{\mu\nu}$".

44 Formally, the definition given in Equation 810 and, therefore, Equation 812 are analogous for all discussed cases, including $A = B, C$.

whose solution breaks down to a tensor reduction of

$$\begin{aligned}&I^{(A,\psi)}_{\mu\nu;\alpha\beta}(u;q_1,q_2)\\&\quad\coloneqq\int d^Dk\,\frac{\mathrm{Tr}\left\{(\not k+\not q_1+m_\psi)\gamma_\mu(\not k+m_\psi)\gamma_\alpha(\not k+\bar u\not P+m_\psi)\gamma_\beta(\not k+\not P+m_\psi)\gamma_\nu\right\}}{\left[k^2-m_\psi^2\right]\left[(k-q_1)^2-m_\psi^2\right]\left[(k+\bar uP)^2-m_\psi^2\right]\left[(k+P)^2-m_\psi^2\right]}.\end{aligned}\tag{813}$$

Apparently, instead of Equation 813 we may equivalently solve (see Figure 28)

$$\begin{aligned}&I^{(A,\psi)}_{\mu\nu;\alpha\beta}(u;q_1,q_2)\Big|_{\text{alt}}\\&=\int d^Dk\,\frac{\mathrm{Tr}\left\{(\not k+\not P+m_\psi)\gamma_\mu(\not k+\not q_2+m_\psi)\gamma_\nu(\not k+m_\psi)\gamma_\alpha(\not k+u\not P+m_\psi)\gamma_\beta\right\}}{D_0D_1D_2D_3},\end{aligned}\tag{814}$$

with the underlying (auxiliary) momenta (cf. Equation 792)

$$p_1^\mu=P^\mu,\quad p_2^\mu=q_2^\mu,\quad p_3^\mu=uP^\mu.\tag{815}$$

This choice exhibits several advantages over the original configuration (see Equation 813) due to a facilitated trace and related denominator decomposition, as implicated by Equation 798 ($p_i^2,f_i=0,\,\forall i=1,2,3$). Appropriately, after applying Equation 798 and further simplifications, Equation 814 can be split up into three different structures[45]

$$\begin{aligned}&\varepsilon^{\alpha\beta}{}_{\rho\tau}q_1^\rho q_2^\tau\,I^{(A,\psi)}_{\mu\nu;\alpha\beta}(u;q_1,q_2)\Big|_{\text{alt}}\\&\sim\varepsilon_{\mu\nu\rho\tau}P^\rho q_2^\tau\left[Q^2\left(uT^3_0[1]-\bar uT^3_0[0]-T^3_0\right)-2\left(T^2_0[0,1]+T^2_0\right)\right]\\&\quad+2\varepsilon_\nu{}^\alpha{}_{\rho\tau}P^\rho q_2^\tau\left[\xi_uQ^2T^4_{\alpha\mu}-P_\mu\xi_uT^3_\alpha[2]+q_{2\mu}T^3_\alpha[1]-(P_\mu+q_{2\mu})T^3_\alpha[0]-2T^3_{\alpha\mu}[0]\right]\\&\quad+2\varepsilon_\mu{}^\alpha{}_{\rho\tau}P^\rho q_2^\tau\left[-\xi_uQ^2T^4_{\alpha\nu}+P_\nu\xi_uT^3_\alpha[2]+q_{2\nu}T^3_\alpha[1]+q_{1\nu}T^3_\alpha[0]+2T^3_{\alpha\nu}[1]\right],\end{aligned}\tag{816}$$

where we adopt the generalization of Equation 802:

$$T^{N-n}_{\mu_1\dots\mu_P}[m_1,\dots,m_n]\coloneqq\frac{(2\pi\mu)^{4-D}}{i\pi^2}\int d^Dk\,\frac{k_{\mu_1}\cdots k_{\mu_P}}{D_0D_1\cdots D_{N-1}}D_{m_1}\cdots D_{m_n}.\tag{817}$$

An extended calculation yields ($p_{12}^2=q_1^2$, $p_{13}^2=0$, $p_{23}^2=uq_1^2$; cf. Equation 815) a formal intermediate result in terms of PV functions (see Section B.1):

$$\begin{aligned}&\varepsilon^{\alpha\beta}{}_{\rho\tau}q_1^\rho q_2^\tau\,I^{(A,\psi)}_{\mu\nu;\alpha\beta}(u;q_1,q_2)\Big|_{\text{alt}}\\&\sim i\varepsilon_{\mu\nu\alpha\beta}q_1^\alpha q_2^\beta\Big\{2-2B_0\left(p_{13}^2;m_\psi^2,m_\psi^2\right)+\frac{1}{\bar u}\left[B_0\left(p_{12}^2;m_\psi^2,m_\psi^2\right)-B_0\left(p_{23}^2;m_\psi^2,m_\psi^2\right)\right]\\&\quad+Q^2\left[\left[\frac{2m_\psi^2}{Q^2}+u\right]C_0\left(p_2^2,p_3^2,p_{23}^2;m_\psi^2,m_\psi^2,m_\psi^2\right)-C_0\left(p_1^2,p_2^2,p_{12}^2;m_\psi^2,m_\psi^2,m_\psi^2\right)\right.\\&\quad+2\left[\frac{m_\psi^2}{Q^2}-\xi_u\right]C_0\left(p_{13}^2,p_{12}^2,p_{23}^2;m_\psi^2,m_\psi^2,m_\psi^2\right)-\bar uC_0\left(p_{13}^2,p_{23}^2,p_{12}^2;m_\psi^2,m_\psi^2,m_\psi^2\right)\\&\quad\left.-4\xi_um_\psi^2D_0\left(p_{13}^2,p_3^2,p_2^2,p_{12}^2,p_1^2,p_{23}^2;m_\psi^2,m_\psi^2,m_\psi^2,m_\psi^2\right)\right]\Big\}.\end{aligned}\tag{818}$$

45 After further tensor reduction, only a single structure will remain, as implied by Equation 731.

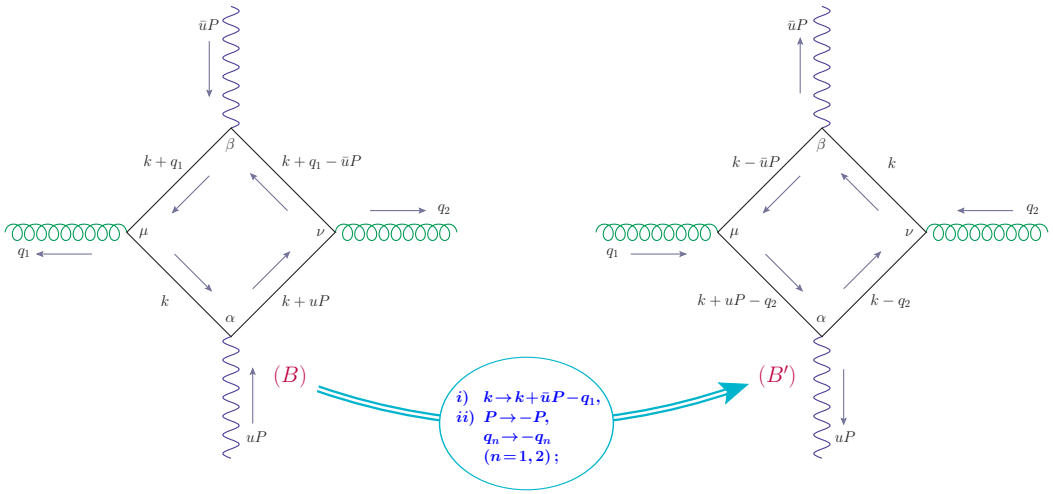

Figure 29: In analogy to Figure 28, (B) as well as (B′) represent the two fundamental choices for a hard subgraph of Figure 24 c). Accordingly, the transition between (B) and (B′) is given by a shift "$k^\mu \to k^\mu + \bar{u}P^\mu - q_1^\mu$" along with an inversion "$P^\mu \to -P^\mu$", "$q_n^\mu \to -q_n^\mu$" ($n = 1, 2$).

This notation enables a compact representation of integral expressions and, hence, is often used in the standard literature (see [417], including references therein). By the same token, (UV) divergences, such as (e. g., [418, 419])

$$(D-4)\,A_0\left(m^2\right) = -2m^2 + \mathcal{O}(D-4)\,, \tag{819}$$

$$(D-4)\,B_0\left(p^2; m_0^2, m_1^2\right) = -2 + \mathcal{O}(D-4)\,, \quad \text{etc.}, \tag{820}$$

are generic[46] and, therefore, easily detectable[47]. Besides, the explicit analytical expression for Equation 818 can always be reconstructed by inserting all necessary master integrals. Moreover, as another validation for our approach, we have also analyzed the shifted amplitude (belonging to Figure 28 (A′))

$$\begin{aligned} &I^{(A,\psi)}_{\mu\nu;\alpha\beta}(u; q_1, q_2)\Big|_{\text{shift}} \\ &= \int d^D k\, \frac{\mathrm{Tr}\left\{(\not{k} - \bar{u}\not{P} + m_\psi)\gamma_\mu(\not{k} + \not{q}_1 - \bar{u}\not{P} + m_\psi)\gamma_\nu(\not{k} + u\not{P} + m_\psi)\gamma_\alpha(\not{k} + m_\psi)\gamma_\beta\right\}}{D_0 D_1 D_2 D_3}, \end{aligned} \tag{821}$$

resulting from Equation 815 via "$k^\mu \to k^\mu - uP^\mu$", followed by "$P^\mu \to -P^\mu$" as well as "$q_i^\mu \to -q_i^\mu$" ($i = 1, 2$). Together with (cf. Equation 792) a tensor decomposition based on "$p_1^\mu\big|_{\text{shift}} = uP^\mu$", "$p_2^\mu\big|_{\text{shift}} = q_1^\mu - \bar{u}P_\mu$" and "$p_3^\mu\big|_{\text{shift}} = -\bar{u}P^\mu$" this (numerically) reproduces Equation 818. Similarly, we have calculated both diagrams of Figure 29 which either correspond to

$$p_1^\mu = q_1^\mu\,, \quad p_2^\mu = uP^\mu\,, \quad p_3^\mu = q_1^\mu - \bar{u}P^\mu\,, \tag{822}$$

46 Besides, several coefficient functions of Equation 794, such as B_1, B_{00}, B_{11}, C_{00}, C_{001}, C_{002} and D_{0000} in general exhibit UV divergences (see [418]).

47 In fact, this constitutes a major advantage of the underlying PV method and formalism, because especially for larger calculations, where strong numerical cancellations and, therefore, instabilities may occur, an algebraic reduction method can be preferable (e. g., [404]). Accordingly, the separation of UV divergences (cf. [418]) needs to be automatized. A prominent example for such a program is given by the LoopTools package (cf. [420–423]), which offers corresponding (numerical) subroutines.

or (including a substitution or "shift", as depicted in Figure 29 (B′))

$$p_1^\mu\big|_{\text{shift}} = -q_1^\mu\,, \quad p_2^\mu\big|_{\text{shift}} = uP^\mu - q_1^\mu\,, \quad p_3^\mu\big|_{\text{shift}} = -\bar{u}P^\mu\,, \tag{823}$$

respectively. For brevity, we only discuss the first case[48]. Accordingly, analogous to Equation 812, Figure 24 c) implies

$$\begin{aligned} M_{\mu\nu}^{(B)} \coloneqq \sum_\psi e_\psi^2 g^2 \mu^{4-D} \int d^D y \int d^D z \left[\prod_{j=1}^{4} \int \frac{d^D k_j}{(2\pi)^D}\right] e^{ix\cdot(k_1-k_2)+iy\cdot(k_2-k_3)+iz\cdot(k_4-k_1)} \times \\ \times \frac{\mathrm{Tr}\{(\not{k}_1+m_\psi)\gamma_\mu(\not{k}_2+m_\psi)\not{A}(y)(\not{k}_3+m_\psi)\gamma_\nu(\not{k}_4+m_\psi)\not{A}(z)\}}{\prod_{l=1}^{4}\left[k_l^2-m_\psi^2+i0^+\right]}\,, \end{aligned} \tag{824}$$

which corresponds to the solution of (after applying Equation 810 and Equation 811)

$$\begin{aligned} &I_{\mu\nu;\alpha\beta}^{(B,\psi)}(u;q_1,q_2) \\ &\quad\coloneqq \int d^D k\, \frac{\mathrm{Tr}\{(\not{k}+\not{q}_1+m_\psi)\gamma_\mu(\not{k}+m_\psi)\gamma_\alpha(\not{k}+u\not{p}+m_\psi)\gamma_\nu(\not{k}+\not{q}_1-\bar{u}\not{p}+m_\psi)\gamma_\beta\}}{D_0D_1D_2D_3}. \end{aligned} \tag{825}$$

Diagram Figure 24 yields only two Lorentz structures[49]

$$\begin{aligned} &\varepsilon^{\alpha\beta}{}_{\rho\tau} q_1^\rho q_2^\tau I_{\mu\nu;\alpha\beta}^{(B,\psi)}(u;q_1,q_2) \\ &\sim \varepsilon_\nu{}^\alpha{}_{\rho\tau} P^\rho q_2^\tau \left\{ \frac{1}{\bar{u}}\left[P_\mu T_\alpha^3[3] + T_{\alpha\mu}^3[3] - uP_\mu T_\alpha^3[1] - \xi_u T_{\alpha\mu}^3[1]\right] + \frac{1}{u}\left[q_{2\mu} T_\alpha^3[2] - T_{\alpha\mu}^3[2]\right.\right. \\ &\quad \left.\left. - (\bar{u}P_\mu + \xi_u q_{1\mu}) T_\alpha^3[0] - \xi_u T_{\alpha\mu}^3[0]\right]\right\} + \varepsilon_\mu{}^\alpha{}_{\rho\tau} P^\rho q_2^\tau \left\{ \frac{1}{\bar{u}}\left[uP_\nu T_\alpha^3[1] - \xi_u T_{\alpha\nu}^3[3]\right.\right. \\ &\quad \left. + T_{\alpha\nu}^3[1] - \frac{1}{2}\left(1+\xi_u^2\right) P_\nu T_\alpha^3[3]\right] - \frac{1}{u}\left[(q_{1\nu} - \bar{u}P_\nu) T_\alpha^3[0] + T_{\alpha\nu}^3[0] + \xi_u T_{\alpha\nu}^3[2]\right. \\ &\quad \left.\left. + \left[\frac{1}{2}\left(1+\xi_u^2\right) P_\nu + \xi_u q_{1\nu}\right] T_\alpha^3[2]\right]\right\}\,, \end{aligned} \tag{826}$$

that ultimately induce $(p_2^2, p_{31}^2, p_{32}^2 = 0,\ p_1^2 = q_1^2,\ p_3^2 = uq_1^2,\ p_{21}^2 = \bar{u}q_1^2)$

$$\begin{aligned} &\varepsilon^{\alpha\beta}{}_{\rho\tau} q_1^\rho q_2^\tau I_{\mu\nu;\alpha\beta}^{(B,\psi)}(u;q_1,q_2) \\ &\sim i\varepsilon_{\mu\nu\alpha\beta} q_1^\alpha q_2^\beta \left\{ \frac{\xi_u}{u\bar{u}}\left[uB_0\left(p_3^2; m_\psi^2, m_\psi^2\right) + \bar{u}B_0\left(p_{21}^2; m_\psi^2, m_\psi^2\right) - B_0\left(p_1^2; m_\psi^2, m_\psi^2\right)\right]\right. \\ &\quad + 2m_\psi^2 \frac{\bar{u}}{u}\left[C_0\left(p_{31}^2, p_1^2, p_3^2; m_\psi^2, m_\psi^2, m_\psi^2\right) - C_0\left(p_{31}^2, p_{23}^2, p_{21}^2; m_\psi^2, m_\psi^2, m_\psi^2\right)\right] \\ &\quad \left. + 2m_\psi^2 \frac{u}{\bar{u}}\left[C_0\left(p_2^2, p_{23}^2, p_3^2; m_\psi^2, m_\psi^2, m_\psi^2\right) - C_0\left(p_2^2, p_1^2, p_{21}^2; m_\psi^2, m_\psi^2, m_\psi^2\right)\right]\right\}\,. \end{aligned} \tag{827}$$

For consistency reasons, let us also have a look at Figure 24 a) (as well as Figure 24 b)), with reversed quark-lines, i. e., assuming $(p_2^2, p_3^2 = 0)$

$$p_1^\mu = q_1^\mu\,, \quad p_2^\mu = P^\mu\,, \quad p_3^\mu = uP^\mu\,. \tag{828}$$

The related subgraph entails

$$\begin{aligned} &I_{\mu\nu;\alpha\beta}^{(C,\psi)}(u;q_1,q_2) \\ &\quad\coloneqq \int d^D k\, \frac{\mathrm{Tr}\{(\not{k}+\not{q}_1+m_\psi)\gamma_\mu(\not{k}+m_\psi)\gamma_\alpha(\not{k}+u\not{p}+m_\psi)\gamma_\beta(\not{k}+\not{p}+m_\psi)\gamma_\nu\}}{D_0D_1D_2D_3}\,, \end{aligned} \tag{829}$$

48 The second case is completely equivalent, although its representation in terms of PV functions may be different.
49 Again, at the end of this calculation only a single tensor structure remains.

which can be rephrased as follows:

$$\begin{aligned}
&\varepsilon^{\alpha\beta}{}_{\rho\tau} q_1^\rho q_2^\tau I^{(C,\psi)}_{\mu\nu;\alpha\beta}(u; q_1, q_2) \\
&\sim \varepsilon_{\mu\nu\rho\tau} q_1^\rho q_2^\tau \Big\{ Q^2 \Big[\bar{u} T_0^3[0] - u T_0^3[2] - T_0^3[3]\Big] - 2\Big[T_0^2[1] + T_0^2[0,2]\Big]\Big\} \\
&\quad - 2\varepsilon_\nu{}^\alpha{}_{\rho\tau} P^\rho q_2^\tau \Big\{ P_\mu \Big[Q^2 \xi_u T_\alpha^4 + \xi_u T_\alpha^3[1] + T_\alpha^3[0]\Big] + Q^2 \xi_u T^4_{\alpha\mu} + q_{1\mu}\Big[T_\alpha^3[2] - T_\alpha^3[0]\Big] \\
&\quad + 2T^3_{\alpha\mu}[2]\Big\} + 2\varepsilon_\mu{}^\alpha{}_{\rho\tau} P^\rho q_2^\tau \Big\{ P_\nu \Big[Q^2 \xi_u T_\alpha^4 + \xi_u T_\alpha^3[1] + T_\alpha^3[0]\Big] + Q^2 \xi_u T^4_{\alpha\nu} \\
&\quad + q_{1\nu}\Big[T_\alpha^3[0] - T_\alpha^3[2]\Big] + 2T^3_{\alpha\nu}[0]\Big\} \,.
\end{aligned} \tag{830}$$

When applying formal relations[50] (using Equation 792 and Equation 828) such as

$$T^4_{\alpha\beta} = \frac{(2\pi\mu)^{4-D}}{i\pi^2\bar{u}} \frac{\partial}{\partial m_0^2} \left\{ \int d^D k \, \frac{k_\alpha k_\beta}{D_0(m_0^2)\, D_1 D_2} - u \int d^D k \, \frac{k_\alpha k_\beta}{D_0(m_0^2)\, D_1 D_3} \right\} \Bigg|_{m_0^2 = m_\psi^2} , \tag{831}$$

Equation 830 can be further reduced to

$$\begin{aligned}
&\varepsilon^{\alpha\beta}{}_{\rho\tau} q_1^\rho q_2^\tau I^{(C,\psi)}_{\mu\nu;\alpha\beta}(u; q_1, q_2) \\
&\sim i\varepsilon_{\mu\nu\alpha\beta} q_1^\alpha q_2^\beta \left\{ \frac{2\xi_u - 1}{u} \Big[B_0\left(p_1^2; m_\psi^2, m_\psi^2\right) - B_0\left(p_{13}^2; m_\psi^2, m_\psi^2\right)\Big] - 2 \right. \\
&\quad + 2B_0\left(p_{23}^2; m_\psi^2, m_\psi^2\right) - Q^2 \left[\left[\xi_u - \bar{u} + \frac{2m_\psi^2}{Q^2} \right] C_0\left(p_3^2, p_1^2, p_{31}^2; m_\psi^2, m_\psi^2, m_\psi^2\right) \right. \\
&\quad - C_0\left(p_2^2, p_{21}^2, p_1^2; m_\psi^2, m_\psi^2, m_\psi^2\right) + \left[\bar{u} + \frac{2m_\psi^2}{Q^2} \right] C_0\left(p_{23}^2, p_{21}^2, p_{13}^2; m_\psi^2, m_\psi^2, m_\psi^2\right) \\
&\quad \left. \left. + 2m_\psi^2 \xi_u D_0\left(p_1^2, p_{21}^2, p_{23}^2, p_3^2, p_2^2, p_{31}^2; m_\psi^2, m_\psi^2, m_\psi^2, m_\psi^2\right) \right] \right\} .
\end{aligned} \tag{832}$$

Notably, Equation 831 is the direct consequence of a simple partial fraction decomposition as entailed by (set $\alpha \in \mathbb{R} \setminus \{0\}$, while using cf. Equation 792)

$$D_m = \alpha D_n + (1-\alpha) D_0 + 2k\cdot(p_m - \alpha p_n) + (f_m - \alpha f_n) \,. \tag{833}$$

The latter unfolds its full power for a collinear setup (such as $p_m^\mu = \alpha p_n^\mu$) together with equal quark masses ($m_k = m_\psi$, $\forall k$) and $p_n^2 = 0$. Most importantly, in this context several more useful identities can be derived, e. g., ($p_3^\mu = u p_2^\mu$ and p_1^μ not collinear to p_2^μ)

$$\begin{aligned}
&C_0\left(p_1^2, p_{12}^2, p_2^2; m_\psi^2, m_\psi^2, m_\psi^2\right) \\
&\quad = u C_0\left(p_1^2, p_{31}^2, p_3^2; m_\psi^2, m_\psi^2, m_\psi^2\right) + \bar{u} C_0\left(p_{21}^2, p_{23}^2, p_{31}^2; m_\psi^2, m_\psi^2, m_\psi^2\right) \,,
\end{aligned} \tag{834}$$

as well as (without additional simplifications)

$$\begin{aligned}
&\bar{u} D_0\left(p_1^2, p_{21}^2, p_{23}^2, p_3^2, p_2^2, p_{31}^2; m_\psi^2, m_\psi^2, m_\psi^2, m_\psi^2\right) \\
&\quad = \frac{\partial}{\partial m_0^2} \Big[C_0\left(p_1^2, p_{21}^2, p_2^2; m_0^2, m_\psi^2, m_\psi^2\right) - u C_0\left(p_1^2, p_{31}^2, p_3^2; m_0^2, m_\psi^2, m_\psi^2\right) \Big] \Bigg|_{m_0^2 = m_\psi^2} ,
\end{aligned} \tag{835}$$

50 In fact, such relations are normally not shown explicitly, because roughly speaking, all derivatives of C_0 with respect to any of its mass arguments can be expressed via B_0s (e. g., [404]). However, this decomposition (along with Equation 835) is beyond the standard reduction algorithm and may, therefore, be seen as a corresponding extension.

which facilitate all calculations that involve (formal) four-point PV functions[51] considerably. This being said, let us now piece together the complete result:

$$\begin{aligned} F_{\mu\nu}^{\text{NLO}}(q_1,q_2) \sim \sum_{\psi} e_\psi^2 C_f \frac{\alpha_S}{2\pi}\frac{f_M^0}{Q^2}\varepsilon^{\alpha\beta}{}_{\rho\tau}q_1^\rho q_2^\tau \int_0^1 du\, \frac{\phi_M^g(u)}{u\bar{u}} \Big[2\Big(I_{\mu\nu;\alpha\beta}^{(A,\psi)}(u;q_1,q_2) \\ -I_{\mu\nu;\alpha\beta}^{(A,\psi)}(\bar{u};q_1,q_2)\Big) + I_{\mu\nu;\alpha\beta}^{(B,\psi)}(u;q_1,q_2) - I_{\mu\nu;\alpha\beta}^{(B,\psi)}(\bar{u};q_1,q_2)\Big] . \end{aligned} \tag{836}$$

Apparently, Equation 836 has been conflated distinctively by utilizing the identity[52]

$$\begin{aligned} &\varepsilon^{\alpha\beta}{}_{\rho\tau}q_1^\rho q_2^\tau \int_0^1 du\, \frac{\phi_M^g(u)}{u\bar{u}}\Big(I_{\mu\nu;\alpha\beta}^{(A,\psi)}(u;q_1,q_2) - I_{\mu\nu;\alpha\beta}^{(A,\psi)}(\bar{u};q_1,q_2)\Big) \\ &= \varepsilon^{\alpha\beta}{}_{\rho\tau}q_1^\rho q_2^\tau \int_0^1 du\, \frac{\phi_M^g(u)}{u\bar{u}}\Big(I_{\mu\nu;\alpha\beta}^{(C,\psi)}(u;q_1,q_2) - I_{\mu\nu;\alpha\beta}^{(C,\psi)}(\bar{u};q_1,q_2)\Big) . \end{aligned} \tag{837}$$

Nevertheless, the explicit result of Equation 836 would still be unintelligibly long and, therefore, has to be abbreviated even more. A canonical approach for this endeavor is given by the implementation of various logarithmic identities[53], such as

$$\text{Li}_2\left(\frac{2}{1+\beta_m(Q^2)}\right) + \text{Li}_2\left(\frac{2}{1-\beta_m(Q^2)}\right) = -\frac{1}{2}\log^2\left(\frac{\beta_m(Q^2)+1}{\beta_m(Q^2)-1}\right) , \tag{838}$$

that include non-negative arguments m^2, Q^2 and

$$\beta_m\left(Q^2\right) \coloneqq \sqrt{1+\tfrac{4m^2}{Q^2}} . \tag{839}$$

When incorporating symmetry properties of Equation 303, the charm quark contribution of Equation 751 can be expressed as[54] (now including all omitted prefactors)

$$\begin{aligned} T_H^{(g)}\left(x,Q^2;\mu,\alpha_S(\mu)\right)\Big|_{\text{charm}} = -C_f\frac{\alpha_S(\mu)}{2\pi}\frac{2}{3}\frac{1}{u\bar{u}^2Q^2}\Big\{u\log^2\left(\frac{\beta_{m_c}(uQ^2)+1}{\beta_{m_c}(uQ^2)-1}\right) \\ -\log^2\left(\frac{\beta_{m_c}(Q^2)+1}{\beta_{m_c}(Q^2)-1}\right) + 4\beta_{m_c}\left(Q^2\right)\log\left(\frac{\beta_{m_c}(Q^2)+1}{\beta_{m_c}(Q^2)-1}\right) \\ -2\left(u+\xi_u\right)\log\left(\frac{\beta_{m_c}(uQ^2)+1}{\beta_{m_c}(uQ^2)-1}\right)\Big\} . \end{aligned} \tag{840}$$

Analogously, the bottom quark corrections can be deduced from Equation 840 simply by replacing[55] "$m_c \to m_b$" and a subsequent multiplication with an extra factor[56] "$1/4$". However, for the whole experimentally accessible region $Q^2 \lesssim 100\ \text{GeV}^2$ only charm and light quark corrections turn out to be sizable, while already bottom admixtures are numerically negligible. Consequently, the inclusion of the former plays an important role within further phenomenological investigations.

For similar reasons, soft effects related to the real photon limit will be closely studied in the next section. This can be realized within the LCSR framework which allows a systematic incorporation of perturbative-, mass- and non-perturbative corrections.

51 Hence, Equation 835 provides a welcome tool for the calculation of required scalar four-point integrals. The latter, are more complicated than, e. g., their three-point counterparts, particularly, when considering a general setup, where (depending on their representation) they have to be written in terms of either 72 or 32 dilogarithms (cf. [388, 424]).

52 Equation 837 serves as another (numerical) cross-check for the overall result.

53 Particularly, that includes functional equations for the dilogarithm.

54 Again, when expanding Equation 840 in powers of m_c (around $m_c \to 0$) the massless result (cf. Equation 789) can be reproduced.

55 As discussed in Section 4.3, we may prefer pole masses (e. g., $m_c \approx 1.42$ GeV [43]) for the present numerical calculations.

56 Evidently, this factor compensates the different electric charge $e_c^2 \to e_b^2$.

4.2 LIGHT-CONE SUM RULE APPROACH

Based on Section 2.4, Section 4.1.2 and Section 4.1.3 we may now derive corresponding LCSRs for the $\gamma^*\gamma \to (\eta, \eta')$ TFFs. Considering the intended purpose, this following section covers all required concepts and techniques as well as a short presentation of the related new results. The latter will be depicted in two separate steps:

a) First, the specific techniques, as originally developed for $\gamma^*\gamma \to \pi^0$ transitions (cf. [1, 280, 281, 425–432]) will be adapted to the $\eta^{(\prime)}$ case.

b) Secondly, all relevant results, including the new leading twist NLO spectral densities as well as higher twist and mass corrections will be listed and calculated explicitly.

Point **b)** is particularly important for the destined phenomenological study of light-cone DAs in Section 4.3. However, before pursuing these objectives, a few general remarks concerning the LCSR method should be made.

4.2.1 *Theoretical foundations*

Since confinement plays an important role in the formation of hadrons, the resulting effects and hadronic properties can in general not be fully described by short distance quark-gluon interactions. However, for lack of an exact analytical solution for this problem, one may instead resort to adequate approximation methods, such as low energy theorems, models or QCD sum rules (see, e. g., [109, 114, 117, 433–439]).

Being among the most widely used working tools in hadron phenomenology, QCD sum rules allow a more or less[57] model independent approach to baryons and mesons which are represented in terms of interpolating quark-gluon currents[58] taken at large virtualities (see [97, 440] for a review). In their original version (commonly referred to as Shifman-Vainshtein-Zakharov sum rules [109, 114, 117]), the calculations are carried out in the framework of Wilson's OPE and pQCD, where soft effects are parametrized in terms of universal vacuum condensates (cf. Section 2.4). Combined with dispersion relations, the perturbatively calculated amplitudes can then be related to corresponding observables that are typically associated with a sum over hadronic states. Usually, this matching procedure necessitates an ansatz for the underlying hadronic spectrum and the related physical spectral density, which indirectly implies a model dependence (see Section 5.1.1 for a detailed discussion). Nevertheless, sum rules obtained in this way give access to a vast number of hadronic observables, while also providing qualitative insight into the QCD vacuum (see [97] for an extended discussion). However, due to the truncated OPE and inevitable deviations of the implemented spectral density from its physical counterpart, QCD sum rules possess an irreducible systematic error $\sim 10\% - 20\%$ (see, e. g., [440]). Besides, channels, where the conventional OPE is not applicable (see, e. g., [109, 114, 441, 442]), are also inaccessible for the standard SVZ sum rule method. However, apart from the special cases, the application of QCD sum rules shows a remarkable consistency with the experimental data (see [97, 440] and references therein).

57 As discussed below (cf. Section 5.1.1), some model dependence arises from quark-hadron duality and the Borel transformation (see Section B.3).

58 SVZ sum rules allow a qualitative description of the quantum vacuum structure [96, 440] and resulting interactions with quark-gluon operators, which crucially depend on the involved spin, as well as flavor structure (see also [94, 97, 109]). Therefore, by expressing hadrons with corresponding interpolation currents, one may understand their properties and differences on the basis of related quantum numbers.

As roughly sketched in Section 2.4 and Section 4.1.1, the rather complicated kinematics of light-cone dominated processes at large momentum transfer necessitate an elaborate theoretical description that systematically includes corresponding hard (perturbative) as well as soft (end-point) contributions. In order to meet these requirements, the LCSR approach has been proposed (see [141–143, 443–445]), representing an adaption of the standard QCD sum rule method (cf. [109, 114, 117]) to hard exclusive processes. This leads to a powerful hybrid of both theories [33, 97, 141–143, 301–303, 446–448] which essentially rests on three major pillars:

i) QCD factorization (i. e., factorization of hard exclusive processes in QCD),

ii) dispersion theory,

iii) quark-hadron duality.

Since point i) has already been dealt with in Section 4.1.1, let us now briefly discuss the remaining two items on this list[59]. Analogous to the pion case [1, 280, 281, 425–428, 430–432, 449] the correlation function given in Equation 731 encodes all dynamical (QCD) effects and, most importantly, is defined for a wide range of momentum transfers. That includes the preferred experimental set-up, as mentioned in Equation 733. Accordingly, the idea is to consider a more general TFF with two non-vanishing photon virtualities[60] $\left(\text{i. e., } q_1^2 = -Q^2 \ll 0,\ q_2^2 = -q^2\right)$ and perform an analytic continuation to the real photon limit $q^2 = 0$, by employing dispersion relations (cf. [3]). The latter may either follow from first principles in QFT or are justifiable on general grounds, by applying the Schwarz reflection principle (see Section B.4) and Cauchy's theorem to perturbation theory [98, 282, 450–456]:

- HADRONIC REPRESENTATION: Within the realm of time-like virtualities $\left(q_2^2 > 0\right)$ long distance quark-gluon interactions and, eventually, the associated particle formation (as induced by $\mathcal{J}_\mu^{\text{em}}$ – cf. Equation 20) becomes important (see, e. g., [97]). Under these circumstances, the investigated correlation function has a very complicated decomposition in terms of hadronic observables (cf. [64, 97]). In fact, this can be quantified by inserting a complete set of intermediate hadronic states (see also [97])

$$\mathbb{1} = \sum_h \int_0^\infty \mathrm{d}s \int \mathrm{d}^4 p\, \theta(p_0)\, \delta\left(p^2 - m_h^2\right) \delta\left(s - m_h^2\right) |h(p)\rangle\langle h(p)| \tag{841}$$

into Equation 731, implying (subtraction terms are omitted):

$$\begin{aligned} \mathrm{i}e^2 \varepsilon_{\mu\nu\alpha\beta}\, q_1^\alpha q_2^\beta F_{\gamma^*\gamma^*\to M}\left(Q^2, q^2\right) &= \sum_h \frac{\langle M(P)|\mathcal{J}_\mu^{\text{em}}|h(q_2)\rangle\langle h(q_2)|\mathcal{J}_\nu^{\text{em}}|0\rangle}{m_h^2 - q_2^2} \\ &= \int_0^\infty \mathrm{d}s \frac{1}{s + q^2} \rho_{\mu\nu}^{\text{had}}(q_1, q_2; s)\ . \end{aligned} \tag{842}$$

The hadronic dispersion relation of Equation 842 includes a formal spectral density (cf. Equation 1352 and the discussion below)

$$\begin{aligned} \rho_{\mu\nu}^{\text{had}}(q_1, q_2; s) &:= \sum_h \delta\left(s - m_h^2\right) \langle M(P)|\mathcal{J}_\mu^{\text{em}}|h(q_2)\rangle\langle h(q_2)|\mathcal{J}_\nu^{\text{em}}|0\rangle \\ &= \mathrm{i}e^2 \varepsilon_{\mu\nu\alpha\beta}\, q_1^\alpha q_2^\beta \frac{1}{\pi} \mathrm{Im}_s F_{\gamma^*\gamma^*\to M}\left(Q^2, -s\right)\ . \end{aligned} \tag{843}$$

59 Focusing on the relevant aspects for the $\gamma^*\gamma \to (\eta, \eta')$ TFFs.

60 Considering this behavior, some authors refer to the correlation function as an object of dual nature (e. g., [97]).

Apparently, its analytical properties are in one-to-one correspondence with the associated QCD particle spectrum (cf. [64, 97, 109, 450]). The relevant singularities, branch points and related branch cuts [97, 282, 450, 455, 456] on the first Riemann sheet are shown in Figure 30 (see, e. g., [97, 451, 457] for further explanations). Nevertheless, already the ground-state vector meson $\left(\varepsilon_\nu^{(\rho)}\right.$ being an adequate rho-meson polarization vector, with $\left.\varepsilon^{(\rho)}\cdot q_2 = 0\right)$

$$\langle \rho^0(q_2)|\mathcal{J}_\nu^{\mathrm{em}}|0\rangle = \frac{f_\rho}{\sqrt{2}} m_\rho \varepsilon_\nu^{(\rho)*}\,, \tag{844}$$

$$\langle M(P)|\mathcal{J}_\mu^{\mathrm{em}}|\rho^0(q_2)\rangle = -i\frac{1}{m_\rho}\varepsilon_{\mu\lambda\alpha\beta}\varepsilon^{(\rho)\lambda}P^\alpha q_2^\beta F_{\gamma^*\rho\to M}\left(Q^2\right)\,, \tag{845}$$

not only entails two additional non-perturbative input parameters ($f_\rho \approx 200$ MeV, $m_\rho \approx 775$ MeV), but also yields two distinct TFFs ($M = \eta, \eta'$) "$F_{\gamma^*\rho\to M}(Q^2)$" for the related $\gamma^*\rho^0 \to M$ transitions. Similar structures could be assigned to other resonances within this channel, e. g., for the almost equally light ($m_\omega \approx m_\rho$) ω meson, resulting in a plethora of required, yet most likely unknown hadronic parameters. Instead, one canonically [1, 280, 281, 426, 430] combines the ρ and ω contributions within one resonance term,[61] while collecting all remaining excited, bound and continuum states with total mass squared above an adequate hadronic threshold "s_0^h" in a dispersion integral. In reality, however, the numerical value of s_0^h is only approximately known. We may, therefore, use an effective parameter[62] "s_0" instead. On these grounds, the form factor's Källén-Lehmann representation (using the Sokhotski-Plemelj formula Equation 1352) arises:

$$F_{\gamma^*\gamma^*\to M}\left(Q^2, q^2\right) = \frac{\sqrt{2}f_\rho F_{\gamma^*\rho\to M}\left(Q^2\right)}{m_\rho^2 + q^2} + \frac{1}{\pi}\int_{s_0}^\infty ds\, \frac{\mathrm{Im}_s F_{\gamma^*\gamma^*\to M}\left(Q^2, -s\right)}{s + q^2}\,. \tag{846}$$

- QCD AND DISPERSION RELATIONS: The same FF can be derived by using the QCD factorization framework [3]. Indeed, when applying Cauchy's integral formula, along with the Schwarz reflection principle (see [458] and Section B.4) to perturbatively calculated QCD amplitudes, they will obey similar dispersion relations, such as those given by Equation 846 ($q^2, Q^2 \gg \Lambda_{\mathrm{QCD}}^2$, Q^2 fixed; see Figure 30):

$$\begin{aligned} F_{\gamma^*\gamma^*\to M}^{\mathrm{QCD}}\left(Q^2, q^2\right) &= \frac{1}{2\pi i}\oint_{C_1} dz\, \frac{F_{\gamma^*\gamma^*\to M}^{\mathrm{QCD}}(Q^2, -z)}{z + q^2} \\ &= \int_0^R ds\, \frac{\frac{1}{\pi}\mathrm{Im}_s F_{\gamma^*\gamma^*\to M}^{\mathrm{QCD}}(Q^2, -s)}{s + q^2} + \oint_{|z|=R} dz\, \frac{F_{\gamma^*\gamma^*\to M}^{\mathrm{QCD}}(Q^2, z)}{2\pi i\left(z - q^2\right)}\,. \end{aligned} \tag{847}$$

Depending on the form factor's UV behavior (see, e. g., [97, 373, 454]) Equation 847 may require a modification to ensure that the limit at $R \to \infty$ exits. This is due to possible

61 Here, one assumes $m_\omega \approx m_\rho$ and uses the zero-width approximation.

62 Both parameters s_0^h and s_0 are correlated with the onset of excited states in the underlying photon channel (see, e. g., [97]). Yet, they do not necessarily coincide with each other.

divergences which can be removed by appropriate subtraction terms (marked in blue), such as[63] ($n \in \mathbb{N}$ sufficiently large)

$$\begin{aligned}\widetilde{F}^{\text{QCD}}_{\gamma^*\gamma^*\to M}\left(Q^2,q^2\right) &= F^{\text{QCD}}_{\gamma^*\gamma^*\to M}\left(Q^2,q^2\right) - \sum_{k=0}^{n-1}\frac{x^k}{k!}\frac{d^k}{dx^k}F^{\text{QCD}}_{\gamma^*\gamma^*\to M}\left(Q^2,x\right)\Big|_{x=0} \\ &= \frac{[q^2]^n}{2\pi i}\oint\limits_{C_1} dz\,\frac{F^{\text{QCD}}_{\gamma^*\gamma^*\to M}(Q^2,z)}{z^n\left(z-q^2\right)}\,. \end{aligned} \tag{848}$$

However, at asymptotically large momentum transfer (i. e., $Q^2, q^2 \to \infty$) the QCD result for $F^{\text{QCD}}_{\gamma^*\gamma^*\to M}$ vanishes sufficiently fast, implying an unsubtracted dispersion relation [3, 280]:

$$F^{\text{QCD}}_{\gamma^*\gamma^*\to M}\left(Q^2,q^2\right) = \int_0^\infty ds\,\frac{\frac{1}{\pi}\,\text{Im}_s F^{\text{QCD}}_{\gamma^*\gamma^*\to M}(Q^2,-s)}{s+q^2}\,. \tag{849}$$

While dispersion theory constitutes an important pillar of this ansatz, one more element is needed to eventually bridge the apparent gap between a description in terms of hadronic (see Equation 846) and partonic (cf. Equation 849) parameters. In other words, the contributions to Equation 731 (with $Q^2 \gg \Lambda^2_{\text{QCD}}$ fixed) for space- and time-like photon virtualities q^2 must be related in a reasonable way[64]. Based on the original sum rule method [109, 114, 117], this can be done by analytically continuing each term of a given truncated theoretical spectral density from positive to negative q^2 values. After reassembling these contributions, they constitute an approximation for the actual hadronic spectral density (see, e. g., [95, 172, 459, 460]). Thus, for lack of exact equality, "$\text{Im}_s F^{\text{QCD}}_{\gamma^*\gamma^*\to M}$" is said to be[65] "dual" [459, 460] to its physical counterpart "$\text{Im}_s F_{\gamma^*\gamma^*\to M}$". Conventionally, duality is either implemented via some kind of local or non-local procedure [3, 97, 459, 460].

- LOCAL QUARK-HADRON DUALITY: This usually refers to a point-by-point comparison of the theoretical and experimental spectral density, for instance at $s \to \infty$ [97]. In general, however, the pQCD predictions are very different from their hadronic counterparts. While the former are smooth functions[66], e. g., $\left(C^q := \sqrt{2}\left(e_u^2 + e_d^2\right),\, C^s := 2e_s^2\right)$

$$\begin{aligned}\frac{1}{\pi}\,\text{Im}_s F^{\text{QCD}}_{\gamma^*\gamma^*\to M}\left(Q^2,-s\right) &= \sum_{R=q,s} C^R f^R_M \int_0^1 dx\,\frac{\phi^R_M(x)}{x}\,\delta\left(\tfrac{\bar{x}}{x}Q^2 - s\right) + \dots \\ &= \sum_{R=q,s} C^R f^R_M\,\frac{1}{s+Q^2}\,\phi^R_M\left(\tfrac{Q^2}{s+Q^2}\right) + \dots\,, \end{aligned} \tag{850}$$

which do not necessarily vanish at small $s \to 0$, the latter (i. e., $\text{Im}_s F_{\gamma^*\gamma^*\to M}$) contain generalized functions, such as[67] "$\delta\left(s - m_\rho^2\right)$" [3]. Thus, one might prefer the use of weaker assumption; in some cases, those can even be attributed to dispersion integrals.

63 The modified integrand of Equation 848 is sufficiently suppressed at $z \to \infty$ to give a finite result.

64 Any practical calculation within this formalism is considered to be an approximation (cf. Section 4.1.1). Consequently, a mere analytical continuation of one result, as obtained within its specific domain to the complementary region can most likely not reproduce the related exact counterpart. Hence, when taking the current approach, the associated ignorance has to be parametrized in a reasonable manner (see [95, 172, 459, 460] and references therein).

65 In other words, the integral of the QCD spectral density over a certain region of energies coincides with the physical spectral density over the same region [3]. Hence, in this sense the QCD description of correlation functions in terms of quarks and gluons is dual to the description using hadronic states [3].

66 The ellipses in Equation 850 represent omitted higher order and higher twist contributions.

67 This contribution is written in the limit of a vanishing width.

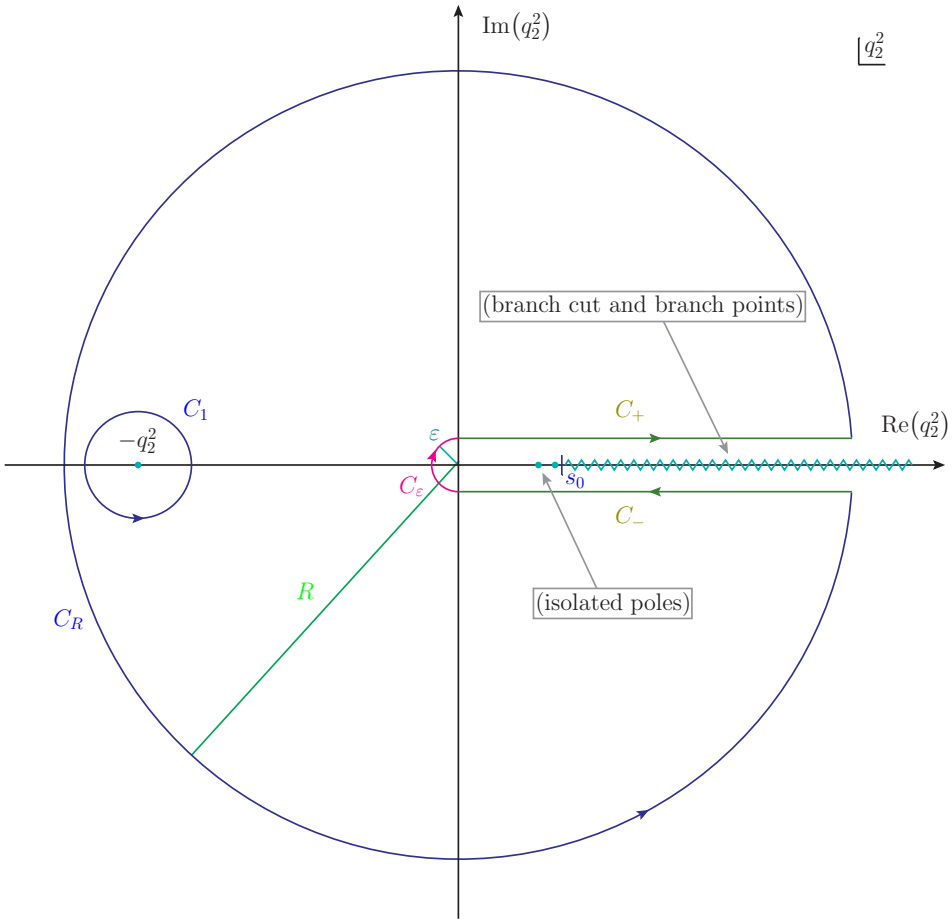

Figure 30: The (qualitative) analytic structure of $F^{\mathrm{QCD}}_{\gamma^*\gamma^*\to M}(Q^2,-q_2^2)$ $(Q^2 \gg \Lambda^2_{\mathrm{QCD}}$, fixed), as depicted in the complex q_2^2-plane, exhibits isolated poles, branch points and associated branch cuts. While the former may be induced by one-particle or bound states, the latter are, e. g., related to multiparticle contributions (see [64, 97, 450]). Besides, the integration contour of Equation 847 is shown. After deforming C_1 and taking the limits $\varepsilon \to 0$ and $R \to \infty$ all contributions related to C_ε and C_R vanish (cf. [373]).

- GLOBAL QUARK-HADRON DUALITY: Accordingly, this concept compares the spectral densities $F^{\mathrm{QCD}}_{\gamma^*\gamma^*\to M}$ and $F_{\gamma^*\gamma^*\to M}$ multiplied with a suitable weight function[68] $w(s)$ and averaged over an *ad hoc* interval $(a,b) \subset \mathbb{R}$:

$$\int_a^b \mathrm{d}s\, w(s)\, \mathrm{Im}_s F^{\mathrm{QCD}}_{\gamma^*\gamma^*\to M}\Big(Q^2,-s\Big) \approx \int_a^b \mathrm{d}s\, w(s)\, \mathrm{Im}_s F_{\gamma^*\gamma^*\to M}\Big(Q^2,-s\Big). \tag{851}$$

  For instance, when assuming that both spectral densities coincide if their arguments are above an effective threshold $s > s_0$, the comparison of Equation 846 with Equation 849 at $|q^2| \to \infty$ yields [3]

$$\sqrt{2} f_\rho F_{\gamma^*\rho\to M}\Big(Q^2\Big) = \int_0^{s_0} \mathrm{d}s\, \frac{1}{\pi}\, \mathrm{Im}_s F^{\mathrm{QCD}}_{\gamma^*\gamma^*\to M}\Big(Q^2,-s\Big)\,. \tag{852}$$

68 Instead of this weight function one may also use a (smooth) test function [3]. The latter is less restricted and may depend on additional (external) parameters.

That explains, why s_0 is usually referred to as interval of duality [3, 445, 461].

In practical applications one usually combines this approximation with a trick borrowed from SVZ sum rules [109, 114, 117], i. e., the Borel transformation (see Section B.3). If applicable[69], this mathematical method reduces the sensitivity to the duality assumption and additionally suppresses contributions arising from higher order terms in the OPE [3]. In fact, by going over to the Borel representation [3] of each involved integrand, its corresponding weight factor may change, e. g., $1/(s+q^2) \to \exp(-s/M^2)$. Hence, together with an adequate choice of the Borel parameter M^2 this approach entails the desired properties[70] (see Section B.3). As an illustration, we may equate the Borel transform of Equation 846 and Equation 849 with each other which implies a LCSR for the $\gamma^*\rho^0 \to (\eta, \eta')$ FFs [3]:

$$\sqrt{2} f_\rho F_{\gamma^*\rho\to M}\left(Q^2\right) = \frac{1}{\pi}\int_0^{s_0} ds\, e^{-\frac{s-m_\rho^2}{M^2}}\, \mathrm{Im}_s F^{\mathrm{QCD}}_{\gamma^*\gamma^*\to M}\left(Q^2, -s\right) . \tag{853}$$

In contrast to Equation 852, the spectral density of Equation 853 is at this point exponentially weighted. By varying the now present Borel parameter within a certain window, e. g., for different (each time fixed) high photon virtualities Q^2 (cf. [3, 280]), one may test the form factor's sensitivity to a chosen spectral density[71] (see Chapter 5). Ideally, the FF displays a negligible dependence on M^2 when restricted to this[72] "working window" [3].

With these refinements, we may now substitute Equation 853 in Equation 846, while using the duality assumption[73] [3]. Since there are no massless states within the related vector channel, the real photon limit can be recovered by simply substituting $q^2 \to 0$ [3]. That results in the desired LCSR [3] $(M = \eta, \eta')$

$$\begin{aligned} F^{\mathrm{LCSR}}_{\gamma^*\gamma\to M}\left(Q^2\right) = {} & \frac{1}{\pi}\int_0^{s_0} \frac{ds}{m_\rho^2}\, e^{\frac{m_\rho^2 - s}{M^2}}\, \mathrm{Im}_s F^{\mathrm{QCD}}_{\gamma^*\gamma^*\to M}\left(Q^2, -s\right) \\ & + \frac{1}{\pi}\int_{s_0}^{\infty} \frac{ds}{s}\, \mathrm{Im}_s F^{\mathrm{QCD}}_{\gamma^*\gamma^*\to M}\left(Q^2, -s\right) \end{aligned} \tag{854}$$

for the $\gamma^*\gamma \to (\eta, \eta')$ TFFs. Most importantly, compared to a "pure" pQCD calculation this expression contains two additional non-perturbative parameters, i.e., the vector meson mass m_ρ along with s_0. This feature is linked to the general phenomenological scope of LCSRs and will be discussed below. Both of the subsequent subsections are, therefore, complementary and will lay the theoretical foundation for a numerical evaluation later on (see Section 4.3). Let us now briefly discuss the general limitations of the QCD sum rule method as well as the form factor's soft contributions at very high energies.

69 The named properties depend on an adequate choice the Borel parameter and the associated "window of stability" (cf. Section B.3). The latter does not exist for all physical problems (see [94, 97]). Fortunately, the analyzed cases do not belong to this specific category.

70 As discussed above, when applying the Borel transformation to Equation 846 and Equation 849, the original dispersion integral gets replaced by an exponentially weighted one. However, reiterating this procedure results in Bessel or hypergeometric functions instead of the desired positive definite exponential factor [109]. Furthermore, a similar exponential fall-off of the continuum part, along with (heavy) resonances can be seen in lattice QCD [43, 462]. This specific exponential suppression, however, is a consequence of the Euclidean time (cf. [97, 450, 463]).

71 In this sense, the inserted (and analytically continued) QCD spectral density serves as a model for its physical counterpart. Conventionally, one tests the resulting sum rule's sensitivity, by plotting it as a function of M^2 (cf. [280, 464, 465]). Flat curves indicate a good accuracy of the underlying QCD sum rule [464].

72 This interval is also referred to as "Borel window" [97] or "window of stability"[111].

73 Here, we employ Equation 851 for $a \to s_0$ and $b \to \infty$.

4.2.2 *Soft corrections vs. the large Q^2 limit*

In the previous subsection, we have derived the LCSRs for the $\gamma^*\gamma\to\eta$ and $\gamma^*\gamma\to\eta'$ TFFs, which will be analyzed at different realms of momentum transfer. This includes the case of asymptotically large photon virtualities which is dominated by LO and related leading twist effects. Especially, the numerical impact of related soft corrections is important for Section 4.3 where the η and η' TFFs are studied at $|Q^2|=112\ \text{GeV}^2$.

To this end, associated end-point contributions for $Q^2\gg\Lambda^2_{\text{QCD}}$ have to be quantified. Within the LCSR approach, those corrections correspond to deviations from a "pure" QCD calculation. In other words, when taking into account Equation 849, we may rewrite the same result as [3]

$$F^{\text{LCSR}}_{\gamma^*\gamma\to M}\left(Q^2\right)=F^{\text{QCD}}_{\gamma^*\gamma^*\to M}\left(Q^2\right)+\frac{1}{\pi}\int_0^{s_0}\frac{ds}{m_\rho^2}\left[e^{\frac{m_\rho^2-s}{M^2}}-\frac{m_\rho^2}{s}\right]\text{Im}_s F^{\text{QCD}}_{\gamma^*\gamma^*\to M}\left(Q^2,-s\right), \tag{855}$$

separating both components, i. e., "pure" pQCD and LCSR admixtures from each other. To get an impression of how this modification affects the QCD results, we may, therefore, insert the mentioned LO and leading twist expressions for $\text{Im}_s F^{\text{QCD}}_{\gamma^*\gamma^*\to M}$ into Equation 855. Apparently, the involved dispersion integral should also be modified to enable a clear-cut physical interpretation. Most conveniently, this is done by substituting the integration variable s with the associated spectator quark's momentum fraction $x=Q^2/(s+Q^2)$ (and analogously $x_0=Q^2/(s_0+Q^2)$):

$$Q^2F^{\text{LCSR}}_{\gamma^*\gamma\to M}\left(Q^2\right)=\sum_{A=0,8}C^A f_M^A\left[\int_0^1\frac{dx}{\bar{x}}\,\phi_M^A(x)+\int_{x_0}^1\frac{dx}{\bar{x}}\left(\frac{\bar{x}Q^2}{xm_\rho^2}e^{\frac{xm_\rho^2-\bar{x}Q^2}{xM^2}}-1\right)\phi_M^A(x)\right]. \tag{856}$$

Referring to [20], $C^0=\frac{2}{\sqrt{3}}\left(e_u^2+e_d^2+e_s^2\right)$ and $C^8=\sqrt{\frac{2}{3}}\left(e_u^2+e_d^2-2e_s^2\right)$ are flavor factors[74], as caused by the quark content of the related SO DAs. Consequently, the first contribution of Equation 856 is the unmodified LO pQCD result for $F_{\gamma^*\gamma\to M}$, while the second part represents an end-point correction from the region $x>x_0=1-s_0/Q^2+\mathcal{O}(s_0^2/Q^4)$, as implied by the LCSR framework. For a rough estimate of the soft corrections, we may expand Equation 856 near[75] $1-x_0\approx 0$ (i. e., at $Q^2\gg\Lambda^2_{\text{QCD}}$):

$$Q^2F^{\text{LCSR}}_{\gamma^*\gamma\to M}\left(Q^2\right)\approx\sum_{A=0,8}C^A f_M^A\left[\int_0^1\frac{dx}{\bar{x}}\,\phi_M^A(x)+\bar{x}_0\left(\frac{s_0}{2m_\rho^2}e^{\frac{m_\rho^2-s_0}{M^2}}-1\right)\frac{d}{dx}\phi_M^A(x)\Big|_{x=0}\right]. \tag{857}$$

This can be further simplified, by using the identities[76]

$$\int_0^1\frac{dx}{\bar{x}}\,\phi_M^A(x)=3\left[1+\sum_{n=1}^{\infty}c^A_{2n,M}\right], \tag{858}$$

$$\frac{d}{dx}\phi_M^A(x)\Big|_{x=0}=6\left[1+\sum_{n=1}^{\infty}(2n+1)\,(n+1)\,c^A_{2n,M}\right]. \tag{859}$$

For the intended phenomenological study of soft contributions to $\gamma^*\gamma\to(\eta,\eta')$ TFFs at very large momentum transfers $|Q^2|\sim 112\ \text{GeV}^2$ Equation 857 is of particular importance (see Section 4.3).

74 Analogous to Equation 267 we have adapted the definitions to ensure $\begin{pmatrix}C^8\\C^0\end{pmatrix}=\begin{pmatrix}\sqrt{\frac{1}{3}}&-\sqrt{\frac{2}{3}}\\\sqrt{\frac{2}{3}}&\sqrt{\frac{1}{3}}\end{pmatrix}\begin{pmatrix}C^q\\C^s\end{pmatrix}$ (cf. definitions of Equation 850).

75 According to their conformal expansions, we may assume, that all involved twist-two DAs vanish linearly at the end points (see [3]).

76 For the derivation of Equation 858 and Equation 859 reference [466] can be used.

4.2.3 *Predictive power of QCD sum rules*

Let us discuss some selected aspects of QCD sum rules which are relevant for an intended error analysis in the subsequent phenomenological chapters.

For assessing the general predictive power of QCD sum rules, their actual theoretical uncertainties have to be estimated. Those originate from the following sources (cf. [97, 464, 465] and references therein):

a) Being an approximation method, QCD sum rules entail a numerical dependence on the Borel parameter as well as s_0. Hence, large instabilities due to M^2 would indicate the absence of important higher order corrections or even may cast doubt over the duality assumption and its reliability.

b) An inaccurate knowledge of the (universal) DAs and condensates.

c) The use of a truncated[77] OPE, including a finite order perturbative calculation.

Fortunately, errors linked to point c) can be decreased by further theoretical endeavor, while continuing phenomenological and experimental progress may push back the ignorance concerning item b) (see [97, 464, 465] for a further discussion). In other words, this conveys two important messages (see, e. g., [97]):

i) The accuracy of QCD sum rules can be systematically improved, but not beyond certain limits.

ii) Within these inherent limitations of the sum rule method, one is able to estimate theoretical uncertainties of the predicted hadronic parameters based on QCD. Similar conclusions cannot be drawn out of, e. g., quark models which may use a non-universal input that is not directly related to QCD.

After this justification, we may now focus on the calculation of required imaginary parts.

4.2.4 *Twist-two spectral densities*

Based on the previous chapters, we can now calculate all required twist-two spectral densities. It is convenient to write the necessary imaginary parts[78]

$$\frac{1}{\pi}\,\mathrm{Im}_s F^{\mathrm{QCD}}_{\gamma^*\gamma^*\to M}\Big(Q^2,-s\Big)=\sum_{A=0,8,g}\frac{1}{\pi}\,\mathrm{Im}_s F^{\mathrm{QCD};\,A}_{\gamma^*\gamma^*\to M}\Big(Q^2,-s\Big) \tag{860}$$

in terms of conformal coefficients, as induced by the DA's Gegenbauer expansion. For $A=0,8$ we have (the case $A=g$ is discussed below):[79]

$$\frac{1}{\pi}\,\mathrm{Im}_s F^{\mathrm{QCD};\,A}_{\gamma^*\gamma^*\to M}\Big(Q^2,-s\Big)=\frac{1}{2}C^A f_M^A\sum_{n=0}^{\infty}c^A_{n,M}\left(\mu^2\right)\left[\sum_{k=0}^{\infty}\left(\frac{C_f\alpha_S}{2\pi}\right)^k\rho_n^{(k)}\left(Q^2,s;\mu^2\right)\right], \tag{861}$$

including $C^0=\frac{4}{3\sqrt{3}}$ and $C^8=\frac{2}{3\sqrt{6}}$ (see [3]). Here, we encounter two types of contributions. First of all, there are the (NLO) twist-two quark components which can be obtained from related

77 The truncated tail of this series is usually not ignored, but instead incorporated into soft corrections, such as those given by the related condensates (see discussion in [111]).

78 This strategy is restricted to the leading twist accuracy.

79 By introducing, e. g., additional superscripts also the gluon case can be absorbed in Equation 861. However, we prefer to tackle this problem separately.

expressions, as presented in our previous work [281]. Notably, the flavor-octet contribution and its corresponding singlet counterpart rely on identical LO $\left(x = Q^2/(s+Q^2)\right)$

$$\rho_n^{(0)}\left(Q^2,s\right) = 2\frac{x}{Q^2}\varphi_n(x)\,, \quad \varphi_n(x) \coloneqq 6x\bar{x}\,C_n^{(3/2)}(\xi_x)\,, \tag{862}$$

as well as NLO spectral densities (cf. Section B.5):

$$\begin{aligned}\rho_n^{(1)}\left(Q^2,s;\mu^2\right) = \frac{x}{Q^2}\Bigg\{\varphi_n(x)\Bigg[-3\left[1+2\left(\psi(2)-\psi(2+n)\right)\right]+\frac{\pi^2}{3}-\frac{\gamma_n^{(0)}}{C_f}\log\left(\frac{\bar{x}Q^2}{x\mu^2}\right)\\ -\log^2\left(\tfrac{\bar{x}}{x}\right)\Bigg]-2\left[\int_x^1 du\,\frac{\varphi_n(u)-\varphi_n(x)}{u-x}\log\left(1-\tfrac{x}{u}\right)+(x\leftrightarrow\bar{x})\right]\\ +\frac{\gamma_n^{(0)}}{C_f}\int_0^{\bar{x}}du\,\frac{\varphi_n(u)-\varphi_n(\bar{x})}{u-\bar{x}}\Bigg\}\,.\end{aligned} \tag{863}$$

Hence, all differences, besides the apparent flavor factors are encoded in the decay constants and associated expansion coefficients $c_{n,M}^{A}$. Conversely, the second type of contributions, i. e., NLO twist-two gluon LCSR corrections are completely new and might, therefore, need some more explanation. With the results of Section 4.1 at hand, the corresponding imaginary parts can be straightforwardly calculated (see Section B.4 and Equation 856). After the analytic continuation $q^2 \to -s$ and some simplifications, we get (see Equation 788)

$$\begin{aligned}\frac{1}{\pi}\operatorname{Im}_s T_H^{(g)}\left(u,Q^2,-s;\mu^2\right)\Big|_{\text{light}} = -\frac{2x}{Q^2}\Bigg\{\frac{1}{u^2\bar{u}^2}\Theta(u-x)\Big[\left(x\bar{u}^2+\bar{x}u^2\right)\log\left(1-\tfrac{\bar{u}}{\bar{x}}\right)+u\bar{u}\Big]\\ +\left[\Theta(u-x)\frac{x}{u^2}-\Theta(x-u)\frac{\bar{x}}{\bar{u}^2}\right]\left[\log\left(\frac{\bar{x}Q^2}{x\mu^2}\right)-2\right]\Bigg\}\,.\end{aligned} \tag{864}$$

This rather compact expression is a natural consequence of the gluon distribution amplitude's transformation properties (cf. Equation 306). Analogously, the involved convolution integral projects Equation 864 on each related Gegenbauer polynomial (see Section A.12)

$$\rho_n^{(g)}\left(Q^2,s;\mu^2\right) \coloneqq \frac{1}{\pi}\int_0^1 du\,\omega_n(u)\operatorname{Im}_s T_H^{(g)}\left(u,Q^2,-s;\mu^2\right)\Big|_{\text{light}}\,, \tag{865}$$

that is given by the underlying conformal expansion of (cf. Equation 424, Equation 862)

$$\phi_M^g(x,\mu) = \sum_{n=1}^{\infty} c_{2n,M}^g(\mu)\,\omega_{2n}(x)\,, \quad \omega_n(x) \coloneqq 30x^2\bar{x}^2C_{n-1}^{(5/2)}(\xi_x)\,. \tag{866}$$

The intended numerical implementation, however, depends on an adequate reformulation of these gluon spectral densities, i. e., similar to the quark-antiquark case (cf. Section B.5), Equation 865 should be expanded into orthogonal polynomials and logarithms. In this way no auxiliary integrals[80], except those of Equation 854, will remain.[81] Accordingly, it is reasonable to divide Equation 864 into two parts:

$$\frac{1}{\pi}\operatorname{Im}_s T_H^{(g)}\left(u,Q^2,-s;\mu^2\right)\Big|_{\text{light}} = \sum_{a=1}^{2} K_a\left(Q^2,x,u;\mu^2\right)\,, \tag{867}$$

80 Moreover, the integrals of Equation 854, corresponding to hard parts are taken analytically (see also [281]). Only the remaining soft corrections have to be solved in a different way, e. g., via numerical integration.

81 In fact, this is of fundamental importance for the intended computer-assisted LCSR analysis, leading to a faster running (Wolfram *Mathematica*® 8) code. That is certainly true for the quark-antiquark case (cf. Section B.5) which serves us as a prototype.

which are defined by the integral kernels (cf. Equation 1422 in Section C.3)

$$Q^2 K_1\Big(Q^2,x,u;\mu^2\Big) \coloneqq -\frac{x}{C_f}\left[\log\Big(\tfrac{\bar{x}Q^2}{x\mu^2}\Big)-2\right] {}^{qg}V_D^{(1)}(x,u)\,, \tag{868}$$

$$Q^2 K_2\Big(Q^2,x,u;\mu^2\Big) \coloneqq -2x\,\Theta(u-x)\left[\frac{1}{u\bar{u}}+\frac{x\bar{u}^2+\bar{x}u^2}{u^2\bar{u}^2}\log\big(1-\tfrac{\bar{u}}{\bar{x}}\big)\right]. \tag{869}$$

In fact, this approach is justified by Equation 865, because those contributions have a very different structure, when considering their convolution with $\omega_n(x)$. Thus, the form of

$$\int_0^1 du\,\omega_n(u)\,Q^2K_1\Big(Q^2,x,u;\mu^2\Big) = -\frac{5x}{C_f}\varphi_n(x)\left[\log\Big(\tfrac{\bar{x}Q^2}{x\mu^2}\Big)-2\right] {}^{gq}\gamma_n^{(0)}\,, \tag{870}$$

is determined by the embedded LO evolution kernel "${}^{qg}V_D^{(1)}$" (see Equation 1422), whereas

$$R_n^{(\mathrm{aux})}(x) \coloneqq \int_0^1 du\,\omega_n(u)\,Q^2K_2\Big(Q^2,x,u;\mu^2\Big) = x\bar{x}\sum_{k=0}^{n+1}\tilde{a}_k x^k \quad (n=2m,\ m\in\mathbb{N}) \tag{871}$$

is simply a real-valued $\big(\tilde{a}_k\in\mathbb{R}\big)$ polynomial. However, similar to the quark-antiquark case, Equation 871 may also be expanded into a series of related Gegenbauer polynomials[82], e. g., via

$$R_n^{(\pm)}(x) \coloneqq \frac{1}{2}\Big(R_n^{(\mathrm{aux})}(x)\pm R_n^{(\mathrm{aux})}(\bar{x})\Big) \tag{872}$$

and the coefficients $\Big(\mathcal{N}_k\coloneqq\frac{2(2k+3)}{3(k+1)(k+2)}$; see also Section B.5 as well as Table 11$\Big)$

$$\widetilde{G}_n^k \coloneqq \mathcal{N}_k\int_0^1 dx\,C_k^{(3/2)}(\xi_x)\,R_n^{(+)}(x)\,,\quad \widetilde{H}_n^k \coloneqq \mathcal{N}_{k+1}\int_0^1 dx\,C_{k+1}^{(3/2)}(\xi_x)\,R_n^{(-)}(x)\,. \tag{873}$$

Consequently, the gluonic spectral density (cf. Equation 865) can be written as

$$\rho_n^{(g)}\Big(Q^2,s;\mu^2\Big) = \frac{1}{Q^2}\left[\sum_{k=0}^{n/2}\Big[\widetilde{H}_n^{2k}\varphi_{2k+1}(x)+\widetilde{G}_n^{2k}\varphi_{2k}(x)\Big]-{}^{gq}\gamma_n^{(0)}\frac{5x}{C_f}\left[\log\Big(\tfrac{\bar{x}Q^2}{x\mu^2}\Big)-2\right]\varphi_n(x)\right]. \tag{874}$$

In particular, we obtain for $n=2$ and $n=4$ the following explicit expressions (cf. Table 11)

$$\rho_2^{(g)}\Big(Q^2,s;\mu^2\Big) = \frac{5x}{Q^2}\left[\frac{5}{6}\bar{x}^2\Big(65x^2-30x+1\Big)-{}^{gq}\gamma_n^{(0)}\left[\log\Big(\tfrac{\bar{x}Q^2}{x\mu^2}\Big)-2\right]\varphi_2(x)\right], \tag{875}$$

$$\begin{aligned}\rho_4^{(g)}\Big(Q^2,s;\mu^2\Big) = \frac{5x}{Q^2}\Bigg[&\frac{14}{15}\bar{x}^2\Big(1827x^4-2457x^3+959x^2-105x+1\Big)\\ &-{}^{gq}\gamma_n^{(0)}\left[\log\Big(\tfrac{\bar{x}Q^2}{x\mu^2}\Big)-2\right]\varphi_4(x)\Bigg].\end{aligned} \tag{876}$$

After collecting all these partial results, we may formulate the final expression for NLO twist-two gluonic spectral densities, as they enter the LCSR calculation (cf. Equation 865):

$$\frac{1}{\pi}\,\mathrm{Im}_s F^{\mathrm{QCD};\,g}_{\gamma^*\gamma^*\to M}\Big(Q^2,-s\Big) = \frac{1}{2}C^0 f_M^0\sum_{n=1}^{\infty}c_{2n,M}^g\Big(\mu^2\Big)\frac{C_f\alpha_S}{2\pi}\rho_{2n}^{(g)}\Big(Q^2,s;\mu^2\Big)\,. \tag{877}$$

This represents the imaginary parts, as entailed by the (light-quark) box diagrams. As mentioned in [3], the charm quark corrections do not need to be written in this form, as they are not affected by the LCSR subtractions. Therefore, that concludes the necessary discussion of twist-two (NLO) spectral densities.

82 Due to the structure of Equation 871 an expansion in terms of $\varphi_n(x)$ seems canonical.

$\widetilde{G}_n^k$	$k=0$	$k=2$	$k=4$	$k=6$	$k=8$	$k=10$
$n=2$	$\frac{25}{36}$	$-\frac{25}{432}$	0	0	0	0
$n=4$	$\frac{7}{36}$	$\frac{49}{54}$	$-\frac{7}{20}$	0	0	0
$n=6$	$\frac{27}{280}$	$\frac{23}{80}$	$\frac{55}{56}$	$-\frac{1809}{3136}$	0	0
$n=8$	$\frac{11}{189}$	$\frac{88}{567}$	$\frac{3751}{11340}$	$\frac{55}{54}$	$-\frac{25751}{34020}$	0
$n=10$	$\frac{325}{8316}$	$\frac{19825}{199584}$	$\frac{845}{4536}$	$\frac{845}{2376}$	$\frac{1235}{1188}$	$-\frac{1987765}{2195424}$
$\widetilde{H}_n^k$	$k=0$	$k=2$	$k=4$	$k=6$	$k=8$	$k=10$
$n=2$	$\frac{725}{756}$	$-\frac{325}{1008}$	0	0	0	0
$n=4$	$\frac{35}{108}$	$\frac{931}{990}$	$-\frac{203}{396}$	0	0	0
$n=6$	$\frac{9}{56}$	$\frac{45}{112}$	$\frac{1707}{1960}$	$-\frac{1443}{2240}$	0	0
$n=8$	$\frac{55}{567}$	$\frac{22}{105}$	$\frac{143}{324}$	$\frac{51865}{64638}$	$-\frac{53471}{71820}$	0
$n=10$	$\frac{1625}{24948}$	$\frac{325}{2464}$	$\frac{845}{3564}$	$\frac{1105}{2376}$	$\frac{3117335}{4207896}$	$-\frac{3789565}{4590432}$

Table 11: All NLO gluonic spectral densities of Equation 874 can be calculated with matching LO anomalous dimensions ${}^{gq}\gamma_n^{(0)}$ and the related expansion coefficients $\widetilde{G}_n^k$ and $\widetilde{H}_n^k$, as defined in Equation 873. Here, the non-vanishing contributions for even $k, n \leqslant 10$ are listed.

4.2.5 *Twist-three, twist-four and meson mass corrections*

Let us extend our discussion to (meson) mass and higher twist corrections which are especially important for the intended investigation of FFs at moderate momentum transfer Q^2 (see Section 4.3). Accordingly, we have to calculate all related spectral densities, as implied by Section 4.1. The main results of this subsection have been published in [3].

All things considered (cf. [3, 281]), the bulk of higher twist effects is linked to two-particle and three-particle twist-four DAs which have been investigated in Chapter 3. Consequently, we may focus on the prepared result of Chapter 3 and Section 4.1, including the investigated mass corrections. As a brief reminder: there are two main sources for such admixtures to the TFF. First of all, the QCD EOM lead to quark-mass and anomalous contributions within the associated DAs. Hence, at LO twist-four accuracy particularly the non-perturbative components engender possible $\mathcal{O}(m_\psi)$ and $\mathcal{O}(h_M^R)$ terms (cf. Chapter 3). Additionally, one has to take care of the twist-three DAs, which appear, when assuming a non-vanishing strange quark mass. Furthermore, an extra meson mass correction $\sim m_M^2$ is introduced by a corresponding expression of the LO pQCD amplitude (see Section 4.1).

For convenience, we may restrict ourselves to the QF basis, while collecting all the above mentioned results within suitable spectral densities, such as:

$$\rho_M^{(i)}\left(Q^2, s\right) \coloneqq \frac{1}{\pi}\,\mathrm{Im}_s F_{\gamma^*\gamma^*\to M}^{\mathrm{QCD};(i)}\left(Q^2, -s\right) . \tag{878}$$

Here, we may assign to each specific contribution the superscript $i = m, 3, 4$ – denoting meson mass, twist-three or twist-four densities, respectively. Moreover, Equation 878 can be further decomposed into summands of different quark flavors:

$$\rho_M^{(i)}\left(Q^2, s\right) = 2e_s^2 \rho_M^{(i),s}\left(Q^2, s\right) + \sqrt{2}\left(e_u^2 + e_d^2\right) \rho_M^{(i),q}\left(Q^2, s\right) . \tag{879}$$

Thus, all occurring matrix elements can be written in terms of FKS parameters, particularly, when consequently applying the state mixing ansatz (cf. Section 3.1). For instance, the meson mass corrections boil down to $(R = q, s)$

$$\rho_M^{(m),R}\left(Q^2, s\right) = \sum_{n=0}^{\infty} c_{n,M}^R h_M^R \frac{x^2}{Q^4}\left(\xi_x \varphi_n(x) - x\bar{x}\frac{d}{dx}\varphi_n(x)\right) , \tag{880}$$

after consistently applying Equation 1353 (see Section B.4) and Equation 729.[83] Similarly, for the contributions of twist-three and four DAs (see Chapter 3) up to NLO accuracy (in conformal spin) we find:

$$\rho_M^{(3),R}\left(Q^2, s\right) = -\frac{x^2}{Q^4}\left(h_M^R \xi_x + 60 m_R f_{3M}^R C_3^{(1/2)}(\xi_x)\right) , \tag{881}$$

$$\begin{aligned}\rho_M^{(4),R}\left(Q^2, s\right) = -\frac{x\xi_x}{Q^4}\Bigg\{ &\frac{160}{3} f_M^R \left(\delta_M^R\right)^2 x\bar{x} + m_R f_{3M}^R [60 - 210 x\bar{x}(3 - x\bar{x})] \\ &+ h_M^R\left[1 - x\bar{x}\left(\frac{13}{6} - \frac{21}{2}x\bar{x}\right) + c_{2M}^R x\bar{x}(21 - 135 x\bar{x})\right]\Bigg\} .\end{aligned} \tag{882}$$

According to the standard approach[84] [281, 352], comparable higher-order conformal spin corrections are absent in the corresponding pion case.

4.2.6 *Rough estimate of twist-six corrections*

Let us conclude this section with an estimate for possible twist-six corrections to the meson-photon TFF. At this point, we will also take up some ideas which have originally been developed in our previous work [281, 373] and adapt them to the $\eta^{(\prime)}$ TFFs.

In the present context, arguments based on power counting (cf. Chapter 2) would suggest that contributions of higher Fock states to the OPE are strongly suppressed and may, therefore, be neglected. Nonetheless, so-called factorizable contributions [140] can still be sizable, even for large photon virtualities. The latter result from light-cone operators that can be factorized into a product of two gauge invariant lower twist operators [140]. In fact, while impossible for the twist-four case [140, 467], several twist-six light-cone operators exist, which can be written as a product of two twist-three, or alternatively one twist-two and an adequate twist-four operator. When sandwiched between vacuum and one-meson state, this either implies a low-twist two-particle DA multiplied with a quark/gluon condensate or gives rise to genuine multiparton twist-six DAs [140]. As we have shown in [281], twist-six contributions to the $\gamma^*\gamma \to \pi^0$ TFF can be calculated within this factorization approximation. An extension of these results to the $\gamma^*\gamma \to (\eta, \eta')$ transitions, however, is not immediate, as corresponding $SU(3)_F$ violation effects are yet missing.

Consequently, all related diagrams, such as those mentioned in Figure 31 would have to be

83 This approximation ensures a compatibility with the calculated twist-four contributions.
84 Here, one normally works in the strict chiral limit, including $m_\pi^2 \approx 0$ (see [281]).

recalculated, while this time one must also keep terms linear in the (strange) quark mass. Especially, for the occurring soft gluon contributions (cf. Figure 31 c), d)) this might require an adapted reevaluation of the quark propagator's light-cone expansion in a background gluon field [75]. Hence, we should first examine the basic structure of these quark-mass corrections.

Let us for example consider diagram Figure 31 a) which contributes to the OPE of Equation 731 if both photon virtualities $Q^2, q^2 \gg \Lambda^2_{\text{QCD}}$ are sufficiently large. Then, we get[85] (cf. Equation 139)

$$
\begin{aligned}
&-\sum_{\psi} e_\psi^2 g_S^2 \int d^4x \int d^4z_1 \int d^4z_2\, e^{-iq_1\cdot x} \times \\
&\times \Big[\langle M(P)|\bar\psi(z_1)\, \underbrace{\not{A}(z_1)\, \overbrace{\psi(z_1)\,\bar\psi}(x)\,\gamma_\mu\psi(x)\,\bar\psi(0)\,\gamma_\nu\overbrace{\psi(0)\,\bar\psi}(z_2)\,\not{A}(z_2)}\,\psi(z_2)\,|0\rangle \\
&+ \langle M(P)|\bar\psi(z_2)\, \underbrace{\not{A}(z_2)\, \overbrace{\psi(z_2)\,\bar\psi}(0)\,\gamma_\nu\psi(0)\,\bar\psi(x)\,\gamma_\mu\overbrace{\psi(x)\,\bar\psi}(z_1)\,\not{A}(z_1)}\,\psi(z_1)\,|0\rangle \Big] \\
=&-\sum_{\psi} e_\psi^2 g_S^2 \int d^4x \int d^4z_1 \int d^4z_2\, e^{-iq_1\cdot x} \Bigg[\frac{(z_1-x)^\beta\, z_2^\alpha}{16\pi^6\,(z_1-x)^4\, z_2^4\,(z_1-z_2)^2} \times \\
&\times \Big(\langle M(P)|\bar\psi_i^a(z_1)\big[\gamma^\rho\gamma_\beta\gamma_\mu\big]_{ij}\Big[T^A\Big]^{ab}\psi_j^b(x)\,\bar\psi_k^c(0)\big[\gamma_\nu\gamma_\alpha\gamma_\rho\big]_{kl}\Big[T^A\Big]^{cd}\psi_l^d(z_2)\,|0\rangle \\
&+ \langle M(P)|\bar\psi_i^a(z_2)\big[\gamma^\rho\gamma_\alpha\gamma_\nu\big]_{ij}\Big[T^A\Big]^{ab}\psi_j^b(0)\,\bar\psi_k^c(x)\big[\gamma_\mu\gamma_\beta\gamma_\rho\big]_{kl}\Big[T^A\Big]^{cd}\psi_l^d(z_1)\,|0\rangle\Big) \\
&+ \Big(\langle M(P)|\bar\psi_i^a(z_1)\big[\gamma^\rho\gamma_\mu\big]_{ij}\Big[T^A\Big]^{ab}\psi_j^b(x)\,\bar\psi_k^c(0)\big[\gamma_\nu\gamma_\alpha\gamma_\rho\big]_{kl}\Big[T^A\Big]^{cd}\psi_l^d(z_2)\,|0\rangle \\
&- \langle M(P)|\bar\psi_i^a(z_2)\big[\gamma^\rho\gamma_\alpha\gamma_\nu\big]_{ij}\Big[T^A\Big]^{ab}\psi_j^b(0)\,\bar\psi_k^c(x)\big[\gamma_\mu\gamma_\rho\big]_{kl}\Big[T^A\Big]^{cd}\psi_l^d(z_1)\,|0\rangle\Big) \times \\
&\times im_\psi \frac{z_2^\alpha}{32\pi^6\,(z_1-x)^2\, z_2^4\,(z_1-z_2)^2} + im_\psi \frac{(z_1-x)^\beta}{32\pi^6\,(z_1-x)^4\, z_2^2\,(z_1-z_2)^2} \times \\
&\times \Big(\langle M(P)|\bar\psi_i^a(z_2)\big[\gamma^\rho\gamma_\nu\big]_{ij}\Big[T^A\Big]^{ab}\psi_j^b(0)\,\bar\psi_k^c(x)\big[\gamma_\mu\gamma_\beta\gamma_\rho\big]_{kl}\Big[T^A\Big]^{cd}\psi_l^d(z_1)\,|0\rangle \\
&- \langle M(P)|\bar\psi_i^a(z_1)\big[\gamma^\rho\gamma_\beta\gamma_\mu\big]_{ij}\Big[T^A\Big]^{ab}\psi_j^b(x)\,\bar\psi_k^c(0)\big[\gamma_\nu\gamma_\rho\big]_{kl}\Big[T^A\Big]^{cd}\psi_l^d(z_2)\,|0\rangle\Big)\Bigg] + \ldots, \qquad (883)
\end{aligned}
$$

where the fields marked in blue have to be understood as soft external fields, which may generate quark condensates [74, 97], i. e., as given by Equation 100. Based on this assumption, all factorizable matrix elements can be approximated according to[86]

$$
\begin{aligned}
&\langle M(P)|\bar\psi_i^a(z_1)\,\big[\gamma^\rho\gamma_\beta\gamma_\mu\big]_{ij}\Big[T^A\Big]^{ab}\psi_j^b(x)\,\bar\psi_k^c(0)\,\big[\gamma_\nu\gamma_\alpha\gamma_\rho\big]_{kl}\Big[T^A\Big]^{cd}\psi_l^d(z_2)\,|0\rangle \\
&\approx \frac{C_f}{3}\langle\bar\psi\psi\rangle\varepsilon_{\mu\nu\alpha\beta}\langle M(P)|\bar\psi(z_1)\,i\gamma_5\psi(z_2)\,|0\rangle - m_\psi\langle\bar\psi\psi\rangle\frac{C_f}{24}x^\tau\big(g_{\alpha\nu}\varepsilon_{\beta\mu\tau\kappa} - g_{\alpha\tau}\varepsilon_{\beta\mu\nu\kappa} \\
&\quad - g_{\beta\mu}\varepsilon_{\alpha\nu\tau\kappa} + g_{\nu\tau}\varepsilon_{\alpha\beta\mu\kappa} + g_{\mu\kappa}\varepsilon_{\alpha\beta\nu\tau} - g_{\beta\kappa}\varepsilon_{\alpha\mu\nu\tau}\big)\langle M(P)|\bar\psi(z_1)\gamma^\kappa\gamma_5\psi(z_2)\,|0\rangle + \ldots, \qquad (884)
\end{aligned}
$$

or similarly

$$
\begin{aligned}
&\langle M(P)|\bar\psi_i^a(z_1)\,\big[\gamma^\rho\gamma_\beta\gamma_\mu\big]_{ij}\Big[T^A\Big]^{ab}\psi_j^b(x)\,\bar\psi_k^c(0)\,\big[\gamma_\nu\gamma_\rho\big]_{kl}\Big[T^A\Big]^{cd}\psi_l^d(z_2)\,|0\rangle \\
&\approx \frac{C_f}{6i}\langle\bar\psi\psi\rangle\varepsilon_{\mu\nu\beta\kappa}\Big(\langle M(P)|\bar\psi(z_1)\,\gamma^\kappa\gamma_5\psi(z_2)\,|0\rangle + \frac{m_\psi}{2}x^\kappa\langle M(P)|\bar\psi(z_1)\,i\gamma_5\psi(z_2)\,|0\rangle\Big) + \ldots. \qquad (885)
\end{aligned}
$$

85 The ellipses represent higher order quark-mass correction.

86 Here, we may focus on the strange quark case. Nevertheless, the light-quark contributions have a similar formal structure.

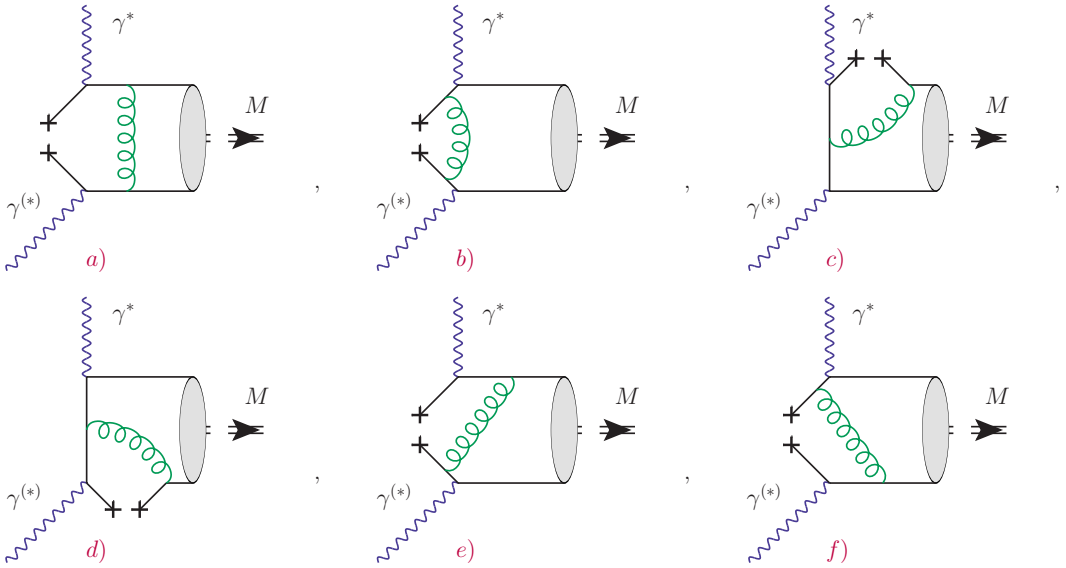

Figure 31: Selected examples (see, e. g., [281, 468]) for two-body (cat's ears) contributions to the $\gamma^*\gamma^{(*)} \to (\eta, \eta')$ TFFs. These correspond to twist-six four-quark corrections in the "factorization" approximation (cf. [140, 280, 281]), where broken quark lines with crosses stand for quark condensates. Of particular note are the diagrams c) and d), which contain the emission of a soft gluon.

Therefore, in case of equally large virtualities $Q^2 = q^2$ the (new) partial result for $\psi = s$

$$F^{\text{QCD;(Figure 31a))}}_{\gamma^*\gamma^*\to M}\left(Q^2, q^2\right)\Big|_{\psi=s} = -e_s^2 8\pi\alpha_S C_f \langle\bar{s}s\rangle \int_0^1 dx \frac{\mathbb{F}^{(s)}_{6M}(x)}{Q^2 q^2 \left(\bar{x}Q^2 + x q^2\right)}, \tag{886}$$

$$\mathbb{F}^{(s)}_{6M}(x) \coloneqq \frac{1}{6m_s}\overline{\Phi}^{(s);p}_{3M}(x) + \frac{5}{12} m_s F^{(s)}_M \phi^{(s)}_M(x)\,, \tag{887}$$

fits with the naive power counting assumption, i. e., it is suppressed by two extra powers of $1/Q^2$

$$F^{\text{QCD;(Figure 31a))}}_{\gamma^*\gamma^*\to M}\left(Q^2, Q^2\right)\Big|_{\psi=s} = -e_s^2 8\pi\alpha_S C_f \frac{\langle\bar{s}s\rangle}{Q^6}\left[\frac{H^{(s)}_M}{6m_s} + \frac{5}{12} m_s F^{(s)}_M\right], \tag{888}$$

when compared to the leading (twist-two) term[87]. On the other hand, Equation 886 cannot describe the real photon limit, since it exhibits a clearly unphysical pole at $q^2 = 0$ (cf. [281]). In fact, this singularity appears due to missing soft quark-photon interactions which are beyond the standard OPE and pQCD description (cf. [281]). Accordingly, additional non-perturbative corrections are needed that correspond to photon emissions from long distances and would be present in the full theory (cf. Section 4.1.1). As discussed in Section 4.2.1 (and [281]), the LCSR approach regulates these divergences, by correcting the underlying QCD spectral density (cf. Equation 849)

$$\begin{aligned}&\frac{1}{\pi}\operatorname{Im}_s F^{\text{QCD;(Figure 31a))}}_{\gamma^*\gamma^*\to M}\left(Q^2, -s\right)\Big|_{\psi=s}\\ &= -e_s^2 8\pi\alpha_S C_f \frac{\langle\bar{s}s\rangle}{Q^4}\int_0^1 \frac{dx}{\bar{x}}\left[\delta(-s) - \delta\left(\frac{\bar{x}}{x}Q^2 - s\right)\right]\mathbb{F}^{(s)}_{6M}(x)\,,\end{aligned} \tag{889}$$

87 The leading pion counterpart of Equation 888 would be proportional to $\langle\bar{q}q\rangle^2/Q^6$ (cf. [281]).

via an inclusion of the ρ and ω resonances as well as continuum states[88] $(x_0 = Q^2/(s_0 + Q^2))$:

$$F^{\text{LCSR;(Figure 31 a))}}_{\gamma^*\gamma\to M}\left(Q^2\right)\Big|_{\psi=s} = e_s^2 8\pi\alpha_S C_f \left(\frac{\langle\bar{s}s\rangle}{m_\rho^2 Q^4}\left[\int_0^1 dx \left[\frac{1}{\bar{x}}\right]_+ \mathbb{F}^{(s)}_{6M}(x)\, e^{\frac{x m_\rho^2 - \bar{x} Q^2}{x M^2}} - \int_0^{x_0}\frac{dx}{\bar{x}}\mathbb{F}^{(s)}_{6M}(x)\, e^{\frac{x m_\rho^2 - \bar{x} Q^2}{x M^2}}\right] - \frac{\langle\bar{s}s\rangle}{Q^6}\int_0^{x_0} dx \frac{x\,\mathbb{F}^{(s)}_{6M}(x)}{\bar{x}^2}\right). \quad (890)$$

This new result, however, is of order $1/Q^4$ not $1/Q^6$ which entails the mentioned enhancement within the complete sum rule (cf. [281]). Indeed, the remaining factorizable twist-six corrections would exhibit a similar formal structure (see also [3]), as they are largely analogous to the (leading) pion case. Furthermore, when employing both Equation 890 and Equation 888, we can roughly estimate the $SU(3)_F$ corrections of Figure 31 a) to be less than 10 % relative to their $\mathcal{O}(m_s^0)$ counterparts[89].

Based on this heuristic analysis, we can estimate the numerical impact of possible factorizable twist-six contributions to the η and η' TFFs. The latter should amount to an additional uncertainty of $2\,\% - 3\,\%$ [3, 281] which is beyond the existing experimental precision. For this reason and theoretical consistency, we should omit such corrections at this point entirely.

4.3 PHENOMENOLOGICAL ANALYSIS OF $\eta^{(\prime)}$-MESON-PHOTON TRANSITIONS

Based on the previously presented theoretical findings, we are now able to perform an improved numerical analysis of the existing space- and time-like data sets, as measured by CLEO and *BABAR* [7, 8, 351]. This includes a careful survey of the associated uncertainties and possible prospects to constrain the two-gluon $\eta^{(\prime)}$ DAs, in particular, when more precise data on TFFs become available.

The presentation is organized as follows (using our work published in [1, 3]):

- **THE BABAR PUZZLE (I)**: In Section 4.3.1 a brief review of the "*BABAR* puzzle" [5] and its[90] implications on the (η, η') TFFs is given. This is supplemented by an explanation of several essential techniques, necessary for the intended extraction of DA related parameters from experimental FF data. Furthermore, we present a new model for the pion DA that is used to describe the recent Belle measurement [6].

- **THE BABAR PUZZLE (II)**: Building on this know-how, we resume our previous discussion on the FKS state mixing approximation (cf. Section 3.1) by including phenomenological aspects that result from the CLEO and *BABAR* measurements [7, 8].

- **THE ASYMPTOTIC LIMIT**: Section 4.3.3 is devoted to study the formal "$Q^2 \to \infty$" limit. Most importantly, by including finite renormalization corrections into the flavor singlet contributions[91], we are able to remove an apparent discrepancy between the expected asymptotic behavior of the $\gamma^*\gamma \to \eta'$ FF and the (experimental) data [7, 351].

- **THE TIME-LIKE FFS**: Furthermore, in Section 4.3.4 we discuss the crucial difference between time- and space-like FFs, based on a pQCD approach. That is followed by a comparison of the theoretical results with existing data [351] at $|Q^2| = 112\ \text{GeV}^2$.

88 For an integrable function "f", we here encounter a "plus" distribution, i. e., $\int_0^1 dx \left[\frac{1}{\bar{x}}\right]_+ f(x) = \int_0^1 dx \frac{1}{\bar{x}}(f(x) - f(1))$.
89 Here, we are focusing on the asymptotic DAs. Otherwise, Equation 888 suggests a relative size of about 6 %.
90 Here, we mean the puzzle proposed by the *BABAR* data [5] on $\gamma^*\gamma \to \pi^0$ transitions.
91 To our best knowledge, this has not been done before.

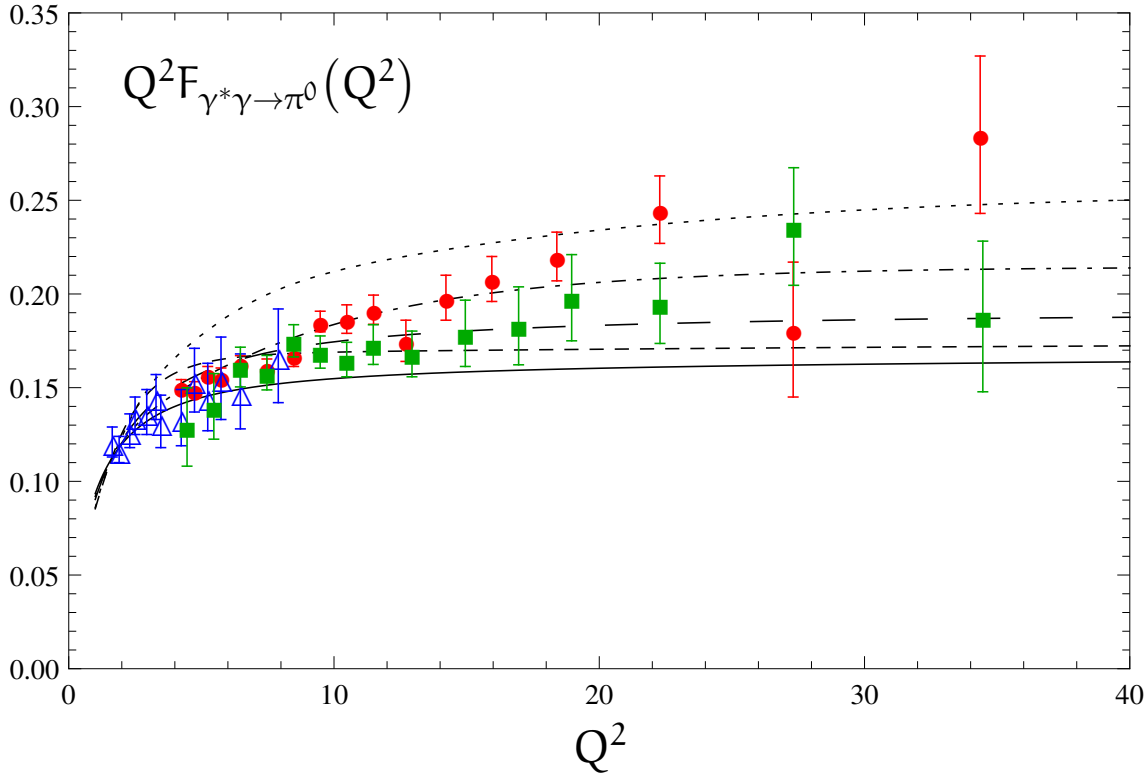

Figure 32: Based on [1] the scaled TFF (in [GeV]) is plotted against the momentum transfer (in $[\text{GeV}]^2$) for LCSR calculations (cf. [1, 281]), that include the "asymptotic" $\phi_\pi^{\text{AS}}(x) = 6x\bar{x}$ (solid line), BMS [469] (short dashes), "holographic" $\phi_\pi^{\text{hol}}(x) = \frac{8}{\pi}\sqrt{x\bar{x}}$ [470] (long dashes), "model II" of Ref. [281] (dash-dotted) and "flat" $\phi_\pi^{\text{flat}}(x) = 1$ [471] (dots) pion DA. The experimental data are from Belle [6] (squares), *BABAR* [5] (circles) and CLEO [8] (open triangles).

- NUMERICAL LCSR ANALYSIS: In Section 4.3.5 we provide a detailed numerical analysis of the available space-like data within the LCSR framework. In particular, we present three possible models for the η and η' DAs which may be used to describe the $\gamma^*\gamma \to \eta^{(\prime)}$ TFF measurements of [7, 8].

Accordingly, this section is of central importance for this work.

4.3.1 *The BABAR puzzle – part I*

Meson-photon TFFs and in particular the $\pi^0\gamma^*\gamma$ FF have been a hot subject over the last several years (cf. [1, 281]). This has been further fueled[92] by the *BABAR* measurement[93] [5] which suggested a strong scaling violation of $Q^2 F_{\gamma^*\gamma\to\pi^0}(Q^2)$. In order to identify the main challenges posed by this "*BABAR* puzzle", some basic facts about $\gamma^*\gamma \to P$ $(P = \pi^0, \eta, \eta')$ TFFs should be reconsidered. This includes several phenomenological concepts, used to determine the underlying

92 As discussed in our earlier work [281] and the corresponding addendum [1], the *BABAR* measurement caused a flurry of theoretical activity.

93 As reported in [3, 7, 351], the differential cross section for the two-photon fusion reaction $e^+e^- \to e^+e^-P$ (P is a pseudoscalar meson) has been measured by using the single tag mode (cf. Figure 18). In fact $\frac{d}{dQ^2}\sigma(e^+e^- \to e^+e^-P)$ is related to the TFF $F_{\gamma^*\gamma\to\pi^0}(Q^2)$ via a simple formula analogous to [472, Equation 2.1, 4.5] (cf. [7, 351]).

distribution amplitude's shape[94]. Based on an analytical approach towards QCD, only the low- and high energy limits of $F_{\gamma^*\gamma\to P}$ are at this point constrained. In fact, by defining the FF via[95] Equation 731 we have implicitly accepted the standard choice [7, 8] for its normalization which allows an extrapolation to the two-photon decay width $\Gamma(P\to 2\gamma)$ (i. e., $Q^2\to 0$). For instance, when considering the neutral pion decay [6, 8] (analogously for $M=\eta,\eta'$)

$$\lim_{Q^2\to 0}\left|F_{\gamma^*\gamma\to\pi^0}\left(Q^2\right)\right|^2=\frac{4\Gamma\left(\pi^0\to 2\gamma\right)}{\pi\alpha_{QED}^2 m_\pi^3}\,, \tag{891}$$

the Adler-Bell-Jackiw anomaly[96] [51, 52] predicts (cf. Equation 2) a corresponding lower bound:

$$\lim_{Q^2\to 0}F_{\gamma^*\gamma\to\pi^0}\left(Q^2\right)=\frac{\sqrt{2}}{4\pi^2 f_\pi}\,. \tag{892}$$

On the other hand, at sufficiently large momentum transfer pQCD can be applied $(\mu^2=Q^2)$:

$$Q^2F^{QCD}_{\gamma^*\gamma\to\pi^0}\left(Q^2\right)=\frac{\sqrt{2}f_\pi}{3}\int_0^1 dx\,\frac{\phi_\pi(x,\mu)}{x}+\mathcal{O}(\alpha_S)+\mathcal{O}\left(\frac{\Lambda_{QCD}^2}{Q^2}\right)\,, \tag{893}$$

which implicates the famous Brodsky-Lepage limit[97] [301]

$$\lim_{Q^2\to\infty}Q^2F^{QCD}_{\gamma^*\gamma\to\pi^0}\left(Q^2\right)=\sqrt{2}f_\pi\approx 0.185\ \text{GeV}\,. \tag{894}$$

For any finite value of Q^2, however, the meson-photon TFF exhibits a rather nontrivial behavior. In short, any attempts to describe the FF entirely in the framework of pQCD is futile[98] (cf. [1, 281]). Instead, non-perturbative and (other) soft corrections must be taken into account, e. g., with a modified approach, such as the Musatov-Radyushkin (cf. Equation 748) model or LCSRs (see Section 4.2.1). Here, it is useful to discuss some facts about the interplay of DAs and FFs. As mentioned in [281], those modifications effectively suppress contributions of higher order terms within the Gegenbauer expansion[99] (similarly for η and η' DAs)

$$\phi_\pi(x,\mu)=6x\bar{x}\left[1+\sum_{k=1}^{\infty}a_{2k}^\pi(\mu)\,C_{2k}^{(3/2)}(\xi_x)\right]\,, \tag{895}$$

i. e., contributions beyond $k=2$ have a small impact on the TFF. This can be illustrated[100] by the discussed Musatov-Radyushkin model (i. e., we use Equation 748 for $\sigma=0.53\ \text{GeV}^2$)

$$Q^2F^{\bar{q}q}_{\gamma^*\gamma\to\pi^0}\left(Q^2{=}20\,\text{GeV}^2\right)=\sqrt{2}f_\pi[0.908+0.556\,a_2^\pi+0.221\,a_4^\pi+0.052\,a_6^\pi+0.006\,a_8^\pi+\ldots]\,, \tag{896}$$

94 Here, we mainly describe the pion TFF. However, the strategies and implied conclusions for the $\eta^{(\prime)}$ case are completely analogous.

95 Evidently, for $M=\pi^0$ Equation 731 also describes the pion TFF.

96 Usually calculated in the chiral limit (cf. [49]).

97 For $Q^2\to\infty$ only the asymptotic DA contributes. In this way Equation 894 can be deduced from Equation 893.

98 Estimates for soft contributions within the LCSR approach are power suppressed compared to their hard counterparts. However, in this context, soft corrections are sizable for a moderate momentum transfer $Q^2\sim 2-6\ \text{GeV}^2$ and can still account for ca. 25% of the $(\gamma^*\gamma\to\pi^0$ FF) at $Q^2=30\ \text{GeV}^2$ [281]. Accordingly, a pure pQCD calculation of the TFF with one real photon and in the collinear factorization approach should not be expected to have a high accuracy (e. g., [281]).

99 This may also restrict the relevance of the involved end-point behavior.

100 The problem, whether such soft corrections can be estimated in a model independent way has been addressed in Section 4.1.1. For the chosen LCSR approach, those non-perturbative modifications are in general somewhat smaller, but sizable (see, e. g., [281]).

which manifests such corrections[101], as compared to a LO pQCD result (e. g., also at $Q^2 = 20\ \mathrm{GeV}^2$)

$$Q^2 F^{\mathrm{QCD}}_{\gamma^*\gamma\to\pi^0}\left(Q^2\right) = \sqrt{2} f_\pi \left[1 + a_2^\pi + a_4^\pi + a_6^\pi + a_8^\pi + \ldots\right] . \tag{897}$$

Here, we have omitted RG effects (e. g., with $a_n^\pi \triangleq a_n^\pi(\mu)$ and $\mu^2 = Q^2$) for brevity and a better visibility of the non-perturbative admixtures. As discussed in Section 4.2.1, similar soft contributions exist in the LCSR approach for each Gegenbauer moment, yet with a more complicated, but also individually different scale dependence. Especially, the latter could, therefore, be made responsible for the role which the different regions of momentum transfer play, when one is extracting information on the DAs from FF measurements (following [1]):

- MODERATE MOMENTUM TRANSFER: A sensitivity to the meson DA within this realm of momentum transfer, i. e., $Q^2 \sim 2 - 6\ \mathrm{GeV}^2$ is mostly limited to the second-order coefficient in the Gegenbauer expansion[102]. Correspondingly, that second moment (e. g., a_2^π) can be roughly determined via fits of LCSR calculations to the experimental data at lower or moderate Q^2 values, while all other Gegenbauer coefficients are temporarily put to zero. Moreover, in the case of $Q^2 \lesssim 6\ \mathrm{GeV}^2$ higher twist corrections appear to be significant for QCD and LCSR predictions. For moderate Q^2 values, however, the sum rule method relies rather heavily on the duality assumption which is used to model soft contributions (cf. Section 4.2.1). According to [459, 460], the accuracy of such approximations is difficult to quantify and should, therefore, be tested. At NLO in α_S, we may roughly estimate an irreducible theoretical uncertainty for this region of about $\pm 5\%$ [1].

- INTERMEDIATE MOMENTUM TRANSFER: QCD predictions in the region of intermediate momentum transfer are particularly sensitive to higher-order shape parameters, such as the fourth and sixth Gegenbauer coefficients. More precisely, the experimental data at $Q^2 \sim 10\ \mathrm{GeV}^2$ allows access to quantitative information on the fourth moment, while data points around $Q^2 \lesssim 20\ \mathrm{GeV}^2$ can be used to further constrain a_6^π. This can be done as follows: provided that a_2^π has already been determined, another fitting procedure can be carried out, which iteratively incorporates additional non-vanishing Gegenbauer coefficients into the considerations. Unfortunately, this strategy is strongly dependent on the data quality. Furthermore, it should be noted that the shape parameters seem to be interdependent. For instance, a sizable coefficient a_6^π leads to a decreasing value of a_4^π (cf. [1, 281]). Let us return to the original problem. Regarding the *BABAR* and Belle experiment [5, 6], the difference between their data points within this region is statistically the most significant (cf. [1]). If the values reported by *BABAR* [5] are true, a description based on QCD collinear factorization which does not use unconventional models for the pion DA (e. g., with large end-point enhancements) seems hard to maintain. In the context of Gegenbauer moments, this is manifested by an inverse hierarchy $a_4^\pi > a_2^\pi$ [1, 281]. Conversely, the Belle data [6] at $Q^2 \sim 9 - 12\ \mathrm{GeV}^2$ is much easier to accommodate within a "standard" scenario, e. g., by using the holographic model (see Figure 32).

- LARGE MOMENTUM TRANSFER: In accordance with pQCD the TFF is expected to approach the Brodsky-Lepage limit in this region, i. e., for $Q^2 > 20\ \mathrm{GeV}^2$. Nevertheless, since an

101 The mentioned soft corrections within Equation 896 (cf. Equation 748) would vanish in the limit $Q^2 \to \infty$, formally restoring Equation 897. However, the (not shown) RG effects will at some point become dominant, leading to an additional suppression of the Gegenbauer moments.

102 This second Gegenbauer coefficient a_2^π has been calculated rather precisely (e. g., [11]) on the lattice. When used as an input, a comparison of the resulting LCSR calculations with the form factor data may allow a better assessment concerning the theoretical accuracy that is presently available [1]. Especially with the expected BES III experiment [473], which plan a significant improvement over the CLEO, *BABAR* and Belle results in this region, there can be quantitative progress [1]. That will be important in a broader context, e. g., for QCD calculations of semileptonic heavy to light meson form factors and comparable weak decays, which involve similar relatively low scales (cf. [1]).

Measurement	$a_2^\pi(\mu_0)$	$a_4^\pi(\mu_0)$	$a_6^\pi(\mu_0)$	$a_8^\pi(\mu_0)$
BABAR [5]	0.140	0.230	0.180	0.050
Belle [6]	0.100	0.100	0.100	0.034

Table 12: Two different models for the pion DA $\left(a_n^\pi \equiv 0,\ n \geqslant 10\right)$, either describing the *BABAR* [5] or Belle [6] measurement (cf. [1]). All involved Gegenbauer coefficients are taken at the generic scale $\mu_0 = 1$ GeV.

asymptotic behavior in QCD is generally achieved for very large scales, it seems unlikely to observe this prediction within the *BABAR* range (cf. [1]). Additionally, much of the excitement caused by the *BABAR* experiment resulted from the associated power-law fit [5] $\left(A = 0.182 \pm 0.002\ \text{GeV},\ \beta = 0.25 \pm 0.02\right)$

$$Q^2 F_{\gamma^*\gamma\to\pi^0}\left(Q^2\right) \simeq A\left(\frac{Q^2}{10\ \text{GeV}^2}\right)^\beta \tag{898}$$

to the FF data [1]. This fit, however, is dominated by the data at lower momentum transfer. Thus, the proclaimed rise at large Q^2 values is not warranted (see [1] and references therein for an extended discussion). In fact, a much higher accuracy would be needed to discriminate between different models that include $a_n^\pi \neq 0$ with $n > 6$ and also provide quantitative constraints. Therefore, higher partial waves, such as a_8^π, a_{10}^π, etc., which may become important in this large Q^2 region, cannot be deduced from the existing data with satisfactory accuracy. Apart from that, higher-order Gegenbauer moments contribute only marginally in the *BABAR* Q^2 range due to cut-off effects caused by soft corrections [1, 281]. Unfortunately, this is also true in the $\eta^{(\prime)}$ case.

Broadly speaking, the distribution amplitude's "x"-dependence (cf. Equation 895) is determined by the form factor's Q^2-dependence and vice versa. In this way it is possible to test different (generic) models[103] on the basis of the given experimental data. As an illustration Figure 32 shows a compilation of FF measurements provided by the Belle [6], *BABAR* [5] and CLEO [8] collaborations. Evidently, the *BABAR* data displays a significant scaling violation at $Q^2 > 10\ \text{GeV}^2$, i. e., it exceeds the asymptotic limit and (seemingly) continues to rise. Conversely, the Belle data points [6] are systematically lower than those of *BABAR* [5] within a broad range of photon virtualities Q^2.[104] Consequently, a LCSR analysis based on [281], which is designed to describe each of the two measured data sets separately, will also give rise to two distinct models for the otherwise universal pion DA. In order to obtain a good fit, we may, therefore, use the Gegenbauer coefficients of Table 12 (cf. [1]). Evidently, these shape parameters by design either describe the new Belle experiment [6] or form a model which may be used to interpret the *BABAR* data [5] (cf. [1]). A comparison of those models can be seen in Figure 32 and Figure 33.

In the context of meson structure physics we may, therefore, summarize [1]:

- The measurements reported by the Belle collaboration [6] should somewhat take the heat off theorists struggling to invent new non-perturbative mechanisms (cf. [1] and references therein) which postpone or even invalidate the onset of QCD factorization in the meson TFF.

103 As pointed out in [1], one has to be very careful in comparing statements on the distribution amplitude's shape which have been obtained within different theoretical approaches. Their specific properties can distort the general form of the DA.

104 The discrepancy between those two data sets is within $1.5 - 2.0$ standard deviations (cf. [1]).

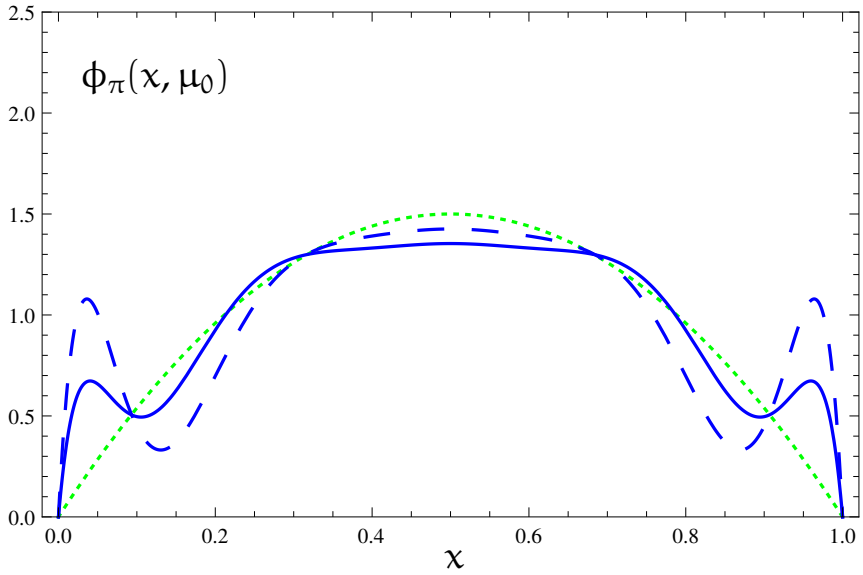

Figure 33: Both models of Table 12 and the asymptotic DA are plotted (picture taken from [1]) against the quark momentum fraction "x" (at $\mu_0 = 1$ GeV). In particular, the corresponding model for [6] (solid line) is compared to "model II" of [281] (dashed) and the asymptotic DA (dotted).

- A new generation of experimental data, e. g., coming from super-B factories (e. g., [473]) could help to settle this question and allow the $\gamma^*\gamma \to \pi^0$ transition to serve its purpose as a gold plated reaction within the theory of hard exclusive reactions.
- Moreover, a global fit of all hard exclusive processes including pions is needed. This may, eventually, also include available lattice data[105].

However, the *BABAR* puzzle is not restricted to the $\gamma^*\gamma \to \pi^0$ FF. Instead, it also affects the analogous measurements of the electromagnetic TFFs $\gamma^*\gamma \to (\eta, \eta')$ at space-like momentum transfers within the interval $Q^2 \sim 4 - 40\ \text{GeV}^2$ [3].

4.3.2 *The BABAR puzzle – part II*

In this section we will discuss the general implications of the *BABAR* puzzle (cf. [1, 3]) on η and η' DAs.

When looking at the $\gamma^*\gamma \to (\eta, \eta')$ *BABAR* data [7] (see Figure 34), it immediately comes to mind that no similar scaling violation, as in the pion case [5] can be observed. Instead, when fitted[106] with the function $\left(Q^2 \text{ in } \text{GeV}^2;\ P = \pi^0, \eta, \eta';\ a_P, b_P \in \mathbb{R}\right)$ [7]

$$Q^2 F_{\gamma^*\gamma \to P}\left(Q^2\right) \simeq b_P + a_P \log\left(\frac{Q^2}{1\ \text{GeV}^2}\right) \tag{899}$$

the observed rise[107] of both η and η' TFFs [7, 351] is about three times weaker [471] than their corresponding counterpart for $\gamma^*\gamma \to \pi^0$ transitions [5] (cf. [7]). But more importantly, the very

105 In recent years, lattice QCD has emerged as a valuable addition to the sum rule method. Both approaches now have a similar precision, e. g., this can be seen in [281, TABLE I.].

106 As reported by [7], this fit uses a combination of the data sets [7] and [351].

107 Here, "rise" is synonymous to the related numerical value "a_P" of this fit (cf. [7]).

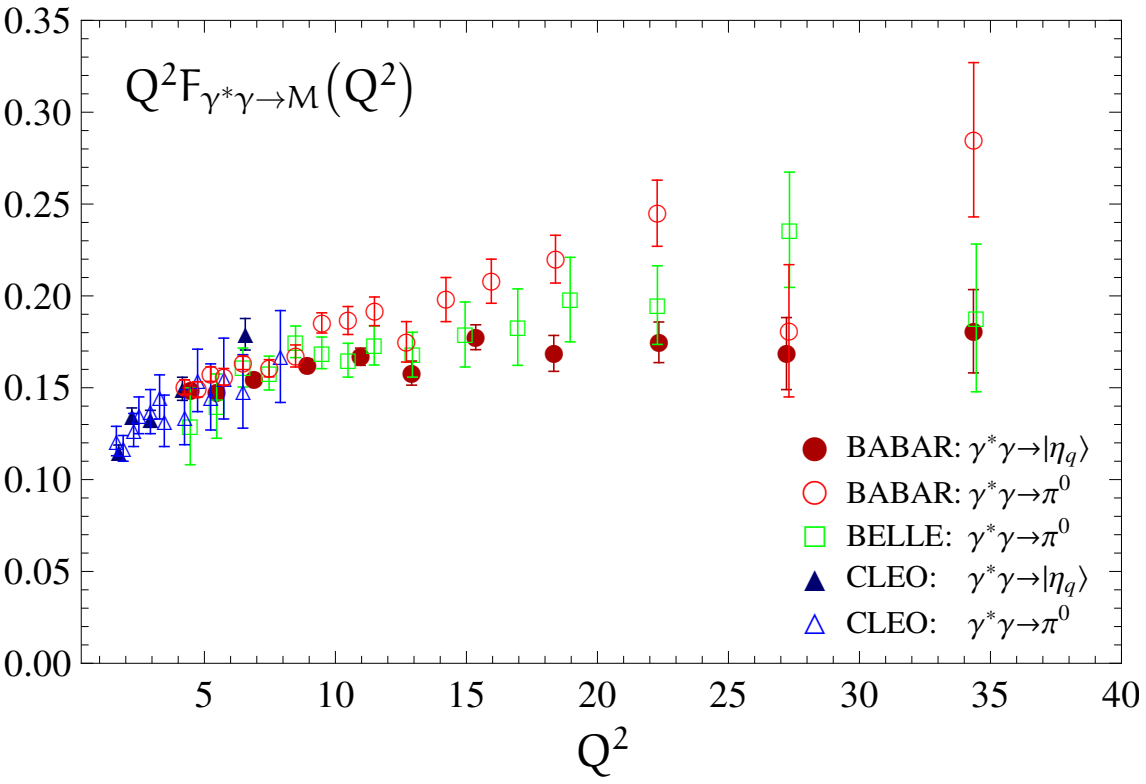

Figure 34: The experimental data on $\gamma^*\gamma \to \pi^0$ [5, 6, 8] (open symbols) compared with the non-strange component of the $\eta^{(\prime)}$ TFFs $\gamma^*\gamma \to |\eta_q\rangle$ (filled symbols), that arise from the combination of *BABAR* or CLEO measurements [7, 8] on η and η' production in the FKS mixing scheme, i. e., by applying the rescaled Equation 900.

same data can be related to each other via a flavor decomposition. In other words, based on the FKS scheme (cf. Section 3.1.1) a comparison of the η and η' data [7] with $\gamma^*\gamma \to \pi^0$ FF measurements [5, 6] is thus also possible via (cf. Equation 315)

$$F_{\gamma^*\gamma\to|\eta_q\rangle}\left(Q^2\right) \coloneqq \cos(\phi)\, F_{\gamma^*\gamma\to\eta}\left(Q^2\right) + \sin(\phi)\, F_{\gamma^*\gamma\to\eta'}\left(Q^2\right) , \tag{900}$$

$$F_{\gamma^*\gamma\to|\eta_s\rangle}\left(Q^2\right) \coloneqq \cos(\phi)\, F_{\gamma^*\gamma\to\eta'}\left(Q^2\right) - \sin(\phi)\, F_{\gamma^*\gamma\to\eta}\left(Q^2\right) . \tag{901}$$

According to [7, 474] the (naive) asymptotic limits are, therefore, given by[108]

$$\lim_{Q^2\to\infty} Q^2 F_{\gamma^*\gamma\to|\eta_q\rangle}\left(Q^2\right) = \frac{5\sqrt{2}}{3} f_q , \tag{902}$$

$$\lim_{Q^2\to\infty} Q^2 F_{\gamma^*\gamma\to|\eta_s\rangle}\left(Q^2\right) = \frac{2}{3} f_s , \tag{903}$$

which are equivalent to the conservative upper bound $\left(M = \eta, \eta', \text{while using Equation 280}\right)$:

$$\lim_{Q^2\to\infty} Q^2 F_{\gamma^*\gamma\to M}\left(Q^2\right) \approx \sqrt{\frac{2}{3}}\left[f_M^{(8)} + 2\sqrt{2} f_M^{(0)}\right] . \tag{904}$$

108 When assuming the (strict) FKS scheme, we may expect, that $\phi_q(x)$ (i. e., the related twist-two DA of $|\eta_q\rangle$ – cf. Section 3.1.4) is close to $\phi_\pi(x)$, except for a prefactor. The latter originates from different quark charges and has to be used when rescaling Equation 900.

In Figure 34 we show a comparison of the $\gamma^*\gamma \to \pi^0$ experimental data with the rescaled non-strange $\gamma^*\gamma \to |\eta_q\rangle$ FF which has been extracted from the *BABAR* [7] and CLEO [8] data for $\gamma^*\gamma \to \eta$ and $\gamma^*\gamma \to \eta'$ transitions, while using Equation 900 (multiplied by $3/5$) [3]. If the FKS scheme were exact, the two FFs would coincide in the whole Q^2 range, i. e., up to tiny isospin breaking corrections (cf. [3]). As can be seen with reference to Figure 34, the existing measurements do not contradict the (assumed) FKS approximation at low-to-intermediate $Q^2 \leqslant 10\ \text{GeV}^2$, whereas at larger virtualities the comparison is inconclusive because of significant discrepancies between the *BABAR* and Belle pion data [5, 6]. Moreover, when taken in isolation, the *BABAR* data exhibits dramatic differences between the $\gamma^*\gamma \to \pi^0$ and $\gamma^*\gamma \to |\eta_q\rangle$ FFs at large momentum transfers which cannot be explained by perturbative effects (see [3]). Most importantly, if these discrepancies were confirmed, it would be a stark indication that the concept of state mixing (cf. Section 3.1.4) is not applicable to the η and η' DAs. Hence, already at a low scale, the corresponding relations between higher-order Gegenbauer coefficients would be strongly broken. We will extend this discussion within Section 4.3.5 in the context of $\eta^{(\prime)}$ TFFs.

It should be emphasized again (cf. Chapter 3), that we use this FKS state mixing assumption for the η and η' DAs $\left(\text{at } \mu_0 = 1\ \text{GeV}\right)$ only as a working hypothesis to avoid a proliferation of parameters. If necessary, we are able to relax those presuppositions in the future[109].

4.3.3 *The asymptotic limit for η and η' transition form factors*

This subsection[110] is devoted to discuss the behavior of η and η' TFFs at very large momentum transfers. In that context we will derive an analogue to the Brodsky-Lepage limit (cf. Equation 894), which, to our best knowledge for the first time includes finite RG effects of the single decay constant (see Equation 462). As further explained in Section 4.3.5, this enables a better compatibility with the experimental data [7, 351].

In the formal $Q^2 \to \infty$ limit the scaled TFFs (cf. Equation 751) have to approach their asymptotic values[111]

$$\lim_{Q^2\to\infty} Q^2 F_{\gamma^*\gamma\to M}\left(Q^2\right) = \sqrt{\frac{2}{3}}\left[f_M^{(8)} + 2\sqrt{2} f_M^{(0)}(\mu_0)\left(1 - \frac{2N_f}{\pi\beta_0}\alpha_S(\mu_0)\right)\right]. \tag{905}$$

Based on Equation 462, the scale dependence of $f_M^{(0)}(\mu_0)$ gives rise to a finite renormalization factor (marked in blue) which is not negligible. Consequently, when using $N_f = 4$, $\mu_0 = 1\ \text{GeV}$, $\alpha_S(\mu_0) \approx 0.5$, and the FKS parameters in Equation 280, we obtain (all numbers in parenthesis correspond to the parameter set of Equation 281):

$$\lim_{Q^2\to\infty} Q^2 F^{\text{asy}}_{\gamma^*\gamma\to\eta}\left(Q^2\right) = 0.173\,(0.158)\ \text{GeV}, \tag{906}$$

$$\lim_{Q^2\to\infty} Q^2 F^{\text{asy}}_{\gamma^*\gamma\to\eta'}\left(Q^2\right) = 0.247\,(0.270)\ \text{GeV}. \tag{907}$$

This finite renormalization correction to the flavor singlet contribution has not been taken into account in [7, 20, 28] (see, e. g., Equation 904). In fact, it causes less than a 5% effect for the η meson, but leads to a 20% reduction of the asymptotic $\gamma^*\gamma \to \eta'$ FF value. In the latter case, this effect is amplified by a cancellation between the flavor singlet and flavor octet contributions, i. e.,

109 For instance, by replacing the Gegenbauer coefficients via particle dependent counterparts.

110 Here, we closely follow our work of [3].

111 Strictly speaking: contributions of heavy quarks have to be added at the corresponding thresholds (cf. Section 2.3), i. e., one has $N_f \alpha_S(\mu_0) \mapsto 3\alpha_S(\mu_0) + \alpha_S(\mu_c) + \alpha_S(\mu_b) + \ldots$. Numerically, however, the difference is not significant.

$f_{\eta'}^{(0)} = 0.15\,(0.17)$, along with $f_{\eta'}^{(8)} = -0.06\,(-0.08)$. As a consequence, the discrepancy between the data [7, 351] and the expected asymptotic behavior of the $\gamma^*\gamma \to \eta'$ FF is removed[112] (see Section 4.3.5).

These renormalization group effects are, therefore, of particular interest in the following chapter.

4.3.4 *The time-like form factors*

In this subsection we analytically continue the η and η' TFFs to large negative photon virtualities which allows a comparison with existing measurements.

It is worth emphasizing that in reference [351] the annihilation processes $e^+e^- \to \gamma^* \to (\eta, \eta')\,\gamma$ (cf. Figure 18) were studied at a center-of-mass energy $\sqrt{s} = 10.58$ GeV. This is especially important, because those measurements can be interpreted in terms of $\gamma^*\gamma \to (\eta, \eta')$ FFs at remarkably high time-like photon virtuality $Q^2 = -s = -112\ \text{GeV}^2$ [3, 351]:

$$\left|Q^2 F_{\gamma^*\gamma\to\eta}\left(Q^2 = -112\ \text{GeV}^2\right)\right| = (0.229 \pm 0.031)\ \text{GeV}\,, \tag{908}$$

$$\left|Q^2 F_{\gamma^*\gamma\to\eta'}\left(Q^2 = -112\ \text{GeV}^2\right)\right| = (0.251 \pm 0.021)\ \text{GeV}\,. \tag{909}$$

Here, we added the statistical and systematic uncertainties (cf. [351]) in quadrature. In general, time-like FFs are complex quantities, whereas only their absolute value is measured [351]:

$$\frac{d\sigma\,(e^+e^- \to M\gamma)}{d\cos(\theta_\gamma^*)} = \frac{\pi^2 \alpha_{\text{QED}}^3}{4} \left|F_{\gamma^*\gamma\to M}(-s)\right|^2 \left(1 + \cos^2(\theta_\gamma^*)\right)\,. \tag{910}$$

For the related center-of-mass frame "θ_γ^*" is the angle between its incoming electron and the outgoing photon (see [351]). At leading twist accuracy, all required time-like FFs can be obtained from their Euclidean (space-like) counterparts via the analytic continuation $(\varepsilon \to 0^+)$

$$Q^2 \longmapsto -s - i\varepsilon\,. \tag{911}$$

In this process imaginary parts arise both from the analytically continued hard coefficient functions as well as involved DAs which become complex at time-like scales $\mu^2 \sim Q^2 = -s$. Particularly, two types of logarithmic corrections become relevant in this context [476]:

- UV logarithms, e. g., originating from the time-like version of α_S, or
- collinear logarithms, e. g., caused by the renormalization of DAs.

Therefore, we encounter functions that contain logarithmic contributions, such as

$$\lim_{\varepsilon\to 0^+} \log\left(\frac{s}{\mu_F^2} - i\varepsilon\right) = \log\left(\frac{Q^2}{\mu_F^2}\right) - i\pi\,, \tag{912}$$

or $(\mu_F^2$ being some fixed mass scale$)$

$$\lim_{\varepsilon\to 0^+} \log\left(\log\left(\frac{s}{\mu_F^2} - i\varepsilon\right)\right) = \log\left(\sqrt{\log^2\left(\frac{Q^2}{\mu_F^2}\right) + \pi^2}\right) - i \arctan\left(\frac{\pi}{\log\left(\frac{Q^2}{\mu_F^2}\right)}\right)\,. \tag{913}$$

112 The *BABAR* data [7, 351] suggests, that $F_{\gamma^*\gamma\to\eta}(Q^2)$ has a slightly different scaling behavior than the $\gamma^*\gamma \to \eta'$ FF. As reported by [7], the preferred description for the combined data [7, 351] corresponding to $Q^2 F_{\gamma^*\gamma\to\eta}(Q^2)$ FFs is given by Equation 899. This function, however, corresponds to a model with a finite DA at the end points [7] (as proposed [471, 475] for the $\gamma^*\gamma \to \pi^0$ TFF [5]). Conversely, the η' TFF can be better described (cf. [7]) via models with a conventional DA, yielding a flat scaled FF for (very) large momentum transfers.

Unfortunately, the transition from space-like to corresponding (mirror) time-like momenta engenders rather cumbersome expressions which we prefer not to show explicitly for their sole evaluation at $Q^2 = -112\ \text{GeV}^2$. Thus, let us instead focus on the numerical evaluation. Since Equation 751 is applicable, both TFFs are linear functions of the DAs. By using the inherent conformal expansion of the latter, each FF can be written as a formal sum over the different Gegenbauer moments[113] (see Equation 447, Equation 467 and Equation 751)

$$\begin{aligned} F^{\text{QCD}}_{\gamma^*\gamma\to M}\left(Q^2\right) = \sum_{A=0,8} 3C^A f_M^{(A)}(\mu) \Bigg[& \int_0^1 dx\, x\bar{x}\, T_H^{(A)}\left(x, Q^2; \mu, \alpha_S(\mu)\right) \\ & + \sum_{n=1}^{\infty} c_{2n;M}^{(A)}(\mu) \int_0^1 dx\, x\bar{x}\, C_{2n}^{(3/2)}(\xi_x)\, T_H^{(A)}\left(x, Q^2; \mu, \alpha_S(\mu)\right) \Bigg] \\ & + 15C^0 f_M^{(g)}(\mu) \sum_{n=1}^{\infty} c_{2n;M}^{(g)}(\mu) \int_0^1 dx\, x^2\bar{x}^2 C_{2n-1}^{(5/2)}(\xi_x)\, T_H^{(g)}\left(x, Q^2; \mu, \alpha_S(\mu)\right), \end{aligned} \tag{914}$$

that are most conveniently taken at a low reference scale $\left(\check{I}_{QF} := \{q, s, g\}\right)$:

$$Q^2 F_{\gamma^*\gamma\to\eta}\left(Q^2 = -112\ \text{GeV}^2\right) = 0.161\ \text{GeV} + \sum_{p\in\check{I}_{QF}} \sum_{n=1}^{\infty} f_{\eta;2n}^{(p)}\left(\frac{Q^2}{\mu^2}, \alpha_S(\mu); \mu_0\right) c_{2n}^{(p)}(\mu_0), \tag{915}$$

$$Q^2 F_{\gamma^*\gamma\to\eta'}\left(Q^2 = -112\ \text{GeV}^2\right) = 0.241\ \text{GeV} + \sum_{p\in\check{I}_{QF}} \sum_{n=1}^{\infty} f_{\eta';2n}^{(p)}\left(\frac{Q^2}{\mu^2}, \alpha_S(\mu); \mu_0\right) c_{2n}^{(p)}(\mu_0). \tag{916}$$

Essentially all scale dependencies can be absorbed[114] in the coefficient functions $f_{M;n}^{(p)}$, while analogous contributions of the asymptotic DA may be written separately[115]. For their numerical evaluation, we also choose the factorizations scale $\mu^2 = Q^2$ and analytically continue the results via Equation 911 to time-like momentum transfers. A comparison between numerical values of possible space- and time-like coefficients for the η and η' mesons, with focus on $n = 2, 4$ are given in Table 13. It should be noted that the functions $f_{M;n}^{(p)}$ have been (originally) calculated without further restrictions, while the corresponding shape parameters $c_{2n}^{(p)}$ are assumed to be particle independent, as implied by the used FKS state mixing ansatz. Accordingly, the parameters of Equation 280 have been used as a default input. Besides, by varying the scale μ^2 we may additionally estimate related perturbative uncertainties which result from a truncation of higher-order $\mathcal{O}\left(\alpha_S^2\right)$ corrections. As a conventional range of variation [37, 42], we choose[116] [3]

$$\frac{Q^2}{2} < \mu^2 < 2Q^2. \tag{917}$$

Consequently, the given numbers of Table 13 will change by at most 10%. Moreover, we see, that the coefficients of higher order Gegenbauer polynomials are in general rather small which is due to a suppression caused by the anomalous dimensions. These coefficients acquire rather large phases. However, for realistic values of the Gegenbauer moments, e. g., $c_n^{(q)} \sim c_n^{(s)} \approx 0.1 - 0.2$

113 Here, we set $f_M^{(8)}(\mu) = f_M^{(8)}$. Moreover, for consistency reasons, we keep particle dependence at this point.

114 This includes RG effects, which are also encoded in the coefficients $f_{M;n}^{(p)}$.

115 Their absolute values $\left(\text{i. e., } f_{M;0}^{(p)}\right)$ are almost the same in the time-like and space-like regions.

116 The residual uncertainty $\mathcal{O}\left(\alpha_S^{N+1}\right)$ of a finite perturbative series, such as $\sum_{k=0}^{N} c_k \left(\frac{\alpha_S}{\pi}\right)^k$ $(N \geqslant 0)$ is associated with the ambiguity in choosing a factorization scale. Hence, varying this scale can be an input in estimating uncertainties on predictions (see [37, 42]).

Meson	Scale	$f_{M;2}^{(q)}$	$f_{M;2}^{(s)}$	$f_{M;2}^{(g)}$
η	space-like	0.126	-0.037	0.010
	time-like	$0.113 + 0.032i$	$-0.033 + 0.009i$	$0.011 - 0.001i$
η'	space-like	0.103	0.045	0.061
	time-like	$0.093 + 0.026i$	$0.040 + 0.011i$	$0.069 - 0.005i$
Meson	Scale	$f_{M;4}^{(q)}$	$f_{M;4}^{(s)}$	$f_{M;4}^{(g)}$
η	space-like	0.105	-0.030	0.006
	time-like	$0.086 + 0.039i$	$-0.025 - 0.011i$	$0.006 + 0.001i$
η'	space-like	0.086	0.037	0.037
	time-like	$0.070 + 0.032i$	$0.030 + 0.014i$	$0.040 + 0.005i$

Table 13: Based on their conformal structure, the twist-two DAs give rise to a similar Gegenbauer expansion of the related TFFs, e. g., as it has been implemented in Equation 915 or Equation 916. Accordingly, we list the first few coefficients ($n = 2, 4$) for the FFs at time-like ($Q^2 = -112\ \text{GeV}^2$) and space-like ($Q^2 = 112\ \text{GeV}^2$) momentum transfer. Here, all numbers are given in units of [GeV], while assuming validity of the FKS scheme at the reference scale $\mu_0 = 1$ GeV.

($n = 2, 4$) the corresponding contributions to the FF appear to be marginal as compared to the leading terms in Equation 915 and Equation 916 (cf. [3]). Thus, the overall phase is small and the related absolute values of the FF in the space- and time-like regions remain close to each other. This result is in agreement with the conclusion in [476], stating that perturbative corrections cannot generate a significant difference between the space-like and time-like FFs.

Unfortunately, the situation beyond the discussed leading power accuracy is less well understood. For instance, the overall $1/Q^2$ corrections to the space-like TFFs is negative[117] and by virtue of the sign change in Q^2, one expects a positive correction to the time-like FF if the analytic continuation is justified to power accuracy which is, however, not obvious (cf. [3]). In general, the higher twist contributions correspond to less singular terms within the light-cone OPE of the product $J_\mu^{\text{em}}(x)\, J_\nu^{\text{em}}(0)$ are small and tend to have alternating signs [3] (see, e. g., Equation 773). In particular, they are unlikely to play any role at $|Q^2| \sim 112\ \text{GeV}^2$. Conversely, soft contributions can be significant, even for very large momentum transfers. As discussed in [3, 281], within the LCSR approach the magnitude of soft corrections is correlated with the leading-twist distribution amplitude's shape, i. e., broader DAs generally lead to larger soft corrections and vice versa. A rough estimate can be given by Equation 857 when assuming numerically equal values for octet and singlet Gegenabuer moments (at leading twist accuracy and Q^2 sufficiently large):

$$Q^2 F_{\gamma^*\gamma\to M}\left(Q^2\right) = Q^2 F_{\gamma^*\gamma\to M}^{\text{QCD}}\left(Q^2\right)\left[1 - \frac{(3-7)\,\text{GeV}^2}{Q^2}\right]. \tag{918}$$

Here, the larger number corresponds to a broad DA of the type [281] (cf. Section 4.3.1) required to describe the *BABAR* data [5] on $\gamma^*\gamma \to \pi^0$ transitions, and the smaller one is obtained from the asymptotic DA. If the soft correction changes sign in the time-like region, we may conclude that the difference between related time- and space-like FFs at $|Q^2| = 112\ \text{GeV}^2$ can be between $\sim 5\%$

117 This can be shown in many ways, see, e. g., [1, 281].

and ∼ 13% for the "narrow" and "broad" meson DA, respectively[118]. It is interesting that the experimental result for $\gamma^*\gamma \to \eta'$ transitions at $Q^2 = -112$ GeV^2 [351] is very close to the contribution of an asymptotic η' meson DA in Equation 916, whereas the asymptotic contribution to $\gamma^*\gamma \to \eta$ is almost 50% below the data (cf. Equation 909). This result urgently needs verification! If correct, it can probably only be explained by much larger soft contributions, e. g., as implied by a much broader η meson DA, as compared to the η' case. This conclusion, however, would also be in conflict with the state mixing approximation for DAs.

We, therefore, conclude that the performed analysis, which is based on an analytical continuation of the $\gamma^*\gamma \to (\eta, \eta')$ FFs to a large negative momentum transfer, entails important constraints on the possible structure of involved meson DAs as well as the allowed approximation methods.

4.3.5 *Numerical analysis of the space-like $\gamma^*\gamma \to (\eta, \eta')$ transition form factors*

The following section is devoted to the phenomenological study of η and η' meson DAs based on available space-like TFF measurements. Correspondingly, it is one of the core components of this thesis.

In addition to a detailed numerical LCSR analysis, the available experimental data will be used to find models for the η and η' meson DAs. As shown below (see also Section 4.3.1), the given data sets do not suffice for more than a reasonable determination of the first two shape parameters, that are engendered by $\phi_M^{(q)}(x, \mu)$ or $\phi_M^{(s)}(x, \mu)$. In the case of the gluon DAs $\phi_M^{(g)}(x, \mu)$ only the first non-trivial moment can be constrained. As discussed in [28], these quantities are only effective parameters which carry an error due to the truncated Gegenbauer expansion. Higher order terms of the latter, however, should be sufficiently suppressed by soft effects (cf. Section 4.3.1).

According to Section 4.3.1, it is, therefore, necessary for such a procedure to name the involved input, i. e., sum rule parameters first.

4.3.5.1 *Light-cone sum rule parameters*

All numerical results in this subsection are obtained by using the two-loop running QCD coupling of Equation 74 (with Equation 67) for $N_f = 4$ active flavors and $\Lambda_{\text{QCD}}^{(4)} = 326$ MeV (cf. Equation 81). Based on Chapter 3 we assume that the FKS mixing scheme is valid for all involved DAs at the generic renormalization scale $\mu_0 = 1$ GeV $\left(\alpha_S(\mu_0) = 0.494\right)$. Unless stated otherwise, we use the set of FKS parameters, as specified in Equation 280. Moreover, all given values of non-perturbative parameters refer to the same reference scale $\mu_0^2 = 1$ GeV^2. Furthermore, a natural factorization and renormalization scale μ for the pQCD calculation of meson TFFs with two large photon virtualities $Q^2, q^2 \gg \Lambda_{\text{QCD}}^2$ is given by the virtuality of the quark propagator $\left(x \in [0, 1]\right)$

$$\mu^2 \sim \bar{x}Q^2 + xq^2 \,. \tag{919}$$

In the LCSR framework, with $q^2 \to 0$, the relevant factorization scale becomes [140]

$$\mu^2 \sim \bar{x}Q^2 + xM^2 \,, \tag{920}$$

or, if $M^2 \gg s_0$ one has [3]

$$\mu^2 \sim \bar{x}Q^2 + xs_0 \,. \tag{921}$$

118 This difference can further be enhanced by Sudakov-type corrections [3]. For a discussion see, e. g., [476] and references therein.

Nevertheless, using an x-dependent factorization scale is rather inconvenient. Hence, we replace "x" by the average $\langle x \rangle$ which is varied within a certain range [3]:

$$\mu^2 = \langle x \rangle Q^2 + \langle x \rangle s_0 \,, \quad \frac{1}{4} < \langle x \rangle < \frac{3}{4} \,. \tag{922}$$

By the same token, the Borel parameter M^2 in LCSRs has to be selected carefully (cf. [464, 465]). In contrast to "classical" QCD sum rules, the twist expansion in LCSRs goes in powers of $1/(xM^2)$ rather than $1/M^2$. Therefore, in order to ensure the same hierarchy of contributions for two point functions within the SVZ approach, one has to use somewhat larger values of M^2 in the LCSR framework [3]. We choose the working window (cf. Section 4.2.1)

$$1 \text{ GeV} < M^2 < 2 \text{ GeV} \tag{923}$$

and $M^2 = 1.5 \text{ GeV}^2$ as the default value in our calculations. Similarly, we use the standard value $s_0 = 1.5 \text{ GeV}^2$ for the continuum threshold as well as the range

$$1.3 \text{ GeV}^2 < s_0 < 1.7 \text{ GeV}^2 \tag{924}$$

for the error estimates.

Possible corrections due to the finite widths of the ρ and ω resonances have not been considered. The estimates in [430] for such modifications suggest a possible enhancement of the FF by $2\% - 4\%$ in the small-to-medium Q^2 region, i. e., where the resonance part dominates. We believe, that these uncertainties are effectively covered by our (conservative) choice of the continuum threshold [3]. Finally, we use the values of the twist-three parameters h_q and h_s [265] specified in Table 8 and also use $\delta_M^{2(q)} = \delta_M^{2(q)} = 0.2 \pm 0.04 \text{ GeV}^2$ [428, 477] (at the scale $\mu_0 = 1$ GeV) for the normalization parameter of twist-four DAs (cf. Section 3.4.3).

4.3.5.2 *Models of distribution amplitudes and comparison with the data*

This part summarizes all results concerning models of $\eta^{(\prime)}$ distribution amplitudes which we have published in our recent work [3].

Based on Section 4.2, the corresponding LCSR calculations for $\gamma^*\gamma \to (\eta, \eta')$ TFFs, together with the experimental data [7, 8] is shown in Figure 35. In this context, the sum rule's dependence on the Borel parameter, continuum threshold, the normalization of higher twist contributions and, to a lesser extend, the factorization scale can be interpreted as an intrinsic irreducible uncertainty of the LCSR method (see [3]). Within Figure 35, these "errors" are shown as dark blue bands. Besides, in order to reduce the number of required parameters, the FKS mixing scheme [9, 15] is used. By assuming that it holds for complete wave functions, e. g., at an *ad hoc* scale $\mu_0 = 1$ GeV, this working hypothesis can be extended to the level of DAs (cf. Chapter 3). As a possible error estimate for this approach, the parameters given by Equation 280 can be varied around their central values, while studying the implied change of the sum rule results. Consequently, a combination[119] with the intrinsic LCSR uncertainties gives rise to an estimate for the total errors which are depicted in Figure 35 by light blue bands. One may expect, that the bulk part of these uncertainties can be eliminated, when, e. g., first-principle lattice calculations for the coupling constants become available.

Another point concerns the form factors' behavior at large photon virtualities which has been

119 Here, we assume, that all errors are statistically independent, i. e., we may add them in quadrature.

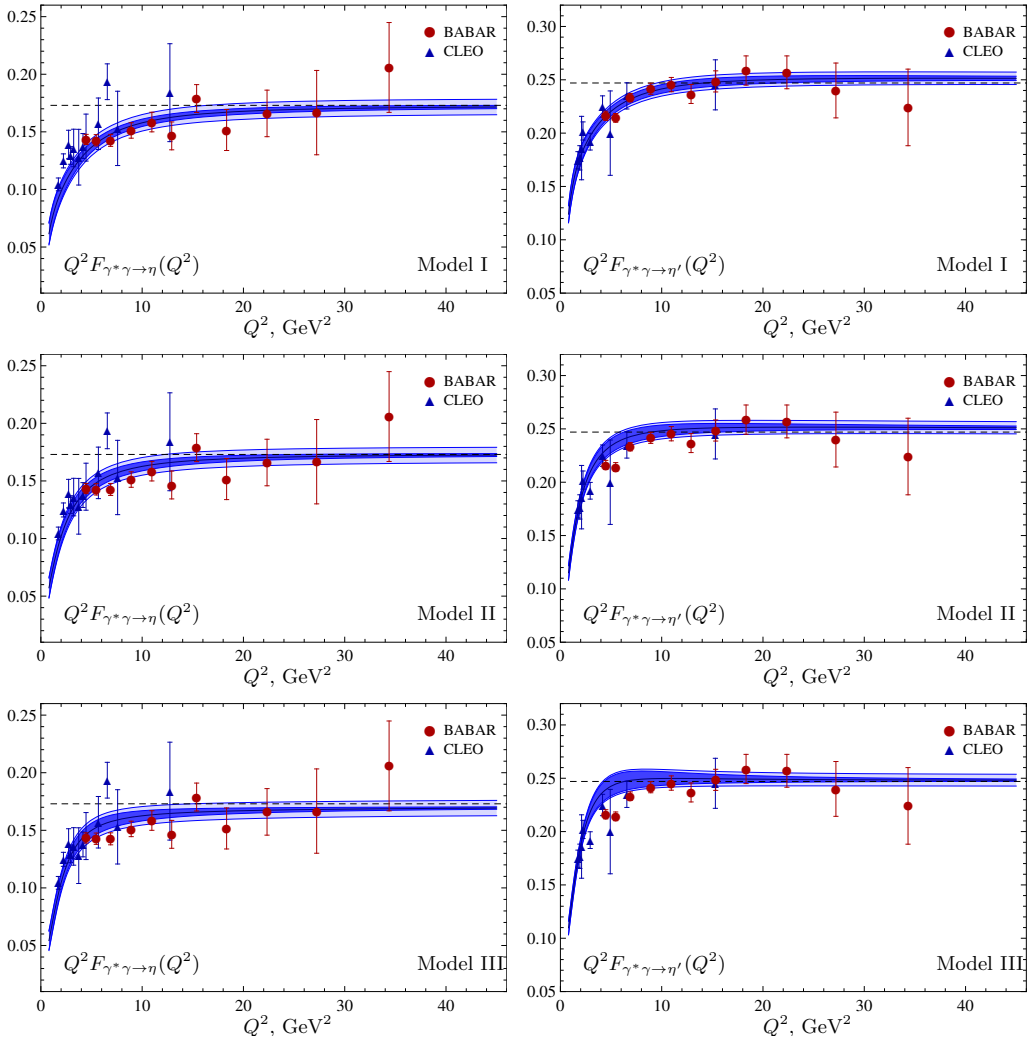

Figure 35: Based on [7, 8] the scaled FFs (in GeV) for $\gamma^*\gamma \to \eta$ (left panels) and $\gamma^*\gamma \to \eta'$ (right panels) transitions are compared to the described LCSR calculations, while using three different models of the twist-two DAs (specified in Table 14) as input. Asymptotic values of the TFFs are shown by the horizontal dashed lines and correspond to the central values mentioned in Equation 280. The depicted dark blue shaded areas correspond to those uncertainties of the calculated scaled FF that are caused by the involved LCSR (M^2, s_0) and higher twist parameters $(h_q, h_s, \delta_M^{2(q)}, \delta_M^{2(s)})$ as well as the varied factorization scale μ (see Section 4.3.5.1). On this basis, the light blue bands are obtained by further adding the error estimates for the FKS parameters, as listed in Equation 280 (see also [3]).

discussed in Section 4.3.3. According to Equation 907, the asymptotic values for $\gamma^*\gamma \to \eta'$ transitions differ considerably from the one assumed in [7, 20, 28]. This is an effect of the finite renormalization correction to the flavor singlet contribution (see Equation 905). Note, that experimental measurements for both η and η' form factors at large momentum transfers are now consistent with the expected asymptotic behavior (see Figure 35).

As a remaining non-perturbative input, we finally require the distribution amplitudes' shape

Model	$c_2^{(q)}$	$c_2^{(s)}$	$c_4^{(q)}$	$c_4^{(s)}$	$c_2^{(g)}$
I	0.10	0.10	0.10	0.10	−0.26
II	0.20	0.20	0.0	0.0	−0.31
III	0.25	0.25	-0.10	-0.10	−0.25

Table 14: Gegenbauer coefficients of three sample models for the η and η' twist-two DAs; both are written in the QF basis at a generic scale $\mu_0 = 1$ GeV.

parameters. In this connection, we do not view that underlying dependence as an "uncertainty". Indeed, the following aspects should be emphasized [3]:

- On the one hand, extraction of information about the DAs is the primary motivation behind this study of TFFs.
- On the other hand, lowest non-trivial moments of DAs can also be studied via lattice QCD [267, 478] which may then serve as input for a possible cross-check with available FF data.

While we strictly focus on the first aspect, such lattice calculations are ongoing and the corresponding parameters will eventually be known to a sufficient precision in the near future[120] [3]. This leads us back to the FKS approximation (cf. Equation 315) where the remaining information on η and η' DAs is encoded in a set of three constants $\left(c_{2n}^{(q)}(\mu_0), c_{2n}^{(s)}(\mu_0), c_{2n}^{(g)}(\mu_0)\right)$, given for each $n \in \mathbb{N}$. The non-strange coefficients $c_{2n}^{(q)}(\mu_0)$ should, in accordance with Section 4.3.1 and Section 4.3.2, be similar to the corresponding pion distribution amplitude's Gegenbauer moments $a_{2n}^{\pi}(\mu_0)$ (see Equation 895). Unfortunately, the situation with the pion DA is far from being settled (cf. [1, 281]). This is due to the discussed *BABAR* puzzle and an insufficient accuracy of the existing QCD sum rule as well as lattice calculations (see [1, 3, 281] and references therein).

Because of this uncertainty, we consider three different models of the $\eta^{(\prime)}$ DA, as specified in Table 14. These results are based on popular models for the pion DA, i. e., we choose $c_n^{(q)}$ to be in the range of a_n^{π}, while $SU(3)_F$-breaking effects were neglected. Appropriately, the related gluonic shape parameters are fitted to describe the experimental data. In particular, we suggest the following models:

- MODEL I: This first model corresponds to the pion DA developed to describe the Belle data (cf. Table 12, truncated at $n \geqslant 6$).
- MODEL II: The second model resembles a typical ansatz used in vast literature on the weak $B \to \pi$ decays.
- MODEL III: The third model with a negative $n = 4$ coefficient is advocated by the Bochum-Dubna group (see [431] and references therein).

On general grounds, it is expected, that the DAs of hadrons containing strange quarks are narrower than those built out of light u and d quarks (cf. [479]; $n \in \mathbb{N}$), i. e.,

$$c_{2n}^{(s)}(\mu_0) < c_{2n}^{(q)}(\mu_0) \,. \tag{925}$$

120 Evidently, this could, among other things, allow further conclusions on the precision of the sum rule method.

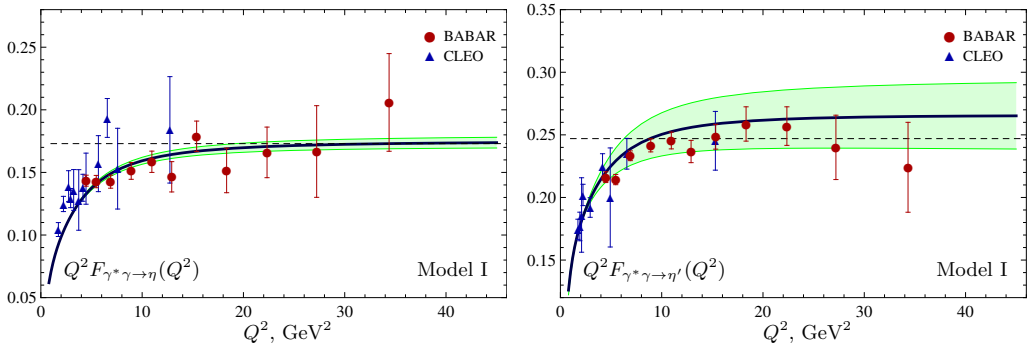

Figure 36: Analogous to Figure 35, the $\eta^{(\prime)}$ TFF is plotted (dark blue line) with all parameters of model I as input (see Table 14), except for the gluon Gegenbauer moment $c_2^{(g)}(\mu_0)$ which is per default set to zero. In order to study the impact of $\phi_M^{(g)}(x,\mu)$, its (remaining) gluonic moment is varied in an *ad hoc* interval $c_2^{(g)} = \pm 0.5$. The shaded area in light green shows the corresponding effect.

Existing numerical estimates of this effect, however, are rather inconclusive [3]. In fact, QCD sum rule calculations (see, e. g., [271, 314]) and lattice calculations [267, 478] do not seem to indicate any large differences at all. Therefore, we may assume $(n \in \mathbb{N})$

$$c_{2n}^{(s)}(\mu_0) \approx c_{2n}^{(q)}(\mu_0) \tag{926}$$

for the present study. To further investigate the influence of this strange quark components, we may assume

$$c_{2n}^{(s)}(\mu_0) \stackrel{!}{=} 0\,, \tag{927}$$

which is probably rather extreme. Consequently, the $\gamma^*\gamma \to \eta$ TFF gets increased by $5\% - 6\%$, while the $\gamma^*\gamma \to \eta'$ FF decreases by about $4\% - 5\%$ for $Q^2 > 5$ GeV^2 as compared to the results shown in Figure 35. Moreover, the gluon DA mainly contributes to the η' FF, whereas its effect on the η meson is small. This dependence is illustrated in Figure 36 where we plot model I for different values of the gluonic coefficient (see Table 14). Note, that the contributions from the gluon DA is significantly enhanced (by a factor $5/3$ for large Q^2) when including the (NLO) charm quark corrections. They are, therefore, an important innovation that goes along with this work. Furthermore, all three models in Table 14 lead to an equally good description of the experimental data at large $Q^2 > 10 - 15$ GeV^2, but differ perceptibly within the realm of small and intermediate momentum transfers, where model I seems to be preferred. Unfortunately, the given uncertainties related to LCSR calculations in this region increase. This is especially true for model III which suffers from a strong dependence on the Borel parameter. For this reason, non of the considered models can at that point be completely excluded. Based on the experiences with $\gamma^*\gamma \to \pi^0$ transitions (cf. Section 4.3.1), future experimental data on $\eta^{(\prime)}$ TFFs alone could be insufficient for a reliable determination of relevant shape parameters. Instead, one needs a combined effort of theory and experiment, e. g., by supplementing FF data with lattice calculations for selected key parameters (cf [3]).

Last but not least, as shown in Figure 37, we extend these results to a logarithmic scale in Q^2, where we have also included the time-like momentum transfer data point [351] at $|Q^2| = 112$ GeV^2 (red star) for comparison. The measurement of $e^+e^- \to \gamma^* \to \eta'\gamma$ appears to be in good agreement with the expected asymptotic behavior in the space-like region, whereas the result for $e^+e^- \to \gamma^* \to \eta\gamma$ is still considerably higher. This difference is interesting and surprising, since

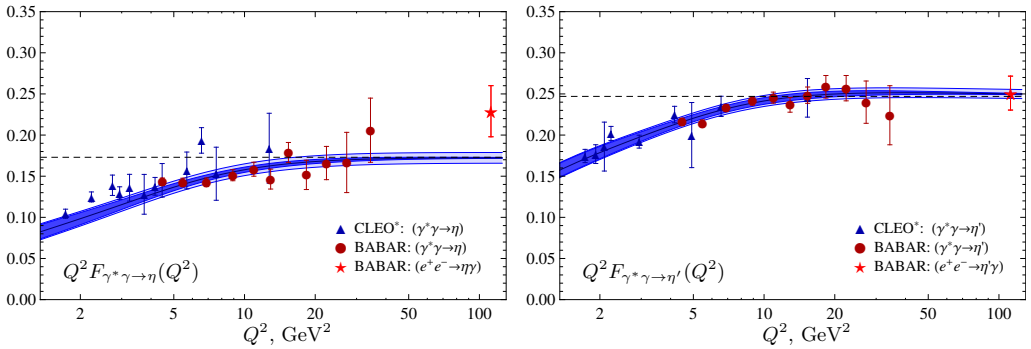

Figure 37: Similar to Figure 35, but here we are applying a logarithmic scale in Q^2. The underlying calculation uses the first model of Table 14. In addition, the time-like data points [351] at $|Q^2| = 112$ GeV^2 are shown by red stars for comparison (see [3]).

QCD effects, such as a possible Sudakov enhancement (see, e. g., [362, 480, 481]) of the time-like form factors compared to their space-like counterparts are universal and should, therefore, affect both η as well as η' production equally strong. Hence, it is natural to attribute the causes of these differences to non-perturbative phenomena, e. g., by considering corrections arising from end-point integration regions. Although a rigorous connection of such contributions to the DAs does not exist, one can plausibly argue, that large soft corrections are correlated with the end-point enhancement in DAs (see [3]). Thus, these are corrections of the same type, as discussed in conjunction with the *BABAR* puzzle (cf. [1, 3]). Accordingly, it is reasonable to expect, that if this large value of the time-like η FF is confirmed, its corresponding space-like counterpart should exhibit a similar scaling violation behavior, as observed by *BABAR* for the pion. In fact, the existing data (i. e., [7]) may support such a trend (see Figure 37), although it is not statistically significant (cf. [3]).

To summarize, in this subsubsection the existing FF data of [7, 8, 351] has been confronted with a refined full NLO LCSR calculation (see previous chapters for details). As a result, we suggest three different models (cf. Table 14) for the twist-two η and η' meson DAs. Moreover, in order to ultimately pin down the shape of these DAs, we conclude, that either more high precision measurements on, e. g., $\gamma^*\gamma \to (\eta, \eta')$ transitions for a wide range of momentum transfer or suitable lattice calculations are needed. Especially, the scaling behavior of the η TFF has to be clarified, which would also answer questions concerning the gluonic content of the $\eta - \eta'$ system, as well as the relevance and impact of possible $SU(3)_F$ corrections.

5 HEAVY TO LIGHT MESON TRANSITION FORM FACTORS

"With four parameters I can fit an elephant,
and with five I can make him wiggle his trunk."

— John v. Neumann (1903 – 1957)

In this chapter, we study the semileptonic $B, D_{(s)} \to \eta^{(\prime)}$ decays using the associated vector form factors f_{HM}^{+} $(H = B, D, D_s;\ M = \eta, \eta')$ within the LCSR approach. The heavy-to-light transitions $D_s \to \eta^{(\prime)} l \nu_l$ have been analyzed phenomenologically [30, 482] and via LO LCSRs [31], that were based on chiral currents, while including finite meson mass corrections. We improve these previous approaches in the following way:

i) Instead of chiral currents, we use standard interpolating and weak currents (see Section 5.1.2 for details). This allows us to take into account a broad spectrum of higher twist effects, including the dominant twist-three LO and NLO quark contributions (cf. Section 5.1.2.1, along with Section 5.1.2.3).

ii) Additionally, NLO twist-two gluon corrections are considered. The latter enable us to extract information on the gluonic content of the η' meson and in particular, its (twist-two) gluon DA.

iii) Moreover, our results for the decay form factors agree (within the given uncertainties) with those of [31] (see, e. g., Section 5.3).

Besides, the decays $B \to \eta/\eta' l \nu_l$ were analyzed in [483] at LO and in [32] at the same level of accuracy as in this work. We improve these calculations by performing an analysis of both, the branching fractions and their ratios (cf. Section 5.3).
Motivation to perform these calculations for all three cases $H = B, D, D_s$ comes from an expected increase in the experimental accuracy (see [2] for an extended discussion). Thus, future experiments for this complete set of meson decays will most likely provide evidence for the underlying gluonic content of the η' particle.

5.1 PQCD APPROACH

This subsection forms the basis for Section 5.2 an the related numerical analysis in Section 5.3. Accordingly, in this context the following issues are elaborated:

- For $B \to \eta^{(\prime)}$ transition form factors the B meson decay constant f_B is needed. By following the standard approach (cf. [320, 322]), we, therefore, prepare corresponding SVZ sum rule calculations and extract f_B from the latter.
- Furthermore, we calculate the $H \to M l \nu_l$ $(H = D, D_s, B;\ M = \eta, \eta')$ transition form factor at LO in α_S within the collinear factorization ansatz, while using the new $\eta^{(\prime)}$ DAs up to twist-four accuracy. Besides, omitted higher twist effects are estimated and discussed below.
- Most importantly, we investigate the applicability of the state mixing ansatz as implied by the FKS scheme. This is done by applying the customized NLO QCD evolution of singlet and octet DAs, including a very short numerical analysis.

Decay mode	axial-vector current	pseudoscalar current
$D^+ \to l^+ \nu_l$	$j_\mu^{D^+} \coloneqq \bar{d}\gamma_\mu\gamma_5 c$	$j_5^{D^+} = (m_c + m_d)\,\bar{d} i\gamma_5 c$
$D_s^+ \to l^+ \nu_l$	$j_\mu^{D_s^+} \coloneqq \bar{s}\gamma_\mu\gamma_5 c$	$j_5^{D_s^+} = (m_c + m_s)\,\bar{s} i\gamma_5 c$
$B^- \to l^- \bar{\nu}_l$	$j_\mu^{B^-} \coloneqq \bar{u}\gamma_\mu\gamma_5 b$	$j_5^{B^-} = (m_b + m_u)\,\bar{u} i\gamma_5 b$

Table 15: Quick reference guide for the underlying axial-vector currents j_μ^H $(H = D, D_s, B)$ of purely leptonic decays $H \to l\nu_l$ as well as related divergences $\partial^\mu j_\mu^H = j_5^H$ (cf. Section 2.6.1).

- Additionally, a strategy is reviewed which allows an inclusion of existing NLO corrections (cf. [32, 320, 322]) as well as their adaption to the $D_{(s)} \to \eta^{(\prime)}$ case.

Therefore, this subsection represents a relevant contribution, extending previous studies.

5.1.1 *Heavy-Meson Decay Constants*

In this subsection we briefly outline the SVZ sum rule method, while focusing on heavy decay constants, such as f_B and $f_{D_{(s)}}$. These are necessary for a subsequent numerical evaluation of the related $B^- \to \eta^{(\prime)} l^- \bar{\nu}_l$ and $D_{(s)}^+ \to \eta^{(\prime)} l^+ \nu_l$ form factors in Section 5.3. Therefore, we present all required basics in the context of an example calculation, while further clarifying the phenomenological necessity for this ansatz.

According to Section 2.6.2, the charged pseudoscalar mesons under consideration can decay into lepton-neutrino pairs $H^+ \to l^+ \nu_l$ (e. g., $H^+ = \pi^+, K^+, D^+, D_s^+, B^+, \dots$), thus providing complementary information to other processes, such as inclusive or exclusive semileptonic decays. Based on the spectator model, purely leptonic decays of heavy mesons, that are formed from valence quarks $\bar{u}_1 d_1$ (u_1 is an up-type and d_1 a down-type quark), can be related to a corresponding decay rate $\Gamma(H \to l\nu_l)$ via the associated subprocess $u_1 \to d_1 + W^+$ (see Table 15). At leading order this annihilation process is, therefore, given by [225, 245]

$$\Gamma(H \to l\nu_l) = \frac{G_F^2}{8\pi} f_H^2 \left|V_{u_1 d_1}\right|^2 m_H m_l^2 \left(1 - \frac{m_l^2}{m_H^2}\right), \tag{928}$$

which includes a product of the decay constant (see Table 15)

$$i f_H P_\mu = \langle 0 | j_\mu^H | H(P) \rangle, \tag{929}$$

and the related CKM matrix element, i. e., its absolute value $\left|V_{u_1 d_1}\right|$. Consequently, by measuring these branching fractions and lifetimes, one may experimentally determine the product $f_H \left|V_{u_1 d_1}\right|$. This, however, offers the opportunity to extract f_H from $\Gamma(H \to l\nu_l)$ if $\left|V_{u_1 d_1}\right|$ is known and vice versa (see [225, 245, 484] for more details). Hence, a precise numerical value of associated CKM matrix elements is crucial for the determination of f_H. Unfortunately, there is a persistent tension [37] between the determination of $\left|V_{u_1 d_1}\right|$ from exclusive $B \to \pi l \nu_l$ and inclusive (charmless semileptonic) $B \to X_u l \nu_l$ decays[1], where X_u denotes all hadronic states, that contain a valence up-quark (see [37, 42, 360, 485–487]). Therefore, extracting f_B from QCD sum

1 As discussed in [37, 245], purely leptonic decays, such as $H \to l\nu_l$ proceed in the SM via axial-vector currents (see Table 15), while semileptonic transitions $H \to M l \nu_l$ $(H = \pi^0, \eta^{(\prime)}, \dots)$ involve weak vector currents (cf. Table 16). Both decay modes may involve the very same CKM matrix elements which can be determined accordingly. Hence, the comparison of these measurements for $\left|V_{u_1 d_1}\right|$ can be used to test the underlying standard model physics, in particular,

rules at $\mathcal{O}(\alpha_S)$ accuracy seems to be a viable solution for this specific problem (cf. also [32]).

The central object of that approach is given by a two-point correlation function [96, 488–502]

$$\Psi\left(q^2\right) \coloneqq i \int d^4x\, e^{iq\cdot x} \langle 0|\, T\left\{ j_5(x)\, j_5^\dagger(0)\right\} |0\rangle\,, \tag{930}$$

which includes the renormalization invariant (see, e. g., Section 2.6.2) operator $j_5 \coloneqq j_5^{B^-}$ (adapted to the notation of [488]). For positive momentum transfers $q^2 > 0$, this interpolating current gives rise to a hadronic spectrum, with corresponding quantum numbers, including the lowest lying resonance B^-. Accordingly, the related phenomenological spectral density [97, 488]

$$\rho_{ph}(s) = m_B^4 f_B^2 \delta\left(s - m_B^2\right) + \rho_{th}(s)\, \Theta\left(s - \bar{s}_0^B\right) \tag{931}$$

implies the Källén-Lehmann representation[2] and its Borel transform (see Section B.3)

$$\Psi\left(q^2\right) = \frac{m_B^4 f_B^2}{m_B^2 - q^2} + \int_{\bar{s}_0^B}^\infty ds \frac{\rho_{th}(s)}{s - q^2} + \text{subtractions} \tag{932}$$

$$\Rightarrow\ \hat{\Psi}\left(\overline{M}_B^2\right) = m_B^4 f_B^2 e^{-\frac{m_B^2}{\overline{M}_B^2}} + \int_{\bar{s}_0^B}^\infty ds\, \rho_{th}(s)\, e^{-\frac{s}{\overline{M}_B^2}}\,. \tag{933}$$

On the other hand, for $-q^2 \ll \Lambda_{QCD}^2$ Equation 930 can be calculated via a short distance OPE (see Section A.15). A posteriori, the resulting amplitudes may exhibit branch cuts along the real axis, which entails a dispersive representation similar to

$$\Psi^{(OPE)}\left(q^2\right) = \frac{1}{\pi} \int_0^\infty ds \frac{\mathrm{Im}_s\left\{\Psi^{(OPE)}(s)\right\}}{s - q^2} + \text{subtractions}\,, \tag{934}$$

$$\Rightarrow\ \hat{\Psi}^{(OPE)}\left(\overline{M}_B^2\right) = \frac{1}{\pi} \int_0^\infty ds\ \mathrm{Im}_s\left\{\Psi^{(OPE)}(s)\right\} e^{-\frac{s}{\overline{M}_B^2}}\,, \tag{935}$$

where $\mathrm{Im}_s\left\{\Psi^{(OPE)}(s)\right\}$ includes terms proportional to $\Theta\left(s - m_b^2\right)$ (see [488] and discussion below). Under the assumption of quark-hadron duality (see Section 4.2.1) Equation 933 and Equation 935 can be related, leading to the SVZ sum rule for f_B (cf. [488]):

$$m_B^4 f_B^2 = \frac{1}{\pi} \int_0^{\bar{s}_0^B} ds\ \mathrm{Im}_s\left\{\Psi^{(OPE)}(s)\right\} e^{\frac{m_B^2 - s}{\overline{M}_B^2}}\,. \tag{936}$$

its electroweak charged-current interactions and corresponding $(V-A)$ structure. Thus, large discrepancies between associated measurements for $\left|V_{u_1 d_1}\right|$ could be caused by (small) right-handed admixtures to the standard model weak currents, indicating effects beyond the SM (see [32, 37, 245]).

2 The subtraction polynomials, which depend on q^2 (see Section 4.2) will not be specified at this point (see [503] for details), since they are removed via a Borel transformation.

The input of Equation 936 can be calculated with the same tools as discussed in Section 2.4. For instance, at leading order in α_S one easily gets[3] $(\delta m_\pm \coloneqq m_b \pm m_u)$

$$\begin{aligned}
\Psi^{(\mathrm{OPE})}\left(q^2\right)\Big|_{\text{bubble}} &= \delta m_+^2\, i \int d^4x\, e^{iq\cdot x} \langle 0|\bar{u}(x) i\gamma_5 \underbrace{b(x)\bar{b}(0)} i\gamma_5 u(0)|0\rangle \\
&= 3\delta m_+^2\, i \int \frac{d^4k}{(2\pi)^4}\, \mathrm{Tr}\left\{ \frac{\not{k}+m_u}{k^2-m_u^2} i\gamma_5 \frac{\not{k}+\not{q}+m_b}{(k+q)^2-m_b^2} i\gamma_5 \right\} \\
&= \frac{3\delta m_+^2}{8\pi^2}\left[\left(q^2-\delta m_-^2\right) B_0\left(q^2; m_u^2, m_b^2\right) - A_0\left(m_u^2\right) - A_0\left(m_b^2\right) \right] \\
&= \frac{3m_b^2}{8\pi^2}\left[\left(q^2-m_b^2\right) B_0\left(q^2; 0, m_b^2\right) - A_0\left(m_b^2\right) \right] + \mathcal{O}\left(m_u^2\right) ,
\end{aligned} \tag{937}$$

as well as (see Equation 100)

$$\begin{aligned}
\Psi^{(\mathrm{OPE})}\left(q^2\right)\Big|_{\langle\bar{q}q\rangle} &= \delta m_+^2\, i \int d^4x\, e^{iq\cdot x} \langle 0|\bar{u}(x) i\gamma_5 \underbrace{b(x)\bar{b}(0)} i\gamma_5 u(0)|0\rangle \\
&= \delta m_+^2\, i \int d^4x\, e^{iq\cdot x} \langle 0|\bar{u}_\alpha^a(x) u_\omega^f(0)|0\rangle \left[i\gamma_5\right]_{\alpha\beta} \underbrace{b_\beta^a(x)\bar{b}_\rho^f(0)} \left[i\gamma_5\right]_{\rho\omega} \\
&= \frac{m_b^3\langle\bar{u}u\rangle}{q^2-m_b^2} + \mathcal{O}\left(m_u^2\right) .
\end{aligned} \tag{938}$$

When neglecting all light-quark mass corrections, the analytical continuation $q^2 \to s$ implies[4]:

$$\mathrm{Im}_s\left\{\Psi^{(\mathrm{OPE})}\left(q^2\right)\right\}\Big|_{\text{bubble}} = \frac{3m_b^2}{8\pi}\frac{\left(s-m_b^2\right)^2}{s}\Theta\left(s-m_b^2\right) , \tag{939}$$

$$\mathrm{Im}_s\left\{\Psi^{(\mathrm{OPE})}\left(q^2\right)\right\}\Big|_{\langle\bar{q}q\rangle} = -\pi m_b^3\langle\bar{u}u\rangle\,\delta\left(s-m_b^2\right) . \tag{940}$$

As a result, we reproduce the well-known findings of [244, 257, 488]:

$$f_B^2 = \frac{3m_b^2}{8\pi^2 m_B^4}\int_{m_b^2}^{\bar{s}_0^B} ds \frac{\left(s-m_b^2\right)^2}{s} e^{\frac{m_B^2-s}{M_B^2}} - \frac{m_b^3\langle\bar{u}u\rangle}{m_B^4} e^{\frac{m_B^2-m_b^2}{M_B^2}} + \mathcal{O}(\alpha_S) . \tag{941}$$

For the intended accuracy, however, Equation 941 has to be retrofitted with NLO perturbative and condensate contributions which can be borrowed from [488] (see Section A.17).

The subsequent numerical evaluation is carried out in two basic steps (see also Section 4.2.1):

i) One starts with a determination of the Borel window (see Section B.3), i. e., a domain for $\overline{M}_B^2$, where truncation errors are sufficiently suppressed, while continuum contributions[5] amount to less than ~ 30% (see, e. g., [95, 97, 244, 322]).[6]

ii) For a given Borel window the continuum threshold $\bar{s}_0^B$ can be determined via an additional sum rule (resulting from Equation 936)

$$m_B^2 = \frac{\overline{M}_B^4 \frac{d}{d\overline{M}_B^2}\left\{ f_B^2 m_B^4 \exp\left(-\frac{m_B^2}{\overline{M}_B^2}\right)\right\}}{f_B^2 m_B^4 \exp\left(-\frac{m_B^2}{\overline{M}_B^2}\right)} = \frac{\int_0^{\bar{s}_0^B} ds\, s\, \mathrm{Im}_s\left\{\Psi^{(\mathrm{OPE})}(s)\right\} e^{-\frac{s}{\overline{M}_B^2}}}{\int_0^{\bar{s}_0^B} ds\, \mathrm{Im}_s\left\{\Psi^{(\mathrm{OPE})}(s)\right\} e^{-\frac{s}{\overline{M}_B^2}}} \tag{942}$$

3 Here, we use the same formalism as in Section 4.1.4.

4 The imaginary part of Equation 939 corresponds to a simple free-quark approximation. Therefore, it is a purely mathematical object (see, e. g., [97]).

5 This refers to the part of the dispersion integral with $s \geqslant \bar{s}_0^B$.

6 The first restriction sets a rough lower bound for $\overline{M}_B^2$, whereas the second condition leads to an upper bound for the Borel parameter.

Decay mode	meson interpolating current	weak current
$D^+ \to \eta^{(\prime)} l^+ \nu_l$	$j_{D^+} \coloneqq m_c \bar{d} i\gamma_5 c$	$V_\mu^{D^+\eta^{(\prime)}} \coloneqq \bar{d}\gamma_\mu c$
$D_s^+ \to \eta^{(\prime)} l^+ \nu_l$	$j_{D_s^+} \coloneqq m_c \bar{s} i\gamma_5 c$	$V_\mu^{D_s^+\eta^{(\prime)}} \coloneqq \bar{s}\gamma_\mu c$
$B^- \to \eta^{(\prime)} l^- \bar{\nu}_l$	$j_{B^-} \coloneqq m_b \bar{u} i\gamma_5 b$	$V_\mu^{B^-\eta^{(\prime)}} \coloneqq \bar{u}\gamma_\mu b$

Table 16: Currents entering the correlation function of Equation 946 (see also [2]).

and the related experimental value of m_B (see also [488]).

As a result, we determine the following set of parameters ($m_{B^+} = (5279.26 \pm 0.17)$ MeV [42]):

$$\bar{s}_0^B = (35.75 \pm 0.25)\ \text{GeV}^2\,, \quad \overline{M}_B^2 = (5 \pm 1)\ \text{GeV}^2\,, \tag{943}$$

which are close to the ones obtained in [319, 320]. This issue will be further elaborated in Section 5.3, where the discussed two-point sum rule is embedded within a corresponding LCSR for $B \to \eta^{(\prime)} l \nu_l$ transition form factors.

Thus, all necessary analytical tools are now at hand, and we may focus on the actual (numerical) calculation of heavy-to-light form factors.

5.1.2 *Perturbative calculations*

This subsection provides all required analytical results to formulate the associated LCSR in Section 5.2. In the following, we, therefore, explicitly calculate LO corrections up to twist-four accuracy and adjust existing NLO contributions accordingly. This allows a state-of-the-art phenomenological analysis as carried out in Section 5.3.

For the exploration of meson-to-meson transition amplitudes standard three-point sum rules proved to be particularly useful, since they successfully describe a multitude of different problems, including pion electromagnetic form factors at intermediate momentum transfers and semileptonic D_s decays (see, e. g., [30, 97, 445, 504, 505]). Nevertheless, this extension of the standard SVZ sum rule method to three-point functions possesses several major problems, which decisively restrict its applicability (following [445]):

- The underlying short distance OPE and associated condensate expansion can be inadequate, causing problems within the systematics of power counting. This in some cases leads to a breakdown of the OPE beyond a relatively narrow kinematical interval[7].
- The calculation of three-point functions usually includes double dispersion relations which are connected to another fundamental issue of this ansatz. In fact, the underlying hadronic representation exhibits associated matrix elements at zero momentum transfer, leading to a contamination of the ground state by its excitations. On a theoretical level the latter are

7 As discussed in [97, 445], three-point sum rules for the pion electromagnetic form factor $F_\pi(Q^2)$ are only legitimate in the interval of intermediate momentum transfers $0.5\ \text{GeV}^2 \leqslant Q^2 \leqslant 1.5\ \text{GeV}^2$. For larger values of Q^2, the contributions related to higher dimensional condensates contain terms $\sim Q^2/M^2$, overpowering lower dimensional corrections and leading to an unphysical rise at $Q^2 \geqslant 3-5\ \text{GeV}^2$ (see also [97, 445, 504, 505]). A similar hierarchy can be detected within the $A_1^{B\to\rho}$ form factor for $B \to \rho e \nu_e$ decays at maximum recoil, thus indicating a general problem of this approach (cf. [445, 506]).

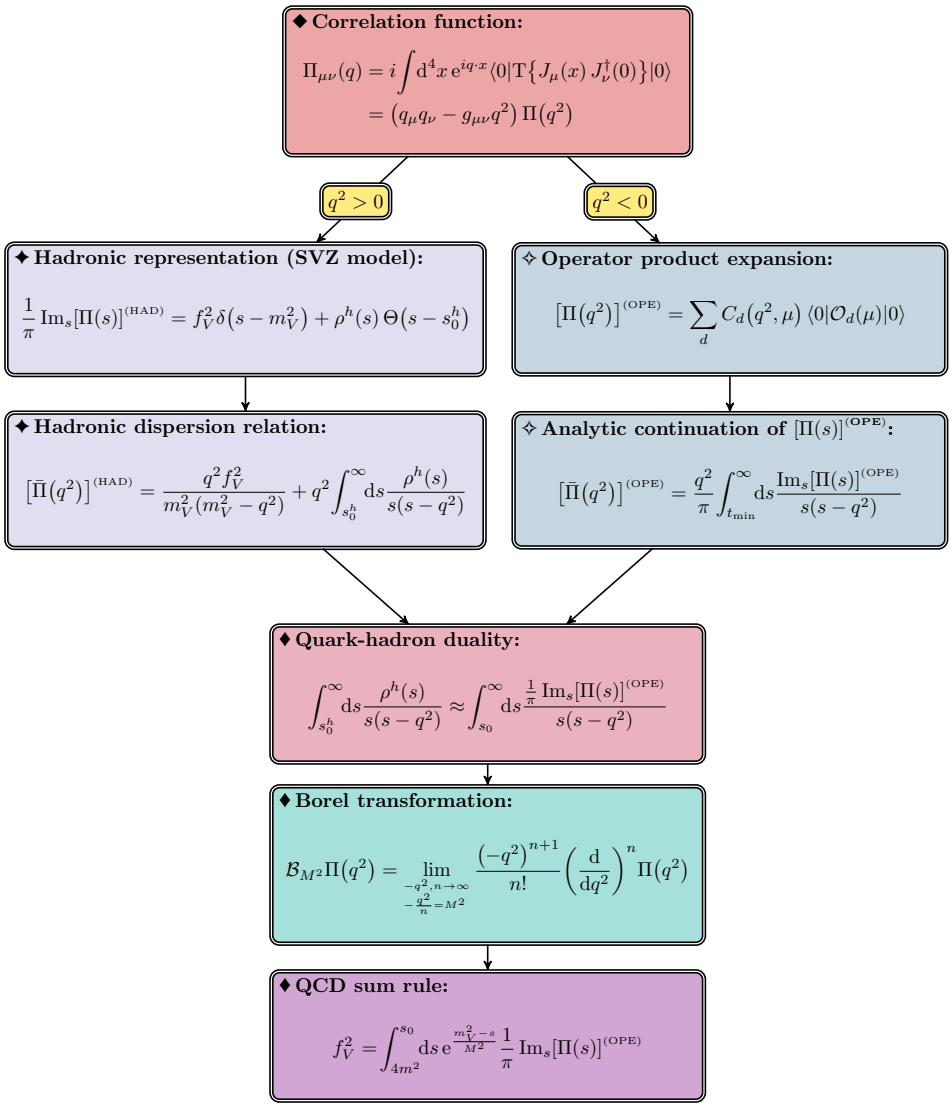

Figure 38: Basic steps towards the SVZ sum rules for a generic decay constant f_V (see also [97, 257]). This observable is related to the ground-state vector meson $\langle V(q)|J_\mu|0\rangle = f_V m_V \varepsilon_\mu^*$ ($\varepsilon\cdot q = 0$) in the channel of the current J_μ (e. g., $J_\mu \equiv \partial_\mu^{\mathrm{em}}$). A similar example has been considered in Section 2.4, assuming the light-quark case $m^2 \ll \Lambda_{\mathrm{QCD}}^2 \ll Q^2$ at large Euclidean virtualities (cf. Section 4.2.1).

represented by single-pole terms, while in this particular case the contribution of interest corresponds to a double-pole correction which cannot simply be isolated via the standard Borel transformation (cf. [97, 445]). Instead, more modifications are needed (cf. [443, 504, 505, 507, 508]). A posteriori, these and analogous[8] technical problems entail a considerable loss of accuracy for the sum rule (see [445] and references therein).

8 For instance, (see [445]) transition matrix elements with large mass differences are also problematic.

Historically, light-cone sum rules [141–143, 443, 444] were developed to circumvent these problems as far as possible, by implementing a modified factorization approach (see Section 4.2.1), which substitutes the expansion at short distances, with one in the transverse distances between partons within the infinite momentum frame [445, 464]. That also solves another critical problem concerning the end-point corrections. While in this context three-point sum rules[9] may become unreliable, LCSRs are fully consistent with QCD, i. e., both hard scattering as well as soft contributions can be systematically taken into account, hence, reproducing the observed behavior (for a detailed discussion see [97, 445, 464]). The most compelling evidence, that LCSRs are implementing the correct physical assumptions and quantum numbers (e. g., conformal spin, etc.) to describe heavy-to-light form factors, would be given by a good agreement with experimental data. Fortunately, the LCSR program, with its steady improvements, has been successfully applied to various problems in heavy-meson physics (see [32, 257, 320] and references therein).

This motivates the following considerations which are largely inspired by [32, 319, 320, 322]. As a starting point, we may resume the discussion on heavy-to-light form factors of Section 2.6.2. They are defined by on-shell matrix elements[10] [2, 322] $(q^\mu := p_H^\mu - p^\mu)$

$$\begin{aligned}\langle M(p)|V_\mu^{HM}|H(p_H)\rangle &= \left((p+p_H)_\mu - \frac{m_H^2-m_M^2}{q^2}q_\mu\right)f_{HM}^+\left(q^2\right) + \frac{m_H^2-m_M^2}{q^2}q_\mu f_{HM}^0\left(q^2\right)\\ &= 2f_{HM}^+\left(q^2\right)p_\mu + \left(f_{HM}^+\left(q^2\right)+f_{HM}^-\left(q^2\right)\right)q_\mu\,,\end{aligned} \tag{944}$$

describing an underlying $H\to M l\nu_l$ transition $\left(H = D^+, D_s^+, B^-;\, M = \pi, K, \eta, \eta'\right)$ via the standard weak current V_μ^{HM} (see Table 16). An important kinematic constraint arises from the chosen parametrization in Equation 944, i. e.,

$$f_{HM}^0\left(q^2\right) = f_{HM}^+\left(q^2\right) + \frac{q^2}{m_H^2-m_M^2}f_{HM}^-\left(q^2\right)\,. \tag{945}$$

Within the limit $q^2\to 0 \Rightarrow f_{HM}^+(0) = f_{HM}^0(0)$ (see also Section 2.6.2). Furthermore, $f_{HM}^0\left(q^2\right)$ enters semileptonic decays proportional to $\sim m_l^2$ and is, therefore, irrelevant for light leptons $(l = e, \mu)$, where the vector form factor dominates (see Section 2.6.2). Most importantly, both form factors can be extracted from [2, 320, 322]

$$\begin{aligned}F_\mu^{HM}(p,q) &= i\int d^4x\, e^{iq\cdot x}\langle M(p)|T\left\{V_\mu^{HM}(x)\, j_H^\dagger(0)\right\}|0\rangle\\ &= F^{HM}\left(q^2,(p+q)^2\right)p_\mu + \tilde{F}^{HM}\left(q^2,(p+q)^2\right)q_\mu\,,\end{aligned} \tag{946}$$

9 As discussed in Section 2.4, an expansion in slowly varying vacuum fields is inadequate, if short distance subprocesses are involved [445, 464], as it holds true for hard exclusive processes.

10 Another possible form factor parametrizes matrix elements similar to [322] $\left(\text{e. g., } H = B^-,\, M = \eta^{(\prime)}\right)$

$$\langle M(p)|J_\mu^{HM}|H(p_H)\rangle = \frac{if_{HM}^T(q^2)}{m_H+m_M}\left[q^2(p_H+p)_\mu - \left(m_H^2-m_M^2\right)q_\mu\right]\,,$$

that include penguin currents, such as $J_\mu^{B\eta^{(\prime)}} = \bar{u}\sigma_{\mu\nu}q^\nu b$. Those operators may occur in the construction of weak effective Hamiltonians, e. g., within those describing gluomagnetic penguins [509]

$$T = i\bar{s}_R\sigma_{\mu\nu}T^A d_L G^{A,\mu\nu}\,,$$

with a corresponding Wilson coefficient that is then proportional to the strange quark mass m_s. For convenience, we have omitted the resulting renormalization scale dependence of $f_{HM}^T\left(q^2\right)$ (see also [322]). Nevertheless, this tensor form factor is only relevant in rare decays, such as $B\to\pi l^+l^-$ or $B_s\to\eta^{(\prime)}l^+l^-$.

which yields two separate dispersion relations in the variable $(p+q)^2$ (omitting subtractions)

$$F^{HM}\left(q^2,(p+q)^2\right)=\frac{2m_H^2 f_H f_{HM}^{+}(q^2)}{m_H^2-(p+q)^2}+\int_{s_0^h}^{\infty}\mathrm{d}s\,\frac{\rho_{HM}(q^2,s)}{s-(p+q)^2}\,, \tag{947}$$

$$\widetilde{F}^{HM}\left(q^2,(p+q)^2\right)=\frac{m_H^2 f_H\left(f_{HM}^{+}(q^2)+f_{HM}^{-}(q^2)\right)}{m_H^2-(p+q)^2}+\int_{\tilde{s}_0^h}^{\infty}\mathrm{d}s\,\frac{\widetilde{\rho}_{HM}(q^2,s)}{s-(p+q)^2}\,, \tag{948}$$

after inserting a complete set of hadronic states[11] between the interpolating currents j_H (see Table 16) and V_μ^{HM}, while separating the associated ground states. Those correspond to the two independent Lorentz structures of Equation 946, which are also accessible via a conformal OPE, particularly, for $(p+q)^2\ll m_Q^2$ as well as fixed momentum transfers $m_Q^2-q^2\geqslant\mathcal{O}(\Lambda_{QCD}m_Q)$ [322, 445] (cf. Section 5.1.2.1), where they can be written in the general form (cp. Equation 738; analogously for $F^{HM}\leftrightarrow\widetilde{F}^{HM}$, along with $T_n^{(t)}\leftrightarrow\widetilde{T}_n^{(t)}$)

$$\left[F^{HM}\left(q^2,(p+q)^2\right)\right]_{OPE}=\sum_{n=0}^{\infty}\sum_{t}\left(\frac{\alpha_S C_f}{4\pi}\right)^n F_{n,t}^{HM}\left(q^2,(p+q)^2\right)\,, \tag{949}$$

with associated convolutions[12] $\left(\int\mathcal{D}\underline{\alpha}=\left[\prod_i\int_0^1\mathrm{d}\alpha_i\right]\delta\left(1-\sum_j\alpha_j\right)\right)$

$$F_{n,t}^{HM}\left(q^2,(p+q)^2\right)=\int\mathcal{D}\underline{\alpha}\,T_n^{(t)}\left(q^2,(p+q)^2,m_Q^2,\underline{\alpha},\mu^2\right)\phi_M^{(t)}\left(\underline{\alpha},\mu^2\right)\,. \tag{950}$$

Here, "t" denotes the collinear twist, "μ" represents the chosen factorization scale and "$\underline{\alpha}$" collects all related parton momentum fractions.[13] Besides, the process-dependent perturbative kernels $T_n^{(t)}$, in general, exhibit a heavy-quark propagator, whereas $T_{n\geqslant 1}^{(t)}$ also include hard-gluon exchanges. Moreover, apart from the present notation in Equation 950, the universal meson DAs $\phi_M^{(t)}$ coincide with those of Chapter 3, i. e., we may use $\phi_M^{(2)}\in\left\{\phi_M^{A}\right\}_{A=8,0,g}$ and so forth. Without reprising previous arguments, this approach provides a good approximation for the two-point correlation function of Equation 946, i. e., higher twist effects are in general subdominant (cf. [142, 269, 319, 320]) and can be neglected[14] at $t\geqslant 5$ (see discussion in Section 5.1.2.1).

In the next subsections we can, therefore, focus our attention on corrections up to twist-four.

5.1.2.1 *Leading-order higher twist corrections*

Higher twist corrections to $B\to\pi,K$ transition form factors have been known since the early 1990s [510] and were constantly improved since then, culminating in the inclusion of $SU(3)_F$-breaking as well as quark along with meson mass corrections at LO accuracy (cf. [246, 320–322, 371, 511–519]). Among other reasons, this was possible due to advances in the exploration of pseudoscalar non-singlet meson DAs (cf. [269, 271, 272, 314, 520, 521]). Nevertheless, the research of $B^-\to\eta^{(\prime)}l^-\bar{\nu}_l$ and $D_{(s)}^+\to\eta^{(\prime)}l^+\nu_l$ decays has received much less attention, leading to

11 Only those with H-meson quantum numbers will contribute.
12 Similar to Equation 334, for $\underline{\alpha}\in\mathbb{R}^n$ we use $\underline{\alpha}=(\alpha_1,\ldots,\alpha_n)$.
13 At this point, we use a notation complementary to Equation 738.
14 As mentioned in [257], multi-parton corrections, as well as terms with twist larger than four should amount to ∼ 1% of the total LCSR result for $B\to\pi$ transition form factors. On the other hand, twist-three effects turn out to be numerically significant (cf. [320]).

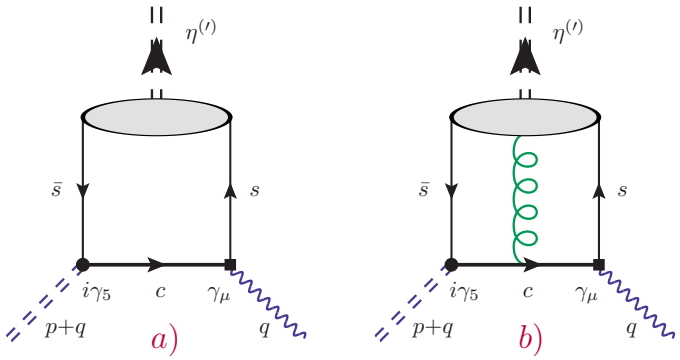

Figure 39: LO two- and three-particle contributions to the operator product expansion of Equation 946 for $D_s^+ \to \eta^{(\prime)} l^+ \nu_l$ transitions. Here, the vertex depicted by a black square (■) corresponds to $V_\mu^{D_s^+ \eta^{(\prime)}}$, while its dotted counterpart (●) represents $j_{D_s^+}$ (see Table 16). Accordingly, related external currents are represented by wave and double-dashed lines and heavy quark flavors are shown as thick black lines. See also Figure 41) for corresponding NLO diagrams.

only a handful of theoretical (see [31, 32, 483]) and phenomenological studies[15] (e. g., [30, 482, 522]). Furthermore, let us emphasize that the calculations within [31, 483] are actually restricted to $B, D_s \to \eta$ form factors and have been carried out for correlation functions with so called chiral currents $\bar{b} i (1+\gamma_5) u$, $\bar{c} i (1-\gamma_5) s$, which are designed to exclude twist-three corrections. Besides, the authors of [31, 483] assume non-singlet, i. e., pion-like η DAs as established by [314]. Accordingly, the $D_s^+ \to \eta' l^+ \nu_l$ case has been extracted from the related analysis of $D_s^+ \to \eta l^+ \nu_l$ form factors via an approximation, based on the QF state mixing ansatz (see Equation 315):

$$\frac{f^\pm_{D_s^+\eta}}{f^\pm_{D_s^+\eta'}} = \frac{\cot\phi \frac{f^\pm_{D_s^+\eta_q}}{f^\pm_{D_s^+\eta_s}} - 1}{\tan\phi \frac{f^\pm_{D_s^+\eta_q}}{f^\pm_{D_s^+\eta_s}} + 1} \tan\phi = -\tan\phi + \frac{f^\pm_{D_s^+\eta_q}}{\cos^2\phi\, f^\pm_{D_s^+\eta_s}} + \mathcal{O}\left(\left[\frac{f^\pm_{D_s^+\eta_q}}{f^\pm_{D_s^+\eta_s}}\right]^2\right), \tag{951}$$

while assuming a vanishing non-strange component[16] $f^+_{D_s^+\eta_q}$.[17] At this point, we are not using any of these assumptions, but instead follow the strategy suggested by [32, 320, 519], while extending it to the $\eta - \eta'$ system. Therefore, we recalculate all LO corrections up to twist-four accuracy, by using the updated η and η' meson DAs. This is complemented by a short discussion concerning the numerical impact of neglected higher twist effects.

As mentioned above, for $q^2, (q+p)^2 \ll m_Q^2$ the correlation function of Equation 946 is dominated by light-like distances $x^2 \sim 0$, justifying a conformal expansion similar to Equation 949 (see also [97, 517, 523]). Thus, the leading contributions to $F_\mu^{HM}(p,q)$ are given by Figure 39,

15 In general, form factors of semileptonic heavy-to-light or similar non-leptonic two-body decays can be used to extract CKM matrix elements from corresponding processes. Thus, it seems plausible, that the rather complicated anatomy of the involved flavor singlet sector made decay modes, such as $D_s^+ \to \eta^{(\prime)} l^+ \nu_l$ transitions less favorable for flavor physics. Instead, they are especially interesting for probing the underlying $\eta - \eta'$ systems gluonic content (see, e. g., [482]).

16 In other words, the authors of [31] assume that at LO in α_S both form factors are related by $f^\pm_{D_s^+\eta} = -\tan\phi\, f^\pm_{D_s^+\eta'}$.

17 In Equation 951 a perturbative expansion of the involved form factors is assumed, i. e., compared to $f^+_{D_s^+\eta_s}$ the function $f^+_{D_s^+\eta_q}$ is suppressed by extra powers of α_S.

where a highly virtual heavy quark propagates near the light-cone, while interacting with soft background fields. Formally, this can be expressed by (flavors are specified in Table 16)

$$F_\mu^{HM}(p,q)\Big|_{LO} = i\int d^4x\, e^{iq\cdot x}\langle M(p)\,|\bar\psi(x)\gamma_\mu \underbrace{Q(x)\overline{Q}(0)}i\gamma_5\psi(0)|0\rangle m_Q\,, \tag{952}$$

with the heavy-quark propagator of Equation 754. Hence, Equation 952 entails the anticipated two-particle

$$\begin{aligned} F_\mu^{(a)}(p,q) \coloneqq im_Q\int d^4x\int\frac{d^4k}{(2\pi)^4}e^{ix\cdot(q-k)}\frac{1}{m_Q^2-k^2}\big[&m_Q\langle M(p)\,|\bar\psi(x)\,\gamma_\mu\gamma_5\psi(0)|0\rangle \\ &-ik_\mu\langle M(p)\,|\bar\psi(x)\,i\gamma_5\psi(0)|0\rangle - ik^\nu\langle M(p)\,|\bar\psi(x)\,\sigma_{\mu\nu}\gamma_5\psi(0)|0\rangle\big]\,, \end{aligned} \tag{953}$$

as well as three-particle corrections

$$\begin{aligned} F_\mu^{(b)}(p,q) \coloneqq im_Q\int d^4x\int\frac{d^4k}{(2\pi)^4}\frac{e^{ix\cdot(q-k)}}{m_Q^2-k^2}\int_0^1 dv\Bigg[&\frac{v}{i}x_\rho\langle M(p)\,|\bar\psi(x)\,\sigma_{\mu\lambda}\gamma_5 g\mathcal{G}^{\rho\lambda}(vx)\,\psi(0)|0\rangle \\ &+\frac{k^\nu}{m_Q^2-k^2}\Big(\langle M(p)\,|\bar\psi(x)\,\sigma_{\mu\lambda}\gamma_5 g\mathcal{G}_\nu{}^\lambda(vx)\,\psi(0)|0\rangle \\ &-\frac{1}{4}g^{\alpha\beta}\varepsilon_{\nu\rho\lambda\alpha}\varepsilon_{\mu\beta\omega\tau}\langle M(p)\,|\bar\psi(x)\,\sigma^{\omega\tau}\gamma_5 g\mathcal{G}^{\rho\lambda}(vx)\,\psi(0)|0\rangle\Big) \\ &+\frac{m_Q}{m_Q^2-k^2}\Big(i\langle M(p)\,|\bar\psi(x)\,\gamma_\lambda\gamma_5 g\mathcal{G}_\mu{}^\lambda(vx)\,\psi(0)|0\rangle \\ &+\langle M(p)\,|\bar\psi(x)\,\gamma^\delta g\widetilde{\mathcal{G}}_{\mu\delta}(vx)\,\psi(0)|0\rangle\Big)\Bigg]\,, \end{aligned} \tag{954}$$

corresponding to diagram a) and b) of Figure 39, respectively. Analogous to [371, 501] the derivation of Equation 953 and Equation 954 requires several matrix identities which can be found in Section A.2. Besides, for the implementation of two-particle DAs (see Equation 325) one may prefer a slightly modified version as realized by the substitution (identical for $s \leftrightarrow q$)

$$F_M^{(s)}\frac{ix_\mu}{2p\cdot x}\int_0^1 du\, e^{iup\cdot x}\psi_{4M}^{(s)}(u) = F_M^{(s)}\frac{x_\mu}{2}\int_0^1 du\, e^{iup\cdot x}\int_0^u dv\,\psi_{4M}^{(s)}(v)\,. \tag{955}$$

Together with Equation 955 and comparable transformations[18] all occurring tensor integrals end up having a similar structure (f is an integrable and well behaved function, $n\in\mathbb{N}_0$)

$$\mathcal{I}_{\mu_1\cdots\mu_n}(up,q) = \int d^4x\int\frac{d^4k}{(2\pi)^4}f(k)\,x_{\mu_1}\cdots x_{\mu_1}e^{ix\cdot(q-k+up)}\,, \tag{956}$$

18 Here, we include definite integrals, such as

$$i\int_0^u dw\, e^{ip\cdot x(u-w)} = \frac{e^{iup\cdot x}-1}{p\cdot x}\,,$$

which are needed to get rid of $(p\cdot x)^{-1}$ terms.

which can be immediately solved via[19]

$$\begin{aligned}\mathcal{I}_{\mu_1\cdots\mu_n}(up,q) &= \left(-i\frac{\partial}{\partial q_{\mu_1}}\right)\cdots\left(-i\frac{\partial}{\partial q_{\mu_n}}\right)\int d^4x\int\frac{d^4k}{(2\pi)^4}f(k)\,e^{i(q-k+up)\cdot x}\\ &= \left(-i\frac{\partial}{\partial q_{\mu_1}}\right)\cdots\left(-i\frac{\partial}{\partial q_{\mu_n}}\right)\int d^4k\,\delta^{(4)}(q-k+up)\,f(k)\\ &= \left(-i\frac{\partial}{\partial q_{\mu_1}}\right)\cdots\left(-i\frac{\partial}{\partial q_{\mu_n}}\right)f(q+up)\;. \end{aligned}\tag{957}$$

In the next step, each remaining mixed scalar product, such as

$$\frac{2p\cdot(up+q)}{\left(m_Q^2-(up+q)^2\right)^2} = -\frac{1}{u}\left[1-\frac{m_Q^2-q^2+u^2p^2}{m_Q^2-(up+q)^2}\right]\frac{1}{m_Q^2-(up+q)^2}\,,\tag{958}$$

has to be simplified accordingly. As a partial result, we obtain for[20] Equation 953:

$$\begin{aligned}F_\mu^{(a)}(p,q) = p_\mu m_Q^2 F_M^{(\psi)}\int_0^1 du\frac{1}{m_Q^2-(up+q)^2}\Bigg[&\phi_M^{(\psi)}(u)-\frac{m_Q^2\phi_{4M}^{(\psi)}(u)}{2\left(m_Q^2-(up+q)^2\right)^2}\\ &-\frac{u}{m_Q^2-(up+q)^2}\int_0^u dv\,\psi_{4M}^{(\psi)}(v)+\frac{1}{2m_Q m_\psi F_M^{(\psi)}}\Bigg(u\bar{\Phi}_{3M}^{(\psi);p}(u)\\ &+\left[2+\frac{m_Q^2+q^2-u^2p^2}{m_Q^2-(up+q)^2}\right]\frac{\bar{\Phi}_{3M}^{(\psi);\sigma}(u)}{6}\Bigg)\Bigg]\\ &+q_\mu m_Q^2 F_M^{(\psi)}\int_0^1 du\frac{1}{m_Q^2-(up+q)^2}\Bigg[\frac{1}{2m_Q m_\psi F_M^{(\psi)}}\Bigg(\bar{\Phi}_{3M}^{(\psi);p}(u)\\ &+\left[1-\frac{m_Q^2-q^2+u^2p^2}{m_Q^2-(up+q)^2}\right]\frac{\bar{\Phi}_{3M}^{(\psi);\sigma}(u)}{6u}\Bigg)-\frac{1}{m_Q^2-(up+q)^2}\int_0^u dv\,\psi_{4M}^{(\psi)}(v)\Bigg]\,.\end{aligned}\tag{959}$$

The calculation of three-particle corrections involve somewhat lengthy tensor structures which will not be explicitly shown at this point. Instead, let us emphasize, that the relevant contributions, e. g., possible twist-three matrix elements of Equation 954 boil down to rather compact terms, i. e.,

$$\langle M(p)\,|\bar{\psi}(x)\,\gamma_\mu\gamma_\nu\sigma_{\rho\lambda}\gamma_5 g\mathcal{G}^{\rho\lambda}(vx)\,\psi(0)|0\rangle = 6if_{3M}^{(\psi)}g_{\mu\nu}p^2\int\mathcal{D}\underline{\alpha}\,e^{i(\alpha_1+v\alpha_2)p\cdot x}\Phi_{3M}^{(\psi)}(\underline{\alpha})\,,\tag{960}$$

along with $\left(X\equiv X(v,\alpha_1,\alpha_2)\coloneqq\alpha_1+v\alpha_2\right)$

$$\langle M(p)\,|\bar{\psi}(x)\,\gamma_\mu\gamma_\lambda\gamma_5 g\mathcal{G}^{\rho\lambda}(vx)\,\psi(0)|0\rangle = f_{3M}^{(\psi)}\left(2p_\mu p^\rho+p^2 g_\mu{}^\rho\right)\int\mathcal{D}\underline{\alpha}\,e^{iXp\cdot x}\Phi_{3M}^{(\psi)}(\underline{\alpha})\,,\tag{961}$$

19 Since Equation 957 is a standard "trick", it seems hardly possible to specify a unique source (e. g., the special case $n=1$ can also be found in [244]). However, the resulting representation is clearly preferable to a calculation in position space (cf. [483]).

20 With this result the well-known pion case [319, 320] can be reproduced, by applying the following substitutions: $p^2, m_M^2, a_M \mapsto 0$, $F_M^{(\psi)}\mapsto f_\pi$, $\phi_M^{(\psi)}\mapsto\phi_\pi$, $\psi_{4M}^{(\psi)}\mapsto\psi_{4\pi}$, $\phi_{4M}^{(\psi)}\mapsto\phi_{4\pi}$, $(2m_\psi)^{-1}\,\bar{\Phi}_{3M}^{(\psi);\sigma}\mapsto f_\pi\mu_\pi\phi_{3\pi}^\sigma$ as well as $(2m_\psi)^{-1}\,\bar{\Phi}_{3M}^{(\psi);p}\mapsto f_\pi\mu_\pi\phi_{3\pi}^p$. Similarly, the kaon case can be generated, however, this time $SU(3)_F$-breaking effects (see Section C.9) have to be included.

after performing all required contractions properly. As a result, we get

$$\begin{aligned}
F_\mu^{(b)}(p,q) = p_\mu \int_0^1 dv \int \mathcal{D}\underline{\alpha} \, \frac{1}{\left(m_Q^2 - (q + Xp)^2\right)^2} \Big[m_Q f_{3M}^{(\psi)} \Phi_{3M}^{(\psi)}(\underline{\alpha}) \left(4v\, p\cdot q + 3\xi_v X p^2\right) \\
+ m_Q^2 f_M^{(\psi)} \left(2\left[\Psi_{4M}^{(\psi)}(\underline{\alpha}) + \widetilde{\Psi}_{4M}^{(\psi)}(\underline{\alpha})\right] - \left[\Phi_{4M}^{(\psi)}(\underline{\alpha}) + \widetilde{\Phi}_{4M}^{(\psi)}(\underline{\alpha})\right]\right)\Big] \\
+ p_\mu \int_0^1 dv \int \mathcal{D}\underline{\alpha} \int_0^X dw \, \frac{4 m_Q^2 f_M^{(\psi)} (X-w)\, p^2}{\left(m_Q^2 - (q + (X-w)\, p)^2\right)^3} \mathcal{A}_{4M}^{(\psi)}(\underline{\alpha}) \\
+ q_\mu \int_0^1 dv \int \mathcal{D}\underline{\alpha} \, \frac{m_Q f_{3M}^{(\psi)} (\xi_v - 2)\, p^2}{\left(m_Q^2 - (q + Xp)^2\right)^2} \Phi_{3M}^{(\psi)}(\underline{\alpha}) \\
+ q_\mu \int_0^1 dv \int \mathcal{D}\underline{\alpha} \int_0^X dw \, \frac{4 m_Q^2 f_M^{(\psi)} p^2}{\left(m_Q^2 - (q + (X-w)\, p)^2\right)^3} \mathcal{A}_{4M}^{(\psi)}(\underline{\alpha}) \, ,
\end{aligned} \tag{962}$$

with the auxiliary function[21]

$$\mathcal{A}_{4M}^{(\psi)}(\underline{\alpha}) \coloneqq \Psi_{4M}^{(\psi)}(\underline{\alpha}) + \widetilde{\Psi}_{4M}^{(\psi)}(\underline{\alpha}) + \Phi_{4M}^{(\psi)}(\underline{\alpha}) + \widetilde{\Phi}_{4M}^{(\psi)}(\underline{\alpha}) \, . \tag{963}$$

Again, Equation 962 can be used to correctly reproduce the corresponding LO pion [320] and kaon [519] results, except for an additional factor "3" (marked blue in Equation 962) that is missing[22] in [519, Equation 10]. Since the latter results from Equation 960 and Equation 961, which also entail rather nontrivial combinations, such as terms proportional to $\sim \xi_v X p^2$, an absent factor is clearly a literal error. Thus, [519] is still valid for further cross-checks. In fact, after performing an integration by parts, i. e., when inserting

$$\begin{aligned}
\int_0^X dw \, \frac{4(X-w)}{\left(m_Q^2 - (q + (X-w)\, p)^2\right)^3} = \frac{X \left(p\cdot q + X p^2\right)^{-1}}{\left(m_Q^2 - (q + Xp)^2\right)^2} \\
- \int_0^X dw \, \frac{p\cdot q \left(p\cdot q + (X-w)\, p^2\right)^{-2}}{\left(m_Q^2 - (q + (X-w)\, p)^2\right)^2}
\end{aligned} \tag{964}$$

into Equation 962, the notation of [335, 519] can be fully reproduced. Before proceeding, let us briefly reconsider the involved convolution integrals and structure of Equation 954 and Equation 962 with respect to their numerical impact [2]:

- Every additional two units of collinear twist are accompanied by an extra power of the denominator $(u \in [0,1])$

$$\frac{1}{D} \coloneqq \frac{1}{m_Q^2 - (q + up)^2} = \frac{1}{m_Q^2 - u\,(p+q)^2 - \bar{u} q^2 + u \bar{u} p^2} \, . \tag{965}$$

  Thus, to ensure a converging light-cone OPE, the momentum transfer q^2 is severely constrained. For instance, the natural hierarchy of this expansion can be justified for a sufficiently large virtuality $(p+q)^2 \ll m_Q^2$ and $m_Q^2 - q^2 \geqslant \mathcal{O}(\Lambda_{QCD} m_Q)$.

21 Note, that surface terms proportional to $\int \mathcal{D}\underline{\alpha} \, \mathcal{A}_{4M}^{(\psi)}(\underline{\alpha})$ vanish (at least up to NLO in conformal spin).

22 However, within a recent paper (see [335]) this factor has been recovered, at least on the level of related imaginary parts. Besides, this paper builds on [3], i. e., it includes spectral densities that have been retrofitted with corresponding $\eta^{(\prime)}$ DAs borrowed from [3]. Most importantly, those coincide with our findings of Section 5.2.2.

- Contributions with odd twist $\left(\text{e.g., } t_{\text{odd}} = 2k+1,\ k \in \mathbb{N} \text{ fixed}\right)$ may arise from mass terms of the heavy-quark propagator (see Equation 754) and are, therefore, subleading in $1/m_Q^2$ compared to their even counterparts $\left(\text{here } t_{\text{even}} = 2k\right)$. However, this does not automatically result in a numerical suppression of the corresponding convolutions. For example, the two-particle twist-three corrections, appearing in Equation 954, mitigate the effects caused by inverse powers of m_Q via an extra prefactor $\sim (H_M^{(\psi)}/m_\psi)$ (see Chapter 3) which comes from the related DAs. As exhibited by the subsequent numerical analysis, $\overline{\Phi}_{3M}^{(\psi);p}$ and $\overline{\Phi}_{3M}^{(\psi);\sigma}$ entail dominant[23] LO as well as NLO QCD corrections to the correlation function (see also [2, 319, 320]). On the other hand, for similar reasons, the mostly unknown twist-five corrections could exceed their twist-four counterparts. To get at least a rough impression of the resulting uncertainty in associated LCSR calculations, we follow [319] and assume an approximate equality for the ratios (see Section 5.2)

$$\frac{f_{HM}^{+}(q^2)\big|_{\text{twist-4}}}{f_{HM}^{+}(q^2)\big|_{\text{twist-2}}} \approx \frac{f_{HM}^{+}(q^2)\big|_{\text{twist-5}}}{f_{HM}^{+}(q^2)\big|_{\text{twist-3}}}, \tag{966}$$

  where $f_{HM}^{+}(q^2)\big|_{\text{twist-t}}$ represent the underlying LO twist-t $\left(t \in \mathbb{N}\right)$ contributions. This would cause an additional error, varying from 4% $\left(\text{for } q^2 = -2\ \text{GeV}^2\right)$ to 2.5% $\left(\text{for } q^2 = 0\right)$.

Furthermore, a recent study (see [524]) dedicated to the exploration of factorizable twist-five and twist-six corrections in LCSRs for $B \to \pi$ form factors $\left(\text{i.e., } f_{B\pi}^{+}\right)$ reveals an extreme numerical suppression[24] of corresponding higher twist effects. Hence, justifying a conventional truncation of the OPE up to twist-four accuracy.

With Equation 954 and Equation 962 all required LO corrections up to twist-four accuracy are now at hand. In the next step, NLO contributions have to be included.

5.1.2.2 *Evolution effects and pseudoscalar meson mixing*

For the intended inclusion of NLO QCD corrections to the corresponding hard-scattering kernels of Equation 949, it is sensible to reconsider existing strategies, such as those outlined in [20, 28, 32, 525]. All of these approaches are ultimately affected by renormalization group effects. The following part is, therefore, dedicated to investigate and justify the selected method including an updated discussion based on the NLO evolution of singlet as well as octet DAs (see Chapter 3).

As a special feature, the complete description of semileptonic $B, D_{(s)} \to \eta^{(\prime)}$ form factors requires specific gluonic contributions which at NLO in α_S are given by diagrams similar to Figure 40. Here, the mechanism responsible for the annihilation of a heavy pseudoscalar meson into two gluons is depicted. The latter may create η or η' particles that undergo a complicated mixing mechanism, as caused by general features of the underlying $\eta - \eta'$ system[25], including

23 The given twist-four two-particle contributions are proportional to $\delta_M^{2(\psi)} D^{-1}$, while twist-three three-particle terms include (numerically small) factors of $f_{3M}^{(\psi)}$. Besides, the remaining twist-four three-particle convolution integrals of equation are suppressed by extra powers of D^{-1}. Consequently, the presented higher twist corrections are in general subdominant when compared to their twist-two counterparts.

24 Within the whole domain of momentum transfers, where the LCSR is applicable, the relative contributions of these higher twist effects do not exceed 0.05% (see [524, 5 Conclusion]).

25 As mentioned above, one could also take into account mixing with other pseudoscalar mesons, such as the closely related neutral pion. However, the induced mixing effects are found to be at the level of a few percent [13–15, 152, 526]. Similarly, the small intrinsic charm component $\bar{c}c$ within the $\eta^{(\prime)}$ meson (see [9]) can be neglected in the present situation. Therefore, we follow [152] and focus on the $\eta - \eta'$ system.

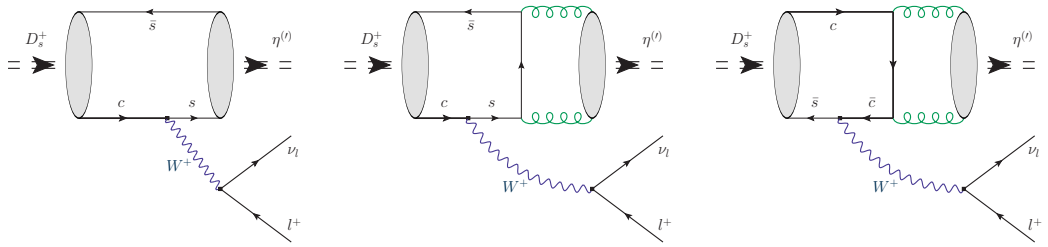

Figure 40: SU(3)-flavor singlet and octet contributions to the $D_s^+ \to \eta^{(\prime)} l^+ \nu_l$ transition form factors.

OZI rule violating subprocesses[26] and the $U(1)_A$ anomaly in particular (see Section 3.1.4). Since no analytical solution for those phenomena has yet been found, we resort to the phenomenologically motivated FKS scheme (see discussion in Section 3.1.4). Thus, this mixing scheme forms the starting point for the developed $\eta^{(\prime)}$ DAs (see Chapter 4), absorbing all relevant physical parameters of the $\eta - \eta'$ system (cf. [9, 15]). Apart from that, the applied RG methods rest on strong theoretical foundations that go beyond a mere phenomenological approach. However, unlike for $\gamma^*\gamma^{(*)} \to \eta^{(\prime)}$ TFFs, no comparably large momentum transfers occur in $B, D_{(s)} \to \eta^{(\prime)}$ decays. For instance, the mass of an arbitrary hadron "H" $\left(\text{e.g., } H = D, D_s, B;\right)$ that contains a heavy quark "Q" can be expressed via [238]

$$m_H = m_Q + \overline{\Lambda} + \mathcal{O}\left(\frac{1}{m_Q}\right) . \tag{967}$$

Accordingly, the mass independent parameter $\overline{\Lambda}$ (sometimes referred to as "binding energy" [238]) gives a rough estimate for the involved characteristic transverse parton momenta. Consequently, the factorization scale μ_F for heavy-to-light decays should be roughly given by $\mu_F \approx \mu_H := \sqrt{m_H^2 - m_Q^2}$ (see also [2, 319, 320, 322]). On these grounds, let us reconsider our strategy:

- The numerical impact of higher Gegenbauer moments has, e.g., been investigated for ϕ_π in $B \to \pi$ transitions, concluding (cf. [281, 299, 527]), that heavy-to-light decays are only slightly influenced by higher order coefficients $n \geqslant 4$. Hence, we expect a similar behavior for f_{HM}^+ $(M = \eta, \eta')$. Consequently, we truncate the conformal expansions (see Section 3.2) of ϕ_{2M}^A ($A = 0, 8$ or $A = q, s$) as well as $\phi_{2M}^{(g)}$ at $n > 2$.
- Since we are using the $\overline{\text{MS}}$-scheme throughout our calculations, all renormalized quantities, such as quark masses or Gegenbauer moments have to be evolved from their individual reference scale μ_0 to the preferred renormalization point μ_F. For the latter, we may choose $\mu_F = \mu_H$.
- This leaves the question about the relative size of RG effects and their impact on the discussed $H \to M l \nu_l$ transition form factors. According to Chapter 3, the evolution of singlet and octet Gegenbauer coefficients can be cast into the form $\left(\text{for } a = 0, 8, g, \text{ where } \alpha_{8g} \equiv \alpha_{g8} \equiv \alpha_{08} \equiv \alpha_{80} \equiv 0\right)$

$$c_{2,M}^{(a)}(\mu) = \sum_{b \in \{0,8,g\}} \alpha_{ab}(\mu, \mu_0)\, c_{2,M}^{(b)}(\mu_0) + \beta_a(\mu, \mu_0) , \tag{968}$$

with continuous coefficient functions α_{ab} and β_a, which are defined on $\mu \in [\mu_0, \mu_H]$. Here, $\alpha_{gg}(\mu, \mu_0)$, $\alpha_{00}(\mu, \mu_0)$, $\alpha_{88}(\mu, \mu_0) \leqslant 1$ and $\beta_0(\mu, \mu_0)$, $\beta_8(\mu, \mu_0) \leqslant 0$ are strictly decreasing,

26 Those effects are of order $\mathcal{O}(N_c^{-1})$ in a formal N_c^{-1} expansion and are phenomenologically found to be small [13, 14]. Thus, in this case, OZI violating contributions can be safely neglected, leaving the $U(1)_A$ anomaly as the main mixing mechanism.

	$\mu = 1.4$ GeV	$\mu = 1.5$ GeV	$\mu = 2.5$ GeV
$\alpha_{88}(\mu, \mu_0)$	0.904426	0.888145	0.790773
$\beta_8(\mu, \mu_0)$	−0.001725	−0.001996	−0.003461
$\alpha_{00}(\mu, \mu_0)$	0.914812	0.900010	0.809757
$\alpha_{0g}(\mu, \mu_0)$	0.067888	0.078594	0.136372
$\beta_0(\mu, \mu_0)$	−0.002468	−0.002827	−0.004598
$\alpha_{gg}(\mu, \mu_0)$	0.832543	0.804931	0.646365
$\alpha_{g0}(\mu, \mu_0)$	0.005523	0.006343	0.010485
$\beta_g(\mu, \mu_0)$	0.002587	0.002961	0.004787

Table 17: Coefficients of Equation 968, evaluated for $\mu_0 = 1.0$ GeV and $\mu = \mu_H = \sqrt{m_h - m_Q}$ ($H = B, D, D_s$). The induced uncertainties are estimated by varying Λ^2_{QCD} by 10%, resulting in approximate relative errors $(\Delta\alpha_{00}/\alpha_{00}) \approx 2\%$, $(\Delta\alpha_{88}/\alpha_{88}) \approx 3\%$, $(\Delta\alpha_{gg}/\alpha_{gg}) \approx 4\%$, $(\Delta\alpha_{0g}/\alpha_{0g}) \approx 6\%$, $(\Delta\alpha_{g0}/\alpha_{g0}) \approx 9\%$, $(\Delta\beta_0/\beta_0) \approx 17\% \approx (\Delta\beta_g/\beta_g)$ and $(\Delta\beta_8/\beta_8) \approx 19\%$ (taken at $\mu = 2.5$ GeV).

while $0 \leqslant \alpha_{0g}(\mu, \mu_0)$, $\alpha_{g0}(\mu, \mu_0)$, along with $\beta_g(\mu, \mu_0) \geqslant 0$ are strictly increasing (see Table 17). Similar to [32, 525], but this time with a NLO evolution of the involved Gegenbauer moments we may analyze (for simplicity, we are dropping the subscript M)

$$\Delta_0(\mu, \mu_0) := \left| \frac{c_2^{(0)}(\mu) - c_2^{(8)}(\mu)}{c_2^{(0)}(\mu)} \right| . \tag{969}$$

Since we expect the most significant changes for B meson decays, we favor the interval $\mu \in [1.0 \text{ GeV}, 2.5 \text{ GeV}]$. Thus, the generic parameters $c_2^{(0)}(\mu_0) = 0.25 \pm 0.15 = c_2^{(8)}(\mu_0)$ and $c_2^{(g)}(\mu_0) = \pm 0.67$ imply[27] (neglecting correlations)

$$\Delta_0(2.5 \text{ GeV}, 1.0 \text{ GeV}) = 0.018 \pm 0.453\Big|_{c_2^{(g)}(\mu_0)} \pm 0.603\Big|_{c_2^{(0)}(\mu_0)} \pm 0.600\Big|_{c_2^{(8)}(\mu_0)} . \tag{970}$$

The central value in Equation 970 is calculated with those of the Gegenbauer moments, while all uncertainties are due to the variation of the latter. In other words, for $c_2^{(g)}(\mu_0) \approx 0$ and $c_2^{(0)}(\mu_0) \approx c_2^{(8)}(\mu_0)$ the relative deviation Δ_0 amounts to less than 2% over the range $1.0 \text{ GeV} < \mu < 2.5$ GeV. Otherwise, RG mixing effects would not be negligible.

Furthermore, for $c_2^{(0)}(\mu_0) \approx 0.25$, $\mu \in [1.0 \text{ GeV}, 2.5 \text{ GeV}]$ and the rather conservative estimate $c_2^{(g)}(\mu_0) = \pm 0.67$, the gluon Gegenbauer moment changes by at most 36% due to QCD evolution. Based on Chapter 3 and Section A.14, we may, therefore, proceed as follows:

- As discussed in Chapter 3, the QF basis can be beneficial when considering meson DAs, because it prevents a proliferation of largely unknown parameters. One reason for this finding is its inherent state mixing approach (see Equation 315) which we want to exploit

27 In principle, a knowledge of the monotonicity of all coefficient functions as well as the recorded values in Table 17 are sufficient for an evaluation of Equation 970.

in Section 5.1.2.3. Nevertheless, the associated omission of OZI-rule violating contributions, i. e., (see Section A.14 for further details)

$$|\eta_q(p)\rangle \propto \phi_2^{(q)}(u,\mu)\,|q\bar{q}\rangle + \phi_2^{\mathrm{OZI}}(u,\mu)\,|s\bar{s}\rangle + \dots\,, \tag{971}$$

$$|\eta_s(p)\rangle \propto \phi_2^{\mathrm{OZI}}(u,\mu)\,|q\bar{q}\rangle + \phi_2^{(s)}(u,\mu)\,|s\bar{s}\rangle + \dots\,, \tag{972}$$

also implies a loss of scale dependence in the corresponding parameters, such as the decay constants[28] or mixing angles. Fortunately, this does not necessarily affect the involved DAs

$$\phi_2^{(q)}(u,\mu) = \frac{1}{3}\Big(\phi_2^{(8)}(u,\mu) + 2\,\phi_2^{(0)}(u,\mu)\Big)\,, \tag{973}$$

$$\phi_2^{(s)}(u,\mu) = \frac{1}{3}\Big(\phi_2^{(0)}(u,\mu) + 2\,\phi_2^{(8)}(u,\mu)\Big)\,, \tag{974}$$

$$\phi_2^{\mathrm{OZI}}(u,\mu) = \frac{\sqrt{2}}{3}\Big(\phi_2^{(0)}(u,\mu) - \phi_2^{(8)}(u,\mu)\Big)\,, \tag{975}$$

as long as we consistently implement the condition

$$\phi_2^{\mathrm{OZI}}(u,\mu) \stackrel{!}{=} 0\,. \tag{976}$$

However, according to the above preparations Equation 976 can be approximately fulfilled if we demand the subsequent rules:

i) At the refernce scale $\mu_0 = 1$ GeV, we may set

$$\phi_2^{(0)}(u,\mu_0) \stackrel{!}{=} \phi_2^{(8)}(u,\mu_0)\,, \tag{977}$$

or equivalently (see Equation 973 and Equation 974)

$$\phi_2^{(q)}(u,\mu_0) \stackrel{!}{=} \phi_2^{(s)}(u,\mu_0)\,. \tag{978}$$

ii) We can then model $\phi_2^{(q)}$ and $\phi_2^{(s)}$ via ($a = 0, 8$)

$$\phi_2^{(a)}(u,\mu) = 6u\bar{u}\Big(1 + c_2^{(a)}(\mu)\,C_2^{(3/2)}(\xi_x)\Big)\,, \tag{979}$$

and evolve the remaining coefficient

$$c_2(\mu_0) \coloneqq c_2^{(a)}(\mu_0) \tag{980}$$

according to the scaling-law for the octet Gegenbauer moments (cf. Section 3.3):

$$c_2(\mu) \approx \left[\frac{\alpha_S(\mu)}{\alpha_S(\mu_0)}\right]^{\frac{50}{9\beta_0}} c_2(\mu_0)\,. \tag{981}$$

iii) Furthermore, we can assume that (see[29] Section A.14)

$$\phi_{2\eta}^{(g)}(u,\mu) = \phi_{2\eta'}^{(g)}(u,\mu)\,, \tag{982}$$

and entailed $\mathrm{SU}(3)_F$-breaking corrections have only a small impact on $f_{HM}^{+}(q^2)$. This is consistent with our general assumption, that the bulk part of flavor symmetry breaking effects are encoded in the decay constants, while they are subleading in the Gegenbauer coefficients [3, 271, 525].

28 Since the scale dependence of $f_0(\mu)$ is a subleading two-loop effect, its impact is numerically insignificant, i. e., at least for $\mu_0 \approx 1$ GeV and $\mu \approx \mu_H$.

29 As discussed in Section A.14, Equation 982 is a consequence of point i) and ii).

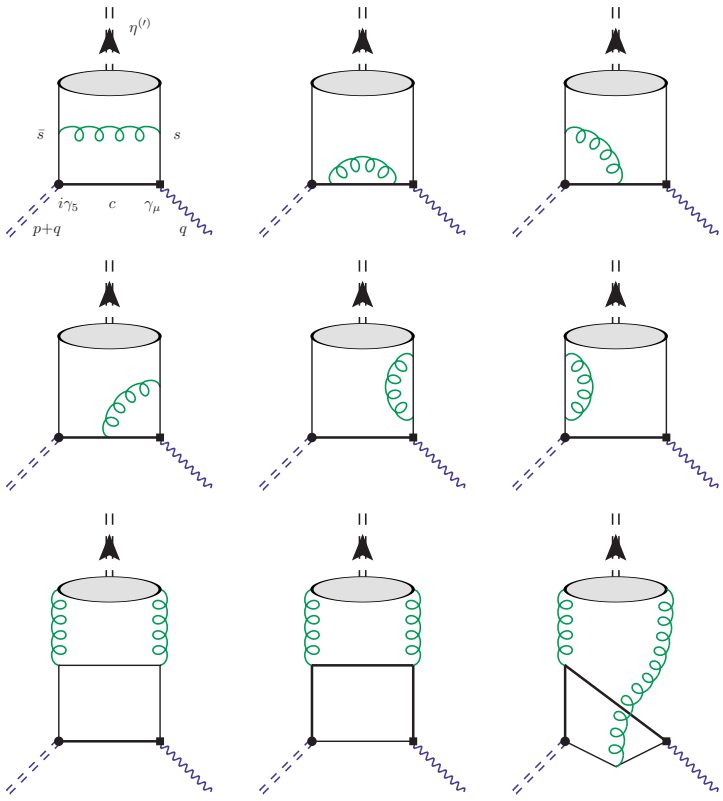

Figure 41: NLO contributions to the operator product expansion of Equation 946 for $D_s^+ \to \eta^{(\prime)} l^+ \nu_l$ transitions.

In conclusion, by reconsidering the original ansatz of [20, 28, 32, 525], we are able to confirm their findings, particularly concerning the implemented models for Gegenbauer moments and related RG techniques.

Thus, in the light of this ansatz, we may now turn to the remaining NLO corrections.

5.1.2.3 *Inclusion of next-to-leading order corrections*

In this sub-subsection, we devote our attention to the inclusion of NLO QCD corrections into the OPE of Equation 946. Those corrections can in principle be reconstructed from existing calculations, such as[30] [32, 320, 322], to describe $D_s^+, D^+ \to \eta^{(\prime)} l^+ \nu_l$ transition form factors. For this purpose, some adaptations have to be made which go beyond the existing strategies.

In accordance with Section 5.1.2.2, we neglect all OZI-rule violating effects, allowing us to apply Equation 315 which relates the physical $|\eta^{(\prime)}\rangle$ states and the QF basis states $|\eta_{q,s}\rangle$ with each

30 The twist-three corrections have been calculated in [2, 320], while gluonic twist-two contributions were studied by [32, 525].

other. As a consequence, the correlation function of Equation 946 can be decomposed into formal contributions similar to (this analogously applies to $\widetilde{F}^{HM}$) [2]

$$F^{D_s\eta}\left(q^2,(p+q)^2\right) = -F^{D_s\eta_s}\left(q^2,(p+q)^2\right)\sin\phi + F^{D_s\eta_q}\left(q^2,(p+q)^2\right)\cos\phi\,, \tag{983}$$

$$F^{D_s\eta'}\left(q^2,(p+q)^2\right) = F^{D_s\eta_s}\left(q^2,(p+q)^2\right)\cos\phi + F^{D_s\eta_q}\left(q^2,(p+q)^2\right)\sin\phi\,, \tag{984}$$

$$F^{D\eta}\left(q^2,(p+q)^2\right) = F^{D\eta_q}\left(q^2,(p+q)^2\right)\cos\phi - F^{D\eta_s}\left(q^2,(p+q)^2\right)\sin\phi\,, \tag{985}$$

$$F^{D\eta'}\left(q^2,(p+q)^2\right) = F^{D\eta_q}\left(q^2,(p+q)^2\right)\sin\phi + F^{D\eta_s}\left(q^2,(p+q)^2\right)\cos\phi\,. \tag{986}$$

Here, the main difference with respect to [32], besides using $\overline{MS}$ masses for m_b and m_c, is that in the case of $D_s\to\eta^{(\prime)}$ decays we probe the $\eta^{(\prime)}$ meson's strange quark (viz. $\bar{s}s$) content. This implies a different dependence on the mixing angle, when compared to $B\to\eta^{(\prime)}$ transitions, which resemble the $D\to\eta^{(\prime)}$ case after replacing all particle specific masses, i. e., $m_c\leftrightarrow m_b$, $m_D\leftrightarrow m_B$, along with related sum rule parameters (e. g., the Borel parameter and continuum threshold). In other words (see Figure 41), according to the given interpolating current within Equation 946, the second summand in each equation of Equation 983 – Equation 986 only receives non-vanishing contributions[31] at NLO accuracy, coming from gluonic singlet diagrams, while the first summand is a combination of LO as well as NLO quark and gluonic QCD corrections. The most striking aspect of this approach, where $SU(3)_F$-flavor violations are exclusively taken into account via the decay constants[32], concerns twist-three two-particle DAs. In fact, by consistently applying the strict FKS scheme (see Equation 551), we receive a simplified set of parameters which entail the following replacement rules for existing NLO quark contributions [2]:

$$f_\pi \mapsto f_{q,s}\,, \quad f_\pi\frac{m_\pi^2}{2m_q} \mapsto f_q\frac{m_\pi^2}{2m_q}\,, \quad f_\pi\frac{m_\pi^2}{2m_q} \mapsto f_s\frac{2m_K^2-m_\pi^2}{2m_s}\,. \tag{987}$$

The latter allow a straight forward implementation of the corresponding results, based on the pion and kaon case [319, 320]. Besides, our results do not change significantly if meson and quark mass corrections are included (see also [2]). However, keeping all $SU(3)_F$-breaking effects would not only force us to respect every possible mass dependence in the correlation function, but also to use Equation 534 and Equation 535 instead of Equation 551. As already discussed in Section 3.4.2, these quantities are only weakly constrained and their inclusion would lead to uncertainties at the level of 200%, i. e., if one assumes uncorrelated errors within the twist-three part (see also [2, 32]). This, however, would be inconsistent with the chosen ansatz that automatically avoids these uncertainties.

Together with Equation 983 – Equation 986 and the associated replacement rules, we can now consistently implement NLO QCD corrections into our considerations.

5.2 LIGHT-CONE SUM RULES FOR HEAVY-TO-LIGHT DECAYS

In this subsection the LCSRs for $B, D_{(s)}\to\eta^{(\prime)}l\nu_l$ transition form factors are derived. Based on Section 5.1, where we also discuss some of the underlying historical developments, which led to the currently used method (see Section 5.1.2), we may now place our main focus on the following three goals:

31 All remaining LO and NLO corrections, however, have the wrong flavor content (see Figure 41) and can thus only contribute to the first terms in Equation 983 – Equation 986.

32 In [319, 519] it was shown, that for heavy-to-light decays into pions and kaons, this is indeed a good approximation [2].

i) As mentioned above, the subsequent part represents an extension of previous studies, in particular, those concerning $B \to \pi$ decays which are among the most important applications for the LCSR method[33] (see [245, 269, 322, 335, 445, 519, 523]). Consequently, we have to reconsider the techniques which have been developed for similar approaches and apply the required minor changes accordingly.

ii) As a showcase, we calculate the LO spectral densities, while all remaining NLO results of [32, 320] are included via Equation 983 – Equation 986.

iii) The collected formulas are extended by complementary sum rules for physical observables, such as m_H^2, as needed to fix related LCSR parameters. This is done as a preparation for the intended numerical analysis, carried out in Section 5.3.

Thus, the present subsection is essential for this work.

5.2.1 *General structure and special features*

The basic concepts of the LCSR method are outlined in Section 4.2 and will not be repeated at this point. However, there are specific features which have to be considered. For this purpose, it is reasonable to resume the discussion of Section 5.1.2.

In this context, the two hadronic dispersion relations Equation 947 and Equation 948 were derived, which can be equated with (again omitting subtraction terms; similar for $F^{HM} \leftrightarrow \widetilde{F}^{HM}$)

$$\left[F^{HM}\left(q^2,(p+q)^2\right)\right]_{OPE} = \frac{1}{\pi}\int_{m_Q^2}^{\infty} ds \frac{\mathrm{Im}_s\left[F^{HM}(q^2,s)\right]_{OPE}}{s-(p+q)^2} \tag{988}$$

after assuming approximate quark-hadron duality, i. e.,

$$\int_{s_0^h}^{\infty} ds \frac{\rho_{HM}(q^2,s)}{s-(p+q)^2} \approx \frac{1}{\pi}\int_{s_0}^{\infty} ds \frac{\mathrm{Im}_s\left[F^{HM}(q^2,s)\right]_{OPE}}{s-(p+q)^2}\,. \tag{989}$$

Here, the substitution (as resulting from Equation 965)

$$s(u) = \frac{m_Q^2 - \bar{u}q^2 + u\bar{u}p^2}{u} \;\Rightarrow\; u = \frac{q^2+p^2-s+\sqrt{\left(s-q^2-p^2\right)^2+4p^2\left(m_Q^2-q^2\right)}}{2p^2} \tag{990}$$

has been applied, which entails the named integration limits, while Equation 989 is assumed to hold for a certain continuum threshold s_0 which not necessarily coincides with its hadronic counterpart s_0^h. After subtracting Equation 989 from both sides of the resulting equation

$$\frac{1}{\pi}\int_{m_Q^2}^{\infty} ds \frac{\mathrm{Im}_s\left[F^{HM}(q^2,s)\right]_{OPE}}{s-(p+q)^2} \approx \frac{2m_H^2 f_H f_{HM}^+(q^2)}{m_H^2-(p+q)^2} + \int_{s_0^h}^{\infty} ds \frac{\rho_{HM}(q^2,s)}{s-(p+q)^2} + \text{subtractions}, \tag{991}$$

one usually performs a Borel transformation[34] in the variable $(p+q)^2$ (see Section B.3; $n \in \mathbb{N}$):

$$\hat{\mathcal{B}}_{(p+q)^2\to M^2}\left\{\frac{1}{D^n}\right\} = \frac{\exp\left[-\frac{m_Q^2-\bar{u}q^2+u\bar{u}p^2}{uM^2}\right]}{(n-1)!\left(M^2\right)^{n-1}u^n}\,. \tag{992}$$

33 Among other things, this is a consequence of its use in flavor physics (see, e. g., [97, 320, 322, 445, 464]).

34 The Borel transformation provides an exponential suppression of the mostly unknown continuum contribution, while it also leads to a factorial suppression of remaining power-corrections. Thus, the impact of neglected higher twist effects gets reduced accordingly.

As discussed above, this operation removes all subtractions and gives rise to the LCSRs for the $D_{(s)}, B \to \eta^{(\prime)} l \nu_l$ form factors (later on, we use $M^2 \mapsto M_H^2$)

$$f_{HM}^{+}\left(q^2\right) = \frac{e^{\frac{m_H^2}{M^2}}}{2m_H^2 f_H} \int_{m_Q^2}^{s_0} ds\, \frac{1}{\pi}\, \mathrm{Im}_s \left[F^{HM}\left(q^2, s\right)\right]_{OPE} e^{-\frac{s}{M^2}}\,, \tag{993}$$

$$f_{HM}^{+}\left(q^2\right) + f_{HM}^{-}\left(q^2\right) = \frac{e^{\frac{m_H^2}{M^2}}}{m_H^2 f_H} \int_{m_Q^2}^{s_0} ds\, \frac{1}{\pi}\, \mathrm{Im}_s \left[\widetilde{F}^{HM}\left(q^2, s\right)\right]_{OPE} e^{-\frac{s}{M^2}}\,. \tag{994}$$

Both sum rules require an adequate Borel window[35] which is determined in Section 5.3.1 (see Section 5.1.1 and Section B.3 for more details). If the latter has been roughly determined, we may use the following sum rule (m_H^2 results from experimental data)

$$\begin{aligned} m_H^2 &= M^4 \frac{d}{d\,M^2} \log\left[2m_H^2 f_H f_{HM}^{+}\left(q^2\right) e^{-\frac{m_H^2}{M^2}}\right] \\ &= M^4 \frac{d}{d\,M^2} \left\{\int_{m_Q^2}^{s_0} ds\, \frac{1}{\pi}\, \mathrm{Im}_s \left[F^{HM}\left(q^2, s\right)\right]_{OPE} e^{-\frac{s}{M^2}}\right\} \end{aligned} \tag{995}$$

to fix[36] the numerical value of s_0.

In conclusion, Equation 993, Equation 994 and Equation 995 thus provide all formal foundations for an actual determination of the corresponding LCSRs.

5.2.2 *Leading-order and next-to-leading order spectral densities*

In this subsection, we explicitly formulate the LCSRs for the f_{HM}^{+} form factor. For this purpose, we show the calculation of all considered LO spectral densities, while following the strategy of Section 5.1.2.3 to include existing NLO QCD corrections. The resulting LCSRs then allow a phenomenological NLO analysis of the $D_{(s)}, B \to \eta^{(\prime)}$ transition form factors.

Before proceeding with an actual calculation, let us reconsider the expected structure of the included contributions. According to the factorization theorem (see Equation 949), all relevant results can be written in the general form (cf. [2]; $p_H^{\mu} = (p+q)^{\mu}$):

$$\left[F^{HM}\left(q^2, p_H^2\right)\right]_{OPE} = \sum_{t=2,3,4} F_{0,t}^{HM}\left(q^2, p_H^2\right) + \frac{\alpha_S C_f}{4\pi} \sum_{t=2,3} F_{1,t}^{HM}\left(q^2, p_H^2\right) + \dots\,, \tag{996}$$

where the ellipses represent neglected higher order corrections. For the subsequent determination of imaginary parts, we may use Equation 988 after performing a Borel transformation in $(p+q)^2$ on it:

$$\begin{aligned} &\hat{\mathcal{B}}_{(p+q)^2 \to M^2} \left\{\left[F^{HM}\left(q^2, (p+q)^2\right)\right]_{OPE}\right\} \\ &= \int_0^1 du\, \exp\left[-\frac{m_Q^2 - \bar{u} q^2 + u \bar{u} p^2}{u M^2}\right] \frac{m_Q^2 - q^2 + u^2 p^2}{u^2} \frac{1}{\pi}\, \mathrm{Im}_{s(u)} \left[F^{HM}\left(q^2, s(u)\right)\right]_{OPE}\,. \end{aligned} \tag{997}$$

35 Along with the continuum threshold s_0, a variation of M^2 is required to have only a negligible numerical impact on the given sum rule. The interval of Borel parameters (if existing), where this behavior is guaranteed, is usually named a Borel window.

36 Based on [322], the threshold parameter s_0 is roughly determined by its SVZ counterpart for f_B. Thus, the optimal value for s_0 has to be found in connection with the determination of M^2.

In this way, the formally similar QCD amplitudes (see Equation 959 and Equation 962) give rise to corresponding imaginary parts, simply by means of partial integration. This is necessary to remove the contributions that depend on inverse powers of the Borel parameter. Since the latter can be generated via $\left(-M^2\right)^{-n} e^{-\frac{s}{M^2}} = \frac{d^n}{ds^n} e^{-\frac{s}{M^2}}$ ($n \in \mathbb{N}_0$), integration by parts offers the opportunity to shift derivatives between different functions of the integrand. In this way all $\left(-M^2\right)^{-n}$ terms can be absorbed into derivatives. For instance, Equation 959 entails corrections similar to (here all surface terms $\sim \phi_{4M}^{(\psi)}$ are omitted)

$$\int_0^1 du\, \frac{\phi_{4M}^{(\psi)}(u)}{u^3 M^4} e^{-\frac{m_Q^2-\bar{u}q^2+u\bar{u}p^2}{uM^2}} = \int_0^1 du\, e^{-\frac{m_Q^2-\bar{u}q^2+u\bar{u}p^2}{uM^2}} \left(\frac{12u^3p^4\phi_{4M}^{(\psi)}(u)}{\left[m_Q^2-q^2+u^2p^2\right]^4} - \frac{6u^2p^2\frac{d\,\phi_{4M}^{(\psi)}(u)}{du}}{\left[m_Q^2-q^2+u^2p^2\right]^3} + \frac{u\frac{d^2\phi_{4M}^{(\psi)}(u)}{du^2}}{\left[m_Q^2-q^2+u^2p^2\right]^2} \right). \tag{998}$$

Thus, as a result, we get for Equation 959 (terms marked in blue are a difference to [319, 335, 519])

$$\begin{aligned}
&\hat{\mathcal{B}}_{(p+q)^2\to M^2} \left\{ \left[F^{HM}\left(q^2,(p+q)^2\right)\right]_{OPE} \right\}\Big|_{LO} \\
&= m_Q^2 F_M^{(\psi)} \int_0^1 du\, e^{-\frac{m_Q^2-\bar{u}q^2+u\bar{u}p^2}{uM^2}} \left\{ \frac{\phi_M^{(\psi)}(u)}{u} + \frac{1}{2m_\psi m_Q F_M^{(\psi)}} \left(\overline{\phi}_{3M}^{(\psi);p}(u) \right.\right. \\
&\quad \left.\left. + \left[\frac{2}{u} + \frac{4m_Q^2up^2}{\left(m_Q^2-q^2+u^2p^2\right)^2} - \frac{m_Q^2+q^2-u^2p^2}{m_Q^2-q^2+u^2p^2}\frac{d}{du} \right] \frac{\overline{\phi}_{3M}^{(\psi);\sigma}(u)}{6} \right) \right. \\
&\quad - \frac{m_Q^2 u}{4\left(m_Q^2-q^2+u^2p^2\right)^2} \left[\frac{12u^2p^4}{\left(m_Q^2-q^2+u^2p^2\right)^2} - \frac{6up^2}{m_Q^2-q^2+u^2p^2}\frac{d}{du} \right. \\
&\quad \left.\left. + \frac{d^2}{du^2} \right] \phi_{4M}^{(\psi)}(u) + \frac{1}{m_Q^2-q^2+u^2p^2} \left[u\psi_{4M}^{(\psi)}(u) + \frac{m_Q^2-q^2-u^2p^2}{m_Q^2-q^2+u^2p^2} \int_0^u dv\, \psi_{4M}^{(\psi)}(v) \right] \right\} \\
&\quad + \frac{m_Q^4 F_M^{(\psi)} e^{-\frac{m_Q^2}{M^2}}}{4\left(m_Q^2-q^2+p^2\right)^2} \left\{ \frac{d}{dx}\phi_{4M}^{(\psi)}(x) \right\}\Big|_{x=1},
\end{aligned} \tag{999}$$

with the surface term (cf. Equation 997)

$$\frac{1}{\pi}\,\mathrm{Im}_{s(u)} \left[F^{HM}\left(q^2,s(u)\right)\right]_{OPE}\Big|_{surface} = \frac{m_Q^4 F_M^{(\psi)} u^3 \delta(\bar{u})}{4\left(m_Q^2-q^2+u^2p^2\right)^3} \left\{ \frac{d}{dx}\phi_{4M}^{(\psi)}(x) \right\}\Big|_{x=u}. \tag{1000}$$

All remaining imaginary parts can be extracted from Equation 999 in the same manner, i. e., within the corresponding sum rules only the integration limits will change[37] (see Equation 993). Similarly, the three-particle corrections can be resolved, in particular, after introducing the identity ("f" represents a well-behaved function)

$$\int_0^1 dv \int \mathcal{D}\underline{\alpha}\, f(\underline{\alpha},v) = \int_0^1 du \int_0^u d\alpha_1 \int_{\frac{u-\alpha_1}{1-\alpha_1}}^1 dv\, \frac{1}{v} f(\underline{\alpha},v)\Big|_{\substack{\alpha_2=1-\alpha_1-\alpha_3 \\ \alpha_3=\frac{u-\alpha_1}{v}}}. \tag{1001}$$

37 In other words, by replacing $\int_0^1 du \mapsto \int_{u_0}^1 du$ within Equation 999 the corresponding LCSRs can be derived.

Based on Equation 1001, we may, therefore, define

$$I_{3M}^{(\psi)}(u) \coloneqq \int_0^u d\alpha_1 \int_{\frac{u-\alpha_1}{1-\alpha_1}}^1 dv\, \frac{1}{v} \Phi_{3M}^{(\psi)}(\underline{\alpha}) \left(4v\, p\cdot q + 3\xi_v u p^2\right) \Big|_{\substack{\alpha_2=1-\alpha_1-\alpha_3 \\ \alpha_3=\frac{u-\alpha_1}{v}}}, \tag{1002}$$

$$I_{4M}^{(\psi)}(u) \coloneqq \int_0^u d\alpha_1 \int_{\frac{u-\alpha_1}{1-\alpha_1}}^1 \frac{dv}{v} \left(2\left[\Psi_{4M}^{(\psi)}(\underline{\alpha}) + \widetilde{\Psi}_{4M}^{(\psi)}(\underline{\alpha})\right] - \left[\Phi_{4M}^{(\psi)}(\underline{\alpha}) + \widetilde{\Phi}_{4M}^{(\psi)}(\underline{\alpha})\right]\right) \Big|_{\substack{\alpha_2=1-\alpha_1-\alpha_3 \\ \alpha_3=\frac{u-\alpha_1}{v}}}, \tag{1003}$$

$$\bar{I}_{4M}^{(\psi)}(u) \coloneqq \int_0^u d\alpha_1 \int_{\frac{u-\alpha_1}{1-\alpha_1}}^1 \frac{dv}{v} \left(\Psi_{4M}^{(\psi)}(\underline{\alpha}) + \widetilde{\Psi}_{4M}^{(\psi)}(\underline{\alpha}) + \Phi_{4M}^{(\psi)}(\underline{\alpha}) + \widetilde{\Phi}_{4M}^{(\psi)}(\underline{\alpha})\right) \Big|_{\substack{\alpha_2=1-\alpha_1-\alpha_3 \\ \alpha_3=\frac{u-\alpha_1}{v}}}, \tag{1004}$$

$$\widetilde{I}_{3M}^{(\psi)}(u) \coloneqq \int_0^u d\alpha_1 \int_{\frac{u-\alpha_1}{1-\alpha_1}}^1 dv\, \frac{1}{v} \left(2-\xi_v\right) \Phi_{3M}^{(\psi)}(\underline{\alpha}) \Big|_{\substack{\alpha_2=1-\alpha_1-\alpha_3 \\ \alpha_3=\frac{u-\alpha_1}{v}}}, \tag{1005}$$

which together with

$$\int_0^1 du \int_0^u dw\, \frac{(u-w)\, \bar{I}_{4M}^{(\psi)}(u)}{\left[m_Q^2 - (q+(u-w)\,p)^2\right]^3} = \int_0^1 du\, \frac{1}{\left[m_Q^2 - (q+up)^2\right]^3} \int_u^1 dw\, \bar{I}_{4M}^{(\psi)}(w)\,, \tag{1006}$$

$$\int_0^1 du \int_0^u dw\, \frac{\bar{I}_{4M}^{(\psi)}(u)}{\left[m_Q^2 - (q+(u-w)\,p)^2\right]^3} = \int_0^1 du\, \frac{1}{\left[m_Q^2 - (q+up)^2\right]^3} \int_u^1 dw\, \bar{I}_{4M}^{(\psi)}(w)\,, \tag{1007}$$

imply a modified version of Equation 962

$$\begin{aligned} F_\mu^{(b)}(p,q) = p_\mu \int_0^1 du\, \frac{m_Q^2 F_M^{(\psi)}}{\left[m_Q^2 - (q+up)^2\right]^2} \Bigg[& \frac{f_{3M}^{(\psi)}}{m_Q F_M^{(\psi)}} I_{3M}^{(\psi)}(u) + I_{4M}^{(\psi)}(u) \\ & + \frac{4up^2}{m_Q^2 - (q+up)^2} \int_u^1 dw\, \bar{I}_{4M}^{(\psi)}(w) \Bigg] \\ - q_\mu \int_0^1 du\, \frac{m_Q^2 F_M^{(\psi)}}{\left[m_Q^2 - (q+up)^2\right]^2} \Bigg[& \frac{f_{3M}^{(\psi)}}{m_Q F_M^{(\psi)}} p^2 \widetilde{I}_{3M}^{(\psi)}(u) \\ & - \frac{4p^2}{m_Q^2 - (q+up)^2} \int_u^1 dw\, \bar{I}_{4M}^{(\psi)}(w) \Bigg]\,. \end{aligned} \tag{1008}$$

Consequently, the Borel transformation of Equation 1008 can again be simplified via integration by parts. Thus, for Equation 1008 we finally get the result

$$\begin{aligned}
&\hat{\mathcal{B}}_{(p+q)^2\to M^2}\left\{\left[F^{HM}\left(q^2,(p+q)^2\right)\right]_{OPE}\right\}\Big|_{LO}\\
&= m_Q^2 F_M^{(\psi)}\int_0^1 du\, e^{-\frac{m_Q^2-\bar{u}q^2+u\bar{u}p^2}{uM^2}}\left\{\frac{1}{m_Q^2-q^2+u^2p^2}\times\right.\\
&\quad\times\left[\frac{2up^2}{m_Q^2-q^2+u^2p^2}-\frac{d}{du}\right]\left(\frac{f_{3M}^{(\psi)}}{m_Q F_M^{(\psi)}}I_{3M}^{(\psi)}(u)+I_{4M}^{(\psi)}(u)\right)\\
&\quad-\frac{2up^2}{\left[m_Q^2-q^2+u^2p^2\right]^2}\left[\left(u\frac{d}{du}+2\frac{m_Q^2-q^2-2u^2p^2}{m_Q^2-q^2+u^2p^2}\right)\bar{I}_{4M}^{(\psi)}(u)\right.\\
&\quad\left.\left.+\frac{6up^2\left(m_Q^2-q^2-u^2p^2\right)}{\left[m_Q^2-q^2+u^2p^2\right]^2}\int_u^1 dw\,\bar{I}_{4M}^{(\psi)}(w)\right]\right\},
\end{aligned}\tag{1009}$$

which can be used to reproduce the findings of [335, 519], i. e., after applying

$$\begin{aligned}
&\left(1-\frac{4u^2p^2}{m_Q^2-q^2+u^2p^2}+u\frac{d}{du}\right)\bar{I}_{4M}^{(\psi)}(u)\\
&+\frac{m_Q^2-q^2-u^2p^2}{m_Q^2-q^2+u^2p^2}\left(\frac{6up^2}{m_Q^2-q^2+u^2p^2}-\frac{d}{du}\right)\int_u^1 dw\,\bar{I}_{4M}^{(\psi)}(w)\\
&=\left(2\frac{m_Q^2-q^2-2u^2p^2}{m_Q^2-q^2+u^2p^2}+u\frac{d}{du}\right)\bar{I}_{4M}^{(\psi)}(u)+6up^2\frac{m_Q^2-q^2-u^2p^2}{m_Q^2-q^2+u^2p^2}\int_u^1 dw\,\bar{I}_{4M}^{(\psi)}(w)
\end{aligned}\tag{1010}$$

and related replacement rules (see Section 5.1.2.1). In accordance with Section 5.1.2.2, the remaining NLO QCD corrections can be introduced by inserting the given spectral densities of [32, 320] into Equation 983 – Equation 986 and subsequently Equation 993. Since the resulting expressions are in general kept unchanged, we refer to the original works [32, 257, 320, 525] for a detailed review. Let us instead mention the extent of all included corrections (cf. Equation 996):

- At LO in α_S the vector form factor f_{HM}^+ is calculated up to twist-four accuracy, while in general keeping $\mathcal{O}(m_s)$ as well as $\mathcal{O}\left(m_H^2\right)$ effects in the meson DAs and $F_{0,t}^{HM}$.
- For the hard scattering kernels $F_{1,t}^{HM}$, however, only $\mathcal{O}(m_s)\sim\mathcal{O}\left(m_H^2\right)$ and $\mathcal{O}(\alpha_S)$ contributions, but not $\mathcal{O}(m_s\alpha_S)$ admixtures are taken into account, since the latter would induce a mixing between different twist components which is beyond the scope of this study[38] (see [319, 335] for more details).

Hence, we adopt similar assumptions, such as those made in [32, 319, 519]. Correspondingly, the intended numerical evaluation exhibits constraints analogous to those of [32].

With this in mind and the NLO LCSRs ready to use, we may now focus on a phenomenological analysis of f_{HM}^+ form factors.

38 Those corrections originate from finite mass-terms proportional to m_s or $p^2=m_M^2$ within the NLO diagrams (see Figure 41). Therefore, these effects would require a recalculation of related hard scattering kernels, including a dedicated study of the various higher twist DAs (see [319, 322, 335] for an extended discussion).

5.3 NUMERICAL EVALUATION

The discussed upcoming high luminosity experiments at B-factories and other collider facilities, such as Belle II (at the SuperKEKB accelerator complex) [528], *BABAR* (PEP-II collider at the SLAC laboratory) [529], BES III (BEPC II) [530] or $\overline{\text{P}}$ANDA (FAIR) [29], may produce crucial statistics needed for a phenomenological study of $B, D_{(s)} \to \eta^{(\prime)} X$ decays (see [35, 42] for details). Most importantly, the semileptonic decay modes $\left(\text{e.g., } X = l\nu_l, \text{ with } l = e, \mu\right)$ are expected to be mainly driven by SM dynamics. Thus, their detailed analysis could reveal the underlying non-perturbative mechanisms, responsible for mixing effects and meson transitions. Moreover, the weak decays $D_s^+ \to \eta^{(\prime)} l^+ \nu_l$, $D^+ \to \eta^{(\prime)} l^+ \nu_l$ and $B^+ \to \eta^{(\prime)} l^+ \nu_l$ proceed on greatly different time scales [35, 522], since they are driven by Cabibbo-allowed, Cabibbo-suppressed and Kobayashi-Maskawa-suppressed subprocesses [225], respectively. Additionally, all three processes could provide highly complementary information on the $\eta^{(\prime)}$ meson's flavor structure, because the latter is produced via a $s\bar{s}$, $d\bar{d}$, $u\bar{u}$ or gg valence Fock-state (see Section A.14). Accordingly, there are several ways to approach this topic, i. e., our strategy could be as follows (see also [2, 244, 525]):

i) When focusing on the aspects related to flavor physics, we could analyze the spectrum $\frac{d\,\Gamma(H \to \eta^{(\prime)} l \nu_l)}{d\,q^2}$ which allows an extraction of CKM matrix elements $[V_{CKM}]_{ij} \equiv V_{ij}$ (see Section 2.6.1).

ii) Alternatively, one may use ratios of branching fractions to constrain the gluonic Gegenbauer moment.

Since our primary goal is an investigation of $\eta^{(\prime)}$ DAs, we follow the second path, while using $|V_{ij}|$ as an external input parameter. Furthermore, we extract f_{HM}^+ form factors from LCSRs for all three decay modes, starting with an analysis at $q^2 = 0$ (see Section 5.3.2). This is followed by a calculation of Branching fractions which we compare to the existing experimental data (cf. Section 5.3.4). However, for that purpose, a corresponding extrapolation method[39] is needed, which we also discuss in detail.

5.3.1 *Choice of input parameters*

In this subsection, all necessary input parameters are introduced, while some important aspects concerning the assumed numerical values of Gegenbauer moments at a preferred reference scale $\mu_0 = 1$ GeV are discussed. Here, we closely follow our publication [2].

As mentioned above, we consistently use the $\overline{\text{MS}}$ scheme and one universal scale $\mu^2 \approx m_H^2 - m_Q^2$ (see Table 16) throughout our calculations. Correspondingly, all quantities are evolved to this renormalization point, using a two-loop running coupling constant α_s (see Section 2.3) for parameters related to DAs, while the scale dependence of $\overline{\text{MS}}$ masses are calculated up to one-loop accuracy (see [2, 319, 320] for more details).

The choice for the implemented Gegenbauer moments requires some explanation (see also Section 5.1.2.2), since it is affected by the chronological order of our own publications that have been included in this work. Since [3] has been published after [2] we make use of a very general ansatz for the applied input parameters, including the Gegenbauer moments $c_{2,M}^{(a)}(\mu_0)$ $\left(a = 0, 8, g;\ M = \eta, \eta'\right)$. The latter were mostly unknown, and to our best knowledge have only been investigated in [20, 28, 531, 532]. In fact, within the recent perturbative analysis of [20, 28] $\eta^{(\prime)}$ DAs

39 In Section 5.3.3 we give an introduction to the used extrapolation methods and their nontrivial physical content.

and, in particular, their two-gluon components were studied, giving rise to the following values (see Section 3.1.4) [20, 28]:

$$c_2^{(8)}(\mu_0)\big|_{\text{Kroll}} = -0.05 \pm 0.02\,,\; c_2^{(0)}(\mu_0)\big|_{\text{Kroll}} = -0.12 \pm 0.01\,,\; c_2^{(g)}(\mu_0)\big|_{\text{Kroll}} = 0.67 \pm 0.16\,. \tag{1011}$$

According to [28] these parameters are contaminated by effects related to omitted higher order Gegenbauer coefficients and neglected power corrections. Nevertheless, both of these effects are sizable for the underlying pion and η, η' transition form factors at intermediate momentum transfer, as we were able to show in [1, 3, 281], and should, therefore, not be neglected. For instance, within the accessible kinematic region of the $\gamma^*\gamma^{(*)} \to \pi^0$ form factor they imply a considerable difference between the moments obtained in [1, 281] $\left(c_{2,\pi}(\mu_0) \approx 0.14 \pm 0.02\right)$ and those given by [28] $\left(c_{2,\pi}(\mu_0) \approx -0.02 \pm 0.02\right)$. In other words, by including corresponding generic power corrections, one may create a shift in the parameters of Equation 1011 which roughly amounts to $c_2^{(8)}(\mu_0)\big|_{\text{Kroll}} \approx 0.06 \pm 0.05$. Consequently, Equation 1011 should be taken with a grain of salt. Instead of retrofitting these older studies, we will use the more general average value [2]:

$$c_2(\mu_0) \coloneqq 0.25 \pm 0.15\,. \tag{1012}$$

The latter results from a combination of lattice QCD and sum rule calculations which also includes LCSR fits to experimental data (see [1, 2, 281] for more details). Thus, in accordance with Section 5.1.2.2, we implement the QCD evolution of Gegenbauer moments via Equation 981, i. e., by neglecting all higher order coefficients except for

$$c_2^{(0)}(\mu_0) \stackrel{!}{=} c_2^{(8)}(\mu_0) \stackrel{!}{=} c_2(\mu_0)\,. \tag{1013}$$

A posteriori (see, e. g., [2, 3, 271, 319, 525]), there is no indication of large $\mathrm{SU}(3)_F$-flavor violations in pion or kaon DAs, i. e., $c_{2,\pi} \approx c_{2,K}$. Thus, Equation 1013 and the ansatz described in Section 5.1.2.2 should imply an acceptable approximation. Moreover, due to a rather moderate mixing between $c_2^{(0)}$ and $c_2^{(g)}$ (see Section 5.1.2.2), we may treat the latter as a free parameter and vary it over the same conservative range $c_2^{(0)}(\mu_0) = \pm 0.67$ as done in [2, 32]. For the quark and meson masses, we adopt their current values $(\mu_{\text{aux}} \coloneqq 2\text{ GeV})$, as given by [2, 225]:

$$m_c(m_c) = (1.275 \pm 0.025)\text{ GeV}\,, \quad m_u(\mu_{\text{aux}}) = \left(2.3^{+0.7}_{-0.5}\right)\text{ MeV}\,, \tag{1014}$$

$$m_d(\mu_{\text{aux}}) = \left(4.8^{+0.7}_{-0.3}\right)\text{ MeV}\,, \quad m_s(\mu_{\text{aux}}) = (95 \pm 5)\text{ MeV}\,, \tag{1015}$$

$$m_{D^+} = 1869.6\text{ MeV}\,, \quad m_{D_s^+} = 1968.5\text{ MeV}\,, \tag{1016}$$

$$m_{\pi^0} = 134.98\text{ MeV}\,, \quad m_{K^0} = 497.61\text{ MeV}\,. \tag{1017}$$

Here, Equation 1017 is needed to determine the hypothetical masses of the $|\eta_q\rangle$ and $|\eta_s\rangle$ states (see Equation 541). Furthermore, in order to reduce the involved uncertainties, we use the corresponding experimental values for [225]

$$f_D = (206.7 \pm 8.5 \pm 2.5)\text{ MeV}\,, \quad f_{D_s} = (260 \pm 5.4)\text{ MeV}\,, \tag{1018}$$

while f_B is extracted from a NLO two-point QCD sum rule (see Section 5.1.1). In this context also the quark-, gluon- and mixed condensate, as listed in Section 2.4 are employed. Finally, at the given order of accuracy, we require the standard twist-three and twist-four parameter (cf. [2, 271]), as mentioned in Table 7, along with Section 3.4.3. Besides, we need [2, 271]

$$\varepsilon_\pi = \frac{21}{8}\,(0.2 \pm 0.1)\text{ GeV}\,. \tag{1019}$$

This concludes the list of necessary numerical parameters.

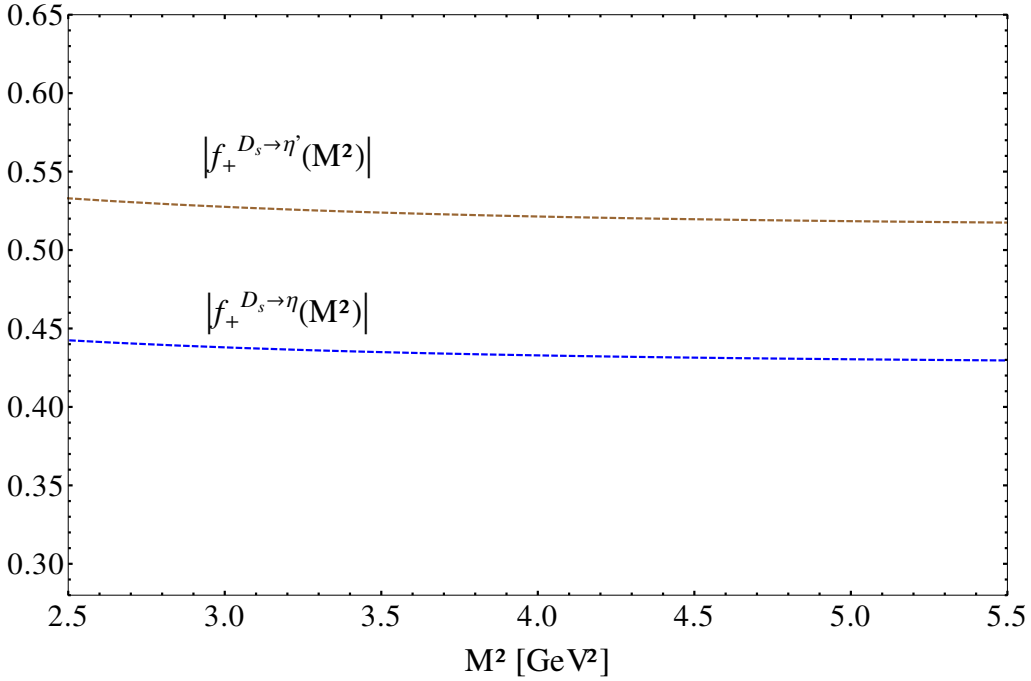

Figure 42: The vector form factors $|f_+^{D_s\to\eta}(M^2)|$, $|f_+^{D_s\to\eta'}(M^2)|$ plotted as functions of the Borel parameter M^2. Here, the blue dashed line corresponds to $|f_+^{D_s\to\eta}(M^2)|$, while the brown dashed line represents $|f_+^{D_s\to\eta'}(M^2)|$ (the plots are taken from [2]).

5.3.2 *Phenomenological results for* $q^2 = 0$

We now turn to the numerical evaluation of LCSRs for f_{HM}^+ form factors, as introduced in Equation 993. The code used in this analysis is partially based on an older program, written by N. Offen, which provides the required NLO quark spectral densities. We extend the underlying program code by including gluonic NLO contributions and other subroutines which allow an extended statistical analysis of all input parameters.

As a starting point for an evaluation of Equation 993, the inherent Borel window and effective threshold parameter have to be determined. For an illustration, we show the dependence of $f_{HM}^+(0)$ on M^2 (i. e., let us use $f_{HM}^+(0, M^2) =: f_+^{H\to M}(M^2)$) in Figure 42. In fact, the sum rule exhibits a stable behavior over a wide range of input parameters. Thus, the optimal values should lie within the intervals [2]

$$s_0^D = (7 \pm 0.6)\ \text{GeV}^2\,, \qquad s_0^B = (35.75 \pm 0.25)\ \text{GeV}^2\,, \tag{1020}$$

$$M_D^2 = (4.4 \pm 1.1)\ \text{GeV}^2\,, \quad M_B^2 = (18 \pm 3)\ \text{GeV}^2\,. \tag{1021}$$

The corresponding LCSR results for $q^2=0$ can be written as

$$|f^+_{D_s^+\eta}(0)| = 0.432 \pm 0.003\Big|_{M^2} \pm 0.026\Big|_{\mu} \pm 0.010\Big|_{s_0} \pm 0.013\Big|_{c_2} \pm 0.001\Big|_{c_2^{(g)}} \pm 0.025\Big|_{(f_q,f_s,\phi)} \pm 0.014\Big|_{\text{twist-3}} \pm 0.002\Big|_{\text{twist-4}} \pm 0.005\Big|_{(\text{condensates},m_c)}, \tag{1022}$$

$$|f^+_{D_s^+\eta'}(0)| = 0.520 \pm 0.003\Big|_{M^2} \pm 0.032\Big|_{\mu} \pm 0.012\Big|_{s_0} \pm 0.015\Big|_{c_2} \pm 0.070\Big|_{c_2^{(g)}} \pm 0.028\Big|_{(f_q,f_s,\phi)} \pm 0.016\Big|_{\text{twist-3}} \pm 0.002\Big|_{\text{twist-4}} \pm 0.006\Big|_{(\text{condensates},m_c)}, \tag{1023}$$

which include an error analysis of all relevant parameters, i. e., the latter are varied within their respective ranges (see discussion above). Similarly, we get [2]

$$|f^+_{D^+\eta}(0)| = 0.552 \pm 0.008\Big|_{M^2} \pm 0.034\Big|_{\mu} \pm 0.013\Big|_{s_0} \pm 0.016\Big|_{c_2} \pm 0.002\Big|_{c_2^{(g)}} \pm 0.015\Big|_{(f_q,f_s,\phi)} \pm 0.036\Big|_{\text{twist-3}} \pm 0.002\Big|_{\text{twist-4}} \pm 0.007\Big|_{(\text{condensates},m_c)}, \tag{1024}$$

$$|f^+_{D^+\eta'}(0)| = 0.458 \pm 0.007\Big|_{M^2} \pm 0.028\Big|_{\mu} \pm 0.011\Big|_{s_0} \pm 0.013\Big|_{c_2} \pm 0.096\Big|_{c_2^{(g)}} \pm 0.025\Big|_{(f_q,f_s,\phi)} \pm 0.030\Big|_{\text{twist-3}} \pm 0.002\Big|_{\text{twist-4}} \pm 0.006\Big|_{(\text{condensates},m_c)}, \tag{1025}$$

$$|f^+_{B^+\eta}(0)| = 0.238 \pm 0.002\Big|_{M^2} \pm 0.013\Big|_{\mu} \pm 0.002\Big|_{s_0} \pm 0.004\Big|_{c_2} \pm 0.001\Big|_{c_2^{(g)}} \pm 0.006\Big|_{(f_q,f_s,\phi)} \pm 0.011\Big|_{\text{twist-3}} \pm 0.0002\Big|_{\text{twist-4}} \pm 0.007\Big|_{(\text{condensates},m_b)}, \tag{1026}$$

$$|f^+_{B^+\eta'}(0)| = 0.198 \pm 0.001\Big|_{M^2} \pm 0.011\Big|_{\mu} \pm 0.002\Big|_{s_0} \pm 0.003\Big|_{c_2} \pm 0.061\Big|_{c_2^{(g)}} \pm 0.007\Big|_{(f_q,f_s,\phi)} \pm 0.009\Big|_{\text{twist-3}} \pm 0.0001\Big|_{\text{twist-4}} \pm 0.006\Big|_{(\text{condensates},m_b)}. \tag{1027}$$

Inspired by [319], we also consider the variation $1\text{ GeV} < \mu < 3\text{ GeV}$ as a possible source of uncertainty. Most importantly, ratios of the $f^+_{H\eta'}(0)$ and $f^+_{H\eta}(0)$ form factors are particularly interesting, since for such quantities most of the related uncertainties cancel [2]:

$$\left|\frac{f^+_{D_s^+\eta'}(0)}{f^+_{D_s^+\eta}(0)}\right| = 1.20 \pm 1\cdot 10^{-13}\Big|_{M^2} \pm 1\cdot 10^{-12}\Big|_{\mu} \pm 6\cdot 10^{-13}\Big|_{s_0} \pm 7\cdot 10^{-14}\Big|_{c_2} \pm 0.16\Big|_{c_2^{(g)}} \pm 0.06\Big|_{(f_q,f_s,\phi)} \pm 3\cdot 10^{-12}\Big|_{\text{twist-3}} \pm 3\cdot 10^{-14}\Big|_{\text{twist-4}} \pm 2\cdot 10^{-14}\Big|_{(\text{condensates},m_b)}, \tag{1028}$$

$$\left|\frac{f^+_{D^+\eta'}(0)}{f^+_{D^+\eta}(0)}\right| = 0.83 \pm 5\cdot 10^{-13}\Big|_{M^2} \pm 9\cdot 10^{-13}\Big|_{\mu} \pm 2\cdot 10^{-13}\Big|_{s_0} \pm 5\cdot 10^{-15}\Big|_{c_2} \pm 0.18\Big|_{c_2^{(g)}} \pm 0.04\Big|_{(f_q,f_s,\phi)} \pm 8\cdot 10^{-13}\Big|_{\text{twist-3}} \pm 3\cdot 10^{-14}\Big|_{\text{twist-4}} \pm 5\cdot 10^{-14}\Big|_{(\text{condensates},m_b)}, \tag{1029}$$

$$\left|\frac{f^+_{B^+\eta'}(0)}{f^+_{B^+\eta}(0)}\right| = 0.83 \pm 8\cdot 10^{-13}\Big|_{M^2} \pm 6\cdot 10^{-13}\Big|_{\mu} \pm 1\cdot 10^{-13}\Big|_{s_0} \pm 1\cdot 10^{-13}\Big|_{c_2} \pm 0.26\Big|_{c_2^{(g)}} \pm 0.04\Big|_{(f_q,f_s,\phi)} \pm 8\cdot 10^{-13}\Big|_{\text{twist-3}} \pm 2\cdot 10^{-14}\Big|_{\text{twist-4}} \pm 2\cdot 10^{-13}\Big|_{(\text{condensates},m_b)}. \tag{1030}$$

Here, we should recall, that by assuming $SU(3)_F$-breaking effects in the gluonic Gegenbauer moments, i. e., $c^{(g)}_{2,\eta'} \approx c^{(g)}_{2,\eta}$, no similar behavior can be inferred for the associated TFFs. Instead,

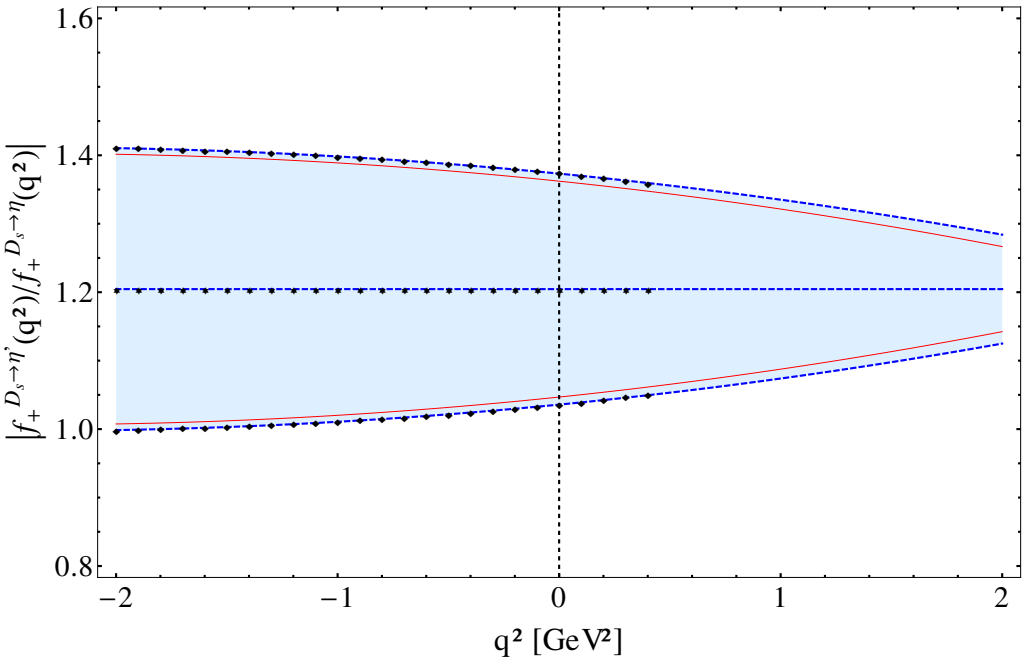

Figure 43: Based on [2] $\left|f^+_{D_s^+\eta'}(q^2)/f^+_{D_s^+\eta}(q^2)\right| \equiv \left|f_+^{D_s^+\to\eta'}(q^2)/f_+^{D_s^+\to\eta}(q^2)\right|$ is plotted as a function of q^2. Again, the black dots are calculated sum rule results, where the upper and lower line correspond to the uncertainties of our calculation. Those are completely dominated by the gluonic contributions (red lines).

contributions to the form factor are vastly different, because the gluonic admixtures of the singlet part are determined by (see Chapter 3)

$$f_\eta^{(0)} = \sqrt{\frac{2}{3}} f_q \cos\phi - \sqrt{\frac{1}{3}} f_s \sin\phi\,, \tag{1031}$$

$$f_{\eta'}^{(0)} = \sqrt{\frac{2}{3}} f_q \sin\phi + \sqrt{\frac{1}{3}} f_s \cos\phi\,. \tag{1032}$$

Therefore, the corresponding dependence on the gluonic Gegenbauer moment does not cancel. In fact, as listed in Equation 1028 – Equation 1030, almost the entire uncertainty in $\left|f^+_{H\eta'}(0)/f^+_{H\eta}(0)\right|$ comes from $c_2^{(g)}(\mu_0)$, thus offering a possibility to constrain the gluonic DAs, if more precise experimental data becomes available. In the next step, we may study the behavior of $\left|f^+_{H\eta'}(0)/f^+_{H\eta}(0)\right|$ for different q^2 values. The results for $D_s \to \eta^{(\prime)}$ form factors are shown in Figure 43. As expected, the given uncertainties are completely governed by gluonic contributions. However, this evaluation anticipates a peculiarity of the LCSR method which is only applicable for $q^2 \lesssim m_Q^2 - 2m_Q\chi$ ($\chi = \mathcal{O}(1\text{ GeV})$, see [257, 517, 523]).

Correspondingly, the plots of Figure 43 actually require an adequate extrapolation method which is discussed in the next subsection.

5.3.3 *Parametrizations of heavy-to-light form factors*

In this subsection, we summarize and compare some of the most popular extrapolation methods[40], that are used in form factor calculations. While focusing on the nontrivial physics behind those different parametrizations, we also address the resulting impact on observables and their statistical interpretation. This forms a theoretical basis for the subsequently performed phenomenological analysis.

As mentioned above, the LCSR method for "heavy (H)→light (M)" transitions is restricted to a kinematical regime of sufficiently large meson energies $E_M \coloneqq \frac{p_H \cdot p_M}{m_H} \gg \Lambda_{QCD}$ which translates into small or moderate values of momentum transfers[41]:

$$q^2 = m_H^2 - 2m_H E_M + m_M^2 \,. \tag{1033}$$

In other words, it cannot access the entire physical region[42] $0 \leqslant q^2 \leqslant (m_H - m_M)^2 = q^2_{max}$, as needed to obtain the corresponding semileptonic branching ratios. Consequently, a parametrization that reliably reproduces the data beyond this accessible realm is required[43]. For this purpose, one may start from first principles which ideally imply the required general structure of $f_+^{HM}(q^2)$ as well as $f_0^{HM}(q^2)$. Indeed, due to their inherent Lorentz invariance both form factors are analytic functions in q^2 satisfying unsubtracted dispersion relations [542–544]:

$$f_+^{HM}\left(q^2\right) = \frac{\mathrm{Res}_{t=m_{H^*}^2}\left\{f_+^{HM}(t)\right\}}{m_{H^*}^2 - q^2} + \frac{1}{\pi}\int_{t_0}^{\infty} \mathrm{d}t\, \frac{\mathrm{Im}_t\, f_+^{HM}(t)}{t - q^2}\,, \tag{1034}$$

$$f_0^{HM}\left(q^2\right) = \frac{1}{\pi}\int_{t_0}^{\infty} \mathrm{d}t\, \frac{\mathrm{Im}_t\, f_0^{HM}(t)}{t - q^2}\,. \tag{1035}$$

As implied by the associated quantum numbers of f_+ $\left(J^P = 1^-\right)$, or its scalar counterpart f_0 $\left(J^P = 0^+\right)$, each imaginary part contains all possible poles and branch points/cuts which are situated above the generic two-particle threshold $t_0 = (m_H + m_\pi)^2$. It is worth highlighting that the vector form factor exhibits an isolated pole below t_0, while possible analogous contributions to f_0 are effectively hidden within the related dispersive term (cf. [322, 542]). Moreover, the residue of[44] f_+ at $q^2 = m_{H^*}^2$ (see [322, 371, 542])

$$c_{H^*} \coloneqq \frac{f_{H^*} g_{H^*HM}}{2m_{H^*}} = \frac{\mathrm{Res}_{q^2=m_{H^*}^2}\left\{f_+^{HM}\left(q^2\right)\right\}}{m_{H^*}^2} = \lim_{q^2 \to m_{H^*}^2}\left(1 - \frac{q^2}{m_{H^*}^2}\right) f_+^{HM}\left(q^2\right) \tag{1036}$$

40 Strictly speaking, those techniques have been developed mainly for $B \to \pi l \nu_l$ decays, but can be straightforwardly adapted to similar problems. Here, we do not include other approaches and parametrizations, as described by [533–537] or [538, 539].

41 Here, E_M is the light hadron's energy in the rest frame of the heavy meson.

42 A similar problem arises in lattice QCD calculations of the form factors for $B^0 \to \pi^- l^+ \nu_l$ decays near zero recoil (see, e. g., [540]), where f_+ and f_0 are usually extrapolated to the full recoil range via adequate models, such as Equation 1042. Correspondingly, the present LCSR and lattice studies access complementary realms of the given physical region. For instance, when focusing on $B \to \pi l \nu_l$ decays, the related QCD sum rule results are restricted to $0 \leqslant q^2 \leqslant 14\ \mathrm{GeV}^2$, while analogous lattice simulations are limited to $16\ \mathrm{GeV}^2 \leqslant q^2 \leqslant 26.4\ \mathrm{GeV}^2$ (cf. [322, 541]).

43 As discussed in [322], a multitude of processes do not require any knowledge or specific extrapolation method beyond this accessible realm. Prominent examples are non-leptonic B or rare $B \to P l^+ l^-$ $(P = \pi, K, \eta)$ decays. Thus, the discussed $H \to M l \nu_l$ transitions are an important exception.

44 Based on the fundamental principles of dispersion relations and the S-matrix theory, each semileptonic decay $H \to M l \nu_l$ can be (kinematically) connected to $HM \to l \nu_l$ via crossing symmetries. This reaction, however, indirectly includes an elastic strong scattering process $HM \to HM$, which may exhibit every intermediate state (e. g., $HM \to H^* \to HM$) with quantum numbers similar to the related vector meson "H^*". In terms of coupling constants, which describe the corresponding hadronic transitions, this gives rise to contributions that involve g_{H^*HM}. The analytic continuation of f_+^{HM} based on dispersion relations, therefore, contains a term proportional to $\sim g_{H^*HM}\left(m_{H^*}^2 - q^2\right)^{-1}$.

can be expressed by hadronic on-shell matrix elements similar to (ε^μ is the H^* meson's polarization vector, cf. [371, 542])

$$\langle 0|V_\mu^M|H^*(p,\varepsilon)\rangle = f_{H^*} m_{H^*} \varepsilon_\mu \,, \tag{1037}$$

$$\langle H^*(p,\varepsilon)\, M(q)\, |H(p+q)\rangle = -g_{H^*HM}\ (q\cdot\varepsilon)\,, \tag{1038}$$

which involve two additional non-perturbative parameters, such as the hadronic H^*HM coupling g_{H^*HM}, along with the vector meson decay constant f_{H^*} (compare with [334, 371, 542, 545]). This relation is particularly useful when studying H^*HM (on-shell) vertices, such as[45] $D^*D\pi$, $B^*B\pi$ or $D_s^*D_s\eta^{(\prime)}$ (see [334]), where the implied normalization factor $f_{H^*} g_{H^*HM}$ approximately determines the associated heavy-to-light form factor's behavior near zero (pionic) recoil (cf. [322, 371, 546, 553]):

$$f_+^{HM}\left(q^2 \approx q^2_{\max}\right) \approx \frac{f_{H^*} g_{H^*HM}}{2m_{H^*}\left[1-\frac{q^2}{m^2_{H^*}}\right]}\,. \tag{1039}$$

Accordingly, it is connected to an important input parameter which should not be dropped. As discussed in [537], the remaining dispersion integrals can be approximated to any desired accuracy by introducing a sufficient number of finely-spread effective poles ($N \geqslant 1$)

$$f_+(x) \approx \frac{c_{H^*}}{1-x} + \sum_{k=1}^{N} \frac{\rho_k}{1-\frac{x}{\gamma_k}}\,, \quad f_0(x) \approx \sum_{k=1}^{N} \frac{\sigma_k}{1-\frac{x}{\beta_k}}\,, \quad x \coloneqq \frac{q^2}{m^2_{H^*}}\,, \tag{1040}$$

with formal coefficients $\beta_k > 0$, σ_k, and ($t_0 \leqslant t_1 < \ldots < t_{n+1} < \infty$) [537]

$$\rho_k = \frac{1}{\pi}\int_{t_k}^{t_{k+1}} dt\, \frac{\operatorname{Im}_t f_+(t)}{t}\,, \quad \gamma_k = \frac{t_k}{m^2_{H^*}}\,. \tag{1041}$$

The present generation of experimental and lattice QCD data, however, cannot yet resolve[46] scenarios beyond $N = 1$ (cf. [537, 556]). Thus, many popular approaches are based on the (four-parameter) Bečirević-Kaidalov parametrization [542] which not only retains the first isolated pole, but also models all remaining contributions by a single effective pole [542, 554] (α, β, $\gamma > 0$)

$$f_+(x) = \frac{c_{H^*}}{1-x} + \frac{c_{H^*}\alpha}{1-\frac{x}{\gamma}}\,, \quad f_0(x) = \frac{c_{H^*}(1-\alpha)}{1-\frac{x}{\beta}}\,. \tag{1042}$$

In other words, this ansatz entails an additional parameter for each effective pole squared mass, i. e., $m^2_{1^-} = \gamma m^2_{H^*}$ and $m^2_{0^+} = \beta m^2_{H^*}$ as well as α to further quantify the corresponding impact of higher states. We observe in passing that the relative slope of f_+ and f_0 at large recoil is determined by (neglecting $\mathcal{O}(m^2_{H^*}/m^2_H)$ corrections, along with powers of "$1 - m^2_{H^*}/m^2_H$") [556]

$$\delta \coloneqq 1 - \frac{m_H^2 - m_M^2}{f_+(0)}\left(\left.\frac{d\, f_+(q^2)}{d\, q^2}\right|_{q^2=0} - \left.\frac{d\, f_0(q^2)}{d\, q^2}\right|_{q^2=0}\right)\,, \tag{1043}$$

$$\frac{1}{\beta} \coloneqq \left.\frac{m_H^2 - m_M^2}{f_+(0)}\,\frac{d\, f_0(q^2)}{d\, q^2}\right|_{q^2=0}\,, \tag{1044}$$

45 Both couplings, i. e., $D^*D\pi$ and $B^*B\pi$ have been studied with a variety of different approaches, e. g., [97, 109, 371, 546–548]. Hence, they may serve as prime models for other coupling constants. It should be emphasized that $g_{D^*D\pi}$ is directly related to the decay width $\Gamma(D^* \to D\pi)$ [546, 549], while the analogous process $B^* \to B\pi$ is kinematically forbidden. Instead, one encounters $B^* \to B\gamma$ as the dominant decay mode (cf. [42, 546]). Nevertheless, the $B^*B\pi$ on-shell vertex may occur as a fundamental parameter of chiral effective Lagrangians with heavy-light mesons (cf. [371, 465, 550–552]) and (as mentioned above) can constrain the $B \to \pi l \nu_l$ form factor (see also [371, 546]).

46 This has to be understood in the sense that the inclusion of additional fit parameters would not significantly improve the corresponding results for $\Gamma(H \to M \nu_l l)$, etc. (see also [537]).

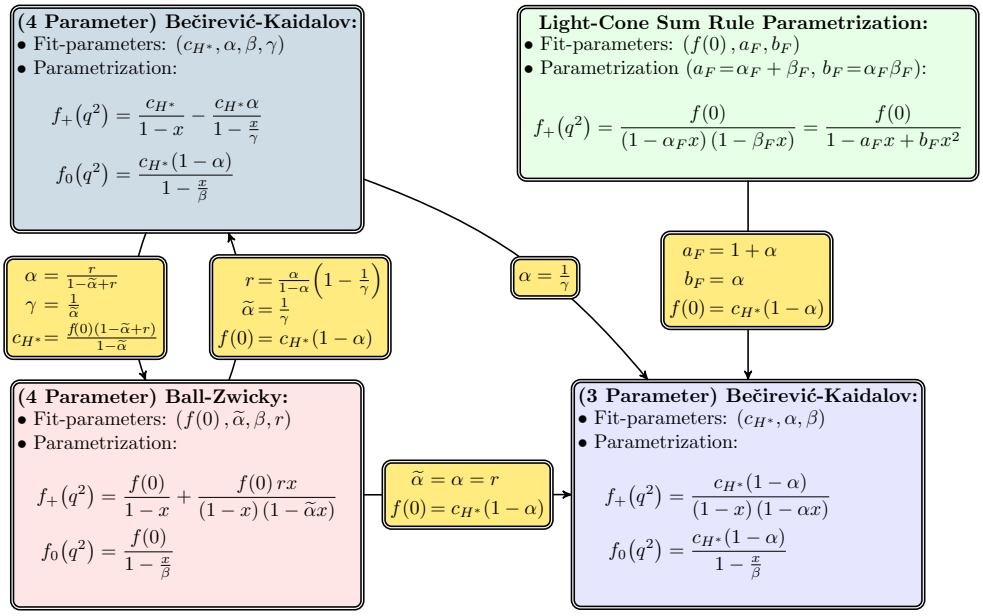

Figure 44: This is a contrasting juxtaposition of the most common extrapolation methods for f_+ and f_0. While using $x = q^2/m^2_{H^*}$, the listed examples involve the Bečirević-Kaidalov [542, 554], Ball-Zwicky [555], along with a conventional LCSR parametrization (where originally $a = (m^2_H/m^2_{H^*})\,a_F$ and $b = (m^2_H/m^2_{H^*})^2\,b_F$ is used) [515].

implying $\left(\gamma \equiv \gamma(\alpha, \beta, \delta)\right)$

$$\frac{1}{\gamma} = 1 - \frac{1-\alpha}{\alpha}\left(\frac{1}{\beta} - 1 + \frac{m^2_{H^*}}{m^2_H - m^2_M}(1-\delta)\right) \approx 1 - \frac{1-\alpha}{\alpha}\left(\frac{1}{\beta} - \delta\right). \tag{1045}$$

Additionally, the parameter δ is implicitly measuring the relative size of hard-scattering and soft-overlap contributions[47] in the $H \to M l \nu_l$ form factors (for a detailed discussion see [557, 558]). This reveals a deeper connection between the scalar and vector form factor which is also encoded in the following relations (cf. [537, 556]):

47 Based on the soft-collinear effective theory (SCET) formalism (E being the light hadron energy) [557–563]

$$f_+(E) = \sqrt{m_H}\left[\hat{\zeta}_M(E) + \left(\frac{4E}{m_H} - 1\right)\hat{H}_M(E)\right], \quad f_0(E) = \frac{2E}{\sqrt{m_H}}\left[\hat{\zeta}_M(E) + \hat{H}_M(E)\right],$$

both form factors can be decomposed into contributions of hard-scattering $(\hat{H}_M)$ and soft-overlap $(\hat{\zeta}_M)$ terms. At large recoil $E \approx \frac{m_H}{2}$, the heavy quark expansion gives rise to [556]

$$\delta = \left.\frac{2\hat{H}_M}{\hat{\zeta}_M + \hat{H}_M}\right|_{E=\frac{m_H}{2}} + \dots.$$

Here, the ellipses correspond to corrections beyond leading order in m_Q^{-1} and $\alpha_s(m_Q)$. Consequently, two opposing scenarios may occur:

i) The case $\delta \approx 0$ indicates a negligible presence of hard-scattering contributions.

ii) For $\delta \approx 2$ the form factor is dominated by hard-scattering effects.

Those may serve as a simple guideline to assess the underlying heavy quark physics.

i) The kinematical constraint $f_+(0) = f_0(0)$ (cf. Equation 945), as already implemented in Equation 1042, entails the generic parameter (cf. Figure 44)

$$f_+(0) = c_{H^*}(1-\alpha) =: f(0) \,. \tag{1046}$$

According to this equation, c_{H^*} and the normalization $f(0)$ can be used equivalently.

ii) For a renormalization point $\mu_F \lesssim m_Q$ ("Q" being a heavy quark flavor), at which $\alpha_S(m_Q)$ is still a sufficiently small expansion parameter, the underlying physics can be approximately described by an effective field theory, such as heavy quark effective theory (HQET) [248, 564–566]. In the heavy quark limit $(m_Q \to \infty)$ and near zero recoil $(q^2 \approx q^2_{max})$, one will encounter the famous Isgur-Wise scaling law [557]:

$$f_+\left(q^2 \approx q^2_{max}\right) \sim \sqrt{m_H}\,, \quad f_0\left(q^2 \approx q^2_{max}\right) \sim \frac{1}{\sqrt{m_H}}\,. \tag{1047}$$

iii) A similar heavy quark (meson) scaling law exists for both form factors in the low $q^2 \to 0$ region, i. e., at large recoil:

$$f_+\left(q^2 \approx 0\right) \sim m_H^{-\frac{3}{2}} \sim f_0\left(q^2 \approx 0\right) \,. \tag{1048}$$

This has been originally predicted by [141] using the LCSR method and was later on confirmed within the large energy effective theory (LEET) framework (cf. [248, 567]).

iv) Another nontrivial symmetry relation between the form factors emerges within the heavy quark limit and for large recoils $(m_Q \to \infty,\, E \to \infty)$ [248, 249]:

$$f_+\left(q^2 \approx q^2_{max}\right) = \frac{2E}{m_H} f_+\left(q^2 \approx q^2_{max}\right) \,. \tag{1049}$$

Based on these general restrictions[48], one may finally test the chosen model for its consistency. For instance, in accordance with [371] the resulting scaling behavior of Equation 1036 is given by $c_{H^*} \sim \frac{1}{\sqrt{m_H}}$. In combination with point iii), a pole dominance ansatz is, therefore, excluded (see also [542, 556]). Thus, it is essential to understand the effects caused by all remaining hadronic states within the related vector meson channel, e. g., as encoded in the scaling laws for γ and α.

Due to[49] ii) $\alpha\gamma$ and $(1-\gamma)m_H$ scale as constants, while i) combined with iii) imply: $1/(1-\alpha) \sim m_H$. In summary, when omitting logarithmic and higher order mass corrections, i) – iii) lead to the

48 When applying the Lehmann-Symanzik-Zimmermann (LSZ) reduction formula to corresponding heavy-to-light decays, additional nontrivial equations for the related coupling constants may arise. For example, the resulting Callan-Treiman relation for $B \to \pi \nu_l l$ decays implies [554, 568] $(p_\pi^\mu \to 0,\, m_\pi^2 \to 0)$

$$f_0\left(m_B^2\right) = \frac{f_B}{f_\pi}\,,$$

which can be relevant in associated numerical calculations (cf. [322, 554]).

49 For the assumed heavy quark limit, it is reasonable to apply $q^2_{max} \approx m_H^2$. Consequently, a dimensional analysis according to ii) implies (while neglecting light meson mass corrections)

$$f_+\left(q^2_{max}\right) = c_{H^*}\left[\frac{m_{H^*}^2}{m_{H^*}^2 - m_H^2} + \frac{\alpha\gamma}{1-\gamma} + \mathcal{O}\left(m_H^2 - m_{H^*}^2\right)\right] \approx c_{H^*} m_H \left(1 + \frac{\alpha\gamma}{(1-\gamma)\, m_H} + \dots\right)\,,$$

which reproduces [542, Equation 13]. Based on this heuristic approach, one may deduce the discussed scaling laws. A similar argument is valid for the scalar form factor in Equation 1042.

simple estimate[50] $\alpha, \gamma \sim 1 + \frac{\text{const.}}{m_H} + \dots$ (for further discussion see [542]). Besides, these well-known findings have been confirmed within the SCET approach [556]. The latter additionally predicts δ to be of $\mathcal{O}(1)$ in the power counting. Consequently, Equation 1045 has the following structure (cf. Figure 44)

$$\frac{1}{\gamma} = \alpha + (1-\alpha)\delta + \mathcal{O}\left(m_H^{-2}\right) = \alpha + \mathcal{O}\left(m_H^{-1}\right) , \tag{1050}$$

approximately yielding two independent parametrizations for f_+ and f_0 that are valid within the whole physical region. Alternatively, when taking point iv) into consideration, one may analogously deduce $\frac{1}{\gamma} = \alpha + \mathcal{O}(1/m_H)$ (see [542] for details). Hence, in order to satisfy relation iv) (cf. Equation 1049), while neglecting $\mathcal{O}(1/m_H)$ corrections, the number of free fit parameters can be even further reduced (see Figure 44).

A posteriori, the parameter set $(c_{H^*}, \alpha, \beta, \gamma)$ is, therefore, sufficient to describe the currently available data without contradicting general physical constraints (see also [322, 542, 554, 556]). Conversely, Equation 1042 allows a physically interpretable extrapolation of available data points, e. g., as produced by the given vector and scalar form factor calculations. Nonetheless, in reference to previous LCSR and recent lattice studies, such as [12, 319, 319, 322, 541], we use a modified[51] version of Equation 1042 [2, 555] $(\alpha_{BZ} := (m_H^2/m_{H^*}^2)\,\widetilde{\alpha})$:

$$f_+\left(q^2\right) = f(0)\left(\frac{1}{1-x} + \frac{rx}{(1-x)(1-\widetilde{\alpha}x)}\right) , \qquad f_0\left(q^2\right) = \frac{f(0)}{1-\frac{x}{\beta}} , \tag{1051}$$

known as the (four parameter) Ball-Zwicky parametrization (see Figure 44). As intended, this approach fulfills all the mentioned requirements and is valid for $q^2 \in (-\infty, q^2_{max})$, but unfortunately represents another source of error.

In general, however, it is difficult to isolate and quantify possible uncertainties on the form factor shape inherent to LCSR calculations. Or to put it differently: some observables imply a tightly constrained fit that is less dependent on the chosen parametrization, while other important physical quantities are sensitive to the inclusion of more parameters than can be constrained by the given data points (see, e. g., [537] for a detailed discussion). Fortunately, for certain observables, such as the total semileptonic decay rates, comparable existing studies indicate a rather mild dependence of $\Gamma(B \to \pi l \nu_l)$ on the method used to extrapolate $f_+^{B\pi}$. In fact, it has been pointed out by[52] [322], that $\Gamma(B \to \pi l \nu_l)$ changes at most 6 % for three different extrapolations[53] (see [322]) of their LCSR results[54]. Similar studies have been carried out for $|V_{ub}| f_+(0)$, using

50 Similarly, β scales as $1 + \frac{\text{const.}}{m_H} + \dots$, since ii) and iii) have to be fulfilled simultaneously (see, e. g., [542, 554]).

51 At this level of accuracy, the parameters of Equation 1042 and Equation 1051 can be related via (cf. Figure 44):

$$r = \frac{1}{\beta} - \delta = \frac{\alpha}{1-\alpha}\left(1 - \frac{1}{\gamma}\right) , \quad \widetilde{\alpha} = \frac{1}{\gamma} = 1 - \frac{1-\alpha}{\alpha}\left(\frac{1}{\beta} - \delta\right) .$$

52 Other LCSR studies (cf. [319, 320, 569]) come to similar conclusions when comparing the results of different parametrizations as based on [533–536] or [538, 539].

53 Those parametrizations are based on Equation 1042:

$$f_+^{(i)}\left(q^2\right) = \frac{r_1}{1-\frac{q^2}{m_1^2}} + \frac{r_2}{1-\frac{q^2}{m_{fit}^2}} , \quad f_+^{(ii)}\left(q^2\right) = \frac{f_+(0)}{\left(1-\frac{q^2}{m_1^2}\right)\left(1-\frac{q^2}{m_{fit}^2}\right)} , \quad f_+^{(iii)}\left(q^2\right) = \frac{r_1}{1-\frac{q^2}{m_{fit}^2}} + \frac{r_2}{\left(1-\frac{q^2}{m_{fit}^2}\right)^2} ,$$

while using $m_1^{\pi,\eta} \to m_{B^*}$, $m_1^K \to m_{B_s^*}$ and (r_1, r_2, m_{fit}) as fit parameters (cf. [322]).

54 According to [537], that is also true for other quantities, such as $|V_{ub}| f_+(0)$, $|V_{ub}|$ and $f_+(0)$, which have been extracted from experimental [570–573] as well as lattice [574, 575] data. In fact, a corresponding rigorous error estimate

Decay mode	r	α_{BZ}	$\lvert f^+_{HM}(0)\rvert$
$D_s^+ \to \eta l^+ \nu_l$	$0.284^{+0.003}_{-0.002}$	$0.252^{+0.107}_{-0.082}$	$0.432^{+0.033}_{-0.033}$
$D_s^+ \to \eta' l^+ \nu_l$	$0.284^{+0.137}_{-0.095}$	$0.252^{+0.382}_{-0.395}$	$0.520^{+0.080}_{-0.080}$
$D^+ \to \eta l^+ \nu_l$	$0.174^{+0.001}_{-0.001}$	$-0.043^{+0.068}_{-0.052}$	$0.552^{+0.051}_{-0.051}$
$D^+ \to \eta' l^+ \nu_l$	$0.174^{+0.243}_{-0.142}$	$-0.043^{+0.526}_{-0.596}$	$0.458^{+0.105}_{-0.105}$

Table 18: Shape parameters for the vector form factor $f^+_{HM}(q^2)$ $(H = D, D_s;\ M = \eta, \eta')$ as input for the Ball-Zwicky parametrization, see Equation 1051 (cf. [2]). For reasons of numerical stability we use Equation 1051 with α_{BZ} instead of $\widetilde{\alpha}$.

the rather different Ball-Zwicky [322], Albertus-Flynn-Hernandez-Nieves [538, 576] and Boyd-Grinstein-Lebed [534, 536] parametrizations to estimate the inherent model dependence of this observable (cf. [577]). Indeed, it has been reported in [577], that the uncertainty induced by each set of related shape parameters does not exceed $\sim 6\,\%$. Most interestingly, for $q^2 \lesssim q^2_{max}$ the named parametrizations yield (to within 2% accuracy) the same numerical results, indicating a model independence [577].

Thus, the systematic error introduced by this fitting procedure would be considerably smaller than the estimated intrinsic and irreducible uncertainty of the sum rule method, which should amount to $\sim 7\,\% - 15\,\%$ (see [109, 114, 117, 320–322, 464, 515]). Since our present basic problem is completely compatible with these findings, they may be used to establish a rough order of magnitude estimate for corresponding systematic uncertainties of $\Gamma(H \to M l \nu_l)$.

If accepted being only slightly dependent on the chosen Ball-Zwicky parametrization, which again could be seamlessly absorbed into the total systematic errors, the subsequent phenomenological analysis lends itself to a straightforward statistical interpretation (see also [322, 537, 556]).

5.3.4 *Heavy-to-light form factors and their shape* $(q^2 \neq 0)$

According to Section 5.3.3, the LCSR method cannot access the entire physical region. Thus, the form factors are calculated for sufficiently small momentum transfers $q^2 \lesssim q^2_\chi \approx m_Q^2 - 2m_Q\chi$ where the sum rule is easily applicable. All corresponding results are then extrapolated to the remaining interval. On the one hand, this allows for the calculation of branching fractions, but on the other hand a necessary error analysis gets more difficult. Therefore, both of these aspects are described in the following subsection.

As a starting point, the results for $f^+_{D_s^+\eta}(q^2)$ and $f^+_{D_s^+\eta'}(q^2)$ are shown in Figure 45 as well as Figure 46. In order to get the related error bands, we perform a statistical analysis for all input parameters at each grid point $q^2 \lesssim q^2_\chi$, while assuming Gaussian uncertainties. Then we extrapolate all results in the same way as the plotted central values. Again, we note, that the uncertainty coming from the unknown gluon DAs is almost negligible for the $f^+_{H\eta}$ $(H = D, D_s, B)$ form factors. This supports the notion of the η meson being almost an ideal octet state. On the other hand, there is a considerable impact of gluonic singlet contributions on the $f^+_{H\eta'}$ form

has been carried out by [537] for arbitrary many parameters, while assuming very loose dispersive bounds (cf. Equation 1040), i. e., $\sum_k |\rho_k| \sim \sqrt{\Lambda_{QCD}/m_b} < 10$. The resulting estimates for uncertainties on $f_+(0)$ and $|V_{ub}|$, as introduced by the form factor shape, do not exceed $\sim 4\,\% - 6\,\%$ (see [537]).

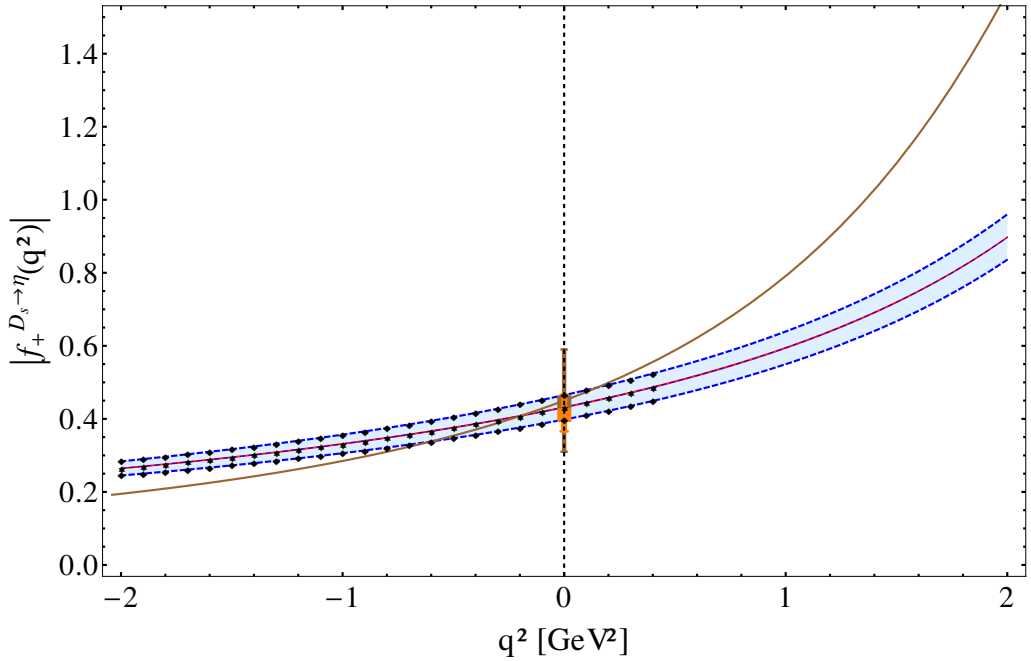

Figure 45: $f^+_{D_s^+\eta}(q^2)$ plotted as a function of q^2 (cf. [2]). Black dots represent the calculated sum rule values. Correspondingly, the straight blue line is the fit to central values. Here, the blue dashed band depicts the full uncertainty of our result, while red lines are limited to uncertainties coming from gluonic contributions. The latter have a very small numerical impact on $f^+_{D_s^+\eta}(q^2)$, thus almost concealing the blue line. Results of [31] are included via brown lines. The orange point illustrates recent lattice results from [12, 578] (see [2] for details).

factors. The associated fit parameters can be found in Table 18 which employ a slightly modified version of the Ball-Zwicky model to guarantee a better numerical stability. Furthermore, Figure 45 and Figure 46 also contain results from the first lattice simulation for these quantities [2, 578], supporting our present calculations. Unfortunately, there is no experimental data for the previously discussed form factors themselves. Then again, with an extrapolation of $f^+_{HM}(q^2)$ to the entire kinematic region, we can calculate corresponding branching fractions, for which experimental results are available (see Table 19). Based on Section 2.6.2, the decay rate for massless leptons is given by[55] (similarly for $H = D, D_s, B$; $M = \eta, \eta'$; $l = e, \mu$; $|V_{qQ}|$ from Table 16)

$$\Gamma(H^+ \to M l^+ \nu_l) = \frac{G_F^2 |V_{qQ}|^2}{24\pi^3} \int_0^{q^2_{max}} dq^2 \, \lambda^{3/2}\left(q^2, m_H^2, m_M^2\right) \left|f^+_{HM}\left(q^2\right)\right|^2 \tag{1052}$$

$$\lambda\left(q^2, m_H^2, m_M^2\right) = \frac{1}{4m_H^2}\left[\left(m_H^2 + m_M^2 - q^2\right)^2 - 4m_H^2 m_M^2\right] . \tag{1053}$$

After a multiplication with the mean lifetime of the considered meson, we get the relevant branching fractions. In order to extract the underlying uncertainties, we again assume Gaussian errors of $\left|f^+_{HM}(q^2)\right|^2$ with different fit functions from $q^2 \lesssim q^2_\chi$ to the physical region. The entailed deviations are incorporated into the error budget. Our results and associated experimental values are shown in Table 19. Again, the ratios $\Gamma(H^+\to\eta' l^+\nu_l)/\Gamma(H^+\to\eta l^+\nu_l)$ turn out to be especially interesting, since most of the given theoretical uncertainties cancel. The remaining

55 For the currently available data only transitions with electrons or muons (i. e., $l = e, \mu$) in the final state have been measured [360]. Thus, Equation 1052 is a reasonable approximation. Here, contributions of f^0_{HM} can be safely neglected.

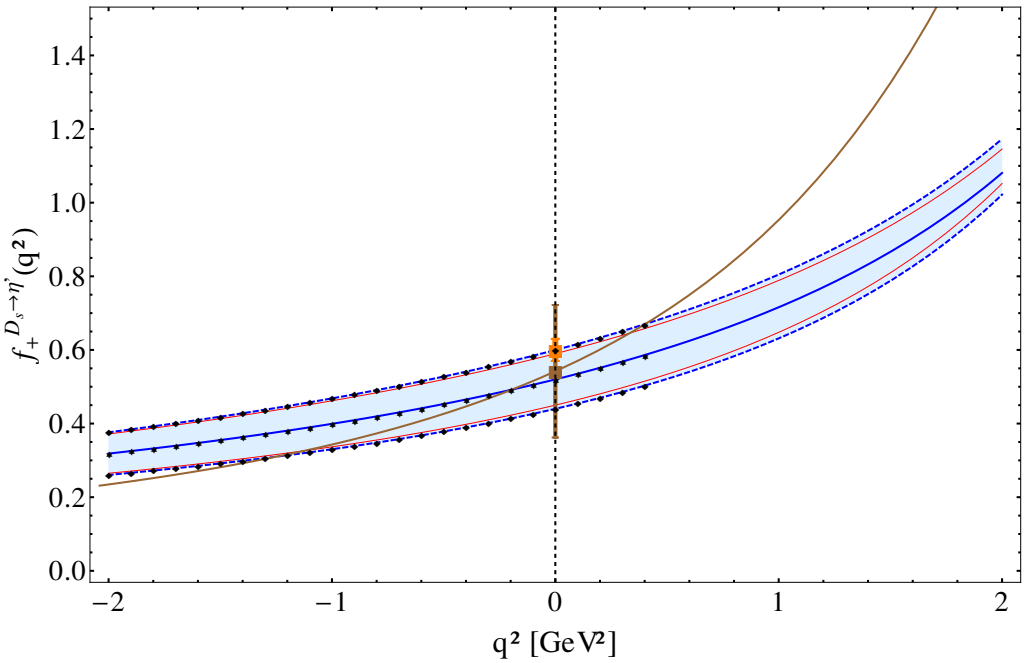

Figure 46: $f^+_{D_s^+\eta'}(q^2)$ plotted as a function of q^2. Here, we use the same conventions as in Figure 45.

error bars are dominated by contributions of the gluonic Gegenbauer moment as well as FKS parameters. A comparison with the available data reveals an overall good agreement of the theoretical predictions with the experiment, see Table 20. Nevertheless, the achievable experimental precision is up to now insufficient to draw any conclusion on $c_2^{(g)}(\mu_0)$.

In this chapter we have calculated the form factors and branching fractions of the decays $D^+_{(s)} \to \eta^{(\prime)} l^+ \nu_l$ as well as $B^+ \to \eta^{(\prime)} l^+ \nu_l$ within the LCSR framework for massless leptons. Both form factors were shown to agree within the available lattice results, while the determined branching rations also concur with the experimental data. Thus, the overall picture implies a general agreement of these complementary sources. Our main result, however, is related to the performed statistical analysis. For all studied quantities $c_2^{(g)}(\mu_0)$ dominates the resulting uncertainties.[56] Therefore, even a moderate increase in the experimental accuracy or quality of lattice data could provide decisive contributions to a better understanding of η, along with η' DAs, and, in particular, concerning their gluonic content. Accordingly, precision measurements of the discussed different branching ratios (see Table 20) would allow us to settle this long-standing issue.

56 Within the recent publication [335] a possible shortcoming of [32] has been pointed out which is related to the γ_5 problem in D dimensions. In fact, resulting ambiguities have led to a difference between the findings of [32] and [335]. As a consequence, the gluonic singlet contributions would change accordingly. E. g., at $q^2 = 0$ the relative change of related numerical results would amount to approximately 30% for $D_{(s)} \to \eta^{(\prime)}$ and up to 50% for $B \to \eta^{(\prime)}$ decays. Fortunately, this does not affect any qualitative or quantitative findings of this work, except for a possible decrease in the uncertainty related to the gluonic Gegenbauer moments.

Decay mode	LCSRs (this work)	Experiment	
$D_s^+ \to \eta' e^+ \nu_e$	(0.75 ± 0.23) %	(0.91 ± 0.33) %	[579]
$D_s^+ \to \eta e^+ \nu_e$	(2.00 ± 0.32) %	(2.48 ± 0.29) %	[579]
$D^+ \to \eta' e^+ \nu_e$	$(3.86 \pm 1.77) \cdot 10^{-4}$	$(2.16 \pm 0.53 \pm 0.07) \cdot 10^{-4}$	[580]
$D^+ \to \eta e^+ \nu_e$	$(24.5 \pm 5.26) \cdot 10^{-4}$	$(11.4 \pm 0.9 \pm 0.4) \cdot 10^{-4}$	[580]
$B^+ \to \eta' e^+ \nu_e$	$(0.36 \pm 0.22) \cdot 10^{-4}$	$(2.66 \pm 0.80 \pm 0.56) \cdot 10^{-4}$	[581]
		$(0.24 \pm 0.08 \pm 0.03) \cdot 10^{-4}$	[582]
$B^+ \to \eta e^+ \nu_e$	$(0.73 \pm 0.20) \cdot 10^{-4}$	$(0.44 \pm 0.23 \pm 0.11) \cdot 10^{-4}$	[581]
		$(0.36 \pm 0.05 \pm 0.04) \cdot 10^{-4}$	[582]

Table 19: Branching fractions for the different decays, including a comparison of LCSR results and experimental data.

Ratio	LCSRs (this work)	Experiment	
$\Gamma(D_s^+ \to \eta' l^+ \nu_l)/\Gamma(D_s^+ \to \eta l^+ \nu_l)$	$0.37 \pm 0.09\big\vert_{c_2^{(g)}} \pm 0.04\big\vert_{\text{rest}}$	0.36 ± 0.14	[271]
$\Gamma(D^+ \to \eta' l^+ \nu_l)/\Gamma(D^+ \to \eta l^+ \nu_l)$	$0.16 \pm 0.06\big\vert_{c_2^{(g)}} \pm 0.02\big\vert_{\text{rest}}$	0.19 ± 0.09	[579]
$\Gamma(B^+ \to \eta' l^+ \nu_l)/\Gamma(B^+ \to \eta l^+ \nu_l)$	$0.50 \pm 0.29\big\vert_{c_2^{(g)}} \pm 0.05\big\vert_{\text{rest}}$	0.67 ± 0.26	[581]

Table 20: Ratios of branching fractions for the different decay modes (see [2]). Here, we explicitly indicate the uncertainties caused by $c_2^{(g)}(\mu_0)$, while all residual errors are collected accordingly.

6 CONCLUSION

"The effort to understand the universe is one of the very few things which lifts human life a little above the level of farce and gives it some of the grace of tragedy."

— Steven Weinberg

In this thesis, we provide a state-of-the-art NLO analysis of corresponding $\gamma^*\gamma \to \eta^{(\prime)}$ and $D_{(s)} \to \eta^{(\prime)} l \nu_l$ transition form factors within the LCSR framework. The obtained results can be presented in the following way [2, 3]:

In anticipation for the possibility of high-precision measurements of the transition form factors $\gamma^*\gamma \to \eta$ and $\gamma^*\gamma \to \eta'$ at the upgraded KEKB facility, in this work we update the corresponding theoretical framework. The presented formalism incorporates several new elements in comparison to the existing calculations, in particular a full NLO analysis of perturbative corrections, the charm quark contribution, and revisited twist-four contributions taking into account SU(3)-flavor breaking and the axial anomaly. A numerical analysis of the existing experimental data is performed with these improvements.

For the numerical analysis we have used the FKS state mixing assumption for the η, η' DAs at a low scale 1 GeV as a working hypothesis to avoid proliferation of parameters. This assumption does not contradict the data on the FFs at small-to-moderate photon virtualities and can be relaxed in future, if necessary.

The most important effect of the NLO improvement is due to the finite renormalization of the flavor-singlet axial current which results in a 20% reduction of the the expected asymptotic value of the $\gamma^*\gamma \to \eta'$ form factor at large photon virtualities. Taking into account this correction brings the result in agreement with *BABAR* measurements [7].

We also want to emphasize the importance of taking into account the charm quark corrections. This effect is negligible at small Q^2, but increases the contribution of the most interesting two-gluon DA by a factor $5/3$ at large scales, so that a consistent implementation of the charm-quark mass threshold effects is mandatory.

The update of the higher twist corrections does not have a large numerical impact, but is necessary for theoretical consistency when taking into account the meson mass corrections to the leading-twist diagrams. Identifying the hadron mass corrections in hard exclusive reactions is in general a nontrivial problem [583], and it is made even harder by the axial anomaly. We have calculated the anomalous contribution to the twist-four DA for one particular case and found a specific mechanism how this contribution can restore the relations between η, η' masses implied by the state-mixing assumption for higher twist.

Our results for the FFs at Euclidean virtualities are, in general, in good agreement with the experimental data [7], although the present statistical accuracy of the measurements is insufficient to distinguish between different models of the DAs specified in Chapter 4. We expect that experimental errors will become smaller in future, and also that some of the parameters, most importantly the decay constants f_η, $f_{\eta'}$, will be calculated with high precision on the lattice. In this way the comparison of the QCD calculation with experiment will allow one to study the structure of η, η' mesons at short interquark separations, encoded in the DAs, on a quantitative level.

We have given a short discussion of the transition form factors in the time-like region. The result by *BABAR* [351] suggesting a large enhancement of the η form factor in the time-like as compared to the space-like region, and at the same time no such enhancement for η' is rather puzzling. If confirmed, this difference would imply a significant difference in the end-point behavior of η and η' DAs.

Furthermore, we have calculated the form factors and branching fractions of the $D_{(s)} \to \eta^{(\prime)} l\nu$ and $B \to \eta^{(\prime)} l\nu$ decays in the framework of LCSR for massless leptons. The form factors were shown to agree with available lattice results and the branching ratios Chapter 5 with experiment. So the overall picture is nicely consistent. Our main result is, however, the error budget given in Chapter 5 clearly showing that $c_2^{(g)}$ dominates the uncertainties in all cases. Therefore, already a moderate increase in experimental accuracy will allow to determine the gluonic contribution to η and η' from all three ratios, providing a sensitive consistency check. FAIR and Super-KEKB should even provide precision measurements of these ratios and thus allow to settle this long-standing issue.

Gratitude is the memory of the heart.

— Roch-Ambroise Cucurron Sicard (1742 – 1822)

ACKNOWLEDGEMENTS

First and foremost, I would like to express my gratitude to Professor Dr. *Andreas Schäfer* who gave me the opportunity of writing this thesis. I have greatly benefited from his scientific guidance and invaluable support.
I would also like to thank Prof. Dr. *Vladimir M. Braun* for his patience and kind encouragement throughout these years. It has been a great pleasure to participate in his interesting research projects and a fantastic learning experience.
I am indebted to Dr. *Nils Offen*, for the pleasant collaboration and always finding the time to quell my confusion. Also, I want to thank him for useful comments on the draft. Special thanks to Dr. *Shahin Agaev* who was a great help during our long and productive collaboration.

Furthermore, I am much obliged to *Monika Maschek* and *Heidi Decock* for taking care of all administrative issues. Moreover, I am deeply grateful to *Philipp Wein* for proofreading the draft and his friendly support.

I would also like to thank my former office colleagues *Sebastian Schierenberg*, *Tobias Lautenschlager*, *Issaku Kanamori*, *Gordon Donald*, *Alessandro Amato*, along with *Fabian Hutzler*, and the many other friends who have made my time in Regensburg so enjoyable.

Last, but not least, I want to thank my parents and my brother *André* for their unconditional love and neverending support.

A

APPENDIX – MISCELLANEOUS TOPICS

In the following appendix chapter, several topics are collected, that are required for this work. If not stated otherwise we use the Einstein notation (cf. [584]) which shortens the given expressions considerably.

A.1 PAULI AND GELL-MANN MATRICES

In general, the special unitary group of degree $N \in \mathbb{N}$ is a Lie group formed by unitary $N \times N$ matrices $U \in \mathbb{C}^{N \times N}$ with determinant $\det(U) = 1$ (see, e. g., [83, 156, 283, 585] for details). The corresponding (infinitesimal) generators of $SU(N)$ are usually represented as traceless Hermitian matrices. Accordingly, in the fundamental representation these N^2-1 generators T^A are given by $N \times N$ matrices $(A = 1, \ldots, N^2-1)$, obeying the following relations[1]:

$$\left[T^A, T^B\right]_- \equiv \left[T^A, T^B\right] = i \sum_{C=1}^{N^2-1} f^{ABC} T^C \,, \tag{1054}$$

$$\left[T^A, T^B\right]_+ \equiv \left\{T^A, T^B\right\} = \frac{1}{N} \delta^{AB} \mathbb{1}_{N \times N} + \sum_{C=1}^{N^2-1} d^{ABC} T^C \,. \tag{1055}$$

The involved structure constants f^{ABC} and coefficients d^{ABC} can be extracted from[2]

$$f^{ABC} = -i T_F^{-1} \operatorname{Tr}\left\{ \left[T^A, T^B\right]_- T^C \right\} , \tag{1056}$$

$$d^{ABC} = T_F^{-1} \operatorname{Tr}\left\{ \left[T^A, T^B\right]_+ T^C \right\} , \tag{1057}$$

which themselves result from the relations $\left(C_A = N,\ C_f = \frac{N^2-1}{2N} \text{ and } T_F = \frac{1}{2}\right)$

$$\delta^{AB} C_A = \operatorname{Tr}\left\{ \mathcal{T}^A \mathcal{T}^B \right\} = \sum_{C=1}^{N^2-1} \sum_{D=1}^{N^2-1} f^{ACD} f^{BCD} \,, \tag{1058}$$

$$\delta_{ab} C_f = \left(T^A T^A\right)_{ab} = \sum_{A=1}^{N^2-1} \sum_{c=1}^{N} \left(T^A\right)_{ac} \left(T^A\right)_{cb} \,, \tag{1059}$$

$$\delta^{AB} T_F = \operatorname{Tr}\left\{ T^A T^B \right\} = \sum_{a=1}^{N} \sum_{b=1}^{N} \left(T^A\right)_{ab} \left(T^B\right)_{ba} \,. \tag{1060}$$

In this context, the (N^2-1)-dimensional adjoint representation of the generators occurs. The latter correspond to $(N^2-1) \times (N^2-1)$ matrices, whose elements can be defined by

$$\left(\mathcal{T}^A\right)_{BC} = -i f^{ABC} \,. \tag{1061}$$

1 Here, we imply $\mathbb{1}_{N \times N} \equiv \mathbb{1}_N = \operatorname{diag}(1, \ldots, 1)$ to be the $N \times N$ identity matrix $(N \in \mathbb{N})$.

2 According to Equation 1056 and Equation 1057 the structure constants are antisymmetric in all indices, whilst the d^{ABC} are totally symmetric under any permutation of the given indices A, B, C.

Moreover, these generators again fulfill the commutation relation

$$\left[\mathcal{T}^A, \mathcal{T}^B\right] = i \sum_{C=1}^{N^2-1} f^{ABC}\mathcal{T}^C \,. \tag{1062}$$

Besides, for the fundamental representation of $SU(N)$ we get the completeness relation [325]

$$\sum_{A=1}^{N^2-1} \left(T^A\right)_{ab}\left(T^A\right)_{cd} = T_F\left(\delta_{ad}\delta_{cb} - \frac{1}{N}\delta_{ab}\delta_{cd}\right), \tag{1063}$$

giving rise to $\left(\text{i.e., } M\in\mathbb{C}^{N\times N} \text{ with } (M)_{ij}\in\mathbb{C}\right)$

$$\frac{1}{T_F}\sum_{A=1}^{N^2-1}\sum_{t=1}^{N}\left(T^A M\right)_{tt}\left(T^A\right)_{ij} + \frac{1}{T_F}\sum_{r=1}^{N}\left(\sqrt{\frac{T_F}{N}}\mathbb{1}_{N\times N}M\right)_{rr}\left(\sqrt{\frac{T_F}{N}}\mathbb{1}_{N\times N}\right)_{ij} = (M)_{ij} \,. \tag{1064}$$

In fact, Equation 1064 is particularly useful for the decomposition of arbitrary matrices M. For the construction of a basis it is, therefore, reasonable to include (see Equation 1063)

$$T^0 \coloneqq \sqrt{\frac{T_F}{N}}\mathbb{1}_{N\times N} \quad\Rightarrow\quad \sum_{A=0}^{N^2-1}\left(T^A\right)_{ab}\left(T^A\right)_{cd} = T_F\delta_{ad}\delta_{cb}\,, \tag{1065}$$

which entails the general identity $\left(\text{using } T_F^{-1}\equiv 2\right)$

$$M = \sum_{A=0}^{N^2-1} 2\,\mathrm{Tr}\left\{MT^A\right\}T^A \,. \tag{1066}$$

Two important examples for special unitary groups have to be discussed in detail, including $N=2$, along with $N=3$. Starting with the Pauli matrices $\left\{\sigma_j\right\}_{j=1,2,3}$ $\left(\text{here } f^{ijk}\equiv\varepsilon^{ijk}\right)$ [323]

$$\sigma_1 = \begin{pmatrix} 0 & 1 \\ 1 & 0 \end{pmatrix}, \qquad \sigma_2 = \begin{pmatrix} 0 & -i \\ i & 0 \end{pmatrix}, \qquad \sigma_3 = \begin{pmatrix} 1 & 0 \\ 0 & -1 \end{pmatrix}, \tag{1067}$$

we get the generic generators of $SU(2)$ via $T^j \equiv \frac{1}{2}\sigma_j$. The latter are also embedded in the first three Gell-Mann matrices $\left\{\lambda^A\right\}_{A=1,\ldots,8}$, which are given by (see [38]):

$$\left.\begin{aligned} \lambda^1 &= \begin{pmatrix} 0 & 1 & 0 \\ 1 & 0 & 0 \\ 0 & 0 & 0 \end{pmatrix}, \quad \lambda^2 = \begin{pmatrix} 0 & -i & 0 \\ i & 0 & 0 \\ 0 & 0 & 0 \end{pmatrix}, \quad \lambda^3 = \begin{pmatrix} 1 & 0 & 0 \\ 0 & -1 & 0 \\ 0 & 0 & 0 \end{pmatrix}, \\ \lambda^4 &= \begin{pmatrix} 0 & 0 & 1 \\ 0 & 0 & 0 \\ 1 & 0 & 0 \end{pmatrix}, \quad \lambda^5 = \begin{pmatrix} 0 & 0 & -i \\ 0 & 0 & 0 \\ i & 0 & 0 \end{pmatrix}, \\ \lambda^6 &= \begin{pmatrix} 0 & 0 & 0 \\ 0 & 0 & 1 \\ 0 & 1 & 0 \end{pmatrix}, \quad \lambda^7 = \begin{pmatrix} 0 & 0 & 0 \\ 0 & 0 & -i \\ 0 & i & 0 \end{pmatrix}, \quad \lambda^8 = \frac{1}{\sqrt{3}}\begin{pmatrix} 1 & 0 & 0 \\ 0 & 1 & 0 \\ 0 & 0 & -2 \end{pmatrix}. \end{aligned}\right\} \tag{1068}$$

	$A=0$	$A=8$	$A=3$	$R=q$	$R=s$	$R=3$
α_{0A}	$\frac{2(2m_q+m_s)}{3}$	$\frac{2\sqrt{2}(m_q-m_s)}{3}$	$\frac{\sqrt{2}(m_u-m_d)}{\sqrt{3}}$			
α_{8A}	$\frac{2\sqrt{2}(m_q-m_s)}{3}$	$\frac{2(m_q+2m_s)}{3}$	$\frac{(m_u-m_d)}{\sqrt{3}}$			
α_{3A}	$\frac{\sqrt{2}(m_u-m_d)}{\sqrt{3}}$	$\frac{(m_u-m_d)}{\sqrt{3}}$	$2m_q$			
α_{qR}				$2m_q$	0	m_u-m_d
α_{sR}				0	$2m_s$	0
α_{3R}				m_u-m_d	0	$2m_q$

Table 21: Selected coefficients of Equation 1070 in the SO and QF basis.

Those can be used to define the generic $SU(3)$ generators $T^A \equiv \frac{\lambda^A}{2}$. On the other hand, in Chapter 3 an alternative definition of the subspace "$\text{span}\left(\{T^8, T^0\}\right)_{\mathbb{C}}$" via the generators T^q, T^s has been discussed. Accordingly, the following identity is valid for $A \in I = \{0, 1, \ldots, 8\}$ as well as $A \in I = \{q, s, 1, \ldots, 7\}$ (see Equation 150):

$$\begin{aligned}\sum_{f,f'} A_f \left[\sqrt{2}T^A, \hat{m}\right]_{\pm}^{ff'} B_{f'} &= 2\sum_{B\in I}\sum_{f,f'} \text{Tr}\left\{\left[T^A, \hat{m}\right]_{\pm} T^B\right\} A_f \left[\sqrt{2}T^B\right]^{ff'} B_{f'} \\ &= \sum_{f,f'} \pm(m_f \pm m_{f'})\, A_f \left[\sqrt{2}T^A\right]^{ff'} B_{f'}\,, \end{aligned} \tag{1069}$$

where A_f and B_f are components of arbitrary complex vectors $\vec{A}$, $\vec{B} \in \mathbb{C}^3$. Besides, it is useful to introduce the following abbreviations:

$$\alpha_{AB} = 2\,\text{Tr}\left\{\left[T^A, \hat{m}\right]_+ T^B\right\}, \tag{1070}$$

$$\beta_{AB} = 2\,\text{Tr}\left\{\left[T^A, \hat{m}\right]_- T^B\right\}, \tag{1071}$$

with $\alpha_{AB} = \alpha_{BA}$ and $\beta_{AB} = -\beta_{BA}$. The relevant coefficients of Equation 1070 are collected in Table 21. For the discussed SO and QF basis, all contributions of Equation 1071 vanish:

$$\begin{aligned} &\beta_{0A} \equiv \beta_{8A} \equiv \beta_{3A} \equiv 0\,, \quad \forall A = 0, 1, \ldots, 8\,, \\ \Leftrightarrow\ &\beta_{qR} \equiv \beta_{sR} \equiv \beta_{3R} \equiv 0\,, \quad \forall R = q, s, 1, \ldots, 7\,. \end{aligned} \tag{1072}$$

In a nutshell, the "raison d'être" for Equation 1070 and Equation 1071 may be found in the local and non-local operator identities, such as Equation 178 or Equation 1485, which are relating the different symmetry currents in a closed form.

Furthermore, the operators to construct the weight diagrams (see discussion in [38, 44]) of $SU(3)_F$ should be mentioned. For instance, the related isospin operator and its third component can be represented (using the first three generators of $SU(3)$) by $\hat{T}^2 = \sum_{i=A}^{3} \left(T^A\right)^2$ and $\hat{T}_3 = T^3$, respectively. Additionally, the hypercharge can be related to $\hat{Y} = \frac{2}{\sqrt{3}} T^8$, fulfilling $\left[\hat{Y}, \hat{T}_3\right] = 0$.[3] Since both operators can be diagonalized simultaneously, they can be

3 Both $\hat{Y}$ and $\hat{T}_3$ are part of the Cartan-Weyl basis which implies a multitude of different commutation relations. The latter can be used to construct a irreducible representation of $SU(3)$ (see [586] for details).

used to label different states $|I, I_z, Y\rangle$ (i. e., related to a given eigenvalue of the isospin Casimir operator $\hat{T}^2|I, I_z, Y\rangle = I(I+1)|I, I_z, Y\rangle$) by the associated eigenvalues of $\hat{Y}$ and $\hat{T}_3$, e. g., via $\hat{Y}|I, I_z, Y\rangle = Y|I, I_z, Y\rangle$ and $\hat{T}_3|I, I_z, Y\rangle = I_z|I, I_z, Y\rangle$. Thus, they give rise to the anticipated weight diagrams, that are usually depicted in the $I_z - Y$ plane. By including other quantum numbers (e. g., charm), they can be extended to supermultiplets similar to Figure 1.

A.2 DIRAC ALGEBRA AND CHIRAL PROJECTION OPERATORS

This is a short collection of required identities concerning Dirac matrices and spinors.

Most of the time we only need the defining property (a more complete list can be found in [64, 98, 323, 324]) for the four-dimensional complex 4×4 gamma matrices $\{\gamma^0, \gamma^1, \ldots, \gamma^4\}$ to generate a Clifford algebra (see [64, 98]), i. e.,

$$\{\gamma^\mu, \gamma^\nu\} = 2g^{\mu\nu}\mathbb{1}_4 \tag{1073}$$

along with relations implied by $\gamma_5 = i\gamma^0\gamma^1\gamma^2\gamma^3$ $(\varepsilon_{0123} = +1)$, such as

$$\{\gamma^\mu, \gamma_5\} = 0\,. \tag{1074}$$

Analogous to Equation 1073, one may additionally define $\sigma_{\mu\nu}$, which can bee seen as the anti-symmetric counterpart of $g_{\mu\nu}$:

$$i\,[\gamma_\mu, \gamma_\nu] = 2\sigma_{\mu\nu}\,. \tag{1075}$$

Nevertheless, in the context of projection operators (see Equation 144), with the characteristic properties

$$P_{R,L}^2 = P_{R,L}\,, \quad P_L P_R = 0 = P_R P_L\,, \quad P_L + P_R = \mathbb{1}_4 \tag{1076}$$

it is sometimes needed to choose a specific basis for the gamma matrices. The two most common choices are the Weyl, or chiral basis $\left(\text{with } \sigma^\mu = (\mathbb{1}_2, \vec{\sigma})\,,\ \bar{\sigma}^\mu = (\mathbb{1}_2, -\vec{\sigma})\right)$

$$\gamma^\mu = \begin{pmatrix} 0 & \sigma^\mu \\ \bar{\sigma}^\mu & 0 \end{pmatrix}\,, \quad \gamma^5 = \gamma_5 = \begin{pmatrix} -\mathbb{1}_2 & 0 \\ 0 & \mathbb{1}_2 \end{pmatrix} \tag{1077}$$

and the Dirac basis[4] $(k = 1, 2, 3)$:

$$\gamma^5_{\text{Dirac}} = \gamma^0_{\text{Weyl}}\,, \quad \gamma^k_{\text{Dirac}} = \gamma^k_{\text{Weyl}}\,, \quad \gamma^0_{\text{Dirac}} = -\gamma^5_{\text{Weyl}} \quad . \tag{1078}$$

The Weyl basis has several advantages, when expressing Dirac spinors [64]

$$\psi = \begin{pmatrix} \psi^W_L \\ \psi^W_R \end{pmatrix} \tag{1079}$$

in terms of left- and right-handed Weyl spinors $\psi^W_{L,R}$, which obey the following chiral projections

$$P_L\psi = \begin{pmatrix} \psi^W_L \\ 0 \end{pmatrix}\,, \quad P_R\psi = \begin{pmatrix} 0 \\ \psi^W_R \end{pmatrix}\,. \tag{1080}$$

4 Here, we use the subscripts "Dirac" and "Weyl" to point out the specific basis.

In this notation, the massless free Dirac equation implies two separate Weyl equations [64, 188]

$$i\not{\partial}\psi = 0 \Rightarrow \begin{cases} i\bar{\sigma}^{\mu}\partial_{\mu}\psi_{L}^{W} = 0 \\ i\sigma^{\mu}\partial_{\mu}\psi_{R}^{W} = 0 \end{cases} . \tag{1081}$$

On the other hand, e. g., when focusing on a set-up with massless particles, it is easier to clarify the connection between chirality and helicity by using the Dirac representation [188]. For instance, each Dirac spinor describing massive ($m \neq 0$) spin-$\frac{1}{2}$ fermions in momentum-space

$$u^{s}(p) = \mathcal{N}\begin{pmatrix} \chi^{s} \\ \frac{\vec{\sigma}\cdot\vec{p}}{E+m}\chi^{s} \end{pmatrix} \xrightarrow[(E\to|\vec{p}|)]{m\to 0} \tilde{\mathcal{N}}\begin{pmatrix} \chi^{s} \\ \frac{\vec{\sigma}\cdot\vec{p}}{|\vec{p}|}\chi^{s} \end{pmatrix} \tag{1082}$$

can be decomposed into adequate normalization factors[5] $\mathcal{N}$, $\tilde{\mathcal{N}}$ (cf. [64, 66, 76]) and an arbitrary two-spinor χ^{s}. The latter can be defined as an eigenvector

$$\chi^{s} = \begin{cases} \binom{1}{0}, s = 1 \\ \binom{0}{1}, s = 2 \end{cases} \tag{1083}$$

of the related eigenequation (with eigenvalues $h_{s} = \pm 1$)

$$\frac{\vec{\sigma}\cdot\vec{p}}{|\vec{p}|}\chi^{s} = h_{s}\chi^{s} , \tag{1084}$$

which itself results from the underlying helicity operator (cf. [64, 188])

$$\Lambda_{h} = \vec{\Sigma}\cdot\frac{\vec{p}}{|\vec{p}|} = \begin{pmatrix} \frac{\vec{\sigma}\cdot\vec{p}}{|\vec{p}|} & 0 \\ 0 & \frac{\vec{\sigma}\cdot\vec{p}}{|\vec{p}|} \end{pmatrix} . \tag{1085}$$

Therefore, we may conclude, that in the massless limit a given chiral projector $\left(\text{e. g., } P_{R} \text{ or } P_{L}\right)$

$$\frac{1}{2}\left(\mathbb{1}_{4} \pm \gamma^{5}_{\text{Dirac}}\right) u^{s}(p) = \frac{1}{2}\tilde{\mathcal{N}}\begin{pmatrix} (1 \pm h_{s})\,\chi^{s} \\ \pm(1 \pm h_{s})\,\chi^{s} \end{pmatrix} \tag{1086}$$

projects on right-handed/left-handed states (i. e., $h_{s} = 1$ or $h_{s} = -1$ respectively) [76]. Here, $u^{s}(p)$ describes particles $\left(\text{set } \mathcal{N} = \sqrt{E+m}\right)$, while anti-particles are given by

$$v^{s}(p) = \mathcal{N}\begin{pmatrix} \frac{\vec{\sigma}\cdot\vec{p}}{E+m}\chi^{s} \\ \chi^{s} \end{pmatrix} . \tag{1087}$$

Accordingly, in Equation 242 we apply the completeness relations for the four-spinors u and v $\left(\not{p} = p_{\mu}\gamma^{\mu},\ \bar{u} = u^{\dagger}\gamma_{0}\right)$ [64]

$$\sum_{s} u^{s}(p)\,\bar{u}^{s}(p) = \not{p} + m , \tag{1088}$$

$$\sum_{s} v^{s}(p)\,\bar{v}^{s}(p) = \not{p} - m . \tag{1089}$$

Besides, we have to mention the following relation (for $\alpha \in \mathbb{R}$), which can be easily proven[6]:

$$\frac{1}{2}\left(\mathbb{1}_{4} + \gamma_{5}\right)e^{i\alpha} + \frac{1}{2}\left(\mathbb{1}_{4} - \gamma_{5}\right)e^{-i\alpha} = \mathbb{1}_{4}\cos(\alpha) + \gamma_{5}\sin(\alpha) = \exp(i\alpha\gamma_{5}) , \tag{1090}$$

5 For a particle with mass m and three-momentum $\vec{p}$ the energy is given by $E \equiv E_{\vec{p}} = \sqrt{m^{2} + \vec{p}^{2}}$.

6 For instance with properties of the involved nilpotent matrix γ^{5}.

when using the Taylor expansions of the involved matrix functions (see, e. g., [323, 324]). Additionally, we use identities based on (see also [323, 324, 371, 501])

$$\gamma_\mu\gamma_\alpha\gamma_\nu = g_{\mu\alpha}\gamma_\nu + g_{\alpha\nu}\gamma_\mu - g_{\mu\nu}\gamma_\alpha + i\varepsilon_{\mu\nu\alpha\beta}\gamma^\beta\gamma_5\,, \tag{1091}$$

as well as $(2i\sigma_{\alpha\beta}\gamma_5 = \varepsilon_{\alpha\beta\mu\nu}\sigma^{\mu\nu})$

$$\gamma_\mu\sigma_{\rho\lambda} = i\big(g_{\mu\rho}\gamma_\lambda - g_{\mu\lambda}\gamma_\rho\big) + \varepsilon_{\mu\rho\lambda\delta}\gamma^\delta\gamma_5 \quad \Rightarrow \quad \{\gamma_\mu, \sigma_{\nu\lambda}\} = 2\varepsilon_{\mu\nu\lambda\rho}\gamma^\rho\gamma_5, \tag{1092}$$

$$\gamma_\mu\gamma_\nu + i\sigma_{\mu\nu} = g_{\mu\nu}\mathbb{1}_4 \;\Leftrightarrow\; \gamma_\mu\gamma_\lambda\gamma_5 = -i\sigma_{\mu\lambda}\gamma_5 + g_{\mu\lambda}\gamma_5, \tag{1093}$$

$$\gamma_\mu\gamma_\nu\sigma_{\rho\lambda} = \sigma_{\mu\lambda}g_{\nu\rho} - \sigma_{\mu\rho}g_{\nu\lambda} + i\big(g_{\mu\lambda}g_{\nu\rho} - g_{\mu\rho}g_{\nu\lambda}\big) - \varepsilon_{\mu\nu\rho\lambda}\gamma_5 - i\varepsilon_{\nu\rho\lambda\alpha}g^{\alpha\beta}\sigma_{\mu\beta}\gamma_5. \tag{1094}$$

Furthermore, the Fierz identity (see, e. g., [322])

$$\begin{aligned}\delta_{\alpha'\beta}\delta_{\alpha\beta'} = \frac{1}{4}\Big[&(\mathbb{1}_4)_{\alpha\alpha'}(\mathbb{1}_4)_{\beta\beta'} - (i\gamma_5)_{\alpha\alpha'}(i\gamma_5)_{\beta\beta'} + (\gamma_\mu)_{\alpha\alpha'}(\gamma^\mu)_{\beta\beta'} \\ &- (\gamma_\mu\gamma_5)_{\alpha\alpha'}(\gamma^\mu\gamma_5)_{\beta\beta'} + \frac{1}{2}(\sigma_{\mu\nu})_{\alpha\alpha'}(\sigma^{\mu\nu})_{\beta\beta'}\Big]\end{aligned} \tag{1095}$$

is very useful for the parametrization of quark-antiquark matrix elements, especially with

$$(\sigma_{\mu\nu})_{\alpha\alpha'}(\sigma^{\mu\nu})_{\beta\beta'} = (\sigma_{\mu\nu}\gamma_5)_{\alpha\alpha'}(\sigma^{\mu\nu}\gamma_5)_{\beta\beta'}\,. \tag{1096}$$

Moreover, we make use of several trace theorems, in particular (for more, see [98, 323, 324])

$$\mathrm{Tr}\{\gamma_\mu\gamma_\nu\gamma_\alpha\gamma_\beta\} = 4\big[g_{\mu\nu}g_{\alpha\beta} + g_{\mu\beta}g_{\alpha\nu} - g_{\mu\alpha}g_{\nu\beta}\big]\,, \tag{1097}$$

$$\mathrm{Tr}\{\gamma_\mu\gamma_\nu\gamma_\alpha\gamma_\beta\gamma_5\} = 4i\varepsilon_{\mu\nu\alpha\beta}\,, \tag{1098}$$

$$\mathrm{Tr}\{\gamma_{\mu_1}\gamma_{\mu_2}\cdots\gamma_{\mu_{2n+1}}\} = 0 = \mathrm{Tr}\{\gamma_{\mu_1}\gamma_{\mu_2}\cdots\gamma_{\mu_{2n+1}}\gamma_5\} \quad (n \in \mathbb{N}_0)\,. \tag{1099}$$

For generalized D-dimensional identities, we refer to [64, 98, 323, 324, 587].

A.3 OPERATOR IDENTITIES

This short supplement collects several operator identities for Section 3.4.3. Here, we did not intend to circumvent possible redundancies because the listed expressions are supposed to be some sort of "cheat sheet" for the actual calculations.
Hence, we get for (cf. Chapter 2)

$$\vec{D}_\mu = \vec{\partial}_\mu\mathbb{1}_3 - ig\mathcal{A}^A_\mu T^A\,, \tag{1100}$$

$$\overleftarrow{D}_\mu = \overleftarrow{\partial}_\mu\mathbb{1}_3 + ig\mathcal{A}^A_\mu T^A\,, \tag{1101}$$

$$\partial_\mu = \vec{\partial}_\mu + \overleftarrow{\partial}_\mu = \vec{D}_\mu + \overleftarrow{D}_\mu\,, \tag{1102}$$

$$\overleftrightarrow{D}_\mu = \vec{D}_\mu - \overleftarrow{D}_\mu\,, \tag{1103}$$

the standard relations:

$$\vec{\not{D}}\gamma_5\psi = im_\psi\gamma_5\psi\,, \tag{1104}$$

$$-\vec{\not{D}}\psi = im_\psi\psi\,, \tag{1105}$$

$$\bar{\psi}\overleftarrow{\not{D}} = im_\psi\bar{\psi}\,, \tag{1106}$$

as well as

$$\vec{D}^2 = \vec{\not{D}}^2 + \frac{1}{2}\sigma_{\mu\nu}g\mathcal{G}^{\mu\nu}\,, \tag{1107}$$

$$\overleftrightarrow{D}^2 = 2\vec{D}^2 + 2\overleftarrow{D}^2 - \partial^2\,, \tag{1108}$$

$$\partial^\mu \overleftrightarrow{D}_\mu = \vec{D}^2 - \overleftarrow{D}^2\,, \tag{1109}$$

$$\overleftrightarrow{D}_\alpha \overleftrightarrow{D}_\beta + \partial_\alpha\partial_\beta = 2\vec{D}_\alpha\vec{D}_\beta + 2\overleftarrow{D}_\alpha\overleftarrow{D}_\beta\,, \tag{1110}$$

$$\overleftrightarrow{D}^2 = \overleftrightarrow{\not{D}}^2 + 2g\sigma^{\mu\nu}\mathcal{G}_{\mu\nu}\,, \tag{1111}$$

$$\left[\vec{D}_\mu, \vec{D}_\nu\right] = -ig\mathcal{G}_{\mu\nu} = \left[\overleftarrow{D}_\mu, \overleftarrow{D}_\nu\right]\,, \tag{1112}$$

$$\left[\overleftrightarrow{D}_\mu, \overleftrightarrow{D}_\nu\right] = -4ig\mathcal{G}_{\mu\nu}\,, \tag{1113}$$

$$\left[\overleftarrow{D}_\mu, \vec{D}_\nu\right] = ig\mathcal{G}_{\mu\nu} = \left[\vec{D}_\mu, \overleftarrow{D}_\nu\right]\,, \tag{1114}$$

$$\left[\vec{D}_\mu, \overleftrightarrow{D}_\nu\right] = -2ig\mathcal{G}_{\mu\nu} = \left[\overleftarrow{D}_\nu, \overleftrightarrow{D}_\mu\right]\,, \tag{1115}$$

$$\left[\partial_\mu, \overleftrightarrow{D}_\nu\right] = 0\,. \tag{1116}$$

Besides, we use relations for the gluon field strength tensor, such as

$$\varepsilon_{\xi\beta\rho\sigma}\mathcal{G}^{\xi}_{\ \alpha} = g_{\beta\alpha}\widetilde{\mathcal{G}}_{\rho\sigma}\,. \tag{1117}$$

A.4 RESTRICTIONS ON THE LAGRANGIAN

The structure of the general Lagrangian is based on Lorentz invariance, including an invariance under space inversions and time reversal as well as renormalizability (following [45]). The latter is particularly important for a reasonable formulation of the underlying theory, since covariance and gauge-invariance alone would not only allow terms proportional to (for definitions see Section 2.2)

$$\bar{\psi}\psi\,, \quad \bar{\psi}\not{D}\psi\,, \quad G^A_{\mu\nu}G^{A,\mu\nu}\,, \tag{1118}$$

but also to

$$\bar{\psi}\sigma^{\mu\nu}G_{\mu\nu}\psi\,, \quad \bar{\psi}\not{D}\psi\bar{\psi}\psi\,, \quad \ldots\,. \tag{1119}$$

Thus, owing to renormalizability irrepressible contributions (denoted by the ellipsis)

$$\mathcal{L} = \sum_\psi \left(a_1\bar{\psi}\psi + a_2\bar{\psi}\not{D}\psi\right) + a_3 G^A_{\mu\nu}G^{A,\mu\nu} + \sum_\psi a_4\bar{\psi}\sigma^{\mu\nu}G_{\mu\nu}\psi + \ldots \tag{1120}$$

to the invariant Lagrangian density can be ruled out. Based on the corresponding operator dimension (for $D=4$)

$$\dim\left[\bar{\psi}\psi\right] = 3\,,\ \dim\left[\bar{\psi}\not{D}\psi\right] = 4\,,\ \dim\left[G^A_{\mu\nu}G^{A,\mu\nu}\right] = 4\,,\ \dim\left[\bar{\psi}\sigma^{\mu\nu}G_{\mu\nu}\psi\right] = 5\,,\ \ldots \tag{1121}$$

the mass dimension of each coefficient a_i ($i = 1,2,3,\ldots$) can be deduced. For instance, the coefficients a_1, a_2 and a_3 have positive or vanishing mass dimensions "$\dim[a_i]$", while a_4, etc. have a negative canonical dimension. According to [45] the sign of $\dim[a_i]$ is related to the renormalizability of the underlying theory which is ultimately governed by the corresponding Lagrangian. Therefore, terms with $\dim[a_i] \geqslant 0$ are renormalizable, while those with $\dim[a_i] < 0$ are non-renormalizable and have to be discarded. Furthermore, the flavor-independence of gluon fields excludes terms proportional to γ_5 and $\gamma_\mu\gamma_5$ in the QCD Lagrangian (see, e. g., [44] for a detailed discussion).

A.5 ELEMENTS OF QUANTIZATION

In the following subsection we collect some selected facts concerning Feynman path integrals in the continuum. As mentioned in Section 2.2, this approach provides a self consistent formalism to introduce gauge-fixing and Faddeev-Popov ghosts (the original ansatz can be found in [72, 588]). Thus, we may focus on the main features of this method, while closely following [45].

As a starting point, we note, that within this formalism one can calculate any Green's function as a (functional) derivative

$$\frac{\delta Z[J(x)]}{\delta J(y)} = \lim_{\varepsilon \to 0} \frac{Z[J(x) + \varepsilon\delta(x-y)] - Z[J(x)]}{\varepsilon} \tag{1122}$$

of the generating functional $Z[J(x)]$. For convenience, one may choose a massive scalar field theory to introduce the notation. Accordingly, we encounter a self-coupling of the related field ϕ, as denoted by $V(\phi)$, i. e.,

$$\mathcal{L}_{\text{scal}} = \frac{1}{2}\left(\partial^\mu\phi\partial_\mu\phi - m^2\phi^2\right) - V(\phi) \ . \tag{1123}$$

Moreover, this generic notation includes an artificial source function $J(x)$

$$Z[J] = \int [d\,\phi]\, \exp\left\{ i \int d^4x\, (\mathcal{L} + \phi J) \right\} , \tag{1124}$$

which is needed to generate the actual Green's function[7]

$$\langle 0|T\{\hat{\phi}(x_1)\dots\hat{\phi}(x_n)\}|0\rangle = \frac{(-i)^n}{Z[0]} \frac{\delta^n Z[J]}{\delta J(x_1)\dots\delta J(x_n)}\bigg|_{J=0} \ . \tag{1125}$$

In the case of QCD for each field a corresponding source function has to be introduced. Let us start with the pure gluonic case

$$Z[J] = \int [d\,\mathcal{A}]\, \exp\left\{ i \int d^4x \left(\mathcal{L}_G + \mathcal{A}^A_\mu J^{A,\mu}\right) \right\} . \tag{1126}$$

The need for a gauge fixing condition, similar to Equation 25 in the path integral approach is essential, since it prevents the emergence of divergences. In fact, the action $S = \int d^4x\, \mathcal{L}_G$ is invariant for all gluon fields related to a specific gauge-transformation, corresponding to the same physical configuration. Since S is constant for all those configurations of the subset, $Z[0]$ diverges as the region of the integration is infinite. Hence, it is necessary to implement the condition introduced by Equation 25 into Equation 1126. As a consequence, the integration is restricted to physically different field configurations and one can additionally factor out a (divergent) formal constant. In the next step one inserts[8] (in the limit $n \to \infty$)

$$\det \mathcal{M}_G \int \prod_A \left[d\,\theta^A\right] \delta^{(n)}\left(G^\mu \mathcal{A}^A_\mu(x) - \mathcal{B}^A(x)\right) = 1 \tag{1127}$$

$$[\mathcal{M}_G(x,y)]^{AB} = \frac{\delta\left(G^\mu \mathcal{A}^{A,\theta}_\mu(x)\right)}{\delta\theta^B(y)} \tag{1128}$$

7 Here, a distinction between the field ϕ and the corresponding operator $\hat{\phi}$ should be made.

8 The existence and structure of $\mathcal{M}_G$ is caused by the underlying theory and involved gauge transformations (see, e. g., [44, 45]).

into Equation 1126. After exponentiating the inherent delta-function (using, that $\mathcal{B}^A$ can be arbitrarily chosen) we see, that Equation 1127 is effectively a modification of the action:

$$Z[J] = \int [d\mathcal{A}]\ \det\mathcal{M}_G e^{i\int d^4x\left(\mathcal{L}_G - \frac{1}{2\xi}\left[G^\mu \mathcal{A}^A_\mu\right]^2 + \mathcal{A}^A_\mu J^{A,\mu}\right)}\,. \tag{1129}$$

Let us now include fermions, e. g., by replacing the underlying Lagrangian and introduce adequate source functions:

$$Z[J,\eta,\bar\eta] = \int [d\mathcal{A}][d\psi]\left[d\bar\psi\right]\ \det\mathcal{M}_G e^{i\int d^4x\left(\mathcal{L}_G+\mathcal{L}_F - \frac{1}{2\xi}\left[G^\mu \mathcal{A}^A_\mu\right]^2 + \mathcal{A}^A_\mu J^{A,\mu} + \bar\psi\eta + \bar\eta\psi\right)}\,. \tag{1130}$$

When calculating $\mathcal{M}_G$ for the assumed gauge-fixing condition one finds

$$\frac{\delta\left(G^\mu \mathcal{A}^{A,\theta}_\mu(x)\right)}{\delta\theta^B(y)} = -\frac{1}{g}\left[\delta^{AB}\,G^\mu\partial_\mu - g f^{ABC}\,G^\mu \mathcal{A}^C_\mu\right]\delta^{(4)}(x-y)\,. \tag{1131}$$

Thus, there are two completely different scenarios concerning the choice of G^μ (see discussion in Section 2.2). For some cases, such as $G^\mu \equiv n^\mu$ (n^μ being an adequate four-vector) and $n^\mu \mathcal{A}^A_\mu = 0$, the matrix is independent of the gluon fields and, therefore, a constant. On the other hand, i. e., for choices similar to the Lorentz gauge $G^\mu \equiv \partial^\mu$ (with $\partial^\mu \mathcal{A}^A_\mu = 0$) the dependence on the gauge-field in the determinant of $\mathcal{M}_G$ does not vanish. As a result it has to be included in the dynamics of the physical theory. As a consequence, the effects of $\det\mathcal{M}_G$ have to be included into the effective Lagrangian. For the fermionic contributions, one may use an identity developed for Grassmann numbers. As discussed in [45], for Grassmann variables ψ, $\bar\psi$, along with diagonalizable matrices A, one may find

$$\int [d\psi]\left[d\bar\psi\right]\ \exp\left\{\int d^4x \int d^4y\ \bar\psi A(x,y)\psi\right\} = \det A\,. \tag{1132}$$

The same "trick" can be used to exponentiate the determinant $\det\mathcal{M}_G$ when introducing the complex fictitious fields $\tilde\chi^A$, $\tilde\chi^{A*}$ that are in the adjoint representation of $SU(3)_c$. These Faddeev-Popov ghost[9] fields are complex scalar fields (see Section A.6), which anti-commute, similar to fermions. For a general choice of the gauge-fixing condition one may, therefore, get

$$\begin{aligned} Z\left[J,\tilde\xi,\tilde\xi^*,\eta,\bar\eta\right] = \int [d\mathcal{A}][d\psi]\left[d\bar\psi\right][d\tilde\chi][d\tilde\chi^*]\ \exp\Bigg\{ & i\int d^4x\,(\mathcal{L}_G+\mathcal{L}_F) \\ & + i\int d^4x\,\left(\mathcal{A}^A_\mu J^{A,\mu} + \bar\psi\eta + \bar\eta\psi + \tilde\chi^{A*}\tilde\xi^A + \tilde\xi^{A*}\tilde\chi^A\right) \\ & - i\int d^4x\,d^4y\,\tilde\chi^{A*}(x)\,[\mathcal{M}_G(x,y)]^{AB}\,\tilde\chi^B(y) - i\int d^4x\,\frac{1}{2\xi}\left[G^\mu\mathcal{A}^A_\mu\right]^2\Bigg\}\,. \end{aligned} \tag{1133}$$

After redefining the ghost fields and involved generating functions in Equation 1133, the full quantum Lagrangian of QCD (as mentioned in Section 2.2) can be derived.

A.6 FEYNMAN RULES OF QCD

In this subsection the explicit expressions for the propagators and vertices (see Section 2.2) are collected.

9 They are necessary as computational tools, but do not correspond to any real particles.

According to Equation 29 the quantum Lagrangian of QCD can be split up into a free component $\mathcal{L}^{(0)}_{\text{QCD}}$, giving rise to possible propagators and an interactive part $\mathcal{L}^{(1)}_{\text{QCD}}$, which entails all vertices of the theory. In fact, the free Lagrangian can be written as (using Equation 6, Equation 22 and Equation 26)

$$\mathcal{L}^{(0)}_{\text{QCD}} = \mathcal{L}^{(0)}_{\text{F}} + \mathcal{L}^{(0)}_{\text{G}} + \mathcal{L}_{\text{GF}} + \mathcal{L}^{(0)}_{\text{FP}}\,, \quad \mathcal{L}^{(0)}_{\text{FP}} = -\chi^{A*}\delta^{AB}\,G^{\mu}\partial_{\mu}\chi^{B}\,. \tag{1134}$$

Let us start with the derivation of the gluon propagator. For the latter the gauge-fixing condition has to be incorporated:

$$\mathcal{L}^{(0)}_{\text{G}} + \mathcal{L}_{\text{GF}} = -\frac{1}{2}\mathcal{A}^{A}_{\nu}\left[-g^{\mu\nu}\partial^{2} + \partial^{\mu}\partial^{\nu}\right]\mathcal{A}^{A}_{\mu} - \frac{1}{2\xi}\left[G^{\mu}\mathcal{A}^{A}_{\mu}\right]\left[G^{\nu}\mathcal{A}^{A}_{\nu}\right]\,. \tag{1135}$$

Thus, when choosing "$G^{\mu}=\partial^{\mu}$", Equation 1135 implies the invertible operator $\mathcal{K}^{AB}_{\mu\nu}$:

$$\mathcal{L}^{(0)}_{\text{G}} + \mathcal{L}_{\text{GF}}\Big|_{G^{\mu}=\partial^{\mu}} = -\frac{1}{2}\mathcal{A}^{A}_{\mu}\mathcal{K}^{AB}_{\mu\nu}\mathcal{A}^{B}_{\nu}\,, \quad \mathcal{K}^{AB}_{\mu\nu} = \delta^{AB}\left[-g_{\mu\nu}\partial^{2} + \left(1-\frac{1}{\xi}\right)\partial_{\mu}\partial_{\nu}\right]\,. \tag{1136}$$

Similarly, the classical field equations for the propagators of the quark and ghost fields can be found. Correspondingly, the following differential equations arise

$$-g^{\lambda\rho}\mathcal{K}^{AC}_{\mu\lambda}D^{CB}_{\rho\nu}(x) = \delta^{AB}g_{\mu\nu}\delta^{(4)}(x)\,, \tag{1137}$$

$$-\delta^{AB}\partial^{2}D^{BC}(x) = \delta^{AC}\delta^{(4)}(x)\,, \tag{1138}$$

$$\left\{\left[i\gamma_{\mu}\partial^{\mu} - m_{\psi}\right]S_{\psi}(x)\right\}^{ab}_{\alpha\beta} = \delta^{ab}\delta_{\alpha\beta}\delta^{(4)}(x)\,, \tag{1139}$$

which have the formal solutions $(\varepsilon \to 0^{+})$

$$D^{AB}_{\mu\nu}(x) = \delta^{AB}\int\frac{d^{4}k}{(2\pi)^{4}}\,d_{\mu\nu}(k,\xi)\,\frac{e^{-ik\cdot x}}{k^{2}+i\varepsilon}\,, \tag{1140}$$

$$D^{AB}(x) = \delta^{AB}\int\frac{d^{4}k}{(2\pi)^{4}}\,\frac{e^{-ik\cdot x}}{k^{2}+i\varepsilon}\,, \tag{1141}$$

$$\left[S_{\psi}(x)\right]^{ab}_{\alpha\beta} = \delta^{ab}\int\frac{d^{4}p}{(2\pi)^{4}}\,\frac{\left[\not{p}+m_{\psi}\right]_{\alpha\beta}}{p^{2}-m^{2}_{\psi}+i\varepsilon}\,e^{-ip\cdot x}\,. \tag{1142}$$

Those describe the gluon propagator $D^{AB}_{\mu\nu}$, the (free) quark-propagator $\left[S_{\psi}\right]^{ab}_{\alpha\beta}$, and the ghost propagator D^{AB} in position space, respectively. Additionally, we define the auxiliary function:

$$D_{\mu\nu}(x) = \int\frac{d^{4}k}{(2\pi)^{4}}\,d_{\mu\nu}(k,\xi)\,\frac{e^{-ik\cdot x}}{k^{2}+i\varepsilon}\,. \tag{1143}$$

It is important to note that the related Lagrangian of Equation 1141 describes a massless charged scalar particle. Besides, the tensor structure of the gluon propagator in Equation 1140 is given by

$$d_{\mu\nu}(k,\xi) = \left(-g_{\mu\nu} + (1-\xi)\,\frac{k_{\mu}k_{\nu}}{k^{2}}\right)\,, \tag{1144}$$

where the choice $\xi=1$ is usually referred to as "Feynman gauge", while $\xi=0$ is known as "Landau gauge". Note that a non-covariant gauge-fixing condition, such as the axial gauge $n^{\mu}\mathcal{A}^{A}_{\mu}=0$ not only implies a decoupling of the ghost from the gluon fields, but also a quite complicated form for the associated gluon propagator:

$$d_{\mu\nu}(k,\xi) = \left(-g_{\mu\nu} + \frac{k_{\mu}n_{\nu}+k_{\nu}n_{\mu}}{(k\cdot n)} - \frac{n^{2}+\xi k^{2}}{(k\cdot n)^{2}}\right)\,. \tag{1145}$$

On the other hand, $\mathcal{L}^{(1)}_{\text{QCD}}$ can be written as (using Equation 18)

$$\begin{aligned}\mathcal{L}^{(1)}_{\text{QCD}} = &-\frac{g}{2} f^{ABC}\left(\partial_\mu \mathcal{A}^A_\nu - \partial_\nu \mathcal{A}^A_\mu\right)\mathcal{A}^{B,\mu}\mathcal{A}^{C,\nu} - \frac{g^2}{4} f^{ABE} f^{CDE}\mathcal{A}^A_\mu \mathcal{A}^B_\nu \mathcal{A}^{C,\mu}\mathcal{A}^{D,\nu} \\ &+ g f^{ABC}\chi^{A*} G^\mu \mathcal{A}^C_\mu \chi^B + g\mathcal{A}^A_\mu \partial^{A,\mu}\,,\end{aligned} \tag{1146}$$

which gives rise to the quark-gluon vertex, three-gluon vertex and four-gluon vertex. For a complete set of (SM) Feynman rules (consistent with the given formulas) we refer to [45, 198, 589].

A.7 RENORMALIZATION GROUP – BASICS

Based on Section 2.3 let us consider two different renormalization procedures $\mathfrak{R}$ and $\mathfrak{R}'$ (for a detailed discussion see [45]). Since both schemes start with the same unique Lagrangian (following [44, 45])

$$\mathcal{L}_{\mathfrak{R}} = \mathcal{L} = \mathcal{L}_{\mathfrak{R}'} \tag{1147}$$

they can be related accordingly. In terms of a generic unrenormalized field ϕ_0 and the corresponding scheme dependent renormalization constants $\mathcal{Z}_\phi\left(\mathfrak{R}^{(\prime)}\right)$

$$\phi_{\mathfrak{R}} = \mathcal{Z}_\phi(\mathfrak{R})\,\phi_0\,, \quad \phi_{\mathfrak{R}'} = \mathcal{Z}_\phi\left(\mathfrak{R}'\right)\phi_0\,, \tag{1148}$$

therefore, implies the relation

$$\phi_{\mathfrak{R}'} = Z_\phi\left(\mathfrak{R}', \mathfrak{R}\right)\phi_{\mathfrak{R}}\,, \qquad Z_\phi\left(\mathfrak{R}', \mathfrak{R}\right) = \frac{Z_\phi(\mathfrak{R}')}{Z_\phi(\mathfrak{R})}\,. \tag{1149}$$

Thus, fields in different subtraction schemes are related by a multiplicative factor. The latter has to be a finite quantity, because the renormalized fields are themselves finite. Besides, the complete set of transformations $\left\{Z_\phi(\mathfrak{R}', \mathfrak{R})\right\}_{\mathfrak{R}', \mathfrak{R}}$ forms an abelian group, usually referred to as RG. The formal group axioms can be easily confirmed via Equation 1149 and

$$\left.\begin{aligned} &Z_\phi(\mathfrak{R}'', \mathfrak{R}) = Z_\phi(\mathfrak{R}'', \mathfrak{R}')\, Z_\phi(\mathfrak{R}', \mathfrak{R}) && \text{(composition)}\,, \\ &Z_\phi(\mathfrak{R}, \mathfrak{R}) = 1 && \text{(unity)}\,, \\ &Z_\phi(\mathfrak{R}', \mathfrak{R})^{-1} = Z_\phi(\mathfrak{R}, \mathfrak{R}') && \text{(inverse)}\,, \end{aligned}\right\} \tag{1150}$$

which are by definition realized. Note, that the RG is not depending on a perturbative approach.

A.8 CALCULATION OF THE CHIRAL ANOMALY

Within this subsection, we calculate the chiral anomaly. For this purpose, we outline Schwinger's split point regularization approach (e. g., [3, 55, 66]). Moreover, in order to shorten the expressions, we consider the divergence of a current $\left(|\varepsilon_\mu| \ll 1\right)$

$$j^{(\psi)}_{\mu 5}(x) = \bar{\psi}(x+\varepsilon)\,\gamma_\mu\gamma_5\,[x+\varepsilon, x-\varepsilon]\,\psi(x-\varepsilon)\,, \tag{1151}$$

which is defined for one of the N_f active flavors ψ. Throughout the calculation ε_μ will be kept fixed, until the limit $|\varepsilon_\mu| \to 0$ can be taken to obtain the final result. Then the divergence is

$$\begin{aligned}\partial^\mu j^{(\psi)}_{\mu 5}(x) = &\bar{\psi}(x+\varepsilon)\overleftarrow{\not{\partial}}\gamma_5\,[x+\varepsilon, x-\varepsilon]\,\psi(x-\varepsilon) + \bar{\psi}(x+\varepsilon)\,[x+\varepsilon, x-\varepsilon]\overrightarrow{\not{\partial}}\gamma_5\psi(x-\varepsilon) \\ &+ \bar{\psi}(x+\varepsilon)\left(\not{\partial}\gamma_5\,[x+\varepsilon, x-\varepsilon]\right)\psi(x-\varepsilon)\,.\end{aligned} \tag{1152}$$

The derivative of the Wilson-line[10] ($\hat{P}$ denotes the path-ordering operator) [64]

$$[x,y] = \hat{P}\left\{ ig\int_0^1 du\ (x-y)_\mu\, \mathcal{A}^\mu(xu+y\bar{u})\right\} \tag{1153}$$

is proportional to (using a short-distance expansion of the quark fields)

$$\left[\mathcal{A}(x+\varepsilon)-\mathcal{A}(x-\varepsilon)\right] \sim \gamma^\mu \varepsilon^\nu \mathcal{G}_{\mu\nu}(0)\ , \tag{1154}$$

while the QCD EOM for the quark fields imply

$$\overrightarrow{\not\partial}\,\psi = ig\not{\mathcal{A}}\psi - im_\psi\psi \tag{1155}$$

$$\bar{\psi}\overleftarrow{\not\partial} = -ig\bar{\psi}\not{\mathcal{A}} + im_\psi\bar{\psi}\,. \tag{1156}$$

Thus, Equation 1152 gives rise to

$$-ig\not{\mathcal{A}}(x+\varepsilon)\,\gamma_5 - ig\gamma_5\not{\mathcal{A}}(x-\varepsilon) = ig\varepsilon^\rho\gamma^\mu\gamma_5\mathcal{G}_{\mu\rho}(0) + \dots\ , \tag{1157}$$

which results in

$$\partial^\mu j^{(\psi)}_{\mu 5}(x) = 2\bar{\psi}(x+\varepsilon)\left\{m_\psi i\gamma_5 + ig\varepsilon^\rho\gamma^\mu\gamma_5\mathcal{G}_{\mu\rho}(0)\right\}\psi(x-\varepsilon)\ . \tag{1158}$$

In the next step we neglect quark mass terms to get (taking the limit $|\varepsilon_\mu| \to 0$)

$$\begin{aligned}\lim_{m_\psi\to 0}\partial^\mu j^{(\psi)}_{\mu 5}(x) &= \overbrace{\bar{\psi}^a_\alpha(x+\varepsilon)\,2ig\varepsilon^\rho[\gamma^\mu\gamma_5]_{\alpha\beta}[\mathcal{G}_{\mu\rho}(0)]^{ab}\,\psi^b_\beta}(x-\varepsilon)\\ &= 2g\,\mathrm{Tr}\left\{S_\psi(x-\varepsilon,x+\varepsilon)\,\varepsilon^\rho\gamma^\mu\gamma_5\mathcal{G}_{\mu\rho}(0)\right\}\ .\end{aligned} \tag{1159}$$

After inserting the short distance propagator [3]

$$\underbrace{\psi(-x)\,\bar{\psi}}(x) = -\frac{i\not{x}}{16\pi^2x^4} + \frac{ix^\rho g\widetilde{\mathcal{G}}_{\rho\sigma}}{16\pi^2x^2}\gamma^\sigma\gamma_5 + \dots \tag{1160}$$

into Equation 1159 only the structures $\sim\gamma^\varphi\gamma_5$ can contribute. Therefore, we get

$$\begin{aligned}\lim_{m_\psi\to 0}\partial^\mu j^{(\psi)}_{\mu 5} &= \frac{g^2}{8\pi^2}\,\mathrm{Tr}\left\{\frac{\varepsilon^\alpha\varepsilon^\rho}{\varepsilon^2}\gamma^\mu\gamma_5\gamma^\varphi\gamma_5\mathcal{G}_{\mu\rho}\widetilde{\mathcal{G}}_{\alpha\rho}\right\}\\ &= -\frac{g^2}{4\pi^2}\frac{\varepsilon^\alpha\varepsilon^\rho}{\varepsilon^2}\mathcal{G}^A_{\mu\rho}\widetilde{\mathcal{G}}^{A,\mu}_{\alpha}\,.\end{aligned} \tag{1161}$$

Within the symmetric limit (e. g., [64])

$$\varepsilon^\mu\varepsilon^\nu \to \frac{1}{D}\varepsilon^2 g^{\mu\nu} \tag{1162}$$

Equation 1161 reproduces the anticipated identity (at NLO accuracy)

$$\partial^\mu j^{(\psi)}_{\mu 5} = \frac{\alpha_s}{4\pi}\mathcal{G}^A_{\mu\nu}\widetilde{\mathcal{G}}^{A,\mu\nu} + 2m_\psi\bar{\psi}i\gamma_5\psi\,. \tag{1163}$$

Surprisingly, as discussed in [55, 66] Equation 1163 represents the complete answer, which is also valid at higher loop accuracy.

10 Equation 1153 contains soft gluon fields (see, e. g., [64]).

A.9 LIGHT-CONE COORDINATES AND PROJECTION OPERATORS

In this section we discuss the standard conventions concerning light-cone coordinates, which are used throughout this work. For the sake of convenience, we focus on the Brodsky-Lepage (LB) and Kogut-Soper (KS) conventions (see [266] and references therein).
Based on the LB convention, the time- and space-like components (cf. [266]) of the contravariant vector

$$x^\mu = \left(x^0, x^1, x^2, x^3\right)^\mathsf{T} \equiv \left(x^+, x^-, \vec{x}_\perp\right)^\mathsf{T} \tag{1164}$$

are defined via

$$x^\pm = x^0 \pm x^3 \,. \tag{1165}$$

The remaining coordinates form the two-dimensional vector

$$\vec{x}_\perp = \left(x^1, x^2\right)^\mathsf{T} \,. \tag{1166}$$

Covariant vectors are obtained by using the metric tensor

$$g^{\mu\nu} = \begin{pmatrix} 0 & 2 & 0 & 0 \\ 2 & 0 & 0 & 0 \\ 0 & 0 & -1 & 0 \\ 0 & 0 & 0 & -1 \end{pmatrix} \quad \text{and} \quad g_{\mu\nu} = \begin{pmatrix} 0 & \frac{1}{2} & 0 & 0 \\ \frac{1}{2} & 0 & 0 & 0 \\ 0 & 0 & -1 & 0 \\ 0 & 0 & 0 & -1 \end{pmatrix} , \tag{1167}$$

i. e., $x_\mu = g_{\mu\nu} x^\nu$. Accordingly, the scalar product of two four-vectors x^μ and p^μ in the LB convention is given by

$$x \cdot p = x^\mu p_\mu = \frac{1}{2}\left(x^+ p^- + x^- p^+\right) - \vec{x}_\perp \cdot \vec{p}_\perp \,. \tag{1168}$$

In order to avoid extra factors of 2 and $1/2$ the KS convention may be used instead. The latter uses a different definition of the "light-cone time" and "light-cone position" [266], i. e.,

$$x^+ = \frac{1}{\sqrt{2}}\left(x^0 + x^3\right) \quad \text{and} \quad x^- = \frac{1}{\sqrt{2}}\left(x^0 - x^3\right) , \tag{1169}$$

respectively. The definition of the perpendicular components stays the same as in Equation 1166. Consequently, the corresponding metric tensor boils down to

$$g^{\mu\nu} = \begin{pmatrix} 0 & 1 & 0 & 0 \\ 1 & 0 & 0 & 0 \\ 0 & 0 & -1 & 0 \\ 0 & 0 & 0 & -1 \end{pmatrix} = g_{\mu\nu} \,, \tag{1170}$$

which implies the scalar product $\left(x^\pm = x_\mp\right)$

$$\begin{aligned} x \cdot p &= x^\mu p_\mu = x^+ p_+ + x^- p_- + x^1 p_1 + x^2 p_2 \\ &= x^+ p^- + x^- p^+ - \vec{x}_\perp \cdot \vec{p}_\perp \,. \end{aligned} \tag{1171}$$

This formalism is very useful in the context of light-cone dominated processes[11], where the ultra-relativistic particles travel close to the light-cone. Therefore, the light-cone coordinates seem to be a natural choice for this specific set-up.
Moreover, the KS convention is present (following [128]) in the context of conformal operators. It is, therefore, reasonable to introduce several abbreviations. Let us assume two independent light-like vectors, similar to

$$n^\mu = \left(0, 1, \vec{0}_\perp\right)^\mathsf{T}, \quad \bar{n}^\mu = \left(1, 0, \vec{0}_\perp\right)^\mathsf{T}, \tag{1172}$$

which fulfill

$$n^2 = 0 = \bar{n}^2, \quad n \cdot \bar{n} = 1. \tag{1173}$$

Accordingly, the "+"- and "−"-projections of an arbitrary four-vector v^μ correspond to:

$$v^+ = v^\mu n_\mu, \quad v^- = v^\mu \bar{n}_\mu. \tag{1174}$$

Additionally, the notation for a four-vector, that only has (a priori non-vanishing) perpendicular components

$$x_\perp^\mu = g_\perp^{\mu\nu} x_\nu \tag{1175}$$

can be defined, via the metric tensor in the directions orthogonal to the light-cone

$$g_{\mu\nu}^\perp = g_{\mu\nu} - n_\mu \bar{n}_\nu - n_\nu \bar{n}_\mu. \tag{1176}$$

Thus, a decomposition of any four-vector x^μ can be written as[12]

$$x^\mu = x^- n^\mu + x^+ \bar{n}^\mu + x_\perp^\mu. \tag{1177}$$

Consequently, with Equation 1173 it is easy to verify the general relations (cf. [266])

$$\gamma^+\gamma^+ = 0 = \gamma^-\gamma^-, \tag{1178}$$

as well as

$$\gamma^+\gamma^-\gamma^+ = 2\gamma^+, \quad \gamma^-\gamma^+\gamma^- = 2\gamma^-. \tag{1179}$$

Moreover, with Equation 1178 and Equation 1179 the fundamental properties of Equation 354, i. e.,

$$\Pi_+ + \Pi_- = \mathbb{1}_4, \quad \Pi_\pm \Pi_\mp = 0, \quad \Pi_\pm^2 = \Pi_\pm, \tag{1180}$$

can be easily verified. Additionally, the following identities can be useful:

$$\gamma_\mu^\perp = -\frac{1}{2}\left[\gamma_+\gamma_\mu\gamma_- + \gamma_-\gamma_\mu\gamma_+\right], \tag{1181}$$

$$i\varepsilon_{\sigma\mu+-}\gamma^\sigma\gamma_5 = +\frac{1}{2}\left[\gamma_+\gamma_\mu\gamma_- - \gamma_-\gamma_\mu\gamma_+\right]. \tag{1182}$$

11 When using this light-cone formalism, a multitude of expressions can be simplified. For instance, boosts in the z-direction can be calculated in a simpler way, i. e., when compared to the standard notation (see also [590]).

12 In the original work [128] all contravariant vectors are consistently written in a modified way: $x^\mu = (x_+, x_-, \vec{x}_\perp)^\mathsf{T}$.

A.10 CONSTRUCTION OF LIGHT-LIKE VECTORS

This supplement features some common lore about the construction of light-like vectors. In fact, a standard way to construct two light-like vectors n_μ and p_μ from predefined four-vectors x_μ, P_μ is given by (cf. [532])

$$n_\mu = x_\mu - \frac{P_\mu}{P^2}\left[(P\cdot x) - \sqrt{(P\cdot x)^2 - P^2 x^2}\right], \tag{1183}$$

$$p_\mu = P_\mu - \frac{x_\mu P^2}{(P\cdot x) + \sqrt{(P\cdot x)^2 - P^2 x^2}}. \tag{1184}$$

These definitions are particularly useful for $x^2 \approx 0$, $P^2 = m_M^2$ and $P\cdot x \geqslant 0$:

$$n_\mu = x_\mu + \mathcal{O}\left(x^2\right), \tag{1185}$$

$$p_\mu = P_\mu - \frac{x_\mu m_M^2}{2\,(P\cdot x)} + \mathcal{O}\left(x^2\right) = P_\mu - \frac{n_\mu m_M^2}{2\,(P\cdot x)} + \mathcal{O}\left(x^2\right). \tag{1186}$$

Moreover, we may write (neglecting $\mathcal{O}(x^2)$ corrections)

$$p\cdot n = P\cdot n = P\cdot x\,. \tag{1187}$$

Moreover, for this set-up one usually defines (up to the intended order of accuracy)

$$p_\mu = P_\mu - \frac{n_\mu m_M^2}{2\,(P\cdot n)} \quad \Rightarrow \quad \bar{n}_\mu = \frac{p_\mu}{p\cdot n}, \tag{1188}$$

along with the projection operator (cf. Equation 1176)

$$g^{\perp}_{\mu\nu} = g_{\mu\nu} - \frac{1}{(p\cdot n)}\left(p_\mu n_\nu + p_\nu n_\mu\right). \tag{1189}$$

A.11 LIE ALGEBRA OF THE CONFORMAL GROUP

The Lie algebra of the Pointcaré group is generated by the operators (cf. Section 3.2) $\mathbf{P}_\mu$ and $\mathbf{M}_{\mu\nu}$ [55, 128]:

$$i[\mathbf{P}_\mu, \mathbf{P}_\nu] = 0\,, \tag{1190}$$

$$i[\mathbf{M}_{\alpha\beta}, \mathbf{P}_\mu] = g_{\alpha\mu}\mathbf{P}_\beta - g_{\beta\mu}\mathbf{P}_\alpha\,, \tag{1191}$$

$$i[\mathbf{M}_{\alpha\beta}, \mathbf{M}_{\mu\nu}] = g_{\alpha\mu}\mathbf{M}_{\beta\nu} - g_{\beta\mu}\mathbf{M}_{\alpha\nu} - g_{\alpha\nu}\mathbf{M}_{\beta\mu} + g_{\beta\nu}\mathbf{M}_{\alpha\mu}\,, \tag{1192}$$

while the conformal algebra is defined via the extensions

$$i[\mathbf{D}, \mathbf{P}_\mu] = \mathbf{P}_\mu\,, \tag{1193}$$

$$i[\mathbf{D}, \mathbf{K}_\mu] = -\mathbf{K}_\mu\,, \tag{1194}$$

$$i[\mathbf{M}_{\alpha\beta}, \mathbf{K}_\mu] = g_{\alpha\mu}\mathbf{K}_\beta - g_{\beta\mu}\mathbf{K}_\alpha\,, \tag{1195}$$

$$i[\mathbf{P}_\mu, \mathbf{K}_\nu] = -2g_{\mu\nu}\mathbf{D} + 2\mathbf{M}_{\mu\nu}\,, \tag{1196}$$

$$i[\mathbf{D}, \mathbf{M}_{\mu\nu}] = i[\mathbf{K}_\mu, \mathbf{K}_\nu] = 0\,. \tag{1197}$$

The latter include operators that give rise to the special conformal transformations $(\mathbf{K}_\mu)$ and dilatations $(\mathbf{D})$. By using the definitions of Equation 362 and Equation 364, one obtains the following relations (cf. [128])

$$\left.\begin{aligned} [\mathbf{L}_+, \phi(\alpha)] &= -\tfrac{d}{d\alpha}\phi(\alpha) \equiv L_+\phi(\alpha)\ , \\ [\mathbf{L}_-, \phi(\alpha)] &= \left(\alpha^2\tfrac{d}{d\alpha} + 2j\alpha\right)\phi(\alpha) \equiv L_-\phi(\alpha)\ , \\ [\mathbf{L}_0, \phi(\alpha)] &= \left(\alpha\tfrac{d}{d\alpha} + j\right)\phi(\alpha) \equiv L_0\phi(\alpha)\ . \end{aligned}\right\} \tag{1198}$$

Similar to the one-particle case (cf. Equation 384), the adjoint representation for the ladder operators (see Equation 388) may be formulated via[13]:

$$\left.\begin{aligned} L_0\widetilde{\mathcal{P}}_n(\kappa_1,\kappa_2) &= \textstyle\sum_{i=1}^{2}\left(\kappa_i\partial_{\kappa_i} + j_i\right)\widetilde{\mathcal{P}}_n(\kappa_1,\kappa_2)\ , \\ L_-\widetilde{\mathcal{P}}_n(\kappa_1,\kappa_2) &= -\textstyle\sum_{i=1}^{2}\partial_{\kappa_i}\widetilde{\mathcal{P}}_n(\kappa_1,\kappa_2)\ , \\ L_+\widetilde{\mathcal{P}}_n(\kappa_1,\kappa_2) &= \textstyle\sum_{i=1}^{2}\left(\kappa_i\partial_{\kappa_i} + 2j_i\kappa_i\right)\widetilde{\mathcal{P}}_n(\kappa_1,\kappa_2)\ , \end{aligned}\right\} \tag{1199}$$

with the characteristic polynomials $\widetilde{\mathcal{P}}_n(\kappa_1,\kappa_2)$. The latter arise from Equation 387 when applying the substitution of Equation 396 (see [55, 128] for a detailed discussion).

A.12 POLYNOMIALS AND ORTHOGONALITY RELATIONS

This short supplement collects the orthogonality relations of Gegenbauer and Jacobi polynomials as well as some general theorems concerning polynomials used in this work.

The Gegenbauer, or "ultraspherical" polynomials [291]

$$C_n^{(\alpha)}(\xi) = \frac{(-2)^n}{n!}\frac{\Gamma(n+\alpha)\,\Gamma(n+2\alpha)}{\Gamma(\alpha)\,\Gamma(2n+2\alpha)}\left(1-\xi^2\right)^{\frac{1}{2}-\alpha}\frac{d^n}{d\xi^n}\left\{\left(1-\xi^2\right)^{n+\alpha-\frac{1}{2}}\right\} \tag{1200}$$

are a special case (cf. Equation 407) of the Jacobi (or "hypergeometric") polynomials [291, 591]

$$P_n^{(\alpha,\beta)}(\xi) = \frac{(-1)^n}{2^n n!}(1-\xi)^{-\alpha}(1+\xi)^{-\beta}\frac{d^n}{d\xi^n}\left\{(1-\xi)^{\alpha}(1+\xi)^{\beta}\left(1-\xi^2\right)^n\right\}. \tag{1201}$$

Both belong to a class of orthogonal polynomials that have the domain $\xi\in[-1,1]$. For instance, the Gegenbauer polynomials fulfill the orthogonality relation[14] $(\alpha>-\frac{1}{2}$ fixed) [466]

$$\int_{-1}^{1} d\xi\, C_n^{(\alpha)}(\xi)\, C_m^{(\alpha)}(\xi)\,\widetilde{w}^{(\alpha)}(\xi) = \delta_{nm}\widetilde{N}_n^{(\alpha)}\,, \tag{1202}$$

using the weight function [466]

$$\widetilde{w}^{(\alpha)}(\xi) = \left[1-\xi^2\right]^{\alpha-\frac{1}{2}} \tag{1203}$$

and the normalization constant [466]

$$\widetilde{N}_n^{(\alpha)} = \frac{\pi\, 2^{1-2\alpha}\Gamma(n+2\alpha)}{n!\,(n+\alpha)\,[\Gamma(\alpha)]^2}\,. \tag{1204}$$

13 At this point, Equation 1199 could also be formulated with adequate test functions instead of $\widetilde{\mathcal{P}}_n(\kappa_1,\kappa_2)$.
14 Similar orthogonality relations for the hypergeometric polynomials may be found in [466, 592].

The given physical set-up (cf. Section 3.1.4 and in particular Equation 290) restricts us to $x \in [0,1]$. This implies the substitution "$\xi \to \xi_x$" (cf. Equation 128). Therefore, Equation 1202 has to be written as

$$\int_0^1 dx\, C_n^{(\alpha)}(\xi_x)\, C_m^{(\alpha)}(\xi_x)\, w^{(\alpha)}(x) = \delta_{nm} N_n^{(\alpha)} \tag{1205}$$

including the new weight function

$$w^{(\alpha)}(x) = 2^{1-2\alpha} \widetilde{w}^{(\alpha)}(\xi_x) \equiv [x\bar{x}]^{\alpha-\frac{1}{2}} \tag{1206}$$

and the normalization factor

$$N_n^{(\alpha)} = \frac{2^{1-4\alpha}\left[\Gamma\left(\frac{1}{2}\right)\right]^2 \Gamma(n+2\alpha)}{(n+\alpha)\left[\Gamma(\alpha)\right]^2 \Gamma(n+1)} \,. \tag{1207}$$

The latter reproduces the widely used (cf. [20, 26]) conventions:

$$N_n^{(3/2)} = \frac{(n+1)(n+2)}{4(2n+3)}, \quad N_{n-1}^{(5/2)} = \frac{n(n+3)}{36} N_n^{(3/2)} \,. \tag{1208}$$

Analogously, we make use of the corresponding orthogonality condition (cf. [593] when adapted to the domain of definition $x \in [0,1]$):

$$\int_0^1 dx\, P_n^{(\alpha,\beta)}(\xi_x)\, P_m^{(\alpha,\beta)}(\xi_x) = N_n^{(\alpha,\beta)} \delta_{nm} \,, \tag{1209}$$

with the normalization constant

$$N_n^{(\alpha,\beta)} = \frac{1}{n!\,(2n+\alpha+\beta+1)} \frac{\Gamma(n+\alpha+1)\,\Gamma(n+\beta+1)}{\Gamma(n+\alpha+\beta+1)} \,. \tag{1210}$$

Let us now discuss the use of the named orthogonality relations. Apparently, for a given function $\phi(x)$ $\left(x \in [0,1]\right)$, one may consider the (formal) power series[15]

$$\phi(x) = \sum_{n=0}^{\infty} c_{n;\alpha}^{\phi} w^{(\alpha)}(x)\, C_n^{(\alpha)}(\xi_x) \,, \tag{1211}$$

with the Gegenbauer coefficients

$$c_{n;\alpha}^{\phi} = \int_0^1 dx\, \frac{C_n^{(\alpha)}(\xi_x)}{N_n^{(\alpha)}} \phi(x) \,. \tag{1212}$$

The latter have been derived via the assumption

$$\int_0^1 dx \left(\sum_{n=0}^{\infty} c_{n;\alpha}^{\phi} w^{(\alpha)}(x)\, C_n^{(\alpha)}(\xi_x) \right) \phi(x) \equiv \sum_{n=0}^{\infty} c_{n;\alpha}^{\phi} \int_0^1 dx\, w^{(\alpha)}(x)\, C_n^{(\alpha)}(\xi_x)\, \phi(x) \,. \tag{1213}$$

Alternatively, the expansion of "ϕ" may be written as

$$\phi(x) = \sum_{n=0}^{\infty} \tilde{c}_{n;\alpha}^{\phi} C_n^{(\alpha)}(\xi_x) \,, \tag{1214}$$

15 According to Chapter 3, we refer to Equation 1211 as the Gegenbauer expansion, while other sources introduce Equation 1214 with the very same name (cf. [594]).

with the coefficients

$$\tilde{c}^{\phi}_{n;\alpha} = \int_0^1 dx \, \frac{w^{(\alpha)}(x)}{N_n^{(\alpha)}} C_n^{(\alpha)}(\xi_x) \, \phi(x) \; . \tag{1215}$$

Similarly, we encounter functions similar to $f(x)$ $\left(x \in [0,1]\right)$:

$$f(x) = \frac{\Gamma(\alpha+\beta+2)}{\Gamma(\alpha+1)\,\Gamma(\beta+1)} \bar{x}^{\alpha} x^{\beta} \, g(x) \; , \tag{1216}$$

where the power series expansion for "g" is given by:

$$g(x) = \sum_{n=0}^{\infty} \kappa_n^{(\alpha,\beta)} P_n^{(\alpha,\beta)}(\xi_x) \; , \tag{1217}$$

with the coefficients (α, β some given constants)

$$\kappa_n^{(\alpha,\beta)} = \int_0^1 dx \, \frac{\bar{x}^{\alpha} x^{\beta}}{N_n^{(\alpha,\beta)}} g(x) \, P_n^{(\alpha,\beta)}(\xi_x) \; . \tag{1218}$$

Furthermore, among the multitude of possible identities for Gegenbauer and Jacobi polynomials, we emphasize [466, 591, 592]:

$$\left(1-\xi_x^2\right) \frac{d}{d\,\xi_x} C_n^{(\alpha)}(\xi_x) = (n+2\alpha)\,\xi_x C_n^{(\alpha)}(\xi_x) - (n+1)\, C_{n+1}^{(\alpha)}(\xi_x) \, , \tag{1219}$$

$$C_{n+1}^{(\alpha)}(\xi_x) = \xi_x C_n^{(\alpha)}(\xi_x) + \frac{2\alpha+n-1}{2\alpha-2} C_{n+1}^{(\alpha-1)}(\xi_x) \; . \tag{1220}$$

When using Equation 407, Equation 1219 and Equation 1220, we get the important relations:

$$\frac{d}{dx}\left\{ 6x\bar{x} C_n^{(3/2)}(\xi_x) \right\} = -3\,(n+1)\,(n+2)\, C_{n+1}^{(1/2)}(\xi_x) \; , \tag{1221}$$

$$C_n^{(1/2)}(\xi_x) = \bar{x}\, P_n^{(1,0)}(\xi_x) + x\, P_n^{(0,1)}(\xi_x) \; , \tag{1222}$$

$$C_{n+1}^{(1/2)}(\xi_x) = x\, P_n^{(0,1)}(\xi_x) - \bar{x}\, P_n^{(1,0)}(\xi_x) \; . \tag{1223}$$

In order to derive the formal structure of the two-particle twist-three DAs, Equation 1222 and Equation 1223 as well as Equation 1221 has to be used.
Apart from that, for the proper description of generic three-particle operators, such as (cf. Equation 385)

$$\mathcal{O}(\alpha_1,\alpha_2,\alpha_3) = \phi_{j_1}(\alpha_1)\,\phi_{j_2}(\alpha_2)\,\phi_{j_3}(\alpha_3) \tag{1224}$$

a suitable conformal basis has to be constructed. According to [128, 293, 297], a well-defined choice of basis not only requires a definite total three-particle spin ($N \in \mathbb{N}_0$)

$$J = j_1 + j_2 + j_3 + N \, , \tag{1225}$$

but also a fixed value of the conformal spin in the preassigned two-particle channel ($0 \leqslant n \leqslant N$)

$$j = j_1 + j_2 + n \, . \tag{1226}$$

The latter is related to the generic ambiguity of this system to couple all three spins to the total spin "J". Consequently, the following polynomials arise (cf. [128]):

$$Y_{J,j}^{(12)3}(\underline{\alpha}) = \overline{\alpha}_3^n P_{N-n}^{(2j_3-1,2j-1)}(-\xi_{\alpha_3})\, P_n^{(2j_1-1,2j_2-1)}\left(\tfrac{\alpha_2-\alpha_1}{\overline{\alpha}_3}\right) \; , \tag{1227}$$

which obey the relation [128, 293, 297]

$$\int \mathcal{D}\underline{\alpha} \left[\prod_{k=1}^{3} \alpha_k^{2j_k-1} \right] Y_{J,j}^{(12)3}(\underline{\alpha})\, Y_{J',j'}^{(12)3}(\underline{\alpha}) \sim \delta_{JJ'}\delta_{jj'} \,. \tag{1228}$$

In particular, they are orthogonality with respect to the corresponding asymptotic DA (cf. Equation 412). Besides, for a given triplet (j_1, j_2, j_3) of spins, we use the following abbreviation:

$$Y_{J,j}^{(12)3}(\underline{\alpha}) \to Y_{J,j}^{(j_1,j_2)j_3}(\underline{\alpha}) \,. \tag{1229}$$

For instance, $Y_{3,3/2}^{(1,1/2)3/2}(\underline{\alpha})$ corresponds to "$(1, \frac{1}{2}, \frac{3}{2})$". Furthermore, for the derivation of Equation 395 the multinomial theorem ($n, h \in \mathbb{N}_0$)

$$\left(\sum_{k=1}^{n} x_k \right)^h = \sum_{|\alpha|=h} \binom{h}{\alpha} x^\alpha \tag{1230}$$

has been used, where we apply the multi-index notation [595]:

$$\alpha = (\alpha_1, \ldots, \alpha_n) \in \mathbb{N}_0^n \tag{1231}$$

$$|\alpha| = \alpha_1 + \ldots + \alpha_n \tag{1232}$$

$$\binom{h}{\alpha} = \frac{h!}{\alpha_1! \cdots \alpha_n!} \tag{1233}$$

$$x = (x_1, \ldots, x_n) \in \mathbb{R}^n \tag{1234}$$

$$x^\alpha = x_1^{\alpha_1} \cdots x_n^{\alpha_n} \,. \tag{1235}$$

For a detailed discussion see, e. g., [595].

A.13 ASYMPTOTIC EXPANSION

This is a short supplement concerning asymptotic expansions (see Section 2.4) (e. g., [77, 79]). Let us assume a generic observable $R(\alpha_S)$. Since the corresponding asymptotic power series $R(\alpha_S) \approx \sum_n C_n \alpha_S^n$ (cf. Equation 49) does not converge, its partial sums do not provide an arbitrarily accurate approximation to $R(\alpha_S)$ for any fixed value of α_S (cf. [77, 79, 596]). When assuming ($N \in \mathbb{N}$ fixed) a polynomial truncation error ($K_N, a, b \in \mathbb{R}$ being some constants)

$$\left| R(\alpha_S) - \sum_{n=0}^{N-1} C_n \alpha_S^n \right| \leqslant K_N \alpha_S^N \,, \quad K_N \sim a^N N!\, N^b \,, \tag{1236}$$

in $\alpha_S < 1$ the related ratio for successive terms ($n \gg 1$)

$$\frac{K_n \alpha_S^n}{K_{n-1} \alpha_S^{n-1}} = an \left(1 + \frac{1}{n-1} \right)^b \alpha_S \approx an\alpha_S \tag{1237}$$

generally grows with n, e. g., it becomes larger than 1, if $n > (|a|\alpha_S)^{-1}$. Most importantly, the best approximation can be achieved for

$$|a|\alpha_S n \sim 1 \,, \tag{1238}$$

i. e., at this point the inclusion of higher order corrections does not improve the overall accuracy. Thus, when truncating the series at $N_* \sim (|a|\alpha_S)^{-1}$, one may expect an error proportional to ($N_* \gg 1$ applying Stirling's formula) [77]

$$K_{N_*}\alpha_S^{N_*} \sim \left(\frac{1}{|a|\alpha_S}\right)^{\frac{1}{2}+b} e^{-\frac{1}{|a|\alpha_S}} \sim e^{-\frac{1}{|a|\alpha_S}}\,, \tag{1239}$$

implying an exponentially accurate approximation of $R(\alpha_S)$.
This knowledge about the optimal truncation point N_* is applied in Equation 92.

A.14 FOCK STATES AND LIGHT-CONE WAVE FUNCTIONS

Here, is a short supplement collecting heuristic examinations concerning the (hypothetical) flavor states $|\eta_q\rangle$ and $|\eta_s\rangle$ (see Equation 315). In this subsection we also try to further elucidate the relationship between gluon distribution amplitudes and the state-mixing approach. Accordingly, we reconsider the work done by [20, 32, 278] and extend it according to our approach.

In the following we focus on the flavor structure of valence Fock states (cf. Section 2.5, Section 3.1.4). For the quark-antiquark case they are defined by $\Big(\boldsymbol{\Psi} = (u, d, s)^T$, $|\psi\bar{\psi}^q\rangle \equiv |q\bar{q}\rangle$, $|\psi\bar{\psi}^s\rangle \equiv |s\bar{s}\rangle\Big)$

$$|\psi\bar{\psi}^A\rangle = \left|\boldsymbol{\Psi}_a \left[\sqrt{2}T^A\right]_{ab} \overline{\boldsymbol{\Psi}}_b\right\rangle\,, \tag{1240}$$

while $|gg\rangle$ is representing the two-gluon component of a given meson state. In this context, $a, b = 1, 2, 3$ are flavor indices related to corresponding $SU(3)_F$ generators $T^A = \frac{\lambda^A}{2}$ $(e.g., A = q, s, 8, 0)$. Therefore, the decomposition of a given vector $|M\rangle$ $(i.e., M = \eta, \eta'$ labeling the associated element of the underlying Hilbert space$)$ into Fock components [20, 152] can be reduced to[16]

$$|M\rangle = \sum_{A=8,0} \Psi_M^A|A\rangle + \Psi_M^g|gg\rangle + \dots\,, \tag{1241}$$

with the individual light-cone wave functions Ψ_M^A for each Fock state[17] (cf. Equation 288). The latter can be decomposed into a DA $\overline{\phi}_M^A$ and a transverse momentum part Σ_M^A [278, 369, 597]:

$$\Psi_M^A\left(x, \vec{k}_\perp\right) = \frac{f_M^A}{2\sqrt{2N_c}}\overline{\phi}_M^A(x)\,\Sigma_M^A\left(\frac{\vec{k}_\perp}{\sqrt{x\bar{x}}}\right)\,, \tag{1242}$$

which again is normalized as [278]

$$\int\frac{d^2k_\perp}{16\pi^3}\,\Sigma_M^A\left(\frac{\vec{k}_\perp}{\sqrt{x\bar{x}}}\right) = 1 \quad\Rightarrow\quad \int\frac{d^2k_\perp}{16\pi^3}\int_0^1 dx\,\Psi_M^A\left(x, \vec{k}_\perp\right) = \frac{f_M^A}{2\sqrt{2N_c}}\,. \tag{1243}$$

As discussed in [278], we could assume

$$\Sigma_M^A\left(\frac{\vec{k}_\perp}{\sqrt{x\bar{x}}}\right) = \frac{16\pi^2\left[\tilde{a}_M^A\right]^2}{x\bar{x}}\exp\left(-\frac{\left[\tilde{a}_M^A\right]^2\vec{k}_\perp^2}{x\bar{x}}\right)\,. \tag{1244}$$

16 Here, the ellipses represent neglected states.

17 As discussed in Section 3.1.4 (see also [278]), the momentum fraction x and transverse momentum $\vec{k}_\perp$ refer to the involved quark, while the given antiquark is characterized by $\bar{x}$ as well as $-\vec{k}_\perp$.

Here, the associated transverse size parameters $\tilde{a}_M^A$ can be approximated with their pion counterpart, i. e., we may infer $\tilde{a}_M^A \approx \tilde{a}_\pi$. For the given set up, we can, therefore, expect a similar transverse momentum dependence for all involved light-cone wave functions.

Most importantly, by using Equation 268 the quark-antiquark Fock components of Equation 1241 can be rewritten. Together with a formal integration of the light-cone wave functions[18]

$$\frac{f_M^A}{2\sqrt{2N_c}}\phi_M^A\left(x,Q^2\right) = \int_0^{Q^2}\frac{d^2k_\perp}{16\pi^3}\Psi_M^A\left(x,\vec{k}_\perp\right), \tag{1245}$$

while applying the state mixing assumption Equation 315 we get[19]

$$|\eta_q\rangle \sim \left[\sqrt{\frac{1}{3}}h_1 + \sqrt{\frac{2}{3}}h_2\right]|q\bar{q}\rangle + \left[\sqrt{\frac{1}{3}}h_2 - \sqrt{\frac{2}{3}}h_1\right]|s\bar{s}\rangle + g_1|gg\rangle + \ldots \tag{1246}$$

$$|\eta_s\rangle \sim \left[\sqrt{\frac{1}{3}}\tilde{h}_1 + \sqrt{\frac{2}{3}}\tilde{h}_2\right]|q\bar{q}\rangle + \left[\sqrt{\frac{1}{3}}\tilde{h}_2 - \sqrt{\frac{2}{3}}\tilde{h}_1\right]|s\bar{s}\rangle + g_2|gg\rangle + \ldots . \tag{1247}$$

Here, we make use of the following abbreviations[20] $\left(\sigma = \sqrt{\frac{N_f}{C_f}}\right)$:

$$h_1\left(x,\mu^2\right) \coloneqq \cos\phi\, f_\eta^8\phi_\eta^8\left(x,\mu^2\right) + \sin\phi\, f_{\eta'}^8\phi_{\eta'}^8\left(x,\mu^2\right), \tag{1248}$$

$$h_2\left(x,\mu^2\right) \coloneqq \cos\phi\, f_\eta^0\phi_\eta^0\left(x,\mu^2\right) + \sin\phi\, f_{\eta'}^0\phi_{\eta'}^0\left(x,\mu^2\right), \tag{1249}$$

$$\tilde{h}_1\left(x,\mu^2\right) \coloneqq \cos\phi\, f_{\eta'}^8\phi_{\eta'}^8\left(x,\mu^2\right) - \sin\phi\, f_\eta^8\phi_\eta^8\left(x,\mu^2\right), \tag{1250}$$

$$\tilde{h}_2\left(x,\mu^2\right) \coloneqq \cos\phi\, f_{\eta'}^0\phi_{\eta'}^0\left(x,\mu^2\right) - \sin\phi\, f_\eta^0\phi_\eta^0\left(x,\mu^2\right), \tag{1251}$$

$$g_1\left(x,\mu^2\right) \coloneqq \cos\phi\,\frac{f_\eta^0}{\sigma}\phi_\eta^g\left(x,\mu^2\right) + \sin\phi\,\frac{f_{\eta'}^0}{\sigma}\phi_{\eta'}^g\left(x,\mu^2\right), \tag{1252}$$

$$g_2\left(x,\mu^2\right) \coloneqq \cos\phi\,\frac{f_{\eta'}^0}{\sigma}\phi_{\eta'}^g\left(x,\mu^2\right) - \sin\phi\,\frac{f_\eta^0}{\sigma}\phi_\eta^g\left(x,\mu^2\right). \tag{1253}$$

In the next step, relations similar to (cf. [9, 15, 20]):

$$\begin{aligned} \cos(\phi-\theta_8) &= \tfrac{1}{\sqrt{3}}\tfrac{f_q}{f_8}, \quad \cos(\phi-\theta_0) = \tfrac{1}{\sqrt{3}}\tfrac{f_s}{f_0}, \\ \sin(\phi-\theta_8) &= \sqrt{\tfrac{2}{3}}\tfrac{f_s}{f_8}, \quad \sin(\phi-\theta_0) = \sqrt{\tfrac{2}{3}}\tfrac{f_q}{f_0}, \end{aligned} \tag{1254}$$

are useful. Combined with the standard trigonometric identities each amplitude can be further simplified. In parallel, the general relations of Equation 307 can be used to extend these considerations to our approach. Consequently, the different limits imply $(M=\eta,\eta';\ A=8,0,g;\ R=q,s,g)$

$$|\eta_q\rangle \sim \begin{cases} f_q\left(\phi_q^{SO}|q\bar{q}\rangle + \phi_{opp}|s\bar{s}\rangle + \sqrt{\frac{2}{3}}\frac{1}{\sigma}\phi_g|gg\rangle\right), & \phi_M^A=\phi_A \\ f_q\left(\phi_q|q\bar{q}\rangle \qquad\qquad + \sqrt{\frac{2}{3}}\frac{1}{\sigma}\phi_g|gg\rangle\right), & \phi_M^R=\phi_R \end{cases} \tag{1255}$$

$$|\eta_s\rangle \sim \begin{cases} f_s\left(\phi_s^{SO}|s\bar{s}\rangle + \phi_{opp}|q\bar{q}\rangle + \sqrt{\frac{1}{3}}\frac{1}{\sigma}\phi_g|gg\rangle\right), & \phi_M^A=\phi_A \\ f_s\left(\phi_s|s\bar{s}\rangle \qquad\qquad + \sqrt{\frac{1}{3}}\frac{1}{\sigma}\phi_g|gg\rangle\right), & \phi_M^R=\phi_R \end{cases}, \tag{1256}$$

18 A similar ansatz is valid for "$A=g$", however, with an additional prefactor (see discussion below).
19 For convenience, we are omitting possible renormalization scale dependencies, e. g., for f_M^0.
20 The named amplitudes may be shortened even more, however, this would result in rather cryptic expressions. Therefore, we leave them as they are.

where[21] we use Equation 314, along with the abbreviation

$$\phi_q^{SO}\left(x,\mu^2\right) = \frac{1}{3}\left(\phi_8\left(x,\mu^2\right) + 2\,\phi_0\left(x,\mu^2\right)\right)\,, \tag{1257}$$

$$\phi_s^{SO}\left(x,\mu^2\right) = \frac{1}{3}\left(\phi_0\left(x,\mu^2\right) + 2\,\phi_8\left(x,\mu^2\right)\right)\,. \tag{1258}$$

Within this specific limit we, therefore, reproduce the corresponding results of [20]. Furthermore, by assuming $\phi_M^g \approx \phi_g$ and $\frac{f_s}{f_q} \approx \sqrt{2}$ we may also deduce (see Equation 1255 and Equation 1256):

$$\langle 0|\mathcal{G}_{n\xi}(z_2 n)\,\widetilde{\mathcal{G}}^{n\xi}(z_1 n)|\eta_q\rangle \approx \langle 0|\mathcal{G}_{n\xi}(z_2 n)\,\widetilde{\mathcal{G}}^{n\xi}(z_1 n)|\eta_s\rangle\,. \tag{1259}$$

In other words, the assumption of a particle independent gluon DA is (approximately) consistent with the state mixing ansatz (for further discussion, see [3]).

In Chapter 3 we discuss a less-constrained[22] approach which also takes into account the scale dependence of all occurring (leading-twist) DAs and decay constants. Hence, this ansatz is indispensable for a description of $\gamma^*\gamma^{(*)} \to \eta^{(\prime)}$ transition form factors at large momentum transfers. On the other hand, $B, D_{(s)} \to \eta^{(\prime)}$ decays can be easier described by the above method, inter alia, since there are no large factorization scales involved (see Section 5.1.2.2).

A.15 SHORT-DISTANCE CORRELATION FUNCTIONS

The present subsection serves as a supplement, discussing required kinematical conditions necessary for the short distance domination of two-point correlation functions (see, e. g., [97] and references therein).

For this purpose, we may consider the generic example of a hadronic observable which is represented by adequate local operators $\mathcal{J}_{1,2}$ taken at large virtualities[23] $Q^2 = -q^2 \gg \Lambda^2_{QCD}$:

$$\mathcal{P}(q) = i\int d^4x\, e^{iq\cdot x}\langle 0|\,T\{\mathcal{J}_1(x)\,\mathcal{J}_2(0)\}\,|0\rangle\,. \tag{1260}$$

Correspondingly, both interpolation currents $\mathcal{J}_{1,2}$ are chosen to have the correct quantum numbers and intended particle content (see, e. g., Section A.17), while the preferred momentum configuration $Q^2 \to \infty$ turns Equation 1260 into a genuine short distance object. Accordingly, the dominant contributions to Equation 1260 come from partons propagating at small spacial distances and time intervals, such as (R_{had} denoting the typical hadronic size)

$$|\vec{x}| \sim x_0 \sim \frac{1}{\sqrt{Q^2}} \ll R_{had}\,, \tag{1261}$$

which in turn justifies the use of a short distance OPE. Before devoting ourselves to a proof sketch of these assertions, we must distinguish between the following two basic cases:

i) $\mathcal{J}_1$ and $\mathcal{J}_2$ are currents that only involve light quark flavors ($\psi = u, d, s$).

ii) At least one of the two operators $\mathcal{J}_{1,2}$ is a heavy quark current ($Q = c, b, t$).

21 The results mentioned in Equation 1255 and Equation 1256 only list the first view Fock states.
22 Here, no restrictions, such as Equation 313, are needed, allowing wider application possibilities.
23 Here, "q^μ" is the incoming external momentum.

In the second case the mere existence of heavy flavored quarks $m_Q \gg \Lambda_{QCD}$ introduces a similarly large intrinsic energy scale. Therefore, already at small $|q^2| \ll 4m_Q^2$ one may expect asymptotically free quark-antiquark fluctuations. Consequently, the characteristic distances of Equation 1260 are an inverse of the involved heavy quark masses, i. e., $|\vec{x}| \sim x_0 \sim \frac{1}{2m_Q}$ (see also [97]). For light quarks, an approach based on the method of stationary phase can be used (cf. [598, 599]). In fact, when combining the concepts of Fourier analysis with Lorentz invariance:

$$f\left(x^2\right) = i\langle 0|\, T\{j_1(x)\, j_2(0)\}\,|0\rangle = \frac{1}{2\pi}\int_{-\infty}^{\infty} d\tau\, e^{i\tau x^2}\,\tilde{f}(\tau)\ , \tag{1262}$$

Equation 1260 gives rise to (see also [97])

$$\begin{aligned}\int d^4x\, e^{iq\cdot x}\, f\left(x^2\right) &= \int_{-\infty}^{\infty} d\tau \int d^4x\, e^{iq\cdot x} e^{i\tau x^2}\,\frac{\tilde{f}(\tau)}{2\pi} = \int_{-\infty}^{\infty} d\tau \int d^4x\, e^{i\tau\left(x+\frac{1}{2\tau}q\right)^2} e^{i\frac{Q^2}{4\tau}}\,\frac{\tilde{f}(\tau)}{2\pi} \\ &= \int_{-\infty}^{\infty} d\tau \int d^4x\, e^{i\tau x^2} e^{i\frac{Q^2}{4\tau}}\,\frac{\tilde{f}(\tau)}{2\pi}\,.\end{aligned} \tag{1263}$$

Based on [598, 599], Equation 1263 is thus dominated by contributions related to $\tau^2 \sim Q^2/x^2$, i. e., where its phase term $\phi(\tau) := \tau x^2 + \frac{1}{4}\tau^{-1}Q^2$ is (almost) stationary[24], while integrands with rapidly varying phases approximately cancel (see, e. g., Riemann-Lebesgue lemma [600, 601]). In other words, an oscillatory behavior of the involved exponential functions is suppressed if both $\tau \sim 1/x^2$ and $\tau \sim Q^2$ are fulfilled simultaneously, which is equivalent to $x^2 \sim 1/Q^2$. Thus, for $Q^2 \to \infty$ the involved quarks predominantly propagate near the light-cone, which is a necessary, but not yet a sufficient condition for the assumed short distance domination of Equation 1263. To proof the latter, one conveniently (cf. [97]) chooses a reference frame with $q_0 = 0$, i. e., $\vec{q}^2 = Q^2$, implying, that leading terms of the altered correlation function (cf. Equation 1260)

$$\int d^4x\, f\left(x^2\right)\, e^{iq\cdot x} \equiv \int d^4x\, f\left(x^2\right)\, e^{-i\vec{q}\cdot\vec{x}}\,, \tag{1264}$$

arise from regions, where its integrand does not exhibit fast oscillations:

$$|\vec{x}| \sim \frac{1}{\sqrt{Q^2}}\,. \tag{1265}$$

Together with the underlying light-cone dominance, it follows the assertion. In other words, for large values of Q^2 Equation 1260 is mainly determined by short distance QCD effects.

A.16 LIGHT-CONE DOMINATED CORRELATION FUNCTIONS

The following subsection supplements our discussion on hard exclusive processes, while focusing on their specific kinematical structure. For the sake of completeness, we, therefore, extend Section A.15 to (approximately) light-cone dominated phenomena and current correlators in position space with small space-like separations[25] $|x^2| \ll \Lambda_{QCD}^{-2}$.

As an example for the latter, we may consider a two-point correlation function[26]

$$F_{ab}(q_1, q_2) = i\int d^4x\, e^{-iq_1\cdot x}\langle M(P)|\, T\{j_a(x)\, j_b(0)\}\,|0\rangle\,, \tag{1266}$$

24 More precisely, the phase term actually becomes stationary $\left(\phi'(\tau) = 0\right)$ at $\tau^2 = \frac{Q^2}{4x^2}$.

25 At sufficiently small space-like separations, the matrix element in Equation 1266 can be calculated by applying the OPE. When analyzing the corresponding Fourier transform, we therefore have to ensure, that the given kinematical input implies all necessary conditions for such an evaluation.

26 Here, "a" and "b" may, e. g., represent a set of open Lorentz indices.

representing the annihilation of a given hadronic state M into two suitable currents $\mathcal{J}_a$ and $\mathcal{J}_b$. Accordingly, it is sufficient to study the analogous meson-photon transition $(M = \pi^0, \eta, \eta', \ldots)$ $\gamma^*(q_1)\,\gamma^*(q_2) \to M(P)$ which for large space-like momenta $\left(Q^2 := -q_1^2,\ q^2 := -q_2^2\right)$

$$Q^2,\ q^2 \gg \Lambda^2_{\text{QCD}},\ \mu^2 \tag{1267}$$

can be approached perturbatively (cf. Section 4.1.1). In accordance with [97] Equation 1267 already includes a generic mass scale $\mu \sim |\vec{P}| \sim |P_0|$ as introduced by the meson four-momentum. Furthermore, the potentially large scalar product $q_1 \cdot P$ can be expressed via [97, 517]:

$$\xi = \frac{2q_1 \cdot P}{Q^2} = \frac{q^2 - Q^2 + P^2}{Q^2}\,. \tag{1268}$$

It should be noted, that under appropriate conditions this hadronic variable may be used as a generic "small" parameter. For instance, the discussed (cf. Chapter 4) $\gamma^{(*)}\gamma^* \to M$ TFF at LO and leading-twist accuracy boils down to (using Fock-Schwinger gauge):

$$F_{\mu\nu}(q_1, q_2) = -\sum_\psi e_\psi^2 \varepsilon_{\mu\nu\alpha\beta} \int d^4x\, e^{-iq_1\cdot x} \frac{x^\alpha}{\pi^2 x^4} \langle M(P)|\bar\psi(x)\,\gamma^\beta\gamma_5\psi(0)\,|0\rangle\Big|_{\text{twist-2}}\,. \tag{1269}$$

After an expansion into local operators around the origin $x^\rho = 0$

$$\langle M(P)|\bar\psi(x)\,\gamma_\beta\gamma_5\psi(0)\,|0\rangle = \sum_{n=0}^{\infty} \frac{1}{n!} x^{\mu_1}\cdots x^{\mu_n} \langle M(P)|\bar\psi \overleftarrow{D}_{\mu_1}\cdots\overleftarrow{D}_{\mu_n}\gamma_\beta\gamma_5\psi|0\rangle \tag{1270}$$

one can extract traceless $(\text{at } P^2 = 0)$ and totally symmetric components of the arising matrix elements, e. g., via[27] (see also [97, 602, 603]):

$$\langle M(P)|\bar\psi \overleftarrow{D}_{\mu_1}\cdots\overleftarrow{D}_{\mu_n}\gamma_\beta\gamma_5\psi|0\rangle = i^n P_{\mu_1}\cdots P_{\mu_n} P_\beta M_n^{(\psi)} + \ldots\,, \tag{1271}$$

which by definition (cf. Chapter 3)

$$\langle M(P)|\bar\psi(x)\,\gamma^\beta\gamma_5\psi(0)\,|0\rangle = -if_M^{(\psi)} P^\beta \int_0^1 du\, e^{iuP\cdot x}\phi_M^{(\psi)}(u) \tag{1272}$$

also correspond to moments of twist-two DAs:

$$M_n^{(\psi)} = -if_M^{(\psi)} \int_0^1 du\, u^n \phi_M^{(\psi)}(u)\,. \tag{1273}$$

Based on this decomposition one straightforwardly gets a formal power series in ξ for the physical observable[28] (reproducing the findings of [97])

$$\begin{aligned} F_{\mu\nu}(q_1, q_2) = \varepsilon_{\mu\nu\alpha\beta} q_1^\alpha q_2^\beta \frac{2}{Q^2} \sum_\psi e_\psi^2 \Bigg[M_0^{(\psi)} - \xi M_1^{(\psi)} + \left(\cancel{\frac{P^2}{Q^2}} + \xi^2\right) M_2^{(\psi)} \\ - \left(2\cancel{\frac{P^2}{Q^2}}\xi + \xi^3\right) M_3^{(\psi)} + \ldots \Bigg] = \varepsilon_{\mu\nu\alpha\beta} q_1^\alpha q_2^\beta \frac{2}{Q^2} \sum_\psi e_\psi^2 \sum_{n=0}^{\infty} (-\xi)^n M_n^{(\psi)}. \end{aligned} \tag{1274}$$

27 For convenience, possible higher twist corrections, a scale dependence as well as traces are omitted.

28 This is also true for higher twist corrections. Besides, the first few terms of Equation 1274 explicitly contain possible $\mathcal{O}(P^2)$ corrections which would cancel with the traces.

Consequently, when assuming soft pion momenta $|P^\mu| \to 0$, i. e., $|\xi| \approx 0$ the correlation function resembles a short distance object (cf. Section A.15), which can be reasonably well described by a truncated OPE similar to Equation 1274. The preferred kinematical set-up $\xi \sim 1$, however, prohibits such an approach[29] (cf. Section 2.4). Instead a non-local ansatz seems to be favorable (see Section 4.1.1). According to [97] a light-cone dominance of Equation 1266 within the $x_0 - x_3$ plane[30] can be proven. For this purpose, one conveniently defines (see also [97, 257])

$$q_1^\mu := (q_0, 0, 0, q_3)^T \,, \tag{1275}$$

with the related components (while neglecting all other $\mathcal{O}(\mu)$ corrections to q_0 and q_3)

$$q_0 \approx \frac{Q^2\xi}{4\mu}, \quad q_3 \approx \sqrt{Q^2 + q_0^2} = \frac{Q^2\xi}{4\mu} \sum_{n=0}^{\infty} \frac{(-1)^n\,(2n)!}{(1-2n)\,(n!)^2\,4^n} \left[\frac{16\mu^2}{Q^2\xi^2}\right]^n \approx \frac{Q^2\xi}{4\mu} + \frac{2\mu}{\xi}. \tag{1276}$$

Analogous to the statements in Section A.15 one may argue that the integrand of Equation 1266 is suppressed if its related exponential function is rapidly oscillating. Consequently, dominant contributions to Equation 1266 are determined by the phase term

$$q_1 \cdot x = q_0 x_0 - q_3 x_3 \approx \frac{Q^2\xi}{4\mu}(x_0 - x_3) - \frac{2\mu}{\xi} x_3 + \mathcal{O}\left(\tfrac{1}{Q^2}\right) , \tag{1277}$$

and thus arise from regions with

$$x_0 - x_3 \sim \frac{4\mu}{Q^2\xi} \quad \wedge \quad x_3 \sim \frac{\xi}{2\mu} \,. \tag{1278}$$

In other words, within this domain the difference

$$x_0^2 - x_3^2 \sim \frac{4}{Q^2} + \frac{16\mu^2}{Q^4\xi^2} \tag{1279}$$

at $Q^2 \to \infty$ tends to zero, while all involved components remain finite and relatively large

$$x_0 \sim x_3 \sim \frac{\xi}{2\mu} \gg \frac{1}{\sqrt{Q^2}} \,. \tag{1280}$$

By further following this line of argument, one a priori puts no restrictions on the remaining directions in space[31]. But instead of attempting to refine the current proof (for further details see, e. g., [97, 257, 517]), let us assume finite deviations from the light-cone $|x^2| \ll \Lambda_{\text{QCD}}^{-2}$.

The latter can be absorbed into higher twist corrections (cf. [352]) which in general include related $\mathcal{O}(x^2)$ terms[32]. Thus, their Fourier transform exhibits extra inverse powers of the underlying (photon) virtualities as compared to the given leading contributions. For $Q^2, q^2 \gg \Lambda_{\text{QCD}}^2$ the correlation function (cf. Equation 1266) in coordinate space is, therefore, dominated by distances close to the light-cone.

In conclusion, the present kinematical set-up justifies an approach based on conformal symmetry and QCD factorization (see also [128, 604, 605]). Moreover, a similar discussion concerning the light-cone dominance for heavy-to-light correlation functions (see e. g.Equation 946), can be found in [517, 523]. Here, the arguments presented in [97] are extended to systems with heavy quarks.

29 A priori the series in Equation 1274, with $\xi \sim 1$ cannot be truncated at any finite order.
30 Instead of x_3, one could readily apply the same arguments to x_1 or x_2.
31 This proof incorporates a definition for q_1^μ (see Equation 1275) which essentially allows an arbitrary choice of x_1 and x_2. Hence, while at $Q^2 \to \infty$ the difference $x_0^2 - x_3^2$ tends to zero, $-x_1^2 - x_2^2$ may still be large.
32 It has been pointed out by [352] that the preferred (light-cone) OPE is still applicable for possible small space-like separations.

A.17 SVZ-SUM RULE FOR THE DECAY CONSTANT

The LCSR analysis of Chapter 5 depends on several external input parameters, such as f_B. In particular, this observable will be discussed below. Apart from direct measurements, decay constants of pseudoscalar mesons can also be derived via QCD sum rules for the corresponding two-point correlation functions (cf. Equation 930). Fortunately, the required results are well-known and can, e. g., be found in [488]. For the reader's convenience, however, we collect all needed formulas in the following subsection.

All spectral functions and quark masses are presented in the $\overline{\text{MS}}$ scheme, while being evaluated at the scale (see [488, 606]). Hence, at $\mathcal{O}(\alpha_S)$ accuracy, the SVZ sum rule analysis for f_B can be written as[33] (e. g., $\psi = u, d, s$) [488]

$$\begin{aligned}\frac{m_B^4 f_B^2}{(m_b+m_\psi)^2} = \frac{N_c}{8\pi^2}\int_{m_b^2}^{s_0^B} ds\, e^{\frac{m_B^2-s}{M^2}}\left\{\frac{(s-m_b^2)^2}{s}+\frac{C_f\alpha_S}{2\pi}\rho^{(1)}_{\text{pert}}(s)\right\}\\ + e^{\frac{m_B^2-m_b^2}{M^2}}\left\{\frac{1}{12}\langle\tfrac{\alpha_S}{\pi}\mathcal{G}^A_{\mu\nu}\mathcal{G}^{A,\mu\nu}\rangle - m_b\langle\bar\psi\psi\rangle\left[1+\frac{m_b^2 m_\psi^2}{2M^4}\right.\right.\\ \left.\left.-\left(1+\frac{m_b^2}{M^2}\right)\frac{m_\psi}{2m_b}-\frac{C_f\alpha_S}{2\pi}\rho^{(1)}_{\bar q q}\left(M^2\right)+\frac{m_0^2}{2M^2}\left(1-\frac{m_b^2}{2M^2}\right)\right]\right\},\end{aligned} \tag{1281}$$

which is based on $\left(x = m_b^2 s^{-1}\right)$

$$\begin{aligned}\rho^{(1)}_{\text{pert}}(s) \coloneqq s(1-x)\Big\{&(1-x)\left[4\,\text{Li}_2(x)+2\log(x)\log(1-x)-(5-2x)\log(1-x)\right]\\ &+(1-2x)(3-x)\log(x)+3(1-3x)\log\left(\frac{\mu^2}{m_b^2}\right)+\frac{1}{2}(17-33x)\Big\},\end{aligned} \tag{1282}$$

$$\rho^{(1)}_{\bar q q}\left(M^2\right) \coloneqq 3\left\{\Gamma\left(0,\frac{m_b^2}{M^2}\right)e^{\frac{m_b^2}{M^2}}-\left[1+\left(1-\frac{m_b^2}{M^2}\right)\left(\log\left(\frac{\mu^2}{m_b^2}\right)+\frac{4}{3}\right)\right]\right\}, \tag{1283}$$

and incorporates the incomplete gamma function [593] (using $n>0$)

$$\Gamma(n,z) \coloneqq \int_z^\infty dt\, t^{n-1}e^{-t}, \quad \Gamma(n,0)\equiv\Gamma(n)\ . \tag{1284}$$

While Wilson's OPE may give rise to a plethora of possible higher dimensional operators, only the associated first few condensates, such as $\langle g_S\bar\psi\sigma^{\mu\nu}\mathcal{G}^A_{\mu\nu}\psi\rangle$ (see Equation 105) turn out to be relevant (cf. [125, 488, 607–609]). Although numerically small, we have also included contributions that are related to four-quark condensates (cf. [257, 488]):

$$f_B^2\Big|_{\text{4-quark}} = -\frac{16\pi}{27m_B^4}e^{\frac{m_B^2-m_b^2}{M^2}}\frac{\alpha_S m_b^2\langle\bar\psi\psi\rangle^2}{M^2}\left(1-\frac{m_b^2}{4M^2}-\frac{m_b^4}{12M^4}\right)+\mathcal{O}(m_\psi)\ . \tag{1285}$$

Besides, values for the Borel parameter $M^2 \coloneqq \overline{M}_B^2$ and continuum threshold $s_0^B \coloneqq \bar s_0^B$ are specified in Section 5.1.1. For further details we refer to the discussion in [488] and Chapter 5. To conclude, the presented QCD sum rule exhibits large higher-order corrections, hence excluding an analysis solely relying on the quark pole masses. In fact (see also [488]), the underlying perturbative expansion displays good convergence, indicating a reliable determination of f_B. Thus, the

33 By adequately choosing the input parameters, Equation 1281 can also be used to calculate f_{B_s}, f_D as well as f_{D_s}.

predictive power of this approach is mainly limited by the present error in the heavy ($Q = c, b$) quark mass $m_Q(m_Q)$. The latter relies on[34] [488, 610–613]

$$m(\mu) = m_{\text{pole}}\left[1 + \frac{C_f \alpha_S(\mu)}{2\pi}\left(2 + 3\log\left(\frac{\mu}{m(\mu)}\right)\right) + \mathcal{O}\left(\alpha_S^2\right)\right], \tag{1286}$$

which at this order of accuracy cancels the corresponding logarithmic terms within Equation 1281 (see discussion in [488]). Based on these formulas and considerations, we can refine our analysis in Chapter 5 accordingly.

34 In Equation 1286 m_{pole} denotes the pole mass of a generic quark flavor, while $m(\mu)$ represents its mass in the $\overline{MS}$ scheme.

B

APPENDIX – CALCULATION SUPPLEMENTS

The subsequent appendix section includes supplementary material belonging to the PV reduction algorithm (see Section 4.1.4.2). Accordingly, it provides a basis for the performed NLO calculations of this work. Additionally, we show all required Fourier integrals, including an example calculation.

B.1 SCALAR ONE-LOOP INTEGRALS

Instead of always starting from first principles for each arising tensor integral (cf. Equation 791), the discussed PV algorithm (cf. Section 4.1.4) relies on a standardized and in its limits universal approach. The latter requires an analytical input, as given by four distinct classes of scalar functions. Based on the original work of Passarino [395], Veltman [395, 397–399], 'tHooft [399] and Melrose [400] (cf. also [388]) it is, therefore, sufficient to consider adequate scalar master integrals when applying this reduction algorithm (e. g., Section 4.1.4.1). Correspondingly, the following discussion may be restricted to related one-, two-, three- and four-point functions, which in fact reflect all possible one-loop diagram topologies. In particular, a constructive treatment of the PV functions "D_0", along with our preferred solution method will be addressed below.

According to the standard Feynman parametrization (e. g., [282]) each generic PV function (cf. Equation 791, Equation 792) can be written as

$$T_0^N(p_1,\dots,p_{N-1};m_0,\dots,m_{N-1}) = \Gamma(N)\int d^D k \left[\prod_{j=1}^{N}\int_0^1 d\alpha_j\right] \frac{\delta\left(\sum_{k=1}^{N}\alpha_k - 1\right)}{\left[\sum_{t=1}^{N}\alpha_t D_{t-1}\right]^N}, \tag{1287}$$

which naturally gives rise to $\left(\text{choose a } 1\leqq j\leqq N, \text{ along with } \alpha_j = 1-\sum_{n\neq j}\alpha_n\right)$

$$I_N(A_N) = \int d^D k \frac{1}{\left[k^2 - A_N + i0^+\right]^N}, \tag{1288}$$

$$A_N = \left(\sum_{n=1}^{N}\alpha_n p_{n-1}\right)^2 + \sum_{k=1}^{N}\alpha_k\left(m_{k-1}^2 - p_{k-1}^2\right), \tag{1289}$$

after performing an adequate shift, such as "$k^\mu \to k^\mu - \sum_{n=1}^{N}\alpha_n p_{n-1}^\mu$". This auxiliary integral may then be solved via standard techniques (e. g., [64, 418, 419]), which are

i) performing a Wick rotation in the k_0-plane and introduce generalized spherical coordinates within this underlying euclidean space.

ii) Separately solving the spherical and radial integration.

As a result (e. g., [418, 419]) Equation 1288 engenders $\left(D \neq 4\right)$

$$I_N(A_N) = i\,(-1)^N \pi^{D/2}\frac{\Gamma\left(N-\frac{D}{2}\right)}{\Gamma(N)}\left[A_N - i0^+\right]^{D/2-N}, \tag{1290}$$

whose UV divergences appear as poles in "$(D-4)$". Hence, after an expansion in powers of "$(D-4)$" only the parameter integrals would remain to be determined. This, however, may become a rather nontrivial problem and has, therefore, been the recurring subject of intense research (cf. [388, 392, 393, 395, 397–400, 424]) for several decades. Consequently, we can only mention the basic techniques (e. g., [419]) needed for this work.

When starting with the simplest possible topology, i. e., $N=1$ $\left(A_1 \equiv m_0^2\right)$:

$$A_0\left(m_0^2\right) = \frac{(2\pi\mu)^{4-D}}{i\pi^2} I_1\left(m_0^2\right) = m_0^2\left[\Delta_{4-D} - \log\left(\frac{m_0^2}{\mu^2}\right) + 1\right] + \mathcal{O}(D-4)\,, \tag{1291}$$

$$\Delta_{4-D} \coloneqq \frac{2}{4-D} - \gamma_E + \log 4\pi\,, \tag{1292}$$

one faces a (mass-dependent) UV divergence, as given by Equation 819. Similarly, two-point PV functions, such as $\left(A_2 = x^2p^2 + x\left(m_1^2 - m_0^2 - p^2\right) + m_0^2\right)$

$$\begin{aligned} B_0\left(p^2; m_0^2, m_1^2\right) &= \frac{(2\pi\mu)^{4-D}}{i\pi^2}\int_0^1 dx\, I_2(A_2) \\ &= \Delta_{4-D} - \int_0^1 dx\, \log\left(\frac{A_2 - i0^+}{\mu^2}\right) + \mathcal{O}(D-4)\,, \end{aligned} \tag{1293}$$

can be straightforwardly calculated, revealing (e. g., [388, 417])

$$\begin{aligned} B_0\left(p^2; m_0^2, m_1^2\right) &= \Delta_{4-D} + 2 - \log\left(\frac{m_0 m_1}{\mu^2}\right) + \frac{m_0^2 - m_1^2}{p^2}\log\left(\frac{m_1}{m_0}\right) \\ &\quad - \frac{m_0 m_1}{p^2}\left(\frac{1}{r} - r\right)\log r + \mathcal{O}(D-4)\,, \end{aligned} \tag{1294}$$

where "r" and "$1/r$" are determined by[1]

$$x^2 + \frac{m_0^2 + m_1^2 - p^2 - i0^+}{m_0 m_1}x + 1 = (x+r)\left(x + \frac{1}{r}\right)\,. \tag{1295}$$

Analogous to Equation 819 B_0 possesses a universal UV singularity, as recorded in Equation 820. In fact one- and two-point PV functions are not only both UV divergent, but are additionally interconnected via (e. g., [418]) relations, such as

$$\left(m_0^2 - m_1^2\right) B_0\left(0; m_0^2, m_1^2\right) = A_0\left(m_0^2\right) - A_0\left(m_1^2\right)\,, \tag{1296}$$

$$\left(1 + B_0\left(0; m^2, m^2\right)\right) = A_0\left(m^2\right)\,. \tag{1297}$$

Thus, any use of A_0 can be completely circumvented if desired (see, e. g., Equation 818). In turn, the scalar three-point functions, as denoted by "C_0", are UV convergent (e. g., [388, 418, 419]), i. e.,

$$(D-4)\, C_0\left(p_1^2, p_{21}^2, p_2^2; m_0^2, m_1^2, m_2^2\right) = \mathcal{O}(D-4)\,. \tag{1298}$$

For this reason, they can be safely calculated in the limit $D \to 4$ (see Equation 1300):

$$\begin{aligned} C_0\left(p_1^2, p_{21}^2, p_2^2; m_0^2, m_1^2, m_2^2\right) &= \frac{(2\pi\mu)^{4-D}}{i\pi^2} 2\int_0^1 dx \int_0^{\bar{x}} dy\, I_3(A_3) \\ &= -\int_0^1 dx \int_0^{\bar{x}} dy\, \frac{1}{A_3 - i0^+} + \mathcal{O}(D-4) \end{aligned} \tag{1299}$$

1 This representation ensures that "r" never crosses the negative real axis, i. e., the natural logarithm's branch cut (see [388] for further a discussion).

entailing a rather intricate integration procedure. The latter can be summarized as follows (cf. [399, 419]):

i) As a first step, all y^2-terms of

$$A_3 = x^2 p_1^2 + y^2 p_2^2 + xy\left(p_1^2 + p_2^2 - p_{21}^2\right) + x\left(m_1^2 - m_0^2 - p_1^2\right) + y\left(m_2^2 - m_0^2 - p_2^2\right) + m_0^2 \tag{1300}$$

have to be removed, e. g., via an Euler shift (cf. [392, 399, 419])

$$x \to x + \alpha y\,, \tag{1301}$$

where "α" may be extracted from[2]

$$\alpha^2 p_1^2 + \alpha\left(p_1^2 + p_2^2 - p_{21}^2\right) + p_2^2 = 0\,. \tag{1302}$$

ii) With the application of Equation 1301 all y-integrals become feasible, resulting in structures, similar to $(a, b, c, d \in \mathbb{C})$

$$\int dx \frac{\log(ax+b)}{cx+d}\,. \tag{1303}$$

iii) Further simplifications imply a decomposition of this intermediate result into logarithms and Spence's functions which are defined by[3] (e. g., [388])

$$\mathrm{Li}_2(x) = -\int_0^1 \frac{dt}{t}\log(1-xt)\,, \quad |\arg(1-x)| < \pi\,. \tag{1304}$$

In consequence, the structure of every three-point PV function can be deduced by applying this scheme. Yet, instead of listing all calculated cases[4] for the needed master integrals, we quote a general formula, applicable to real momenta and physical masses (cf. [388]):

$$\begin{aligned} C_0\left(p_1^2, p_{21}^2, p_2^2; m_0^2, m_1^2, m_2^2\right) = \frac{1}{\kappa(p_1^2, p_{21}^2, p_2^2)} \sum_{i=0}^{2} \Bigg\{ \sum_{n=1}^{2} \Bigg[& \mathrm{Li}_2\left(-\frac{\bar{y}_{i0}}{y_{in}}\right) - \mathrm{Li}_2\left(\frac{y_{i0}}{y_{in}}\right) \\ & + \eta\left(\bar{x}_{in}, y_{in}^{-1}\right)\log\left(-\frac{\bar{y}_{i0}}{y_{in}}\right) - \eta\left(-x_{in}, y_{in}^{-1}\right)\log\left(\frac{y_{i0}}{y_{in}}\right)\Bigg] \\ & + \left[\eta(y_{i2}, y_{i1}) + 2\pi i\,\theta\left(-p_{jk}^2\right)\theta(-\mathrm{Im}(y_{i2}y_{i1}))\right. \\ & \left. -\eta(-x_{i2}, -x_{i1})\right]\log\left(-\frac{\bar{y}_{i0}}{y_{i0}}\right)\Bigg\} \end{aligned} \tag{1305}$$

2 Equation 1302 is true for the generic example of Equation 1299 and Equation 1300.

3 This representation of the dilogarithm enables an elegant reformulation of remaining parameter integrals, as given by Equation 1287 and Equation 1303.

4 In fact, a direct calculation of C_0 is always advisable when dealing with general arguments. This ensures a correct representation of the PV function's complex structure.

including $\left((i,j,k) \in \{(0,1,2),(1,2,0),(2,0,1)\};\, n=1,2\right)$

$$y_{i0} \coloneqq \frac{1}{2\kappa\left(p_1^2,p_{21}^2,p_2^2\right)p_{jk}^2}\Big[p_{jk}^2\left(p_{jk}^2-p_{ki}^2-p_{ij}^2+2m_i^2-m_j^2-m_k^2\right) - \left(p_{ki}^2-p_{ij}^2\right)\left(m_j^2-m_k^2\right)+\kappa\left(p_1^2,p_{21}^2,p_2^2\right)\left(p_{jk}^2-m_j^2+m_k^2\right)\Big]\,, \tag{1306}$$

$$x_{in} \coloneqq \frac{1}{2p_{jk}^2}\left[p_{jk}^2-m_j^2+m_k^2+(-1)^n\,\alpha_i\right]\,, \tag{1307}$$

$$\alpha_i \coloneqq \kappa\left(p_{jk}^2,m_j^2,m_k^2\right)\left[1+ip_{jk}^2 0^+\right]\,, \tag{1308}$$

$$y_{in} \coloneqq y_{i0}-x_{in}\,. \tag{1309}$$

Here, one also uses the Källén function

$$\kappa(x,y,z) \coloneqq \sqrt{\lambda(x,y,z)}\,,\quad \lambda(x,y,z)=(x-y-z)^2-4yz\,, \tag{1310}$$

as well as (see [388, 392, 399])

$$\eta(a,b)=\log(ab)-\log(a)-\log(b)\,, \tag{1311}$$

with, e. g., $\left(a,b,c\in\mathbb{C}\setminus(-\infty,0)\right.$ on the first Riemann sheet [614]$)$

$$\eta(a,b)=2\pi i\left[\theta(-\mathrm{Im}(a))\,\theta(-\mathrm{Im}(b))\,\theta(\mathrm{Im}(ab))-\theta(\mathrm{Im}(a))\,\theta(\mathrm{Im}(b))\,\theta(-\mathrm{Im}(ab))\right]. \tag{1312}$$

In a similar manner the scalar four-point integrals (e. g., [388, 392, 399])

$$\begin{aligned}&D_0\left(p_1^2,p_{21}^2,p_{32}^2,p_3^2,p_2^2,p_{31}^2;m_0^2,m_1^2,m_2^2,m_3^2\right)\\&=\Gamma\left(4-\tfrac{D}{2}\right)\left(4\pi\mu^2\right)^{2-D/2}\int_0^1 d\alpha_1\int_0^{\bar\alpha_1} d\alpha_2\int_0^{\bar\alpha_1-\alpha_2} d\alpha_3\,\frac{1}{\left[P(\bar\alpha_1-\alpha_2-\alpha_3,\alpha_1,\alpha_2,\alpha_3)\right]^{4-D/2}},\end{aligned} \tag{1313}$$

as defined by (cf. Equation 808)

$$P(x_0,x_1,x_2,x_3)=\sum_{i=0}^{3}m_i^2x_i^2+\sum_{\substack{i,j=0\\i<j}}^{3}Y_{ij}x_ix_j\,, \tag{1314}$$

can be reduced to logarithms and dilogarithms. The required procedure has been recently reviewed in [392] and will not be shown here. Alternatively, when restricting our discussion to a collinear set-up (cf. discussion of Section 4.1.4.2), while neglecting $\mathcal{O}\left(m_M^2\right)$ $(M=\eta,\eta')$ corrections, all required "four-point" PV functions can be further reduced via[5] Equation 835. This approach, though beyond the standard PV reduction algorithm, ensures a straight forward calculation of all needed D_0's, which is preferable over an otherwise rather tedious solution procedure.

In essence, the latter concludes this short collection of relevant techniques and formulas concerning one-loop scalar integrals, as needed for this work.

5 As mentioned in Section 4.1.4.2, the right hand side of Equation 835 could be further reduced, ultimately leading to (derivatives of) scalar two-point functions.

B.2 PASSARINO-VELTMAN DECOMPOSITION – CALCULATION EXAMPLE

This short supplement mainly serves as a retrofit for Section 4.1.4.1, as well as Section 4.1.4.2, where we focus on the PV reduction algorithm's formal structure and several specific applications. Accordingly, a generic example is given below which explicitly depicts the essential techniques, as used within Section 4.1.4.2.

Let us exemplify the method for[6] C_μ, together with $C_{\mu\nu}$ which are primarily required in Equation 826. Similar to the general case, those two tensor integrals can be iteratively calculated, i. e., when starting at two-point level[7] all interconnected one-loop integrals can be derived step-by-step, in ascending order. Hence, Equation 794 implies

$$B^\mu(p_1; m_0, m_1) = p_1^\mu B_1\left(p_1^2; m_0^2, m_1^2\right) , \tag{1315}$$

which can be solved via Equation 800, i. e., (see also Equation 798)

$$B_1 = \frac{p_1^\mu}{p_1^2} B_\mu(p_1; m_0, m_1) = \frac{1}{2p_1^2}\left[A_0\left(m_0^2\right) - A_0\left(m_1^2\right) - f_1 B_0\left(p_1^2; m_0^2, m_1^2\right)\right] . \tag{1316}$$

Analogously, we may write $\left((p_1\cdot p_2) = \frac{1}{2}\left(p_1^2 + p_2^2 - p_{21}^2\right)\right)$

$$C^\mu(p_1, p_2; m_0, m_1, m_2) = \sum_{k=1}^{2} p_k^\mu C_k\left(p_1^2, p_{21}^2, p_2^2; m_0^2, m_1^2, m_2^2\right) , \tag{1317}$$

giving rise to $\left(\text{cf. Equation 1310, with } \lambda\left(p_1^2, p_2^2, p_{21}^2\right) = 4\left((p_1\cdot p_2)^2 - p_1^2 p_2^2\right)\right)$

$$\begin{pmatrix} C_1 \\ C_2 \end{pmatrix} = -\frac{4}{\lambda\left(p_1^2, p_2^2, p_{21}^2\right)} \begin{pmatrix} p_2^2 & -(p_1\cdot p_2) \\ -(p_1\cdot p_2) & p_1^2 \end{pmatrix} \begin{pmatrix} R_0^{3,1} \\ R_0^{3,2} \end{pmatrix} . \tag{1318}$$

The latter requires $\left(\text{cf. Equation 800, i. e., } R_0^{3,k} = p_k^\mu C_\mu \text{ for } (k,j) \in \{(1,2),(2,1)\}\right)$

$$R_0^{3,k} = \frac{1}{2}\left[B_0\left(p_j^2; m_0^2, m_j^2\right) - B_0\left(p_{21}^2; m_1^2, m_2^2\right) - f_k C_0\left(p_1^2, p_{21}^2, p_2^2; m_0^2, m_1^2, m_2^2\right)\right] . \tag{1319}$$

Notably, the coefficient functions of (while omitting all related arguments)

$$C^{\mu\nu} = g^{\mu\nu} C_{00} + \left(p_1^\mu p_2^\nu + p_1^\nu p_2^\mu\right) C_{12} + p_1^\mu p_1^\nu C_{11} + p_2^\mu p_2^\nu C_{22} , \tag{1320}$$

can only be determined by a subsequent Lorentz decomposition (cf. Equation 803)

$$\begin{pmatrix} R_\mu^{3,1} \\ R_\mu^{3,2} \end{pmatrix} = \begin{pmatrix} R_{11} & R_{12} \\ R_{21} & R_{22} \end{pmatrix} \begin{pmatrix} p_{1\mu} \\ p_{2\mu} \end{pmatrix} , \tag{1321}$$

that entails (see Equation 806)

$$\begin{pmatrix} C_{11} & C_{12} \\ C_{21} & C_{22} \end{pmatrix} = \frac{4}{\lambda\left(p_1^2, p_2^2, p_{21}^2\right)} \begin{pmatrix} -p_2^2 & (p_1\cdot p_2) \\ (p_1\cdot p_2) & -p_1^2 \end{pmatrix} \begin{pmatrix} R_{11} - C_{00} & R_{12} \\ R_{21} & R_{22} - C_{00} \end{pmatrix} . \tag{1322}$$

6 For brevity, we focus on formulas, with finite p_j^2 $(j = 1, 2)$. Other cases can be derived analogously.

7 As the denominator of A_μ (cf. Equation 791) is symmetric under a reflection "$k_\mu \to -k_\mu$", this integral has to vanish. Therefore, there cannot be a one-point one-loop tensor integral.

When eliminating all spurious dependencies[8] within $\left(R_{00} \equiv R_0^{3,00} = g^{\mu\nu} C_{\mu\nu}\right)$

$$C_{00} = \frac{1}{D}\left(R_{00} - 2\,(p_1 \cdot p_2)\,C_{12} - p_1^2 C_{11} - p_2^2 C_{22}\right)\,, \tag{1323}$$

Equation 1322 engenders (cf. Equation 805)

$$C_{00} = \frac{1}{D-2}\left[R_{00} - R_{11} - R_{22}\right]\,, \tag{1324}$$

leaving us with the determination of R_{00}, R_{11}, R_{12} and R_{22}. In fact, the former can be easily derived

$$R_{00} = B_0\left(p_{21}^2; m_1^2, m_2^2\right) + m_0^2 C_0\left(p_1^2, p_{21}^2, p_2^2; m_0^2, m_1^2, m_2^2\right)\,, \tag{1325}$$

while all other coefficients emerge from (again $(k,j) \in \{(1,2),(2,1)\}$)

$$\begin{aligned} R_\mu^{3,k} = \frac{1}{2}\Big[& B_\mu\left(p_j^2; m_0^2, m_j^2\right) - B_\mu\left(p_{21}^2; m_1^2, m_2^2\right) + p_{1\mu} B_0\left(p_{21}^2; m_1^2, m_2^2\right) \\ & - f_k C_\mu(p_1, p_2; m_0, m_1, m_2)\Big]\,, \end{aligned} \tag{1326}$$

after equating coefficients of p_1^μ, along with p_2^μ. This leads to

$$\begin{aligned} R_{11} = {} & f_1 \tfrac{(p_1\cdot p_2) f_2 - p_2^2 f_1}{\lambda(p_1^2,p_2^2,p_{21}^2)} C_0\left(p_1^2, p_{21}^2, p_2^2; m_0^2, m_1^2, m_2^2\right) + \tfrac{m_1^2 - m_2^2}{4p_{21}^2} B_0\left(0; m_1^2, m_2^2\right) \\ & + \frac{1}{4}\left(2 + \tfrac{m_2^2 - m_1^2}{p_{21}^2} + \tfrac{m_0^2 - m_1^2}{p_1^2} + 4 f_1 \tfrac{(p_1\cdot p_2)(p_1^2 - (p_1\cdot p_2))}{p_1^2 \lambda(p_1^2,p_2^2,p_{21}^2)}\right) B_0\left(p_{21}^2; m_1^2, m_2^2\right) \\ & + f_1 \tfrac{p_2^2}{\lambda(p_1^2,p_2^2,p_{21}^2)} B_0\left(p_2^2; m_0^2, m_2^2\right) - f_1 \tfrac{(p_1\cdot p_2)}{\lambda(p_1^2,p_2^2,p_{21}^2)} B_0\left(p_1^2; m_0^2, m_1^2\right)\,, \end{aligned} \tag{1327}$$

$$\begin{aligned} R_{12} = {} & f_1 \tfrac{(p_1\cdot p_2) f_1 - p_1^2 f_2}{\lambda(p_1^2,p_2^2,p_{21}^2)} C_0\left(p_1^2, p_{21}^2, p_2^2; m_0^2, m_1^2, m_2^2\right) + \tfrac{m_0^2 - m_2^2}{4p_2^2} B_0\left(0; m_0^2, m_2^2\right) \\ & + \frac{1}{4}\left(1 + \tfrac{m_1^2 - m_2^2}{p_{21}^2} - 4 f_1 \tfrac{p_1^2 - (p_1\cdot p_2)}{\lambda(p_1^2,p_2^2,p_{21}^2)}\right) B_0\left(p_{21}^2; m_1^2, m_2^2\right) \\ & + \frac{1}{4}\left(\tfrac{m_2^2 - m_0^2}{p_2^2} - 4 f_1 \tfrac{(p_1\cdot p_2)}{\lambda(p_1^2,p_2^2,p_{21}^2)} - 1\right) B_0\left(p_2^2; m_0^2, m_2^2\right) \\ & + f_1 \tfrac{p_1^2}{\lambda(p_1^2,p_2^2,p_{21}^2)} B_0\left(p_1^2; m_0^2, m_1^2\right) + \tfrac{m_2^2 - m_1^2}{4p_{21}^2} B_0\left(0; m_1^2, m_2^2\right)\,, \end{aligned} \tag{1328}$$

$$\begin{aligned} R_{22} = {} & f_2 \tfrac{(p_1\cdot p_2) f_1 - p_1^2 f_2}{\lambda(p_1^2,p_2^2,p_{21}^2)} C_0\left(p_1^2, p_{21}^2, p_2^2; m_0^2, m_1^2, m_2^2\right) + \tfrac{m_2^2 - m_1^2}{4p_{21}^2} B_0\left(0; m_1^2, m_2^2\right) \\ & + \frac{1}{4}\left(2 + \tfrac{m_1^2 - m_2^2}{p_{21}^2} - 4\tfrac{(p_1\cdot p_2)((p_1\cdot p_2) - f_2) + p_1^2(m_0^2 - m_2^2)}{\lambda(p_1^2,p_2^2,p_{21}^2)}\right) B_0\left(p_{21}^2; m_1^2, m_2^2\right) \\ & + f_2 \tfrac{p_1^2}{\lambda(p_1^2,p_2^2,p_{21}^2)} B_0\left(p_1^2; m_0^2, m_1^2\right) - f_2 \tfrac{(p_1\cdot p_2)}{\lambda(p_1^2,p_2^2,p_{21}^2)} B_0\left(p_2^2; m_0^2, m_2^2\right)\,. \end{aligned} \tag{1329}$$

When restricted to a collinear set-up, as discussed in Section 4.1.4.2, we can essentially avoid an explicit derivation of D_μ, along with $D_{\mu\nu}$ via relations, such as Equation 831. Hence, the corresponding formulas are not mentioned at this point.

In conclusion, the mentioned techniques and formulas (including their variations) are sufficient to decompose the bulk part of all encountered tensor integrals within this work.

8 For this purpose, all symmetries of the non-diagonal coefficient functions C_{ij} have been used.

B.3 THE BOREL TRANSFORMATION

This supplement collects several concepts and formulas concerning the Borel transformation, as required to formulate Section 4.2 and Chapter 5. Usually, this transformation is part of the Borel summation method[9] [219, 615, 616, 619–624] which provides a technique to treat divergent series.

For instance (following [625]), suppose the (formal) power series $\left(g, f_k \in \mathbb{C}\right)$

$$f(g) = \sum_{k=0}^{\infty} f_k g^k \,, \tag{1330}$$

which may have a zero radius of convergence, e. g., due to[10] its coefficients ($k \gg 1$, $\alpha \in \mathbb{C}$)

$$f_k \propto (-\alpha)^k \, k! \,. \tag{1331}$$

In order to counter this kind of divergences and eventually obtain a convergent series, the Borel transformation [74, 626] can be applied which is denoted by [630] "$\mathcal{B}[f](\sigma)$" ($\sigma \in \mathbb{C}$). The latter (if it exists) may be interpreted as an inverse Laplace transformation [617], i. e.,

$$f(g) = \int_0^{\infty} \mathrm{d}t \, e^{-t} \mathcal{B}[f](gt) \,, \tag{1332}$$

and is for integer power series[11] defined via[12] [617, 630]:

$$\begin{aligned} &\mathcal{B} : \mathbb{C}[[g]] \longrightarrow \mathbb{C}[[t]] \,, \\ &\Gamma(s+1) \, g^s \longmapsto t^s \quad (s \in \mathbb{N}) \,. \end{aligned} \tag{1333}$$

Consequently, the Borel transform of Equation 1330 is given by its equivalent exponential series

$$\mathcal{B}[f](t) = \sum_{k=0}^{\infty} \frac{f_k}{k!} t^k \,, \tag{1334}$$

which includes the auxiliary (Borel) parameter "t". Alternatively, an analytical approach can be chosen, i. e., using the integral[13] [625]

$$\mathcal{B}[f](t) = \frac{1}{2\pi \mathrm{i}} \oint_{\gamma} \mathrm{d}z \, \frac{e^z}{z} f\left(\tfrac{t}{z}\right) \,, \tag{1335}$$

whose contour "γ" encircles the origin. Significantly, the actual calculation of Equation 1335 can be performed by adopting Cauchy's residue theory (cf. [632]). In fact, when considering a meromorphic function $h(z)$, which possesses a pole of order $n \geqslant 2$ $\left(n \in \mathbb{N}\right)$ at $z_0 \in \mathbb{C}$, the corresponding residue around $z = z_0$ can be found with [632]:

$$\mathrm{Res}_{z_0} h = \frac{1}{(n-1)!} \left. \frac{\mathrm{d}^{n-1}}{\mathrm{d}\, x^{n-1}} \right|_{z_0} (x - z_0)^n \, h(x) \,. \tag{1336}$$

9 The complete method, as discussed in [615–618] is not subject of this supplement.

10 Typically, this behavior can be seen in the context of perturbative calculations [77, 102, 103, 108, 116, 626–629]. For example, in ϕ^4-theory [625] the occurring perturbation series is often factorially divergent.

11 Here, we follow the standard notation of [618, 631]. Accordingly, let $\mathbb{C}[[z]]$ be the space of all formal series in z, i. e., similar to "$\sum_{k=0}^{\infty} c_k z^k$" with complex coefficients $c_k \in \mathbb{C}$ (see also [617]).

12 Equation 1333 arises when adapting the definitions of [617] to our notation.

13 There are several physical problems, such as the polarization operator of Equation 85, which cannot be entirely represented as an infinite series in $1/Q^2$ (see, e. g., [109]). Therefore, the definition of Equation 1335 is required which is additionally compatible with related dispersion relations (see below).

To that effect, after inserting Equation 1330 into Equation 1335, the Equation 1334 can be reproduced.

Yet, the accepted standard definition, as used for QCD sum rules (cf. [97, 109, 464, 465]) has been adapted to suit the specific requirements of this approach. That entails a slightly different appearance. As a matter of convenience, we focus on sum rules for two-point functions[14], which at the end only exhibit a single Borel parameter, along with an effective threshold "s_0". Indeed, the Borel transform of a test function (such as Equation 85 or Equation 930) is given by [97, 109, 588] (including the fixed Borel parameter "M^2")

$$\hat{\mathcal{B}}_{M^2}\left\{\Psi\left(Q^2\right)\right\} \coloneqq \lim_{\substack{n,Q^2\to\infty \\ M^2=Q^2/n}} \frac{1}{(n-1)!}\left[Q^2\right]^n \left(-\frac{d}{d\,Q^2}\right)^n \Psi\left(Q^2\right) \equiv \hat{\Psi}\left(M^2\right) , \tag{1337}$$

which implies two essential results (see also [97, 109, 440], $k \in \mathbb{N}$)

$$\hat{\mathcal{B}}_{M^2}\left\{\frac{1}{s+Q^2}\right\} = \lim_{\substack{n,Q^2\to\infty \\ M^2=Q^2/n}} \frac{1}{\frac{Q^2}{n}} \frac{1}{\left(1+\frac{s}{n}\frac{1}{Q^2/n}\right)^{n+1}} = \frac{1}{M^2} e^{-\frac{s}{M^2}} , \tag{1338}$$

$$\hat{\mathcal{B}}_{M^2}\left\{\left[Q^2\right]^k\right\} = 0 . \tag{1339}$$

An alternative calculation method [440, 633], which is based on the Schwinger parametrization and a tailor-made integral identity (see below, as shown in blue) turns out to be useful for a wide range of problems[15] (see also [440]), e. g.,

$$\begin{aligned}\hat{\mathcal{B}}_{M^2}\left\{\frac{1}{\left(s+Q^2\right)^k}\right\} &= \frac{1}{(k-1)!}\int_0^\infty d\alpha\, \alpha^{k-1} e^{-\alpha s}\, \hat{\mathcal{B}}_{M^2}\left\{e^{-\alpha Q^2}\right\} \\ &= \frac{1}{(k-1)!}\int_0^\infty d\alpha\, \alpha^{k-1} e^{-\alpha s}\, \delta\left(1-\alpha M^2\right) \\ &= \frac{1}{(k-1)!}\left[\frac{1}{M^2}\right]^k e^{-\frac{s}{M^2}} .\end{aligned} \tag{1340}$$

Accordingly, when applied to a dispersion relation, such as[16] [97] (taken from Equation 85, with $Q^2 = -q^2$)

$$\overline{\Pi}\left(q^2\right) = \int_0^\infty ds\, \frac{\frac{1}{\pi}\,\mathrm{Im}_s\Pi(s)}{s+Q^2} - \Pi(0) = \Pi\left(q^2\right) - \Pi(0) , \tag{1341}$$

Equation 1339 implicates the removal of all involved (polynomial) subtraction terms. Moreover, contributions of higher resonances and continuum states become exponentially suppressed[17] (see Equation 1338), i. e.,

$$\hat{\mathcal{B}}_{M^2}\left\{\overline{\Pi}\left(q^2\right)\right\} = \frac{1}{M^2}\int_0^\infty ds\, e^{-\frac{s}{M^2}}\, \frac{1}{\pi}\,\mathrm{Im}_s\Pi(s) = \hat{\mathcal{B}}_{M^2}\left\{\Pi\left(q^2\right)\right\} , \tag{1342}$$

which effectively reduces their impact on the resulting sum rule (see also [97, 464, 465]). Conversely, for correlation functions that include charm or bottom quark-antiquark (interpolation)

14 Hence, we may again use Equation 85 as a generic example.

15 For "$s \to 0$" Equation 1340 implies the mapping "$[1/Q^2]^k \mapsto \frac{1}{(k-1)!}\,[1/M^2]^k$". This is the analogue of Equation 1333 for $f(1/Q^2)$ (cf. Equation 1330) and its Borel transform $\mathcal{B}[f](1/M^2)$ (cf. Equation 1334).

16 As discussed in [97], the constant subtraction term within Equation 1341 is vanishing. Yet, we formally retain it.

17 Consequently, this reduces the sum rule's sensitivity to the duality approximation (see, e. g., [97]).

currents, already a power suppression of the induced heavy resonances (as well as multiparticle and continuum states) can be sufficient. In other words, a simpler method than the Borel transformation may be applied which is based on general dispersion relations, such as [97, 109] $\left(q_0^2 \leqslant 0\right)$:

$$M_n\left(q_0^2\right) = \frac{(-1)^n}{n!} \frac{d^n}{d\left[Q^2\right]^n} \Pi\left(q^2\right)\Big|_{Q^2=-q_0^2} = \int_0^\infty ds\, \frac{\frac{1}{\pi}\,\mathrm{Im}_s \Pi(s)}{\left(s-q_0^2\right)^{n+1}}\,. \tag{1343}$$

Here, $n \in \mathbb{N}$ is chosen sufficiently large to remove all occurring subtraction terms. E. g., the proper analogue of Equation 1341 would be given by $\left(Q^2 \text{ fixed}\right)$

$$-\frac{d}{d\,Q^2}\Pi\left(q^2\right) = \int_0^\infty ds\, \frac{\frac{1}{\pi}\,\mathrm{Im}_s \Pi(s)}{\left(s+Q^2\right)^2}\,, \tag{1344}$$

which again corresponds to an inverse of[18] Equation 1342 (see also [109])

$$\begin{aligned}\int_0^\infty d\left(\tfrac{Q^2}{M^2}\right)\, e^{-\frac{Q^2}{M^2}}\, \hat{\mathcal{B}}_{M^2}\left\{\overline{\Pi}\left(q^2\right)\right\} &= \int_0^\infty d\left(\tfrac{1}{M^2}\right) \int_0^\infty ds\, \frac{Q^2}{M^2} e^{-\frac{s+Q^2}{M^2}}\, \frac{1}{\pi}\,\mathrm{Im}_s \Pi(s) \\ &= Q^2 \int_0^\infty ds\, \frac{\frac{1}{\pi}\,\mathrm{Im}_s \Pi(s)}{\left(s+Q^2\right)^2} = -Q^2 \frac{d}{d\,Q^2}\Pi\left(q^2\right)\,. \end{aligned} \tag{1345}$$

For practical applications, however, those desired properties also depend on an adequate choice of the Borel parameter and the related continuum threshold[19].

Accordingly, the working window's limits are determined by the subsequent considerations and assumptions (see, e. g., [97, 464, 465]):

i) By demanding a sufficient suppression of higher order OPE corrections, one receives a lower Bound on the possible Borel parameters[20].

ii) Conversely, M^2 cannot be chosen arbitrarily large[21], because otherwise the intended exponential suppression of higher state contributions (with masses[22] $m^2 > s_0$) would become inefficient. In other words [97], when using too large values for the Borel parameter one should be cautioned not to place undue reliance on the quark-hadron duality approximation. Consequently, this method additionally requires an upper bound on M^2 which (together with point i)) results in the named window of stability.

Let us assume, that for the given QCD sum rule such a Borel window exists[23]. In order to test its model dependence (which is, inter alia, caused by s_0, M^2), one may plot the specific sum rule as

18 Equation 1345 results from Equation 1332, after applying the substitution $t = \lambda/g$, along with $\lambda = 1/M^2$ and $g = 1/Q^2$. Moreover, because of their inherent structure, one may set $f(1/Q^2) \equiv \Pi\left(q^2\right)$ and $\mathcal{B}[f](1/M^2) \equiv \hat{\mathcal{B}}_{M^2}\{\overline{\Pi}(q^2)\}$.

19 Due to the sum rule's formal structure, both parameters are interconnected in a nontrivial way [97]. Besides, the numerical value of s_0 is not arbitrary, but can be related to the channel specific resonance activity (see [97, 280]).

20 For example, when considering a truncated short distance OPE (such as Equation 85) terms with the highest included energy dimension are usually supposed to remain a small fraction of all incorporated contributions (see, e. g., [97]). In the context of LCSRs that is still a working assumption, but the involved Borel parameter has to be modified accordingly (see, e. g., Section 4.3). Thus, this required lower limit (ideally) enables a better control over the OPE's convergence and as a result may also reduce the error caused by neglecting higher-dimensional corrections (see, e. g., [97, 634] for an extended discussion):

21 This may be seen when considering the limit $M^2 \to \infty$.

22 Being the sum of all involved (hadron) masses within this specific state.

23 There are cases, where the QCD sum rule method cannot access the lowest lying meson states [94]. Such channels usually exhibit a strong coupling to the vacuum fluctuations [94] and sometimes no Borel window can be found [97]. This may involve a scenario, where the lower limit of M^2 overshoots the upper one [97].

a function of the Borel parameter at different values of the generic momentum transfer and s_0, while keeping all other parameters fixed (see [97, 280, 464, 465]). For instance, the leading twist (LO) LCSR (see Section 4.2), which describes the $\gamma^*\rho \to P$ $\left(P = \eta, \eta'\right)$ transition FF $\left(x_0 = Q^2/(s_0 + Q^2)\right)$

$$\sqrt{2} f_\rho F_{\gamma^*\rho\to P}\left(Q^2\right) = \int_{x_0}^1 dx \left[2e_s^2 f_P^s \frac{\phi_P^{(s)}(x)}{x} + \sqrt{2}\left(e_u^2 + e_d^2\right) f_M^q \frac{\phi_P^{(q)}(x)}{x}\right] e^{\frac{x m_\rho^2 - \bar{x} Q^2}{x M^2}} \tag{1346}$$

can be analyzed in this way[24]. Flat curves, i. e., the negligible dependence on M^2, would indicate a good accuracy of the sum rule [280, 464]. Besides, after narrowing down the Borel window, s_0 can be further studied[25] by demanding maximal stability of the underlying sum rule (see [97, 464]). This leads to a similar working window for the effective threshold parameter[26].

In brief, the introduced techniques and concepts are pivotal for the used QCD sum rule method and all related numerical evaluations. Correspondingly, the most basic facts have been presented, as required for this work.

24 Besides, Equation 1346 reproduces the leading twist structure of [280, Equation 28].
25 This can be done by an adequate fitting procedure, as discussed in [97].
26 A more detailed discussion of this ansatz may be found in [95, 445, 460].

B.4 CALCULATION OF IMAGINARY PARTS

In the following we introduce several concepts and formulas, which are necessary to calculate the occurring imaginary parts within this work. Yet, here we focus on a heuristic discussion, i. e., for brevity no proofs are shown explicitly. Instead, the latter may be found in the named references and textbooks, such as [458, 632, 635, 636].

When considering complex functions, one may encounter a general problem concerning their uniqueness. Already the complex numbers[27] $z = |z|e^{i\arg(z)} \in \mathbb{C}$ in their polar form are multi-valued functions $\big(\arg(z) = \arctan(\mathrm{Im}\, z/\mathrm{Re}\, z)\big)$, because their argument $\arg(z)$ is only defined up to the addition of $2\pi k$, $k \in \mathbb{Z}$. Most easily this ambiguity can be resolved by defining the principal value "Arg" of the function[28] "arg":

$$\mathrm{Arg} : \mathbb{C} \to \big(-\pi, \pi\big] , \quad \text{with} \quad z \mapsto \mathrm{Arg}(z) . \tag{1347}$$

This new function $z = |z|e^{i\,\mathrm{Arg}(z)}$, however, is not continuous anymore, but has a discontinuity along the negative real axis. Analogously, the complex logarithm "Log"

$$\mathrm{Log}(z) = \mathrm{Log}(|z|) + i\arg(z) \quad \big(z \in \mathbb{C}\backslash\{0\}\big) , \tag{1348}$$

is not single-valued before we choose one of its branches. Following the standard approach (e. g., [632]), we select the related principal branch of the logarithmic function[29]:

$$\log : \mathbb{C}\backslash(-\infty, 0] \to \big\{z = x+iy \big| x \in \mathbb{R}, y \in (-\pi, \pi)\big\} , \tag{1349}$$

$$z \mapsto \log(z) = \log(|z|) + i\,\mathrm{Arg}(z) . \tag{1350}$$

Thus, "log" possesses a branch cut along the negative real axis as well as a branch point in the origin, i. e., we may write [587] $(x, x_0 \in \mathbb{R})$

$$\lim_{\varepsilon \to 0^+} \log(x - x_0 \pm i\varepsilon) = \log(|x - x_0|) \pm i\pi\,\Theta(x_0 - x) . \tag{1351}$$

In fact, Equation 1351 is of profound importance for our needs, because it entails the well known Sokhotski-Plemelj formula[30] [587, 637]

$$\begin{aligned} \frac{1}{x - x_0 \pm i0^+} &= \frac{d}{dx} \log\big(x - x_0 \pm i0^+\big) = \frac{1}{x - x_0}\big[\Theta(x - x_0) + \Theta(x_0 - x)\big] \mp i\pi\delta(x - x_0) \\ &= \mathrm{PV}\frac{1}{x - x_0} \mp i\pi\,\delta(x - x_0) , \end{aligned} \tag{1352}$$

which can be generalized[31] [587] via $(n \geqslant 2)$

$$\begin{aligned} \frac{1}{(x - x_0 \pm i0^+)^n} &= \frac{(-1)^{n-1}}{(n-1)!} \frac{d^{n-1}}{dx^{n-1}} \frac{1}{x - x_0 \pm i0^+} \\ &= \frac{1}{(x - x_0)^n}\big[\Theta(x - x_0) + \Theta(x_0 - x)\big] \mp i\pi \frac{(-1)^{n-1}}{(n-1)!} \delta^{(n-1)}(x - x_0) . \end{aligned} \tag{1353}$$

27 Here, $|z|$ is the modulus of z, as defined by $|z|^2 = zz^*$. Without any restrictions, we use $\bar{z}$ as well as z^* to denote the complex conjugate of z. Moreover, the argument of z is written as "$\arg(z)$" (cf. [458, 632, 635, 636]).

28 Thus, we have $\arg(z) = \mathrm{Arg}(z) \pm 2\pi k$, with $k \in \mathbb{Z}$.

29 Here, one commonly uses the restriction $\mathrm{Arg} \in (-\pi, \pi)$.

30 Here, we use $|x - x_0| = (x - x_0)\,\Theta(x - x_0) + (x_0 - x)\,\Theta(x_0 - x)$.

31 As an abbreviation, we use $\frac{d^n}{dx^n}\delta(x) \equiv \delta^{(n)}(x)$.

However, when considering products[32] of functions, such as $\frac{\log(x-x_0\pm i0^+)}{x-x_0\pm i0^+}$ the related complex structure can in general not simply be deduced from the factors' imaginary parts. In order to solve this problem, we may either search for an adequate artifice (see, e. g., [587]) or apply a more straightforward approach (similar to [638]). When choosing the latter, some basic results of complex analysis should be recapitulated[33]:

- ANALYTIC CONTINUATION: In a nutshell [639–642], suppose two analytic functions ($i = 1, 2$) $f_i : U_i \to \mathbb{C}$, that are defined on non-empty open subsets $U_i \subset \mathbb{C}$. If $U_1 \subset U_2$ and $f_1(z) = f_2(z)\ \forall z \in U_1$, then f_2 is an analytic continuation of f_1.

- UNIQUENESS OF ANALYTIC CONTINUATION: Let $\gamma : [t_0, t_1] \to \mathbb{C}$ be a continuous path (cf. [632, 639]). The holomorphic functions $g, \tilde{g} : D_{\varepsilon'}(\gamma(t_1)) \to \mathbb{C}$ may arise from $f : D_\varepsilon(\gamma(t_0)) \to \mathbb{C}$ by analytic continuation along a finite ($n \in \mathbb{N}$) chain of discs[34] $(D_0, \ldots, D_n)$ which themselves run along γ. Then the two functions are identical [632, 639], i. e., $g(z) = \tilde{g}(z)\ \forall z \in D_{\varepsilon'}(\gamma(t_1))$. In other words, the analytic continuation of f is unique (see, e. g., "identity theorem" for analytic functions [458]).

- SCHWARZ REFLECTION PRINCIPLE: Let the non-empty domain $D \subset \mathbb{C}$ be symmetric with respect to the real axis $\mathbb{R}$, i. e., for $z \in D \Rightarrow z^* \in D$. Furthermore, let us define $D_+ := \{z \in D \,|\, \operatorname{Im} z > 0\}$, $D_- := \{z \in D \,|\, \operatorname{Im} z < 0\}$ and $D_0 := D \cap \mathbb{R}$. If a function $f : D_+ \cup D_0 \to \mathbb{C}$ is continuous and $f|_{D_+}$ is analytic, with $f(D_0) \subset \mathbb{R}$, then

$$\tilde{f} : D \to \mathbb{C}\,, \quad \text{as defined by} \quad z \mapsto \tilde{f}(z) := \begin{cases} f(z)\,, & z \in (D_+ \cup D_0) \\ f(z^*)^*\,, & z \in D_- \end{cases} \tag{1354}$$

  is also an analytic function (cf. [458]).

In order to see the full power of these theorems, consider an analytic function f with $f([a, b]) \subset \mathbb{R}$ for an interval $[a, b] \subset \mathbb{R}$. Then the relation ($z \in [a, b]$)

$$f(z) = f(z^*)^*\,, \tag{1355}$$

holds and f can be analytically continued to other parts of the complex plane, where it is single-valued (i. e., well-defined) [450]. Thus, Equation 1355 implies

$$\operatorname{Re} f(z) = \operatorname{Re} f(z^*)\,, \quad \operatorname{Im} f(z) = -\operatorname{Im} f(z^*)\,. \tag{1356}$$

Suppose, that f has a branch cut along the negative real axis. By defining $z = s + i\varepsilon$ $(s, \varepsilon \in \mathbb{R})$ together with [450]

$$\operatorname{disc}_s f(s) := \lim_{\varepsilon \to 0^+} \left(f(s + i\varepsilon) - f(s - i\varepsilon)\right)\,, \tag{1357}$$

we may analyze the underlying discontinuity. Most importantly, Equation 1356 combined with Equation 1357 implicates:

$$\operatorname{disc}_s f(s) = 2i \operatorname{Im}_s f(s)\,. \tag{1358}$$

32 Here, we mean pointwise products of functions.
33 Following the standard notation [632] we define the open ε-disc around z_0: $D_\varepsilon(z_0) := \{z \in \mathbb{C} \,||z - z_0| < \varepsilon\}$.
34 More precisely, we subdivide the parameter interval $t_0 \leqslant \tau_0 \leqslant \ldots \leqslant \tau_n \leqslant t_1$ and define $D_j := D_{\varepsilon_j}(\gamma(\tau_j))$ (with ε_j sufficiently large) to ensure $\gamma|_{[\tau_{i-1}, \tau_i]} \subset (D_{i-1} \cap D_i)\ \forall i = 1, \ldots, n$ and $\forall j = 0, \ldots, n$ (cf. [632]).

Analogously, one may find

$$\mathrm{Re}_s f(s) := \lim_{\varepsilon \to 0^+} \frac{1}{2}\left(f(s+i\varepsilon) + f(s-i\varepsilon)\right) , \tag{1359}$$

which entails[35]

$$f\left(s \pm i0^+\right) = \mathrm{Re}_s f(s) \pm i\,\mathrm{Im}_s f(s) . \tag{1360}$$

Now the machinery is in place to solve our initial problem concerning pointwise products of adequate complex functions, such as f_1 and f_2. By employing the definition of Equation 1359, while using Equation 1360, we get:

$$\begin{aligned} \mathrm{Re}_s f_1(s)\, f_2(s) &= \frac{1}{2}\left(f_1\left(s+i0^+\right) f_2\left(s+i0^+\right) + f_1\left(s-i0^+\right) f_2\left(s-i0^+\right)\right) \\ &= \mathrm{Re}_s f_1(s)\,\mathrm{Re}_s f_2(s) - \mathrm{Im}_s f_1(s)\,\mathrm{Im}_s f_2(s) , \qquad (1361) \\ \mathrm{Im}_s f_1(s)\, f_2(s) &= \mathrm{Re}_s f_1(s)\,\mathrm{Im}_s f_2(s) + \mathrm{Re}_s f_2(s)\,\mathrm{Im}_s f_1(s) . \qquad (1362) \end{aligned}$$

Both results reproduce similar findings of [638]. Moreover, with Equation 1361 and Equation 1362 it is now possible to iteratively calculate the real and imaginary parts of pointwise products, such as $\prod_{i=1}^{N} f_i(s)$ $(N \in \mathbb{N})$, by simply knowing each factor's complex structure. For instance, when considering the case $x - x_0 > 0$ (analogously for $x \leftrightarrow x_0$) we get[36]:

$$\begin{aligned} \frac{1}{\pi}\,\mathrm{Im}_s\left\{\frac{\log(x-x_0 \pm i0^+)}{x-x_0 \pm i0^+}\right\} &= \frac{1}{\pi}\,\mathrm{Re}_s\left\{\log\left(x-x_0 \pm i0^+\right)\right\}\mathrm{Im}_s\left\{\frac{1}{x-x_0 \pm i0^+}\right\} \\ &\quad + \frac{1}{\pi}\,\mathrm{Im}_s\left\{\log\left(x-x_0 \pm i0^+\right)\right\}\mathrm{Re}_s\left\{\frac{1}{x-x_0 \pm i0^+}\right\} \\ &= \pm\left[\frac{\Theta(x_0-x)}{x-x_0} - \delta(x-x_0)\log(x_0-x)\right] . \end{aligned} \tag{1363}$$

With the mentioned techniques and relations all occurring imaginary parts within Chapter 4 as well as Chapter 5 can be calculated.

35 Equation 1360 has been mentioned to show the consistency of Equation 1357 and Equation 1359 with Equation 1355.
36 This reproduces a similar result of [587]. However, the authors of [587] use a different approach.

B.5 NEXT-TO-LEADING ORDER QUARK-ANTIQUARK SPECTRAL DENSITIES

For an elegant numerical implementation[37], the NLO twist-two quark-antiquark spectral density of Equation 1366 has to be reformulated. Fortunately, we have solved this problem in our previous work [281] which can now be adapted to the $\gamma^*\gamma \to (\eta, \eta')$ TFFs.

Thus, we use the definitions of [281, Equation (33), (34), (35)] $\left(\text{including } \mathcal{N}_m \coloneqq \frac{2(2m+3)}{3(m+1)(m+2)}\right)$ for the coefficients H_n^k and G_n^{2k}, i. e., we apply:

$$H_n^m \coloneqq \mathcal{N}_m \int_0^1 dx\, C_m^{(3/2)}(\xi_x) \left[\int_0^{\bar{x}} du\, \frac{\varphi_n(u) - \varphi_n(\bar{x})}{u - \bar{x}} + 3\bar{x}\right], \tag{1364}$$

$$G_n^m \coloneqq \mathcal{N}_m \int_0^1 dx\, C_m^{(3/2)}(\xi_x) \left[\int_1^{x} du\, \frac{\varphi_n(u) - \varphi_n(x)}{u - x} \log\left(1 - \tfrac{x}{u}\right) + \{x \to \bar{x}\}\right]. \tag{1365}$$

The latter basically arise from the integrals of Equation 863 which have been expanded into Gegenbauer polynomials (see Section A.12). Besides, corresponding numerical values for $n, m \leqslant 12$ can be found in [281, Table IV, V]. As a result Equation 863 boils down to $\left(x = Q^2/(s + Q^2)\right)$

$$\rho_n^{(1)}\left(Q^2, s; \mu^2\right) = \frac{\bar{x}}{s}\left[2\sum_{k=0}^{n/2} G_n^{2k}\, \varphi_{2k}(x) - \frac{\gamma_n^{(0)}}{C_f}\left(3\bar{x} - \sum_{k=0}^{n} H_n^k\, \varphi_k(x)\right) + R_n\left(\tfrac{Q^2}{\mu^2}, x\right)\varphi_n(x)\right], \tag{1366}$$

together with the coefficient function (see Equation 863):

$$R_n\left(\tfrac{Q^2}{\mu^2}, x\right) = -3\left[1 + 2\left(\psi(2) - \psi(2+n)\right)\right] + \frac{\pi^2}{3} - \log^2\left(\tfrac{\bar{x}}{x}\right) - \frac{\gamma_n^{(0)}}{C_f}\log\left(\tfrac{\bar{x}Q^2}{x\mu^2}\right). \tag{1367}$$

Accordingly, Equation 1366 will be used for the related numerical analysis. As discussed in Section 4.2.4 a similar method may, therefore, be applied to the new NLO gluon spectral densities.

Finally, it should be pointed out once again that the discussed changes are of fundamental importance for the computer-assisted evaluation[38].

B.6 FOURIER INTEGRALS

In this appendix, we collect several standard integrals which are needed for the calculations of this work (set $D = 4 - 2\varepsilon$).
The necessary Fourier integrals can be derived from (cf. [74, 373, 643] for details)

$$\int \frac{d^D x}{\pi^{D/2}} \frac{e^{iqx}}{\left[-x^2\right]^\alpha} = -i2^{D-2\alpha}\frac{\Gamma\left(\frac{D}{2} - \alpha\right)}{\Gamma(\alpha)}\left[-q^2\right]^{\alpha - D/2} \tag{1368}$$

37 In particular, this version ensures a fast code.
38 In other words, without Equation 1366 an implementation of the related sum rules would be crucially impaired.

after iteratively differentiating both sides with respect to "q_μ". Correspondingly, the first three integrals are given by:

$$-\int \frac{d^D x}{\pi^{D/2}} \frac{x_\mu e^{iqx}}{\left[-x^2\right]^\alpha} = q_\mu 2^{D+1-2\alpha} \frac{\Gamma\left(\frac{D}{2}+1-\alpha\right)}{\Gamma(\alpha)} \left[-q^2\right]^{\alpha-1-D/2}, \tag{1369}$$

$$\int \frac{d^D x}{\pi^{D/2}} \frac{x_\mu x_\nu e^{iqx}}{\left[-x^2\right]^\alpha} = i2^{D+1-2\alpha} \frac{\Gamma\left(\frac{D}{2}+1-\alpha\right)}{\Gamma(\alpha)} \left[-q^2\right]^{\alpha-2-D/2} \times \\ \times \left[g_{\mu\nu}\left(-q^2\right) + 2q_\mu q_\nu \left(\frac{D}{2}+1-\alpha\right)\right], \tag{1370}$$

$$\int \frac{d^D x}{\pi^{D/2}} \frac{x_\mu x_\nu x_\rho e^{iqx}}{\left[-x^2\right]^\alpha} = 2^{D+2-2\alpha} \frac{\Gamma\left(\frac{D}{2}+2-\alpha\right)}{\Gamma(\alpha)} \left[-q^2\right]^{\alpha-3-D/2} \Big[2q_\mu q_\nu q_\rho \left(\frac{D}{2}+2-\alpha\right) \\ - q^2(q_\nu g_{\mu\rho} + q_\mu g_{\nu\rho} + q_\rho g_{\mu\nu})\Big]. \tag{1371}$$

Depending on the value of "α", however, the limit $D \to 4$ has to be taken with great caution. In this context, it is possible to create ill-defined expressions. For instance, Equation 1368 has to be expanded into a Laurent series in "ε" (cf. Equation 43, with $\overline{\mu} \equiv \mu^{\overline{MS}}$), implying

$$\mu^{D-4} \int \frac{d^D x}{\pi^2} \frac{e^{iqx}}{\left[-x^2+i0^+\right]^2} = i\left(\frac{1}{\varepsilon} + \log\left(\frac{-q^2-i0^+}{\overline{\mu}^2}\right)\right) + \mathcal{O}(\varepsilon). \tag{1372}$$

Analogously, Equation 1370 (omitting irrelevant contributions) gives rise to

$$\mu^{D-4} \int \frac{d^D x}{\pi^2} \frac{x_\mu x_\nu e^{iqx}}{\left[-x^2+i0^+\right]^4} = \frac{i}{48}\left(\frac{1}{\varepsilon} + \log\left(\frac{-q^2-i0^+}{\overline{\mu}^2}\right)\right) \times \\ \times \left[\left(-q^2\right) g_{\mu\nu} - 2q_\mu q_\nu\right] + \dots. \tag{1373}$$

Those expressions are particularly useful for calculations in the position space.

B.7 TWO-GLUON CORRELATION FUNCTION

In following we sketch the calculation that results in Equation 709.
The LO ansatz is given by $(n^2 = 0)$

$$\Pi(p) = \frac{i}{4} \int d^D y\, e^{-ipy} \Big[\langle 0|\overbrace{\mathcal{G}_{\mu\nu}(z_1 n)\, \mathcal{G}_{\alpha\beta}(y)}\, \overbrace{\mathcal{G}_{\rho\sigma}(z_2 n)\, \mathcal{G}_{\gamma\delta}(y)}|0\rangle \\ + \langle 0|\underbrace{\mathcal{G}_{\mu\nu}(z_1 n)}\, \mathcal{G}_{\gamma\delta}(y)\, \underbrace{\mathcal{G}_{\rho\sigma}(z_2 n)}\, \mathcal{G}_{\alpha\beta}(y)|0\rangle\Big] \varepsilon^{\mu\nu\rho\sigma} \varepsilon^{\alpha\beta\gamma\delta}, \tag{1374}$$

together with (omitting color matrices and indices)

$$\underbrace{\mathcal{G}_{\mu\nu}(x)\, \mathcal{G}_{\alpha\beta}(0)} = D_{\mu\nu;\alpha\beta}(x) - D_{\nu\mu;\alpha\beta}(x) - D_{\mu\nu;\beta\alpha}(x) + D_{\nu\mu;\beta\alpha}(x), \tag{1375}$$

$$D_{\mu\nu;\alpha\beta}(x) = \frac{g_{\nu\beta}}{2\pi^{D/2}} \left[2x_\mu x_\alpha \frac{\Gamma\left(\frac{D}{2}+1\right)}{\left[-x^2\right]^{D/2+1}} + g_{\mu\alpha} \frac{\Gamma\left(\frac{D}{2}\right)}{\left[-x^2\right]^{D/2}}\right]. \tag{1376}$$

Due to its simple tensor and color structure, i. e.,

$$\varepsilon^{\mu\nu\rho\sigma} \varepsilon^{\alpha\beta\gamma\delta} \langle 0|\overbrace{\mathcal{G}_{\mu\nu}(z_1 n)\, \mathcal{G}_{\alpha\beta}(y)}\, \overbrace{\mathcal{G}_{\rho\sigma}(z_2 n)\, \mathcal{G}_{\gamma\delta}(y)}|0\rangle \\ = 16 \varepsilon^{\mu\nu\rho\sigma} \varepsilon^{\alpha\beta\gamma\delta} \delta^{AA} D_{\mu\nu;\alpha\beta}(z_1 n - y)\, D_{\rho\sigma;\gamma\delta}(z_2 n - y), \tag{1377}$$

one easily gets

$$\Pi(p) = -\frac{32i}{\pi^D}\int d^D y\, e^{-ip\cdot y}\left[\frac{D\left[\Gamma\left(\frac{D}{2}\right)\right]^2}{\left[-x_1^2\right]^{D/2}\left[-x_2^2\right]^{D/2}} - \frac{(x_1\cdot x_2)^2\, D^2\left[\Gamma\left(\frac{D}{2}\right)\right]^2}{\left[-x_1^2\right]^{D/2+1}\left[-x_2^2\right]^{D/2+1}}\right]. \tag{1378}$$

Here, we use the abbreviations

$$x_1^\mu = z_1 n^\mu - y^\mu\,, \quad x_2^\mu = z_2 n^\mu - y^\mu\,. \tag{1379}$$

After further simplifications[39], the Fourier integrals within

$$\begin{aligned}\Pi(p) = -\frac{32D}{\pi^D} i\int_0^1 du\, e^{-iz_{21}^u p\cdot n}\int d^D y\, e^{-ip\cdot y}\Bigg[u\bar u\frac{\Gamma(D)}{\left[-y^2\right]^D}\\ -\frac{4}{D}(D+1)\,u^2\bar u^2\left(D\frac{\Gamma(D)}{\left[-y^2\right]^D} + 2z_{21}\xi_u\frac{\Gamma(D+1)\,(n\cdot y)}{\left[-y^2\right]^{D+1}}\right.\\ \left.+\frac{z_{21}^2\xi_u^2}{D+1}\frac{\Gamma(D+2)\,(n\cdot y)^2}{\left[-y^2\right]^{D+2}}\right)\Bigg]\end{aligned} \tag{1380}$$

can be solved via (Section B.6)

$$i\int d^D y\,\frac{\Gamma(D)}{\left[-y^2\right]^D} e^{-ip\cdot y} = -2^{-D}\pi^{D/2}\Gamma\left(-\tfrac{D}{2}\right)\left[-p^2\right]^{D/2}, \tag{1381}$$

as well as

$$i\int d^D y\,\frac{\Gamma(D+1)}{\left[-y^2\right]^{D+1}} e^{-ip\cdot y}\,(n\cdot y) = -\frac{1}{2} i\,(n\cdot p)\,2^{-D}\pi^{D/2}\Gamma\left(-\tfrac{D}{2}\right)\left[-p^2\right]^{D/2}, \tag{1382}$$

$$i\int d^D y\,\frac{\Gamma(D+2)}{\left[-y^2\right]^{D+2}} e^{-ip\cdot y}\,(n\cdot y)^2 = \frac{1}{4}\,(n\cdot p)^2\,2^{-D}\pi^{D/2}\Gamma\left(-\tfrac{D}{2}\right)\left[-p^2\right]^{D/2}. \tag{1383}$$

Hence, we get (cf. Equation 710)

$$\begin{aligned}\Pi(p) &= D\frac{2^{5-D}}{\pi^{D/2}}\Gamma\left(-\tfrac{D}{2}\right)\left[-p^2\right]^{D/2}\int_0^1 du\left[u\bar u - \frac{4}{D}u^2\bar u^2\left(D(D+1)\right.\right.\\ &\quad\left.\left.+\,(D+1)\,\xi_u\partial_u + \frac{1}{4}\xi_u^2\partial_u^2\right)\right]e^{-iz_{21}^u p\cdot n}\\ &= -2\mathcal{N}\left(p^2\right)\int_0^1 du\, e^{-iz_{21}^u p\cdot n}\left[u\bar u - 20u^2\bar u^2 + 5\partial_u\left\{u^2\bar u^2\xi_u\right\}\right.\\ &\quad\left.-\frac{1}{4}\partial_u^2\left\{u^2\bar u^2\xi_u^2\right\}\right]\\ &= -2\mathcal{N}\left(p^2\right)\int_0^1 du\left[u\bar u\,(1-20u\bar u) + 10u\bar u\,(5u\bar u - 1)\right.\\ &\quad\left.-\frac{1}{4}\left(120u^2\bar u^2 - 36u\bar u + 2\right)\right]e^{-iz_{21}^u p\cdot n},\end{aligned} \tag{1384}$$

which implies Equation 709.

39 The additional integral "$\int_0^1 du$" arises when combining the different propagators via a Feynman parametrization.

C

APPENDIX – RENORMALIZATION AND EVOLUTION

This appendix chapter contains:

- a collection of required projection operators for the evolution procedure, and LO evolution kernels,
- a calculation of the singlet decay constant's evolution,
- a list of all needed (NLO) anomalous dimensions.

Moreover, an adaption of the singlet evolution and related formalism is discussed. In short, based on [13, 20, 26, 27, 129, 304, 385] and Chapter 3, the following supplement represents a stand-alone toolbox which allows a full NLO evolution of η and η' DAs. Furthermore, we present the higher twist kaon DAs, which have been retrofitted with our newly calculated results (see Chapter 3).

C.1 EVOLUTION OF THE SINGLET DECAY CONSTANT

Finding the explicit evolution of the singlet decay constant[1]

$$f_M^0 \sim \langle 0|\mathcal{J}_{+5}(0)|M(P)\rangle \tag{1385}$$

is a standard problem of QCD. In fact, the renormalized decay constant $f_M^0(\mu^2)$ is connected to its bare counterpart $\left[f_M^0\right]_{\text{bare}}$ (cf. [644]) via the corresponding renormalization constant $\mathcal{Z}(\mu^2)$:

$$f_M^0\left(\mu^2\right) = \mathcal{Z}^{-1}\left(\mu^2\right)\left[f_M^0\right]_{\text{bare}} . \tag{1386}$$

The resulting[2] RGE (see, e. g., [45, 644])

$$\left[\mu^2\frac{\partial}{\partial\mu^2} + \beta(\alpha_S)\frac{\partial}{\partial\alpha_S} + \frac{1}{2}\gamma(\alpha_S)\right] f_M^0\left(\mu^2\right) = 0\,, \quad \gamma(\alpha_S) = \frac{2\mu^2}{\mathcal{Z}}\frac{\partial\mathcal{Z}}{\partial\mu^2} \tag{1387}$$

may be solved in a similar to Equation 53. This means, based on an adequate substitution procedure, with proper initial conditions we may use the associated truncated[3] asymptotic expansions of $\beta(\alpha_S)$ as well as $\gamma(\alpha_S)$. Consequently, one gets the general solution (see for example [45, 644])

$$\frac{f_M^0(\mu^2)}{f_M^0(\mu_0^2)} = \left[\frac{\alpha_S(\mu^2)}{\alpha_S(\mu_0^2)}\right]^{-\frac{\gamma^{(0)}}{\beta_0}}\left[\frac{4\pi\beta_0+\beta_1\alpha_S(\mu^2)}{4\pi\beta_0+\beta_1\alpha_S(\mu_0^2)}\right]^{-\frac{2}{\beta_1}\left(\gamma^{(1)}-\frac{\beta_1}{2\beta_0}\gamma^{(0)}\right)} \tag{1388}$$

1 Again, we will swap between f_M^0 and $f_M^{(0)}$, if we see fit. Here, one has to find a compromise between overloading the expressions and precision.

2 The RG of Equation 1387 boils down to Equation 261.

3 The asymptotic expansions will be taken into account up to the intended order of accuracy.

at NLO accuracy[4]. Moreover, in the case of a small strong coupling constant $\alpha_S(Q^2) \ll 1$ (for $Q = \mu, \mu_0$), Equation 1388 can be simplified to [5]

$$\frac{f_M^0(\mu^2)}{f_M^0(\mu_0^2)} \approx \left[\frac{\alpha_S(\mu^2)}{\alpha_S(\mu_0^2)}\right]^{-\frac{\gamma^{(0)}}{\beta_0}} \left(1 + \frac{\alpha_S(\mu_0^2) - \alpha_S(\mu^2)}{2\pi\beta_0}\left(\gamma^{(1)} - \frac{\beta_1}{2\beta_0}\gamma^{(0)}\right)\right). \tag{1389}$$

The latter results in Equation 462 when adapted to the rest of our notation (e. g., $\gamma^{(0)} \to 0$, $\gamma^{(1)} \to -4N_f$).

C.2 LIST OF ANOMALOUS DIMENSIONS

For this work a full NLO evolution of the η and η' DAs is needed. Correspondingly, within the subsequent subsection we list all required anomalous dimensions. For this purpose, we collect and adapt the results of [129, 385] to the formalism of [26, 304]. Besides, the anomalous dimensions of the parity-odd sector, the non-singlet case is listed up to NLO accuracy. Most importantly, the formalism given below, together with Section 3.3.3 and Section C.6 builds a stand-alone toolbox for the intended (NLO) evolution of $\eta^{(\prime)}$ meson DAs.

The literature does not provide us with a (flawless) list of anomalous dimensions ready to use[6]. However, after some modifications and cross-checks with the splitting functions of[7] [129, 385] the subsequent anomalous dimensions for the parity-odd case have been found.

Let us start with the Gegenbauer coefficients of the flavor-octet contributions. The analytically continued LO flavor non-singlet anomalous dimensions are given by [36, 281, 385] ($n \geqslant 0$):

$$\gamma_n^{(0)} = C_f\left[4\psi(n+2) + 4\gamma_E - 3 - \frac{2}{(n+1)(n+2)}\right], \tag{1390}$$

where $\psi(x) = \frac{d}{dx}\Gamma(x)$ is the digamma and $\Gamma(x)$ the usual gamma function. For the NLO case, we will use the definition (cf. Equation 116)

$$\gamma_n^{(1)} = {}^{NS}\gamma_n^{(1)}, \tag{1391}$$

4 When asymptotically expanding $\gamma(\alpha_S)$ in powers of "$\frac{\alpha_S}{2\pi}$", the first two coefficients are $\gamma^{(0)}$ and $\gamma^{(1)}$. This is similar to Equation 262, except for an extra minus signs.

5 Here, we may use $x^b \approx 1 + b\,(x-1)$, because $x \approx 1$ is fulfilled.

6 Due to this lack of information, it seems obligatory to list the used anomalous dimensions explicitly.

7 Unfortunately, the published version uses a different representation compared to the "*arXiv*" version which may lead to some confusion.

with the explicit expression [36, 129, 385] ($n \geqslant 0$)

$$
\begin{aligned}
{}^{\mathrm{NS}}\gamma_n^{(1)} &= 8C_f\tilde{S}_{1,2}(n)\,(C_A - 2C_f) + 4C_A C_f S_3(n-1) \\
&+ \frac{4(2n+3)\,C_f\tilde{S}_2(n)\,(C_A - 2C_f)}{(n+1)\,(n+2)} - 4C_f\tilde{S}_3(n)\,(C_A - 2C_f) \\
&+ \frac{2}{9}C_f S_1(n-1)\left(67C_A - \frac{18C_f\left(4n^4+18n^3+31n^2+24n+8\right)}{n^2\,(n+1)^2\,(n+2)^2}\right) \\
&- 8C_f^2 S_{1,2}(n-1) - 8C_f^2 S_{2,1}(n-1) \\
&+ \frac{2}{3}C_f S_2(n-1)\left(3\left(\frac{n\,(3n+5)}{(n+1)\,(n+2)} - \frac{4}{n}\right)C_f - 11C_A\right) \\
&+ \frac{C_f}{36n^3\,(n+1)^3\,(n+2)^3}\Big(\big(-51n^9+613n^8+6297n^7 \\
&+ 20435n^6+31794n^5+25568n^4+10944n^3+4288n^2 \\
&+ 3072n+1152\big)C_A - 9\big(3n^9+27n^8+51n^7-11n^6 \\
&+ 206n^5+1692n^4+3888n^3+4224n^2+2304n+512\big)C_f\Big) \\
&+ N_f\left(\frac{\left(3n^6-62n^5-309n^4-456n^3-168n^2+128n+96\right)C_f}{18n^2\,(n+1)^2\,(n+2)^2}\right. \\
&\left. - \frac{20}{9}C_f S_1(n-1) + \frac{4}{3}C_f S_2(n-1)\right).
\end{aligned}
\tag{1392}
$$

Here, the following functions have been used [36, 129, 385]

$$
S_r(n) = \sum_{i=1}^{n}\frac{\mathrm{sgn}(r)^i}{i^{|r|}}, \tag{1393}
$$

$$
S_{r,s}(n) = \sum_{k=1}^{n}\sum_{j=1}^{k}\frac{\mathrm{sgn}(r)^k}{k^{|r|}}\frac{\mathrm{sgn}(s)^j}{j^{|s|}}, \tag{1394}
$$

$$
\tilde{S}_r(n) = \sum_{i=1}^{n}\frac{(-1)^i}{i^r}, \tag{1395}
$$

$$
\tilde{S}_{r,s}(n) = \sum_{k=1}^{n}\sum_{j=1}^{k}\frac{1}{k^r}\frac{(-1)^j}{j^s}. \tag{1396}
$$

Moreover, the (cf. Section 3.3.3) off-diagonal mixing coefficients may be introduced

$$
d_n^k\left(\mu^2,\mu_0^2\right) = r_{nk}\left(\mu^2,\mu_0^2\right)M_n^k, \tag{1397}
$$

with the help of

$$
r_{nk}\left(\mu^2,\mu_0^2\right) = \frac{-1}{\gamma_n^{(0)}-\gamma_k^{(0)}-\beta_0}\left\{1-\left[\frac{\alpha_S\left(\mu^2\right)}{\alpha_S\left(\mu_0^2\right)}\right]^{\frac{\gamma_n^{(0)}-\gamma_k^{(0)}-\beta_0}{\beta_0}}\right\} \tag{1398}
$$

and the matrix

$$M_n^k = \frac{(k+1)(k+2)(2n+3)}{(n+1)(n+2)} \left[\gamma_k^{(0)} - \gamma_n^{(0)}\right] \times \\ \times \left\{ \frac{4C_f A_n^k - \gamma_k^{(0)} - \beta_0}{(n-k)(n+k+3)} + 2C_f \frac{A_n^k - \psi(n+2) + \psi(1)}{(k+1)(k+2)} \right\} . \tag{1399}$$

The latter contains the definition

$$A_n^k = \psi\left(\frac{n+k+4}{2}\right) - \psi\left(\frac{n-k}{2}\right) + 2\psi(n-k) - \psi(n+2) - \psi(1) . \tag{1400}$$

For the singlet sector, the forward anomalous dimensions "$\gamma_n^{\mathrm{fw}(m)}$" are formally related to the diagonal anomalous dimensions via [26]

$$\left.\begin{aligned} {}_{qq}\gamma_n^{\mathrm{D}(m)} &= {}_{qq}\gamma_n^{\mathrm{fw}(m)}, \quad {}_{qg}\gamma_n^{\mathrm{D}(m)} = {}_{qg}\gamma_n^{\mathrm{fw}(m)} \tfrac{6}{n}, \\ {}_{gg}\gamma_n^{\mathrm{D}(m)} &= {}_{gg}\gamma_n^{\mathrm{fw}(m)}, \quad {}_{gq}\gamma_n^{\mathrm{D}(m)} = {}_{gq}\gamma_n^{\mathrm{fw}(m)} \tfrac{n}{6}. \end{aligned}\right\} \tag{1401}$$

Here, the original forward anomalous dimensions of Equation 118 have been rescaled by adequate factors of $\left(\frac{1}{2}\right)^m$ (i. e., $m=1$ for LO, $m=2$ for NLO, etc.), while the index $j \to n+1$ has been shifted accordingly. Apart from these modifications, one has to replace $T_f \to N_F T_A$ to get a result for N_f active flavors. Therefore, the LO expressions for singlet anomalous dimensions are given by ($n \geqslant 2$)

$${}_{qq}\gamma_n^{\mathrm{D}(0)} = \gamma_n^{(0)} , \tag{1402}$$

$${}_{qg}\gamma_n^{\mathrm{D}(0)} = \frac{-12N_f}{(n+1)(n+2)} , \tag{1403}$$

$${}_{gq}\gamma_n^{\mathrm{D}(0)} = \frac{-C_f n(n+3)}{3(n+1)(n+2)} , \tag{1404}$$

$${}_{gg}\gamma_n^{\mathrm{D}(0)} = N_c \left[4\psi(n+2) + 4\gamma_E - \frac{8}{(n+1)(n+2)}\right] - \beta_0 . \tag{1405}$$

For the NLO anomalous dimensions, the modification

$${}^{\mathrm{SING}}\gamma_n^{(1)} = N_f \frac{4T_F C_f (n+3)\left(n^3+3n^2+5n+4\right)}{(n+1)^3 (n+2)^3} \tag{1406}$$

is needed to get (cf. [304]):

$${}_{qq}\gamma_n^{\mathrm{D}(1)} = {}^{\mathrm{NS}}\gamma_n^{(1)} + {}^{\mathrm{SING}}\gamma_n^{(1)} . \tag{1407}$$

In the context of the NLO evolution formalism (cf. Section 3.3.3), Equation 1407 connects the singlet and the non-singlet sectors with each other. Besides, the case $n=0$ has to be emphasized:

$${}^{\mathrm{NS}}\gamma_0^{(1)} = 0 , \quad {}^{\mathrm{SING}}\gamma_0^{(1)} = 4N_f , \tag{1408}$$

because it is interconnected with the evolution of the singlet decay constant f_M^0 (cf. Section 3.3.3). Furthermore, the remaining anomalous dimensions are given by:

$$\begin{aligned}
{}^{qg}\gamma_n^{D(1)} = N_f \Bigg(& \frac{48 T_F C_A}{n^2+3n+2} \tilde{S}_2(n) + \frac{24 T_A \left(C_A - C_f\right)}{(n+1)(n+2)} S_1^2(n-1) \\
& - \frac{48 T_F \left(\left(n^2+3n+2\right) C_f - n(2n+3) C_A\right)}{n(n+1)^2 (n+2)^2} S_1(n-1) \\
& - \frac{12 T_F}{n(n+1)^3 (n+2)^3} \Big(2 \Big(n^5 + 6n^4 + 6n^3 - 7n^2 - 18n \\
& - 12) C_A + \left(5n^3 + 30n^2 + 56n + 33\right) n^2 C_f \Big) + \frac{24 T_F (C_A + C_f)}{(n+1)(n+2)} S_2(n-1) \Bigg) , \qquad (1409)
\end{aligned}$$

and

$$\begin{aligned}
{}^{gq}\gamma_n^{D(1)} = & - \frac{n(n+3) C_f \left(C_A - C_f\right)}{3(n+1)(n+2)} S_1^2(n-1) \\
& + \frac{2n(n+3) C_A C_f}{3(n+1)(n+2)} \tilde{S}_2(n) + \frac{n(n+3) C_f (C_A + C_f)}{3(n+1)(n+2)} S_2(n-1) \\
& + \frac{C_f}{9(n+1)^2 (n+2)^2} \Big(\left(11n^4 + 54n^3 + 67n^2 - 12n - 36\right) C_A \\
& - 3 \left(3n^4 + 12n^3 + 3n^2 - 22n - 12\right) C_f \Big) S_1(n-1) \\
& + \frac{C_f}{54n(n+1)^3 (n+2)^3} \Big(9 \Big(9n^7 + 63n^6 + 152n^5 + 159n^4 \\
& + 125n^3 + 180n^2 + 160n + 48 \Big) C_f - 2n \Big(76n^6 + 585n^5 \\
& + 1573n^4 + 1605n^3 + 151n^2 - 678n - 324 \Big) C_A \Big) \\
& + N_f \Bigg(\frac{4 T_F \left(5n^4 + 21n^3 + 10n^2 - 30n - 18\right) C_f}{27(n+1)^2 (n+2)^2} \\
& - \frac{4 T_F n(n+3) C_f}{9(n+1)(n+2)} S_1(n-1) \Bigg) , \qquad (1410)
\end{aligned}$$

as well as

$$
\begin{aligned}
{}^{gg}\gamma_n^{D(1)} = &-\frac{8nC_A^2}{n^2+3n+2}\tilde{S}_2(n) + 4C_A^2\tilde{S}_3(n) - 8C_A^2\tilde{S}_{1,2}(n) \\
&+ \frac{2C_A^2}{9n^2(n+1)^2(n+2)^2}\Big(67n^6+402n^5+799n^4 \\
&+ 588n^3-128n^2-432n-144\Big)S_1(n-1) \\
&+ 4C_A^2 S_3(n-1) - 8C_A^2 S_{1,2}(n-1) - 8C_A^2 S_{2,1}(n-1) \\
&- \frac{8\left(2n^2+3n+2\right)C_A^2}{n(n+1)(n+2)}S_2(n-1) \\
&- \frac{C_A^2}{9n^3(n+1)^3(n+2)^3}\Big(48n^9+164n^8-369n^7 \\
&- 2474n^6-4695n^5-2990n^4+2820n^3+6056n^2 \\
&+ 3888n+864) + N_f\left(\frac{2T_F}{9n(n+1)^3(n+2)^3}\Big(4\Big(3n^7\right. \\
&+ \left. 17n^6+27n^5-23n^4-141n^3-215n^2-150n\right. \\
&- \left. 40\right)C_A + 9n\Big(n^6+9n^5+35n^4+71n^3+70n^2 \\
&+ \left. 30n+8\right)C_f) - \frac{40}{9}T_F C_A S_1(n-1)\Big)\,. \qquad (1411)
\end{aligned}
$$

According to [26, 27] the non-diagonal anomalous dimensions may be defined by

$$
\begin{aligned}
{}^{qq}\gamma_{nm}^{ND(1)} = &\left({}^{qq}\gamma_n^{(0)} - {}^{qq}\gamma_m^{(0)}\right)\left[d_{nm}\left(\beta_0 - {}^{qq}\gamma_m^{(0)}\right) + {}^{qq}g_{nm}\right] \\
&- \left({}^{qg}\gamma_n^{(0)} - {}^{qg}\gamma_m^{(0)}\right)d_{nm}\,{}^{gq}\gamma_m^{(0)} + {}^{qg}\gamma_n^{(0)}\,{}^{gq}g_{nm}\,, \qquad (1412) \\
{}^{qg}\gamma_{nm}^{ND(1)} = &\left({}^{qg}\gamma_n^{(0)} - {}^{qg}\gamma_m^{(0)}\right)d_{nm}\left(\beta_0 - {}^{gg}\gamma_m^{(0)}\right) \\
&- \left({}^{qq}\gamma_n^{(0)} - {}^{qq}\gamma_m^{(0)}\right)d_{nm}\,{}^{qg}\gamma_m^{(0)} + {}^{qg}\gamma_n^{(0)}\,{}^{gg}g_{nm} \\
&- {}^{qg}\gamma_m^{(0)}\,{}^{qq}g_{nm}\,, \qquad (1413) \\
{}^{gq}\gamma_{nm}^{ND(1)} = &\left({}^{gq}\gamma_n^{(0)} - {}^{gq}\gamma_m^{(0)}\right)d_{nm}\left(\beta_0 - {}^{qq}\gamma_m^{(0)}\right) \\
&- \left({}^{gg}\gamma_n^{(0)} - {}^{gg}\gamma_m^{(0)}\right)d_{nm}\,{}^{gq}\gamma_m^{(0)} + {}^{gq}\gamma_n^{(0)}\,{}^{qq}g_{nm} \\
&- {}^{gq}\gamma_m^{(0)}\,{}^{gg}g_{nm} + \left({}^{gg}\gamma_n^{(0)} - {}^{qq}\gamma_m^{(0)}\right){}^{gq}g_{nm}\,, \qquad (1414) \\
{}^{gg}\gamma_{nm}^{ND(1)} = &\left({}^{gg}\gamma_n^{(0)} - {}^{gg}\gamma_m^{(0)}\right)\left[d_{nm}\left(\beta_0 - {}^{gg}\gamma_m^{(0)}\right) + {}^{gg}g_{nm}\right] \\
&- \left({}^{gq}\gamma_n^{(0)} - {}^{gq}\gamma_m^{(0)}\right)d_{nm}\,{}^{qg}\gamma_m^{(0)} - {}^{qg}\gamma_m^{(0)}\,{}^{gq}g_{nm}\,. \qquad (1415)
\end{aligned}
$$

Here, the named definitions contain several abbreviations, such as

$$
d_{nm} = -\frac{1}{2}\frac{(2m+3)\left[1+(-1)^{n-m}\right]}{(n-m)(n+m+3)}\,, \qquad (1416)
$$

along with (see also [26]):

$$
{}^{qq}g_{nm} = 2C_f d_{nm}\theta_{n-2,m}\left\{2A_n^m + (A_n^m - \psi(n+2) + \psi(1))\,\frac{(n-m)\,(n+m+3)}{(m+1)\,(m+2)}\right\}, \tag{1417}
$$

$$
{}^{gq}g_{nm} = C_f d_{nm}\theta_{n-2,m}\frac{(n-m)\,(n+m+3)}{3\,(m+1)\,(m+2)}\,, \tag{1418}
$$

$$
\begin{aligned}
{}^{gg}g_{nm} = {} & 2C_A d_{nm}\theta_{n-2,m}\{2A_n^m + (A_n^m - \psi(n+2) + \psi(1)) \times \\
& \times\left[\frac{\Gamma(n+4)\,\Gamma(m)}{\Gamma(n)\,\Gamma(m+4)} - 1\right] + 2\,(n-m)\,(n+m+3)\,\frac{\Gamma(m)}{\Gamma(m+4)}\right\}\,,
\end{aligned} \tag{1419}
$$

where we use

$$
\theta_{n,m} = \begin{cases} 1 & , n \geqslant m \\ 0 & , n < m \end{cases}\,. \tag{1420}
$$

C.3 LEADING-ORDER EVOLUTION KERNELS

This is a short supplement for the LO evolution kernels. The latter were used for the adaptation of the LO and NLO anomalous dimensions, as discussed in Section C.5 as well as Section C.2. Moreover, in Section 4.2.4, one of these kernels is explicitly needed.
Since they have been investigated in a number of papers, such as [20–27, 645], we only collect the corresponding results:

$$
{}^{qq}V_D^{(1)}(x,y) = -2C_f\left\{\frac{x}{y}\left[1 + \frac{1}{y-x}\right]\theta(y-x) + \left\{\begin{smallmatrix} x\to\bar{x} \\ y\to\bar{y}\end{smallmatrix}\right\}\right\}_+\,, \tag{1421}
$$

$$
{}^{qg}V_D^{(1)}(x,y) = 2C_f\left\{\frac{x}{y^2}\theta(y-x) - \left\{\begin{smallmatrix} x\to\bar{x} \\ y\to\bar{y}\end{smallmatrix}\right\}\right\}\,, \tag{1422}
$$

$$
{}^{gq}V_D^{(1)}(x,y) = -2N_f\left\{\frac{x^2}{y}\theta(y-x) - \left\{\begin{smallmatrix} x\to\bar{x} \\ y\to\bar{y}\end{smallmatrix}\right\}\right\}\,, \tag{1423}
$$

$$
{}^{gg}V_D^{(1)}(x,y) = -2N_c\left\{\frac{x}{y}\left[\left(\frac{\theta(y-x)}{y-x}\right)_+ + \frac{\xi_x}{y}\theta(y-x)\right] + \left\{\begin{smallmatrix} x\to\bar{x} \\ y\to\bar{y}\end{smallmatrix}\right\}\right\} - \beta_0\delta(x-y)\,. \tag{1424}
$$

Here, the plus distribution occurs which is defined by (cf. [20])

$$
[F(x,y)]_+ = F(x,y) - \delta(x-y)\int_0^1 dz\,F(z,y)\,. \tag{1425}
$$

Most importantly, the conversion to the formalism of [20] is given by ($\sigma = \sqrt{C_f/N_f}$ and $a = q, g$):

$$
V_{aa}(x,y) = -{}^{aa}V_D^{(1)}(x,y) \tag{1426}
$$

$$
V_{qg}(x,y) = -{}^{qg}V_D^{(1)}(x,y)\,\sigma^{-1} \tag{1427}
$$

$$
V_{gq}(x,y) = -{}^{gq}V_D^{(1)}(x,y)\,\sigma\,. \tag{1428}
$$

Therefore, the original LO eigenvalue problem (see, e. g., [20]) boils down to ($a, b = q, g$):

$$
\begin{aligned}
& \int_0^1 dy\,\left[{}^{ab}V_D^{(1)}(x,y)\,\varphi_n^{(\nu(b))}(y)\right] = {}^{ba}\gamma_n^{(0)}\varphi_n^{(\nu(a))}(x) \\
\Leftrightarrow \quad & \int_0^1 dy\,\left[V_{ab}(x,y)\,\varphi_n^{(\nu(b))}(y)\right] = \gamma_n^{ab}\varphi_n^{(\nu(a))}(x)\,,
\end{aligned} \tag{1429}
$$

where we have introduced the abbreviations

$$\varphi_n^{(\alpha)}(x) \coloneqq [x\bar{x}]^{\alpha-\frac{1}{2}}\, C_{n+3/2-\alpha}^{(\alpha)}(\xi_x)\,, \tag{1430}$$

$$\nu(a) \coloneqq \begin{cases} 3/2\,, & a=q \\ 5/2\,, & a=g \end{cases}\,, \tag{1431}$$

along with $(a = q, g)$

$$\gamma_n^{aa} = -^{aa}\gamma_n^{(0)}\,, \tag{1432}$$

$$\gamma_n^{qg} = -^{gq}\gamma_n^{(0)}\sigma^{-1}\,, \tag{1433}$$

$$\gamma_n^{gq} = -^{qg}\gamma_n^{(0)}\sigma\,. \tag{1434}$$

Besides, in the context of Equation 1429 and for the given anomalous dimensions (cf. Section C.2, Section A.12) the kernels may also be expressed via[8]

$$V_{ab}(x,y) = \sum_{n=2}^{\infty} \gamma_n^{ab}\varphi_n^{(\nu(a))}(x)\,\frac{C_{n+3/2-\nu(b)}^{(\nu(b))}(\xi_y)}{N_{n+3/2-\nu(b)}^{(\nu(b))}}\,. \tag{1435}$$

Furthermore, the connection to the LO renormalization matrix $\mathfrak{Z}$ is given by (e. g., [20])

$$\mathfrak{Z}\left(x,y;\alpha_S\left(\mu^2\right)\right) = \underbrace{\delta(x-y)\,\mathbb{1}_2}_{=\mathbb{1}^{(x,y)}} + \frac{\alpha_S\left(\mu^2\right)}{4\pi}\frac{1}{\varepsilon}\underbrace{\begin{pmatrix} V_{qq}(x,y) & V_{qg}(x,y) \\ V_{gq}(x,y) & V_{gg}(x,y) \end{pmatrix}}_{=\boldsymbol{V}^{(1)}(x,y)}\,, \tag{1436}$$

which is consistent

$$\begin{aligned} &\int_0^1 \mathrm{d}\,x'\,\mathfrak{Z}^{-1}\left(x,x';\alpha_S\left(\mu^2\right)\right)\mathfrak{Z}\left(x',y;\alpha_S\left(\mu^2\right)\right) \\ &= \int_0^1 \mathrm{d}\,x'\left[\mathbb{1}^{(x,x')} - \frac{\alpha_S\left(\mu^2\right)}{4\pi}\frac{1}{\varepsilon}\boldsymbol{V}^{(1)}\left(x,x'\right)\right]\left[\mathbb{1}^{(x',y)} + \frac{\alpha_S\left(\mu^2\right)}{4\pi}\frac{1}{\varepsilon}\boldsymbol{V}^{(1)}\left(x',y\right)\right] = \mathbb{1}^{(x,y)}\,, \end{aligned} \tag{1437}$$

with the ansatz Equation 430 (up to $\mathcal{O}(\alpha_S)$ accuracy)

$$-\int_0^1 \mathrm{d}\,x'\,\mathfrak{Z}^{-1}\left(x,x';\alpha_S\left(\mu^2\right)\right)\left[\mu^2\frac{\partial}{\partial\mu^2}\mathfrak{Z}\left(x',y;\alpha_S\left(\mu^2\right)\right)\right] = \frac{\alpha_S\left(\mu^2\right)}{4\pi}\boldsymbol{V}^{(1)}(x,y) + \mathcal{O}\left(\alpha_S^2\right)\,. \tag{1438}$$

Here, we use (cf. Equation 64 and [20])

$$\beta\left(\alpha_S\left(\mu^2\right),\varepsilon\right) = -\varepsilon\alpha_S\left(\mu^2\right) - \beta_0\frac{\alpha_S^2\left(\mu^2\right)}{4\pi} + \mathcal{O}\left(\alpha_S^3\right)\,. \tag{1439}$$

Last but not least, the LO non-singlet evolution kernel $V_{NS}^{(1)}$

$$V_{NS}^{(1)}(x,y) = {}^{qq}V_D^{(1)}(x,y)\,. \tag{1440}$$

coincides with the singlet kernel ${}^{qq}V_D^{(1)}$ [3]. This is particularly important for matching the normalization constants of octet and singlet DAs.

8 Here, we also use $\gamma_0^{qq} \equiv 0$.

C.4 PROJECTION OPERATORS FOR THE EVOLUTION PROCEDURE

This is a short supplement concerning the projection operators of Equation 444. The latter effectively decouple the evolution of the Gegenbauer coefficients $c^{(a)}_{n,M}$ (with $a = \pm$; see also Section 3.3.2). That may be most easily seen in the eigenbasis of the $\pm$-modes:

$$\mathbf{P}^{\pm}_n\big|_{\text{eig}} = \frac{\pm 1}{\gamma^{(+)}_n - \gamma^{(-)}_n}\left(\text{diag}\left(\gamma^{(+)}_n, \gamma^{(-)}_n\right) - \gamma^{(\mp)}_n \mathbb{1}_2\right) = \begin{cases} \text{diag}(1,0) & \text{for "+"} \\ \text{diag}(0,1) & \text{for "−"} \end{cases} . \tag{1441}$$

Accordingly, with the change of basis (cf. Equation 437, Equation 440)

$$\mathbf{P}^{\pm}_n = [\mathbf{T}_n \mathbf{D}_n]\left(\mathbf{P}^{\pm}_n\big|_{\text{eig}}\right)\left[\mathbf{D}_n^{-1}\mathbf{T}_n^{-1}\right] \tag{1442}$$

the projection operators of Equation 444, i. e., for the basis related to $c^{(a)}_{n,M}$ (with $a = 1, g$) can be reproduced. Based on the structure of Equation 441, which includes a vanishing gluonic Gegenbauer moment, we may define

$$\mathbf{P}^{+}_0 \coloneqq \begin{pmatrix} 1 & 0 \\ 0 & 0 \end{pmatrix} , \qquad \mathbf{P}^{-}_0 \coloneqq \begin{pmatrix} 0 & 0 \\ 0 & 1 \end{pmatrix} . \tag{1443}$$

This is possible, because the analytic continuation of $\mathbf{P}^{\pm}_n$ to $n = 0$ represents an upper triangular matrix. Furthermore, the operators $\mathbf{P}^{\pm}_n$ act on the eigenstates of the corresponding evolution equation, and fulfill

$$\mathbf{P}^{+}_n + \mathbf{P}^{-}_n = \mathbb{1}_2 , \quad \left(\mathbf{P}^{\pm}_n\right)^2 = \mathbf{P}^{\pm}_n , \quad \mathbf{P}^{+}_n \mathbf{P}^{-}_n = 0 . \tag{1444}$$

C.5 DETAILS OF KROLL'S FORMALISM

In this section, we provide a comparison to other conventions, such as [20, 28]. Furthermore, the following steps have been important when adapting the existing formalism of the singlet evolution. Therefore, it seems reasonable to mention some details.

When focusing on LO accuracy, Equation 434 and Equation 435 lead to the ansatz of [20]

$$\mu \frac{\mathrm{d}}{\mathrm{d}\,\mu}\left[\mathbf{L}\,\vec{c}_{n,M}(\mu)\right] = \tfrac{\alpha_S(\mu)}{4\pi} \mathbf{K} \begin{pmatrix} \gamma^{qq}_n & \gamma^{qg}_n \\ \gamma^{gq}_n & \gamma^{gg}_n \end{pmatrix} \mathbf{K}^{-1}\left[\mathbf{L}\,\vec{c}_{n,M}(\mu)\right] , \tag{1445}$$

which entails the relation

$$\mathbf{K} \begin{pmatrix} \gamma^{qq}_n & \gamma^{qg}_n \\ \gamma^{gq}_n & \gamma^{gg}_n \end{pmatrix} \mathbf{K}^{-1} = -\mathbf{L}\,\mathbf{T}_n \boldsymbol{\gamma}^{\mathrm{D}(0)}_n \mathbf{T}_n \mathbf{L}^{-1} \tag{1446}$$

together with the coefficient matrices

$$\mathbf{L} = \text{diag}(l_1, l_2) , \tag{1447}$$

$$\mathbf{K} = \text{diag}(k_1, k_2) . \tag{1448}$$

Here, the entries of $\mathbf{K}$ correspond to the (chosen) normalization constants of the quark-antiquark and two-gluon leading twist DAs, i. e., for this work, they are given by (cf. Chapter 3):

$$k_1 = 6 , \quad k_2 = 30 , \tag{1449}$$

whereas for [20] they are defined via

$$k_1 = 6\,, \quad k_2 = 1\,. \tag{1450}$$

On the other hand, $\mathbf{L}$ collects the additional factors of $\sigma = \sqrt{C_f/N_f}$ (except for possible constants, that usually cancel in the quotient l_1/l_2), e. g.,

$$\mathbf{L} = \mathrm{diag}\left(1, \sigma^{-1}\right)\,. \tag{1451}$$

According to Equation 1446, the differences between the formalism of [20] and this work will be present in the off-diagonal elements of the anomalous dimension matrices. Thus, it can be absorbed within the gluonic DA (see also [20]). Moreover, by interchanging the off-diagonal elements related to the anomalous dimension matrix $\boldsymbol{\gamma}_n^{D(0)}$, we may reproduce the LO set-up of [20], as well as that mentioned in Section 3.3.2 (again neglecting extra prefactors, such as those of $\mathbf{L}$, $\mathbf{K}$). However, for this purpose the matrix $\mathbf{T}_n$ (cf. Equation 437) has to be constructed. This is possible due to (see also [20]) the relation

$$\frac{qg\gamma_n^{(0)}}{gq\gamma_n^{(0)}} = \frac{N_n^{(3/2)}}{N_{n-1}^{(5/2)}}\frac{N_f}{C_f}\,. \tag{1452}$$

C.6 NEXT-TO-LEADING ORDER SINGLET EVOLUTION

In this section, we collect the definitions used to reformulate the NLO singlet evolution.

As discussed in Section 3.3.3, the general solution of Equation 429 is given in terms of the partial conformal wave expansion [27]

$$\boldsymbol{\phi}_M\left(x, \mu^2\right) = \sum_{j=0}^{\infty}\left[\sum_{k=j}^{\infty}\boldsymbol{\phi}_k(x)\,\mathbf{B}_{kj}\left(\mu^2, \mu_0^2\right)\right]\boldsymbol{\mathcal{E}}_j\left(\mu^2, \mu_0^2\right)\widetilde{\boldsymbol{\phi}}_{j,M}\left(\mu_0^2\right)\,. \tag{1453}$$

Here, the partial conformal wave matrix

$$\boldsymbol{\phi}_j\left(x; \mu^2, \mu_0^2\right) = \sum_{k=j}^{\infty}\boldsymbol{\phi}_k(x)\,\mathbf{B}_{kj}\left(\mu^2, \mu_0^2\right)\,, \tag{1454}$$

with the LO kernel eigenfunctions

$$\boldsymbol{\phi}_k(x) = \mathrm{diag}\left(\frac{x\bar{x}}{N_k^{(3/2)}}C_k^{(3/2)}(\xi_x)\,, \frac{x^2\bar{x}^2}{N_{k-1}^{(5/2)}}C_{k-1}^{(5/2)}(\xi_x)\right)\,, \tag{1455}$$

is an eigenstate of Equation 429 to all orders of α_S (cf. [26]). Moreover, the $\mathbf{B}$-matrix[9]

$$\mathbf{B}_{kj}\left(\mu^2, \mu_0^2\right) = \delta_{kj}\mathbb{1}_2 + \mathbf{B}_{kj}^{(1)}\left(\mu^2, \mu_0^2\right) + \mathcal{O}\left(\alpha_S^2\right) \tag{1456}$$

defines the higher order corrections to the tree-level eigenfunctions, including the non-diagonal behavior of the kernel. It is (up to NLO in α_S) determined by [26]

$$= \frac{1}{\beta_0}\left\{\left[\boldsymbol{\gamma}^{D(0)}, \mathbf{B}^{(1)}\left(\mu^2, \mu_0^2\right)\right] + \frac{\alpha_S\left(\mu^2\right)}{2\pi}\boldsymbol{\gamma}^{ND(1)}\right\} + \mathcal{O}\left(\alpha_S^2\right)\,, \tag{1457}$$

9 We use the abbreviations $\mathbf{B}_{kj}\left(\mu^2, \mu_0^2\right) \equiv \mathbf{B}_{kj}\left(\alpha_S\left(\mu^2\right), \alpha_S\left(\mu_0^2\right)\right)$ and $\boldsymbol{\mathcal{E}}_j\left(\mu^2, \mu_0^2\right) \equiv \boldsymbol{\mathcal{E}}_j\left(\alpha_S\left(\mu^2\right), \alpha_S\left(\mu_0^2\right)\right)$.

with the (NLO) solution (k > j)

$$\mathbf{B}^{(1)}_{kj}\left(\mu^2,\mu_0^2\right) = \frac{\alpha_S\left(\mu^2\right)}{2\pi}\mathcal{D}^j_k\left(\mu^2,\mu_0^2\right), \tag{1458}$$

where we introduce the abbreviation[10]

$$\mathcal{D}^k_n\left(\mu^2,\mu_0^2\right) = \sum_{a,b=\pm}\mathcal{R}^{ab}_{nk}\left(\mu^2,\mu_0^2\right)\mathbf{P}^a_n\mathcal{M}^k_n\mathbf{P}^b_k, \tag{1459}$$

with

$$\mathcal{R}^{ab}_{nk}\left(\mu^2,\mu_0^2\right) = \frac{-1}{\gamma_n^{(a)}-\gamma_k^{(b)}-\beta_0}\left\{1-\left[\frac{\alpha_S\left(\mu^2\right)}{\alpha_S\left(\mu_0^2\right)}\right]^{\frac{\gamma_n^{(a)}-\gamma_k^{(b)}-\beta_0}{\beta_0}}\right\}. \tag{1460}$$

Moreover, the scale dependence of multiplicatively renormalizable moments is encoded in the evolution operator

$$\widetilde{\boldsymbol{\Phi}}_{j,M}\left(\mu^2\right) = \mathcal{E}_j\left(\mu^2,\mu_0^2\right)\widetilde{\boldsymbol{\Phi}}_{j,M}\left(\mu_0^2\right), \tag{1461}$$

which is (up to NLO) determined by [26]

$$\frac{d}{d\ln\alpha_S\left(\mu^2\right)}\mathcal{E}^{NLO}\left(\mu^2,\mu_0^2\right) = \frac{1}{\beta_0}\left\{\gamma_j^{D(0)}+\frac{\alpha_S\left(\mu^2\right)}{2\pi}\Gamma_j\right\}\mathcal{E}^{NLO}\left(\mu^2,\mu_0^2\right)+\mathcal{O}\left(\alpha_S^2\right). \tag{1462}$$

This includes the matrix

$$\Gamma_j = \gamma_j^{D(1)} - \frac{\beta_1}{2\beta_0}\gamma_j^{D(0)} \tag{1463}$$

and the boundary condition

$$\mathcal{E}^{NLO}\left(\mu_0^2,\mu_0^2\right) = \mathbb{1}_2 = \mathcal{E}^{LO}\left(\mu_0^2,\mu_0^2\right). \tag{1464}$$

In order to decouple the evolution of f^0_M and the singlet Gegenbauer moments (cf. Section 3.3.3), one has to replace $\gamma_j^{D(1)} \to \gamma_j^{(1)}$ (cf. Equation 466) in Equation 1463. Nevertheless, for the corresponding NLO solution of Equation 1462 we may write

$$\mathcal{E}^{NLO}_j\left(\mu^2,\mu_0^2\right) = \sum_{a,b=\pm}\left[\delta^{ab}\mathbf{P}^a_j+\frac{\alpha_S\left(\mu^2\right)}{2\pi}\mathcal{R}^{ab}_{jj}\left(\mu^2,\mu_0^2\right)\mathbf{P}^a_j\Gamma_j\mathbf{P}^b_j\right]\left[\frac{\alpha_S\left(\mu^2\right)}{\alpha_S\left(\mu_0^2\right)}\right]^{\frac{\gamma_j^{(b)}}{\beta_0}}. \tag{1465}$$

In general, the definitions of Equation 1465 and Equation 1458 ensure, that there are no radiative corrections at the reference scale μ_0^2. Therefore, the Gegenbauer moments at μ_0^2 are defined via

$$\widetilde{\boldsymbol{\Phi}}_{j,M}\left(\mu_0^2\right) = \int_0^1 dx\, C_j(x)\,\boldsymbol{\Phi}_M\left(x,\mu_0^2\right), \tag{1466}$$

using the matrix (cf. [26])

$$C_j(x) = \mathrm{diag}\left(C_j^{(3/2)}(\xi_x), C_{j-1}^{(5/2)}(\xi_x)\right). \tag{1467}$$

10 These choices create an analogy to Equation 1397 and Equation 1398 of the octet case.

PARTICLE:	VALENCE STATE:	FLAVOR STRUCTURE:
π^-	$\bar{u}d$	$T^1 + iT^2$
K^-	$\bar{u}s$	$T^4 + iT^5$
$\overline{K}^0$	$\bar{d}s$	$T^6 + iT^7$
π^0	$\frac{1}{\sqrt{2}}(\bar{u}u - \bar{d}d)$	$\sqrt{2}T^3$
η, η'	$\left\{ \begin{array}{c} \frac{1}{\sqrt{3}}(\bar{u}u + \bar{d}d + \bar{s}s) \\ \frac{1}{\sqrt{6}}(\bar{u}u + \bar{d}d - 2\bar{s}s) \end{array} \right\}$	$\left\{ \begin{array}{c} \sqrt{2}T^0 \\ \sqrt{2}T^8 \end{array} \right\}$

Table 22: The flavor structure Equation 1470 of the corresponding valence quark state "$\overline{\Psi}\mathcal{F}\Psi$" (omitting the associate Lorentz structure, etc.).

Furthermore, a compatibility with the formalism of this work requires the following substitutions (cf. Section 3.3.3):

$$\widetilde{\Phi}_{j,M}\left(\mu_0^2\right) = f_M^0\left(\mu_0^2\right) \mathbf{T}_j \vec{c}_{j,M}\left(\mu_0^2\right) , \tag{1468}$$

$$\Phi_j(x) = \Psi_j(x)\, \mathbf{T}_j^{-1} , \tag{1469}$$

which may be seen by a straightforward calculation. When inserting Equation 1458, Equation 1465, Equation 1468 and Equation 1469 in the general solution of Equation 1453, we get the NLO expression, as given by Equation 455.

C.7 EQUATIONS OF MOTION

In the following, we provide some basic details, which are needed to derive the necessary EOM. Moreover, in order to shorten the results, we apply Equation 141. The latter is especially useful, when relating the specific flavor structure[11] ($\alpha_A \in \mathbb{C}$)

$$\mathcal{F} = \sum_{A=0}^{8} \alpha_A T^A \tag{1470}$$

to the valence quark content "$\overline{\Psi}_f [\mathcal{F}]^{ff'} \Psi_{f'}$" of a given particle. Thus, for kaons and charged pions we get (cf. Table 22), Equation 1470 boils down to ($A = 1, 4, 6$)

$$\mathcal{F} = T^A \pm iT^{A+1} , \tag{1471}$$

while π^0 along with $\eta^{(\prime)}$ imply ($A = 0, 3, 8$)

$$\mathcal{F} = \sqrt{2}T^A . \tag{1472}$$

Additionally, the abbreviations defined in Equation 1070 and Equation 1071 have to be applied. In a nutshell, a reasonable ansatz to devise relations between DAs is based on non-local operator identities, known as EOM. For this work it is sufficient to analyze the total translation and dilatation of (cf. [313] and references therein)

$$\overline{\Psi}_f(n) \left[\sqrt{2}T^A\right]^{ff'} \sigma_{\mu\nu}\gamma_5 \Psi_{f'}(-n) , \tag{1473}$$

11 In the context of Table 22, the related anti-particles would have a flavor structure proportional to $\mathcal{F}^\dagger$ corresponding to $\mathcal{F}$ of the particle.

along with

$$\overline{\Psi}_f(n)\left[\sqrt{2}T^A\right]^{ff'}\gamma_\mu\gamma_5\Psi_{f'}(-n)\ . \tag{1474}$$

In this context, all required EOM contain the standard QCD EOM (cf. Equation 1155, Equation 1156)

$$\gamma_\mu\frac{\partial}{\partial x_\mu}\psi(x) = ig\mathcal{A}^\mu(x)\,\gamma_\mu\psi(x) - im_\psi\psi(x) \tag{1475}$$

$$\frac{\partial}{\partial x_\mu}\bar{\psi}(x)\,\gamma_\mu = -ig\bar{\psi}(x)\,\gamma_\mu\mathcal{A}^\mu(x) + im_\psi\bar{\psi}(x) \tag{1476}$$

and derivatives of Wilson-lines[12], similar to (cf., e. g., [646])

$$\begin{aligned}\frac{\partial}{\partial h_\mu}\left[x+h,h-x\right]\Big|_{h\to0} &= ig\mathcal{A}^\mu(x)\,[x,-x] - ig\,[x,-x]\,\mathcal{A}^\mu(-x)\\ &\quad - ig\int_{-1}^{1}dv\ [x,vx]\,x_\rho\mathcal{G}^{\rho\mu}(vx)\,[vx,-x]\ ,\end{aligned} \tag{1477}$$

$$\begin{aligned}\frac{\partial}{\partial x_\mu}[x,-x] &= ig\mathcal{A}^\mu(x)\,[x,-x] + ig\,[x,-x]\,\mathcal{A}^\mu(-x)\\ &\quad - ig\int_{-1}^{1}dv\ [x,vx]\,vx_\rho\mathcal{G}^{\rho\mu}(vx)\,[vx,-x]\ .\end{aligned} \tag{1478}$$

In the following, we also use the abbreviation [271]

$$\partial_\rho F(x) = \frac{\partial}{\partial h_\rho}F(x+h)\Big|_{h\to0}\ , \tag{1479}$$

and omit the gauge-links. Furthermore, we assume non-vanishing (light-like) distances. After a short straight forward calculation (applying Equation 1475-Equation 1478), we can reproduce the well known EOMs (cf. [3, 271, 313, 315])

$$\begin{aligned}\frac{\partial}{\partial x_\mu}\{\bar{\chi}(x)\,\sigma_{\mu\nu}\gamma_5\psi(-x)\} &= -\partial_\nu\bar{\chi}(x)\,i\gamma_5\psi(-x) - \left(m_\chi+m_\psi\right)\bar{\chi}(x)\,\gamma_\nu\gamma_5\psi(-x)\\ &\quad - ig\int_{-1}^{1}dv\,\bar{\chi}(x)\,x_\rho\mathcal{G}^\rho{}_\nu(vx)\,i\gamma_5\psi(-x)\\ &\quad - ig\int_{-1}^{1}dv\,\bar{\chi}(x)\,vx_\rho\mathcal{G}^{\rho\mu}(vx)\,\sigma_{\mu\nu}\gamma_5\psi(-x)\ ,\end{aligned} \tag{1480}$$

$$\begin{aligned}\partial^\mu\{\bar{\chi}(x)\,\sigma_{\mu\nu}\gamma_5\psi(-x)\} &= -\frac{\partial}{\partial x_\nu}\bar{\chi}(x)\,i\gamma_5\psi(-x) + \left(m_\psi-m_\chi\right)\bar{\chi}(x)\,\gamma_\nu\gamma_5\psi(-x)\\ &\quad - ig\int_{-1}^{1}dv\,\bar{\chi}(x)\,vx_\rho\mathcal{G}^\rho{}_\nu(vx)\,i\gamma_5\psi(-x)\\ &\quad - ig\int_{-1}^{1}dv\,\bar{\chi}(x)\,x_\rho\mathcal{G}^{\rho\mu}(vx)\,\sigma_{\mu\nu}\gamma_5\psi(-x)\ ,\end{aligned} \tag{1481}$$

12 When calculating the EOM, contributions of gluon-four potentials related to the Dirac equations will cancel with counter terms caused by Equation 1477 and Equation 1478.

along with

$$\frac{\partial}{\partial x_\mu}\{\bar{\chi}(x)\,\gamma_\mu\gamma_5\psi(-x)\} = \left(m_\chi - m_\psi\right)\bar{\chi}(x)\,i\gamma_5\psi(-x) - ig\int_{-1}^{1} d\nu\,\bar{\chi}(x)\,\nu x_\rho\,\mathcal{G}^{\rho\mu}(\nu x)\,\gamma_\mu\gamma_5\psi(-x)\;, \tag{1482}$$

$$\partial^\mu\{\bar{\chi}(x)\,\gamma_\mu\gamma_5\psi(-x)\} = \left(m_\psi + m_\chi\right)\bar{\chi}(x)\,i\gamma_5\psi(-x) - ig\int_{-1}^{1} d\nu\,\bar{\chi}(x)\,x_\rho\,\mathcal{G}^{\rho\mu}(\nu x)\,\gamma_\mu\gamma_5\psi(-x)\;, \tag{1483}$$

which are valid for arbitrary quark flavors χ and ψ, e. g., $\chi,\psi = u, d, s$. We also have to consider a shifted version of Equation 1483 for equal flavors (cf. Section 3.4.3)

$$\partial^\mu\left\{\bar{\psi}(x+a)\,\gamma_\mu\gamma_5\psi(b-x)\right\} = -i\int_0^1 d\nu\,\bar{\psi}(x+a)\,\Delta_\rho g\mathcal{G}^{\rho\mu}(\nu(a+x)+\bar{\nu}\,(b-x))\,\gamma_\mu\gamma_5\psi(b-x) + 2m_\psi\bar{\psi}(x+a)\,i\gamma_5\psi(b-x)\;, \tag{1484}$$

with $\Delta_\rho = (a-b+2x)_\rho$, e. g., $a_\mu = z_1 n_\mu$ and $b_\mu = z_2 n_\mu$ (cf. Chapter 3). Although Equation 1480-Equation 1483 are most suitable for describing kaons and charged pions (cf. Table 22), it seems more convenient to model adequate EOMs in terms of related symmetry currents when considering π^0 and $\eta^{(\prime)}$ mesons. Accordingly, when combining Equation 1480 and Equation 1481 with Equation 1069, we get[13]:

$$\begin{aligned}
&\partial^\mu\left\{\overline{\Psi}_f(x)\,\sigma_{\mu\nu}\gamma_5\left[\sqrt{2}T^A\right]^{ff'}\Psi_{f'}(-x)\right\}\\
&= -\frac{\partial}{\partial x^\nu}\left\{\overline{\Psi}_f(x)\,i\gamma_5\left[\sqrt{2}T^A\right]^{ff'}\Psi_{f'}(-x)\right\} + \sum_{B\in I}\beta_{AB}\overline{\Psi}_f(x)\,\gamma_\nu\gamma_5\left[\sqrt{2}T^B\right]^{ff'}\Psi_{f'}(-x)\\
&\quad - ig\int_{-1}^{1} d\nu\,\overline{\Psi}_f(x)\,\nu x^\rho\mathcal{G}_{\rho\nu}(\nu x)\,i\gamma_5\left[\sqrt{2}T^A\right]^{ff'}\Psi_{f'}(-x)\\
&\quad - ig\int_{-1}^{1} d\nu\,\overline{\Psi}_f(x)\,x^\rho\mathcal{G}_\rho{}^\mu(\nu x)\,\sigma_{\mu\nu}\gamma_5\left[\sqrt{2}T^A\right]^{ff'}\Psi_{f'}(-x)\;,
\end{aligned} \tag{1485}$$

along with

$$\begin{aligned}
&\frac{\partial}{\partial x_\mu}\left\{\overline{\Psi}_f(x)\,\sigma_{\mu\nu}\gamma_5\left[\sqrt{2}T^A\right]^{ff'}\Psi_{f'}(-x)\right\}\\
&= -\partial_\nu\left\{\overline{\Psi}_f(x)\,i\gamma_5\left[\sqrt{2}T^A\right]^{ff'}\Psi_{f'}(-x)\right\} - \sum_{B\in I}\alpha_{AB}\overline{\Psi}_f(x)\,\gamma_\nu\gamma_5\left[\sqrt{2}T^B\right]^{ff'}\Psi_{f'}(-x)\\
&\quad - ig\int_{-1}^{1} d\nu\,\overline{\Psi}_f(x)\,x^\rho\mathcal{G}_{\rho\nu}(\nu x)\,i\gamma_5\left[\sqrt{2}T^A\right]^{ff'}\Psi_{f'}(-x)\\
&\quad - ig\int_{-1}^{1} d\nu\,\overline{\Psi}_f(x)\,\nu x^\rho\mathcal{G}_\rho{}^\mu(\nu x)\,\sigma_{\mu\nu}\gamma_5\left[\sqrt{2}T^A\right]^{ff'}\Psi_{f'}(-x)\;.
\end{aligned} \tag{1486}$$

13 Such a closed form unleashes its full power in the context of the SO basis, where the different flavors a priori belong to fundamentally different currents.

Here, we may either set $I = \{0, 1, \dots, 8\}$ or $I = \{q, s, 1, \dots, 7\}$, while using $A = 8, 0$ or $A = q, s$. Analogously, the two-particle twist four DAs can be constrained with

$$\begin{aligned}
&\partial^\mu \left\{ \overline{\Psi}_f(x)\, \gamma_\mu \gamma_5 \left[\sqrt{2} T^A\right]^{ff'} \Psi_{f'}(-x) \right\} \\
&= -ig \int_{-1}^{1} dv\, \overline{\Psi}_f(x)\, x^\alpha G_{\alpha\mu}(vx)\, \gamma^\mu \gamma_5 \left[\sqrt{2} T^A\right]^{ff'} \Psi_{f'}(-x) \\
&\quad + \sum_{B \in I} \alpha_{AB} \overline{\Psi}_f(x)\, i\gamma_5 \left[\sqrt{2} T^B\right]^{ff'} \Psi_{f'}(-x) \,, \qquad (1487)
\end{aligned}$$

as well as

$$\begin{aligned}
&\frac{\partial}{\partial x_\mu} \left\{ \overline{\Psi}_f(x)\, \gamma_\mu \gamma_5 \left[\sqrt{2} T^A\right]^{ff'} \Psi_{f'}(-x) \right\} \\
&= -ig \int_{-1}^{1} dv\, \overline{\Psi}_f(x)\, vx^\alpha G_{\alpha\mu}(vx)\, \gamma^\mu \gamma_5 \left[\sqrt{2} T^A\right]^{ff'} \Psi_{f'}(-x) \\
&\quad - \sum_{B \in I} \beta_{AB} \overline{\Psi}_f(x)\, i\gamma_5 \left[\sqrt{2} T^B\right]^{ff'} \Psi_{f'}(-x) \,. \qquad (1488)
\end{aligned}$$

With Equation 1485-Equation 1488 at light-like separations, a consistent application of Equation 325 and Equation 327-Equation 331 is possible (cf. Section 3.4).

C.8 TWIST-THREE DISTRIBUTION AMPLITUDES

This short supplement, provides selected details related to the derivation of two-particle twist-three $\eta^{(\prime)}$ meson DAs. In the following we, therefore, take the chance to calculate[14] all involved quantities and cross-check our results with those of the existing pion and kaon case (cf. [142, 271]). The latter are presented in Section C.9.

One method (cf. Section 3.4.2) to derive the explicit solutions for Equation 502, along with Equation 513 is based on a formal expansion of Equation 489 and Equation 490 in powers of $P{\cdot}n = P_+$ (with $n^2 = 0$). As a consequence, the generic expressions

$$\int_0^1 dx\, e^{i\xi_x P_+} \xi_x \phi(x) = \sum_{m=0}^{\infty} \frac{(iP_+)^m}{m!} \left[M^\phi_{m+1} \right] , \qquad (1489)$$

$$iP_+ \int_0^1 dx\, e^{i\xi_x P_+} \phi(x) = \sum_{m=0}^{\infty} \frac{(iP_+)^m}{m!} \left[m\, M^\phi_{m-1} \right] , \qquad (1490)$$

$$iP_+ \int_0^1 dx\, e^{i\xi_x P_+} \xi_x \phi(x) = \sum_{m=0}^{\infty} \frac{(iP_+)^m}{m!} \left[m\, M^\phi_{m} \right] , \qquad (1491)$$

as well as (cf. Equation 494, with $\underline{z} = (-1, 1, v)$)

$$\int_{-1}^{1} dv\, \Phi^A_{3M}(\underline{z}, P_+) = \sum_{m=0}^{\infty} \frac{(iP_+)^m}{m!} \int_{-1}^{1} dv \ll (\alpha_1 - \alpha_2 - v\,\alpha_3)^m \gg , \qquad (1492)$$

$$iP_+ \int_{-1}^{1} dv\, v\, \Phi^A_{3M}(\underline{z}, P_+) = \sum_{m=0}^{\infty} \frac{(iP_+)^m}{m!} \int_{-1}^{1} dv\, vm \ll (\alpha_1 - \alpha_2 - v\,\alpha_3)^{m-1} \gg , \qquad (1493)$$

14 For this purpose, we have reverse engineered the findings of [332] and applied the techniques in a broader context.

arise[15]. Again, the test function "ϕ" represents an arbitrary DA. Evidently, dependencies on the indices "m" may be translated into derivatives with respect to the longitudinal parton momentum fractions, via integration by parts. Hence, we find the identity[16] ($n, k \in \mathbb{N}_0$)

$$2\,(n+k)\,M_n^{\phi} = 2\,(k-1)\,M_n^{\phi} - M_{n+1}^{\phi'} + \xi_x^{n+1}\phi(x)\Big|_0^1 , \tag{1494}$$

which unleashes its full power when used iteratively or as superposition for different values of the involved indices. For instance, Equation 497 implies the pattern (including an auxiliary function $\mathcal{L}(x)$)

$$(n+1)\,M_n^{\phi} - (n-1)\,M_{n-2}^{\phi} = \frac{1}{2} M_{n-1}^{\mathcal{L}} , \tag{1495}$$

with the solution[17] (cf. Equation 1494)

$$\int_0^1 dx\,\xi_x^{n-1}\left[4x\bar{x}\,\tfrac{d}{dx}\phi(x)\right] - \xi_x^{n-1}\left[4x\bar{x}\,\phi(x)\right]\Big|_0^1 = \int_0^1 dx\,\xi_x^{n-1}\mathcal{L}(x) . \tag{1496}$$

According to the formal structure of $\phi_{3M}^{A;p}$ (cf. Equation 479) all surface terms in Equation 1496 vanish, i. e., for the substitution $\phi \to \phi_{3M}^{A;p}$. Surface terms also vanish for the discussed integral equations which can include $\phi_{3M}^{A;\sigma}$, ϕ_M^A, $\varphi_{3M}^{A;(1)}$ as well as $\varphi_{3M}^{A;(2)}$ (see discussion below). Furthermore, for the proper derivation of all source terms, Equation 497 has to be converted into the form of Equation 1496. For example, Equation 497 gives rise to[18]

$$(n+1)\,M_n^{\phi_{3M}^{A;p}} - (n-1)\,M_{n-2}^{\phi_{3M}^{A;p}}\Big|_{\underline{\rho}^M} = \sum_{B\in I}\left[\underline{\rho}^M\right]^{AB}(n+1)\,M_{n-1}^{\phi_M^B}, \tag{1497}$$

which may be solved with Equation 1494:

$$2(n+1)\,M_{n-1}^{\phi} = \xi_x^n\phi(x)|_0^1 + \int_0^1 dx\,\xi_x^{n-1}\left[2\phi(x) - \xi_x\phi'(x)\right] . \tag{1498}$$

The appearance of Equation 1498, however, changes after integration (cf. Equation 505), because the contributions in $(\xi_{\bar{\nu}} = -\xi_\nu)$

$$\frac{1}{\bar{\nu}}\left[2\phi(\nu) - \xi_\nu\phi'(\nu)\right] = \frac{1}{\bar{\nu}}\left[2\phi(\nu) - \phi'(\nu)\right] + 2\phi'(\nu) , \tag{1499}$$

$$\frac{1}{\nu}\left[2\phi(\nu) - \xi_\nu\phi'(\nu)\right] = \frac{1}{\nu}\left[2\phi(\nu) + \phi'(\nu)\right] - 2\phi'(\nu) , \tag{1500}$$

proportional to "$2\phi'(\nu)$" imply vanishing surface terms. Similar considerations lead to the solution Equation 500, along with Equation 503 to Equation 505. Some three-particle contributions cannot be solved by the (multiple) application of Equation 1494 alone. For instance (cf. Equation 497):

$$4(n-1)(n-2)M_{n-3}^{\phi} = M_{n-1}^{\phi''} - \xi_x^{n-2}\left[\xi_x\phi'(x) - 2\,(n-1)\,\phi(x)\right]\Big|_0^1 \tag{1501}$$

15 For the derivation of Equation 1489–Equation 1493 in their present form, the interchangeability of summation and integration has been assumed.

16 Here, we use the abbreviations $\phi'(x) = \frac{d}{dx}\phi(x)$ and $\phi''(x) = \frac{d^2}{dx^2}\phi(x)$.

17 Due to the structure of Equation 1496, all source terms (and involved DAs) are well-defined up to a possible null set. In order to eliminate this apparent ambiguity, one may define adequate equivalent relations and quotient spaces (cf. [647]).

18 Equation 1497 is restricted to the contributions of Equation 497 proportional to $\underline{\rho}^M$.

additionally requires relations similar to

$$4(n+1)(n-1)\,M^{\phi}_{n-2} = \int_0^1 dx\,\xi_x^{n-1}\left[\xi_x\phi''(x) - 2\phi'(x)\right] - \xi_x^{n-1}\left[\xi_x\phi'(x) - 2\,(n+1)\,\phi(x)\right]\Big|_0^1 . \tag{1502}$$

Analogously, the careful use of Equation 1494, e. g.,

$$(n+3)\,M^{\phi}_{n} - (n-1)\,M^{\phi}_{n-2} = 2\int_0^1 dx\,\xi_x^{n-1}\left[\xi_x\phi(x) + x\bar{x}\,\phi'(x)\right] - 2\xi_x^{n-1}x\bar{x}\,\phi(x)\Big|_0^1 \tag{1503}$$

reveals the underlying structure of Equation 512 and $\phi^{A;\sigma}_{3M}$. It should be noted, that similar structures, such as Equation 503–Equation 505 and Equation 514–Equation 516 have been found for the kaon case (cf. [271]). Therefore, we confirm their universal structure for the pseudoscalar meson sector and extend their use to the $\eta^{(\prime)}$ mesons.
Before we proceed, let us discuss the structure of twist-three DAs formulated in the SO basis (cf. Section 3.4.2 for definitions). In analogy to Equation 553 we propose the following definitions ($M = \eta, \eta'$)

$$h^8_M = \alpha_{88} f^8_M h^8_{3M}\,, \quad h^0_M = \alpha_{00} f^0_M h^0_{3M}\,, \tag{1504}$$

which formally give rise to (cf. Equation 524)

$$\frac{h^8_M}{\alpha_{88}} = -\frac{f^8_M m^2_M \alpha_{00} + \sqrt{3}a_M\alpha_{80} - f^0_M m^2_M \alpha_{80}}{\alpha^2_{80} - \alpha_{00}\alpha_{88}}\,, \tag{1505}$$

$$\frac{h^0_M}{\alpha_{00}} = \frac{f^8_M m^2_M \alpha_{80} + \sqrt{3}a_M\alpha_{88} - f^0_M m^2_M \alpha_{88}}{\alpha^2_{80} - \alpha_{00}\alpha_{88}}\,. \tag{1506}$$

The latter are consistent with Equation 559 and Equation 560 (see also Table 8). Additionally, in the $SU(3)_F$ limit, i. e.,

$$\overline{m} = \tfrac{1}{3}\,(m_u + m_d + m_s)\,, \tag{1507}$$

$$\alpha_{00},\ \alpha_{88} \to 2\overline{m}\,, \tag{1508}$$

$$\alpha_{08} \to 0\,, \tag{1509}$$

Equation 1505 and Equation 1506 boil down to

$$h^0_M = m^2_M f^0_M - \sqrt{3}a_M\,, \quad h^8_M = m^2_M f^8_M\,. \tag{1510}$$

This profound simplification may also be seen on the level of twist-three[19] DAs ($A = 0, 8$)

$$h^A_M \phi^{A;\sigma}_{3M}(x) =: \overline{\phi}^{A;\sigma}_{3M}(x)\,, \quad h^A_M \phi^{A;p}_{3M}(x) =: \overline{\phi}^{A;p}_{3M}(x)\,, \tag{1511}$$

which are formally defined via (analogously for "$8 \leftrightarrow 0$")

$$\overline{\phi}^{8;p}_{3M}(x) = h^8_M + \alpha_{88} f^8_{3M}\phi^{8;(g)}_{3M}(x) + \alpha^2_{88} f^8_M \phi^{8;(+)}_{3M}(x) + \alpha_{08}\alpha_{88} f^0_M \phi^{0;(+)}_{3M}(x)\,, \tag{1512}$$

$$\overline{\phi}^{8;\sigma}_{3M}(x) = 6x\bar{x}h^8_M + \alpha_{88} f^8_{3M}\widetilde{\phi}^{8;(g)}_{3M}(x) + \alpha^2_{88} f^8_M \widetilde{\phi}^{8;(+)}_{3M}(x) + \alpha_{08}\alpha_{88} f^0_M \widetilde{\phi}^{0;(+)}_{3M}(x)\,. \tag{1513}$$

19 As discussed in Section 3.4.2, it is reasonable to absorb all h^A_M factors into the corresponding DAs.

According to the assumed NLO accuracy in conformal spin and within the $SU(2)_I$ limit, we, therefore, get (similar for "$8 \leftrightarrow 0$")

$$\begin{aligned}
\overline{\phi}^{8;p}_{3M}(x) &= h^8_M + 3\alpha_{88}\left[\alpha_{08} f^0_M\left(1+6c^{(0)}_{2,M}\right) + \alpha_{88} f^8_M\left(1+6c^{(8)}_{2,M}\right)\right] \\
&\quad + 15\alpha_{88}\left(2f^8_{3M} + \alpha_{08} f^0_M c^{(0)}_{2,M} + \alpha_{88} f^8_M c^{(8)}_{2,M}\right) C_2^{(1/2)}(\xi_x) \\
&\quad - 3\alpha_{88} f^8_{3M}\omega^8_{3M} C_4^{(1/2)}(\xi_x) + \frac{3}{2}\alpha_{88}\left[\alpha_{08} f^0_M\left(1+6c^{(0)}_{2,M}\right)\right. \\
&\quad \left. + \alpha_{88} f^8_M\left(1+6c^{(8)}_{2,M}\right)\right]\log x\bar{x}\,, \qquad (1514)\\
\overline{\phi}^{8;\sigma}_{3M}(x) &= 6x\bar{x}\left\{h^8_M + \frac{3}{2}\alpha_{88}\left[\alpha_{08} f^0_M\left(1+10c^{(0)}_{2,M}\right) + \alpha_{88} f^8_M\left(1+10c^{(8)}_{2,M}\right)\right]\right. \\
&\quad \left. + \frac{1}{2}\alpha_{88}\left[10f^8_{3M} - f^8_{3M}\omega^8_{3M} + 3\alpha_{08} f^0_M c^{(0)}_{2,M} + 3\alpha_{88} f^8_M c^{(8)}_{2,M}\right] C_2^{(3/2)}(\xi_x)\right\} \\
&\quad + 9x\bar{x}\alpha_{88}\left[\alpha_{08} f^0_M\left(1+6c^{(0)}_{2,M}\right) + \alpha_{88} f^8_M\left(1+6c^{(8)}_{2,M}\right)\right]\log x\bar{x}\,. \qquad (1515)
\end{aligned}$$

In particular, the $SU(3)_F$ symmetric DAs ($A = 8, 0$)

$$\begin{aligned}
\overline{\phi}^{A;p}_{3M}(x) &= h^A_M + 12\overline{m}^2 f^A_M\left(1+6c^{(A)}_{2,M}\right) + 60\left(\overline{m} f^A_{3M} + \overline{m}^2 f^A_M c^{(A)}_{2,M}\right) C_2^{(1/2)}(\xi_x) \\
&\quad - 6\overline{m} f^A_{3M}\omega^A_{3M} C_4^{(1/2)}(\xi_x) + 6\overline{m}^2 f^A_M\left(1+6c^{(A)}_{2,M}\right)\log x\bar{x}\,, \qquad (1516)\\
\overline{\phi}^{A;\sigma}_{3M}(x) &= 6x\bar{x}\left[h^A_M + 6\overline{m}^2 f^A_M\left(1+10c^{(A)}_{2,M}\right)\right. \\
&\quad \left. + \left(10\overline{m} f^A_{3M} - \overline{m} f^A_{3M}\omega^A_{3M} + 6\overline{m}^2 f^A_M c^{(A)}_{2,M}\right) C_2^{(3/2)}(\xi_x)\right] \\
&\quad + 36x\bar{x}\overline{m}^2 f^A_M\left(1+6c^{(A)}_{2,M}\right)\log x\bar{x}\,, \qquad (1517)
\end{aligned}$$

formally correspond to their QF counter parts, i. e., as given by Equation 554 and Equation 555, after replacing all relevant parameters, such as "$\{8, 0\} \leftrightarrow \{q, s\}$", along with "$\overline{m} \leftrightarrow m_q, m_s$" the associated quark mass terms.

Nevertheless, the QF DAs rely on milder constraints and consequently have a larger scope of application (cf. discussion in Section 3.4.2). Therefore, let us resume the initial problem statement, i. e., Equation 474 and Equation 475. For the corresponding explicit calculation of $\phi^{R;M}_{\uparrow\downarrow}$ and $\phi^{R;M}_{\downarrow\uparrow}$ ($R = q, s$; $M = \eta, \eta'$), Equation 476 as well as Equation 477 have to be written as[20]:

$$\phi^{R;M}_{\uparrow\downarrow}\left(x,\mu^2\right) = \phi^{R;p}_{3M}\left(x,\mu^2\right) + \frac{1}{6}\frac{d}{dx}\phi^{R;\sigma}_{3M}\left(x,\mu^2\right)\,, \qquad (1518)$$

$$\phi^{R;M}_{\downarrow\uparrow}\left(x,\mu^2\right) = \phi^{R;p}_{3M}\left(x,\mu^2\right) - \frac{1}{6}\frac{d}{dx}\phi^{R;\sigma}_{3M}\left(x,\mu^2\right)\,. \qquad (1519)$$

Based on Equation 554, along with Equation 555 (cf. Section A.12 for the used orthogonality relations) we, therefore, find the conformal coefficients:

$$\left.\begin{aligned}
\kappa^{R;M}_0 &= h^R_M + 12\left[1+6c^{(R)}_{2,M}\right] f^R_M m^2_A = \overline{\kappa}^{R;M}_0\,,\\
\kappa^{R;M}_1 &= -24c^{(R)}_{2,M} f^R_M m^2_R = -\overline{\kappa}^{R;M}_1\,,\\
\kappa^{R;M}_2 &= 12m_R\left[5f^R_{3M} + 3c^{(R)}_{2,M} f^R_M m_R\right] = \overline{\kappa}^{R;M}_2\,,\\
\kappa^{R;M}_3 &= 6f^R_{3M}\omega^R_{3M} m_R = -\overline{\kappa}^{R;M}_3\,.
\end{aligned}\right\} \qquad (1520)$$

20 Note that EOM relations among $\phi^{R;M}_{\uparrow\downarrow}$ (or $\phi^{R;M}_{\downarrow\uparrow}$) and $\phi^{R;\sigma}_{3M}$, as mentioned in [271, Chapter 3, p. 13] can be readily derived from Equation 1518 and Equation 1519.

TWIST-TWO	TWIST-THREE	AUXILIARY QUANTITIES
$\phi_M^R \to \phi_K$	$\Phi_{3M}^A \to \Phi_{3;K}$ $\phi_{3M}^{A;p} \to \phi_{3;K}^p$ $\phi_{3M}^{A;\sigma} \to \phi_{3;K}^\sigma$	$\phi_{3M}^{A;(g)} \to \phi_{3,g}^p$ $\phi_{3M}^{A;(\pm)} \to \phi_{3,\pm}^p$ $\widetilde{\phi}_{3M}^{A;(g)} \to \phi_{3,g}^\sigma$ $\widetilde{\phi}_{3M}^{A;(\pm)} \to \phi_{3,\pm}^\sigma$
$f_M^A \to f_K$ $c_{n,M}^{(R)} \to a_n^K$	$f_{3M}^A \to f_{3K}$ $\lambda_{3M}^A \to \lambda_{3K}$ $\omega_{3M}^A \to \omega_{3K}$	$\sum_{B\in I} \left[\rho_\pm^M\right]^{AB} \phi_{3M}^{B;(\pm)} \to \rho_\pm^K \phi_{3,\pm}^p$ $\sum_{B\in I} \left[\rho_\pm^M\right]^{AB} \widetilde{\phi}_{3M}^{B;(\pm)} \to \rho_\pm^K \phi_{3,\pm}^\sigma$ $R_{3M}^A \to \eta_{3K}$

Table 23: Replacement rules (at NLO in conformal spin), used to reproduce the twist-three kaon DAs (cf. [271]) via the results of Chapter 3.

Moreover, up to the assumed accuracy, we may set $\kappa_n^{R;M} \equiv 0 \equiv \bar{\kappa}_n^{R;M}$ for $n \geqslant 4$, while the related logarithmic corrections (cf. Equation 479, Equation 480) are given by

$$\kappa_{\log}^{R;M} = 12\left[1 + 6c_{2,M}^{(R)}\right] f_M^R m_R^2 = \bar{\kappa}_{\log}^{R;M} . \tag{1521}$$

Before concluding this supplement, we emphasize, that the use of all named identities is not restricted to twist-three DAs. Instead, similar integral equations, such as Equation 665 or Equation 669, with (see Equation 334, while using "$\alpha_3 = 1 - \alpha_1 - \alpha_2$")

$$\int_{-1}^{1} d\nu \int \mathcal{D}\underline{\alpha}\, [\alpha_1 - \alpha_2 - \nu\alpha_3]^{n-1}\, \mathcal{F}(\underline{\alpha}) = \int_0^1 dx\, \xi_x^{n-1} \int_0^x d\alpha_1 \int_0^{\bar{x}} d\alpha_2\, \frac{2\,\mathcal{F}(\underline{\alpha})}{\alpha_3}, \tag{1522}$$

$$\int_{-1}^{1} d\nu\, \nu \int \mathcal{D}\underline{\alpha}\, [\alpha_1 - \alpha_2 - \nu\alpha_3]^{n-1}\, \mathcal{F}(\underline{\alpha}) = \int_0^1 dx\, \xi_x^{n-1} \int_0^x d\alpha_1 \int_0^{\bar{x}} d\alpha_2\, \frac{2\,[\alpha_1 - \alpha_2 - \xi_x]\,\mathcal{F}(\underline{\alpha})}{\alpha_3^2}, \tag{1523}$$

arise for the twist-four case. Hence, their solution is similar to the given approach.

C.9 RETROFITTED HIGHER TWIST KAON DISTRIBUTION AMPLITUDES

This section contains a conversion scheme for kaon twist-three DAs, and most importantly an update of the associated twist-four distributions. For the latter, we also introduce all necessary parameters and common estimates, based on [271].

Starting with the former, Equation 1480-Equation 1483 and Equation 1485 to Equation 1488 evidently lead to analogous operator relations which only vary in their flavor structure. Consequently, all implied DAs share a similar structure which is already present in Equation 503-Equation 505 and Equation 514-Equation 516. Thus, instead of introducing adjusted definitions, e. g., (cf. Equation 1471, Table 22; $A = 4, 6$)

$$\langle 0|\overline{\psi}(z_2 n)\, i\gamma_5 \left[T^A + iT^{A+1}\right] \psi(z_1 n)\, |K(P)\rangle\Big|_{n^2=0} = \frac{f_{3K}}{\eta_{3K}} \int_0^1 dx\, e^{-iz_{21}^x (P\cdot n)}\, \phi_{3;K}^p\left(x, \mu^2\right) , \tag{1524}$$

together with (cf. Equation 520, [271], written for the $\mathrm{SU}(2)_\mathrm{I}$ limit)

$$\langle 0|\overline{\psi}\,\sigma_+{}^{\zeta}\gamma_5 g\mathcal{G}_{+\zeta}\left[T^A+iT^{A+1}\right]\psi|K(P)\rangle = 2if_{3K}P_+^2\,, \tag{1525}$$

$$\langle 0|\overline{\psi}\,\gamma_+\gamma_5\left[T^A+iT^{A+1}\right]\psi|K(P)\rangle = if_K P_+\,, \tag{1526}$$

$$\frac{f_{3K}}{f_K}\frac{m_q+m_s}{m_K^2} = \eta_{3K}\,, \tag{1527}$$

we suggest the following replacement rules. Those are intended to reproduce all kaon twist-three DAs, along with other results of [271] (this excludes the sum rule parameters):

i) Up to NLO in conformal spin, the essential replacements are given by Table 23. Those have to be combined with

$$\sqrt{2}T^R \to \left[T^A+iT^{A+1}\right]\,, \tag{1528}$$

for the involved matrix elements (cf. Chapter 3, Section C.7) of charged pions ($A=1$) or kaons ($A=4,6$). Based on the notation of Section 3.4.2, we are, therefore, not only able to reproduce [271, Equation 3.25, Equation 3.26], but also [271, Equation 3.17], along with [271, Equation 3.18-Equation 3.23].

ii) Furthermore, several auxiliary quantities include the definitions[21] (see Table 23) [271]:

$$\rho_+^K = \frac{(m_s+m_q)^2}{m_K^2}\,,\quad \rho_-^K = \frac{m_s^2-m_q^2}{m_K^2}\,. \tag{1529}$$

Nonetheless, under specific conditions, both notations (i. e., the corresponding definitions of Section 3.4.2 and [271]) may coincide. For instance, when neglecting all anomalous contributions and differences in the Gegenbauer moments, the π^- case as implied by (up to NLO and within the strict $\mathrm{SU}(2)_\mathrm{I}$ limit; see [271])

$$a_1^\pi = 0\,,\quad \rho_-^\pi = 0\,,\quad \lambda_{3\pi} = 0\,,\quad \kappa_{4\pi} = 0\quad \text{etc.}, \tag{1530}$$

has a similar formal structure as Equation 563 or Equation 564. Accordingly, this entails the opportunity for another cross-check with[22] [271, Equation 3.25, Equation 3.26] (in the limit Equation 1530) confirm our findings, i. e., Equation 554 and Equation 555.

Notably, for the twist-four DAs, we are able to provide a substantial update. In this context, the improvements are twofold: on the one hand, as a by-product of our investigations, we have recalculated the operator relations for Equation 583. This leads to adjusted three-particle twist-four[23] DAs (cf. Section 3.4.3 and [271]), i. e.,

$$\Phi_{4K}(\underline{\alpha}) = 120\alpha_1\alpha_2\alpha_3\left[\phi_0^K+\phi_1^K(\alpha_1-\alpha_2)+\phi_2^K(3\alpha_3-1)\right]+\ldots\,, \tag{1531}$$

$$\widetilde{\Phi}_{4K}(\underline{\alpha}) = 120\alpha_1\alpha_2\alpha_3\left[\tilde{\phi}_0^K+\tilde{\phi}_1^K(\alpha_1-\alpha_2)+\tilde{\phi}_2^K(3\alpha_3-1)\right]+\ldots\,, \tag{1532}$$

21 These dimensionless parameters are a scalar analogon of the matrices $\left[\boldsymbol{\rho}_\pm^M\right]^{AB}$ (cf. Equation 491). For instance, when assuming the state mixing ansatz as well as $f_{3q}\to f_{3\pi}$, $f_q\to f_\pi$, one may get $\rho_+^\pi = \frac{4m_q^2}{m_\pi^2} = \lim_{m_\eta\to m_\pi}\left(\lim_{a_\eta\to 0}\left[\boldsymbol{\rho}_+^\eta\right]^{qq}\right)$ (cf. Equation 552) and $\eta_{3\pi} = \frac{f_{3\pi}}{f_\pi}\frac{2m_q}{m_\pi^2} = \lim_{m_\eta\to m_\pi}\left(\lim_{a_\eta\to 0} R_{3\eta}^q\right)$.

22 Based on the results of [271] for Equation 1530, it seems reasonable to reproduce all relevant elements of $\left[\boldsymbol{\rho}_+^M\right]^{AB}$ as well as Equation 563, Equation 564, by another set of adequate substitutions (cf. Section 3.4.3). Nevertheless, a thorough calculation of the latter (as done in Section 3.4.2) is preferable.

23 The ellipses in Equation 1531–Equation 1534 represent contributions of higher order conformal spin.

as well as (the ellipses represent neglected higher order correction)

$$\begin{aligned}\Psi_{4K}(\underline{\alpha}) = 30\alpha_3^2\Big[&\theta_0^K(1-\alpha_3)+\theta_1^K[\alpha_3(1-\alpha_3)-6\alpha_1\alpha_2]\\&+\theta_2^K\left[\alpha_3(1-\alpha_3)-\frac{3}{2}\left(\alpha_1^2+\alpha_2^2\right)\right]\\&-(\alpha_1-\alpha_2)\left[\psi_0^K+\alpha_3\psi_1^K+\frac{1}{2}(5\alpha_3-3)\,\psi_2^K\right]\Big]+\dots\,,\end{aligned} \tag{1533}$$

$$\begin{aligned}\widetilde{\Psi}_{4K}(\underline{\alpha}) = -30\alpha_3^2\Big[&\psi_0^K(1-\alpha_3)+\psi_1^K[\alpha_3(1-\alpha_3)-6\alpha_1\alpha_2]\\&+\psi_2^K\left[\alpha_3(1-\alpha_3)-\frac{3}{2}\left(\alpha_1^2+\alpha_2^2\right)\right]\\&-(\alpha_1-\alpha_2)\left[\theta_0^K+\alpha_3\theta_1^K+\frac{1}{2}(5\alpha_3-3)\,\theta_2^K\right]\Big]+\dots\,,\end{aligned} \tag{1534}$$

with coefficients as discussed below. Here, the $\{\theta_i^K\}_{i\in\mathbb{N}_0}$ represent $SU(3)_F$-breaking corrections which induce G-parity violations. Furthermore, we have calculated a state-of-the-art version of all two-particle twist-four DAs, up to NLO accuracy in conformal spin.
Based on Section 3.4.3 the particle's flavor structure is predominantly present within the corresponding decay constants and quark-mass correction (as well as anomaly contributions), e. g., Equation 626 or Equation 627. For instance, the kaon case may be deduced from the latter via:

$$m_q \longrightarrow \frac{1}{2}\,(m_q + m_s)\,, \tag{1535}$$

combined with Equation 1531–Equation 1534 (cf. [271, Equation 4.8]). Similar to Equation 634, the local limit of Equation 628 and Equation 629 (adapted for the kaon case, e. g., [271, Equation 4.2]) together with Equation 1531 to Equation 1534 further reveals [271] (cf. Table 10)

$$\phi_0^K = -\theta_0^K = \frac{1}{3}m_K^2\kappa_{4K}\,, \tag{1536}$$

$$\langle 0|\bar{q}\gamma^\alpha\gamma_5 ig\mathcal{G}_{\mu\alpha}s|K(P)\rangle = iP_\mu f_K m_K^2\kappa_{4K}\,, \tag{1537}$$

while θ_1^K, θ_2^K and ϕ_2^K may, for example, be roughly estimated with the renormalon model[24] [271, 319, 521]

$$\phi_2^K = -\frac{7}{20}a_1^K\delta_K^2\,,\quad \theta_1^K = \frac{7}{10}a_1^K\delta_K^2\,,\quad \theta_2^K = -\frac{7}{5}a_1^K\delta_K^2\,. \tag{1538}$$

24 As discussed in [271], a consistent treatment of G-parity-breaking corrections (up to $J = 4$) would, e. g., require the exclusive application of [271, Equation 4.8]. Nevertheless, similar to [319], we will use Equation 1538 as the best available estimate.

In combination with our newly calculated coefficients (cf. Equation 657–Equation 661 and Equation 1535):

$$\tilde{\phi}_0^K = \psi_0^K = -\frac{1}{3}\delta_K^2, \tag{1539}$$

$$\tilde{\phi}_2^K = \frac{21}{8}\delta_K^2\omega_{4K}\,, \tag{1540}$$

$$\phi_1^K = \frac{21}{8}\left[\delta_K^2\omega_{4K} + \frac{2}{45}m_K^2\left(1-\frac{18}{7}a_2^K\right)\right], \tag{1541}$$

$$\psi_1^K = \frac{7}{4}\left[\delta_K^2\omega_{4K} + \frac{1}{45}m_K^2\left(1-\frac{18}{7}a_2^K\right) + 2\,(m_s+m_q)\frac{f_{3K}}{f_K}\right], \tag{1542}$$

$$\psi_2^K = \frac{7}{4}\left[2\delta_K^2\omega_{4K} - \frac{1}{45}m_K^2\left(1-\frac{18}{7}a_2^K\right) - 2\,(m_s+m_q)\frac{f_{3K}}{f_K}\right], \tag{1543}$$

all NLO twist-four kaon parameters are specified. Analogous to Equation 675 along with Equation 678 and according to the notation of [271], both twist-four two-particle DAs

$$\psi_{4K}(x) = \psi_{4K}^{T4}(x) + \psi_{4K}^{WW}(x)\,, \tag{1544}$$

$$\phi_{4K}(x) = \phi_{4K}^{T4}(x) + \phi_{4K}^{WW}(x)\,, \tag{1545}$$

can be split up into a genuine twist-four contribution (i. e., ψ_{4K}^{T4}, ϕ_{4K}^{T4}) and a Wandzura-Wilczek type mass correction (see [271] and references therein). Correspondingly, we find

$$\psi_{4K}^{T4}(x) = \frac{20}{3}\delta_K^2 C_2^{(1/2)}(\xi_x) + 5\left(2\theta_1^K - \theta_2^K\right)C_3^{(1/2)}(\xi_x)\,, \tag{1546}$$

as well as (see also Equation 1554)

$$\begin{aligned}
\psi_{4K}^{WW}(x) = {} & 6m_K^2\left[\rho_+^K\left(1+6a_2^K\right) - 3\rho_-^K a_1^K\right]C_0^{(1/2)}(\xi_x) \\
& - 3m_K^2\left[4\kappa_{4K} - 9\rho_+^K a_1^K + \rho_-^K\left(1+18a_2^K\right) + \frac{6}{5}a_1^K\right]C_1^{(1/2)}(\xi_x) \\
& + 2m_K^2\left[\frac{1}{3} + 3\left(5\rho_+^K a_2^K - \rho_-^K a_1^K\right) - \frac{6}{7}a_2^K\right]C_2^{(1/2)}(\xi_x) \\
& + \left\{m_K^2\left[\frac{16}{3}\kappa_{4K} - 9\rho_-^K a_2^K + \frac{18}{5}a_1^K\right] + 20\frac{f_{3K}}{f_K}\,(m_q+m_s)\,\lambda_{3K}\right\}C_3^{(1/2)}(\xi_x) \\
& - \left\{\frac{3}{2}\frac{f_{3K}}{f_K}\,(4\omega_{3K}-5)\,(m_q+m_s) - m_K^2\left[\frac{3}{4}+\frac{45}{14}a_2^K\right]\right\}C_4^{(1/2)}(\xi_x) \\
& - 3m_K^2\left(\rho_-^K - \rho_+^K\right)\left[1+3a_1^K+6a_2^K\right]\log\bar{x} \\
& + 3m_K^2\left(\rho_-^K + \rho_+^K\right)\left[1-3a_1^K+6a_2^K\right]\log x\,.
\end{aligned} \tag{1547}$$

For consistency reasons with [271] and Chapter 3, terms proportional[25] to $\rho_\pm^K$, such as

$$\left(\rho_-^K + \rho_+^K\right)m_K^2 = +2m_s\,(m_q+m_s)\,, \tag{1548}$$

$$\left(\rho_-^K - \rho_+^K\right)m_K^2 = -2m_q\,(m_q+m_s)\,, \tag{1549}$$

25 Along with all other corrections of $\mathcal{O}\left(m_\psi^2\right)$.

have to be omitted. Hence, we get:

$$\begin{aligned}\phi_{4K}^{T4}(x) = {} & \frac{200}{3}\delta_K^2 x^2\bar{x}^2 + 20\xi_x x^2\bar{x}^2\left(4\theta_1^K - 5\theta_2^K\right) \\ & + 21\delta_K^2\omega_{4K}\left(\left[2x^3\left(6x^2-15x+10\right)\log x\right] + [x\leftrightarrow\bar{x}] + x\bar{x}\left(2+13x\bar{x}\right)\right) \\ & + 40\phi_2^K\left(\xi_x x\bar{x}(2+3x\bar{x}) - \left[2x^3(x-2)\log x\right] + [x\leftrightarrow\bar{x}]\right), \end{aligned} \tag{1550}$$

along with

$$\begin{aligned}\phi_{4K}^{WW}(x) = {} & \frac{16}{3}m_K^2\kappa_{4K}\left(\xi_x x\bar{x}\left(1-2x\bar{x}\right) + \left[5x^3(x-2)\log x\right] - [x\leftrightarrow\bar{x}]\right) \\ & + \frac{36}{5}m_K^2 a_1^K\xi_x x\bar{x}\left(1+3x\bar{x}\right) + 4\frac{f_{3K}}{f_K}\left(m_q+m_s\right)x\bar{x}\left(30\left(1+\xi_x\frac{m_q-m_s}{m_q+m_s}\right)\right. \\ & - \omega_{3K}\left[3\xi_x\left(1-7x\bar{x}\right)\frac{m_q-m_s}{m_q+m_s} + 3 - 21x\bar{x} + 28x^2\bar{x}^2\right] \\ & \left. + 10\lambda_{3K}\left[\left(1-5x\bar{x}\right)\frac{m_q-m_s}{m_q+m_s} + \xi_x(1-x\bar{x})\right] + \frac{5}{2}x\bar{x}(14x\bar{x}-63)\right) \\ & + \frac{1}{15}m_K^2\left(x\bar{x}\left(88+117x\bar{x}+210x^2\bar{x}^2\right)\right. \\ & \left. + \left[28x^3\left(6x^2-15x+10\right)\log x\right] + [x\leftrightarrow\bar{x}]\right) \\ & - \frac{6}{5}m_K^2 a_2^K\left(x\bar{x}\left(4-9x\bar{x}+150x^2\bar{x}^2\right)\right. \\ & \left. + \left[4x^3\left(6x^2-15x+10\right)\log x\right] + [x\leftrightarrow\bar{x}]\right). \end{aligned} \tag{1551}$$

In Equation 1546, we have corrected another typo (i. e., the figure marked with blue) which has not been spotted before. As mentioned above, a consistent application of the renormalon model [271, 521] would imply different models for Equation 1544 and Equation 1545, such as

$$\left[\psi_{4K}^{T4}(x)\right]^{ren} = \frac{20}{3}\delta_K^2 C_2^{(1/2)}(\xi_x) + 14\delta_K^2 a_1^K C_3^{(1/2)}(\xi_x), \tag{1552}$$

together with

$$\begin{aligned}\left[\psi_{4K}^{WW}(x)\right]^{ren} = {} & 6m_K^2\left[\rho_+^K\left(1+6a_2^K\right) - 3\rho_-^K a_1^K\right]C_0^{(1/2)}(\xi_x) \\ & + 3m_K^2\left[9\rho_+^K a_1^K - \frac{6}{5}a_1^K - \rho_-^K\left(1+18a_2^K\right)\right]C_1^{(1/2)}(\xi_x) \\ & + 2\left\{m_K^2\left[1-\frac{18}{7}a_2^K - 3\rho_-^K a_1^K + 15\rho_+^K a_2^K\right] + 30\frac{f_{3K}}{f_K}\left(m_q+m_s\right)\right\}C_2^{(1/2)}(\xi_x) \\ & + \left\{m_K^2\left[\frac{18}{5}a_1^K - 9\rho_-^K a_2^K\right] + 20\frac{f_{3K}}{f_K}\left(m_q+m_s\right)\lambda_{3K}\right\}C_3^{(1/2)}(\xi_x) \\ & + 6\left\{\frac{6}{7}m_K^2 a_2^K - \frac{f_{3K}}{f_K}\left(m_q+m_s\right)\omega_{3K}\right\}C_4^{(1/2)}(\xi_x) \\ & - 3m_K^2\left(\rho_-^K - \rho_+^K\right)\left[1+3a_1^K+6a_2^K\right]\log\bar{x} \\ & + 3m_K^2\left(\rho_-^K + \rho_+^K\right)\left[1-3a_1^K+6a_2^K\right]\log x. \end{aligned} \tag{1553}$$

This ansatz, however, would lead astray from our approach and we will, therefore, not further follow this path. Nonetheless, similar to Equation 1551, we suggest to rewrite Equation 1547 according to

$$\begin{aligned}
\psi_{4K}^{WW}(x) = {} & 3m_K^2 a_1^K \left[3\xi_x \left(3\rho_+^K - 4x\bar{x}\right) - 4\rho_-^K (2 - 3x\bar{x})\right] \\
& + \frac{3}{2} m_K^2 a_2^K \left[1 + 44\rho_+^K + 6\rho_-^K \xi_x (10x\bar{x} - 7) + 6x\bar{x}\left(25x\bar{x} - 2\left(10\rho_+^K + 3\right)\right)\right] \\
& + \frac{15}{2}\frac{f_{3K}}{f_K}(m_q + m_s)\left(1 - 20x\bar{x} + 70x^2\bar{x}^2\right) - \frac{20}{3} m_K^2 \kappa_{4K} \xi_x (1 + 8x\bar{x}) \\
& + m_K^2 \left(6\rho_+^K - 3\xi_x \rho_-^K + \frac{17}{12} - 19x\bar{x} + \frac{105}{2}x^2\bar{x}^2\right) \\
& + 20\frac{f_{3K}}{f_K}(m_q + m_s)\lambda_{3K}\xi_x (1 - 10x\bar{x}) \\
& - 6\frac{f_{3K}}{f_K}(m_q + m_s)\omega_{3K}\left(1 - 20x\bar{x} + 70x^2\bar{x}^2\right) \\
& - 3m_K^2\left(1 + 3a_1^K + 6a_2^K\right)\left(\rho_-^K - \rho_+^K\right)\log\bar{x} \\
& + 3m_K^2\left(1 - 3a_1^K + 6a_2^K\right)\left(\rho_-^K + \rho_+^K\right)\log x\,. \qquad (1554)
\end{aligned}$$

This ensures a visible difference to the conformal expansion in Equation 1546. Furthermore, in this way the connection to Equation 676–Equation 677 and Equation 679–Equation 680 is more visible.

BIBLIOGRAPHY

[1] S. S. Agaev, V. M. Braun, N. Offen, and F. A. Porkert, *BELLE Data on the $\pi^0\gamma*\gamma$ Form Factor: A Game Changer?*, *Phys. Rev.* **D86** (2012) 077504, arXiv:1206.3968 [hep-ph].

[2] N. Offen, F. A. Porkert, and A. Schäfer, *Light-cone sum rules for the $D_{(s)} \to \eta^{(\prime)} l\nu_l$ form factor*, *Phys. Rev.* **D88** no. 3, (2013) 034023, arXiv:1307.2797 [hep-ph].

[3] S. S. Agaev, V. M. Braun, N. Offen, F. A. Porkert, and A. Schäfer, *Transition form factors $\gamma^*\gamma \to \eta$ and $\gamma^*\gamma \to \eta'$ in QCD*, *Phys. Rev.* **D90** no. 7, (2014) 074019, arXiv:1409.4311 [hep-ph].

[4] F. Porkert, *Standard model of elementary particles.* , 2016/2018. LaTeX/TikZ file, based on the CERN Webfest 2012 contribution of D. Galbraith, C. Burgard, "Standard Model of the Standard Model," http://davidgalbraith.org/portfolio/ux-standard-model-of-the-standard-model/, as well as http://www.texample.net/tikz/examples/model-physics/. Moreover, the given values are taken from [37, 42, 197].

[5] **BaBar** Collaboration, B. Aubert et al., *Measurement of the $\gamma\gamma^* \to \pi^0$ transition form factor*, *Phys. Rev.* **D80** (2009) 052002, arXiv:0905.4778 [hep-ex].

[6] **Belle** Collaboration, S. Uehara et al., *Measurement of $\gamma\gamma^* \to \pi^0$ transition form factor at Belle*, *Phys. Rev.* **D86** (2012) 092007, arXiv:1205.3249 [hep-ex].

[7] **BaBar** Collaboration, P. del Amo Sanchez et al., *Measurement of the $\gamma\gamma^* \to \eta$ and $\gamma\gamma* \to \eta'$ transition form factors*, *Phys. Rev.* **D84** (2011) 052001, arXiv:1101.1142 [hep-ex].

[8] **CLEO** Collaboration, J. Gronberg et al., *Measurements of the meson - photon transition form-factors of light pseudoscalar mesons at large momentum transfer*, *Phys. Rev.* **D57** (1998) 33–54, arXiv:hep-ex/9707031 [hep-ex].

[9] T. Feldmann, P. Kroll, and B. Stech, *Mixing and decay constants of pseudoscalar mesons*, *Phys. Rev.* **D58** (1998) 114006, arXiv:hep-ph/9802409 [hep-ph].

[10] R. Escribano and J.-M. Frere, *Study of the $\eta - \eta'$ system in the two mixing angle scheme*, *JHEP* **06** (2005) 029, arXiv:hep-ph/0501072 [hep-ph].

[11] V. M. Braun, S. Collins, M. Göckeler, P. Pérez-Rubio, A. Schäfer, R. W. Schiel, and A. Sternbeck, *Second Moment of the Pion Light-cone Distribution Amplitude from Lattice QCD*, *Phys. Rev.* **D92** no. 1, (2015) 014504, arXiv:1503.03656 [hep-lat].

[12] G. S. Bali, S. Collins, S. Dürr, and I. Kanamori, $D_s \to \eta, \eta'$ *semileptonic decay form factors with disconnected quark loop contributions*, *Phys. Rev.* **D91** no. 1, (2015) 014503, arXiv:1406.5449 [hep-lat].

[13] H. Leutwyler, *On the $\frac{1}{N}$ expansion in chiral perturbation theory*, *Nucl. Phys. Proc. Suppl.* **64** (1998) 223–231, arXiv:hep-ph/9709408 [hep-ph].

[14] R. Kaiser and H. Leutwyler, *Large N_c in chiral perturbation theory*, *Eur. Phys. J.* **C17** (2000) 623–649, arXiv:hep-ph/0007101 [hep-ph].

[15] T. Feldmann, P. Kroll, and B. Stech, *Mixing and decay constants of pseudoscalar mesons: The Sequel*, *Phys. Lett.* **B449** (1999) 339–346, arXiv:hep-ph/9812269 [hep-ph].

[16] D. Melikhov, *Dispersion approach to quark binding effects in weak decays of heavy mesons*, *Eur. Phys. J.direct* **4** no. 1, (2002) 2, arXiv:hep-ph/0110087 [hep-ph].

[17] D. Melikhov and B. Stech, *On the $\gamma^*\gamma \to \pi(\eta, \eta')$ transition form factors*, *Phys. Rev.* **D85** (2012) 051901, arXiv:1202.4471 [hep-ph].

[18] D. Melikhov and B. Stech, *Universal behaviour of the $\gamma^*\gamma \to (\pi^0, \eta, \eta')$ transition form factors*, *Phys. Lett.* **B718** (2012) 488–491, arXiv:1206.5764 [hep-ph].

[19] Y. N. Klopot, A. G. Oganesian, and O. V. Teryaev, *Axial anomaly and mixing: from real to highly virtual photons*, *Phys. Rev.* **D84** (2011) 051901, arXiv:1106.3855 [hep-ph].

[20] P. Kroll and K. Passek-Kumericki, *The Two gluon components of the η and η' mesons to leading twist accuracy*, *Phys. Rev.* **D67** (2003) 054017, arXiv:hep-ph/0210045 [hep-ph].

[21] M. V. Terentev, *FACTORIZATION IN EXCLUSIVE PROCESSES. FORM-FACTOR OF SINGLET MESONS IN QUANTUM CHROMODYNAMICS*, *Sov. J. Nucl. Phys.* **33** (1981) 911. [Yad. Fiz.33,1692(1981)].

[22] T. Ohrndorf, *The Q^2 Dependence of the Flavor Singlet Pseudoscalar Meson Wave Function in QCD*, *Nucl. Phys.* **B186** (1981) 153–164.

[23] V. N. Baier and A. G. Grozin, *Meson Wave Functions With Two Gluon States*, *Nucl. Phys.* **B192** (1981) 476–488.

[24] J. Blumlein, B. Geyer, and D. Robaschik, *Twist-2 light ray operators: Anomalous dimensions and evolution equations*, in *Deep inelastic scattering off polarized targets: Theory meets experiment. Physics with polarized protons at HERA. Proceedings, Workshops, SPIN'97, Zeuthen, Germany, September 1-5, 1997 and Hamburg, Germany, March-September 1997*, pp. 196–209. 1997. arXiv:hep-ph/9711405 [hep-ph].

[25] A. V. Belitsky and D. Müller, *Next-to-leading order evolution of twist-2 conformal operators: The Abelian case*, *Nucl. Phys.* **B527** (1998) 207–234, arXiv:hep-ph/9802411 [hep-ph].

[26] A. V. Belitsky, D. Müller, L. Niedermeier, and A. Schäfer, *Evolution of nonforward parton distributions in next-to-leading order: Singlet sector*, *Nucl. Phys.* **B546** (1999) 279–298, arXiv:hep-ph/9810275 [hep-ph].

[27] A. V. Belitsky and D. Müller, *Broken conformal invariance and spectrum of anomalous dimensions in QCD*, *Nucl. Phys.* **B537** (1999) 397–442, arXiv:hep-ph/9804379 [hep-ph].

[28] P. Kroll and K. Passek-Kumericki, *The $\eta(\eta')\gamma$ transition form factor and the gluonâgluon distribution amplitude*, *J. Phys.* **G40** (2013) 075005, arXiv:1206.4870 [hep-ph].

[29] **PANDA** Collaboration, M. F. M. Lutz et al., *Physics Performance Report for PANDA: Strong Interaction Studies with Antiprotons*, arXiv:0903.3905 [hep-ex].

[30] P. Colangelo and F. De Fazio, *D_s decays to η and η' final states: A Phenomenological analysis*, *Phys. Lett.* **B520** (2001) 78–86, arXiv:hep-ph/0107137 [hep-ph].

[31] K. Azizi, R. Khosravi, and F. Falahati, *Exclusive $D_s \to (\eta, \eta')l\nu$ decays in light cone QCD*, *J. Phys.* **G38** (2011) 095001, arXiv:1011.6046 [hep-ph].

[32] P. Ball and G. W. Jones, $B \to \eta^{(\prime)}$ *Form Factors in QCD*, *JHEP* **08** (2007) 025, arXiv:0706.3628 [hep-ph].

[33] G. P. Lepage and S. J. Brodsky, *Exclusive Processes in Quantum Chromodynamics: Evolution Equations for Hadronic Wave Functions and the Form-Factors of Mesons*, *Phys. Lett.* **87B** (1979) 359–365.

[34] W. Heisenberg, *On the structure of atomic nuclei*, *Z. Phys.* **77** (1932) 1–11.

[35] I. I. Bigi, CP *violation*. Cambridge, UK: Univ. Pr. (2009) 485 p, 2009. http://www.cambridge.org/catalogue/catalogue.asp?isbn=9780521847940.

[36] W. R. Inc., *Mathematica, Version 8.0/9.0/10.0*. . Champaign, IL, (2010/2012/2014).

[37] **Particle Data Group** Collaboration, C. Patrignani et al., *Review of Particle Physics*, *Chin. Phys.* **C40** no. 10, (2016) 100001.

[38] M. Gell-Mann, *The Eightfold Way: A Theory of strong interaction symmetry*,.

[39] V. E. Barnes et al., *Confirmation of the existence of the Ω^- hyperon*, *Phys. Lett.* **12** (1964) 134–136.

[40] E. M. Riordan, *The Discovery of quarks*, *Science* **256** (1992) 1287–1293.

[41] **Particle Data Group** Collaboration, W. M. Yao et al., *Review of Particle Physics*, *J. Phys.* **G33** (2006) 1–1232.

[42] **Particle Data Group** Collaboration, K. A. Olive et al., *Review of Particle Physics*, *Chin. Phys.* **C38** (2014) 090001.

[43] **Particle Data Group** Collaboration, K. Nakamura et al., *Review of particle physics*, *J. Phys.* **G37** (2010) 075021.

[44] T. P. Cheng and L. F. Li, *GAUGE THEORY OF ELEMENTARY PARTICLE PHYSICS*. Oxford, Uk: Clarendon (1984) 536 P. (Oxford Science Publications), 1984.

[45] T. Muta, *Foundations of Quantum Chromodynamics: An Introduction to Perturbative Methods in Gauge Theories, (3rd ed.)*, vol. 78 of *World scientific Lecture Notes in Physics*. World Scientific, Hackensack, N.J., 2010. http://www-spires.fnal.gov/spires/find/books/www?cl=QC793.3.Q35M88::2010.

[46] S. Bethke, *Experimental tests of asymptotic freedom*, *Prog. Part. Nucl. Phys.* **58** (2007) 351–386, arXiv:hep-ex/0606035 [hep-ex].

[47] S. Kluth, *Jet physics in e^+e^- annihilation from 14 GeV to 209 GeV*, *Nucl. Phys. Proc. Suppl.* **133** (2004) 36–46, arXiv:hep-ex/0309070 [hep-ex].

[48] D. Binosi and L. Theußl, *Jaxodraw: A graphical user interface for drawing feynman diagrams*, *Computer Physics Communications* **161** no. 1, (2004) 76 – 86. http://www.sciencedirect.com/science/article/pii/S0010465504002115.

[49] S. L. Adler and W. A. Bardeen, *Absence of higher order corrections in the anomalous axial vector divergence equation*, *Phys. Rev.* **182** (1969) 1517–1536.

[50] X. Feng, S. Aoki, H. Fukaya, S. Hashimoto, T. Kaneko, J.-i. Noaki, and E. Shintani, *Two-photon decay of the neutral pion in lattice QCD*, *Phys. Rev. Lett.* **109** (2012) 182001, arXiv:1206.1375 [hep-lat].

[51] S. L. Adler, *Axial vector vertex in spinor electrodynamics*, *Phys. Rev.* **177** (1969) 2426–2438.

[52] J. S. Bell and R. Jackiw, *A PCAC puzzle: $\pi^0 \to \gamma\gamma$ in the σ model*, *Nuovo Cim.* **A60** (1969) 47–61.

[53] A. Pich, *Effective field theory: Course*, in *Probing the standard model of particle interactions. Proceedings, Summer School in Theoretical Physics, NATO Advanced Study Institute, 68th session, Les Houches, France, July 28-September 5, 1997. Pt. 1, 2*, pp. 949–1049. 1998. arXiv:hep-ph/9806303 [hep-ph].

[54] D. V. Shirkov, *Evolution of the Bogolyubov renormalization group*, arXiv:hep-th/9909024 [hep-th].

[55] M. Shifman, *Advanced topics in quantum field theory.* Cambridge Univ. Press, Cambridge, UK, 2012. http://www.cambridge.org/mw/academic/subjects/physics/theoretical-physics-and-mathematical-physics/advanced-topics-quantum-field-theory-lecture-course?format=AR.

[56] A. Perlmutter (Ed.) and B. Kurşunoğlu, *Field theory in elementary particles*. Springer US · Plenum Press, New York , 469 p, 1983.

[57] J. D. Bjorken, *CURRENT ALGEBRA AT SMALL DISTANCES*, *Conf. Proc.* **C670717** (1967) 55–81.

[58] J. D. Bjorken, *Asymptotic Sum Rules at Infinite Momentum*, *Phys. Rev.* **179** (1969) 1547–1553.

[59] A. Ali and G. Kramer, *Jets and QCD: A Historical Review of the Discovery of the Quark and Gluon Jets and its Impact on QCD*, *Eur. Phys. J.* **H36** (2011) 245–326, arXiv:1012.2288 [hep-ph].

[60] A. Zee, *Unity of Forces in the Universe*. World Scientific Pub Co Inc, Singapore, 1982.

[61] S. R. Coleman and D. J. Gross, *Price of asymptotic freedom*, *Phys. Rev. Lett.* **31** (1973) 851–854.

[62] B. R. Stella and H.-J. Meyer, *Υ(9.46 GeV) and the gluon discovery (a critical recollection of PLUTO results)*, *Eur. Phys. J.* **H36** (2011) 203–243, arXiv:1008.1869 [hep-ex].

[63] O. Eberhardt, G. Herbert, H. Lacker, A. Lenz, A. Menzel, U. Nierste, and M. Wiebusch, *Impact of a Higgs boson at a mass of* 126 *GeV on the standard model with three and four fermion generations*, *Phys. Rev. Lett.* **109** (2012) 241802, arXiv:1209.1101 [hep-ph].

[64] M. E. Peskin and D. V. Schroeder, *An Introduction to quantum field theory*. Addison-Wesley, Reading, USA, 1995. http://www.slac.stanford.edu/~mpeskin/QFT.html.

[65] V. Chandra and R. Kumar, *Chromo-electric Yang-Mills gauge fields*, arXiv:0706.0962 [hep-th].

[66] W. Greiner, S. Schramm, and E. Stein, *Quantum chromodynamics*. Berlin, Germany: Springer (2002), 551 p, 2002.

[67] W. Greiner and J. Reinhardt, *Field quantization*. Berlin, Germany: Springer, 440 p, 1996.

[68] G. Parisi and Y.-s. Wu, *Perturbation Theory Without Gauge Fixing*, *Sci. Sin.* **24** (1981) 483.

[69] R. P. Feynman, *Space-time approach to nonrelativistic quantum mechanics*, *Rev. Mod. Phys.* **20** (1948) 367–387.

[70] W. Heisenberg and W. Pauli, *On Quantum Field Theory. (In German)*, *Z. Phys.* **56** (1929) 1–61.

[71] W. Heisenberg and W. Pauli, *On Quantum Field Theory. 2. (In German)*, *Z. Phys.* **59** (1930) 168–190.

[72] L. D. Faddeev and V. N. Popov, *Feynman Diagrams for the Yang-Mills Field*, *Phys. Lett.* **B25** (1967) 29–30.

[73] F. J. Yndurain, *The theory of quark and gluon interactions*. Berlin, Germany: Springer, 413 p, 1999.

[74] V. A. Novikov, M. A. Shifman, A. I. Vainshtein, and V. I. Zakharov, *Calculations in External Fields in Quantum Chromodynamics. Technical Review*, *Fortsch. Phys.* **32** (1984) 585.

[75] I. I. Balitsky and V. M. Braun, *Evolution Equations for QCD String Operators*, *Nucl. Phys.* **B311** (1989) 541–584.

[76] W. Weise, *Introduction to qcd*. . http://www.t39.ph.tum.de/T39_files/Lectures_files/QCD200708.php. Lecture notes, Winter Semester 2007/2008, Technische Universität München (T39).

[77] M. Beneke, *Renormalons*, *Phys. Rept.* **317** (1999) 1–142, arXiv:hep-ph/9807443 [hep-ph].

[78] M. Shifman, *Resurgence, operator product expansion, and remarks on renormalons in supersymmetric Yang-Mills theory*, *J. Exp. Theor. Phys.* **120** no. 3, (2015) 386–398, arXiv:1411.4004 [hep-th].

[79] A. Erdélyi, *Asymptotic Expansions*. Dover Publications, New York: 1987 (paperback 2010), 128 p., 2010.

[80] M. Hans, *AN ELECTROSTATIC EXAMPLE TO ILLUSTRATE DIMENSIONAL REGULARIZATION AND RENORMALIZATION GROUP TECHNIQUE*, *Am. J. Phys.* **51** (1983) 694–698.

[81] F. Olness and R. Scalise, *Regularization, Renormalization, and Dimensional Analysis: Dimensional Regularization meets Freshman E&M*, *Am. J. Phys.* **79** (2011) 306, arXiv:0812.3578 [hep-ph].

[82] J. Collins, *Renormalization: An Introduction to Renormalization, the Renormalization Group and the Operator-product Expansion*. Cambridge University Press (2003), 2003.

[83] B. Hall, *Lie Groups, Lie Algebras, and Representations: An Elementary Introduction (Graduate Texts in Mathematics)*. Springer · Corr. 2nd printing, 2004.

[84] A. A. Slavnov, *Ward Identities in Gauge Theories*, *Theor. Math. Phys.* **10** (1972) 99–107. [Teor. Mat. Fiz.10,153(1972)].

[85] J. C. Taylor, *Ward Identities and Charge Renormalization of the Yang-Mills Field*, *Nucl. Phys.* **B33** (1971) 436–444.

[86] H. Georgi, *Sidney Coleman's Harvard*, arXiv:1606.03738 [physics.hist-ph].

[87] S. Bethke, *The 2009 World Average of α_s*, *Eur. Phys. J.* **C64** (2009) 689–703, arXiv:0908.1135 [hep-ph].

[88] M. Göckeler, R. Horsley, V. Linke, P. E. L. Rakow, G. Schierholz, and H. Stuben, *Is there a Landau pole problem in QED?*, *Phys. Rev. Lett.* **80** (1998) 4119–4122, arXiv:hep-th/9712244 [hep-th].

[89] P. Breitenlohner and D. Maison, *Dimensional Renormalization and the Action Principle*, *Commun. Math. Phys.* **52** (1977) 11.

[90] K. G. Wilson, *Nonlagrangian models of current algebra*, *Phys. Rev.* **179** (1969) 1499–1512.

[91] W. Zimmermann, *Normal products and the short distance expansion in the perturbation theory of renormalizable interactions*, *Annals Phys.* **77** (1973) 570–601. [Lect. Notes Phys.558,278(2000)].

[92] W. Zimmermann, *Local operator products and renormalization in quantum field theory*. Brandeis Lectures (M.I.T. Press, Cambridge, eds. S. Deser), Vol. 1, 395 p, 1970.

[93] V. A. Novikov, M. A. Shifman, A. I. Vainshtein, and V. I. Zakharov, *Wilson's Operator Expansion: Can It Fail?*, *Nucl. Phys.* **B249** (1985) 445–471. [Yad. Fiz.41,1063(1985)].

[94] V. A. Novikov, M. A. Shifman, A. I. Vainshtein, and V. I. Zakharov, *Are All Hadrons Alike? DESY-check = Moscow Inst. Theor. Exp. Phys. Gkae - Itef-81-048 (81,rec.jun.) 32* P *and Nucl. Phys. B191 (1981) 301-369 and Moscow Inst. Theor. Exp. Phys. Gkae - Itef-81-042 (81,rec.apr.) 70* P. *(104907)*, *Nucl. Phys.* **B191** (1981) 301–369.

[95] M. A. Shifman, *Snapshots of hadrons or the story of how the vacuum medium determines the properties of the classical mesons which are produced, live and die in the QCD vacuum*, *Prog. Theor. Phys. Suppl.* **131** (1998) 1–71, arXiv:hep-ph/9802214 [hep-ph].

[96] M. A. Shifman, ed., *Vacuum structure and QCD sum rules*. Amsterdam, Netherlands: North-Holland (Current physics: sources and comments, 10), 516 p, 1992.

[97] P. Colangelo and A. Khodjamirian, *QCD sum rules, a modern perspective*, arXiv:hep-ph/0010175 [hep-ph].

[98] C. Itzykson and J. B. Zuber, *Quantum Field Theory*. International Series In Pure and Applied Physics. McGraw-Hill, New York, 1980. http://dx.doi.org/10.1063/1.2916419.

[99] R. L. Jaffe, *Spin, twist and hadron structure in deep inelastic processes*, in *The spin structure of the nucleon. Proceedings, International School of Nucleon Structure, 1st Course, Erice, Italy, August 3-10, 1995*, pp. 42–129. 1996. arXiv:hep-ph/9602236 [hep-ph].

[100] J. Collins, *Foundations of perturbative QCD*, *Camb. Monogr. Part. Phys. Nucl. Phys. Cosmol.* **32** (2011) 1–624.

[101] S. L. Adler, *Some Simple Vacuum Polarization Phenomenology:* $e^+e^- \to$ *Hadrons: The* μ *- Mesic Atom x-Ray Discrepancy and* $g_\mu{}^{-2}$, *Phys. Rev.* **D10** (1974) 3714.

[102] D. J. Gross and A. Neveu, *Dynamical Symmetry Breaking in Asymptotically Free Field Theories*, *Phys. Rev.* **D10** (1974) 3235.

[103] B. E. Lautrup, *On High Order Estimates in QED*, *Phys. Lett.* **69B** (1977) 109–111.

[104] G. 't Hooft and A. Zichichi (ed.), *Can we make sense out of quantum chromodynamics?*. Publ. in *The Why's on Subnuclear Physics* (proc. int. school, erice, italy, 1977), plenum, new york/london, 943., July, 1977. lectures given at the "Ettore Majorana" Int. School of Subnuclear Physics, Erice.

[105] M. Neubert, *Scale setting in QCD and the momentum flow in Feynman diagrams*, *Phys. Rev.* **D51** (1995) 5924–5941, arXiv:hep-ph/9412265 [hep-ph].

[106] V. I. Zakharov, *QCD perturbative expansions in large orders*, *Nucl. Phys.* **B385** (1992) 452–480.

[107] I. I. Y. Bigi, M. A. Shifman, N. G. Uraltsev, and A. I. Vainshtein, *The Pole mass of the heavy quark. Perturbation theory and beyond*, *Phys. Rev.* **D50** (1994) 2234–2246, arXiv:hep-ph/9402360 [hep-ph].

[108] A. H. Mueller, *On the Structure of Infrared Renormalons in Physical Processes at High-Energies*, *Nucl. Phys.* **B250** (1985) 327–350.

[109] M. A. Shifman, A. I. Vainshtein, and V. I. Zakharov, *QCD and Resonance Physics. Theoretical Foundations*, *Nucl. Phys.* **B147** (1979) 385–447.

[110] M. Shifman, *New and Old about Renormalons: in Memoriam Kolya Uraltsev*, *Int. J. Mod. Phys.* **A30** no. 10, (2015) 1543001, arXiv:1310.1966 [hep-th].

[111] M. A. Shifman, *Shifman-vainshtein-zakharov sum rules*. Scholarpedia (2013), 8(11):8790, 2013. http://www.scholarpedia.org/article/Shifman-Vainshtein-Zakharov_sum_rules.

[112] A. Grozin, *Lectures on QED and QCD: Practical calculation and renormalization of one- and multi-loop Feynman diagrams*. Hackensack, USA: World Scientific, 224 p, 2007.

[113] J. C. Collins, D. E. Soper, and G. F. Sterman, *Factorization of Hard Processes in QCD*, *Adv. Ser. Direct. High Energy Phys.* **5** (1989) 1–91, arXiv:hep-ph/0409313 [hep-ph].

[114] M. A. Shifman, A. I. Vainshtein, and V. I. Zakharov, *QCD and Resonance Physics: Applications*, *Nucl. Phys.* **B147** (1979) 448–518.

[115] F. David, *Nonperturbative Effects and Infrared Renormalons Within the $\frac{1}{N}$ Expansion of the $O(N)$ Nonlinear σ Model*, *Nucl. Phys.* **B209** (1982) 433–460.

[116] F. David, *On the Ambiguity of Composite Operators, IR Renormalons and the Status of the Operator Product Expansion*, *Nucl. Phys.* **B234** (1984) 237–251.

[117] M. A. Shifman, A. I. Vainshtein, and V. I. Zakharov, *QCD and Resonance Physics. The $\rho - \omega$ Mixing*, *Nucl. Phys.* **B147** (1979) 519–534.

[118] V. Braun, *Qcd sum rules*. , Sommersemester 2011. Vorlesungsskript, Universität Regensburg.

[119] M. Shifman, ed., *At the Frontier of Particle Physics : Handbook of QCD (3 Volumes)*. World Scientific Publishing Company, 2188 p, 2001.

[120] D. Diakonov and V. Yu. Petrov, *A Theory of Light Quarks in the Instanton Vacuum*, *Nucl. Phys.* **B272** (1986) 457–489.

[121] E. V. Shuryak and T. Schäfer, *The QCD vacuum as an instanton liquid*, *Ann. Rev. Nucl. Part. Sci.* **47** (1997) 359–394.

[122] C. McNeile, *An Estimate of the chiral condensate from unquenched lattice QCD*, *Phys. Lett.* **B619** (2005) 124–128, arXiv:hep-lat/0504006 [hep-lat].

[123] H. G. Dosch and S. Narison, *Direct extraction of the chiral quark condensate and bounds on the light quark masses*, *Phys. Lett.* **B417** (1998) 173–176, arXiv:hep-ph/9709215 [hep-ph].

[124] B. L. Ioffe, *QCD at low energies*, *Prog. Part. Nucl. Phys.* **56** (2006) 232–277, arXiv:hep-ph/0502148 [hep-ph].

[125] A. A. Ovchinnikov and A. A. Pivovarov, *QCD sum rule calculation of the quark gluon condensate*, *Sov. J. Nucl. Phys.* **48** (1988) 721–723. [Yad. Fiz.48,1135(1988)].

[126] B. L. Ioffe and K. N. Zyablyuk, *Gluon condensate in charmonium sum rules with three loop corrections*, *Eur. Phys. J.* **C27** (2003) 229–241, arXiv:hep-ph/0207183 [hep-ph].

[127] T. Schäfer and E. V. Shuryak, *Instantons in QCD*, *Rev. Mod. Phys.* **70** (1998) 323–426, arXiv:hep-ph/9610451 [hep-ph].

[128] V. M. Braun, G. P. Korchemsky, and D. Müller, *The Uses of conformal symmetry in QCD*, *Prog. Part. Nucl. Phys.* **51** (2003) 311–398, arXiv:hep-ph/0306057 [hep-ph].

[129] R. Mertig and W. L. van Neerven, *The Calculation of the two loop spin splitting functions* $P_{ij}^{(1)}(x)$, *Z. Phys.* **C70** (1996) 637–654, arXiv:hep-ph/9506451 [hep-ph].

[130] M. A. Ahmed and G. G. Ross, *Polarized Lepton - Hadron Scattering in Asymptotically Free Gauge Theories*, *Nucl. Phys.* **B111** (1976) 441–460.

[131] K. Sasaki, *Polarized Electroproduction in Asymptotically Free Gauge Theories*, *Prog. Theor. Phys.* **54** (1975) 1816.

[132] A. Gonzalez-Arroyo and C. Lopez, *Second Order Contributions to the Structure Functions in Deep Inelastic Scattering. 3. The Singlet Case*, *Nucl. Phys.* **B166** (1980) 429–459.

[133] G. Curci, W. Furmanski, and R. Petronzio, *Evolution of Parton Densities Beyond Leading Order: The Nonsinglet Case*, *Nucl. Phys.* **B175** (1980) 27–92.

[134] W. Furmanski and R. Petronzio, *Lepton - Hadron Processes Beyond Leading Order in Quantum Chromodynamics*, *Z. Phys.* **C11** (1982) 293.

[135] W. Furmanski and R. Petronzio, *Singlet Parton Densities Beyond Leading Order*, *Phys. Lett.* **97B** (1980) 437–442.

[136] E. G. Floratos, R. Lacaze, and C. Kounnas, *Space and Timelike Cut Vertices in QCD Beyond the Leading Order. 1. Nonsinglet Sector*, *Phys. Lett.* **98B** (1981) 89–95.

[137] E. G. Floratos, D. A. Ross, and C. T. Sachrajda, *Higher Order Effects in Asymptotically Free Gauge Theories: The Anomalous Dimensions of Wilson Operators*, *Nucl. Phys.* **B129** (1977) 66–88. [Erratum: Nucl. Phys.B139,545(1978)].

[138] A. Gonzalez-Arroyo, C. Lopez, and F. J. Yndurain, *Second Order Contributions to the Structure Functions in Deep Inelastic Scattering. 1. Theoretical Calculations*, *Nucl. Phys.* **B153** (1979) 161–186.

[139] E. G. Floratos, C. Kounnas, and R. Lacaze, *Higher Order QCD Effects in Inclusive Annihilation and Deep Inelastic Scattering*, *Nucl. Phys.* **B192** (1981) 417–462.

[140] V. M. Braun, A. Khodjamirian, and M. Maul, *Pion form-factor in QCD at intermediate momentum transfers*, *Phys. Rev.* **D61** (2000) 073004, arXiv:hep-ph/9907495 [hep-ph].

[141] V. L. Chernyak and I. R. Zhitnitsky, *B meson exclusive decays into baryons*, *Nucl. Phys.* **B345** (1990) 137–172.

[142] V. M. Braun and I. E. Filyanov, *QCD Sum Rules in Exclusive Kinematics and Pion Wave Function*, *Z. Phys.* **C44** (1989) 157. [Yad. Fiz.50,818(1989)].

[143] I. I. Balitsky, V. M. Braun, and A. V. Kolesnichenko, *Radiative Decay $\Sigma^+ \to p\gamma$ in Quantum Chromodynamics*, *Nucl. Phys.* **B312** (1989) 509–550.

[144] V. M. Braun and I. E. Halperin, *Soft contribution to the pion form-factor from light cone QCD sum rules*, *Phys. Lett.* **B328** (1994) 457–465, arXiv:hep-ph/9402270 [hep-ph].

[145] E. Noether, *Invariant Variation Problems*, *Gott. Nachr.* **1918** (1918) 235–257, arXiv:physics/0503066 [physics]. [Transp. Theory Statist. Phys.1,186(1971)].

[146] M. Maggiore, *A Modern introduction to quantum field theory*. Oxford University Press (Oxford Series in Physics, 12. ISBN 0 19 852073 5), 2005.

[147] S. L. Adler, *Remarks on the history of quantum chromodynamics*, *Submitted to: Phys. Today* (2004) , arXiv:hep-ph/0412297 [hep-ph].

[148] T. Y. Cao, *From current algebra to quantum chromodynamics*. Cambridge Univ. Pr., Cambridge, UK, 2010. http://www.cambridge.org/de/knowledge/isbn/item6958617.

[149] S. F. Novaes, *Standard model: An Introduction*, in *Particles and fields. Proceedings, 10th Jorge Andre Swieca Summer School, Sao Paulo, Brazil, February 6-12, 1999*, pp. 5–102. . arXiv:hep-ph/0001283 [hep-ph].

[150] J. S. Schwinger, *On gauge invariance and vacuum polarization*, *Phys. Rev.* **82** (1951) 664–679.

[151] R. Peierls, *STATISTICAL ERROR IN COUNTING EXPERIMENTS*, *Proc. Roy. Soc. Lond.* **A149** (1935) 467–486.

[152] T. Feldmann, *Quark structure of pseudoscalar mesons*, *Int. J. Mod. Phys.* **A15** (2000) 159–207, arXiv:hep-ph/9907491 [hep-ph].

[153] R. D. Peccei, *The Strong* CP *problem and axions*, *Lect. Notes Phys.* **741** (2008) 3–17, arXiv:hep-ph/0607268 [hep-ph].

[154] H. Banerjee, D. Chatterjee, and P. Mitra, *Is there still a strong* CP *problem?*, *Phys. Lett.* **B573** (2003) 109, arXiv:hep-ph/0012284 [hep-ph].

[155] R. D. Peccei and H. R. Quinn, CP *Conservation in the Presence of Instantons*, *Phys. Rev. Lett.* **38** (1977) 1440–1443.

[156] T. Frankel, *The geometry of physics: An introduction*. Cambridge, UK: Univ. Pr., 654 p, 1997.

[157] J. de Vries, E. Mereghetti, and A. Walker-Loud, *Baryon mass splittings and strong* CP *violation in* SU(3) *Chiral Perturbation Theory*, *Phys. Rev.* **C92** no. 4, (2015) 045201, arXiv:1506.06247 [nucl-th].

[158] S. Scherer and M. R. Schindler, *A Primer for Chiral Perturbation Theory*, *Lect. Notes Phys.* **830** (2012) pp.1–338.

[159] J. Goldstone, *Field Theories with Superconductor Solutions*, *Nuovo Cim.* **19** (1961) 154–164.

[160] J. Goldstone, A. Salam, and S. Weinberg, *Broken Symmetries*, *Phys. Rev.* **127** (1962) 965–970.

[161] Y. Nambu, *Quasiparticles and Gauge Invariance in the Theory of Superconductivity*, *Phys. Rev.* **117** (1960) 648–663.

[162] C. A. Meyer and E. S. Swanson, *Hybrid Mesons*, *Prog. Part. Nucl. Phys.* **82** (2015) 21–58, arXiv:1502.07276 [hep-ph].

[163] V. Crede and C. A. Meyer, *The Experimental Status of Glueballs*, *Prog. Part. Nucl. Phys.* **63** (2009) 74–116, arXiv:0812.0600 [hep-ex].

[164] A. R. Dzierba, C. A. Meyer, and A. P. Szczepaniak, *Reviewing the evidence for pentaquarks*, *J. Phys. Conf. Ser.* **9** (2005) 192–204, arXiv:hep-ex/0412077 [hep-ex].

[165] C. A. Meyer, *An Experimental overview of gluonic mesons*, *AIP Conf. Proc.* **698** (2004) 554–558, arXiv:hep-ex/0308010 [hep-ex].

[166] S. Capstick et al., *Key issues in hadronic physics*, in *APS Division of Nuclear Physics Town Meeting on Electromagnetic and Hadronic Physics Newport News, Virginia, December 1-4, 2000*. . arXiv:hep-ph/0012238 [hep-ph]. http://www1.jlab.org/Ul/publications/view_pub.cfm?pub_id=6006.

[167] C. A. Meyer, *Meson spectroscopy and the search for exotics*, *AIP Conf. Proc.* **412** no. 1, (1997) 91–100, arXiv:hep-ex/9707008 [hep-ex].

[168] **Crystal Barrel** Collaboration, H. Koch et al., *Meson spectroscopy and the Crystal Barrel detector at LEAR*, in *Medium-energy physics. Proceedings, International Symposium, Beijing, P.R. China, June 23-28, 1987*, pp. 588–594. .

[169] C. A. Meyer, *Light and exotic mesons*. , June, 2008. http://www.curtismeyer.com/material/lecture.pdf. Lecture notes, Carnegie Mellon University, Pittsburgh, PA 15213.

[170] O. Nachtmann, *Elementary Particle Physics: Concepts and Phenomena*. Berlin, Germany: Springer, 559 p, 1990.

[171] M. Jamin, *Flavor symmetry breaking of the quark condensate and chiral corrections to the Gell-Mann-Oakes-Renner relation*, *Phys. Lett.* **B538** (2002) 71–76, arXiv:hep-ph/0201174 [hep-ph].

[172] M. Shifman, *Vacuum structure and QCD sum rules: Introduction*, *Int. J. Mod. Phys.* **A25** (2010) 226–235.

[173] J. B. Kogut and L. Susskind, *QUARK CONFINEMENT AND THE PUZZLE OF THE NINTH AXIAL CURRENT*, *Phys. Rev.* **D10** (1974) 3468–3475.

[174] J. B. Kogut and L. Susskind, *How to Solve the* $\eta \to 3\pi$ *Problem by Seizing the Vacuum*, *Phys. Rev.* **D11** (1975) 3594.

[175] G. 't Hooft, *How Instantons Solve the* $U(1)$ *Problem*, *Phys. Rept.* **142** (1986) 357–387.

[176] R. Alkofer, C. S. Fischer, and R. Williams, $U_A(1)$ *anomaly and* η' *mass from an infrared singular quark-gluon vertex*, *Eur. Phys. J.* **A38** (2008) 53–60, arXiv:0804.3478 [hep-ph].

[177] G. 't Hooft, *Symmetry Breaking Through Bell-Jackiw Anomalies*, *Phys. Rev. Lett.* **37** (1976) 8–11.

[178] E. Witten, *Large N Chiral Dynamics*, *Annals Phys.* **128** (1980) 363.

[179] E. Witten, *Instantons, the Quark Model, and the* $\frac{1}{N}$ *Expansion*, *Nucl. Phys.* **B149** (1979) 285–320.

[180] G. Veneziano, $U(1)$ *Without Instantons*, *Nucl. Phys.* **B159** (1979) 213–224.

[181] H. Fritzsch, M. Gell-Mann, and H. Leutwyler, *Advantages of the Color Octet Gluon Picture*, *Phys. Lett.* **47B** (1973) 365–368.

[182] R. Kaiser and H. Leutwyler, *Pseudoscalar decay constants at large* N_c, in *Nonperturbative methods in quantum field theory. Proceedings, Workshop, Adelaide, Australia, February 2-13, 1998*, pp. 15–29. . arXiv:hep-ph/9806336 [hep-ph].

[183] L. Venkataraman and G. Kilcup, *The* η' *meson with staggered fermions*, *Submitted to: Phys. Rev. D* (1997) , arXiv:hep-lat/9711006 [hep-lat].

[184] M. Fukugita, Y. Kuramashi, M. Okawa, and A. Ukawa, *Lattice QCD solution to the* $U(1)$ *problem*, *Phys. Rev.* **D51** (1995) 3952–3954.

[185] A. Pich, *The Standard model of electroweak interactions*, in *The Standard model of electroweak interactions*, pp. 1–49. 2008. arXiv:0705.4264 [hep-ph]. http://doc.cern.ch/yellowrep/2007/2007-005/cern-2007-005.pdf.

[186] A. Pich, *The Standard Model of Electroweak Interactions*, in *Proceedings, High-energy Physics. Proceedings, 18th European School (ESHEP 2010): Raseborg, Finland, June 20 - July 3, 2010*, pp. 1–50. 2012. arXiv:1201.0537 [hep-ph].

[187] C. Quigg, *GAUGE THEORIES OF THE STRONG, WEAK AND ELECTROMAGNETIC INTERACTIONS*, *Front. Phys.* **56** (1983) 1–334.

[188] W. Greiner and B. Müller, *Gauge theory of weak interactions*. Berlin, Germany: Springer, 308 p (Theoretical physics, 5), 1993.

[189] B. C. Allanach, *Beyond the Standard Model Lectures for the 2016 European School of High-Energy Physics*, in *Proceedings, 2016 European School of High-Energy Physics (ESHEP2016): Skeikampen, Norway, June 15-28 2016*, pp. 123–152. 2017. arXiv:1609.02015 [hep-ph].

[190] P. Nath, T. Taylor, and S. Pokorski, eds., *Physics from Planck scale to electroweak scale. Proceedings, US - Polish Workshop, Warsaw, Poland, September 21-24, 1994*. 1995.

[191] P. de Aquino, *Beyond Standard Model Phenomenology at the LHC*. PhD thesis, Louvain U., New York, 2012. http://www.springer.com/physics/particle+and+nuclear+physics/book/978-3-319-00761-8.

[192] T. Aliev, N. K. Pak, and M. Serin, *Proceedings, 2nd International Summer School in High Energy Physics on The standard model and beyond*, *Springer Proc. Phys.* **118** (2008) pp.1–197.

[193] G. L. Kane and M. Shifman, eds., *The supersymmetric world: The beginning of the theory*. Singapore, Singapore: World Scientific, 271 p, 2000.

[194] M. Shifman and A. Yung, *Supersymmetric solitons*. Cambridge Monographs on Mathematical Physics. Cambridge University Press, 2009. http://www.cambridge.org/catalogue/catalogue.asp?isbn=9780521516389.

[195] V. P. Wess, J.; Akulov, *Supersymmetry and Quantum Field Theory*. Springer Berlin, 408 p, 2014.

[196] P. Deligne, P. Etingof, D. S. Freed, L. C. Jeffrey, D. Kazhdan, J. W. Morgan, D. R. Morrison, and E. Witten, eds., *Quantum fields and strings: A course for mathematicians. Vol. 1, 2*. Providence, USA: AMS, pp. 1-1501, 1999.

[197] **ATLAS, CMS** Collaboration, T. G. McCarthy, *Top Quark Mass Measurements at the LHC*, in *Proceedings, 51st Rencontres de Moriond on QCD and High Energy Interactions: La Thuile, Italy, March 19-26, 2016*, pp. 13–18. . arXiv:1612.04994 [hep-ex].

[198] J. C. Romao and J. P. Silva, *A resource for signs and Feynman diagrams of the Standard Model*, *Int. J. Mod. Phys.* **A27** (2012) 1230025, arXiv:1209.6213 [hep-ph].

[199] D. J. Gross and F. Wilczek, *Ultraviolet Behavior of Nonabelian Gauge Theories*, *Phys. Rev. Lett.* **30** (1973) 1343–1346.

[200] H. D. Politzer, *Reliable Perturbative Results for Strong Interactions?*, *Phys. Rev. Lett.* **30** (1973) 1346–1349.

[201] G. 't Hooft and M. J. G. Veltman, *Regularization and Renormalization of Gauge Fields*, *Nucl. Phys.* **B44** (1972) 189–213.

[202] G. 't Hooft and M. J. G. Veltman, *Combinatorics of gauge fields*, *Nucl. Phys.* **B50** (1972) 318–353.

[203] S. Weinberg, *A Model of Leptons*, *Phys. Rev. Lett.* **19** (1967) 1264–1266.

[204] S. L. Glashow, *Partial Symmetries of Weak Interactions*, *Nucl. Phys.* **22** (1961) 579–588.

[205] A. Salam, *Weak and Electromagnetic Interactions*, *Conf. Proc.* **C680519** (1968) 367–377.

[206] P. W. Higgs, *Broken symmetries, massless particles and gauge fields*, *Phys. Lett.* **12** (1964) 132–133.

[207] P. W. Higgs, *Spontaneous Symmetry Breakdown without Massless Bosons*, *Phys. Rev.* **145** (1966) 1156–1163.

[208] P. W. Higgs, *Broken Symmetries and the Masses of Gauge Bosons*, *Phys. Rev. Lett.* **13** (1964) 508–509.

[209] G. S. Guralnik, C. R. Hagen, and T. W. B. Kibble, *Global Conservation Laws and Massless Particles*, *Phys. Rev. Lett.* **13** (1964) 585–587.

[210] C. J. Gorter, *A New Suggestion for Aligning Certain Atomic Nuclei*. Physica. 14, p. 504, 1948.

[211] M. E. Rose, *On the production of nuclear polarization*, *Physical Review. 75* (1949) 213.

[212] C. S. Wu, E. Ambler, R. W. Hayward, D. D. Hoppes, and R. P. Hudson, *Experimental Test of Parity Conservation in Beta Decay*, *Phys. Rev.* **105** (1957) 1413–1414.

[213] T. D. Lee and C.-N. Yang, *Question of Parity Conservation in Weak Interactions*, *Phys. Rev.* **104** (1956) 254–258.

[214] J. H. Christenson, J. W. Cronin, V. L. Fitch, and R. Turlay, *Evidence for the 2π Decay of the K_2^0 Meson*, *Phys. Rev. Lett.* **13** (1964) 138–140.

[215] Y. Grossman and P. Tanedo, *Just a Taste: Lectures on Flavor Physics*, in *Proceedings, Theoretical Advanced Study Institute in Elementary Particle Physics : Anticipating the Next Discoveries in Particle Physics (TASI 2016): Boulder, CO, USA, June 6-July 1, 2016*, pp. 109–295. 2018. arXiv:1711.03624 [hep-ph].

[216] S. L. Glashow, *The renormalizability of vector meson interactions*, *Nucl. Phys.* **10** (1959) 107–117.

[217] A. Salam and J. C. Ward, *Weak and electromagnetic interactions*, *Nuovo Cim.* **11** (1959) 568–577.

[218] H. Yukawa, *On the Interaction of Elementary Particles I*, *Proc. Phys. Math. Soc. Jap.* **17** (1935) 48–57. [Prog. Theor. Phys. Suppl.1,1(1935)].

[219] S. Weinberg, *The quantum theory of fields. Vol. 2: Modern applications*. Cambridge University Press, 2013.

[220] A. Pich, *The Standard model of electroweak interactions*, in *2004 European School of High-Energy Physics, Sant Feliu de Guixols, Spain, 30 May - 12 June 2004*, pp. 1–48. 2005. arXiv:hep-ph/0502010 [hep-ph]. http://doc.cern.ch/yellowrep/2006/2006-003/p1.pdf.

[221] S. L. Glashow, J. Iliopoulos, and L. Maiani, *Weak Interactions with Lepton-Hadron Symmetry*, *Phys. Rev.* **D2** (1970) 1285–1292.

[222] J. D. Bjorken and S. L. Glashow, *Elementary Particles and* SU(4), *Phys. Lett.* **11** (1964) 255–257.

[223] N. Cabibbo, *Unitary Symmetry and Leptonic Decays*, *Phys. Rev. Lett.* **10** (1963) 531–533.

[224] M. Kobayashi and T. Maskawa, CP *Violation in the Renormalizable Theory of Weak Interaction*, *Prog. Theor. Phys.* **49** (1973) 652–657.

[225] **Particle Data Group** Collaboration, J. Beringer et al., *Review of Particle Physics (RPP)*, *Phys. Rev.* **D86** (2012) 010001.

[226] A. J. Buras, *Weak Hamiltonian,* CP *violation and rare decays*, in *Probing the standard model of particle interactions. Proceedings, Summer School in Theoretical Physics, NATO Advanced Study Institute, 68th session, Les Houches, France, July 28-September 5, 1997. Pt. 1, 2*, pp. 281–539. 1998. arXiv:hep-ph/9806471 [hep-ph].

[227] G. C. Branco, L. Lavoura, and J. P. Silva, CP *Violation*, *Int. Ser. Monogr. Phys.* **103** (1999) 1–536.

[228] C. P. Burgess and G. D. Moore, *The standard model: A primer*. Cambridge University Press, 2006.

[229] L.-L. Chau and W.-Y. Keung, *Comments on the Parametrization of the Kobayashi-Maskawa Matrix*, *Phys. Rev. Lett.* **53** (1984) 1802.

[230] R. Rückl, *WEAK DECAYS OF HEAVY FLAVORS*. PhD thesis, University of Munich, Oct. 1983.

[231] C. Jarlskog, *Commutator of the Quark Mass Matrices in the Standard Electroweak Model and a Measure of Maximal CP Violation*, *Phys. Rev. Lett.* **55** (1985) 1039.

[232] T. Mannel, *Effective Field Theories in Flavor Physics*, *Springer Tracts Mod. Phys.* **203** (2004) 1–175.

[233] A. J. Buras, *Flavor physics and* CP *violation*, in *2004 European School of High-Energy Physics, Sant Feliu de Guixols, Spain, 30 May - 12 June 2004*, pp. 95–168. 2005. arXiv:hep-ph/0505175 [hep-ph]. http://doc.cern.ch/yellowrep/2006/2006-003/p95.pdf.

[234] I. I. Y. Bigi and N. G. Uraltsev, D_s *Lifetime,* m_b, m_c *and* $|V_{cb}|$ *in the heavy quark expansion*, *Z. Phys.* **C62** (1994) 623–632, arXiv:hep-ph/9311243 [hep-ph].

[235] M. K. Gaillard, B. W. Lee, and J. L. Rosner, *Search for Charm*, *Rev. Mod. Phys.* **47** (1975) 277–310.

[236] J. R. Ellis, M. K. Gaillard, and D. V. Nanopoulos, *On the Weak Decays of High Mass Hadrons*, *Nucl. Phys.* **B100** (1975) 313. [Erratum: Nucl. Phys.B104,547(1976)].

[237] T. E. Browder, K. Honscheid, and D. Pedrini, *Nonleptonic decays and lifetimes of* b *quark and* c *quark hadrons*, *Ann. Rev. Nucl. Part. Sci.* **46** (1996) 395–469, arXiv:hep-ph/9606354 [hep-ph].

[238] M. Neubert, *Heavy quark effective theory*, *Subnucl. Ser.* **34** (1997) 98–165, arXiv:hep-ph/9610266 [hep-ph].

[239] A. Lenz, *Lifetimes and heavy quark expansion*, *Int. J. Mod. Phys.* **A30** no. 10, (2015) 1543005, arXiv:1405.3601 [hep-ph].

[240] J. Chay, H. Georgi, and B. Grinstein, *Lepton energy distributions in heavy meson decays from QCD*, *Phys. Lett.* **B247** (1990) 399–405.

[241] I. I. Y. Bigi, N. G. Uraltsev, and A. I. Vainshtein, *Nonperturbative corrections to inclusive beauty and charm decays: QCD versus phenomenological models*, *Phys. Lett.* **B293** (1992) 430–436, arXiv:hep-ph/9207214 [hep-ph]. [Erratum: Phys. Lett.B297,477(1992)].

[242] I. I. Y. Bigi, M. A. Shifman, N. G. Uraltsev, and A. I. Vainshtein, *QCD predictions for lepton spectra in inclusive heavy flavor decays*, *Phys. Rev. Lett.* **71** (1993) 496–499, arXiv:hep-ph/9304225 [hep-ph].

[243] B. Blok, L. Koyrakh, M. A. Shifman, and A. I. Vainshtein, *Differential distributions in semileptonic decays of the heavy flavors in QCD*, *Phys. Rev.* **D49** (1994) 3356, arXiv:hep-ph/9307247 [hep-ph]. [Erratum: Phys. Rev.D50,3572(1994)].

[244] C. Klein, *Berechnung hadronischer Übergangsamplituden in der Charm-Physik*. PhD thesis, Universiät Siegen, 2011.

[245] J. L. Rosner, S. Stone, and R. S. Van de Water, *Leptonic Decays of Charged Pseudoscalar Mesons - 2015*, *Submitted to: Particle Data Book* (2015) , arXiv:1509.02220 [hep-ph].

[246] A. Khodjamirian, R. Rückl, S. Weinzierl, and O. I. Yakovlev, *Perturbative QCD correction to the* $B \to \pi$ *transition form-factor*, *Phys. Lett.* **B410** (1997) 275–284, arXiv:hep-ph/9706303 [hep-ph].

[247] T. Palmer and J. O. Eeg, *Form factors for semileptonic* D *decays*, *Phys. Rev.* **D89** no. 3, (2014) 034013, arXiv:1306.0365 [hep-ph].

[248] J. Charles, A. Le Yaouanc, L. Oliver, O. Pene, and J. C. Raynal, *Heavy to light form-factors in the heavy mass to large energy limit of QCD*, *Phys. Rev.* **D60** (1999) 014001, arXiv:hep-ph/9812358 [hep-ph].

[249] M. Beneke and T. Feldmann, *Symmetry breaking corrections to heavy to light* B *meson form-factors at large recoil*, *Nucl. Phys.* **B592** (2001) 3–34, arXiv:hep-ph/0008255 [hep-ph].

[250] N. Isgur and M. B. Wise, *Weak Decays of Heavy Mesons in the Static Quark Approximation*, *Phys. Lett.* **B232** (1989) 113–117.

[251] N. Isgur and M. B. Wise, *WEAK TRANSITION FORM-FACTORS BETWEEN HEAVY MESONS*, *Phys. Lett.* **B237** (1990) 527–530.

[252] H. Georgi, *An Effective Field Theory for Heavy Quarks at Low-energies*, *Phys. Lett.* **B240** (1990) 447–450.

[253] A. F. Falk, H. Georgi, B. Grinstein, and M. B. Wise, *Heavy Meson Form-factors From QCD*, *Nucl. Phys.* **B343** (1990) 1–13.

[254] A. F. Falk, *Hadrons of arbitrary spin in the heavy quark effective theory*, *Nucl. Phys.* **B378** (1992) 79–94.

[255] J. D. Bjorken, *New symmetries in heavy flavor physics*, *Conf. Proc.* **C900318** (1990) 583–596.

[256] A. G. Grozin and M. Neubert, *Asymptotics of heavy meson form-factors*, *Phys. Rev.* **D55** (1997) 272–290, arXiv:hep-ph/9607366 [hep-ph].

[257] N. Offen, *B-decay form factors from QCD sum rules*. PhD thesis, Siegen U., 2008. http://dokumentix.ub.uni-siegen.de/opus/volltexte/2008/334/.

[258] E. Byckling and K. Kajantie, *Particle Kinematics*. John Wiley & Sons Ltd, 330 p, 1973.

[259] W. von Schlippe, *Relativistic kinematics of particle interactions*. , March, 2002. http://www.helsinki.fi/~www_sefo/phenomenology/Schlippe_relativistic_kinematics.pdf. Article On Relativisitic Kinematics, St. Petersburg University.

[260] H. Haber, *Two-particle lorentz invariant phase space*. , 2016. http://scipp.ucsc.edu/~haber/ph217/Lips.pdf. Class Handouts, University of California, Santa Cruz.

[261] T. Feldmann, *Mixing and decay constants of pseudoscalar mesons: Octet singlet versus quark flavor basis*, *Nucl. Phys. Proc. Suppl.* **74** (1999) 151–154, arXiv:hep-ph/9807367 [hep-ph].

[262] A. Lenz, $B_s - \bar{B}_s$ *mixing and lifetimes*, *PoS* **Beauty2014** (2014) 002.

[263] R. Kaiser, *Diploma thesis*, Master's thesis, University of Bern, 1997.

[264] T. Feldmann and P. Kroll, *Mixing of pseudoscalar mesons*, *Phys. Scripta* **T99** (2002) 13–22, arXiv:hep-ph/0201044 [hep-ph].

[265] M. Beneke and M. Neubert, *Flavor singlet B decay amplitudes in QCD factorization*, *Nucl. Phys.* **B651** (2003) 225–248, arXiv:hep-ph/0210085 [hep-ph].

[266] S. J. Brodsky, H.-C. Pauli, and S. S. Pinsky, *Quantum chromodynamics and other field theories on the light cone*, *Phys. Rept.* **301** (1998) 299–486, arXiv:hep-ph/9705477 [hep-ph].

[267] V. M. Braun et al., *Moments of pseudoscalar meson distribution amplitudes from the lattice*, *Phys. Rev.* **D74** (2006) 074501, arXiv:hep-lat/0606012 [hep-lat].

[268] S. J. Brodsky, F.-G. Cao, and G. F. de Teramond, *Evolved QCD predictions for the meson-photon transition form factors*, *Phys. Rev.* **D84** (2011) 033001, arXiv:1104.3364 [hep-ph].

[269] V. M. Braun and I. E. Filyanov, *Conformal Invariance and Pion Wave Functions of Nonleading Twist*, *Z. Phys.* **C48** (1990) 239–248. [Yad. Fiz.52,199(1990)].

[270] P. Ball, V. M. Braun, and A. Lenz, *Twist-4 distribution amplitudes of the K^* and ϕ mesons in QCD*, *JHEP* **08** (2007) 090, arXiv:0707.1201 [hep-ph].

[271] P. Ball, V. M. Braun, and A. Lenz, *Higher-twist distribution amplitudes of the K meson in QCD*, *JHEP* **05** (2006) 004, arXiv:hep-ph/0603063 [hep-ph].

[272] V. M. Braun and A. Lenz, *On the $SU(3)$ symmetry-breaking corrections to meson distribution amplitudes*, *Phys. Rev.* **D70** (2004) 074020, arXiv:hep-ph/0407282 [hep-ph].

[273] P. Ball, V. M. Braun, and E. Gardi, *Distribution Amplitudes of the Λ_b Baryon in QCD*, *Phys. Lett.* **B665** (2008) 197–204, arXiv:0804.2424 [hep-ph].

[274] P. Ball, V. M. Braun, and N. Kivel, *Photon distribution amplitudes in QCD*, *Nucl. Phys.* **B649** (2003) 263–296, arXiv:hep-ph/0207307 [hep-ph].

[275] P. Ball and V. M. Braun, *Handbook of higher twist distribution amplitudes of vector mesons in QCD*, in *Continuous advances in QCD. Proceedings, 3rd Workshop, QCD'98, Minneapolis, USA, April 16-19, 1998*, pp. 125–141. 1998. arXiv:hep-ph/9808229 [hep-ph].

[276] A. V. Radyushkin, *Asymmetric gluon distributions and hard diffractive electroproduction*, *Phys. Lett.* **B385** (1996) 333–342, arXiv:hep-ph/9605431 [hep-ph].

[277] J. B. Kogut and D. E. Soper, *Quantum Electrodynamics in the Infinite Momentum Frame*, *Phys. Rev.* **D1** (1970) 2901–2913.

[278] T. Feldmann and P. Kroll, *Flavor symmetry breaking and mixing effects in the $\eta\gamma$ and $\eta'\gamma$ transition form-factors*, *Eur. Phys. J.* **C5** (1998) 327–335, arXiv:hep-ph/9711231 [hep-ph].

[279] S. S. Agaev and M. A. G. Nobary, *Pion distribution amplitude from holographic QCD and the electromagnetic form factor $F_\pi(Q^2)$*, *Phys. Rev.* **D77** (2008) 074014, arXiv:0805.0993 [hep-ph].

[280] A. Khodjamirian, *Form-factors of $\gamma^*\rho \to \pi$ and $\gamma^*\gamma \to \pi^0$ transitions and light cone sum rules*, *Eur. Phys. J.* **C6** (1999) 477–484, arXiv:hep-ph/9712451 [hep-ph].

[281] S. S. Agaev, V. M. Braun, N. Offen, and F. A. Porkert, *Light Cone Sum Rules for the $\pi^0\gamma^*\gamma$ Form Factor Revisited*, *Phys. Rev.* **D83** (2011) 054020, arXiv:1012.4671 [hep-ph].

[282] S. Weinberg, *The Quantum theory of fields. Vol. 1: Foundations*. Cambridge University Press, 2005.

[283] W. K. Tung, *GROUP THEORY IN PHYSICS*. Singapore, Singapore: World Scientific, 344p, 1985.

[284] P. Di Francesco, P. Mathieu, and D. Senechal, *Conformal Field Theory*. Graduate Texts in Contemporary Physics. Springer-Verlag, New York, 1997. http://www-spires.fnal.gov/spires/find/books/www?cl=QC174.52.C66D5::1997.

[285] S. Coleman, *Aspects of Symmetry*. Cambridge University Press, Cambridge, U.K., 1985.

[286] G. Mack and A. Salam, *Finite component field representations of the conformal group*, *Annals Phys.* **53** (1969) 174–202.

[287] N. K. Nielsen, *The Energy Momentum Tensor in a Nonabelian Quark Gluon Theory*, *Nucl. Phys.* **B120** (1977) 212–220.

[288] S. L. Adler, J. C. Collins, and A. Duncan, *Energy-Momentum-Tensor Trace Anomaly in Spin $\frac{1}{2}$ Quantum Electrodynamics*, *Phys. Rev.* **D15** (1977) 1712.

[289] J. C. Collins, A. Duncan, and S. D. Joglekar, *Trace and Dilatation Anomalies in Gauge Theories*, *Phys. Rev.* **D16** (1977) 438–449.

[290] I. E. Halperin, *Conformal symmetry on the light cone and nonleading twist distribution amplitudes of massive vector meson*, *Phys. Rev.* **D57** (1998) 1680–1686, arXiv:hep-ph/9704265 [hep-ph].

[291] P. K. Suetin (originator), *Ultraspherical polynomials*. Encyclopedia of Mathematics, Springer, 2011. http://www.encyclopediaofmath.org/index.php?title=Ultraspherical_polynomials&oldid=14267.

[292] T. Ohrndorf, *Constraints From Conformal Covariance on the Mixing of Operators of Lowest Twist*, *Nucl. Phys.* **B198** (1982) 26–44.

[293] V. M. Braun, S. E. Derkachov, G. P. Korchemsky, and A. N. Manashov, *Baryon distribution amplitudes in QCD*, *Nucl. Phys.* **B553** (1999) 355–426, arXiv:hep-ph/9902375 [hep-ph].

[294] J. Eilers, *Geometric twist decomposition off the light-cone for nonlocal QCD operators*, arXiv:hep-th/0608173 [hep-th].

[295] R. L. Jaffe and X.-D. Ji, *Chiral odd parton distributions and Drell-Yan processes*, *Nucl. Phys.* **B375** (1992) 527–560.

[296] T. Bröcker, *Analysis 2*, vol. 2., korr. Aufl. Spektrum Akademischer Verlag, 1995.

[297] V. M. Braun, G. P. Korchemsky, and A. N. Manashov, *Evolution equation for the structure function $g_2(x, Q^2)$*, *Nucl. Phys.* **B603** (2001) 69–124, arXiv:hep-ph/0102313 [hep-ph].

[298] A. Erdélyi, *Higher Transcendental Functions*. McGraw-Hill Inc.,US, 1953.

[299] P. Ball and A. N. Talbot, *Models for light-cone meson distribution amplitudes*, *JHEP* **06** (2005) 063, arXiv:hep-ph/0502115 [hep-ph].

[300] L. A. Harland-Lang, V. A. Khoze, M. G. Ryskin, and W. J. Stirling, *Central exclusive production as a probe of the gluonic component of the η' and η mesons*, *Eur. Phys. J.* **C73** (2013) 2429, arXiv:1302.2004 [hep-ph].

[301] G. P. Lepage and S. J. Brodsky, *Exclusive Processes in Perturbative Quantum Chromodynamics*, *Phys. Rev.* **D22** (1980) 2157.

[302] A. V. Efremov and A. V. Radyushkin, *Factorization and Asymptotical Behavior of Pion Form-Factor in QCD*, *Phys. Lett.* **94B** (1980) 245–250.

[303] A. V. Efremov and A. V. Radyushkin, *Asymptotical Behavior of Pion Electromagnetic Form-Factor in QCD*, *Theor. Math. Phys.* **42** (1980) 97–110. [Teor. Mat. Fiz.42,147(1980)].

[304] A. V. Belitsky and A. V. Radyushkin, *Unraveling hadron structure with generalized parton distributions*, *Phys. Rept.* **418** (2005) 1–387, arXiv:hep-ph/0504030 [hep-ph].

[305] F. M. Dittes and A. V. Radyushkin, *TWO LOOP CONTRIBUTION TO THE EVOLUTION OF THE PION WAVE FUNCTION*, *Phys. Lett.* **134B** (1984) 359–362.

[306] M. H. Sarmadi, *The Asymptotic Pion Form-factor Beyond the Leading Order*, *Phys. Lett.* **143B** (1984) 471.

[307] G. R. Katz, *Two Loop Feynman Gauge Calculation of the Meson Nonsinglet Evolution Potential*, *Phys. Rev.* **D31** (1985) 652.

[308] S. V. Mikhailov and A. V. Radyushkin, *Evolution Kernels in QCD: Two Loop Calculation in Feynman Gauge*, *Nucl. Phys.* **B254** (1985) 89–126.

[309] D. Müller, *Conformal constraints and the evolution of the nonsinglet meson distribution amplitude*, *Phys. Rev.* **D49** (1994) 2525–2535.

[310] D. Müller, *The Evolution of the pion distribution amplitude in next-to-leading-order*, *Phys. Rev.* **D51** (1995) 3855–3864, arXiv:hep-ph/9411338 [hep-ph].

[311] B. Melic, D. Müller, and K. Passek-Kumericki, *Next-to-next-to-leading prediction for the photon to pion transition form-factor*, *Phys. Rev.* **D68** (2003) 014013, arXiv:hep-ph/0212346 [hep-ph].

[312] R. Escribano, P. Masjuan, and P. Sanchez-Puertas, *The η transition form factor from space- and time-like experimental data*, *Eur. Phys. J.* **C75** no. 9, (2015) 414, arXiv:1504.07742 [hep-ph].

[313] P. Ball, V. M. Braun, Y. Koike, and K. Tanaka, *Higher twist distribution amplitudes of vector mesons in QCD: Formalism and twist-three distributions*, *Nucl. Phys.* **B529** (1998) 323–382, arXiv:hep-ph/9802299 [hep-ph].

[314] P. Ball, *Theoretical update of pseudoscalar meson distribution amplitudes of higher twist: The Nonsinglet case*, *JHEP* **01** (1999) 010, arXiv:hep-ph/9812375 [hep-ph].

[315] P. Ball and V. M. Braun, *Higher twist distribution amplitudes of vector mesons in QCD: Twist-4 distributions and meson mass corrections*, *Nucl. Phys.* **B543** (1999) 201–238, arXiv:hep-ph/9810475 [hep-ph].

[316] V. Braun, R. J. Fries, N. Mahnke, and E. Stein, *Higher twist distribution amplitudes of the nucleon in QCD*, *Nucl. Phys.* **B589** (2000) 381–409, arXiv:hep-ph/0007279 [hep-ph]. [Erratum: Nucl. Phys.B607,433(2001)].

[317] J. P. Singh, *Twist-three distribution amplitudes and octet current decay constants of η and η': A QCD sum rule approach*, *Int. J. Mod. Phys.* **E18** (2009) 1318–1323.

[318] H.-M. Choi and C.-R. Ji, *Two-particle twist-3 distribution amplitudes of the pion and kaon in the light-front quark model*, *Phys. Rev.* **D95** no. 5, (2017) 056002, arXiv:1701.02402 [hep-ph].

[319] A. Khodjamirian, C. Klein, T. Mannel, and N. Offen, *Semileptonic charm decays $D \to \pi l \nu_l$ and $D \to K l \nu_l$ from QCD Light-Cone Sum Rules*, *Phys. Rev.* **D80** (2009) 114005, arXiv:0907.2842 [hep-ph].

[320] G. Duplancic, A. Khodjamirian, T. Mannel, B. Melic, and N. Offen, *Light-cone sum rules for $B \to \pi$ form factors revisited*, *JHEP* **04** (2008) 014, arXiv:0801.1796 [hep-ph].

[321] P. Ball, *$B \to \pi$ and $B \to K$ transitions from QCD sum rules on the light cone*, *JHEP* **09** (1998) 005, arXiv:hep-ph/9802394 [hep-ph].

[322] P. Ball and R. Zwicky, *New results on $B \to \pi, K, \eta$ decay formfactors from light-cone sum rules*, *Phys. Rev.* **D71** (2005) 014015, arXiv:hep-ph/0406232 [hep-ph].

[323] V. I. Borodulin, R. N. Rogalev, and S. R. Slabospitsky, *CORE: COmpendium of RElations: Version 2.1*, arXiv:hep-ph/9507456 [hep-ph].

[324] V. I. Borodulin, R. N. Rogalyov, and S. R. Slabospitskii, *CORE 3.1 (COmpendium of RElations, Version 3.1)*, arXiv:1702.08246 [hep-ph].

[325] C. C. Nishi, *Simple derivation of general Fierz-like identities*, *Am. J. Phys.* **73** (2005) 1160–1163, arXiv:hep-ph/0412245 [hep-ph].

[326] J. F. Nieves and P. B. Pal, *Generalized Fierz identities*, *Am. J. Phys.* **72** (2004) 1100–1108, arXiv:hep-ph/0306087 [hep-ph].

[327] A. P. Bukhvostov, G. V. Frolov, L. N. Lipatov, and E. A. Kuraev, *Evolution Equations for Quasi-Partonic Operators*, *Nucl. Phys.* **B258** (1985) 601–646.

[328] Y. Koike and K. Tanaka, Q^2 *evolution of nucleon's chiral odd twist - three structure function:* $h_L(x, Q^2)$, *Phys. Rev.* **D51** (1995) 6125–6138, arXiv:hep-ph/9412310 [hep-ph].

[329] V. M. Braun, G. P. Korchemsky, and A. N. Manashov, *Evolution of twist - three parton distributions in QCD beyond the large* N_c *limit*, *Phys. Lett.* **B476** (2000) 455–464, arXiv:hep-ph/0001130 [hep-ph].

[330] A. S. Gorsky, *FORM-FACTOR PI RHO GAMMA IN PERTURBATIVE QCD,*.

[331] A. R. Zhitnitsky, I. R. Zhitnitsky, and V. L. Chernyak, *QCD SUM RULES AND PROPERTIES OF WAVE FUNCTIONS OF NONLEADING TWIST. (IN RUSSIAN)*, *Sov. J. Nucl. Phys.* **41** (1985) 284. [Yad. Fiz.41,445(1985)].

[332] P. Ball, *QCD sum rules on the light cone, factorization and SCET*, arXiv:hep-ph/0308249 [hep-ph].

[333] S. Wandzura and F. Wilczek, *Sum Rules for Spin Dependent Electroproduction: Test of Relativistic Constituent Quarks*, *Phys. Lett.* **72B** (1977) 195–198.

[334] S. S. Agaev, K. Azizi, and H. Sundu, *Strong* $D_s^* D_s \eta^{(\prime)}$ *and* $B_s^* B_s \eta^{(\prime)}$ *vertices from QCD light-cone sum rules*, *Phys. Rev.* **D92** no. 11, (2015) 116010, arXiv:1509.08620 [hep-ph].

[335] G. Duplancic and B. Melic, *Form factors of* $B, B_s \to \eta^{(\prime)}$ *and* $D, D_s \to \eta^{(\prime)}$ *transitions from QCD light-cone sum rules*, *JHEP* **11** (2015) 138, arXiv:1508.05287 [hep-ph].

[336] J. S. Schwinger, *Field theory of matter*, *Phys. Rev.* **135**, *B 816* (1964) .

[337] P. Ball and R. Zwicky, *Operator relations for* $SU(3)$ *breaking contributions to* K *and* K^* *distribution amplitudes*, *JHEP* **02** (2006) 034, arXiv:hep-ph/0601086 [hep-ph].

[338] V. M. Braun, A. N. Manashov, and J. Rohrwild, *Renormalization of Twist-Four Operators in QCD*, *Nucl. Phys.* **B826** (2010) 235–293, arXiv:0908.1684 [hep-ph].

[339] C. Shi, C. Chen, L. Chang, C. D. Roberts, S. M. Schmidt, and H.-S. Zong, *Kaon and pion parton distribution amplitudes to twist-three*, *Phys. Rev.* **D92** (2015) 014035, arXiv:1504.00689 [nucl-th].

[340] I. F. Ginzburg, *Two photon physics. Personal recollection*, arXiv:1508.06581 [hep-ph].

[341] M. Krawczyk, *Photon and its hadronic interaction*, *Nucl. Phys. Proc. Suppl.* **126** (2004) 3–4, arXiv:hep-ph/0312340 [hep-ph].

[342] V. I. Telnov, *Photon colliders: The First 25 years*, *Acta Phys. Polon.* **B37** (2006) 633–656, arXiv:physics/0602172 [physics].

[343] V. I. Telnov, *Prospects of high energy photon colliders*, *Nucl. Part. Phys. Proc.* **273-275** (2016) 219–224.

[344] V. I. Telnov, *High-energy photon-photon colliders*, *Proc. SPIE Int. Soc. Opt. Eng.* **3485** (1998) 13–24, arXiv:physics/9710014 [physics.acc-ph].

[345] V. I. Telnov, *Photon Collider Technology Overview*, in *PHOTON 2009, proceedings of the International Conference on the Structure and the Interactions of the Photon including the 18th International Workshop on Photon-Photon Collisions and the International Workshop on High Energy Photon Linear Colliders, May 11-15, 2009 DESY Hamburg, Germany*, pp. 73–82. 2009. arXiv:0908.3136 [physics.acc-ph].

[346] **CLIC Physics Working Group** Collaboration, E. Accomando et al., *Physics at the CLIC multi-TeV linear collider*, in *Proceedings, 11th International Conference on Hadron spectroscopy (Hadron 2005): Rio de Janeiro, Brazil, August 21-26, 2005*. 2004. arXiv:hep-ph/0412251 [hep-ph]. http://weblib.cern.ch/abstract?CERN-2004-005.

[347] G. Baur, K. Hencken, and D. Trautmann, *Photon-photon and photon - hadron interactions at relativistic heavy ion colliders*, *Prog. Part. Nucl. Phys.* **42** (1999) 357–366, arXiv:nucl-th/9810078 [nucl-th].

[348] S. J. Brodsky, *Photon-photon physics*. , August, 2005. http://www.slac.stanford.edu/th/lectures/warsaw.pdf,https://web.archive.org/web/20150712182430/http://www.slac.stanford.edu/th/lectures/warsaw.pdf. Lecture notes, PHOTON2005, Warsaw, Poland.

[349] S. J. Brodsky, *Photon-Photon Collisions: Past and Future*, *Acta Phys. Polon.* **B37** (2006) 619–632.

[350] **L3** Collaboration, M. Acciarri et al., *Measurement of $\eta'(958)$ formation in two photon collisions at LEP-1*, *Phys. Lett.* **B418** (1998) 399–410.

[351] **BaBar** Collaboration, B. Aubert et al., *Measurement of the η and η' transition form-factors at $q^2 = 112$ GeV^2*, *Phys. Rev.* **D74** (2006) 012002, arXiv:hep-ex/0605018 [hep-ex].

[352] V. Braun and D. Müller, *Exclusive processes in position space and the pion distribution amplitude*, *Eur. Phys. J.* **C55** (2008) 349–361, arXiv:0709.1348 [hep-ph].

[353] S. Wallon, *Hard exclusive processes in perturbative qcd: from medium to asymptotical energies*. , June, 2014. http://www.th.u-psud.fr/page_perso/Wallon/cours/exclusif.pdf. Cours d'Ecoles Doctorales, Doctoral Schools ED 107 (Physique de la Région Parisienne) and ED 517 (Particules, Noyaux et Cosmos).

[354] J. C. Collins, *Sudakov form-factors*, *Adv. Ser. Direct. High Energy Phys.* **5** (1989) 573–614, arXiv:hep-ph/0312336 [hep-ph].

[355] M. Beneke and M. Neubert, *QCD factorization for $B \to PP$ and $B \to PV$ decays*, *Nucl. Phys.* **B675** (2003) 333–415, arXiv:hep-ph/0308039 [hep-ph].

[356] M. Beneke, G. Buchalla, M. Neubert, and C. T. Sachrajda, *QCD factorization in $B \to \pi K, \pi\pi$ decays and extraction of Wolfenstein parameters*, *Nucl. Phys.* **B606** (2001) 245–321, arXiv:hep-ph/0104110 [hep-ph].

[357] M. Beneke, G. Buchalla, M. Neubert, and C. T. Sachrajda, *QCD factorization for exclusive, nonleptonic B meson decays: General arguments and the case of heavy light final states*, *Nucl. Phys.* **B591** (2000) 313–418, arXiv:hep-ph/0006124 [hep-ph].

[358] M. Beneke, G. Buchalla, M. Neubert, and C. T. Sachrajda, *QCD factorization for* $B \to \pi\pi$ *decays: Strong phases and* CP *violation in the heavy quark limit*, *Phys. Rev. Lett.* **83** (1999) 1914–1917, arXiv:hep-ph/9905312 [hep-ph].

[359] **CELLO** Collaboration, H. J. Behrend et al., *A Measurement of the* π^0, η *and* η' *electromagnetic form-factors*, *Z. Phys.* **C49** (1991) 401–410.

[360] **Belle, BaBar** Collaboration, A. J. Bevan et al., *The Physics of the* B *Factories*, *Eur. Phys. J.* **C74** (2014) 3026, arXiv:1406.6311 [hep-ex].

[361] D. Vucinic, *Observation of Excited* B *Mesons in Proton - Anti-Proton Collisions at* 1.8 *TeV*. PhD thesis, MIT, 1999. http://lss.fnal.gov/cgi-bin/find_paper.pl?thesis-1998-31.

[362] I. V. Musatov and A. V. Radyushkin, *Transverse momentum and Sudakov effects in exclusive QCD processes:* $\gamma^*\gamma\pi^0$ *form-factor*, *Phys. Rev.* **D56** (1997) 2713–2735, arXiv:hep-ph/9702443 [hep-ph].

[363] A. V. Radyushkin and R. Ruskov, *QCD sum rule calculation of* $\gamma\gamma^* \to \pi^0$ *transition form-factor*, *Phys. Lett.* **B374** (1996) 173–180, arXiv:hep-ph/9511270 [hep-ph].

[364] A. V. Radyushkin and R. T. Ruskov, *Transition form-factor* $\gamma\gamma^* \to \pi^0$ *and QCD sum rules*, *Nucl. Phys.* **B481** (1996) 625–680, arXiv:hep-ph/9603408 [hep-ph].

[365] F. del Aguila and M. K. Chase, *HIGHER ORDER QCD CORRECTIONS TO EXCLUSIVE TWO PHOTON PROCESSES*, *Nucl. Phys.* **B193** (1981) 517–528.

[366] E. Braaten, *QCD CORRECTIONS TO MESON - PHOTON TRANSITION FORM-FACTORS*, *Phys. Rev.* **D28** (1983) 524.

[367] E. P. Kadantseva, S. V. Mikhailov, and A. V. Radyushkin, *Total* α_S *Corrections to Processes* $\gamma^*\gamma^* \to \pi^0$ *and* $\gamma^*\pi \to \pi$ *in a Perturbative QCD*, *Yad. Fiz.* **44** (1986) 507–516. [Sov. J. Nucl. Phys.44,326(1986)].

[368] P. Kroll and M. Raulfs, *The* $\pi\gamma$ *transition form-factor and the pion wave function*, *Phys. Lett.* **B387** (1996) 848–854, arXiv:hep-ph/9605264 [hep-ph].

[369] R. Jakob, P. Kroll, and M. Raulfs, *Meson - photon transition form-factors*, *J. Phys.* **G22** (1996) 45–58, arXiv:hep-ph/9410304 [hep-ph].

[370] S. J. Brodsky, T. Huang, and G. P. Lepage, *Hadronic wave functions and high momentum transfer interactions in quantum chromodynamics*, *Conf. Proc.* **C810816** (1981) 143–199.

[371] V. M. Belyaev, V. M. Braun, A. Khodjamirian, and R. Rückl, $D^*D\pi$ *and* $B^*B\pi$ *couplings in QCD*, *Phys. Rev.* **D51** (1995) 6177–6195, arXiv:hep-ph/9410280 [hep-ph].

[372] P. Ball and V. M. Braun, *Exclusive semileptonic and rare B meson decays in QCD*, *Phys. Rev.* **D58** (1998) 094016, arXiv:hep-ph/9805422 [hep-ph].

[373] F. Porkert, *Photon-pion transition form factor(s)*, Master's thesis, University of Regensburg, 2011.

[374] L. A. Harland-Lang, V. A. Khoze, M. G. Ryskin, and W. J. Stirling, *Central exclusive production within the Durham model: a review*, *Int. J. Mod. Phys.* **A29** (2014) 1430031, arXiv:1405.0018 [hep-ph].

[375] **CDF** Collaboration, M. G. Albrow, *Central Exclusive Production at the Tevatron*, *Int. J. Mod. Phys.* **A29** no. 28, (2014) 1446009, arXiv:1409.0462 [hep-ex].

[376] L. A. Harland-Lang, V. A. Khoze, and M. G. Ryskin, *Exclusive meson pair production and the gluonic component of the η, η′ mesons*, in *Proceedings, 15th conference on Elastic and Diffractive scattering (EDS Blois 2013)*. 2013. arXiv:1310.2759 [hep-ph].

[377] L. A. Harland-Lang, V. A. Khoze, M. G. Ryskin, and W. J. Stirling, *Probing the perturbative dynamics of exclusive meson pair production*, *Phys. Lett.* **B725** (2013) 316–321, arXiv:1304.4262 [hep-ph].

[378] E. Witten, *Heavy Quark Contributions to Deep Inelastic Scattering*, *Nucl. Phys.* **B104** (1976) 445–476.

[379] J. C. Collins, F. Wilczek, and A. Zee, *Low-Energy Manifestations of Heavy Particles: Application to the Neutral Current*, *Phys. Rev.* **D18** (1978) 242.

[380] J. C. Collins and W.-K. Tung, *Calculating Heavy Quark Distributions*, *Nucl. Phys.* **B278** (1986) 934.

[381] W.-K. Tung, *Small x Behavior of Parton Distribution Functions in the Next-To-Leading Order QCD Parton Model*, *Nucl. Phys.* **B315** (1989) 378–390.

[382] J. C. Collins, *Hard scattering factorization with heavy quarks: A General treatment*, *Phys. Rev.* **D58** (1998) 094002, arXiv:hep-ph/9806259 [hep-ph].

[383] H. Kadeer, A. Spiesberger, *General mass variable flavour number scheme in deep inelastic scattering*. , October, 2009. http://www.emg.uni-mainz.de/Dateien/gmvfns.pdf. EMG Klausurtagung.

[384] M. Jamin and M. E. Lautenbacher, *TRACER: Version 1.1: A Mathematica package for gamma algebra in arbitrary dimensions*, *Comput. Phys. Commun.* **74** (1993) 265–288.

[385] R. Mertig, M. Bohm, and A. Denner, *FEYN CALC: Computer algebraic calculation of Feynman amplitudes*, *Comput. Phys. Commun.* **64** (1991) 345–359.

[386] V. Shtabovenko, R. Mertig, and F. Orellana, *New Developments in FeynCalc 9.0*, *Comput. Phys. Commun.* **207** (2016) 432–444, arXiv:1601.01167 [hep-ph].

[387] R. Mertig, *Guide to feyncalc 1.0," instruction manual*. , March, 1992. http://www.feyncalc.org/oldfc/FCGuide3.pdf. Physikalisches Institut der Universität Würzburg.

[388] A. Denner, *Techniques for calculation of electroweak radiative corrections at the one loop level and results for W physics at LEP-200*, *Fortsch. Phys.* **41** (1993) 307–420, arXiv:0709.1075 [hep-ph].

[389] G. 't Hooft, *Renormalizable Lagrangians for Massive Yang-Mills Fields*, *Nucl. Phys.* **B35** (1971) 167–188.

[390] G. 't Hooft, *Renormalization of Massless Yang-Mills Fields*, *Nucl. Phys.* **B33** (1971) 173–199.

[391] **SM and NLO Multileg Working Group** Collaboration, T. Binoth et al., *The SM and NLO Multileg Working Group: Summary report*, in *Physics at TeV colliders. Proceedings, 6th Workshop, dedicated to Thomas Binoth, Les Houches, France, June 8-26, 2009*, pp. 21–189. 2010. arXiv:1003.1241 [hep-ph]. http://www-public.slac.stanford.edu/sciDoc/docMeta.aspx?slacPubNumber=SLAC-PUB-14871.

[392] A. Denner and S. Dittmaier, *Scalar one-loop 4-point integrals*, *Nucl. Phys.* **B844** (2011) 199–242, arXiv:1005.2076 [hep-ph].

[393] R. K. Ellis and G. Zanderighi, *Scalar one-loop integrals for QCD*, *JHEP* **02** (2008) 002, arXiv:0712.1851 [hep-ph].

[394] A. Denner and S. Dittmaier, *Reduction schemes for one-loop tensor integrals*, *Nucl. Phys.* **B734** (2006) 62–115, arXiv:hep-ph/0509141 [hep-ph].

[395] G. Passarino and M. J. G. Veltman, *One Loop Corrections for e^+e^- Annihilation Into $\mu^+\mu^-$ in the Weinberg Model*, *Nucl. Phys.* **B160** (1979) 151–207.

[396] M. Consoli, *One Loop Corrections to $e^+e^- \to e^+e^-$ in the Weinberg Model*, *Nucl. Phys.* **B160** (1979) 208–252.

[397] M. J. G. Veltman, *Radiative Corrections to Vector Boson Masses*, *Phys. Lett.* **91B** (1980) 95–98.

[398] M. Green and M. J. G. Veltman, *Weak and Electromagnetic Radiative Corrections to Low-Energy Processes*, *Nucl. Phys.* **B169** (1980) 137–164. [Erratum: Nucl. Phys.B175,547(1980)].

[399] G. 't Hooft and M. J. G. Veltman, *Scalar One Loop Integrals*, *Nucl. Phys.* **B153** (1979) 365–401.

[400] D. B. Melrose, *Reduction of Feynman diagrams*, *Nuovo Cim.* **40** (1965) 181–213.

[401] M. Guidry, *General relativity, black holes, and cosmology (astronomy 421)*. . http://eagle.phys.utk.edu/guidry/astro421/. Lecture notes, Spring 2016, University of Tennessee, Knoxville,.

[402] R. G. Stuart, *Algebraic Reduction of One Loop Feynman Diagrams to Scalar Integrals*, *Comput. Phys. Commun.* **48** (1988) 367–389.

[403] R. G. Stuart and A. Gongora, *Algebraic Reduction of One Loop Feynman Diagrams to Scalar Integrals. 2.*, *Comput. Phys. Commun.* **56** (1990) 337–350.

[404] G. Devaraj and R. G. Stuart, *Reduction of one loop tensor form-factors to scalar integrals: A General scheme*, *Nucl. Phys.* **B519** (1998) 483–513, arXiv:hep-ph/9704308 [hep-ph].

[405] R. K. Ellis, Z. Kunszt, K. Melnikov, and G. Zanderighi, *One-loop calculations in quantum field theory: from Feynman diagrams to unitarity cuts*, *Phys. Rept.* **518** (2012) 141–250, arXiv:1105.4319 [hep-ph].

[406] G. Duplancic and B. Nizic, *Reduction method for dimensionally regulated one loop N point Feynman integrals*, *Eur. Phys. J.* **C35** (2004) 105–118, arXiv:hep-ph/0303184 [hep-ph].

[407] O. V. Tarasov, *Connection between Feynman integrals having different values of the space-time dimension*, *Phys. Rev.* **D54** (1996) 6479–6490, arXiv:hep-th/9606018 [hep-th].

[408] A. I. Davydychev, *Recursive algorithm of evaluating vertex type Feynman integrals*, *J. Phys.* **A25** (1992) 5587–5596.

[409] K. G. Chetyrkin and F. V. Tkachov, *Integration by Parts: The Algorithm to Calculate beta Functions in 4 Loops*, *Nucl. Phys.* **B192** (1981) 159–204.

[410] F. V. Tkachov, *A Theorem on Analytical Calculability of Four Loop Renormalization Group Functions*, *Phys. Lett.* **100B** (1981) 65–68.

[411] Z. Bern, L. J. Dixon, and D. A. Kosower, *Dimensionally regulated one loop integrals*, *Phys. Lett.* **B302** (1993) 299–308, arXiv:hep-ph/9212308 [hep-ph]. [Erratum: Phys. Lett.B318,649(1993)].

[412] Z. Bern, L. J. Dixon, and D. A. Kosower, *Dimensionally regulated pentagon integrals*, *Nucl. Phys.* **B412** (1994) 751–816, arXiv:hep-ph/9306240 [hep-ph].

[413] J. Fleischer, F. Jegerlehner, and O. V. Tarasov, *Algebraic reduction of one loop Feynman graph amplitudes*, *Nucl. Phys.* **B566** (2000) 423–440, arXiv:hep-ph/9907327 [hep-ph].

[414] T. Binoth, J. P. Guillet, and G. Heinrich, *Reduction formalism for dimensionally regulated one loop* N *point integrals*, *Nucl. Phys.* **B572** (2000) 361–386, arXiv:hep-ph/9911342 [hep-ph].

[415] G. Heinrich and T. Binoth, *A General reduction method for one loop* N *point integrals*, *Nucl. Phys. Proc. Suppl.* **89** (2000) 246–250, arXiv:hep-ph/0005324 [hep-ph].

[416] A. I. Davydychev, *A Simple formula for reducing Feynman diagrams to scalar integrals*, *Phys. Lett.* **B263** (1991) 107–111.

[417] D. Yu. Bardin and G. Passarino, *The standard model in the making: Precision study of the electroweak interactions*. Oxford, UK: Clarendon, 685 p, 1999.

[418] J. Romão, *Modern techniques for one-loop calculations – version* 1.0.263. , September, 2006. http://porthos.ist.utl.pt/OneLoop/one-loop.pdf. Review, Departamento de Física, Instituto Superior Técnico (A. Rovisco Pais, 1049-001 Lisboa, Portugal).

[419] W. Kilian, *Übungen zu strahlungskorrekturen in eichtheorien*. , 2001. der Herbstschule für Hochenergiephysik – Maria Laach 2001, Institut für Theoretische Teilchenphysik, Universität Karlsruhe (D-76128 Karlsruhe, Deutschland).

[420] T. Hahn, *Automatic loop calculations with FeynArts, FormCalc, and LoopTools*, *Nucl. Phys. Proc. Suppl.* **89** (2000) 231–236, arXiv:hep-ph/0005029 [hep-ph].

[421] T. Hahn, *Looptools* 2.8 *user's guide*. , September, 2012. http://www.feynarts.de/looptools/LT28Guide.pdf. Review, Max-Planck-Institut für Physik (Werner-Heisenberg-Institut – Föhringer Ring 6 D-80805 Munich, Germany),.

[422] F. Krinner, A. Lenz, and T. Rauh, *The inclusive decay* $b \to c\bar{c}s$ *revisited*, *Nucl. Phys.* **B876** (2013) 31–54, arXiv:1305.5390 [hep-ph].

[423] T. Hahn and M. Perez-Victoria, *Automatized one loop calculations in four-dimensions and* D*-dimensions*, *Comput. Phys. Commun.* **118** (1999) 153–165, arXiv:hep-ph/9807565 [hep-ph].

[424] A. Denner, U. Nierste, and R. Scharf, *A Compact expression for the scalar one loop four point function*, *Nucl. Phys.* **B367** (1991) 637–656.

[425] A. Schmedding and O. I. Yakovlev, *Perturbative effects in the form-factor* $\gamma\gamma^* \to \pi^0$ *and extraction of the pion wave function from CLEO data*, *Phys. Rev.* **D62** (2000) 116002, arXiv:hep-ph/9905392 [hep-ph].

[426] A. P. Bakulev, S. V. Mikhailov, and N. G. Stefanis, *QCD based pion distribution amplitudes confronting experimental data*, *Phys. Lett.* **B508** (2001) 279–289, arXiv:hep-ph/0103119 [hep-ph]. [Erratum: Phys. Lett.B590,309(2004)].

[427] A. P. Bakulev, S. V. Mikhailov, and N. G. Stefanis, *CLEO and E791 data: A Smoking gun for the pion distribution amplitude?*, *Phys. Lett.* **B578** (2004) 91–98, arXiv:hep-ph/0303039 [hep-ph].

[428] A. P. Bakulev, S. V. Mikhailov, and N. G. Stefanis, *Unbiased analysis of CLEO data at NLO and pion distribution amplitude*, *Phys. Rev.* **D67** (2003) 074012, arXiv:hep-ph/0212250 [hep-ph].

[429] S. S. Agaev, *Impact of the higher twist effects on the $\gamma\gamma^* \to \pi^0$ transition form-factor*, *Phys. Rev.* **D72** (2005) 114010, arXiv:hep-ph/0511192 [hep-ph]. [Erratum: Phys. Rev.D73,059902(2006)].

[430] S. V. Mikhailov and N. G. Stefanis, *Transition form factors of the pion in light-cone QCD sum rules with next-to-next-to-leading order contributions*, *Nucl. Phys.* **B821** (2009) 291–326, arXiv:0905.4004 [hep-ph].

[431] A. P. Bakulev, S. V. Mikhailov, A. V. Pimikov, and N. G. Stefanis, *Comparing antithetic trends of data for the pion-photon transition form factor*, *Phys. Rev.* **D86** (2012) 031501, arXiv:1205.3770 [hep-ph].

[432] N. G. Stefanis, A. P. Bakulev, S. V. Mikhailov, and A. V. Pimikov, *Can We Understand an Auxetic Pion-Photon Transition Form Factor within QCD?*, *Phys. Rev.* **D87** no. 9, (2013) 094025, arXiv:1202.1781 [hep-ph].

[433] Y. Nambu and G. Jona-Lasinio, *Dynamical Model of Elementary Particles Based on an Analogy with Superconductivity. 1.*, *Phys. Rev.* **122** (1961) 345–358.

[434] Y. Nambu and G. Jona-Lasinio, *DYNAMICAL MODEL OF ELEMENTARY PARTICLES BASED ON AN ANALOGY WITH SUPERCONDUCTIVITY. II*, *Phys. Rev.* **124** (1961) 246–254.

[435] T. Hatsuda and T. Kunihiro, *QCD phenomenology based on a chiral effective Lagrangian*, *Phys. Rept.* **247** (1994) 221–367, arXiv:hep-ph/9401310 [hep-ph].

[436] S. P. Klevansky, *The Nambu-Jona-Lasinio model of quantum chromodynamics*, *Rev. Mod. Phys.* **64** (1992) 649–708.

[437] A. Manohar and H. Georgi, *Chiral Quarks and the Nonrelativistic Quark Model*, *Nucl. Phys.* **B234** (1984) 189–212.

[438] D. Espriu, E. de Rafael, and J. Taron, *The QCD Effective Action at Long Distances*, *Nucl. Phys.* **B345** (1990) 22–56. [Erratum: Nucl. Phys.B355,278(1991)].

[439] J. Bijnens, E. Gamiz, E. Lipartia, and J. Prades, *QCD short distance constraints and hadronic approximations*, *JHEP* **04** (2003) 055, arXiv:hep-ph/0304222 [hep-ph].

[440] A. V. Radyushkin, *Introduction into QCD sum rule approach*, in *Strong interactions at low and intermediate energies. Proceedings, 13th Annual Hampton University Graduate Studies, HUGS'98, Newport News, USA, May 26-June 12, 1998*. 1998. arXiv:hep-ph/0101227 [hep-ph]. http://www1.jlab.org/Ul/publications/view_pub.cfm?pub_id=1220.

[441] H. Forkel and M. K. Banerjee, *Direct instantons in QCD nucleon sum rules*, *Phys. Rev. Lett.* **71** (1993) 484–487, arXiv:hep-ph/9309232 [hep-ph].

[442] E. V. Shuryak, *Pseudoscalar Mesons and Instantons*, *Nucl. Phys.* **B214** (1983) 237–252.

[443] P. Ball, V. M. Braun, and H. G. Dosch, *Form-factors of semileptonic* D *decays from QCD sum rules*, *Phys. Rev.* **D44** (1991) 3567–3581.

[444] I. I. Balitsky, V. M. Braun, and A. V. Kolesnichenko, $\Sigma^+ \to \mathrm{P}\gamma$ *Decay in QCD. (In Russian)*, *Sov. J. Nucl. Phys.* **44** (1986) 1028. [Yad. Fiz.44,1582(1986)].

[445] V. M. Braun, *Light cone sum rules*, in *Progress in heavy quark physics. Proceedings, 4th International Workshop, Rostock, Germany, September 20-22, 1997*, pp. 105–118. 1997. arXiv:hep-ph/9801222 [hep-ph].

[446] S. J. Brodsky and G. P. Lepage, *Large Angle Two Photon Exclusive Channels in Quantum Chromodynamics*, *Phys. Rev.* **D24** (1981) 1808.

[447] V. L. Chernyak and A. R. Zhitnitsky, *Asymptotic Behavior of Hadron Form-Factors in Quark Model. (In Russian)*, *JETP Lett.* **25** (1977) 510. [Pisma Zh. Eksp. Teor. Fiz.25,544(1977)].

[448] V. L. Chernyak and A. R. Zhitnitsky, *Asymptotics of Hadronic Form-Factors in the Quantum Chromodynamics. (In Russian)*, *Sov. J. Nucl. Phys.* **31** (1980) 544–552. [Yad. Fiz.31,1053(1980)].

[449] Y. Gao, C. S. Li, and J. J. Liu, *Transverse momentum resummation for Higgs production in soft-collinear effective theory*, *Phys. Rev.* **D72** (2005) 114020, arXiv:hep-ph/0501229 [hep-ph].

[450] R. Zwicky, *A brief Introduction to Dispersion Relations and Analyticity*, in *Proceedings, Quantum Field Theory at the Limits: from Strong Fields to Heavy Quarks (HQ 2016): Dubna, Russia, July 18-30, 2016*, pp. 93–120. 2017. arXiv:1610.06090 [hep-ph].

[451] R. J. Eden, P. V. Landshoff, D. I. Olive, and J. C. Polkinghorne, *The analytic S-matrix*. Cambridge Univ. Press, Cambridge, 1966.

[452] D. Ter Haar (ed.) and I. T. Todorov, *Analytic Properties of Feynman Diagrams in Quantum Field Theory. International Series of Monographs in Natural Philosophy*. Elsevier Reference Monographs, 169 p, 2014.

[453] G. Barton, *Introduction to dispersion techniques in field theory*. W.A. Benjamin (publ.), 242 p, 1965.

[454] E. de Rafael, *An Introduction to sum rules in QCD: Course*, in *Probing the standard model of particle interactions. Proceedings, Summer School in Theoretical Physics, NATO Advanced Study Institute, 68th session, Les Houches, France, July 28-September 5, 1997. Pt. 1, 2*, pp. 1171–1218. 1997. arXiv:hep-ph/9802448 [hep-ph].

[455] G. Kallen, *On the definition of the Renormalization Constants in Quantum Electrodynamics*, *Helv. Phys. Acta* **25** no. 4, (1952) 417.

[456] H. Lehmann, *On the Properties of propagation functions and renormalization contants of quantized fields*, *Nuovo Cim.* **11** (1954) 342–357.

[457] R. E. Cutkosky, *Singularities and discontinuities of Feynman amplitudes*, *J. Math. Phys.* **1** (1960) 429–433.

[458] F. Freitag and R. Busam, *Funktionentheorie 1*. Springer-Lehrbuch. Springer Berlin, 4. aufl., 550 p ed., 2006.

[459] M. Shifman, *QCD sum rules: Bridging the gap between short and large distances*, *Nucl. Phys. Proc. Suppl.* **207-208** (2010) 298–305, arXiv:1101.1122 [hep-ph].

[460] M. A. Shifman, *Quark hadron duality*, in *At the frontier of particle physics. Handbook of QCD. Vol. 1-3*, pp. 1447–1494, World Scientific. World Scientific, Singapore, 2001. arXiv:hep-ph/0009131 [hep-ph]. http://jhep.sissa.it/archive/prhep/preproceeding/hf8/013. [3,1447(2000)].

[461] Y. Klopot, A. Oganesian, and O. Teryaev, *Quark-hadron duality, axial anomaly and mixing*, *JETP Lett.* **94** (2011) 729–733, arXiv:1110.0474 [hep-ph].

[462] I. Montvay and G. Munster, *Quantum fields on a lattice*. Cambridge Monographs on Mathematical Physics. Cambridge University Press, 1997. http://www.cambridge.org/uk/catalogue/catalogue.asp?isbn=0521404320.

[463] T. DeGrand and C. E. Detar, *Lattice methods for quantum chromodynamics*. New Jersey, USA: World Scientific, 345 p, 2006.

[464] P. Ball and V. M. Braun, *Use and misuse of QCD sum rules in heavy to light transitions: The Decay* $B \to \rho e \nu_e$ *reexamined*, *Phys. Rev.* **D55** (1997) 5561–5576, arXiv:hep-ph/9701238 [hep-ph].

[465] A. Ali, V. M. Braun, and H. Simma, *Exclusive radiative* B *decays in the light cone QCD sum rule approach*, *Z. Phys.* **C63** (1994) 437–454, arXiv:hep-ph/9401277 [hep-ph].

[466] E. W. Weisstein, *Gegenbauer polynomial*. , 2017. http://mathworld.wolfram.com/GegenbauerPolynomial.html. From MathWorld – A Wolfram Web Resource.

[467] E. V. Shuryak and A. I. Vainshtein, *Theory of Power Corrections to Deep Inelastic Scattering in Quantum Chromodynamics. 1. Q^2 Effects*, *Nucl. Phys.* **B199** (1982) 451–481.

[468] W. Weise, ed., *QUARKS AND NUCLEI*. Singapore, Singapore: World Scientific (1984) 700 P. (Int. Rev. Nucl. Phys., 1, 1985.

[469] A. P. Bakulev, S. V. Mikhailov, A. V. Pimikov, and N. G. Stefanis. , 2012. For this calculation we use the Gegenbauer coefficients $a_2^\pi = 0.20$ and $a_4^\pi = -0.14$ at $\mu^2 = 1$ GeV^2 as quoted in [431].

[470] S. J. Brodsky and G. F. de Teramond, *Light-Front Dynamics and AdS/QCD Correspondence: The Pion Form Factor in the Space- and Time-Like Regions*, *Phys. Rev.* **D77** (2008) 056007, arXiv:0707.3859 [hep-ph].

[471] A. V. Radyushkin, *Shape of Pion Distribution Amplitude*, *Phys. Rev.* **D80** (2009) 094009, arXiv:0906.0323 [hep-ph].

[472] S. J. Brodsky, T. Kinoshita, and H. Terazawa, *Two Photon Mechanism of Particle Production by High-Energy Colliding Beams*, *Phys. Rev.* **D4** (1971) 1532–1557.

[473] M. Unverzagt, *Light meson physics with Crystal Ball/MAMI and at BES-III*, *J. Phys. Conf. Ser.* **349** (2012) 012015.

[474] T. Feldmann and P. Kroll, *Interpolation formulas for the* $\eta\gamma$ *and* $\eta'\gamma$ *transition form-factors*, *Phys. Rev.* **D58** (1998) 057501, arXiv:hep-ph/9805294 [hep-ph].

[475] M. V. Polyakov, *On the Pion Distribution Amplitude Shape*, *JETP Lett.* **90** (2009) 228–231, arXiv:0906.0538 [hep-ph].

[476] A. P. Bakulev, A. V. Radyushkin, and N. G. Stefanis, *Form-factors and QCD in space - like and time - like region*, *Phys. Rev.* **D62** (2000) 113001, arXiv:hep-ph/0005085 [hep-ph].

[477] V. A. Novikov, M. A. Shifman, A. I. Vainshtein, M. B. Voloshin, and V. I. Zakharov, *Use and Misuse of QCD Sum Rules, Factorization and Related Topics*, *Nucl. Phys.* **B237** (1984) 525–552.

[478] R. Arthur, P. A. Boyle, D. Brommel, M. A. Donnellan, J. M. Flynn, A. Juttner, T. D. Rae, and C. T. C. Sachrajda, *Lattice Results for Low Moments of Light Meson Distribution Amplitudes*, *Phys. Rev.* **D83** (2011) 074505, arXiv:1011.5906 [hep-lat].

[479] V. L. Chernyak and A. R. Zhitnitsky, *Asymptotic Behavior of Exclusive Processes in QCD*, *Phys. Rept.* **112** (1984) 173.

[480] N. G. Stefanis, W. Schroers, and H.-C. Kim, *Analytic coupling and Sudakov effects in exclusive processes: Pion and $\gamma^*\gamma \to \pi^0$ form-factors*, *Eur. Phys. J.* **C18** (2000) 137–156, arXiv:hep-ph/0005218 [hep-ph].

[481] A. H. Mueller, *Perturbative QCD at High-Energies*, *Phys. Rept.* **73** (1981) 237.

[482] P. Ball, J. M. Frere, and M. Tytgat, *Phenomenological evidence for the gluon content of η and η'*, *Phys. Lett.* **B365** (1996) 367–376, arXiv:hep-ph/9508359 [hep-ph].

[483] T. M. Aliev, I. Kanik, and A. Ozpineci, *Semileptonic $B \to \eta l \nu$ decay in light cone QCD*, *Phys. Rev.* **D67** (2003) 094009, arXiv:hep-ph/0210403 [hep-ph].

[484] **CLEO** Collaboration, B. I. Eisenstein et al., *Precision Measurement of $\mathcal{B}(D^+ \to \mu^+ \nu_\mu)$ and the Pseudoscalar Decay Constant f_{D^+}*, *Phys. Rev.* **D78** (2008) 052003, arXiv:0806.2112 [hep-ex].

[485] **Heavy Flavor Averaging Group (HFAG)** Collaboration, Y. Amhis et al., *Averages of b-hadron, c-hadron, and τ-lepton properties as of summer 2014*, arXiv:1412.7515 [hep-ex].

[486] M. Antonelli et al., *Flavor Physics in the Quark Sector*, *Phys. Rept.* **494** (2010) 197–414, arXiv:0907.5386 [hep-ph].

[487] **Quark Flavor Physics Working Group** Collaboration, J. N. Butler et al., *Working Group Report: Quark Flavor Physics*, in *Proceedings, 2013 Community Summer Study on the Future of U.S. Particle Physics: Snowmass on the Mississippi (CSS2013): Minneapolis, MN, USA, July 29-August 6, 2013*. 2013. arXiv:1311.1076 [hep-ex]. http://www.slac.stanford.edu/econf/C1307292/docs/IntensityFrontier/QuarkFl-15.pdf.

[488] M. Jamin and B. O. Lange, *f_B and f_{B_s} from QCD sum rules*, *Phys. Rev.* **D65** (2002) 056005, arXiv:hep-ph/0108135 [hep-ph].

[489] V. A. Novikov, L. B. Okun, M. A. Shifman, A. I. Vainshtein, M. B. Voloshin, and V. I. Zakharov, *Charmonium and Gluons: Basic Experimental Facts and Theoretical Introduction*, *Phys. Rept.* **41** (1978) 1–133.

[490] M. Beneke and V. M. Braun, *Heavy quark effective theory beyond perturbation theory: Renormalons, the pole mass and the residual mass term*, *Nucl. Phys.* **B426** (1994) 301–343, arXiv:hep-ph/9402364 [hep-ph].

[491] K. G. Chetyrkin and M. Steinhauser, *Heavy - light current correlators at order α_S^2 in QCD and HQET*, *Eur. Phys. J.* **C21** (2001) 319–338, arXiv:hep-ph/0108017 [hep-ph].

[492] K. G. Chetyrkin and M. Steinhauser, *Three loop nondiagonal current correlators in QCD and NLO corrections to single top quark production*, *Phys. Lett.* **B502** (2001) 104–114, arXiv:hep-ph/0012002 [hep-ph].

[493] S. Narison, *Extracting $\bar{m}_c(M_c)$ and $f_{D_s,B}$ from the pseudoscalar sum rules*, *Nucl. Phys. Proc. Suppl.* **74** (1999) 304–308, arXiv:hep-ph/9811208 [hep-ph].

[494] L. J. Reinders, S. Yazaki, and H. R. Rubinstein, *Masses and Couplings of Open Beauty States in QCD*, *Phys. Lett.* **104B** (1981) 305–310.

[495] T. M. Aliev and V. L. Eletsky, *On Leptonic Decay Constants of Pseudoscalar D and B Mesons*, *Sov. J. Nucl. Phys.* **38** (1983) 936. [Yad. Fiz.38,1537(1983)].

[496] S. Narison, *Decay Constants of the B and D Mesons from QCD Duality Sum Rules*, *Phys. Lett.* **B198** (1987) 104–112.

[497] L. J. Reinders, *The Leptonic Decay Constant f_B of the $B(b\bar{d})$ Meson and the Beauty Quark Mass*, *Phys. Rev.* **D38** (1988) 947.

[498] C. A. Dominguez and N. Paver, *How large is f_B from QCD sum rules?*, *Phys. Lett.* **B269** (1991) 169–174.

[499] E. Bagan, P. Ball, V. M. Braun, and H. G. Dosch, *QCD sum rules in the effective heavy quark theory*, *Phys. Lett.* **B278** (1992) 457–464.

[500] M. Neubert, *Heavy meson form-factors from QCD sum rules*, *Phys. Rev.* **D45** (1992) 2451–2466.

[501] A. Khodjamirian and R. Rückl, *QCD sum rules for exclusive decays of heavy mesons*, *Adv. Ser. Direct. High Energy Phys.* **15** (1998) 345–401, arXiv:hep-ph/9801443 [hep-ph].

[502] S. Narison, *Decay Constants of Heavy-Light Mesons from QCD*, *Nucl. Part. Phys. Proc.* **270-272** (2016) 143–153, arXiv:1511.05903 [hep-ph].

[503] N. N. Bogolyubov, B. V. Medvedev, and M. K. Polivanov, *Probleme der theorie der dispersionsbeziehungen*, *Fortschritte der Physik, vol. 6, issue 4-5* (1958) 169–245.

[504] V. A. Nesterenko and A. V. Radyushkin, *Sum Rules and Pion Form-Factor in QCD*, *Phys. Lett.* **115B** (1982) 410.

[505] B. L. Ioffe and A. V. Smilga, *Meson Widths and Form-Factors at Intermediate Momentum Transfer in Nonperturbative QCD*, *Nucl. Phys.* **B216** (1983) 373–407.

[506] P. Ball, *The Semileptonic decays $D \to \pi(\rho)e\nu$ and $B \to \pi(\rho)e\nu$ from QCD sum rules*, *Phys. Rev.* **D48** (1993) 3190–3203, arXiv:hep-ph/9305267 [hep-ph].

[507] B. L. Ioffe and A. V. Smilga, *Pion Form-Factor at Intermediate Momentum Transfer in QCD*, *Phys. Lett.* **114B** (1982) 353–358.

[508] B. Blok and M. Lublinsky, *Parton - hadron duality in QCD sum rules: Quantum mechanical examples*, *Phys. Rev.* **D57** (1998) 2676–2690, arXiv:hep-ph/9706484 [hep-ph]. [Erratum: Phys. Rev.D58,019903(1998)].

[509] A. I. Vainshtein, *How penguins started to fly*, *Int. J. Mod. Phys.* **A14** (1999) 4705–4719, arXiv:hep-ph/9906263 [hep-ph].

[510] V. M. Belyaev, A. Khodjamirian, and R. Rückl, *QCD calculation of the $B \to \pi, K$ form-factors*, *Z. Phys.* **C60** (1993) 349–356, arXiv:hep-ph/9305348 [hep-ph].

[511] E. Bagan, P. Ball, and V. M. Braun, *Radiative corrections to the decay* $B \to \pi e \nu$ *and the heavy quark limit*, *Phys. Lett.* **B417** (1998) 154–162, arXiv:hep-ph/9709243 [hep-ph].

[512] A. Khodjamirian, R. Rückl, and C. W. Winhart, *The Scalar* $B \to \pi$ *and* $D \to \pi$ *form-factors in QCD*, *Phys. Rev.* **D58** (1998) 054013, arXiv:hep-ph/9802412 [hep-ph].

[513] A. Khodjamirian, R. Rückl, S. Weinzierl, C. W. Winhart, and O. I. Yakovlev, *Predictions on* $B \to \pi l \bar{\nu}_l$, $D \to \pi l \bar{\nu}_l$ *and* $D \to K l \bar{\nu}_l$ *from QCD light cone sum rules*, *Phys. Rev.* **D62** (2000) 114002, arXiv:hep-ph/0001297 [hep-ph].

[514] Z.-H. Li, F.-Y. Liang, X.-Y. Wu, and T. Huang, *The* $B_s \to K$ *form-factor in the whole kinematically accessible range*, *Phys. Rev.* **D64** (2001) 057901, arXiv:hep-ph/0106186 [hep-ph].

[515] P. Ball and R. Zwicky, *Improved analysis of* $B \to \pi e \nu$ *from QCD sum rules on the light cone*, *JHEP* **10** (2001) 019, arXiv:hep-ph/0110115 [hep-ph].

[516] A. Khodjamirian, T. Mannel, and N. Offen, *B-meson distribution amplitude from the* $B \to \pi$ *form-factor*, *Phys. Lett.* **B620** (2005) 52–60, arXiv:hep-ph/0504091 [hep-ph].

[517] A. Khodjamirian, T. Mannel, and N. Offen, *Form-factors from light-cone sum rules with* B*-meson distribution amplitudes*, *Phys. Rev.* **D75** (2007) 054013, arXiv:hep-ph/0611193 [hep-ph].

[518] F. De Fazio, T. Feldmann, and T. Hurth, *Light-cone sum rules in soft-collinear effective theory*, *Nucl. Phys.* **B733** (2006) 1–30, arXiv:hep-ph/0504088 [hep-ph]. [Erratum: Nucl. Phys.B800,405(2008)].

[519] G. Duplancic and B. Melic, $B, B_s \to K$ *form factors: An Update of light-cone sum rule results*, *Phys. Rev.* **D78** (2008) 054015, arXiv:0805.4170 [hep-ph].

[520] J. Bijnens and A. Khodjamirian, *Exploring light cone sum rules for pion and kaon form-factors*, *Eur. Phys. J.* **C26** (2002) 67–79, arXiv:hep-ph/0206252 [hep-ph].

[521] V. M. Braun, E. Gardi, and S. Gottwald, *Renormalon approach to higher twist distribution amplitudes and the convergence of the conformal expansion*, *Nucl. Phys.* **B685** (2004) 171–226, arXiv:hep-ph/0401158 [hep-ph].

[522] C. Di Donato, G. Ricciardi, and I. Bigi, $\eta - \eta'$ *Mixing - From electromagnetic transitions to weak decays of charm and beauty hadrons*, *Phys. Rev.* **D85** (2012) 013016, arXiv:1105.3557 [hep-ph].

[523] S. Faller, A. Khodjamirian, C. Klein, and T. Mannel, $B \to D^{(*)}$ *Form Factors from QCD Light-Cone Sum Rules*, *Eur. Phys. J.* **C60** (2009) 603–615, arXiv:0809.0222 [hep-ph].

[524] A. V. Rusov, *Higher-twist effects in light-cone sum rule for the* $B \to \pi$ *form factor*, *Eur. Phys. J.* **C77** no. 7, (2017) 442, arXiv:1705.01929 [hep-ph].

[525] G. W. Jones, *Meson distribution amplitudes - applications to weak radiative* B *decays and* B *transition form factors*. PhD thesis, Durham U., 2007. arXiv:0710.4479 [hep-ph].

[526] P. Kroll, *Mixing of pseudoscalar mesons and isospin symmetry breaking*, *Int. J. Mod. Phys.* **A20** (2005) 331–340, arXiv:hep-ph/0409141 [hep-ph].

[527] A. Khodjamirian, T. Mannel, N. Offen, and Y. M. Wang, $B \to \pi l \nu_l$ *Width and* $|V_{ub}|$ *from QCD Light-Cone Sum Rules*, *Phys. Rev.* **D83** (2011) 094031, arXiv:1103.2655 [hep-ph].

[528] **Belle II** Collaboration, E. Kou et al., *The Belle II Physics Book*, arXiv:1808.10567 [hep-ex].

[529] **BaBar** Collaboration, B. Aubert et al., *The BABAR detector*, *Nucl. Instrum. Meth.* **A479** (2002) 1–116, arXiv:hep-ex/0105044 [hep-ex].

[530] D. M. Asner et al., *Physics at BES-III*, *Int. J. Mod. Phys.* **A24** (2009) S1–794, arXiv:0809.1869 [hep-ex].

[531] A. Ali and A. Ya. Parkhomenko, *The $\eta' g^* g^{(*)}$ vertex function in perturbative QCD and η' meson mass effects*, arXiv:hep-ph/0310250 [hep-ph]. [Eur. Phys. J.C33,s518(2004)].

[532] A. Ali and A. Ya. Parkhomenko, *The $\eta' g^* g^{(*)}$ vertex including the η' meson mass*, *Eur. Phys. J.* **C30** (2003) 367–380, arXiv:hep-ph/0307092 [hep-ph].

[533] C. Bourrely, B. Machet, and E. de Rafael, *Semileptonic Decays of Pseudoscalar Particles ($M \to M' \ell \nu_\ell$) and Short Distance Behavior of Quantum Chromodynamics*, *Nucl. Phys.* **B189** (1981) 157–181.

[534] C. G. Boyd, B. Grinstein, and R. F. Lebed, *Constraints on form-factors for exclusive semileptonic heavy to light meson decays*, *Phys. Rev. Lett.* **74** (1995) 4603–4606, arXiv:hep-ph/9412324 [hep-ph].

[535] L. Lellouch, *Lattice constrained unitarity bounds for $\bar{B}_0 \to \pi^+ l \bar{\nu}_l$ decays*, *Nucl. Phys.* **B479** (1996) 353–391, arXiv:hep-ph/9509358 [hep-ph].

[536] C. G. Boyd and M. J. Savage, *Analyticity, shapes of semileptonic form-factors, and $\bar{B} \to \pi \bar{\nu}_l l$*, *Phys. Rev.* **D56** (1997) 303–311, arXiv:hep-ph/9702300 [hep-ph].

[537] T. Becher and R. J. Hill, *Comment on form-factor shape and extraction of $|V_{ub}|$ from $B \to \pi l \nu$*, *Phys. Lett.* **B633** (2006) 61–69, arXiv:hep-ph/0509090 [hep-ph].

[538] C. Albertus, J. M. Flynn, E. Hernandez, J. Nieves, and J. M. Verde-Velasco, *Semileptonic $B \to \pi$ decays from an Omnes improved nonrelativistic constituent quark model*, *Phys. Rev.* **D72** (2005) 033002, arXiv:hep-ph/0506048 [hep-ph].

[539] J. M. Flynn and J. Nieves, *$|V_{ub}|$ from exclusive semileptonic $B \to \pi$ decays revisited*, *Phys. Rev.* **D76** (2007) 031302, arXiv:0705.3553 [hep-ph].

[540] **UKQCD** Collaboration, K. C. Bowler, L. Del Debbio, J. M. Flynn, L. Lellouch, V. Lesk, C. M. Maynard, J. Nieves, and D. G. Richards, *Improved $B \to \pi \nu_l l$ form-factors from the lattice*, *Phys. Lett.* **B486** (2000) 111–117, arXiv:hep-lat/9911011 [hep-lat].

[541] E. Dalgic, A. Gray, M. Wingate, C. T. H. Davies, G. P. Lepage, and J. Shigemitsu, *B meson semileptonic form-factors from unquenched lattice QCD*, *Phys. Rev.* **D73** (2006) 074502, arXiv:hep-lat/0601021 [hep-lat]. [Erratum: Phys. Rev.D75,119906(2007)].

[542] D. Becirevic and A. B. Kaidalov, *Comment on the heavy $\to$ light form-factors*, *Phys. Lett.* **B478** (2000) 417–423, arXiv:hep-ph/9904490 [hep-ph].

[543] S. J. Brodsky and G. R. Farrar, *Scaling Laws at Large Transverse Momentum*, *Phys. Rev. Lett.* **31** (1973) 1153–1156.

[544] S. J. Brodsky and G. R. Farrar, *Scaling Laws for Large Momentum Transfer Processes*, *Phys. Rev.* **D11** (1975) 1309.

[545] P. Gelhausen, A. Khodjamirian, A. A. Pivovarov, and D. Rosenthal, *Decay constants of heavy-light vector mesons from QCD sum rules*, *Phys. Rev.* **D88** (2013) 014015, arXiv:1305.5432 [hep-ph]. [Erratum: Phys. Rev.D91,099901(2015)].

[546] A. Khodjamirian, R. Rückl, S. Weinzierl, and O. I. Yakovlev, *Perturbative QCD correction to the light cone sum rule for the* $B^*B\pi$ *and* $D^*D\pi$ *couplings*, *Phys. Lett.* **B457** (1999) 245–252, arXiv:hep-ph/9903421 [hep-ph].

[547] A. Abada, D. Becirevic, P. Boucaud, G. Herdoiza, J. P. Leroy, A. Le Yaouanc, and O. Pene, *Lattice measurement of the couplings affine* $\hat{g}_\infty$ *and* $g_{B^*B\pi}$, *JHEP* **02** (2004) 016, arXiv:hep-lat/0310050 [hep-lat].

[548] A. Khodjamirian, *QCD sum rules for heavy flavor physics*, *AIP Conf. Proc.* **602** (2001) 194–205, arXiv:hep-ph/0108205 [hep-ph].

[549] **Particle Data Group** Collaboration, C. Caso et al., *Review of particle physics. Particle Data Group*, *Eur. Phys. J.* **C3** (1998) 1–794.

[550] H. Ohki, H. Matsufuru, and T. Onogi, *Determination of* $B^*B\pi$ *coupling in unquenched QCD*, *Phys. Rev.* **D77** (2008) 094509, arXiv:0802.1563 [hep-lat].

[551] H.-Y. Cheng, C.-Y. Cheung, G.-L. Lin, Y. C. Lin, T.-M. Yan, and H.-L. Yu, *Corrections to chiral dynamics of heavy hadrons:* $SU(3)$ *symmetry breaking*, *Phys. Rev.* **D49** (1994) 5857–5881, arXiv:hep-ph/9312304 [hep-ph]. [Erratum: Phys. Rev.D55,5851(1997)].

[552] S. Fajfer and J. F. Kamenik, *Chiral loop corrections to strong decays of positive and negative parity charmed mesons*, *Phys. Rev.* **D74** (2006) 074023, arXiv:hep-ph/0606278 [hep-ph].

[553] B. Grinstein and P. F. Mende, *Form-factors in the heavy quark and chiral limit: Pole dominance in* $\bar{B} \to \pi e \bar{\nu}_e$, *Nucl. Phys.* **B425** (1994) 451–470, arXiv:hep-ph/9401303 [hep-ph].

[554] A. Abada, D. Becirevic, P. Boucaud, J. P. Leroy, V. Lubicz, and F. Mescia, *Heavy* $\to$ *light semileptonic decays of pseudoscalar mesons from lattice QCD*, *Nucl. Phys.* **B619** (2001) 565–587, arXiv:hep-lat/0011065 [hep-lat].

[555] P. Ball and R. Zwicky, $|V_{ub}|$ *and constraints on the leading-twist pion distribution amplitude from* $B \to \pi l \nu$, *Phys. Lett.* **B625** (2005) 225–233, arXiv:hep-ph/0507076 [hep-ph].

[556] R. J. Hill, *Heavy-to-light meson form-factors at large recoil*, *Phys. Rev.* **D73** (2006) 014012, arXiv:hep-ph/0505129 [hep-ph].

[557] N. Isgur and M. B. Wise, *Influence of the b* Resonance on* $\bar{B} \to \pi e \bar{\nu}_e$, *Phys. Rev.* **D41** (1990) 151.

[558] N. Isgur and M. B. Wise, *Relationship Between Form-factors in Semileptonic* $\bar{B}$ *and* D *Decays and Exclusive Rare* $\bar{B}$ *Meson Decays*, *Phys. Rev.* **D42** (1990) 2388–2391.

[559] C. W. Bauer, S. Fleming, and M. E. Luke, *Summing Sudakov logarithms in* $B \to X_s\gamma$ *in effective field theory*, *Phys. Rev.* **D63** (2000) 014006, arXiv:hep-ph/0005275 [hep-ph].

[560] C. W. Bauer, S. Fleming, D. Pirjol, and I. W. Stewart, *An Effective field theory for collinear and soft gluons: Heavy to light decays*, *Phys. Rev.* **D63** (2001) 114020, arXiv:hep-ph/0011336 [hep-ph].

[561] J. Chay and C. Kim, *Collinear effective theory at subleading order and its application to heavy - light currents*, *Phys. Rev.* **D65** (2002) 114016, arXiv:hep-ph/0201197 [hep-ph].

[562] M. Beneke, A. P. Chapovsky, M. Diehl, and T. Feldmann, *Soft collinear effective theory and heavy to light currents beyond leading power*, *Nucl. Phys.* **B643** (2002) 431–476, arXiv:hep-ph/0206152 [hep-ph].

[563] R. J. Hill and M. Neubert, *Spectator interactions in soft collinear effective theory*, *Nucl. Phys.* **B657** (2003) 229–256, arXiv:hep-ph/0211018 [hep-ph].

[564] M. A. Shifman, *Lectures on heavy quarks in quantum chromodynamics*, in *ITEP lectures on particle physics and field theory. Vol. 1, 2*, pp. 409–514. 1995. arXiv:hep-ph/9510377 [hep-ph].

[565] R. Sommer, *Non-perturbative Heavy Quark Effective Theory: Introduction and Status*, *Nucl. Part. Phys. Proc.* **261-262** (2015) 338–367, arXiv:1501.03060 [hep-lat].

[566] M. Neubert, *Heavy quark symmetry*, *Phys. Rept.* **245** (1994) 259–396, arXiv:hep-ph/9306320 [hep-ph].

[567] M. J. Dugan and B. Grinstein, *QCD basis for factorization in decays of heavy mesons*, *Phys. Lett.* **B255** (1991) 583–588.

[568] M. B. Voloshin, *ON B(e3) DECAY*, *Sov. J. Nucl. Phys.* **50** (1989) 105. [Yad. Fiz.50,166(1989)].

[569] G. Duplancic, A. Khodjamirian, T. Mannel, B. Melic, and N. Offen, $|V_{ub}|$ *determination using* $B \to \pi$ *form factor from light-cone sum rule*, *J. Phys. Conf. Ser.* **110** (2008) 052026.

[570] **CLEO** Collaboration, S. B. Athar et al., *Study of the* q^2 *dependence of* $B \to \pi l\nu$ *and* $B \to \rho(\omega) l\nu\nu$ *decay and extraction of* $|V_{ub}|$, *Phys. Rev.* **D68** (2003) 072003, arXiv:hep-ex/0304019 [hep-ex].

[571] **Belle** Collaboration, K. Abe et al., *Measurement of exclusive* $B \to X_u l\nu$ *decays with* $D^* l\nu$ *decay tagging*, in *Proceedings, 32nd International Conference on High Energy Physics (ICHEP 2004): Beijing, China, August 16-22, 2004. Vol. 1+2*. 2004. arXiv:hep-ex/0408145 [hep-ex].

[572] **BaBar** Collaboration, B. Aubert et al., *Study of* $B \to \pi\ell\nu$ *and* $B \to \rho\ell\nu$ *decays and determination of* $|V_{ub}|$, *Phys. Rev.* **D72** (2005) 051102, arXiv:hep-ex/0507003 [hep-ex].

[573] **BaBar** Collaboration, B. Aubert et al., *Branching fraction for* $B^0 \to \pi^-\ell^+\nu$ *and determination of* $|V_{ub}|$ *in* $\Upsilon_{4S} \to B^0\bar{B}^0$ *events tagged by* $\bar{B}^0 \to D^{(*)}\ell^-\bar{\nu}$, in *Lepton and photon interactions at high energies. Proceedings, 22nd International Symposium, LP 2005, Uppsala, Sweden, June 30-July 5, 2005*. 2005. arXiv:hep-ex/0506064 [hep-ex]. https://oraweb.slac.stanford.edu/pls/slacquery/BABAR_DOCUMENTS.Search?P_SLAC_PUB=SLAC-PUB-11314.

[574] M. Okamoto et al., *Semileptonic* $D \to \pi/K$ *and* $B \to \pi/D$ *decays in* $2+1$ *flavor lattice QCD*, *Nucl. Phys. Proc. Suppl.* **140** (2005) 461–463, arXiv:hep-lat/0409116 [hep-lat].

[575] J. Shigemitsu, C. T. H. Davies, A. Dougall, K. Foley, E. Gamiz, A. Gray, E. Dalgic, G. P. Lepage, and M. Wingate, *Semileptonic* B *decays with* $N_f = 2+1$ *dynamical quarks*, *Nucl. Phys. Proc. Suppl.* **140** (2005) 464–466, arXiv:hep-lat/0408019 [hep-lat].

[576] J. M. Flynn and J. Nieves, *Extracting* $|V_{ub}|$ *from* $B \to \pi l\nu_l$ *decays using a multiply-subtracted Omnes dispersion relation*, *Phys. Rev.* **D75** (2007) 013008, arXiv:hep-ph/0607258 [hep-ph].

[577] P. Ball, $|V_{ub}|$ *from UTangles and* $B \to \pi l\nu$, *Phys. Lett.* **B644** (2007) 38–44, arXiv:hep-ph/0611108 [hep-ph].

[578] I. Kanamori, *Lattice calculations of D_s to η and η' decay form factors*, arXiv:1302.6087 [hep-lat]. [PoSConfinementX,143(2012)].

[579] **CLEO** Collaboration, J. Yelton et al., *Absolute Branching Fraction Measurements for Exclusive D_s Semileptonic Decays*, *Phys. Rev.* **D80** (2009) 052007, arXiv:0903.0601 [hep-ex].

[580] **CLEO** Collaboration, J. Yelton et al., *Studies of $D^+ \to \eta', \eta, \phi e^+ \nu_e$*, *Phys. Rev.* **D84** (2011) 032001, arXiv:1011.1195 [hep-ex].

[581] **CLEO** Collaboration, N. E. Adam et al., *A Study of Exclusive Charmless Semileptonic B Decay and $|V_{ub}|$*, *Phys. Rev. Lett.* **99** (2007) 041802, arXiv:hep-ex/0703041 [HEP-EX].

[582] **BaBar** Collaboration, P. del Amo Sanchez et al., *Measurement of the $B^0 \to \pi^0 l^+ \nu_l$ and $B^+ \to \eta^{(\prime)} l^+ \nu_l$ Branching Fractions, the $B^0 \to \pi^- l^+ \nu_l$ and $B^+ \to \eta l^+ \nu_l$ Form-Factor Shapes, and Determination of $|V_{ub}|$*, *Phys. Rev.* **D83** (2011) 052011, arXiv:1010.0987 [hep-ex].

[583] V. M. Braun and A. N. Manashov, *Operator product expansion in QCD in off-forward kinematics: Separation of kinematic and dynamical contributions*, *JHEP* **01** (2012) 085, arXiv:1111.6765 [hep-ph].

[584] A. Einstein, *The Foundation of the General Theory of Relativity*, *Annalen Phys.* **49** no. 7, (1916) 769–822.

[585] G. F. Sterman, *An Introduction to quantum field theory*. Cambridge University Press, 1993.

[586] V. B. Mandel'tsveig, *Irreducible representations of the $su(3)$ group*, *Sov. Phys. JETP* **20** no. 5, (1965) 1237–1243.

[587] K. Passek-Kumericki and G. Peters, *Nucleon Form Factors to Next-to-Leading Order with Light-Cone Sum Rules*, *Phys. Rev.* **D78** (2008) 033009, arXiv:0805.1758 [hep-ph].

[588] V. S. Popov, V. L. Eletsky, and A. V. Turbiner, *HIGHER ORDER THEORY OF PERTURBATIONS AND SUMMING SERIES IN QUANTUM MECHANICS AND FIELD THEORY*, *Zh. Eksp. Teor. Fiz.* **74** (1978) 445–465.

[589] A. Khodjamirian, *Quantum chromodynamics and hadrons: An Elementary introduction*, in *High-energy physics. Proceedings, European School, Tsakhkadzor, Armenia, August 24-September 6, 2003*, pp. 173–222. 2004. arXiv:hep-ph/0403145 [hep-ph]. http://doc.cern.ch/yellowrep/2005/2005-007/p173.pdf.

[590] J. C. Collins, *Light cone variables, rapidity and all that*, arXiv:hep-ph/9705393 [hep-ph].

[591] G. Szegö, *Orthogonal Polynomials*. Providence, American Mathematical Society, 432 p, 1939.

[592] E. W. Weisstein, *Jacobi polynomial*. , 2017. http://mathworld.wolfram.com/JacobiPolynomial.html. From MathWorld – A Wolfram Web Resource.

[593] M. Abramowitz and I. A. Stegun, eds., *Handbook of Mathematical Functions With Formulas, Graphs and Mathematical Tables. National Bureau of Standards Applied Mathematics Series - 55*, vol. Originally issued June 1964 | 10th edition 1972. New York, USA: Dover Publications Inc., 1046 p, 1972. http://people.math.sfu.ca/~cbm/aands/page_260.htm.

[594] E. D. Micheli and G. A. Viano, *The expansion in gegenbauer polynomials: A simple method for the fast computation of the gegenbauer coefficients*, *Journal of Computational Physics* **239** (2013) 112 – 122. http://www.sciencedirect.com/science/article/pii/S0021999113000387.

[595] T. Bröcker, *Analysis III*. BI Wissenschaftsverlag (Hersteller: Spektrum Akademischer Verlag); Auflage: 1. Auflage, 209 p, 1992.

[596] A. Crisanti, *Asymptotic expansions*. , 2017/2018. http://www2.phys.uniroma1.it/doc/crisanti/Teach/MetNum/Notes/AsExp.pdf. Dipartimento di Fisica - Sapienza Universitàdi Roma, Corso di Metodi Computazionali per la Fisica, A.A.

[597] R. Jakob and P. Kroll, *The Pion form-factor: Sudakov suppressions and intrinsic transverse momentum*, *Phys. Lett.* **B315** (1993) 463–470, arXiv:hep-ph/9306259 [hep-ph]. [Erratum: Phys. Lett.B319,545(1993)].

[598] M. V. Fedoryuk (originator), *Stationary phase, method of the,*. http://www.encyclopediaofmath.org/index.php?title=Stationary_phase,_method_of_the&oldid=24568.

[599] M. Hazewinkel, ed., *Encyclopaedia of Mathematics (set)*. Kluwer Academic Publishers (Verlag), 5402 p, (1992 | 1994 ed.).

[600] S. Bochner and K. Chandrasekharan, *Fourier Transforms. (AM-19)*, vol. Volume 19. Princeton University Press, 219 p, 1949.

[601] I. S. Gradshteyn and I. M. Ryzhik, *Table of Integrals, Series, and Products*, vol. 1. Auflage. Elsevier Science (Verlag), 1206 p, 2014.

[602] V. Braun, *Quantenchromodynamik*. , Wintersemester 2008/2009. Vorlesungsskript, Universität Regensburg.

[603] X. Ji, *Parton Physics on a Euclidean Lattice*, *Phys. Rev. Lett.* **110** (2013) 262002, arXiv:1305.1539 [hep-ph].

[604] D. Müller, *Restricted conformal invariance in QCD and its predictive power for virtual two photon processes*, *Phys. Rev.* **D58** (1998) 054005, arXiv:hep-ph/9704406 [hep-ph].

[605] A. V. Belitsky and D. Müller, *Predictions from conformal algebra for the deeply virtual Compton scattering*, *Phys. Lett.* **B417** (1998) 129–140, arXiv:hep-ph/9709379 [hep-ph].

[606] W. A. Bardeen, A. J. Buras, D. W. Duke, and T. Muta, *Deep Inelastic Scattering Beyond the Leading Order in Asymptotically Free Gauge Theories*, *Phys. Rev.* **D18** (1978) 3998.

[607] D. J. Broadhurst, *Chiral Symmetry Breaking and Perturbative QCD*, *Phys. Lett.* **101B** (1981) 423–426.

[608] S. C. Generalis, *QCD sum rules. 1: Perturbative results for current correlators*, *J. Phys.* **G16** (1990) 785–793.

[609] S. C. Generalis, *QCD sum rules. II: A note on the mass of the strange quark*, *J. Phys.* **G16** (1990) L117–L120.

[610] K. G. Chetyrkin, J. H. Kuhn, and M. Steinhauser, *Three loop polarization function and $\mathcal{O}(\alpha_s^2)$ corrections to the production of heavy quarks*, *Nucl. Phys.* **B482** (1996) 213–240, arXiv:hep-ph/9606230 [hep-ph].

[611] P. Pascual and R. Tarrach, *QCD: RENORMALIZATION FOR THE PRACTITIONER*, *Lect. Notes Phys.* **194** (1984) 1–277.

[612] R. Tarrach, *The Pole Mass in Perturbative QCD*, *Nucl. Phys.* **B183** (1981) 384–396.

[613] N. Gray, D. J. Broadhurst, W. Grafe, and K. Schilcher, *Three Loop Relation of Quark (Modified) Ms and Pole Masses*, *Z. Phys.* **C48** (1990) 673–680.

[614] E. D. Solomentsev (originator), *Riemann surface*. Encyclopedia of mathematics, springer, 2012. https://www.encyclopediaofmath.org/index.php?title=Riemann_surface&oldid=23963.

[615] G. H. Hardy, *Divergent series*, vol. 2nd Revised edition. American Mathematical Society, 396 p, 2000.

[616] A. A. Zakharov and M. Hazewinkel, *Borel summation method*. Encyclopedia of mathematics, springer, 2001. https://www.encyclopediaofmath.org/index.php/Borel_summation_method.

[617] O. Costin, *Asymptotics and Borel Summability. Monographs and Surveys in Pure and Applied Mathematics*. Chapman & Hall/CRC, 256 p, 2008.

[618] J. Berstel and C. Reutenauer, *Noncommutative Rational Series with Applications. Encyclopedia of Mathematics and its Applications 137*, vol. 1st edition. Cambridge University Press, 262 p, 2010.

[619] E. Borel, *Lectures on divergent series, Collection of Monographs on the Theory of Functions, École Normale Supérieure, Paris - France (1927); Translation - Los Alamos Scientific Laboratory of the University of California (LA-6140-TR), U.S., Energy Research and Development Administration (1975).* (1927) .

[620] E. Borel, *Mémoire sur les séries divergentes, Ann. Sci. École Norm. Sup. (3) , 16 (1899)* (1899) 9–131.

[621] W. Beekmann and K. Zeller, *Theorie der Limitierungsverfahren*, vol. 2., erweiterte und verbesserte Aufl. Springer-Verlag Berlin Heidelberg, 1970.

[622] J. Glimm and A. M. Jaffe, *QUANTUM PHYSICS. A FUNCTIONAL INTEGRAL POINT OF VIEW*. Springer-Verlag New York Inc., 535 p, 1987.

[623] M. Reed and B. Simon, *Methods Of Mathematical Physics. Vol. 4: Analysis of Operators*. Academic Press Inc. (Verlag) San Diego, 325 p, 1978.

[624] G. Sansone and J. Gerretsen, *Lectures on the Theory of Functions of a Complex Variable: Volume I: Holomorphic Functions. Volume II: Geometric Theory*. Kluwer Academic Publishers, Dordrecht, 1188 p, 1969.

[625] H. Kleinert and V. Schulte-Frohlinde, *Critical properties of* phi^4*-theories*. River Edge, USA: World Scientific, 489 p, 2001.

[626] G. Parisi, *Singularities of the Borel Transform in Renormalizable Theories*, *Phys. Lett.* **76B** (1978) 65–66.

[627] A. Zichichi, *THE WHYS OF SUBNUCLEAR PHYSICS. PROCEEDINGS OF THE 1977 INTERNATIONAL SCHOOL OF SUBNUCLEAR PHYSICS, HELD IN ERICE, TRAPANI, SICILY, JULY 23 - AUGUST 10, 1977*. New york, usa: Plenum pr.(1979) 1247 p.(the subnuclear series, vol.15), July, 1979.

[628] G. Parisi, *On Infrared Divergences*, *Nucl. Phys.* **B150** (1979) 163–172.

[629] F. David, *The Operator Product Expansion and Renormalons: A Comment*, *Nucl. Phys.* **B263** (1986) 637–648.

[630] J. J. Aubert, R. Gastmans, and J. M. Gerard, eds., *Proceedings, NATO Advanced Study Institute on Particle Physics: Ideas and Recent Developments*, vol. 555. 2000. http://link.springer.com/book/10.1007/978-94-011-4128-4.

[631] N. Bourbaki, *Algebra II: Chapters 4 – 7. Elements of Mathematics*. Springer Berlin (1st ed. 1990. | 2nd printing 2003), 453 p, .

[632] K. Jänich, *Funktionentheorie*, vol. 6. Aufl. Springer Berlin, 123 p, 2004.

[633] V. A. Nesterenko and A. V. Radyushkin, *Quark - Hadron Duality and Nucleon Form-factors in QCD*, *Sov. J. Nucl. Phys.* **39** (1984) 811. [Yad. Fiz.39,1287(1984)].

[634] A. Khodjamirian, *QCD sum rules: A Working tool for hadronic physics*, in *Continuous advances in QCD. Proceedings, Conference, Minneapolis, USA, May 17-23, 2002*, pp. 58–79. 2002. arXiv:hep-ph/0209166 [hep-ph].

[635] K. Jänich, *Analysis für Physiker und Ingenieure*, vol. 4. Aufl. Springer Berlin, 419 p, 2001.

[636] J. Figueroa-O'Farrill, *Complex analysis*. , 1998. http://www.maths.ed.ac.uk/~jmf/Teaching/MT3/ComplexAnalysis.pdf. Mathematical Techniques III – Lecture notes, Autumn term of 1998, University of Edinburgh (School of Mathematics), Scotland UK.

[637] V. PeOinova (ed.), M. W. Evans, A. Luks, and J. Perina (ed.), *Phase in Optics. World Scientific Series in Contemporary Chemical Physics; 15*. World Scientific Publishing Co. Pte. Ltd., Singapore, 464 p, 1998.

[638] M. Melcher, B *decays from QCD sum rules*. PhD thesis, Siegen U., 2006. http://dokumentix.ub.uni-siegen.de/opus/volltexte/2006/212/.

[639] E. Chirka (originator), *Analytic continuation*. Encyclopedia of mathematics, springer, 2012. https://www.encyclopediaofmath.org//index.php?title=Analytic_continuation&oldid=24365.

[640] L. Ahlfors, *Complex Analysis: An Introduction to The Theory of Analytic Functions of One Complex Variable (International Series in Pure and Applied Mathematics)*, vol. 3rd edition. McGraw-Hill Professional, 352 p, 1978.

[641] L. Bieberbach, *Analytische Fortsetzung. Ergebnisse der Mathematik und ihrer Grenzgebiete. 2. Folge; 3*. Springer Berlin, 168 p, (2013 | 1955).

[642] P. Dienes, *The Taylor series: An introduction to the theory of functions of a complex variable*, vol. 1st edition. Dover Publications, 552 p, 1957.

[643] N. Mahnke, *QCD Summenregelbeiträge zu den elektromagnetischen Formfaktoren des Nukleons im Bereich mittleren Energieübertrags*. PhD thesis, Universität Regensburg, 2003.

[644] V. Barone and P. G. Ratcliffe, *Transverse spin physics*. River Edge, USA: World Scientific, 294 p, 2003.

[645] M. A. Shifman and M. I. Vysotsky, *FORM-FACTORS OF HEAVY MESONS IN QCD*, *Nucl. Phys.* **B186** (1981) 475–518.

[646] I. I. Balitsky and V. M. Braun, *The Nonlocal operator expansion for inclusive particle production in e^+e^- annihilation*, *Nucl. Phys.* **B361** (1991) 93–140.

[647] G. Münster, *Quantentheorie*. De Gruyter (Verlag), Berlin · New York, 2006.

This document was typeset using the typographical look-and-feel `classicthesis` developed by André Miede. The style was inspired by Robert Bringhurst's seminal book on typography "*The Elements of Typographic Style*". `classicthesis` is available for both LaTeX and LyX:

http://code.google.com/p/classicthesis/